IRC 868

THE UNITED STATES GEOLOGICAL SURVEY IN ALASKA: ACCOMPLISHMENTS DURING 1981

Geological Survey Circular 868

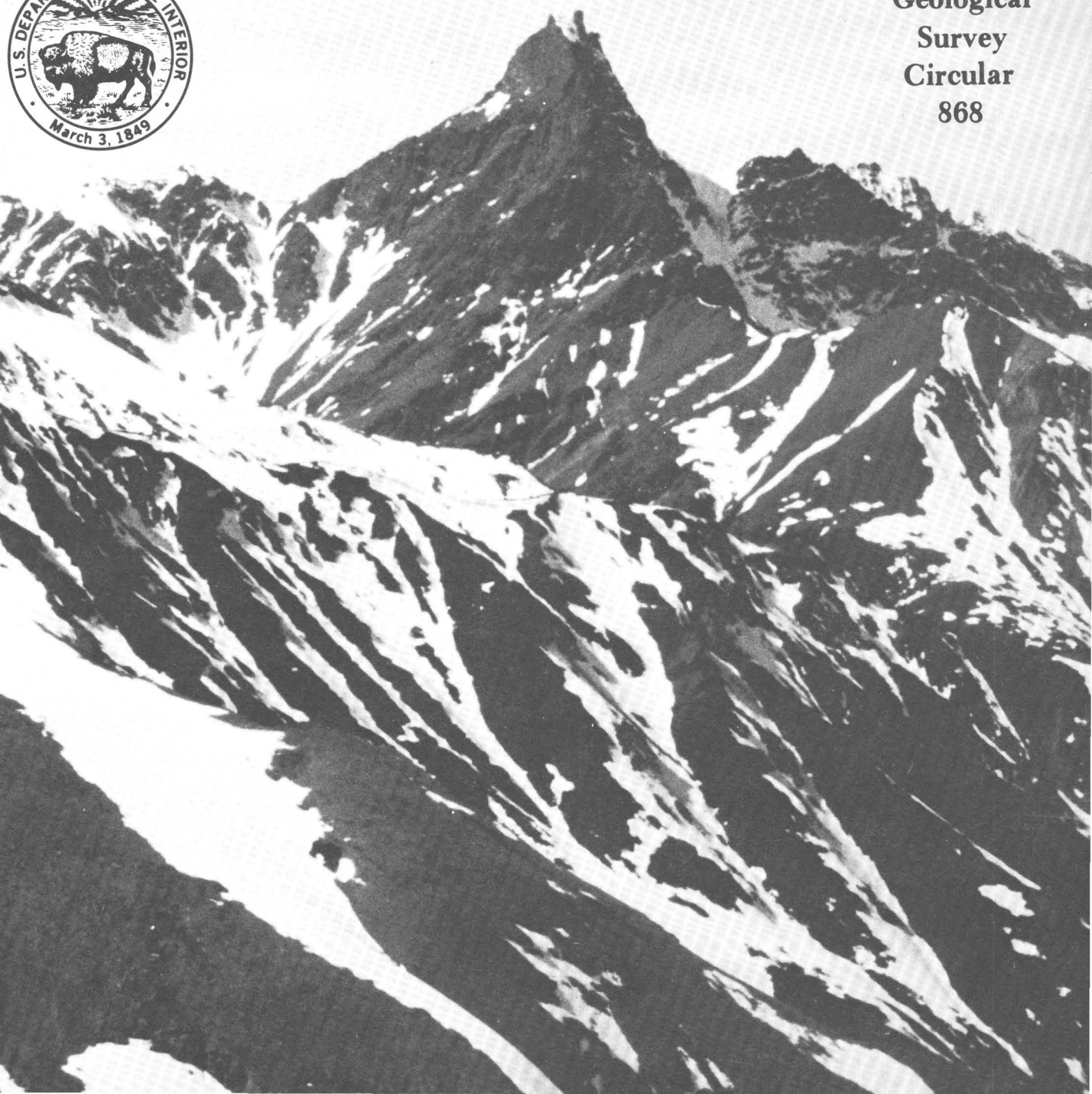

FRONT COVER

The front cover is a photograph of Mount Doonerak, one of the highest mountains in the Brooks Range (see Dutro and others, this volume).

The United States Geological Survey in Alaska: Accomplishments During 1981

Warren L. Coonrad and Raymond L. Elliott, Editors

U.S. GEOLOGICAL SURVEY CIRCULAR 868

1984

Department of the Interior
WILLIAM P. CLARK, *Secretary*

U.S. Geological Survey
Dallas L. Peck, *Director*

Library of Congress Catalog Card Number 76-608093

Free on application to Distribution Branch, Text Products Section,
U.S. Geological Survey, 604 South Pickett Street, Alexandria, VA 22304

CONTENTS

ILLUSTRATIONS

TABLES

Any use of trade names and trademarks in this report is for descriptive purposes only and does not constitute endorsement by the U.S. Geological Survey. Underlining of items in the text of this Circular substitutes for italic typography and is not necessarily used for emphasis.

THE UNITED STATES GEOLOGICAL SURVEY IN ALASKA: ACCOMPLISHMENTS DURING 1981

Warren L. Coonrad and Raymond L. Elliott, Editors

ABSTRACT

This report of accomplishments of the U.S. Geological Survey in Alaska during 1981 contains summary and topical accounts of the results of studies on a wide range of topics of economic and scientific interest. In addition, many more detailed maps and reports are included in the lists of references cited for each article and in the appended compilations of 277 reports on Alaska published by the U.S. Geological Survey and of 103 reports by U.S. Geological Survey authors in various other scientific publications.

SUMMARY OF IMPORTANT RESULTS

The U.S. Geological Survey is engaged in many scientific investigations on various aspects of the land and water in Alaska. Products of the Survey's investigations include reports describing the physical findings and their significance. This volume includes summary discussions, topical results, and some narratives of the course of the studies on just a few of the various Earth-science subjects currently being investigated in Alaska. For the reader's convenience in perusing reports that cover specific areas of interest, the articles are grouped by areas corresponding to the six regional geographic onshore subdivisions shown in figure 1, by offshore coverage, and by those articles that cover more than one geographical region or are Statewide in scope. Index maps showing the study areas or sites discussed are included near the beginning of each subdivision (figs. 1, 5, 13, 19, 23, 44, 72, 90). An author index at the back of the volume should assist in identifying and locating work by specific authors reported herein or in the appended compilations of current reports on Alaska by U.S. Geological Survey authors and their associates.

STATEWIDE ALASKA

(Figure 1 shows the quadrangles and regions referred to in this volume)

Summary of Landsat quadrangle studies in Alaska

By James R. Le Compte, William Clinton Steele, and Nairn R. D. Albert

Landsat-image interpretation and (or) Landsat-feature maps for 27 Alaskan 1:250,000-scale quadrangles (fig. 2) have been completed. These maps are the major summary products of the U.S. Geological Survey's Branch of Alaskan Geology's telegeologic research effort, funded under the auspices of the Alaskan Mineral Resource Assessment Program. Synthesis of the data compiled from these studies indicates that the major features commonly observable on Landsat images of Alaska are lineaments, circular and arcuate features, and anomalously colored areas.

Lineaments

Lineaments observed in Alaska can generally be divided into three groups on the basis of scale: (1) Statewide lineament trends (northwest, north-south, northeast, and east-west; see Lathram and Raynolds, 1977), corresponding to the regmatic shear pattern, that not only transect tectonic and stratigraphic boundaries but also coincide with these boundaries in places; (2) regional trends, such as for the set of lineaments along the Denali fault in the Talkeetna quadrangle (Steele and Albert, 1978a) or along the Coast Range megalineament in the Ketchikan quadrangle; and (3) local trends that are commonly restricted to specific terranes and various geologic phenomena, or to structures caused by unknown (local) tectonic events.

That many lineaments (generally from several kilometers to several tens of kilometers long) which make up sets of subparallel to parallel lineaments detected on Landsat images may reflect relatively narrow (generally less than 10 km wide) zones of associated(?) fractures is particularly well shown in the Ketchikan quadrangle (Steele and Albert, 1978b; Le Compte, 1981b). Only a few (1-10 percent) of the lineaments there are faults, although many faults that are mappable at 1:250,000 scale can be detected on Landsat images. Lineament extensions beyond the terminations of the many faults mapped by field methods are also evident in places.

Circular and Arcuate Features

Circular and arcuate features detected on Landsat images of Alaska can generally be divided into two groups. The first group consists of circular and arcuate features larger than 50 km in diameter, such as several circular features in the eastern Brooks Range (Le Compte, 1979a); few logical explanations have been found for features this large. The second group

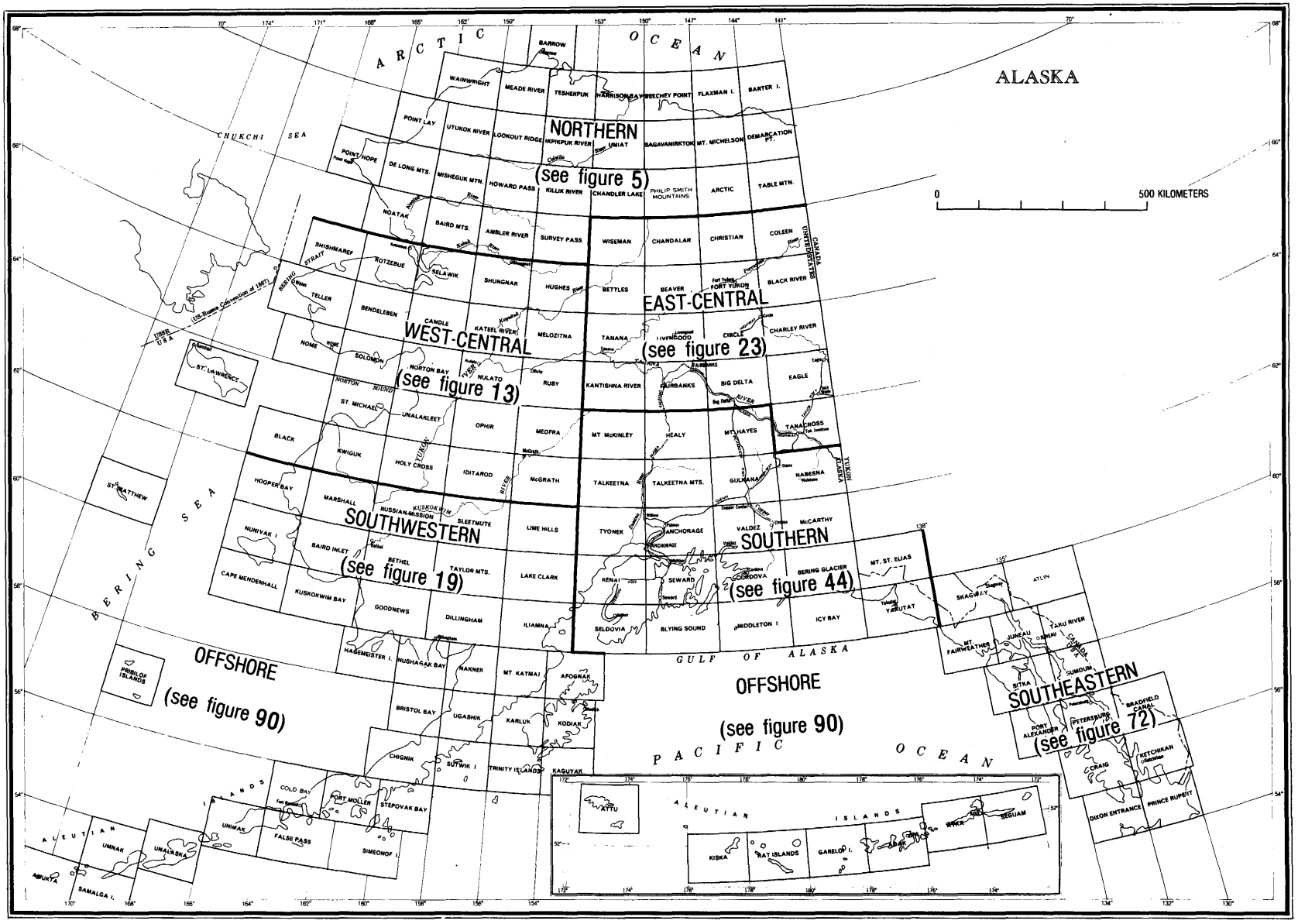

Figure 1.—Regions of Alaska used in this report. Referenced figures indicate regional index maps showing areas discussed in this volume.

consists of circular and arcuate features smaller than 50 km in diameter. Approximately half of these smaller features are spatially related to known geologic bodies or structures: (1) Concentric ("nested") circular features—to batholiths and plutons; (2) solitary circular features—to batholiths, plutons, volcanic cones, craters, and calderas; and (3) "nested" arcuate features—to folds.

Anomalously Colored Areas

Numerous anomalously colored areas are noted statewide from computer-enhanced "true-color" imagery of the quadrangles studied. These areas are typically marked by iron-oxide-stained (gossanlike) surface colorations. Many of these areas have proven to be associated with either mineralized plutonic bodies, such as in the Healy quadrangle (Le Compte, 1981h), or (mineralized or nonmineralized) hydrothermally altered rocks, such as in the Talkeetna Mountains quadrangle (Steele and Le Compte, 1978).

REFERENCES CITED

Albert, N. R. D., 1975, Interpretation of Earth Resources Technology Satellite imagery of the Nabesna quadrangle, Alaska: U.S. Geological Survey Miscellaneous Field Studies Map MF-655-J, scale 1:250,000, 2 sheets.

———1978, Map showing interpretation of Landsat imagery of the Ambler River quadrangle, Alaska: U.S. Geological Survey Open-File Report 78-120-J, scale 1:250,000, 2 sheets.

Albert, N. R. D., Le Compte, J. R., and Steele, W. C., 1978, Map showing interpretation of Landsat imagery of the Chandalar quadrangle, Alaska: U.S. Geological Survey Miscellaneous Field Studies Map MF-878-J, scale 1:250,000, 2 sheets.

Albert, N. R. D., and Steele, W. C., 1976a, Interpretation of Landsat imagery of the McCarthy quadrangle, Alaska: U.S. Geological Survey Miscellaneous Field Studies Map MF-773-N, scale 1:250,000, 3 sheets.

———1976b, Interpretation of Landsat imagery of the Tanacross quadrangle, Alaska: U.S. Geological Survey Miscellaneous Field Studies Map MF-767-C, scale 1:250,000, 3 sheets.

———1978, Maps showing interpretation of Landsat imagery of the Big Delta quadrangle, Alaska: U.S. Geological Survey Open-File Report 78-529-C, scale 1:250,000, 2 sheets.

Lathram, E. H., and Raynolds, R. G. H., 1977, Tectonic deductions from Alaskan space imagery, in Woll, P. W., and Fischer, W. A., eds., Proceedings of the first annual William T. Pecora Memorial Symposium, October 1975, Sioux Falls, South Dakota: U.S. Geological Survey Professional Paper 1015, p. 179-191.

Le Compte, J. R., 1979a, Map showing interpretation of Landsat imagery of the Philip Smith Mountains quadrangle, Alaska: U.S. Geological Survey Miscellaneous Field Studies Map MF-879-F, scale 1:250,000, 2 sheets.

———1979b, Map showing interpretation of Landsat imagery of the Seward and Blying Sound quadrangles, Alaska: U.S. Geological Survey Open-File Report 78-737, scale 1:250,000, 2 sheets.

———1981a, Landsat features maps of the Circle quadrangle, Alaska: U.S. Geological Survey Open-File Report 81-782, scale 1:250,000, 2 sheets.

———1981b, Landsat features maps of the Ketchikan and Prince Rupert quadrangles, Alaska: U.S. Geological Survey Open-File Report 81-1139, scale 1:250,000, 2 sheets.

———1981c, Landsat features maps of the Petersburg quadrangle and vicinity, southeastern Alaska: U.S. Geological Survey Open-File Report 81-799, scale 1:250,000, 2 sheets.

———1981d, Maps showing interpretation of Landsat imagery of the Bradfield Canal quadrangle, southeastern Alaska: U.S. Geological Survey Open-File Report 81-728-L, scale 1:250,000, 2 sheets.

———1981e, Maps showing interpretation of Landsat imagery of the Medfra quadrangle, Alaska: U.S. Geological Survey Open-File Report 80-811-D, scale 1:250,000, 2 sheets.

———1981f, Maps showing interpretation of Landsat imagery of the Survey Pass quadrangle, Alaska: U.S. Geological Survey Miscellaneous Field Studies Map MF-1176-H, scale 1:250,000, 2 sheets.

———1981g, Map showing interpretation of Landsat imagery of the Valdez $1^{\circ}x3^{\circ}$ quadrangle, southern Alaska: U.S. Geological Survey Open-File Report 80-892-F, scale 1:250,000.

———1981h, Preliminary maps showing interpretation of Landsat imagery of the Healy quadrangle, Alaska: U.S. Geological Survey Open-File Report 81-768, scale 1:250,000, 2 sheets.

———1981i, Preliminary maps showing interpretation of Landsat imagery of the Ugashik and Karluk quadrangles, Alaska: U.S. Geological Survey Open-File Report 81-776, scale 1:250,000, 2 sheets.

Le Compte, J. R. and Steele, W. C., 1981, Maps showing interpretation of Landsat imagery of the Chignik and Sutwik Island quadrangles, Alaska: U.S. Geological Survey Miscellaneous Field Studies Map MF-1053-O, scale 1:250,000, 2 sheets.

Steele, W. C., 1978, Interpretation of Landsat imagery of the Goodnews and Hagemeister Island quadrangles region, southwestern Alaska: U.S. Geological Survey Open-File Report 78-9-D, scale 1:250,000.

———1983, Map showing interpretation of Landsat imagery of the Lake Clark quadrangle, Alaska: U.S. Geological Survey Miscellaneous Field Studies Map MF-1114-K, scale 1:250,000 [in press].

Steele, W. C., and Albert, N. R. D., 1978a, Interpretation of Landsat imagery of the Talkeetna quadrangle, Alaska: U.S. Geological Survey Miscellaneous Field Studies Map MF-870-C, scale 1:250,000, 2 sheets.

——— 1978b, Map showing interpretation of Landsat imagery of the Ketchikan and Prince Rupert quadrangles, Alaska: U.S. Geological Survey Open-File Report 78-73-K, scale 1:250,000, 2 sheets.

Steele, W. C., and Le Compte, J. R., 1978, Map showing interpretation of Landsat imagery of the Talkeetna Mountains quadrangle, Alaska: U.S. Geological Survey Open-File Report 78-558-D, scale 1:250,000, 2 sheets.

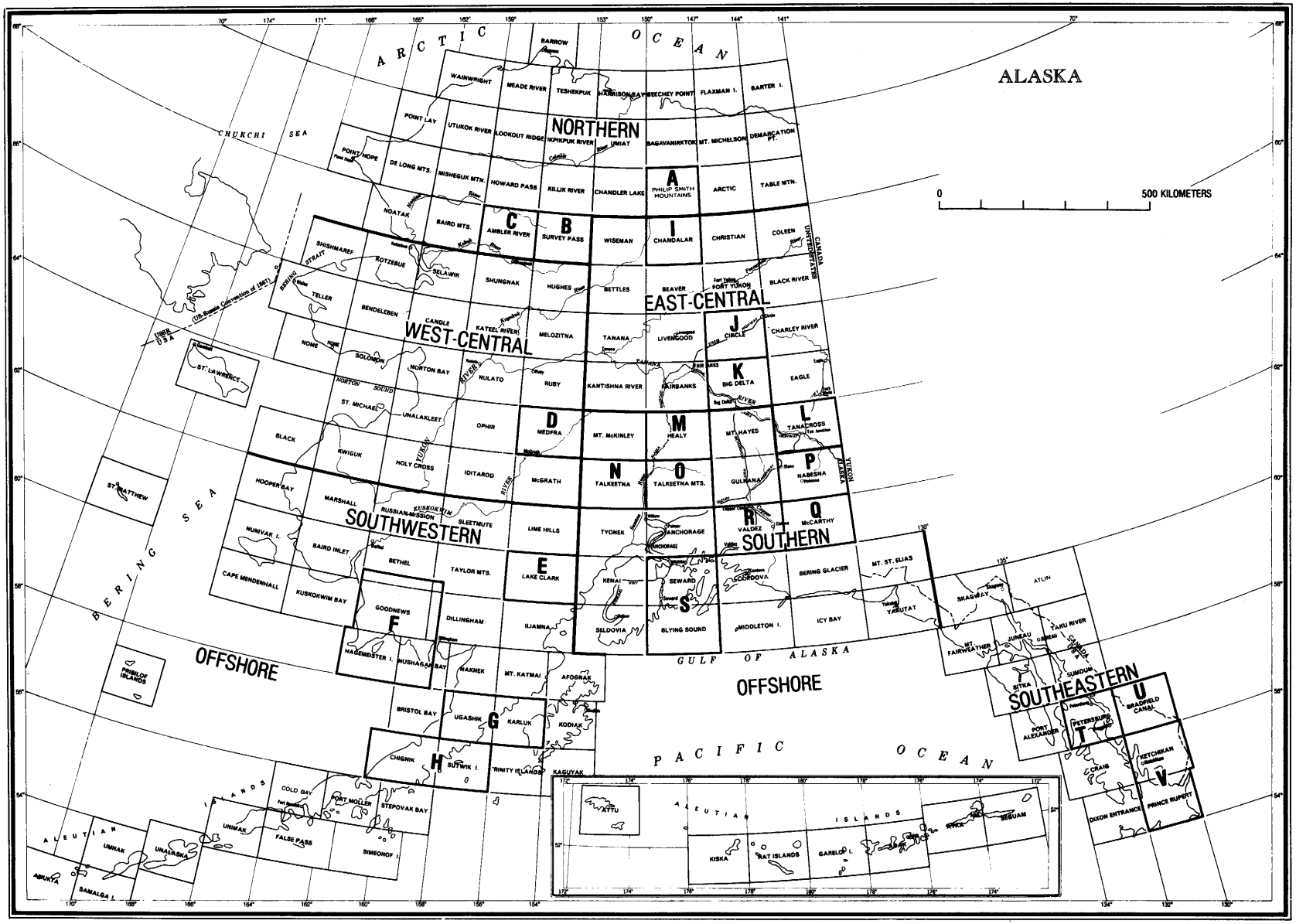
ALASKA
ARCTIC OCEAN
CHUKCHI SEA
BERING SEA
PACIFIC OCEAN
GULF OF ALASKA
NORTHERN
EAST-CENTRAL
WEST-CENTRAL
SOUTHWESTERN
SOUTHERN
SOUTHEASTERN
OFFSHORE
OFFSHORE
A PHILIP SMITH MOUNTAINS
B SURVEY PASS
C AMBLER RIVER
D MEDFRA
E LAKE CLARK
F GOODNEWS
G KARLUK
H CHIGNIK
I CHANDALAR
J CIRCLE
K BIG DELTA
L TANACROSS
M HEALY
N TALKEETNA
O TALKEETNA MTS.
P NABESNA
Q McCARTHY
R VALDEZ
S SEWARD
T PETERSBURG
U BRADFIELD CANAL
V PRINCE RUPERT
0
500 KILOMETERS
BARROW
WAINWRIGHT
MEADE RIVER
TESHEKPUK
HARRISON BAY
BEECHEY POINT
FLAXMAN I.
BARTER I.
POINT LAY
UTUKOK RIVER
LOOKOUT RIDGE
IKPIKPUK RIVER
UMIAT
BAGAVANIRKTOK
MT. MICHELSON
DEMARCATION PT.
POINT HOPE
DE LONG MTS.
MISHEGUK MTN.
HOWARD PASS
KILLIK RIVER
CHANDLER LAKE
ARCTIC
TABLE MTN.
NOATAK
BAIRD MTS.
WISEMAN
COLEEN
SHISHMAREF
KOTZEBUE
SELAWIK
SHUNGNAK
HUGHES
BETTLES
BEAVER
FORT YUKON
BLACK RIVER
CANADA
UNITED STATES
BERING STRAIT
TELLER
BENDELEBEN
CANDLE
KATEEL RIVER
MELOZITNA
TANANA
LIVENGOOD
CHARLEY RIVER
NOME
SOLOMON
NORTON BAY
NULATO
RUBY
KANTISHNA RIVER
FAIRBANKS
EAGLE
ST. LAWRENCE
NORTON SOUND
ST. MICHAEL
UNALAKLEET
OPHIR
MT. McKINLEY
MT. HAYES
BLACK
KWIGUK
HOLY CROSS
IDITAROD
McGRATH
TALKEETNA
GULKANA
HOOPER BAY
MARSHALL
RUSSIAN MISSION
KUSKOKWIM
SLEETMUTE
LIME HILLS
TYONEK
ANCHORAGE
NUNIVAK I.
BAIRD INLET
BETHEL
TAYLOR MTS.
KENAI
CORDOVA
BERING GLACIER
MT. ST. ELIAS
CAPE MENDENHALL
KUSKOKWIM BAY
DILLINGHAM
ILIAMNA
SELDOVIA
MIDDLETON I.
ICY BAY
YAKUTAT
SKAGWAY
ATLIN
HAGEMEISTER I.
BUSHAGAN BAY
WAKNEK
MT. KATMAI
AFOGNAK
PRIBILOF ISLANDS
BRISTOL BAY
UGASHIK
KODIAK
CHIGNIK
SUTWIK I.
TRINITY ISLANDS
KAGUYAK
MT FAIRWEATHER
JUNEAU
TAKU RIVER
SITKA
SUMDUM
PORT ALEXANDER
CRAIG
KETCHIKAN
DIXON ENTRANCE
ALEUTIAN ISLANDS
UNIMAK
UNALASKA
COLD BAY
PORT MOLLER
STEPOVAK BAY
FALSE PASS
SIMEONOF I.
ABUNTA
SAMALGA I.
ATTU
KISKA
RAT ISLANDS
GARELOI I.
KYAK
SEGUAM

Digital elevation models improve processing of Alaskan gravity data

By David F. Barnes

The recent availability of an almost complete file of digital elevation models (DEM's) for the State of Alaska makes possible new maps and calculations, including the terrain and isostatic correction of the gravity data used to prepare the previous gravity map of Alaska (Barnes, 1977). This refinement of data, once suitable only for small-scale regional maps of mountainous areas, now makes the same data useful for larger scale maps and for such quantitative interpretative procedures as digital modeling. The DEM's consist of metric elevations on a nearly square (commonly 3 by 6 second) geographic grid derived from 1:250,000-scale topographic maps and available on magnetic tapes distributed by the U.S. Geological Survey's (USGS) National Cartographic Information Center in Reston, Va. (documentation available from that office). New computer techniques to read these tapes now permit terrain corrections on the gravity data accumulated over the past 20 to 30 years, and future programs will provide isostatic, mean-elevation, and other maps. Use of digital models for terrain corrections on gravity data from the conterminous 48 States has been possible for the past 6 years, but the procedures used on Alaska data are newer and not yet so well perfected.

The differences in Alaskan procedures result from several factors, including: (1) the scarcity of Alaskan survey elevation control, which has prevented most topographic maps from meeting national map-accuracy standards; (2) the resulting abundant use of altimetry; (3) the convergence of meridians at high latitudes; and (4) the DEM format of the elevation tapes, which are now available for Alaska. In contrast, data-reduction and terrain-correction procedures for the conterminous 48 States have been influenced by such factors as: (1) the conformance of most topographic maps to national map standards, (2) the nearly square geographic grid at low latitudes, (3) a file of manually averaged mean-compartment elevations (mostly 1,000-yd or 1-km grids plus 1- and 3-minute grids) that gradually accumulated between 1960 and 1980, and (4) the preliminary planar format (elevations on a cartesian grid requiring map-projection transformations) of the early digital elevation tapes.

The Alaskan techniques have profited greatly from papers, discussions, and communications from many who helped to develop the techniques used in the conterminous 48 States. Particularly significant were the contributions of: (1) G. P. Woollard (in Thiel and others, 1958), who recognized that Alaskan maps required the identification of elevation sources in computer files; (2) Donald Plouff (1966, 1977), who developed a fundamental computer terrain-correction program, using a geographic grid; (3) Atef Elassal (written commun., 1975), who provided a method of reading planar-elevation-model tapes and calculating mean-compartment elevations; (4) Donald Plouff, who adapted Elassal's programming to his terrain-correction system; and (5) R. L. Godson (written commun., 1980), who integrated many of the conterminous-48-States contributions into a user-oriented system of gravity reduction designed for the USGS's Honeywell Multics computer. The present USGS Alaskan system, following a parallel development assisted by these and other contributors, now handles the problems peculiar to Alaskan gravity and elevation data, but it so far operates only on the USGS Multics system (a large-scale virtual-memory system designed primarily for interactive low-speed use, although programs written for it may be difficult to transfer to other systems).

The problems that caused the computer processing of Alaskan gravity data to differ from procedures used in the conterminous 48 States became evident during the earliest USGS Alaskan gravity surveys, which began in the Copper River basin in 1958. Those first-year measurements revealed a broad but poorly defined area in which altimeter elevations differed from spot elevations on 1:63,360-scale maps by as much as 15 m. Repeated altimeter measurements the following year and a leveling line several years later confirmed the accuracy of the altimetry, although the cause of the spot-elevation errors has never been determined. Similar spot-elevation errors were later found in other parts of Alaska, although poor weather conditions on some days also caused altimeter measurements to be almost equally erroneous. The most consistent contours were obtained from altimeter measurements, but only map elevations could be used for accurate terrain corrections. These problems suggested that the best results would be obtained by maintaining both altimetry and map-derived elevations in the computer data file and labeling the sources of all the elevations. The tendency of altimeter elevations to worsen on individual days of poor weather also suggested that each day's data files should be separately accessed and that all computer listings should

Figure 2.—Alaska, showing quadrangles for which Landsat studies have been completed. NORTHERN ALASKA: A, Philip Smith Mountains quadrangle (Le Compte, 1979a); B, Survey Pass quadrangle (Le Compte, 1981f); C, Ambler River quadrangle (Albert, 1978). WEST-CENTRAL ALASKA: D, Medfra quadrangle (Le Compte, 1981e). SOUTHWESTERN ALASKA: E, Lake Clark quadrangle (Steele, 1983); F, Goodnews and Hagemeister Island quadrangles region (Steele, 1978); G, Ugashik and Karluk quadrangles (Le Compte, 1981i); H, Chignik and Sutwik Island quadrangles (Le Compte and Steele, 1981). EAST-CENTRAL ALASKA: I, Chandalar quadrangle (Albert and others, 1978); J, Circle quadrangle (Le Compte, 1981a); K, Big Delta quadrangle (Albert and Steele, 1978); L, Tanacross quadrangle (Albert and Steele, 1976b). SOUTHERN ALASKA: M, Healy quadrangle (Le Compte, 1981h); N, Talkeetna quadrangle (Steele and Albert, 1978a); O, Talkeetna Mountains quadrangle (Steele and Le Compte, 1978); P, Nabesna quadrangle (Albert, 1975); Q, McCarthy quadrangle (Albert and Steele, 1976a); R, Valdez quadrangle (Le Compte, 1981g); S, Seward and Blying Sound quadrangles (Le Compte, 1979b). SOUTHEASTERN ALASKA: T, Petersburg quadrangle and vicinity (Le Compte, 1981c); U, Bradfield Canal quadrangle (Le Compte, 1981d); V, Ketchikan and Prince Rupert quadrangles (Steele and Albert, 1978b; LeCompte, 1981b).

have an easy reference to that day's data set. Once a bad altimetry elevation is verified, all other altimetry elevations on that day can be easily checked and possibly corrected. This procedure of data storage worked well when most calculations were performed by hand but has proved to be even more useful on modern large computers, although much specialized programming has been needed.

The earliest magnetic tapes of digital terrain were received in a "planar" format (elevations calculated on a 0.01-in. grid [about 68 m] for a few available 1:250,000-scale maps). These tapes were used for preliminary tests of the suitability of such models for terrain corrections, but only a limited number of tapes were received. A much more comprehensive data set is now available in the DEM format, which in Alaska provides elevations on a 3- by 6-second geographic grid (3 by 9 seconds north of lat 70° N.). When the tapes are read, these elevations are combined to form files of mean elevations for compartments of nominal 1/4-minute (15 by 30 second), 1-minute (60 by 120 second), and 3-minute (3 by 6 minute) size, which are organized into map files suitable for use by the Plouff terrain-correction program. For computer storage, the map files are organized into storage segments that include all the maps within each square degree, except that 3-minute compartments are stored in 1- by 2-degree "quadrangle" squares. The DEM tapes are also organized into files of elevation data for individual square degrees, so that the computer can calculate the segment name, map names, and other label data from the identifying information in each tape file. Each map label includes the tape name and date of reading, in case tape or program errors are discovered at a later date. Mean-compartment elevations are calculated from elevations that have been so weighted that the importance of elevations on compartment boundaries and corners is proportionately decreased. The geographic arrangement of the DEM format thus permits a more precise determination of mean elevation than could be readily obtained from the planar-format tapes. Naming and map-arrangement conventions permit the area covered by each segment to be apparent after printing only the first two lines of any segment. All the segments containing compartment elevations are permanently stored on a mountable disc from which the files needed for a terrain-correction job may be readily retrieved.

Data-processing procedures still include various steps and formats that are gradually being streamlined and improved. The input data are still in card-image format, and each day's data are separated into individual data sets preceded by lead cards providing base, drift and altimetry-control information for that day's data. This card-image format still conforms to some earlier systems, which limited the station identification, data-set designation, and source-code fields to four characters each. Preliminary processing provides a comparison of the simple Bouguer anomalies resulting from use of altimetry and map, bench-mark, or other elevations. Study of this comparison commonly results in small relocations of stations where the altimetry has indicated probable errors in the positions plotted by the field observer; geographic positions are also checked by computer plots. Then, a final run of the preliminary reduction program produces a listing of station identification, latitude, longitude, and map elevations formatted for input to the terrain-correction program.

The terrain-correction program uses this listing, as well as files of the 1/4-minute, 1-minute, and 3-minute mean-compartment elevations obtained from the DEM tapes. Compilation of the terrain-data files is accomplished partly by an interactive selection program and partly on the Multics computer text editor from files stored on a mountable disc after the initial tape reading. This part of the compilation procedure is now being improved, but once the files are available, the terrain-correction procedure is established by an interactive program that requests file names, radii of hand corrections, outer radius, densities, and other parameters. The inner-zone corrections may be provided by hand calculations, or the computer will calculate a complete correction by assuming that the innermost compartment has a gravitational attraction which depends on the station elevation and the mean elevations of adjacent compartments. The outer radius is currently limited by the number of maps that can be handled by the program, and most Alaskan corrections have been made to a radius of only 99 km (outer radius of Hayford zone N), although a standard 166.7 km (Hayford zone 0) should be possible in the future. The terrain-correction program produces an output file of station names and terrain corrections for two densities, as well as a descriptive run summary that reports calculation parameters along with warnings about missing maps and other possible errors.

A supplementary program merges the output file with the original data file so that terrain corrections are now part of the basic data file. The data can then be recalculated to obtain a complete Bouguer anomaly, which uses the altimetry elevation for the slab part of the correction and the map elevation for the relative-terrain part of the correction. This combination generally provides the most contourable data, although data from days with weather conditions unfavorable for altimetry may conform better if only the map elevations are used. Maintenance of the basic data as individual data sets with each day's data, including the basic base, drift, and altimetry control as well as terrain corrections, optimizes reprocessing with other systems of elevation control. As the file of Alaskan gravity data gradually improves with increasing station density, the possibilities for recognizing errors in earlier data also steadily increase. A final factor that facilitates the improvement of elevation control is that the data file also includes, for as many stations as possible, the height difference between the measurement site and any nearby elevation-reference surfaces, such as rivers, lakes, sea surface, highway, hilltop, or other features that may eventually have a spot elevation on updated maps.

REFERENCES CITED

Barnes, D. F., 1977, Bouguer gravity map of Alaska: U.S. Geological Survey Geophysical Investigations Map GP-913, scale 1:2,500,000.

Plouff, Donald, 1966, Digital terrain corrections based on geographic coordinates [abs.]: Geophysics, v. 31, no. 12, p. 1208.

——1977, Preliminary documentation for a FORTRAN program to compute gravity terrain corrections based on topography digitized on a geographic grid: U.S. Geological Survey Open-File Report 77-535, 45 p.

Thiel, Edward, Bonini, W. E., Ostenso, N. A., and Woollard, G. P., 1958, Gravity measurements in Alaska: Woods Hole Oceanographic Institution Reports, Reference 58-54, 104 p.

Seismic studies in southern Alaska

By Christopher D. Stephens, John C. Lahr, and Robert A. Page

During the past year, analysis of seismic data from the network in southern Alaska has focused on shallow seismicity in three areas: the Yakataga seismic gap along the northeastern Gulf of Alaska, the southern Kenai Peninsula, and the active volcanoes west of Cook Inlet. A summary of the results for each of these areas is presented below.

YAKATAGA SEISMIC GAP

Continued monitoring of the seismicity in and near the Yakataga seismic gap has revealed some interesting variations in the rates of activity during the past 2 years. Figure 3 shows the epicenters of earthquakes that occurred between October 1, 1979, and September 14, 1981. As noted in earlier reports (for example, Stephens and others, 1981), the spatial pattern of the seismicity is remarkably stable. Most of the activity occurs at or near the perimeter of the Yakataga gap, as defined by McCann and others (1980) and Lahr and others (1980), and is dominated by aftershocks from the 1979 St. Elias earthquake. Figure 4 plots the rate of activity as a function of time for various subregions of figure 3. The most striking feature in these curves is a twofold to threefold increase in the monthly number of located events that began about October 1980 for the Waxell Ridge, Copper River delta, St. Elias, and Wrangell subregions. These elevated levels of activity continued for about 6 to 8 months and then returned to near those observed during the earlier period. The increased level of activity within the aftershock zone of the 1979 St. Elias earthquakes appears to be superimposed on a long-term decay in the rate of aftershock activity that approximates the expected inverse time decay for aftershocks. The offshore subregion underwent a gradual increase beginning about June 1980 and returned to normal in November 1980. A review of the data-processing procedures and station-operation history for the period since October 1979 suggests that although these factors may introduce some apparent changes in activity rate, they are not likely sources of systematic errors which could account for the observed long-term variations in seismicity rates. The seismicity rates for the subregions of northern Prince William Sound and Yakutat Bay were also reviewed, but actual changes in the rates of seismicity cannot be reliably established owing to the systematic biases known to exist. For Prince William Sound, a change in the timing criteria to reduce the number of small events to be located coincides with an apparent sharp decrease in activity beginning in October 1980. In the Yakutat Bay subregion, a reduction in the number of operating stations may have introduced the apparent decrease in seismicity beginning in August 1980.

These observations suggest that a perturbation occurred in the regional stress field in and around the Yakataga seismic gap. The possible significance of this change in seismicity as a precursor to a gap-filling earthquake is being weighed.

The Waxell Ridge subregion is the most seismically active area within the Yakataga seismic gap, as defined in figure 3. Whether this shallow seismicity occurs at the thrust interface between the Pacific plate and the overriding North American plate, which is thought to underlie this subregion at a depth of 10 to 20 km, or on faults within the overlying plate is uncertain, primarily because the focal depths of events located in this area are poorly constrained. Preliminary results from a study of selected events in the Waxell Ridge subregion suggest that the earthquakes occur at depths shallower than 20 km. Although the coverage of the focal sphere for P-wave first motions is inadequate to distinguish between dip-slip or strike-slip motion for the earthquake mechanisms, the orientations of the axes of maximum compressive stress are constrained to be northwest-southeastward. This result is compatible with the direction of convergence between the North American and Pacific plates inferred from adjacent areas along this part of the plate boundary (for example, Perez and Jacob, 1980).

SOUTHERN KENAI PENINSULA

Using data from the Bradley Lake network (northeast of Homer) for December 1980 through July 1981, a preliminary review was made of the first-motion data for crustal earthquakes that occurred beneath the southern Kenai Peninsula. This review was made in conjunction with Woodward-Clyde Consultants, who are under contract with the U.S. Army Corps of Engineers to assess the seismic hazards in the region of a proposed hydroelectric project. Composite focal mechanisms were made for a few of the clusters of earthquakes that occurred near the mapped surface traces of major faults. These focal mechanisms were clearly consistent with normal faulting, notwithstanding the ordinary systematic errors in properly locating the first arrivals on the focal sphere due to uncertainties in the velocity structure. The orientation of the principal tension axis was constrained to be within about 20° of east-west. This result, in a region of northwest-directed subduction, was not expected. One possible explanation is that the crust is locally in tension now, since the 1964 earthquake, but that the stress pattern will change to northwest-southeastward-oriented compression in the future as stresses build up before another large thrust earthquake.

WESTERN COOK INLET VOLCANOES

With partial support from the U.S. Geological Survey's Volcano Hazards Program, seismicity in the vicinity of three active volcanoes—Spurr, Redoubt and Iliamna—west of Cook Inlet was examined in detail for

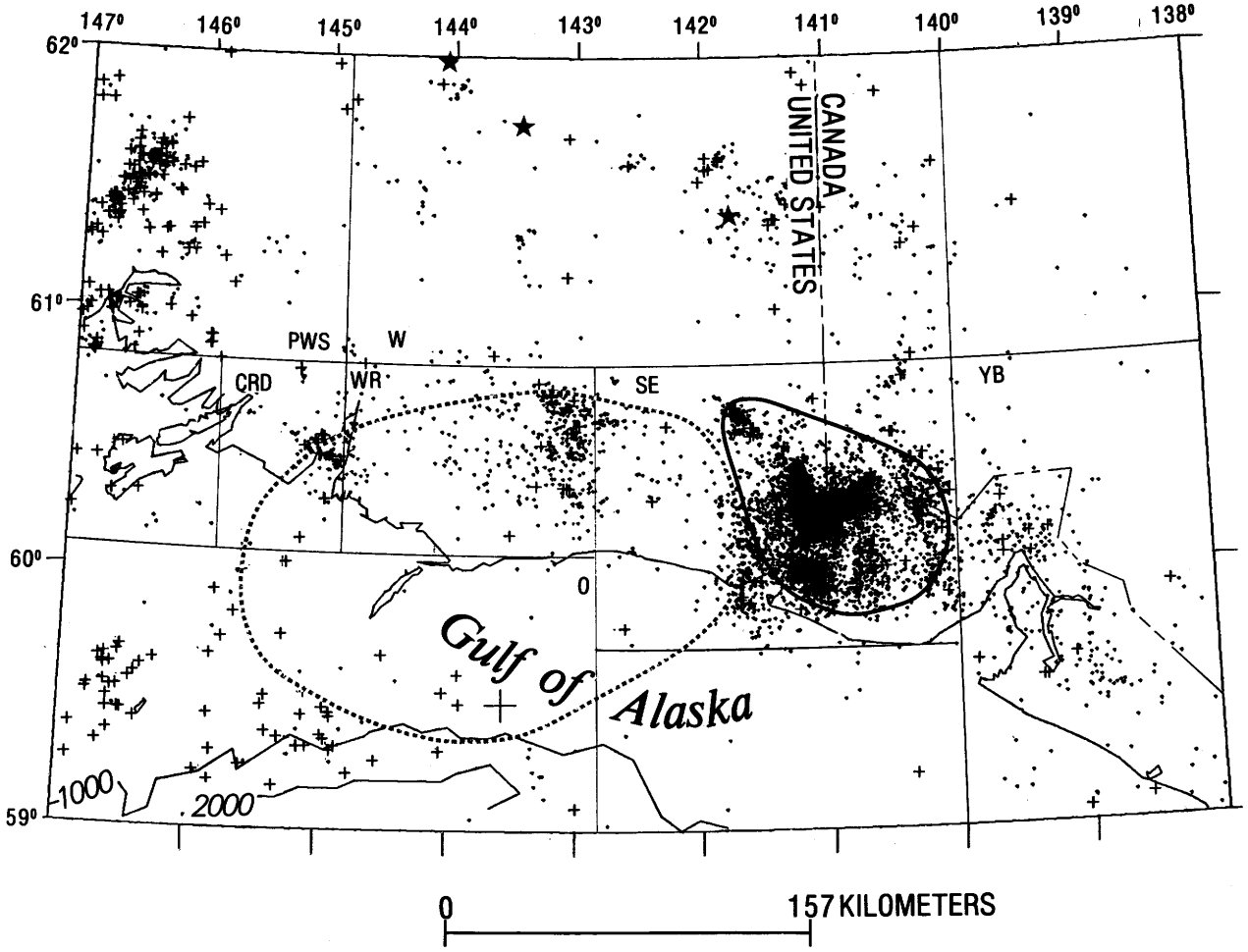

Figure 3.—Epicenters of 7,298 earthquakes in the Gulf of Alaska and southern Alaska region between October 1, 1979, and September 30, 1981. Three symbol sizes (small to large) correspond to earthquakes of magnitudes less than 2 (dot), 2.0-3.9 (small cross), and greater than 3.9 (large cross). Solid curve, rupture zone of 1979 St. Elias earthquake (M_S=7.1); dashed stippled curve, Yakataga seismic gap. Lettered areas correspond to subregions in figure 4, as follows: O, offshore; CRD, Copper River delta; WR, Waxell Ridge; SE, St. Elias; W, Wrangell; YB, Yakutat Bay; PWS, northern Prince William Sound. Stars denote locations of Quaternary volcanoes. Depth contours in fathoms.

the interval October 1980 through June 1981. Locations were determined for all shallow-focus earthquakes with four or more P and S phases recorded at three or more stations. During this interval, no pronounced swarms of shallow earthquakes were observed within 20 km of any of the three volcanic centers. Epicenters of five shallow shocks, ranging in depth from 0 to 10 km and in magnitude from 0 to 1.0, were located within 3 km of the summit of Spurr. In addition, a cluster of 14 events scattered over time was located 10 to 20 km south of the summit. Spurr, which is the closest volcano to the Anchorage metropolitan area, last erupted in 1953 and deposited about 5 mm of ash in Anchorage. On September 9, 1979, a swarm of 47 events with magnitudes as high as 0.7 occurred near the summit of Spurr in an 11-hour interval; no similar activity was observed during the recent 9-month interval. A total of 16 earthquakes shallower than 20 km were located in a diffuse pattern within 20 km of Redoubt, the largest of which was of magnitude 2.0. The most recent eruptions of Redoubt consisted of a series of explosive ash eruptions in 1966-68. Fewer shocks were located in the vicinity of Iliamna Volcano—two events within 5 km of the volcano summit but no others within 20 km. Iliamna has been quiescent over the past 3 decades.

REFERENCES CITED

Lahr, J. C., Stephens, C. D., Hasegawa, H. S., Boatwright, John, and Plafker, George, 1980, Alaska seismic gap only partially filled by 28 February 1979 earthquake: Science, v. 207, no. 4437, p. 1351-1353.

McCann, W. R., Perez, O. J., and Sykes, L. R., 1980, Yakataga seismic gap, southern Alaska: Seismic history and earthquake potential: Science, v. 207, no. 4437, p.1309-1314.

Perez, O. J., and Jacob, K. H., 1980, Tectonic model and seismic potential of the eastern Gulf of Alaska and Yakataga seismic gap: Journal of Geophysical Research, v. 85, no. 12, p. 7132-7150.

Stephens, C. D., Lahr, J. C., and Rogers, J. A., 1981, Eastern Gulf of Alaska seismicity: Annual report to the National Oceanic and Atmospheric Administration for April 1, 1980, through March 31, 1981: U.S. Geological Survey Open-File Report 81-897, 35 p.

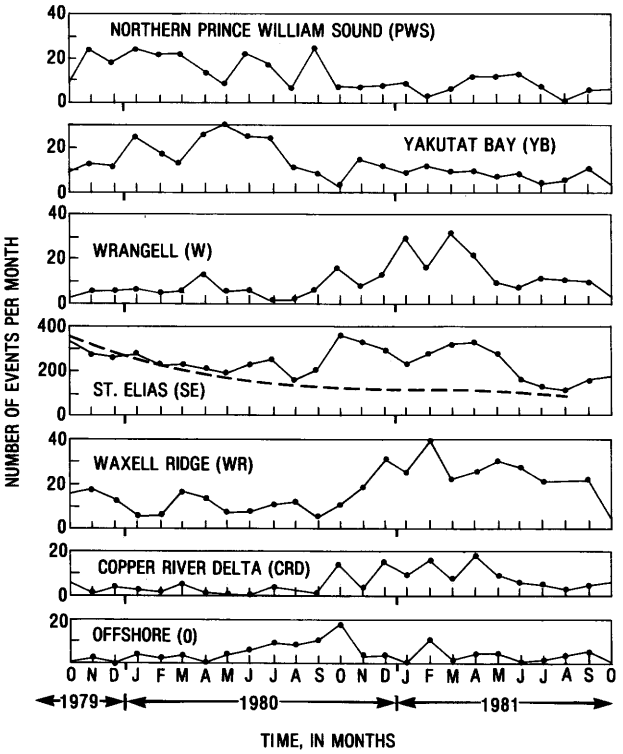

Figure 4.—Number of located earthquakes as a function of time for subregions of figure 3. Data extend through end of October 1981. Dashed curve in St. Elias graph represents an inverse time decay in aftershock activity; note difference in scale for St. Elias region.

Horizontal-strain observations in the Shumagin Island and Yakataga seismic gaps, Alaska

By Michael Lisowski, James C. Savage, and William H. Prescott

The crustal-strain project established a trilateration network near Cape Yakataga in 1979 and in the Shumagin Islands in 1980. Both nets were remeasured after 1 year, and both networks had some observations in common with earlier triangulation or traverse surveys. Comparison of these observations over both the short and long periods has allowed us to put some constraints on the rates of strain accumulation in these two seismic gaps.

In the Shumagin Islands, a trilateration network of 38 lines was measured in 1980 and 1981. The network is 30 km wide parallel to the plate boundary and covers the area between 150 and 250 km northwest of the Aleutian Trench, along which subduction of the Pacific plate occurs. The network has 18 angles in common with a 1913 third-order triangulation survey, and 5 angles in common with a 1954 first-order triangulation survey. A total of 22 of the length measurements made in 1980 were repeated in 1981. Comparison of observations over the period 1913-80 gave shear strain rates with a standard deviation of 0.10 μstrain/yr (engineering); the 1954-80 comparison had a standard deviation of 0.10 μstrain/yr, and the 1980-81 comparison of 0.20 μstrain/yr. The increased precision of the newer observations is offset by the shorter period. The only significant strain rate observed at the two-standard- deviation level was for the period 1954-80, during which a change in $\dot{\gamma}_1$ (which measures left-lateral shear parallel to the northeast-striking plate boundary) at a rate -0.25 ± 0.10 μstrain/yr indicates a right-lateral component of slip on the thrust. Compression or extension normal to the plate boundary would be reflected in $\dot{\gamma}_2$, which had a rate of 0.10 ± 0.13 μstrain/yr during the period 1954-80—not significantly different from zero. Comparisons for other periods indicated that the strain rates are below the two-standard-deviation level in the observations.

For comparison, theoretical strain-accumulation rates near a subduction zone were calculated from a dislocation model (Savage, 1983). The geometry of this model is based on hypocentral locations for recent earthquakes in the Shumagin seismic gap (Davies and House, 1979). Table 1 compares the strain rates calculated from the model with rates observed over various periods. A plate-convergence rate of 7 cm/yr was assumed for the model.

Table 1.--Comparison of strain rates in the Shumagin network

[N, number of common angles or distances; $\dot{\gamma}_1$, rate of engineering shear across a northwest-southeast-oriented plane (right-lateral is positive); $\dot{\gamma}_2$, rate of engineering shear across an east-west-oriented plane (right-lateral is positive); Θ, bearing of direction of maximum contraction; $\dot{\Delta}$, rate of areal dilatation (increasing area is positive)]

Period	N	$\dot{\gamma}_1$ (μrad/yr)	$\dot{\gamma}_2$ (μrad/yr)	Θ	$\dot{\Delta}$ (μppm/yr)
Model	--	0.09	0.16	N. 28° W.	---
1913-80	18	.04±0.06	.06±0.05	N. 26°±26° W.	---
1954-80	5	-.25±0.10	.10±0.13	N. 79°±14° W.	---
1980-81	22	.06±0.18	-.27±0.19	N. 51°±9° W.	-.53±0.40

For the period 1913-80, although the sensitivity in $\dot{\gamma}_2$ was apparently sufficient to detect the model-predicted deformation, such deformation was not observed, possibly because of strain release during the 1938 or 1946 Aleutian earthquakes. Davies and others

(1981) argued that neither earthquake ruptured into the Shumagin gap, but the evidence is circumstantial. Strain release during 1938 (or 1946) seems at least a possible explanation for the absence of any observed strain accumulation.

At Cape Yakataga, an 18-line trilateration network with a 35-km aperture was measured in 1979 and 1980; included within this network is a section of a 1959 electronic distance traverse. Comparison of the 1959 and 1979-80 surveys shows that the west edge of the Yakataga network has been displaced 3.4 m S. 40° E. with respect to the east edge. We attribute this deformation primarily to the 1964 Alaska earthquake, the effects of which apparently penetrated into what is now known as the Yakataga seismic gap. A comparison of five lengths common to the 1979 and 1980 surveys shows no significant strain accumulation at the 0.5-μstrain level.

REFERENCES CITED

Davies, J. N., and House, L. S., 1979, Aleutian subduction zone seismicity, volcano-trench separation, and their relation to great thrust-type earthquakes: Journal of Geophysical Research, v. 84, no. B9, p. 4583-4591.

Davies, J. N., Sykes, L. R., House, L. S., and Jacob, K. H., 1981, Shumagin seismic gap, Alaska Peninsula: History of great earthquakes, tectonic setting, and evidence for high seismic potential: Journal of Geophysical Research, v. 86, no. B5, p. 3821-3855.

Savage, J. C., 1983, A dislocation model of strain accumulation and release at a subduction zone: Journal of Geophysical Research [in press].

Alaskan geochemical field laboratories

By Richard M. O'Leary and James D. Hoffman

The Anchorage geochemical field laboratory was in operation during summer 1981 at 5500 Oilwell Road, Elmendorf AFB, Alaska, as it has been since 1967. The laboratory is managed and operated by the U.S. Geological Survey, Golden, Colo. It is equipped with a drying oven, rock crushers, pulverizers, and sieve shakers to prepare samples of rock, stream sediment, glacial debris, and soil for geochemical analysis. The analytical laboratory includes two emission spectrographs capable of generating semiquantitative analyses for 31 elements on each sample. Atomic-absorption spectrophotometry and mercury-vapor-detection instruments complement the analytical capabilities. To provide additional space and facilities, a self-contained wet-chemical mobile unit (housed in a 7-m-long fifth-wheel trailer) was brought to Anchorage from Denver in 1980. A minicomputer system, added in recent years, is used to enter, edit, update, and retrieve analytical data from the rock-analysis storage system (RASS) while the laboratory is in normal operation. This system circumvents the keypunch operation and timelag involved in processing data through the office in Golden.

The field laboratory offers the advantage of central location for fast mail service and is able to handle a large volume of samples within a short period. The quick turnaround of analytical results allows further sampling or checking of anomalous or critical areas while crews are still in their field areas.

During the 3-1/2-month period in 1981 when the laboratory was in operation, about 7,000 samples collected from the Mount Hayes, Bristol Bay-Ugashik-Karluk, Healy, Circle, Wiseman, Chandler Lake, Killik River, Bendeleben-Solomon, Baird Mountains, and Petersburg quadrangles and the Chugach RARE II project area were processed. The results of these analyses were used mainly to generate geochemical maps that aid in mineral-resource assessments and help locate possible mineral deposits.

Computer-generated latitude and longitude templates for rapid determination of geographic positions in Alaska

By David F. Barnes and Donald Plouff

For the past 8 years, U.S. Geological Survey scientists working in Alaska have been aided by computer-generated latitude and longitude templates. These templates were prepared by digital computers and are reproduced on transparent film, which can be easily laid over maps and plotting sheets. Various scales and formats have already been prepared and more may become available in the future. Reproduction problems hampered the early distribution of the templates, and their use was originally restricted to Government workers. However, their popularity has shown a need for wider distribution, which has recently been met by improved reproduction and distribution methods; templates are now available to the public through specified offices in Anchorage and Denver per information in the last paragraph below.

Geographic coordinates are an essential component of any data base designed to show map locations of field data, but the methods of measuring, recording, and plotting these locations vary. Cartesian coordinates, such as the State grid systems or universal transverse mercator (UTM) grid, are satisfactory for plotting data within local areas, and the coordinates can be measured by linear map scales. However, cartesian systems do not provide accurate representations of locations over large areas of the Earth's spherical surface, and so the global system of latitude and longitude is the conventional way of recording geographic locations in data bases covering large areas. Although most modern topographic maps of the United States include the State grid and UTM coordinates on their margins, latitudes and longitudes are better labeled and generally include gridmark ticks within the maps. On most map projections, meridional convergence causes longitude scale changes that at high latitudes can be significant even within a single map. Digital computer programs now provide systems for converting from geographic to cartesian coordinates and vice versa, and electronic plotters and digitizers may be used for more accurate measurement and plotting of locations. Computers, however, are expensive facilities that generally require space, electric power, and significant setup time. The templates

were designed to improve the accuracy and encourage the use of latitude and longitude for recording geographic positions in the field and office, where expensive computer facilities might not be readily available. Use of a computer to generate templates serves as a method of extending the precision and flexibility of computer facilities to work areas where only less sophisticated facilities are available.

The Survey's use of templates for determining geographic coordinates was started in 1974, when systematic collection of geochemical and geophysical data was accelerating in the Alaskan Mineral Resource Assessment Program (AMRAP). They were, however, an outgrowth of older techniques that had developed during the previous 25 years for determining the geographic coordinates required for early files of gravity data used in U.S. Geological Survey computers. Such geographic coordinates were generally measured by interpolating from linear scales and using multiplication factors for scale conversion. Later, adjustable 10-point dividers and elastic scales were commonly used. To calculate gravity anomalies in the field, D. F. Barnes began using hand-drawn latitude templates covering 5- by 10-minute areas on all Alaskan 1:63,360-scale maps, and for detailed surveys these were supplemented by hand-drawn longitude templates covering the full height of a few maps. Meanwhile, Plouff (1968) had written computer programs to plot station locations on UTM and polyconic projections and to verify these locations before further data processing. Many of these plots revealed location-measurement errors, and the advantages of the geographic over the cartesian system sometimes seemed less important than the errors made in measurements involving scales and conversion factors. After discussions of mutual needs and problems, Plouff wrote a computer program to produce templates that combined the features of D. F. Barnes' hand-drawn individual latitude and longitude templates. Flexibility was provided in the computer program for drawing templates at any latitude, any map scale, on either of two map projections, and at any multiple of 1 second for fine interpolation. Discussions with Henry C. Berg and other geologists assisted in improving format, line spacing, and labeling to standardize the three principal template types now used with Alaskan topographic maps.

The principal topographic-map scales in Alaska are 1:250,000, or 4 miles to the inch (covering a 1-degree latitude range and either 2 or 3 square degrees), and 1:63,360, or 1 mile to the inch (covering a 15-minute latitude range with widths varying from 20 to 36 minutes). Standard templates cover the full north-south dimension of each map, and 30 minutes of longitudinal width of the 1:250,000-scale maps and 10 minutes longitudinal width of the 1:63,360-scale maps so that each template is about 10 by 45 cm. The 1:250,000-scale templates have lines every minute of longitude and every half-minute of latitude, and every fifth line is usually drawn thicker and labeled. There are two categories of 1:63,360-scale templates: One with each minute divided into units representing seconds, and the other with each minute divided into decimal parts. Templates with divisions in seconds have lines every 10 seconds (each minute divided into six parts), and the lines at every minute are thicker and labeled. Templates with minutes divided decimally have lines every 0.1 minute of latitude and every 0.5 minute of longitude, and the lines at every minute or half-minute are thicker and labeled. The separate sets of templates, one with minutes divided into seconds and the other into decimal parts, were prepared because both these systems of recording locations are in common use. Templates in decimal parts of degrees or other scales (some new Alaskan maps are now being published at scales of 1:25,000 and 1:50,000) can be easily prepared if (when) needed in the future.

The templates were originally plotted on paper on a drum plotter and were photographically duplicated as contact prints on either positive clear film or negative film. Attempts to plot directly on Mylar have been only partly successful, mainly because of pen-and-ink problems. The high cost of photographic reproduction initially limited widespread template distribution. However, a set of negatives for template reproduction has recently been sent to the National Cartographic Information Center, U.S. Geological Survey, 218 E. Street, Anchorage, AK 99501. Upon request, the Center can arrange for the distribution of clear-film copies of the templates to the public in Alaska. In addition, a copy of the computer program was transmitted to Denver, where it was used to produce a set of smaller templates (Campbell and Van Trump, 1982a, b) covering half the latitude range of each tier of standard quadrangle maps. Copies of these templates are reproduced on xerographic film for distribution through the Open-File Services Section, Western Distribution Branch, U.S. Geological Survey, Box 25425, Federal Center, Denver, CO 80255.

REFERENCES CITED

Campbell, W. L., and VanTrump, George, Jr., 1982a, Catalog of available clear mylar templates used to determine latitude and longitude of sample localities between the latitudes of 51°00'00" and 71°30'00" at the scale of 1:63,360, and between the latitude of 49°00'00" and 71°30'00" N. or S. at the scale of 1:250,000: U.S. Geological Survey Open-File Report 82-723, 4 p.

——1982b, Clear mylar templates used to measure latitude and longitude of sample localities at scales 1:63,360, and 1:250,000 between the latitudes of 49°00'00" and 71°30'00" N. or S.: U.S. Geological Survey Open-File Report 82-724, 214 p.

Plouff, Donald, 1968, Determination of rectangular coordinates for map projections—modification of basic formulas and application to computer plottings, in Geological Survey research 1968: U.S. Geological Survey Professional Paper 600-C, p. C174-C176.

The U.S. Geological Survey Public Inquiries Office in Anchorage

By Elizabeth C. Behrendt

The Public Inquiries Office (PIO) in downtown Anchorage (Skyline Building, 218 "E" Street) is part of a network of 10 such U.S. Geological Survey PIO facilities throughout the country. These offices serve

the public as a contact point for obtaining information about the activities and products of the Survey, as over-the-counter sources of map and report products of the U.S. Geological Survey, and they provide referral service for individuals seeking technical information.

In fiscal year 1981 the Anchorage PIO, staffed by two full-time and two part-time employees, replied to more than 30,000 information requests received in person, by telephone, and by mail. More than 112,000 topographic and thermatic maps and 2,000 publications were sold. Some 1,100 people used the reference library, and more than 800 patrons were assisted in consulting the files of U.S. Geological Survey Open-File Reports on Alaska.

NORTHERN ALASKA

(Figure 5 shows study areas discussed)

The Kanayut Conglomerate in the westernmost Brooks Range, Alaska

By Tor H. Nilsen and Thomas E. Moore

The Upper Devonian and Lower Mississippian(?) Kanayut Conglomerate is an allochthonous coarse-grained clastic unit that forms a distinctive and mappable stratigraphic unit in the central and eastern Brooks Range (Bowsher and Dutro, 1957; Porter, 1966). It is as thick as 3,000 m and has been divided, in ascending order, into the Ear Peak Member, Shainin Lake Member, and Stuver Member. The Ear Peak and Stuver members typically contain multiple fining- and thinning-upward cycles that appear to be characteristic of deposition by meandering streams, whereas the Shainin Lake Member typically contains more massive outcrops of conglomerate and sandstone that appear to be characteristic of deposition by braided streams (Nilsen and others, 1980, 1981b, 1982). Conglomerate of the Kanayut is composed of chert, quartzite, and quartz clasts, and the sandstone is typically orthoquartzitic in composition. The Kanayut records outbuilding of a major dominantly fluvial delta to the south and west (Nilsen and others, 1981a). It has generally been considered to pinch out laterally to the south and west into age-equivalent units. Herein, and in a recently released Open-File Report (Nilsen and Moore, 1982), we document its presence in Paleozoic stratigraphic sequences in the "Husky Mountains" and the Mulgrave Hills at the westernmost margin of the Brooks Range (area 6, fig. 5; fig. 6).

In the central and eastern Brooks Range (between about long 156°-147°) the Kanayut Conglomerate rests conformably on the marine Upper Devonian

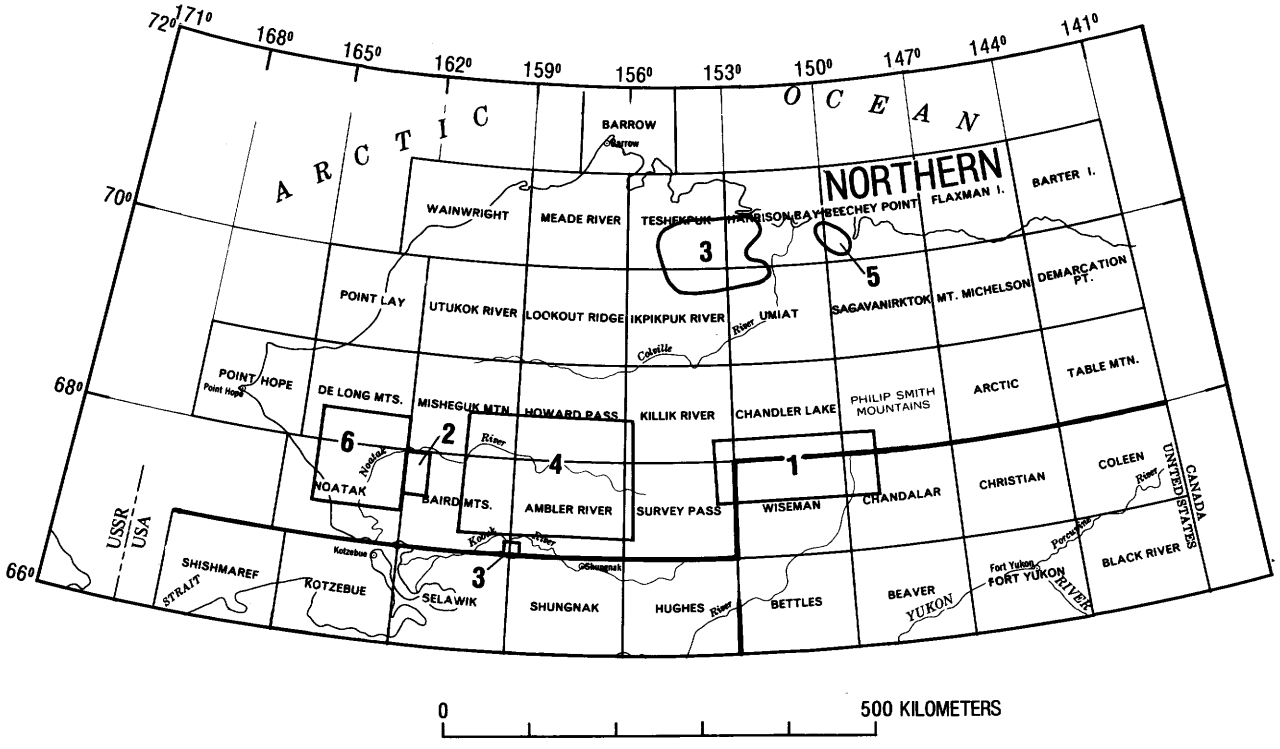

Figure 5.—Areas in northern Alaska discussed in this volume. A listing of authorship, applicable figures and tables, and article pagination (in parentheses) relating to the numbered areas follows. 1, Dutro and others, front-cover photograph, figure 9 (p. 17-19); 2, Ellersieck and others, figure 8 (p. 16-17); 3, Galloway and Koster, figures 10 and 11, table 2 (p. 20-21); 4, Hamilton and Van Etten, figure 12 (p. 21-23); 5, Lachenbruch and others (p. 19-20); 6, Nilsen and Moore, figures 6 and 7 (p. 12-16).

Noatak Sandstone and is overlain conformably by the marine Lower Mississippian Kayak Shale (Brosgé and Pessel, 1977; Mayfield and Tailleur, 1978; Brosgé and others, 1979a, b; Nelson and Grybeck, 1980). Where the Noatak Sandstone, previously mapped as the marine basal sandstone member of the Kanayut Conglomerate, is missing, the Kanayut rests directly on the marine Upper Devonian Hunt Fork Shale. The Kanayut has been mapped together with the Noatak Sandstone as an undivided Devonian and Mississippian unit as far west as the Misheguk Mountain quadrangle and the south half of the National Petroleum Reserve in Alaska (Mayfield and others, 1978, 1982; Ellersieck and others, 1978, 1982; Curtis and others, 1982). In this area, it forms a major unit of the Brooks Range allochthon (Mayfield and others, 1982).

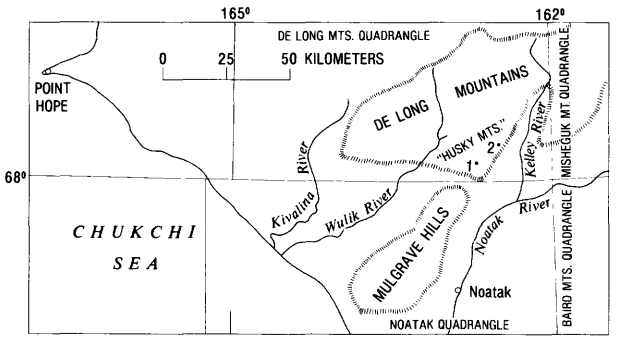

Figure 6.—Index map of "Husky Mountains" and Mulgrave Hills, western Brooks Range, Alaska, showing locations of measured sections B (1) and C (2) (see fig. 7).

Although Martin (1970) applied the name "Kanayut Conglomerate" to part of the Upper Devonian and Lower Mississippian sequence in the westernmost Brooks Range, most workers have described the sequence as consisting, in ascending order, of the following marine units: the Hunt Fork Shale or an unnamed fine-grained clastic unit, the Noatak Sandstone, the Kayak Shale, and the Utukok Formation (Dutro, 1953; Gryc and others, 1967; Tailleur and others, 1967). However, as a result of our work during the 1981 field season in the "Husky Mountains" and Mulgrave Hills in the De Long Mountains and Noatak quadrangles, we differentiate a nonmarine unit above the Noatak Sandstone and below the Kayak Shale that we assign to the Kanayut Conglomerate (fig. 7, col. A). We describe this unit herein and provide criteria for distinguishing it from overlying and underlying clastic units. This assignment confirms the transgressive-regressive conditions within the Endicott Group noted by Tailleur and others (1967) in the western Brooks Range and records a major offlap-onlap cycle similar to that of the central and eastern Brooks Range.

The Hunt Fork Shale, which crops out in the Mulgrave Hills and the "Husky Mountains" in low hills, consists primarily of brown phyllitic siltstone. The common presence of thin beds of fine-grained to very fine grained sandstone that are locally graded suggests that they are thin-bedded turbidites deposited in slope or prodelta settings. Because of tectonic thickening and thinning, low-grade metamorphism, and the absence of any well-exposed complete sections, the true thickness of the Hunt Fork is unknown.

The Hunt Fork Shale grades upward into the Noatak Sandstone, which is probably more than 100 m thick. The Noatak consists of trough-cross-stratified carbonate-cemented quartzose sandstone that contains abundant red-orange-weathering carbonate concretions. It is characterized by alternating layers of brown-weathering fine- to medium-grained sandstone and gray-weathering commonly pebbly coarse-grained sandstone. Bioturbated silty intervals that contain abundant mica and plant fragments are locally present. The sandstone beds are not organized into fining-upward cycles. We interpret the Noatak to represent deposition in inner-shelf and shoreline environments.

The overlying Kanayut Conglomerate consists mainly of thinning- and fining-upward fluvial cycles of conglomerate, sandstone, and shale (fig. 7, col. B). The lower parts of the cycles consist, in ascending order, of channeled light-gray-weathering basal massive or crudely parallel stratified conglomerate, trough-cross-stratified medium-bedded sandstone, and thin-bedded fine-grained sandstone and siltstone characterized by abundant current-ripple marks. The upper parts of the cycles consist of red- or brown-weathering shale and siltstone that contain abundant plant and root fossils, paleosols marked by oxidized red, orange, or yellow horizons, and, locally, coal. The lower, sandy parts of the cycles, which average 5 to 7 m in thickness, represent channel, point-bar, and levee deposits of meandering streams; the upper, shaly parts record deposition on adjacent flood plains. The cycles are characterized by erosional truncation of underlying shale and by upward fining of grain size, thinning of beds, and decrease in the amplitude of cross-strata. The conglomerate contains clasts as large as 3 cm. The sandstone is composed chiefly of detrital quartz and chert grains, and has, in contrast with the Noatak Sandstone, a silica cement.

Local interdigitation of the Kanayut Conglomerate with the underlying Noatak Sandstone results in composite cycles that contain a middle marine unit which does not fine upward. Cycles 1 and 3 contain a basal channeled conglomerate that is incised into underlying shale and fines upward into trough-cross-stratified sandstone (fig. 7, col. C). The middle parts of the cycles consist of alternating carbonate-cemented coarser and finer layers with abundant trough cross-stratification that are identical to the Noatak Sandstone. The upper parts of the cycles fine upward from cross-stratified silica-cemented fluvial sandstone into ripple-marked siltstone and flood-plain shale deposits containing paleosols. Cycle 2 shows a similar composite cycle but lacks the basal fining-upward fluvial interval. Cycle 4 is a typical Kanayut fluvial cycle. We believe that these composite cycles represent mixed fluvial and marine deposition, possibly under estuarine conditions, along the strandline.

The Kayak Shale, which is at least 40 m thick, overlies the Kanayut Conglomerate. Its lower part contains thin coarsening-upward cycles that consist of

a lower black or gray fissile shale and an upper thin-bedded fine-grained sandstone with abundant ripple markings and burrows. Black or gray siltstone, with some intercalated thin-bedded sandstone and carbonate turbidites, forms the upper part of the Kayak. The Kayak records a marine transgression over the dominantly fluvial Kanayut delta and gradually deepening conditions.

The Kanayut Conglomerate is distinguishable from other units of the Endicott Group in the "Husky Mountains" and the Mulgrave Hills by: (1) fining-upward cycles of conglomerate, sandstone, and shale; (2) the presence of red or brown shale intervals that commonly contain brightly colored oxidized paleosols; (3) highly indurated silica-cemented sandstone and conglomerate; and (4) erosional truncation of shale and paleosol intervals by overlying channeled conglomerate and sandstone. The minimum thickness of the Kanayut that we have measured in the western Brooks Range is 240 m. However, we have not identified the various members of the Kanayut in this area.

Substantiation of the presence of Kanayut Conglomerate lithofacies in the westernmost Brooks Range broadens our understanding of: (1) The lateral extent of the large mid-Paleozoic and dominantly fluvial delta on which the Kanayut was deposited

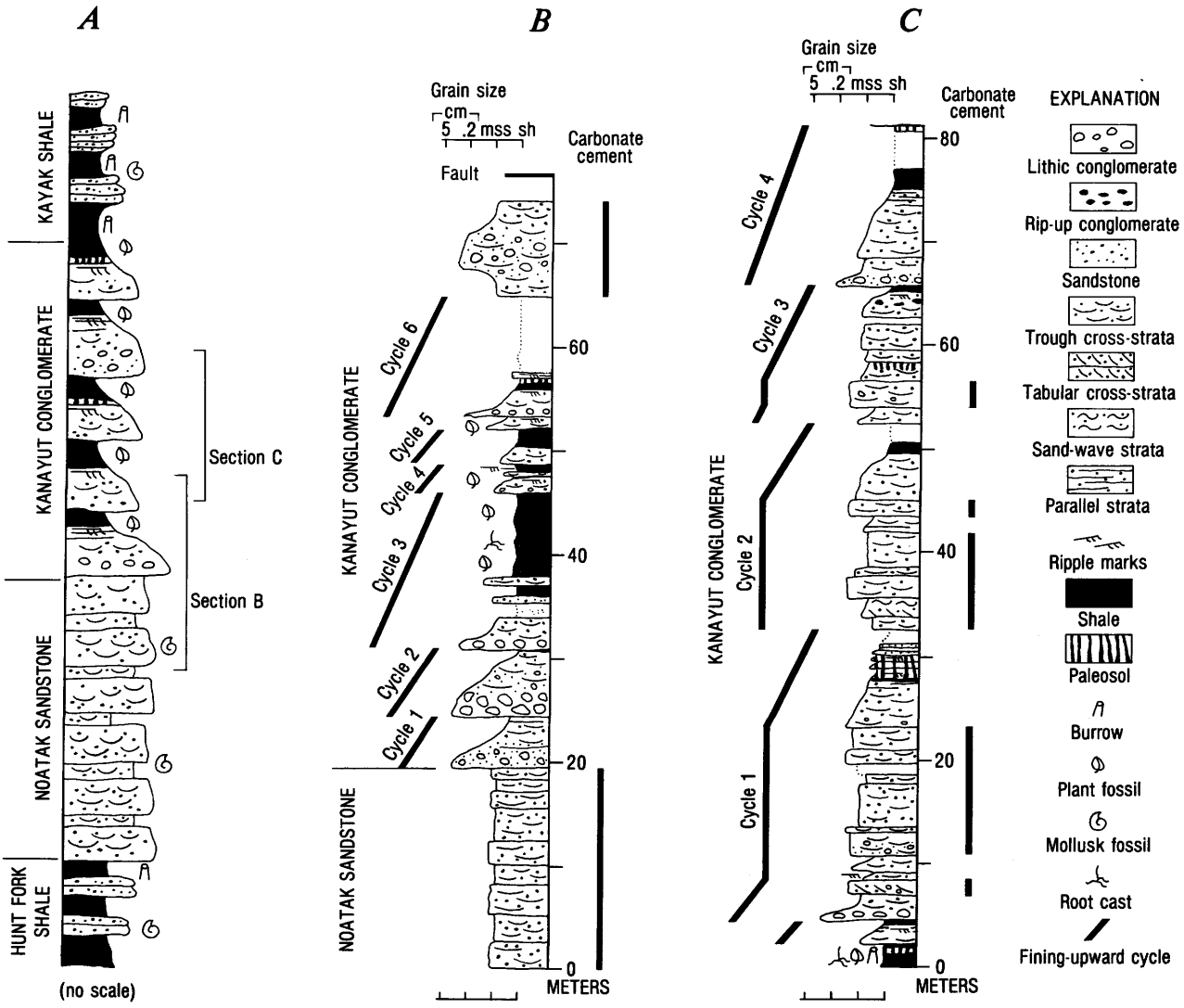

Figure 7.—Stratigraphic sections of the Kanayut Conglomerate in "Husky Mountains" and Mulgrave Hills, western Brooks Range, Alaska (fig. 6). A, Schematic stratigraphic column of the Endicott Group. B, Measured section showing fining-upward fluvial cycles in the Kanayut Conglomerate. C, Measured section showing composite fluvial and marine cycles in the Kanayut Conglomerate. Grain-size scale for sections shows increasing width from shale (sh) to medium-grained sandstone (mss) to conglomerate with maximum clast sizes of 0.2 and 5 cm.

(Nilsen and others, 1981a); (2) facies changes within the delta; and (3) the components of the stratigraphic sequence in this area. The Kanayut Conglomerate could possibly extend farther west. Although our fieldwork in 1982 suggests that coal-bearing Mississippian rocks on the Lisburne Peninsula, described by Tailleur (1965), are not equivalent to the Kanayut, Devonian red beds on Wrangel Island, which is located off the north coast of Siberia, may possibly be equivalent to the Kanayut Conglomerate (Bogdanov and Tilman, 1964). The present known thickness and lateral extent of the Kanayut Conglomerate indicates that it is one of the most significant fluvial deposits in North America and that it records major uplift and orogeny in the Brooks Range area. In the westernmost Brooks Range, it is clearly thinner (several hundred meters to 3,000 m), finer grained (maximum clast size, 1-3 to 23 cm), contains more intercalated marine strata in its lower part, and is less easily divisible or not divisible into its three members. However, it is clearly present in an Upper Devonian and Lower Mississippian stratigraphic sequence that, to us, is remarkably similar to that of the central and eastern Brooks Range, rather than markedly different, as some previous workers had reported.

REFERENCES CITED

Bogdanof, N. A., and Tilman, S. M., 1964, Obshchie cherty razxiliia paleozoiskikh struktur ostrova vrangelia i zabadnoi chasti khrebta Bruksa (Aliaska) [Similarities in the development of the Paleozoic structure of Wrangel Island and the western part of the Brooks Range (Alaska)], in Soveshchanie po problem tektoniki: Skadchatye Oblasti Evrazii, Materialy, Moskva, Nauka, p. 219-230.

Bowsher, A. L., and Dutro, J. T., Jr., 1957, The Paleozoic section in the Shainin Lake area, central Brooks Range, Alaska: U.S. Geological Survey Professional Paper 303-A, p. 1-39.

Brosgé, W. P., and Pessel, G. H., 1977, Preliminary reconnaissance geologic map of Survey Pass quadrangle, Alaska: U.S. Geological Survey Open-File Report 77-27, scale 1:250,000.

Brosgé, W. P., Reiser, H. N., Dutro, J. T., Jr., and Detterman, R. L., 1979a, Bedrock geologic map of the Philip Smith Mountains quadrangle, Alaska: U.S. Geological Survey Miscellaneous Field Studies Map MF-879-B, scale 1:250,000, 2 sheets.

Brosgé, W. P., Reiser, H. N., Dutro, J. T., Jr., and Nilsen, T. H., 1979b, Geologic map of Devonian rocks in parts of the Chandler Lake and Killik River quadrangles, Alaska: U.S. Geological Survey Open-File Report 79-1224, scale 1:200,000.

Curtis, S. M., Ellersieck, Inyo, Mayfield, C. F., and Tailleur, I. L., 1982, Reconnaissance geologic map of southwestern Misheguk Mountain quadrangle, Alaska: U.S. Geological Survey Open-File Report 82-611, scale 1:63,360.

Dutro, J. T., Jr., 1953, Stratigraphy and paleontology of the Noatak and associated formations, Brooks Range, Alaska: New Haven, Conn., Yale University, Ph. D. thesis, 154 p.

Ellersieck, Inyo, Curtis, S. M., Mayfield, C. F., and Tailleur, I. L., 1982, Reconnaissance geologic map of south-central Misheguk Mountain quadrangle, Alaska: U.S. Geological Survey Open-File Report 82-612, scale 1:63,360.

Ellersieck, Inyo, Mayfield, C. F., Tailleur, I. L., and Curtis, S. M., 1979, Thrust sequences in the Misheguk Mountain quadrangle, Brooks Range, Alaska, in Johnson, K. M., and Williams, J. R., eds., The United States Geological Survey in Alaska: Accomplishments during 1978: U.S. Geological Survey Circular 804-B, p. B8-B9.

Gryc, George, Dutro, J. T., Jr., Brosgé, W. P., Tailleur, I. L., and Churkin, Michael, Jr., 1967, Devonian of Alaska, in Oswald, D. H., ed., International Symposium on the Devonian System: Calgary, Alberta, Canada, Alberta Society of Petroleum Geologists, v. 1, p. 703-716.

Mayfield, C. F., Curtis, S. M., Ellersieck, Inyo, and Tailleur, I. L., 1982, Reconnaissance geologic map of southeastern Mishaguk Mountain quadrangle, Alaska: U.S. Geological Survey Open-File Report 82-613, scale 1:63,360.

Mayfield, C. F., and Tailleur, I. L., 1978, Bedrock geologic map of the Ambler River quadrangle, Alaska: U.S. Geological Survey Open-File Report 78-120-A, scale 1:250,000.

Mayfield, C. F., Tailleur, I. L., Mull, C. G., and Sable, E. G., 1978, Bedrock geologic map of the south half of National Petroleum Reserve in Alaska: U.S. Geological Survey Open-File Report 78-70-B, scale 1:500,000, 2 sheets.

Nelson, S. W., and Grybeck, Donald, 1980, Geologic map of the Survey Pass quadrangle, Brooks Range, Alaska: U.S. Geological Survey Miscellaneous Field Studies Map MF-1176-A, scale 1:250,000, 2 sheets.

Nilsen, T. H., Brosgé, W. P., Dutro, J. T., Jr., and Moore, T. E., 1981a, Depositional model for the fluvial Upper Devonian Kanayut Conglomerate, Brooks Range, Alaska, in Albert, N. R. D., and Hudson, Travis, eds., The United States Geological Survey in Alaska: Accomplishments during 1979: U.S. Geological Survey Circular 823-B, p. B20-B21.

Nilsen, T. H., and Moore, T. E., 1982, Sedimentology and stratigraphy of the Kanayut Conglomerate, central and western Brooks Range, Alaska—report of 1981 field season: U.S. Geological Survey Open-File Report 82-674, 64 p.

Nilsen, T. H., Moore, T. E., Balin, D. F., and Johnson, S. Y., 1982, Sedimentology and stratigraphy of the Kanayut Conglomerate, central Brooks Range, Alaska—report of 1980 field season: U.S. Geological Survey Open-File Report 82-199, 81 p.

Nilsen, T. H., Moore, T. E., Brosgé, W. P., and Dutro, J. T., Jr., 1981b, Sedimentology and stratigraphy of the Kanayut Conglomerate and associated units, Brooks Range, Alaska—report of 1981 field season: U.S. Geological Survey Open-File Report 81-506, 39 p.

Nilsen, T. H., Moore, T. E., Dutro, J. T., Jr., Brosgé, W. P., and Orchard, D. M., 1980, Sedimentology and stratigraphy of the Kanayut Conglomerate and associated units, central and eastern Brooks

Range, Alaska—report of 1978 field season: U.S. Geological Survey Open-File Report 80-888, 40 p.

Porter, S. C., 1966, Stratigraphy and deformation of Paleozoic section at Anaktuvuk Pass, central Brooks Range, Alaska: American Association of Petroleum Geologists Bulletin, v. 50, no. 5, p. 952-980.

Tailleur, I. L., 1965, Low-volatile bituminous coal of Mississippian age on the Lisburne Peninsula, northwestern Alaska, in Geological Survey research 1965: U.S. Geological Survey Professional Paper 525-B, p. B34-B38.

Tailleur, I. L., Brosgé, W. P., and Reiser, H. N., 1967, Palinspastic analysis of Devonian rocks in northwestern Alaska, in Oswald, D. H., ed., International Symposium on the Devonian System: Calgary, Alberta, Canada, Alberta Society of Petroleum Geologists, v. 2, p. 1345-1361.

Kivivik Creek: A possible zinc-lead-silver occurrence in the Kuna Formation, western Baird Mountains, Alaska

By Inyo Ellersieck, David C. Blanchard, Steven M. Curtis, Charles F. Mayfield, and Irvin L. Tailleur

Zinc-lead-silver deposits in carbonaceous black shale and chert of the Mississippian and Pennsylvanian Kuna Formation (Mull and others, 1982) are currently attracting mining-company interest in the Red Dog district in the western De Long Mountains. The Red Dog deposit was recently reported to contain 85 million t of ore containing 17.1 weight percent Zn, 5.0 weight percent Pb, and 2.4 troy oz Ag/t, and the nearby Lik deposit 25 million t of ore containing 12 weight percent combined Pb-Zn and 1.3 troy oz Ag/t (Jones, 1982). Reconnaissance geologic mapping in the northwestern Baird Mountains (area 2 of fig. 5) has revealed an extension of the strata known to contain the Red Dog and Lik deposits, and stream-sediment geochemical sampling has identified an area with lead, zinc, and silver anomalies similar to those in the Red Dog district.

The northwestern part of the Baird Mountains is made up of a stack of thrust sheets that have been warped into a northeast-striking antiform, the Agashashok anticlinorium (fig. 8). Facies contrasts occur between coeval rocks in different thrust sheets. Thrust sheets containing a similar lithostratigraphic sequence are grouped into tectonostratigraphic units called allochthons; these allochthons are extensions of the allochthons (previously called thrust sequences) in the De Long Mountains (Ellersieck and others, 1979). The structurally lowest allochthon in the Agashashok anticlinorium is the Brooks Range allochthon, which is made up of at least five thrust sheets larger than 50 km^2 and numerous smaller ones. Each of these thrust sheets contains part or all of a single lithostratigraphic sequence that is distinct from coeval sequences in the structurally higher allochthons. This stratigraphic sequence, called the Key Creek sequence after Key Creek in the De Long Mountains (Mull and others, 1982), is easily recognizable because it is the only sequence in the anticlinorium

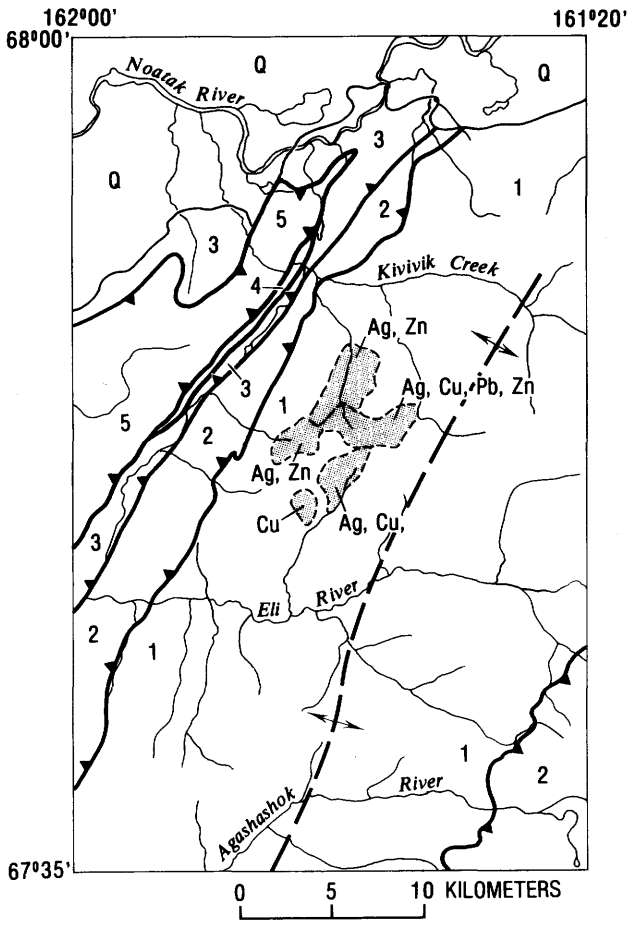

Figure 8.—Sketch map of northwest corner of Baird Mountains quadrangle, showing tectonostratigraphic units and location of anomalous stream-sediment samples.

that contains the Upper Devonian Hunt Fork Shale and Kanayut Conglomerate, and the Mississippian and Pennsylvanian Kuna Formation. Recognition of the Brooks Range allochthon in the Baird Mountains is important because all the known significant mineral occurrences in the De Long Mountains are in this allochthon (Mayfield and others, 1979).

The Kivivik Creek drainage is in the northwest corner of the Baird Mountains quadrangle and lies within the Noatak National Wilderness and Preserve. Attention was initially drawn to this area because it contains several red-stained creeks similar to those in the Red Dog area. Investigations in 1978 revealed a few high geochemical values, and gamma-ray intensities as high as 24 times the average value (Curtis and others, 1979). Followup stream-sediment geochemical sampling in 1979 and 1981 showed that several drainages in one area have anomalously high elemental concentrations (stippling, fig. 8). Copper, lead, and zinc were measured by both atomic absorption and semiquantitative emission-spectrographic methods, and silver by emission spectrography only. Copper values range as high as 320 parts per million (ppm), lead values as high as 360 ppm, zinc values as high as 1,200 ppm, and silver values as high as 20 ppm. The absolute abundances of, and the ratios between, copper, lead, and zinc are nearly identical to those in samples from streams draining the Lik and Red Dog deposits (Ellersieck and others, 1980). Nearly all the samples with the higher values are from streams that drain the Kuna Formation. No sulfides were found in place during reconnaissance mapping, other than some finely disseminated pyrite. On the basis of its geologic and geochemical similarities to rocks in the Red Dog district, the Brooks Range allochthon in the Agashashok anticlinorium should be considered highly prospective for zinc-lead-silver deposits of the Red Dog type.

REFERENCES CITED

Curtis, S. M., Rossiter, Richard, Ellersieck, I. F., Mayfield, C. F., and Tailleur, I. L., 1979, Gamma-ray values in the Misheguk Mountain region and in parts of Barrow, Teshekpuk, and Harrison Bay quadrangles, Alaska, in Johnson, K. M., and Williams, J. R., eds., The United States Geological Survey in Alaska: Accomplishments during 1978: U.S. Geological Survey Circular 804-B, p. B14.

Ellersieck, Inyo, Mayfield, C. F., Tailleur, I. L., and Curtis, S. M., 1979, Thrust sequences in the Misheguk Mountain quadrangle, Brooks Range, Alaska, in Johnson, K. M., and Williams, J. R., eds., The United States Geological Survey in Alaska: Accomplishments during 1978: U.S. Geological Survey Circular 804-B, p. B8-B9.

Ellersieck, Inyo, Curtis, S. M., Gruzensky, A. L., Mayfield, C. F., and Tailleur, I. L., 1980, Copper, lead, and zinc in stream-sediment samples from the De Long Mountains quadrangle, Alaska: U.S. Geological Survey Open-File Report 80-795, scale 1:63,360, 3 sheets.

Jones, Allan, 1982, Red Dog ore deposit said spectacular: Northern Miner, v. 67, no. 51, p. 1.

Mayfield, C. F., Curtis, S. M., Ellersieck, Inyo., and Tailleur, I. L., 1979, Reconnaissance geology of the Ginny Creek Zn-Pb-Ag and Nimiuktuk barite deposits, northwestern Brooks Range, Alaska: U.S. Geological Survey Open-File Report 79-1092, 20 p.

Mull, C. G., Tailleur, I. L., Mayfield, C. F., Ellersieck, Inyo, and Curtis, S. M., 1982, New late Paleozoic and early Mesozoic stratigraphic units, central and western Brooks Range, Alaska: American Association of Petroleum Geologists Bulletin, v. 66, no. 3, p. 348-362.

The Doonerak anticlinorium revisited

By J. Thomas Dutro, Jr., Allison R. Palmer, John E. Repetski, Jr., and William P. Brosgé

The recalcitrant rocks of Doonerak (cover photograph; area 1, fig. 5) yield their secrets grudgingly. For many years, we have probed and sampled this ancient anticlinorium, part of the autochthonous basement of the central Brooks Range, Alaska (Dutro and others, 1976), in which folded and faulted volcanic rocks, metamorphosed fine-grained clastic rocks, and marble are intruded by dikes and sills of two ages (470 m.y. and 350 m.y.). Upper Devonian (Frasnian) strata lie unconformably on parts of the anticlinorium, and Lower Carboniferous beds truncate all older structures with angular unconformity (Brosgé and Reiser, 1971). During the Late Jurassic and Cretaceous building of the ancient Brooks Range, all these rocks were intruded, folded, faulted, thrust northward, and uplifted to initiate Early Cretaceous coarse clastic sedimentation on the Arctic slope.

What is the age of the old metamorphic terrane of Doonerak? Because it is intruded by dikes as old as 470 m.y., we opined in 1976 that the sedimentary rocks might be Cambrian or Ordovician. This was not an uninformed guess because similar anticlinoria in the northeastern autochthonous Brooks Range contain fossiliferous Lower and Upper Cambrian and Middle Ordovician rocks in analogous terranes that also include volcanic rocks (Reiser and others, 1971, 1980). Of course, it may be possible that only Precambrian strata are present near Doonerak.

In previous summers, we spent many hours looking for graptolites in the fine-grained rocks, but to no avail. Several samples were processed for possible microfossils, again with no results.

At last, during the 1981 summer field season, we found megafossils in sandy limestone that is intimately associated with the black fine-grained clastic sequence. In the hills south of Wolf Creek, near the north margin of the anticlinorium (fig. 9), several isolated gray marble bodies are surrounded by black siltstone and argillite and intruded by greenstone dikes. Just above one of these marble bodies, in brown-weathering sandy limestone, we found many trilobite fragments and a few brachiopods. According to A. R. Palmer, these trilobites include Kootenia cf. K. anabarensis Lermontova, "Parehmania" lata Chernysheva, and Pagetia sp. and are most likely early Middle Cambrian, correlative with the Amgan Stage of Siberia. The brachiopods are Nisusia sp., a common Middle Cambrian genus. A sample from the same beds was processed for microfossils by J. E. Repetski, Jr.,

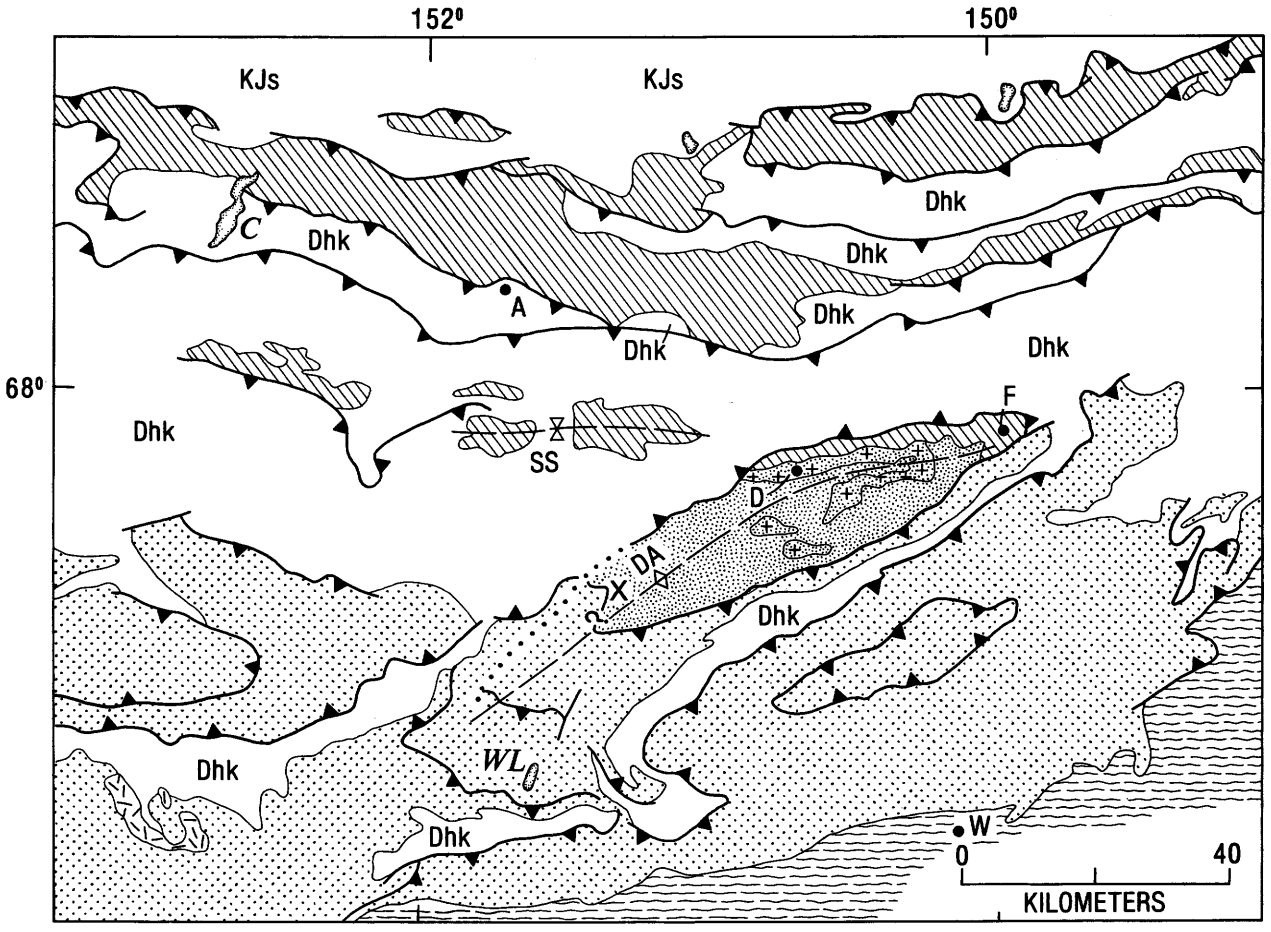

EXPLANATION

KJs	Cretaceous and Jurassic sedimentary rocks
	Triassic, Permian, and Carboniferous sedimentary rocks
Dhk	Upper Devonian sedimentary rocks—Hunt Fork Shale and Kanayut Conglomerate
	Devonian sedimentary rocks older than the Hunt Fork Shale
	Ordovician or Cambrian sedimentary rocks
+ + +	Volcanic rocks of Mount Doonerak
	Quartz-mica and calcareous schists
	Granite
———	Contact
▲——▲	Thrust fault; dotted where inferred

Figure 9.—Generalized geologic and structural map of Doonerak anticlinorium and adjacent areas. X, location of trilobite beds; A, Anaktuvuk Pass; C, Chandler Lake; DA, axis of Doonerak anticlinorium; D, Mount Doonerak; F, Falsoola Mountain; SS, Savioyuk synclinorium; W, Wiseman; WL, Wild Lake (from Dutro and others, 1976, fig. 1).

who found Westergaardodina sp., possible hyolithids, and undetermined acrotretid brachiopods. Other samples, from two localities in the gray marble bodies, contain microfossils that, according to Repetski, also include Westergaardodina sp., a paraconodont which ranges in age from Middle Cambrian into Early Ordovician in many parts of the world.

It is now clear why we were unable to find graptolites in this sequence: it is probably entirely Cambrian.

The marble bodies and associated beds provide a key to the geologic mapping of these old rocks. The brown limestone and gray marble are found as far west as Tobin Creek, on the west-plunging nose of the anticlinorium, where they are isoclinally folded within the clastic sequence and intruded by greenstone dikes.

Thus, part of the mystery of Doonerak has been solved. Its Cambrian rocks can be correlated with those of the northeastern Brooks Range (Dutro and others, 1972) and may be related to the Arctic Cambrian sequences in Siberia, Ellesmereland, North Greenland, and other parts of the North Atlantic Caledonides.

These are the oldest fossiliferous rocks thus far discovered in the central or western Brooks Range. Further search in the probable southwestward extension of this structural trend should turn up additional discoveries. The search goes on.

REFERENCES CITED

Brosgé, W. P. and Reiser, H. N., 1971, Preliminary bedrock geologic map, Wiseman and eastern Survey Pass quadrangles, Alaska: U.S. Geological Survey open-file map, scale 1:250,000, 2 sheets.

Dutro, J. T., Jr., Brosgé, W. P., and Reiser, H. N., 1972, Significance of recently discovered Cambrian fossils and reinterpretation of Neruokpuk Formation, northeastern Alaska: American Association of Petroleum Geologists Bulletin, v. 56, no. 4, p. 808-815.

Dutro, J. T., Jr., Brosgé, W. P., Lanphere, M. A., and Reiser, H. N., 1976, Geologic significance of Doonerak structural high, central Brooks Range, Alaska: American Association of Petroleum Geologists Bulletin, v. 60, no. 6, p. 952-961.

Reiser, H. N., Brosgé, W. P., Dutro, J. T., Jr., and Detterman, R. L., 1971, Preliminary geologic map, Mt. Michelson quadrangle, Alaska: U.S. Geological Survey open-file map, scale 1:200,000, 2 sheets.

Reiser, H. N., Brosgé, W. P., Dutro, J. T., Jr., and Detterman, R. L., 1980, Geologic map of the Demarcation Point quadrangle, Alaska: U.S. Geological Survey Miscellaneous Investigation Series Map I-1133, scale 1:250,000.

Geothermal studies in Alaska: Conditions at Prudhoe Bay

By Arthur H. Lachenbruch, John H. Sass, B. Vaughn Marshall, Thomas H. Moses, Jr., Robert J. Munroe, and Eugene P. Smith

The U.S. Geological Survey's Geothermal Studies Project is continuing to obtain heat-flow measurements in Alaska as opportunities arise in holes drilled for other purposes. Our objective is a better understanding of the tectonics and geothermal-energy resources, and of the geothermal regime of permafrost.

This year, we completed a study of the thermal regime in the Prudhoe Bay area on the coast of the Beaufort Sea (area 5 of fig. 5), on the basis of temperature measurements through permafrost in the Prudhoe Bay oilfield that we obtained through the cooperation of BP Alaska, Inc., and the Atlantic Richfield Oil Co. An analysis of these data, and of thermal-conductivity measurements on samples of drill cuttings and frozen core, leads to the following conclusions (Lachenbruch and Marshall, 1977; Lachenbruch and others, 1983):

1. The heat flow from the Earth's interior is 1.3±0.2 heat-flow units (HFU) (55±8 mW/m^2), a value typical of stable continental regions, similar to the values measured at Cape Thompson (Lachenbruch and others, 1966) and estimated at Barrow (Lachenbruch and Brewer, 1959).
2. The permafrost on land near Prudhoe Bay extends to a depth of 630+ m, 50 to 100 percent deeper than permafrost in the Barrow area. This greater depth is caused by the high thermal conductivity of the coarse ice-rich siliceous sediment in the Prudhoe Bay area; only a small thermal gradient is required to transport the heat flowing from the Earth's interior through such conductive material.
3. As at other sites along the Arctic Alaskan the mean annual temperature of the Earth's surface has increased sharply in the past hundred years. In the Prudhoe Bay area, we estimate that this increase averages about 1.8°C (from -10.9° to -9.1°C) and that it is associated with a net accumulation of 5 to 6 $kcal/cm^2$ by the Earth's surface during this period.
4. Rising sea level (Hopkins, 1983) and thawing seacliffs (Barnes and others, 1977) probably caused the shoreline to advance tens of kilometers in the past 20,000 years, so that a part of the Continental Shelf that is presently the target of intensive oil exploration was inundated. A simple heat-conduction model suggests that the warm seabed will cause the base of ice-rich permafrost to rise about 10 m (from 600± m) during the first 2,000 years after inundation, and thereafter it will rise about 15 m per 1,000 years. Accordingly, this recently inundated region is probably underlain by near-melting ice-rich permafrost to depths of 300 to 500 m; its presence is important to seismic interpretations in oil exploration and to engineering considerations in oil production. With confirmation of the permafrost configuration by offshore drilling, conduction models can yield reliable new information on the chronology of Arctic shorelines.

REFERENCES CITED

Barnes, Peter, Reimnitz, Erk, Smith, Greg, and Melchior, John, 1977, Bathymetric and shoreline changes, northwestern Prudhoe Bay, Alaska: U.S. Geological Survey Open-File Report 77-161, 10 p.

Hopkins, D. M., 1983, Aspects of the paleogeography of Beringia during the late Pleistocene, in Hopkins, D. M., Matthews, J. V., Jr., Schweger, C. E., and Young, S. B., eds., Paleogeography of Beringia: New York, Academic Press, p. 3-28.

Lachenbruch, A. H., and Brewer, M. C., 1959, Dissipation of the temperature effect of drilling a well in Arctic Alaska: U.S. Geological Survey Bulletin 1083-C, p. 73-109.

Lachenbruch, A. H., Greene, G. W., and Marshall, B. V., 1966, Permafrost and the geothermal regimes, in Wilimovsky, N. J., and Wolfe, J. N., eds., Environment of the Cape Thompson region, Alaska: U.S. Atomic Energy Commission, Division of Technical Information Report PNE-481, p. 149-163.

Lachenbruch, A. H., and Marshall, B. V., 1977, Sub-sea temperatures and a simple tentative model for offshore permafrost at Prudhoe Bay, Alaska: U.S. Geological Survey Open-File Report 77-395, 54 p.

Lachenbruch, A. H., Sass, J. H., Marshall, B. V., and Moses, T. H., Jr., 1983, Permafrost, heat flow, and geothermal regime at Prudhoe Bay, Alaska: U.S. Geological Survey Open-File Report [in press].

Comparison of grain-size statistics from two northern Alaska dune fields

By John P. Galloway and Eduard A. Koster[1]

Grain-size parameters were determined for 40 eolian samples collected from two Alaskan dune fields north of the Arctic Circle (area 3, fig. 5; fig. 10). A total of 20 samples were collected from the Great Kobuk Sand Dunes during summer 1981. The Great Kobuk Sand Dunes compose one of two active dune fields located in the central Kobuk Valley and cover an area of 78 km^2 (Fernald, 1964). The other 20 samples were collected from a stabilized Pleistocene dune field that covers more than 7,000 km^2 of the National Petroleum Reserve in Alaska (Carter, 1981). Grain-size analyses of samples from this stabilized dune field have been reported elsewhere (Galloway, 1981).

All samples were analyzed using standard techniques, as described by Folk (1964). Sieving of the sand fraction was done at 1/2Ø intervals, and, when necessary, the fine fraction (material greater than 4Ø, mud) was analyzed with a hydrophotometer. Only two of the samples from the active Great Kobuk Sand Dunes had a mud content greater than 2 percent; the average mud content was 1.16 percent. None of the Great Kobuk Sand Dunes samples were analyzed with the hydrophotometer. The mud content of the samples from the northern (Pleistocene) dune field ranged from less than 0.5 to 12.5 percent, and analysis of the fines with the hydrophotometer was necessary for samples with a mud content greater than 2 percent. Because most of the fines settled out after the first six hydrophotometer readings (7Ø, fine silt), a limit of 8.0Ø (silt/clay boundary) was used in the computer program (Pierce and Good, 1966) for generation of the cumulative curves from which the graphical statistics were derived (Folk and Ward, 1957). Cumulative-frequency curves for a coarse- and a fine-grained sample collected from the north end of the Great Kobuk Sand Dunes were previously published by Fernald (1964, p. K24).

[1]Physical Geography and Soil Science Laboratory, University of Amsterdam, The Netherlands.

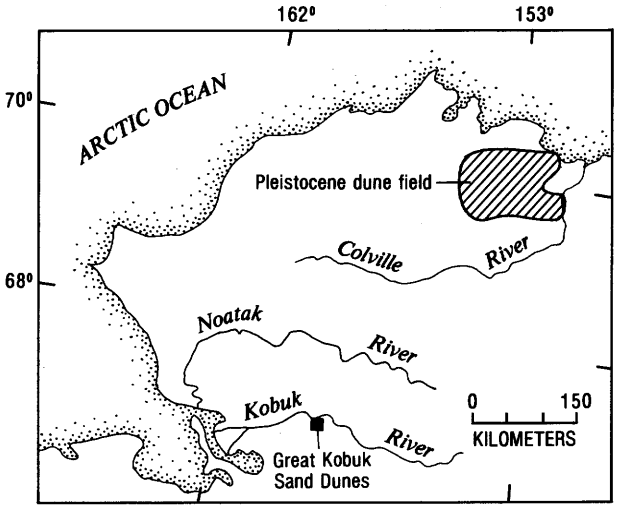

Figure 10.—Index map showing approximate locations of two major dune fields north of the Arctic Circle, northern Alaska.

Table 2.--Summary of graphical statistics

[Graphical statistics in Ø (phi) units]

Mean grain size	Sorting	Skewness
Great Kobuk Sand Dunes		
2.6005, fine sand (1.8465-3.0065)	0.5654, moderately well sorted (0.8657-0.3566)	0.0456, symmetrical (-0.1767-0.3636)
Northern Alaska (Pleistocene) dune field		
2.6838, fine sand (2.1433-3.8706)	0.7960, moderately sorted (1.4086-0.3858)	0.1259, fine (-0.2922-0.4937)

Table 2 lists the means and ranges for the following graphical statistics: mean grain size, sorting, and skewness. Figure 11 is a composite of all the cumulative curves determined for each dune field. Both dune fields consist of fine sand that is moderately to moderately well sorted; granules are absent, and the largest size is -0.5ϕ, very coarse sand. The northern (Pleistocene) dune field exhibits a wider range of sorting and skewness than the active Great Kobuk Sand Dunes; however, the statistics for both fields are consistent with those reported for other inland dune fields (Ahlbrandt, 1979).

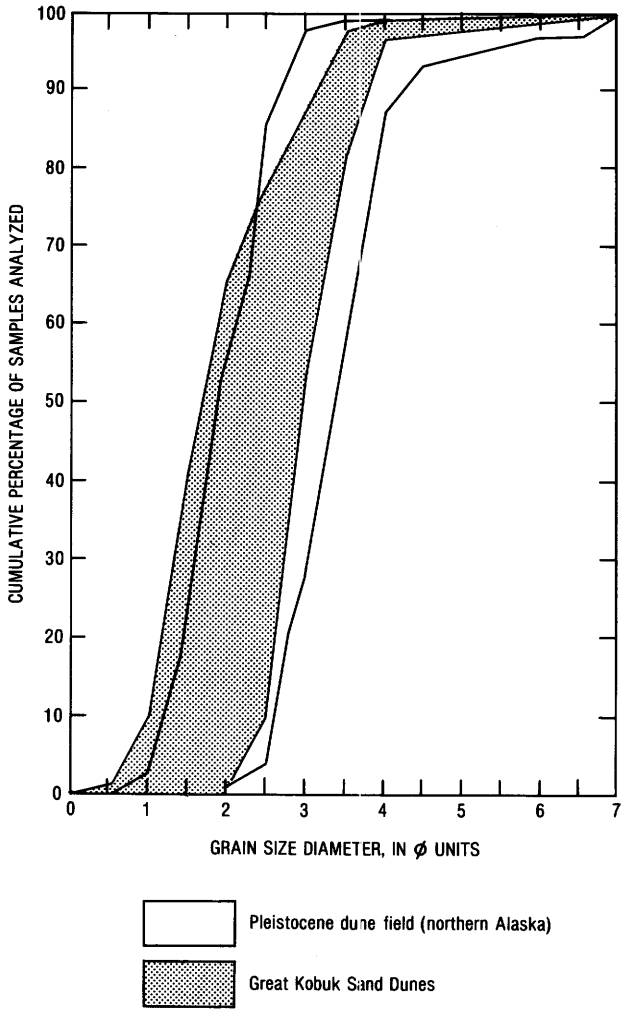

Figure 11.—Cumulative percentage of samples analyzed versus grain size.

REFERENCES CITED

Ahlbrandt, T. S., 1979, Textural parameters of eolian deposits, chap. B of McKee, E. D., ed., A study of global sand seas: U.S. Geological Survey Professional Paper 1052, p. 21-52.

Carter, L. D., 1981, A Pleistocene sand sea on the Alaskan Arctic Coastal Plain: Science, v. 211, no. 4480, p. 381-383.

Fernald, A. T., 1964, Surficial geology of the central Kobuk River valley, northwestern Alaska: U.S. Geological Survey Bulletin 1181-K, p. K1-K31.

Folk, R. L., 1974, Petrology of sedimentary rocks: Austin, Tex., Hemphill, 182 p.

Folk, R. L., and Ward, W. C., 1957, Brazos River Bar: A study of the significance of grain size parameters: Journal of Sedimentary Petrology, v. 47, no. 2, p. 931-932.

Galloway, J. P., 1981, Grain-size analyses of 20 eolian samples from northern Alaska, in Coonrad, W. L., ed., The United States Geological Survey in Alaska: Accomplishments during 1980: U.S. Geological Survey Circular 844, p. 51-53.

Pierce, J. W., and Good, D. I., 1966, FORTRAN II program for standard size analysis of unconsolidated sediments using an IBM 1620 computer: Kansas State Geological Survey Special Distribution Publication 28, 19 p.

Late Pleistocene glacial dams in the Noatak Valley

By Thomas D. Hamilton and Douglas P. Van Etten

Field studies within the upper Noatak Valley in 1981 indicate that proglacial lakes occupied the valley floor during at least two episodes of late Pleistocene glaciation (area 4, fig. 5; fig. 12). These lakes were confined by ice lobes that originated in the De Long Mountains and flowed southeastward to dam an unglaciated stretch of the Noatak Valley. A smaller ice tongue was generated at the head of the valley during each glaciation but did not coalesce with ice from the De Long Mountains. Few glaciers developed within the Baird Mountains along the south flank of the Noatak Valley, and none originated in the hills that lie to the north. The distribution of glaciers around the upper Noatak Valley is approximately that shown by Coulter and others (1965) for their two latest ice advances of Pleistocene age, but the presence of corresponding glacier-dammed lakes evidently was not recognized by those workers.

During the earlier glacial advance, ice streams from the De Long Mountains coalesced to form a large lobe that filled the floor of the Noatak Valley and extended eastward to the present mouth of the Cutler River (fig. 12A). A separate glacier flowed westward down the Noatak Valley and terminated about 25 km from the De Long Mountains ice tongue. Smaller glaciers extended down the valleys of the Cutler River and several of its tributaries, but none of these ice bodies reached the floor of the Noatak Valley. Extensive lacustrine plains, fine-grained glaciolacustrine and slack-water deposits exposed along the Cutler River, and weakly defined shorelines around the margins of the basin document the presence of a large proglacial lake that covered an area of approximately 1,400 km^2 and filled the valley to about 450 m altitude.

During the later glaciation, ice streams originating in the De Long Mountains flowed southeastward through the Nimiuktuk drainage system and once again coalesced to form a broad lobe that blocked the

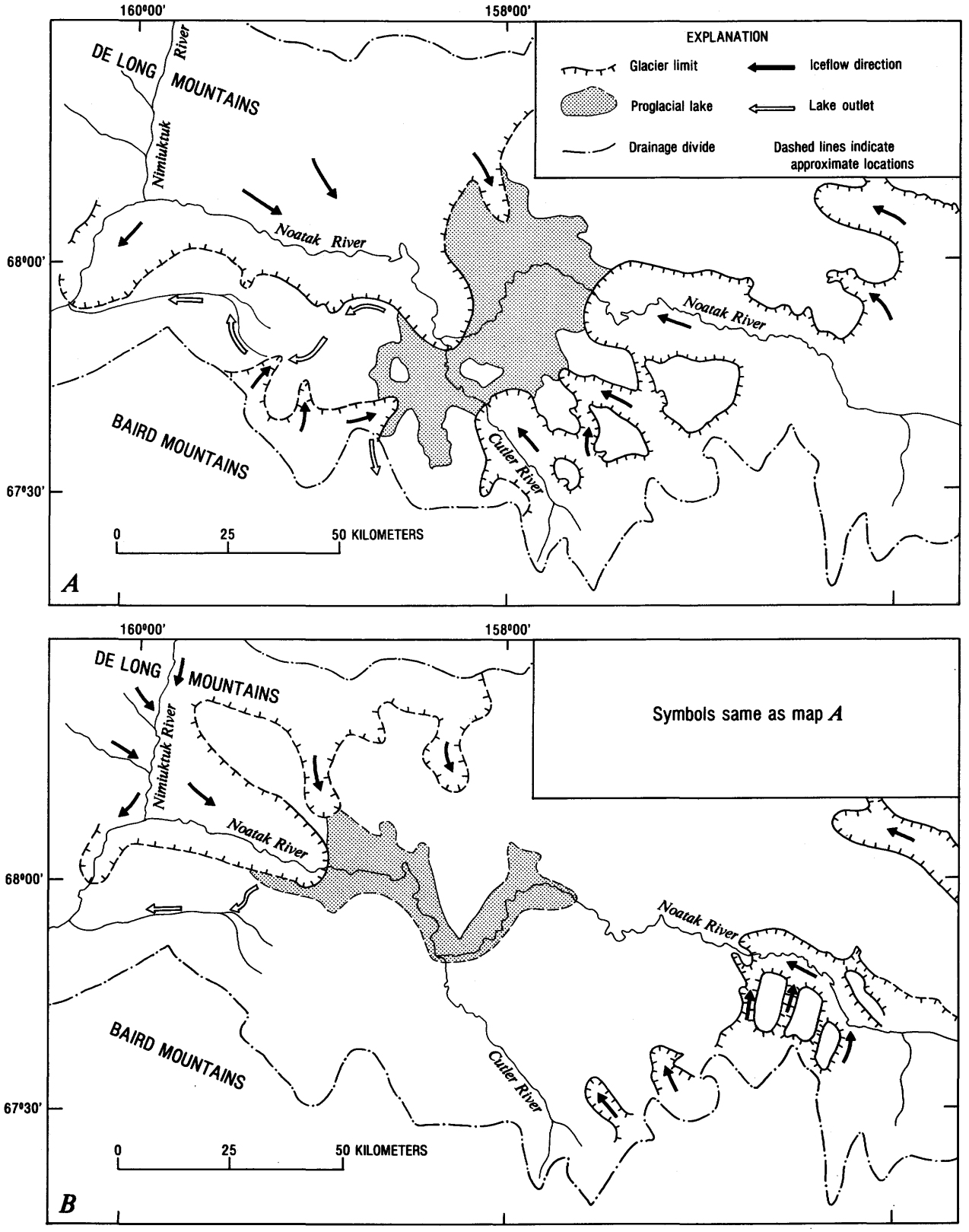

Figure 12.—Paleogeography of upper Noatak Valley during the Itkillik Glaciation (A) and subsequent Walker Lake Glaciation (B).

Noatak Valley (fig. 12B). This ice lobe extended eastward up the Noatak to terminate about 30 km northwest of the mouth of the Cutler River; a smaller glacier extended about 100 km down the upper Noatak Valley and terminated 65 km east of the Cutler River. Only the extreme southeastern part of the Cutler drainage system was glaciated at this time, and no glaciers formed in the low mountains north of the Noatak Valley. The proglacial lake dammed by the De Long Mountains ice tongue rose to about 350 m altitude and covered an area of about 700 km^2; it was confined to the center of the Noatak Valley and inset within ground-moraine and lake deposits dating from the earlier glaciation. The lake drained southward into the lower course of the Noatak Valley via a spillway across a northern outlier of the Baird Mountains. Glaciolacustrine sediment exposed in bluffs along the Noatak Valley consists of weakly bedded silt containing dropstones that unconformably overlies compact peat and organic silt.

The earlier and later intervals of glacial expansion and lake formation in the Noatak Valley can be correlated, respectively, with the Itkillik Glaciation of the central Brooks Range, as defined by Detterman and others (1958), and with the Walker Lake Glaciation of the Kobuk Valley (Fernald, 1964). Recent radiocarbon dating has shown that the Walker Lake Glaciation began about 24,000 yr B.P. and ended by 11,800 yr B.P. or shortly thereafter (Hamilton, 1982). The Itkillik Glaciation was earlier than the maximum time range of conventional radiocarbon dating (approx 55,000 ^{14}C yr), and its exact age is uncertain. Correlative deposits in the Alaska Range are inferred to be early Wisconsinan (Weber and others, 1981), and the absence of soils, weathering profiles, or interglacial fossils between deposits of Itkillik and Walker Lake age in the Brooks Range appears to support this age assignment.

The presence of ancient proglacial lakes in the upper Noatak Valley has important environmental implications. Silt- and clay-rich lacustrine and deltaic sediment is widespread in the valley center, and fine-grained slack-water deposits extend far up into unglaciated tributary valleys. This sediment is poorly drained, frost susceptible, and commonly ice rich; it is subject to failure along river bluffs and to frost heave, thaw settlement, and thaw-lake formation across the valley floor. Large stream icings occur around the perimeter of the former lake basin in places where permeable stream gravel grades laterally into finer grained lacustrine and deltaic deposits.

Late Pleistocene environments throughout much of the Brooks Range could have been strongly affected by the proglacial lakes. Although outlets from the earlier (450 m) lake stage are uncertain at present, these may have included flows across lightly glaciated passes into the Hunt River drainage system of the Kobuk Valley or into the lower Noatak Valley (fig. 12A). Outburst floods resulting from breaching of the ice dam west of the Cutler River may have occurred intermittently during the maximum glacial phases, and such floods almost certainly took place when the ice dam was smaller during growth and recession toward the beginning and end of each glaciation. Such floods would have greatly affected the lower Noatak Valley and should have created slack-water deposits within its unglaciated tributaries (for example, Waitt, 1980), as well as large-scale alluvial deposits and erosional forms along the main valley. The large lake of Itkillik age should have been an important moisture source during summer and fall for mountains near the heads of the Noatak, Alatna, and Kobuk Valleys that lie along the paths of storm tracks moving inland from the coast. Presence of the lake may account in part for extensive Itkillik-age glaciation in the western Brooks Range.

In view of mounting evidence for late Pleistocene aridity in northern Alaska and the Yukon Territory (Cwynar and Ritchie, 1980; Carter, 1981; Hamilton, 1982), large proglacial lakes in the Noatak Valley could also have had a major influence on the distribution of large grazing mammals and their predators, possibly including early man. The lakes not only could have provided a local water source in a generally arid region but also might have induced locally higher rainfall and locally milder temperatures during late summer and early autumn. Access into the upper Noatak lake basin would have been readily accomplished via unglaciated passes to the north and via additional passes to the south during Walker Lake time.

REFERENCES CITED

Carter, L. D., 1981, A Pleistocene sand sea on the Alaskan Arctic Coastal Plain: Science, v. 211, no. 4480, p. 381-383.

Coulter, H. W., Hopkins, D. M., Karlstrom, T. N. V., Péwé, T. L., Wahrhaftig, Clyde, and Williams, J. R., compilers, 1965, Map showing extent of glaciations in Alaska: U.S. Geological Survey Miscellaneous Geologic Investigations Series Map I-415, scale 1:2,500,000.

Cwynar, L. C., and Ritchie, J. C., 1980, Arctic steppe-tundra: A Yukon perspective: Science, v. 208, no. 4450, p. 1375-1377.

Detterman, R. L., Bowsher, A. L., and Dutro, J. T., Jr., 1958, Glaciation on the Arctic slope of the Brooks Range, northern Alaska: Arctic, v. 11, no. 1, p. 43-61.

Fernald, A. T., 1964, Surficial geology of the central Kobuk River Valley, northwestern Alaska: U.S. Geological Survey Bulletin 1181-K, p. K1-K31.

Hamilton, T. D., 1980, Surficial geologic map of the Killik River quadrangle, Alaska: U.S. Geological Survey Miscellaneous Field Studies Map MF-1234, scale 1:250,000.

———1981, Surficial geologic map of the Survey Pass quadrangle, Alaska: U.S. Geological Survey Miscellaneous Field Studies Map MF-1320, scale 1:250,000.

——1982, A late Pleistocene glacial chronology for the southern Brooks Range: Stratigraphic record and regional significance: Geological Society of America Bulletin, v. 93, no. 8, p. 6853-6864.

Waitt, R. B., Jr., 1980, About forty last-glacial Lake Missoula jökulhlaups through southern Washington: Journal of Geology, v. 88, no. 6, p. 653-679.

Weber, F. R., Hamilton, T. D., Hopkins, D. M., Repenning, C. A., and Haas, Herbert, 1981, Canyon Creek: A Late Pleistocene vertebrate locality in interior Alaska: Quaternary Research, v. 16, no. 2, p. 167-180.

WEST-CENTRAL ALASKA

(Figure 13 shows study areas discussed)

Reconnaissance geology of the northern part of the Unalakleet quadrangle

By William W. Patton, Jr., and Elizabeth J. Moll

The Unalakleet quadrangle lies wholly within the Yukon-Koyukuk basin and is underlain chiefly by Cretaceous sedimentary rocks and Cretaceous or lower Tertiary volcanic rocks (area 2, fig. 13; fig. 14). Pre-Cretaceous volcanic and plutonic rocks crop out on a structural high between the Chiroskey and Anvik faults in the central part of the quadrangle, and Quaternary and(?) upper Tertiary flood basalt occurs along the shore of Norton Sound in the southwestern part of the quadrangle.

The pre-Cretaceous volcanic and plutonic rocks exposed on the structural high between the Chiroskey and Anvik faults include altered basalt, the age of which is uncertain but no younger than Middle Jurassic, and diorite and tonalite of Middle and Late Jurassic age (table 3). The basalt is faulted against Jurassic

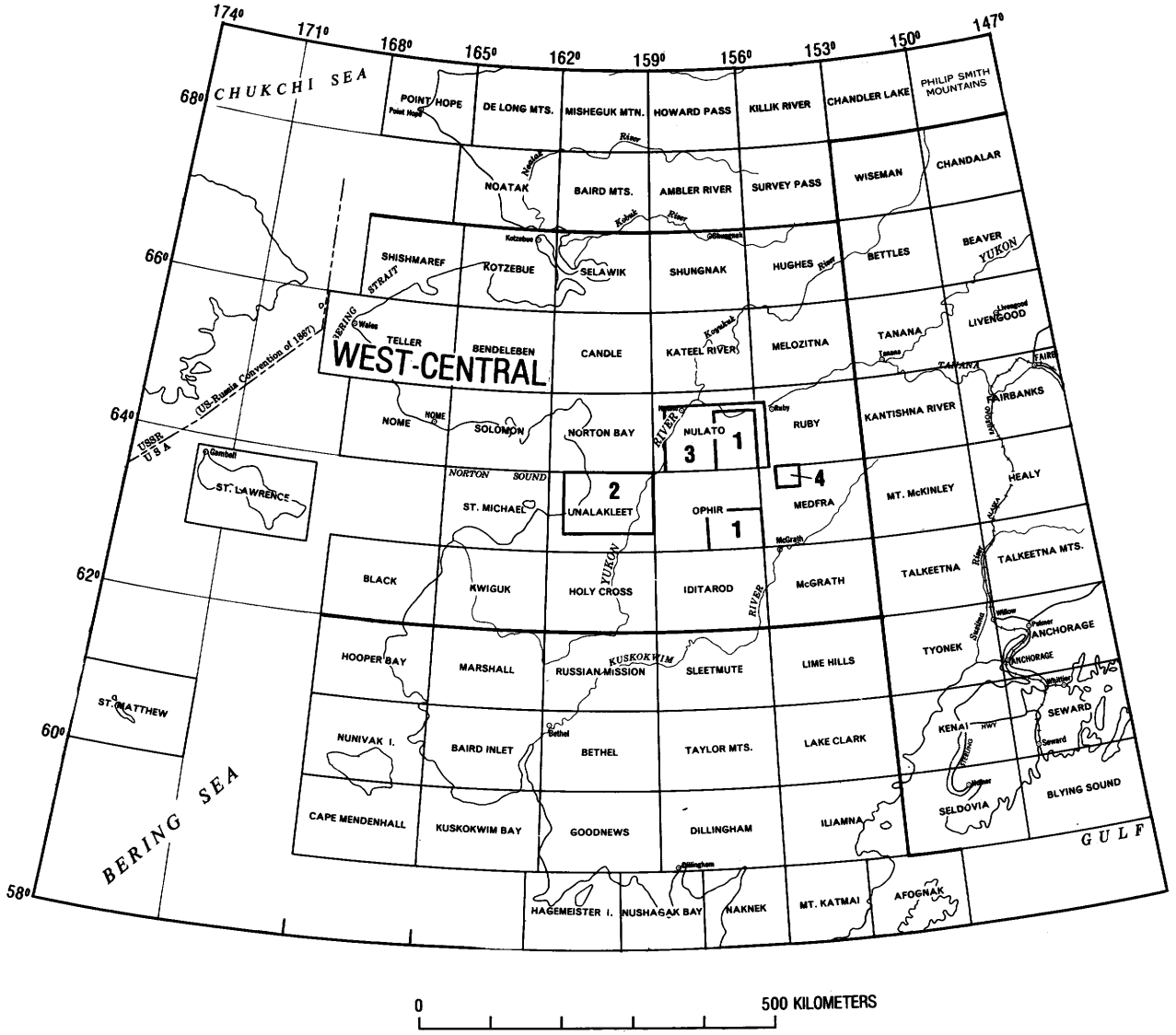

Figure 13.—Areas in west-central Alaska discussed in this volume. A listing of authorship, applicable figures and tables, and article pagination (in parentheses) relating to the numbered areas follows. 1, Loney and Himmelberg, figures 15 and 16 (p. 27-30); 2, Patton and Moll, figure 14, table 3 (p. 24-27); 3, Patton and others, figure 17, table 4 (p. 30-32); 4, Silberman and others, figure 18, table 5 (p. 32-34).

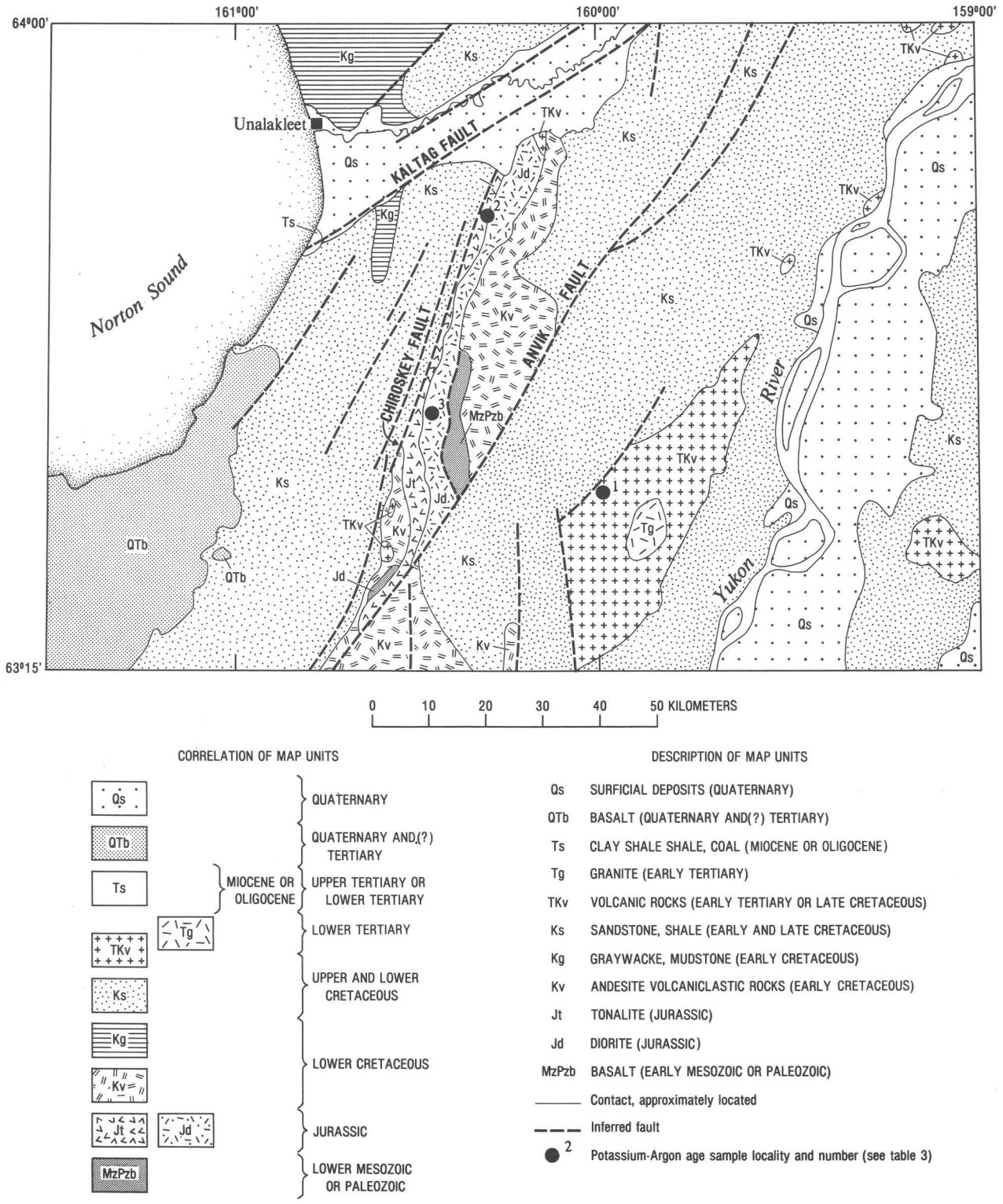

Figure 14.—Generalized geologic map of northern part of Unalakleet quadrangle.

intrusive rocks within the map area but a short distance to the south is intruded and altered by them (J. M. Hoare, written commun., 1981). The diorite and tonalite occur as narrow elongate bodies paralleling the Chiroskey fault along the west side of the structural high. Both bodies are extensively sheared, and their field relations uncertain; however, newly determined K-Ar ages (table 3) suggest that the tonalite is younger than the diorite.

Table 3.--Potassium-argon age determinations

[^{40}K decay constants: λ_e=0.581x10^{-10} yr^{-1}; λ_β=4.963x10^{-10} yr^{-1}; abundance ratio: $^{40}K/K$=1.167x10^{-4} atom percent. Potassium analyses by Paul Klock; argon analyses and age calculations by Krueger Enterprises, Geochron Laboratories, and M. L. Silberman]

Map No.	Field No.	Mineral	Map symbol	K_2O (wt pct)	$^{40}Ar_{rad}$ (10^{10} mol/g)	$\frac{^{40}Ar_{rad}}{^{40}Ar_{total}}$	Calculated age (m.y.)
1	80AMl 12B	Hornblende--	TKv	0.668 .669	0.6920 .5865	0.35 .29	65.2±3.9
2	80APa 15A	Biotite-----	Jt	4.52 4.51	10.33 10.55	.67 .79	154±6
3	80AMl 25	do--------	Jd	2.32 2.33	5.645 5.990	.70 .68	166±7
		Hornblende----------		.662 .660	1.730 1.729	.62 .42	173±9

Andesitic volcaniclastic rocks of probable island-arc affinities unconformably overlie the pre-Cretaceous rocks along the Chiroskey-Anvik structural high. These volcaniclastic rocks are characterized by cyclically repeated sequences that grade upward from volcanic breccia and crystal-lithic tuff to fine-grained cherty tuff and chert. Locally, along the south edge of the map area, the volcanic unit also includes andesite and basalt flows. Radiolarians (D. L. Jones and others, written commun., 1981) and poorly preserved fragments of Buchia(?) indicate a probable Early Cretaceous age for this volcanic unit.

The Cretaceous sedimentary section, which may aggregate as much as 8,000 m in thickness, is composed of a lower unit of graywacke and mudstone submarine-fan turbidites and an upper unit of shallow marine and fluvial deltaic deposits of sandstone and shale. The graywacke and mudstone unit crops out along the Norton Sound coast north of Unalakleet and in a small area southeast of Unalakleet. Although no fossils have been found in the turbidite unit in the map area, correlation with similar strata elsewhere in the Yukon-Koyukuk basin suggests a late Early Cretaceous (Albian) age (Patton, 1973). The sandstone and shale unit is widely exposed over nearly the entire map area. In the vicinity of Unalakleet, it appears to overlie the graywacke and mudstone unit, but along the Chiroskey-Anvik structural high it rests directly on the andesitic volcaniclastic rocks. These shallow-water deposits contain abundant marine mollusks of late Early and early Late Cretaceous (Albian-Cenomanian) age, and plant fossils of Late Cretaceous age (Patton, 1973).

Calc-alkalic subaerial volcanic rocks unconformably overlie the Cretaceous sandstone and shale unit in the eastern and central parts of the map area. Between the Anvik fault and the Yukon River, a volcanic pile of more than 1,000 m of basalt and andesite flows in its lower part and of rhyolite tuff, breccia, and domes in its upper part is preserved in a large partly fault bounded southwest-plunging syncline. This pile is intruded by fine-grained granodiorite of probable early Tertiary age along the axis of the syncline. A single K-Ar determination on hornblende from an andesite flow near the base of the volcanic pile gave a latest Cretaceous or earliest Tertiary age (table 3).

Tertiary sedimentary rocks are confined to a small patch of variegated clay shale and lignitic coal exposed in badly slumped beach bluffs south of Unalakleet on the shore of Norton Sound. These rocks have been dated at late Oligocene or early Miocene on the basis of their pollen flora.

Alkali-olivine basalt of Quaternary and possible late Tertiary age forms a broad lava field covering the coastal lowlands that border Norton Sound in the southwestern part of the map area. Locally, this unit includes fresh, unmodified cinder cones and flows of probable Holocene age.

All the pre-latest Cretaceous rocks in the map area are tightly folded and broken by closely spaced high-angle faults. The latest Cretaceous or earliest Tertiary volcanic rocks are broadly warped and dip generally less than 40°; the late Tertiary or Quaternary basalt flows are essentially undeformed. The Kaltag fault, a major strike-slip fault that can be traced eastward across central Alaska at least as far as the mouth of the Tanana River, is believed to have between 100 and 130 km of right-lateral offset since Cretaceous time (Patton and Hoare, 1968). The Anvik fault, which may be a splay of the Kaltag fault, could have as much as 35 km of right-lateral offset, judging

from displacement of the contact between the andesitic volcanic rocks and the sandstone and shale unit in the central part of the map area. All other faults, including the Chiroskey fault, appear to be high-angle normal or reverse faults.

REFERENCES CITED

Patton, W. W., Jr., 1973, Reconnaissance geology of the northern Yukon-Koyukuk province, Alaska: U.S. Geological Survey Professional Paper 774-A, p. A1-A17.

Patton, W. W., Jr., and Hoare, J. M., 1968, The Kaltag fault, west-central Alaska, in Geological Survey research 1968: U.S. Geological Survey Professional Paper 600-D, p. D147-D153.

Preliminary report on ophiolites in the Yuki River and Mount Hurst areas, west-central Alaska

By Robert A. Loney and Glen R. Himmelberg

Reconnaissance mapping of ultramafic bodies in the Yuki River and Mount Hurst areas, west-central Alaska (areas 1, fig. 13; figs. 15, 16), though incomplete, supports the conclusion of Patton and others (1977) that the widely scattered ultramafic bodies in west-central Alaska are parts of dismembered ophiolite complexes (herein informally called the Mount Hurst and Yuki River ophiolites). The ultramafic bodies of both areas are composed of similar parts of the ophiolite complex, the basal harzburgite tectonite and the ultramafic cumulate, and occur in similar terranes. The ophiolite bodies in the Yuki River area, which occur in a belt of basalt, gabbro, and chert of Mississippian to Triassic age (W. W. Patton, Jr., written commun., 1981), were considered by Patton and others (1977) to be part the Rampart ophiolite belt. They interpreted the ophiolites of this belt to be slablike remnants of allochthonous sheets thrust southward from the Yukon-Koyokuk root zone. Though not part of the Rampart belt, the ophiolite body in the Mount Hurst area occurs in a similar terrane, consisting of chert, tuff, argillite, and basalt of Mississippian to Jurassic(?) age that is part of the Innoko terrane (Patton, 1978). As yet, the thrust-sheet interpretation has not been extended to this ophiolite.

The Yuki River ophiolite occurs mostly as narrow elongate masses that extend northeastward for more than 50 km along the southeast side of the river valley (fig. 15). The largest mass is the southwesternmost body, which forms the mountain on which triangulation station Kede is located. This is the only body in which the harzburgite tectonite-cumulate contact has been mapped. This contact trends diagonally across the Kede body, which it divides into two nearly equal parts of dominantly harzburgite tectonite to the southwest and dominantly ultramafic cumulate to the northeast. The contact appears to be subvertical and may, in part, be a fault. The relation of the harzburgite in the extreme northeastern part to the rest of the body is as yet unresolved.

The Mount Hurst ophiolite is divided longitudinally into a northwestern belt of harzburgite tectonite and a southeastern belt of ultramafic cumulate (fig. 16). Near the top of Mount Hurst, the units form belts of nearly equal width, but to the northeast and southwest the contact, because of a gentle (26°) northwestward dip, swings northwestward, and the cumulate unit becomes the wider. Thus, contrary to the ophiolite model, in which the harzburgite is the basal unit (Penrose Field Conference participants, 1972), here the ultramafic cumulate is structurally lower. Although the nature of the contact is as yet unknown, folding in the rocks on both sides has created foliation attitudes that strike at high angles to the contact. Therefore, the contact must also be folded, or, if not, it must be a fault. A thrust fault would explain the upside-down order of the section.

Although the ultramafic rocks are partially serpentinized, their primary mineralogy and structure are readily distinguishable. The harzburgite tectonite units in the Yuki River and Mount Hurst ophiolites exhibit all the characteristics described for harzburgite in other ophiolite complexes (Loney and others, 1971; Himmelberg and Loney, 1980). The harzburgite tectonite consists dominantly of harzburgite and 25 to 30 percent orthopyroxene. Dunite occurs locally in the harzburgite as centimeter-scale layers and as lenses as much as tens of meters thick. Structurally the harzburgite ranges from massive to well foliated; the foliation results from gradational variation in the ratio of olivine to orthopyroxene.

The cumulate sequence in the Yuki River and Mount Hurst ophiolites consists dominantly of dunite and includes units of wehrlite and olivine clinopyroxenite that range in thickness from a few meters to tens of meters. The ratio of dunite to clinopyroxene-rich rocks is greater in the cumulate sequence of the Yuki River ophiolite than in the Mount Hurst body. In the Mount Hurst body, harzburgite cumulate is locally interlayered with dunite and olivine clinopyroxenite. In the Yuki River ophiolite, harzburgite occurs in the cumulate sequence, but it is tentatively interpreted to be part of the harzburgite tectonite unit infolded into the cumulate sequence. Isoclinal folding of cumulate layers at Mount Hurst and of chromitite seams in dunite cumulate in the Yuki River ophiolite indicates deformation of at least parts of the cumulate sequences.

Two exposures of massive chromitite, as much as 1.5 m thick, were observed in dunite cumulate in the Yuki River ophiolite. Generally, however, in both complexes, chromite is restricted to centimeter-scale layers in dunite and is an accessory mineral.

Gabbro, consisting dominantly of plagioclase and clinopyroxene in a hypautomorphic granular texture, is exposed at two localities northwest of Mount Hurst. At one of these localities, where the contact of the gabbro with limestone is well exposed, the absence of evidence of intrusive effects in the limestone suggests that the gabbro is fault emplaced. Isolated exposures of gabbro also occur in the area of the Yuki River ophiolite. At this time, we do not know whether the gabbro constitutes dismembered parts of the ophiolite complexes.

REFERENCES CITED

Himmelberg, G. R., and Loney, R. A., 1980, Petrology of ultramafic and gabbroic rocks of the Canyon

Mountain ophiolite, Oregon: American Journal of Science, v. 280-A, pt. 1, p. 232-268.
Loney, R. A., Himmelberg, G. R., and Coleman, R. G., 1971, Structure and petrology of the alpine-type peridotite at Burro Mountain, California, U.S.A.: Journal of Petrology, v. 12, no. 2, p. 245-309.
Patton, W. W., Jr., 1978, Juxtaposed continental and oceanic-island arc terranes in the Medfra quadrangle, west-central Alaska, in Johnson, K. M., ed., The United States Geological Survey in Alaska: Accomplishments during 1977: U.S. Geological Survey Circular 772-B, p. B38-B39.
Patton, W. W., Jr., Tailleur, I. L., Brosgé, W. P., and Lanphere, M. A., 1977, Preliminary report on the ophiolites of northern and western Alaska, in Coleman, R. G. and Irwin, W. P., eds., North American ophiolites: Oregon Department of

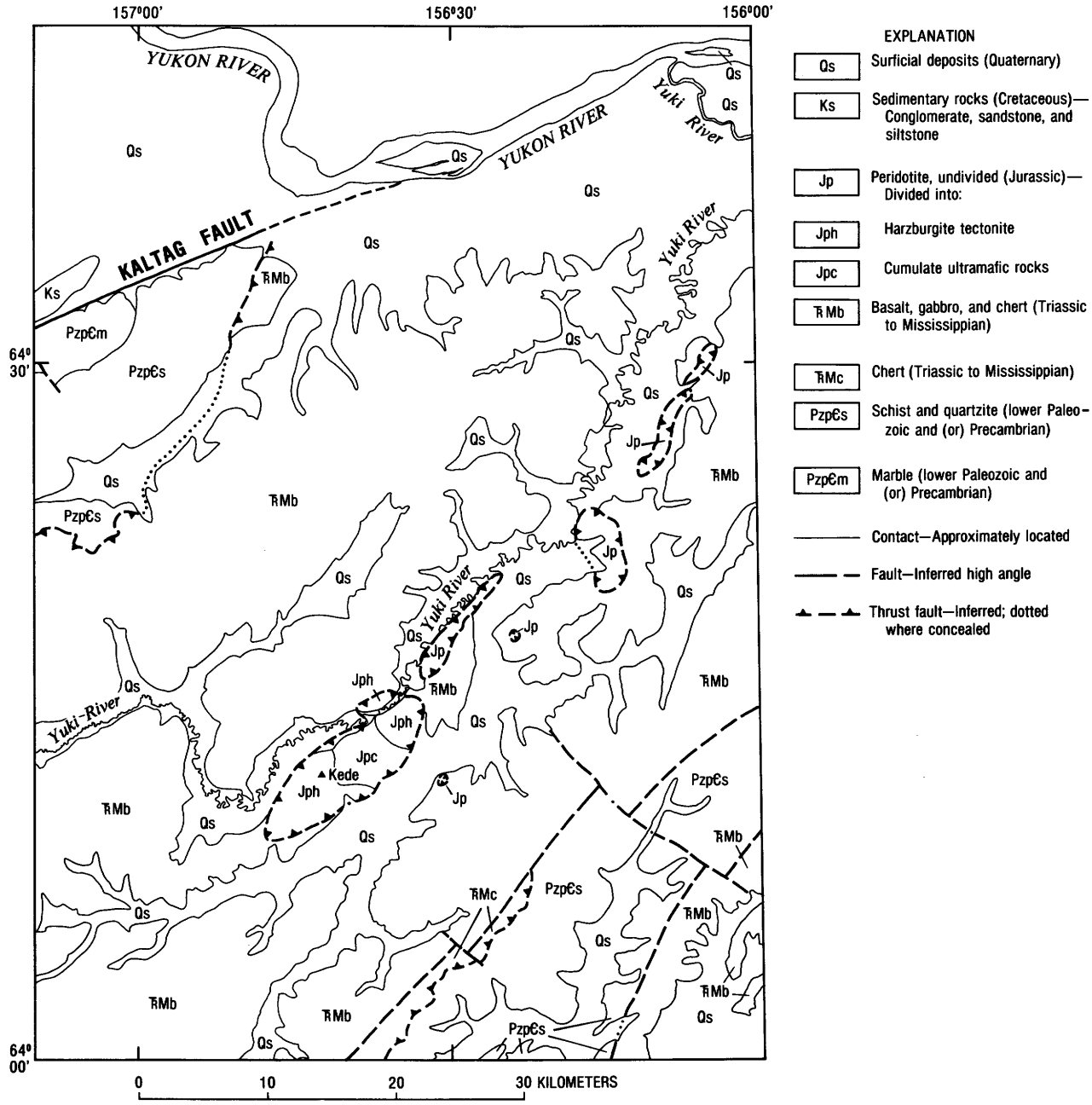

Figure 15.—Geologic map of southeastern part of Nulato quadrangle, Alaska (from W. W. Patton, Jr., written commun. 1981).

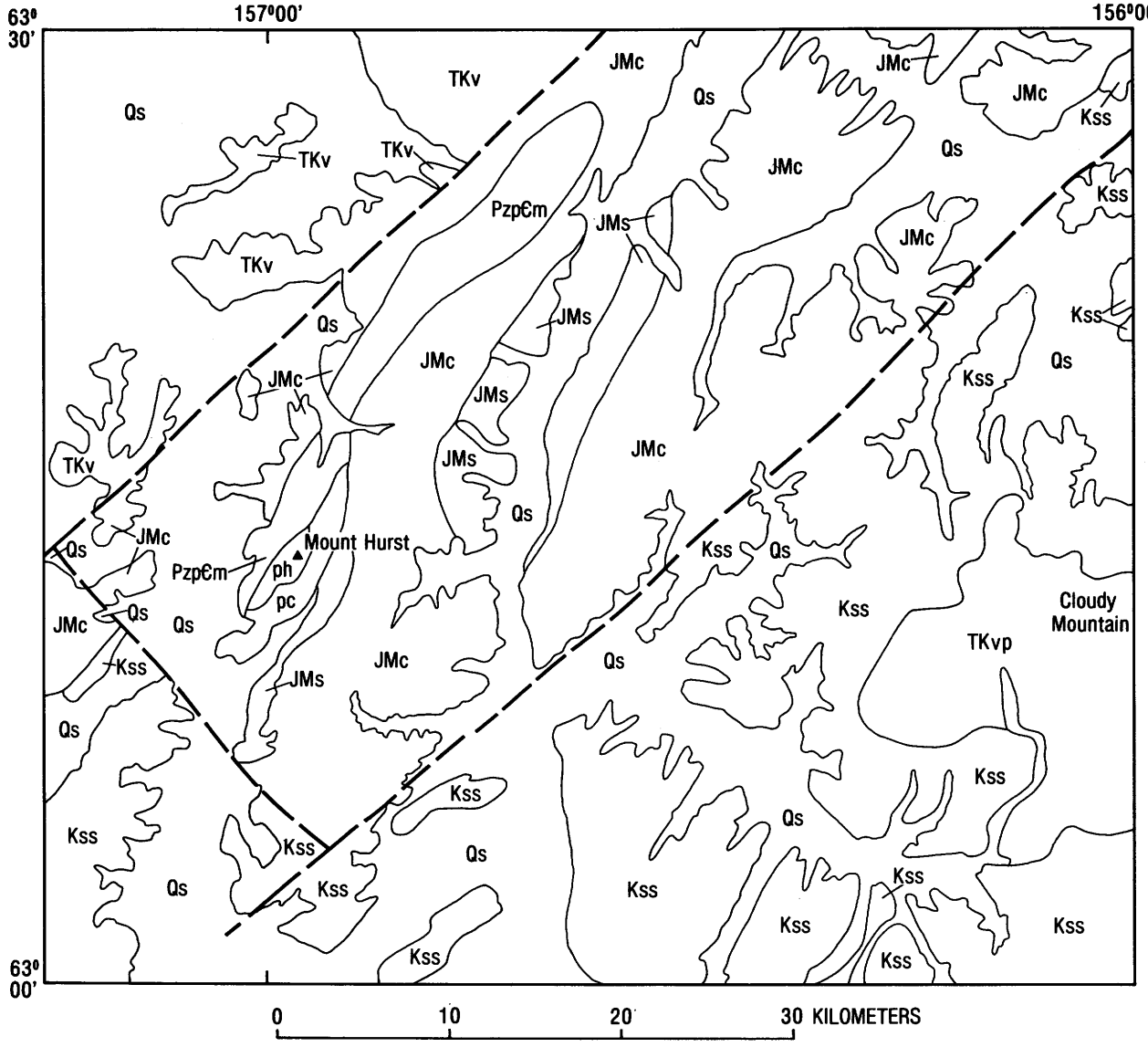

EXPLANATION

Qs	Surficial deposits (Quaternary)	JMs	Sandstone, grit, and argillite (Jurassic? to Mississippian)
TKv	Volcanic rocks (Tertiary and (or) Cretaceous)	Pzp€m	Metamorphic rocks (lower Paleozoic and Precambrian?)
TKvp	Volcanic and plutonic complex (Tertiary and (or) Cretaceous)		Peridotite (age uncertain)—Divided into:
Kss	Sandstone and shale (Cretaceous)	ph	Harzburgite tectonite
JMc	Chert, tuff, argillite, and basalt (Jurassic? to Mississippian)	pc	Cumulate ultramafic rocks
———	Contact—Approximately located	— — —	Fault—Inferred high angle

Figure 16.—Geologic map of southeastern part of Ophir quadrangle, Alaska (from R. M. Chapman and others, written commun. 1981).

Geology and Mineral Industries Bulletin 95, p. 51-57.

Penrose Field Conference participants, 1972, Ophiolites: Geotimes, v. 17, no. 12, p. 24-25.

New age data for the Kaiyuh Mountains, west-central Alaska

By William W. Patton, Jr., Elizabeth J. Moll, Marvin A. Lanphere, and David L. Jones

The Kaiyuh Mountains, situated in the Nulato quadrangle along the southeast margin of the Cretaceous Yukon-Koyukuk basin (area 3, fig. 13), are composed of a Precambrian and (or) Paleozoic metamorphic complex that is overlain by a late Paleozoic and early Mesozoic assemblage of mafic and ultramafic rocks and intruded by Cretaceous granitic rocks (fig. 17). The mafic and ultramafic rocks make up a reversely stacked dismembered ophiolite assemblage that appears to have been thrust southeastward across the metamorphic complex from a root zone at the margin of the Yukon-Koyukuk basin (Patton and others, 1977; Patton and Moll, 1981). This report presents new potassium-argon and fossil age determinations for the metamorphic complex, the ophiolite assemblage, and the granitic intrusive rocks.

1. Two potassium-argon age determinations on metamorphic muscovite from glaucophane-bearing schist in the metamorphic complex gave ages of 134 m.y. and 136 m.y. (latest Jurassic-earliest Cretaceous) (samples 1 and 2, respectively, fig. 17; table 4). These ages are thought to reflect metamorphic events associated with overthrusting of the ophiolites. A similar interpretation has been given for Early Cretaceous metamorphic ages from the schist belt in the southern Brooks Range (Turner and others, 1979; Dillon and others, 1980).
2. Radiolarians were collected from chert interlayered with basalt and gabbro in the lower thrust sheet of the ophiolite assemblage (fig. 17). Four of these collections were determined to be Late Mississippian and (or) Early Pennsylvanian, and one Late Triassic. These ages generally accord with the Mississippian to Triassic fossil ages previously reported from interlayered basalt, gabbro, and chert suites in ophiolite assemblages elsewhere around the borders of the Yukon-Koyukuk basin (Patton and others, 1977; Plafker and others, 1978).
3. Potassium-argon ages of 151 m.y. (Late Jurassic) and 269 m.y. (Permian) were measured on hornblende from hornblende pegmatite (sample 3, fig. 17, table 4) and hornblendite dikes (sample 5, fig. 17, table 4) cutting peridotite and layered gabbro in the upper thrust sheet of the ophiolite assemblage. The Jurassic age agrees with previously published potassium-argon ages on gabbro and hornblende-bearing dikes from ophiolite assemblages elsewhere around the Yukon-Koyukuk basin (Patton and others, 1977), but the Permian age is anomalous and cannot be reconciled with any previously reported ages. An age of 172 m.y. (Middle Jurassic) was measured on hornblende from garnet-bearing amphibolite (sample 4) collected near the base of the upper thrust sheet of the ophiolite. Ages of 155 and 161 m.y. were obtained previously on amphibolite associated with other ophiolite assemblages elsewhere along the southeast margin of the Yukon-Koyukuk basin (Patton and others, 1977).
4. A potassium-argon age of 112 m.y. (Early Cretaceous) was obtained on a biotite mineral separate (sample 6, table 4) from the granitic pluton in the southwestern the Kaiyuh Mountains (fig. 17). This age is of interest because it suggests that this pluton may represent the south end of the Melozitna pluton, offset approximately 160 km to the west along the Kaltag fault. The Melozitna pluton, north of and apparently cut off by the fault, has yielded a potassium-argon age of 111 m.y. and is compositionally similar to the Kaiyuh Mountains pluton (Patton and others, 1978; Chapman and Patton, 1978). Both plutons intrude lithologically similar metamorphic complexes. A previous estimate of 130 km of strike-slip movement along this segment of the Kaltag fault is based on right-lateral separation of the southeast margin of the Yukon-Koyukuk basin (Patton and Hoare, 1968). North of the fault, this margin lies along the Melozitna River valley a short distance west of the Melozitna pluton; south of the fault, it appears to lie between the Kaiyuh Mountains and the Yukon River.

REFERENCES CITED

Chapman, R. M., and Patton, W. W., Jr., 1978, Preliminary summary of the geology in the northwest part of the Ruby quadrangle, in Johnson, K. M., ed., The United States Geological Survey in Alaska: Accomplishments during 1977: U.S. Geological Survey Circular 772-B, p. B39-B41.

Dillon, J. T., Pessel, G. H., Chen, J. H., and Veach, N. C., 1980, Middle Paleozoic magnetism and orogenesis in the Brooks Range, Alaska: Geology, v. 8, no. 7, p. 338-343.

Patton, W. W., Jr., and Hoare, J. M., 1968, The Kaltag fault, west-central Alaska, in Geological Survey research 1968: U.S. Geological Survey Professional Paper 600-D, p. D147-D153.

Patton, W. W., Jr., Miller, T. P., Chapman, R. M., and Yeend, Warren, 1978, Geologic map of Melozitna quadrangle, Alaska: U.S. Geological Survey Miscellaneous Investigations Series Map I-1071, scale 1:250,000.

Patton, W. W., Jr., and Moll, E. J., 1981, Structural and stratigraphic sections along a transect between the Alaska Range and Norton Sound, in Coonrad, W. L., ed., The United States Geological Survey in Alaska: Accomplishments during 1980: U.S. Geological Survey Circular 844, p. 76-78.

Patton, W. W., Jr., Tailleur, I. L., Brosgé, W. P., and Lanphere, M. A., 1977, Preliminary report on the ophiolites of northern and western Alaska, in Coleman, R. G., and Irwin, W. P., eds., North American ophiolites: Oregon Department of Geology and Mineral Industries Bulletin 95, p. 51-58.

Plafker, George, Hudson, Travis, and Jones, D. L., 1978, Upper Triassic radiolarian chert from the Kobuk volcanic sequence in the southern Brooks Range, in Johnson, K. M., ed., The United States Geological Survey in Alaska: Accomplishments during 1977: U.S. Geological Survey Circular 772-B, p. B45-B47.

Turner, D. L., Forbes, R. B., and Dillon, J. T., 1979, K-Ar geochronology of the southwestern Brooks Range, Alaska: Canadian Journal of Earth Sciences, v. 16, no. 9, p. 1789-1804.

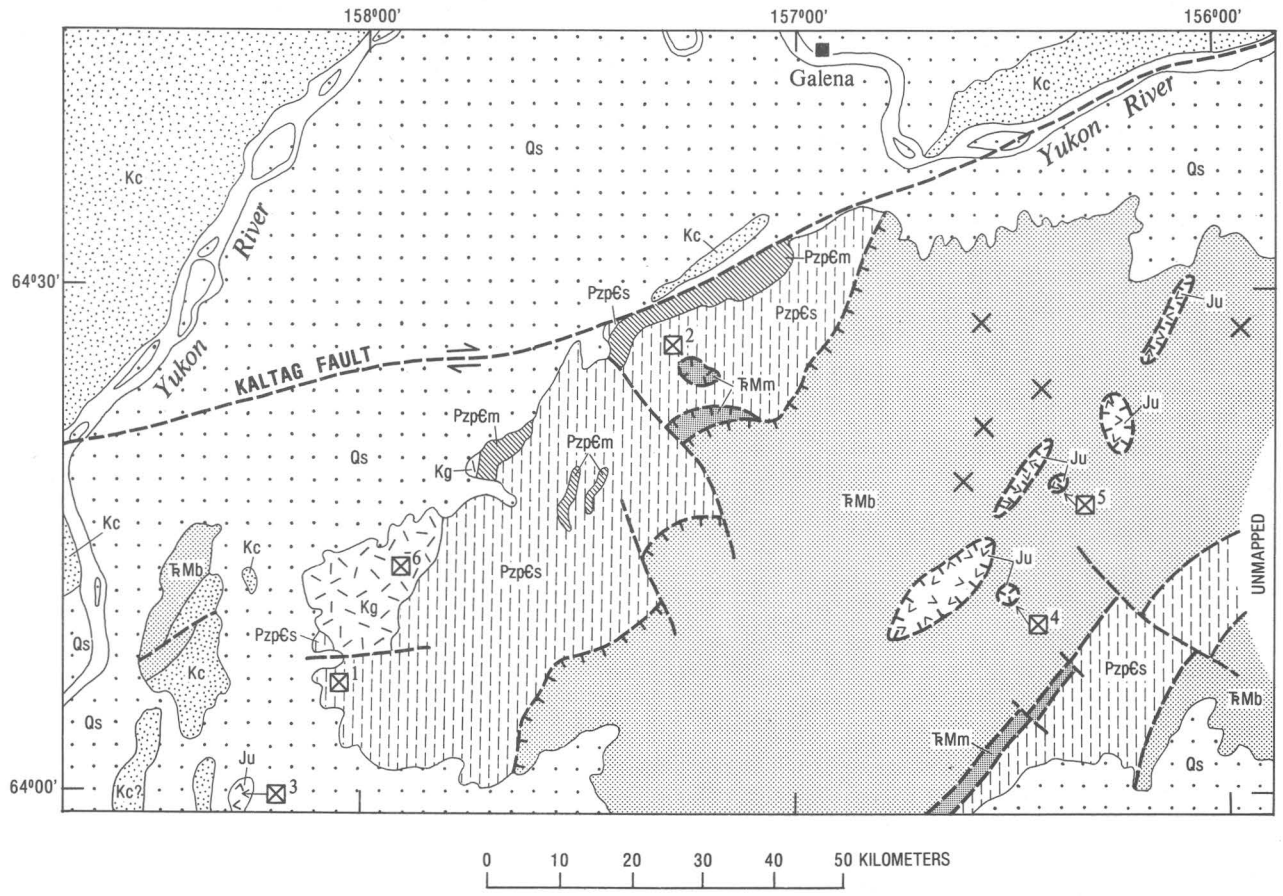

CORRELATION OF MAP UNITS

- Qs — QUATERNARY
- Kc, Kg — CRETACEOUS
- Ju — JURASSIC
- TrMb, TrMm — TRIASSIC TO MISSISSIPPIAN
- PzpЄm, PzpЄs — LOWER PALEOZOIC AND (OR) PRECAMBRIAN

DESCRIPTION OF MAP UNITS

Qs	SURFICIAL DEPOSITS (QUATERNARY)
Kc	CONGLOMERATE, SANDSTONE, AND SILTSTONE (CRETACEOUS)
Kg	GRANITIC ROCKS (CRETACEOUS)
Ju	ULTRAMAFIC ROCKS (JURASSIC)
TrMb	BASALT, GABBRO, AND CHERT (TRIASSIC TO MISSISSIPPIAN)
TrMm	METACHERT (TRIASSIC TO MISSISSIPPIAN)
PzpЄm	MARBLE (LOWER PALEOZOIC AND (OR) PRECAMBRIAN)
PzpЄs	SCHIST AND QUARTZITE (LOWER PALEOZOIC AND (OR) PRECAMBRIAN)

Contact, approximately located

Inferred high-angle fault

Inferred thrust fault; barbs on upper plate

Location of radiolarian collection

Location of potassium-argon age sample. Number refers to sample in table 4.

Figure 17.—Generalized geologic map of the Kaiyuh Mountains, showing potassium-argon-age sample localities and radiolarian-fossil localities.

Table 4.--Potassium-argon ages and analytical data for samples from the Kaiyuh Mountains

[Constants used in calculation of ages: $^{+}\lambda_{\varepsilon}=0.581\times10^{-10}$ yr^{-1}; $\lambda_{\beta}=4.962\times10^{-10}$ yr^{-1}; $^{40}K/K=1.167\times10^{-4}$ mol/mol. Limits of accuracy are estimates of analytical precision at the 68-percent-confidence level]

Map No. (fig. 17)	Field No.	Lat N., long W.	Mineral	Map unit	Mean K_2O (wt pct)	$^{40}Ar_{rad}$ (10^{10} mol/g)	$^{40}Ar_{rad}$ (percent)	Calculated age (m.y.)
1	79APa 551	64°08', 158°05'	Muscovite----	PzpCs	9.895±0.015	19.85	88.6	134±4.0
2	79APa 526	64°27', 157°18'	--do---------	PzpCs	8.805±0.015	17.96	90.9	136±4.1
3	79APa 552A	64°00', 158°16'	Hornblende---	Ju	.270±0.001	.6106	55.0	151±4.5
4	79APa 525A	64°12', 156°31'	--do---------	Ju	.120±0.001	.3111	29.0	172±5.2
5	79APa 521C	64°18', 156°23'	--do---------	Ju	.214±0.004	.8954	56.2	269±8
6	79APa 548	64°14', 157°56'	Biotite------	Kg	9.36±0.0	15.62	85.2	112±3.4

Trace-metal anomalies associated with silicification and argillic alteration in a rhyolite flow-dome complex in volcanic rocks of the Nowitna River area, Medfra quadrangle, Alaska

By Miles L. Silberman, Richard M. O'Leary, Leda Beth Gray, and William W. Patton, Jr.

Several small (less than 5 km^2 area) rhyolite flow-dome complexes of Late Cretaceous and (or) early Tertiary age intrude and overlie dominantly andesitic volcanic rocks of the Nowitna River area (area 4, fig. 13) in the northwestern part of the Medfra quadrangle (Patton and others, 1980). The rhyolitic rocks are exposed as flows and tuff within the more mafic volcanic rocks, and as domes consisting of platy rhyolite and tuff containing sparse quartz and partially altered feldspar crystals. The matrix consists of alkali feldspar and quartz (Moll and others, 1981). Alteration, quite common, consists largely of deposition of minor amounts of quartz in open spaces, oxidation of sulfides, devitrification of the matrix, and formation of spherulites. The most intense alteration observed is restricted to a small dome at the confluence of the Susulatna River and Sunrise Creek (sample traverse E, fig. 18), informally called Sunrise dome, which has a mineral assemblage dominated by quartz and kaolinite containing significant amounts of iron oxides, evidence of hydrothermal brecciation, and anomalous amounts of mercury, arsenic, and antimony.

PETROGRAPHY AND PHYSICAL CHARACTERISTICS

The rocks of Sunrise dome appear to consist of crystal-poor flow-banded rhyolite and tuff; the original textures are largely obscured by alteration. The rocks are mostly light tan, brown, or reddish, with mottled gray streaks from addition of fine-grained quartz veinlets and wisps. Hydrothermal brecciation is common, and the breccia fragments are largely angular, fractured, and surrounded by a matrix of iron oxide or iron-oxide-stained fine-grained to chalcedonic silica. Some areas have stockwork fractures coated with iron oxide, including hematite, and, locally, alined vugs are filled with botryoidal hematite. The rocks are fine grained and largely recrystallized. The most common mineral is quartz, present as fine-grained to very fine grained aggregates, patches, wispy veins, and vug and vesicle fillings. Original feldspars are, in most places, completely replaced by kaolinite, and patches of kaolinite occur in the recrystallized groundmass as well. No sulfides were seen in hand specimen or thin section, although heavy disseminations of limonite and hematite are common, as are the numerous thin fracture coatings and veinlets of iron oxides mentioned previously. The large amount of iron oxide (Fe content of samples ranges as high as 10-20 percent by spectrographic analyses) suggests the prior occurrence of sulfides in the rocks. A single sample (39, table 5) contained disseminated tourmaline and minor sericite as well as quartz and kaolinite.

The mineral assemblage of the rocks would be considered argillic, rather than advanced argillic, because of the absence of other minerals commonly found in advanced argillic suites, such as pyrophyllite, diaspore, alunite, etc. (Meyer and Hemley, 1967; Hudson, 1977). We suggest that the kaolinite formed late, probably by alteration of feldspars and the matrix that were not replaced by silica during early stages of alteration, as a response to acid-sulfate waters generated by the weathering of pyrite and other sulfides. This part of Alaska has been exposed to weathering for much of the Tertiary and has not been glaciated at the elevations of this occurrence. An alternative origin for the kaolinite could be solfataric alteration from

condensed oxidized H_2S-bearing vapors generated by boiling above a shallow water table. We believe that the absence of other advanced argillic minerals, however, favors a cool, supergene-type origin for the kaolinite.

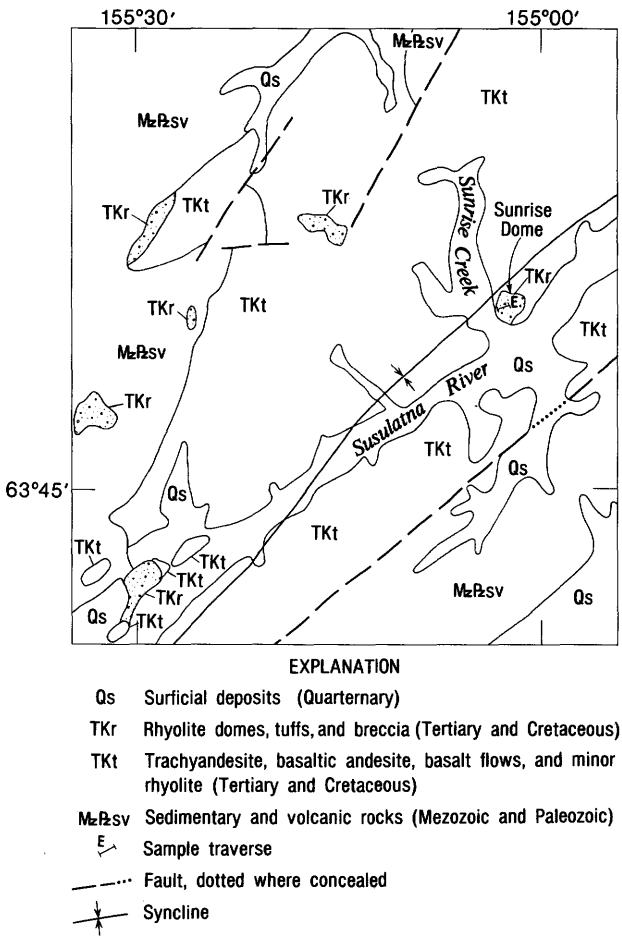

Figure 18.—Generalized geologic map of Sunrise dome area, Medfra quadrangle, west-central Alaska (modified from Patton and others, 1980).

GEOCHEMISTRY

Table 5 lists partial spectrographic and selected chemical analyses of the samples from Sunrise dome. In contrast to the generally low values of trace metals found in the partially altered and unaltered volcanic rocks of the Nowitna River area, the samples from the severely altered Sunrise dome (table 5) are strongly anomalous in Hg (avg 2.1 ppm), As (avg 57 ppm), and Sb (avg 21 ppm) relative to the crustal averages for felsic rocks (Parker, 1967). In the Sunrise dome samples, Au and Ag are below the limits of detectability for the analytical methods used (0.05 and 0.5 ppm, respectively), although these limits themselves are considerably higher than the crustal averages reported by Parker (1967). Two samples contain anomalous Zn, but Cu and Pb contents are quite low. Two other samples contain detectable Mo, but only at the 5-ppm level.

Table 5.--Selected trace-element geochemistry of altered rocks from Sunrise dome

[All values in parts per million. Au and Sb determined by atomic-absorption method, Hg by instrumental method, As and Zn by colorimetric method, and Ag, Cu, Mo, and Pb by semiquantitative spectrographic method. N, not detected at analytical limit (in parentheses); L, detected, but below analytical limit]

Sample	Au (0.05)	Hg (0.02)	As (10)	Sb (1)	Zn (5)	Ag (0.5)	Cu (5)	Mo (5)	Pb (10)
37	N	1.20	40	8	10	N	5	N	20
38	N	3.70	80	10	140	N	10	N	20
38A	N	.95	40	5	55	N	7	N	10
39	N	2.60	80	5	35	N	10	5	10
40	N	2.50	60	10	N	N	L	N	10
41	N	4.20	80	20	N	N	L	N	N
42	N	.80	20	4	N	N	5	N	L
43	N	1.45	20	130	N	N	L	N	N
43A	N	1.00	20	15	200	N	15	N	L
44	N	1.10	20	4	L	N	L	N	10
45	N	1.00	80	10	L	N	5	5	10
176	N	4.10	140	30	20	N	10	N	50
Average		2.1	57	21					

DISCUSSION

Considering the very limited geologic and geochemical work to date at Sunrise dome, we cannot state that this is a mineralized system, although it does satisfy four of the important criteria that have been identified as exploration guides for hot-spring precious-metal systems (M. L. Silberman, unpub. data, 1981): (1) Silicification—addition of chalcedonic silica in large amounts in the altered zones; (2) hydrothermal brecciation—indicative of repeated boiling episodes, which appear to be important in mineralizing processes (Buchanan, 1981); (3) anomalous contents of trace elements (As, Sb, Hg), which are commonly associated with thermal-spring systems and used as guides to these deposits (Radtke and others, 1980; M. L. Silberman, unpub. data, 1981); (4) argillic alteration, associated with partial silicification.

The argillic assemblage and partial silicification are typical of the upper zones of several hot-spring and stockwork gold deposits where they overlie densely silicified and mineralized rocks. At Cinola (Kimbach and others, 1981) and in other deposits of this type, Au and Ag contents are very low in the upper parts of the system. The apparent absence of silver at Sunrise dome might be explainable if the process of formation of kaolinite was as we have suggested. Silver could have been transported downwards by supergene solutions and enriched at depth, as occurred at Pueblo Viejo (Kessler and others, 1981). Gold, though generally less mobile than silver in an oxidizing environment, can and does migrate, particularly if it was deposited within sulfides or as very fine grained native gold (Boyle, 1979). It is equally likely, however, that gold was not present in significant amounts at this level of the system. Analytical techniques with lower limits of detectability, such as instrumental neutron-activation

analyses, might determine whether the Au and Ag contents of the oxidized zone are considerably above the crustal averages, which would indicate mineralization within the system. Such analyses have not yet been made.

SUMMARY

Several features characteristic of hot-spring and stockwork gold deposits occur at Sunrise dome in the Nowitna River area, including silicification, argillic alteration, hydrothermal brecciation, significant trace-metal anomalies in Hg, As, and Sb, and high concentration of iron oxides, probably from the weathering of sulfides (Berger and Tingley, 1980; Wallace, 1980; M. L. Silberman, unpub. data, 1981).

The geometry of the hydrothermal system is not known, although the features present suggest it to be very shallow. Although no detectable (at the limits of the analytical techniques used) gold or silver are present at the surface, it may be that supergene and (or) hypogene leaching has resulted in their enrichment at depth. It may also be that mineralization was limited to deeper parts of the system, possibly within a densely silicified and (or) stockwork zone, as is common in many deposits of the type described.

REFERENCES CITED

Berger, B. R., and Tingley, J. V., 1980, Geochemistry of the Round Mountain gold deposit, Nye Co., Nevada [abs.]: Society of Mining Engineers of AIME, Northern Nevada Section Precious Metals Symposium, Reno, Nev., Abstracts, p. 18c.

Boyle, R. W., 1979, The geochemistry of gold and its deposits: Geological Survey of Canada Bulletin 280, 584 p.

Buchanan, L. J., 1981, Precious metal deposits associated with volcanic environments in the southwest: Arizona Geological Society Digest, v. 14, p. 237-262.

Kessler, S. E., Russell, N., Seaword, M., Rivera, J., McCurdy, K., Cumming, G. L., and Sutter, J. F., 1981, Geology and geochemistry of sulfide mineralization underlying the Pueblo Viejo gold-silver deposit, Dominican Republic: Economic Geology, v. 76, no. 5, p. 1096-1117.

Kimbach, F. W., Cruzon, M. G., and Brooks, R. A., 1981, Geology of stockwork gold deposits as exemplified by the Cinola deposit: Denver, Colorado Mining Association, Mining Year Book 1981, p. 122-129.

Hudson, D. M., 1977, Geology and alteration of the Wedekind and part of the Peavine districts, Washoe County, Nevada: Reno, University of Nevada, M. Sc. thesis, 103 p.

Meyer, Charles, and Hemley, J. J., 1967, Wall rock alteration, in Barnes, H. L., ed., Geochemistry of hydrothermal ore deposits: New York, Holt, Rinehart and Winston, p. 167-235.

Parker, R. L., 1967, Composition of the Earth's crust, chap. D of Fleischer, Michael, ed., Data of geochemistry (6th ed.): U.S. Geological Survey Professional Paper 440-D, p. D1-D19.

Moll, E. J., Silberman, M. L., and Patton, W. W., Jr., 1981, Chemistry, mineralogy, and K-Ar ages of igneous and metamorphic rocks of the Medfra quadrangle, Alaska: U.S. Geological Survey Open-File Report 80-811-C, 19 p.

Patton, W. W., Jr., Moll, E. J., Dutro, J. T., Jr., Silberman, M. L., and Chapman, R. M., 1980, Preliminary geologic map of the Medfra quadrangle, Alaska: U.S. Geological Survey Open-File Report 80-811-A, scale 1:250,000.

Radtke, A. S., Rye, R. O., and Dickson, F. W., 1980, Geology and stable isotope studies of the Carlin gold deposit, Nevada: Economic Geology, v. 75, no. 5, p. 641-672.

Wallace, A. B., 1980, Geology of the Sulphur district, southwestern Humboldt County, Nevada: Society of Economic Geologists Field Conference, Reno, 1980, Road Log and Articles, p. 80-91.

SOUTHWESTERN ALASKA

(Figure 19 shows study areas discussed)

Newly recognized sedimentary environments in the Shelikof Formation, Alaska

By William H. Allaway, Jr., and John W. Miller

The Shelikof Formation was named by Capps (1922) for the rocks that form most of the bold headlands along the northwest shore of Shelikof Strait between Katmai Bay and the southwest end of Wide Bay. During summer 1981, a stratigraphic study of the Shelikof Formation was conducted as part of the Alaskan Mineral Resource Assessment Program (AMRAP), Ugashik and Karluk quadrangles. The areas investigated (area 1, fig. 19; fig. 20) included the peninsula between Puale and Alinchak Bays, an area near the head of Big Creek (north end of Wide Bay), and the ridge southwest of Alai Creek (south end of Wide Bay).

Environmental interpretations of the Shelikof Formation in the literature are few. On the basis of ammonite assemblages, Imlay (1953; oral communs., 1979, 1980) interpreted the Shelikof Formation to have been deposited on a steep slope fronting an open ocean. Burk (1965) suggested a deep neritic environment for the Shelikof. Other early workers (Capps, 1922; Martin, 1926; Smith, 1926; Kellum and others, 1945) reported marine molluscan fossils but otherwise made no environmental interpretations of the Shelikof. Recent work on radiolarians collected from a limestone lens in the middle of the Shelikof Formation at Puale Bay shows that this part of the section was deposited in a deep basinal environment (C. D. Blome, oral commun., 1981).

Our investigations indicate that the Shelikof Formation not only consists of marine facies but also is locally nonmarine (see stratigraphic section in fig. 21). The rocks in the lower part of the section at Puale Bay were almost entirely deposited in a fairly deep shelf submarine-fan environment. The sandstone units consist mainly of turbidites of facies B (Mutti and Ricci Lucci, 1972) and some of facies A and C; the interbedded siltstone is mainly of facies E and G. This sequence is interpreted to represent an inner-fan to mid-fan sequence. Although several thinning-upward cycles occur within the section, the overall trend is

thickening upward, and the thinning-upward cycles occur above the thickening-upward cycles. This relation suggests that the sea was regressing during that time and that the depositional cycles ended owing to channel migration. The upper part of the Shelikof Formation in this area varies considerably in composition. On the north shore of Puale Bay, turbidite facies are transitional to nearshore facies containing the bivalve Corbicula sp.; on the south side, turbidite deposition continued to the top of the formation. The contact with the overlying Naknek Formation in the Puale Bay area is Shelikof siltstone overlain by Naknek conglomerate.

The Shelikof Formation in the Big Creek area also suggests a regressive sequence. Here, the succession of environments is more complete. On the shore of Wide Bay between Des Moines and Big Creeks, a coarse channel conglomerate was reported (Capps, 1922; Kellum and others, 1945) at the base of the Shelikof. We interpret this conglomerate to be an inner-fan-channel deposit. The rocks at the base of the section thin upward to shelf siltstone. The section between the shore of Wide Bay and the head of Big Creek consists of shallow subneritic sandstone, interbedded with thick sections of siltstone that were probably deposited on a shelf below wave base. The upper 460 m of the Shelikof Formation at the head of Big Creek is transitional from nearshore marine sandstone to nonmarine deposits. The lower part consists of nearshore sandstone containing the pelecypods Corbicula sp. and Gryphaea sp.; these fossils suggest a brackish-water to very shallow marine environment. The upper part consists of magnetite-rich sandstone, with inclined laminations of granules and pebbles here interpreted to be beach deposits, overlain by carbonaceous shale and sandstone that locally contain preserved roots. The uppermost 60 m consists of massive channelized conglomerate, with lenses of carbonaceous shale and sandstone interpreted to be levee deposits preserved within it. We interpret this conglomerate and the associated finer grained rocks to be nonmarine deltaic or fluvial deposits. The entire section at the northeast end of Wide Bay is about 1,500 m thick.

The Shelikof Formation thins considerably to only 820 m at Alai Creek near the southwest end of Wide Bay. In this area, the base of the section consists

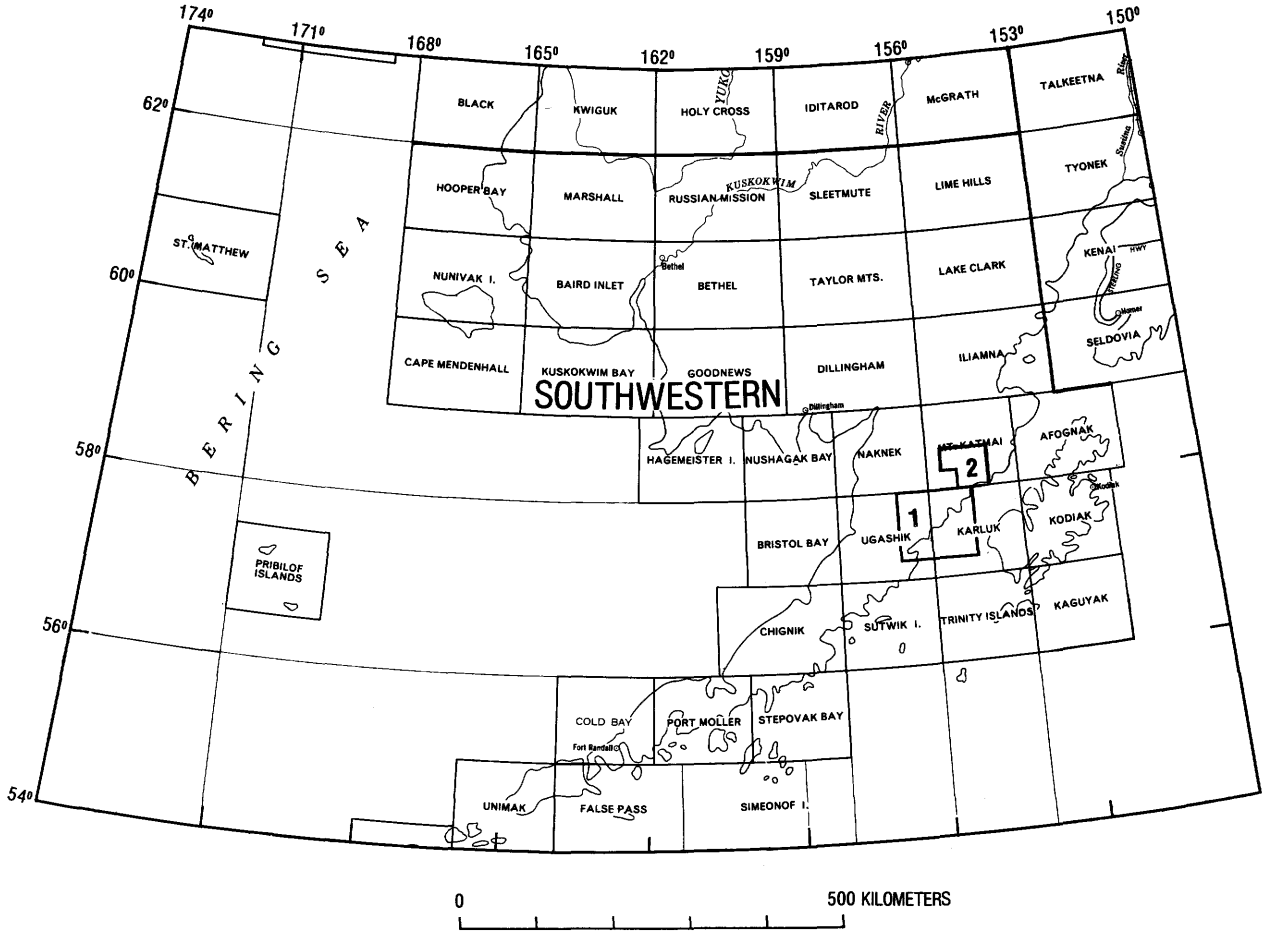

Figure 19.—Areas in southwestern Alaska discussed in this volume. A listing of authorship, applicable figures, and article paging (in parentheses) relating to the numbered areas follows. 1, Allaway and Miller, figures 20 and 21 (p. 34-37); 2, Hildreth and others, figure 22 (p. 37-39).

of shallow neritic sandstone containing Corbicula sp. and small ammonites identified by R. L. Detterman (oral commun., 1981) as Pseudocadoceras sp. Above this sandstone interval is approximately 460 m of massive laminated siltstone containing locally abundant limy concretions and a few pelecypods and small ammonites similar to those mentioned above, interbedded with a few thin sandstone beds, some of which show turbidite structures. We interpret this interval to represent a shelf environment well below wave base. The top of this interval is transitional to the overlying thin- to thick-bedded massive laminated and crosslaminated sandstone representing a nearshore facies. The sandstone, which consists of volcanic wacke and arenite containing a few limy concretions, sharply contacts the conglomerate at the top of the section, which is nonmarine, channeled, massive, and contains lenses of crossbedded and graded sandstone. This upper interval is about 60 m thick.

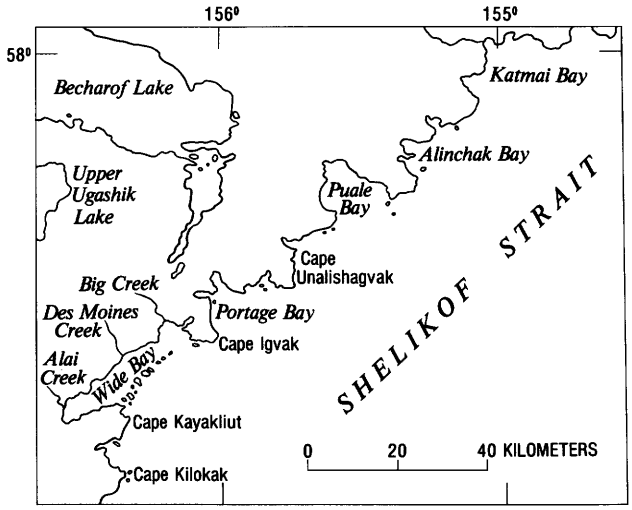

Figure 20.—Wide Bay-Puale Bay area on the Alaska Peninsula.

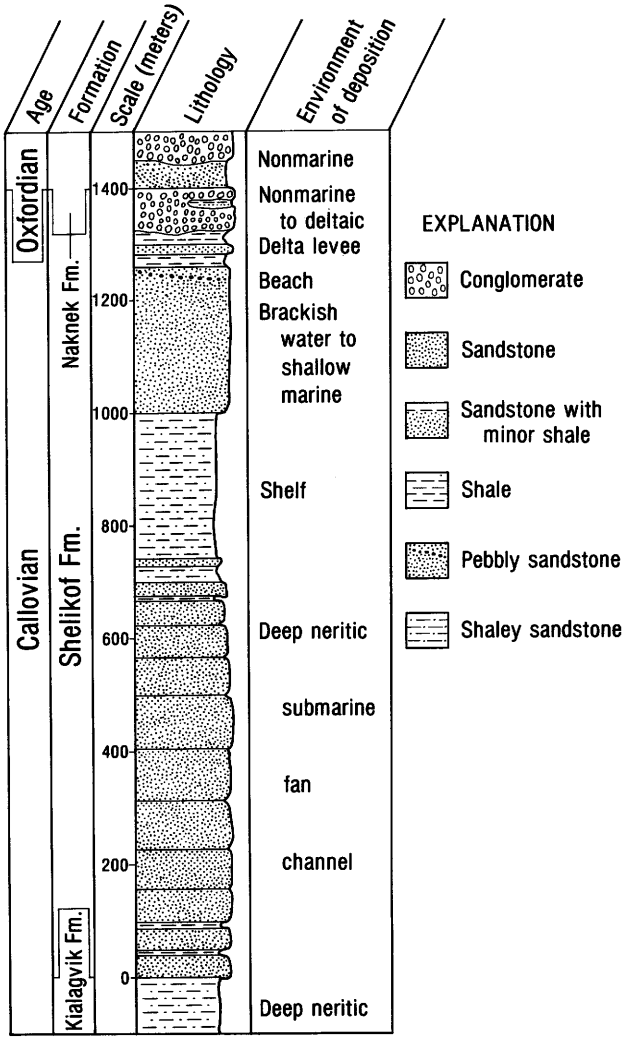

Figure 21.—Composite stratigraphic section of the Shelikof Formation, showing general lithology and environment of deposition.

In the Wide Bay area, the Shelikof Formation mainly contacts crossbedded and laminated arkosic sandstone of the overlying Naknek Formation. Locally, however, the Naknek conglomerate channels downward to the Shelikof conglomerate, and in these places the contact is transitional through about 8 m of conglomeratic section. The abundance of volcanic clasts gradually decreases, and that of granitic clasts gradually increases. This transitional contact, between two formations that generally sharply contact each other, is probably the result of reworking of the Shelikof conglomerate at the base of the Naknek.

In summary, fieldwork conducted in 1981 has shown that the Shelikof Formation consists of both nonmarine and marine facies. The overall trend in the outcrop area is from a deeper water facies near the base of the formation to a shallow-water or nonmarine facies at the top. At Puale Bay, the Shelikof Formation was deposited in a deeper water environment than at Wide Bay. This difference indicates that the paleoshoreline trended more northerly than the present axis of the Alaska Peninsula.

REFERENCES CITED

Burk, C. A., 1965, Geology of the Alaska Peninsula—island arc and continental margin: Geological Society of America Memoir 99, 250 p.

Capps, S. R., 1923, The Cold Bay district, in Mineral resources of Alaska: Report on progress of investigations in 1921: U.S. Geological Survey Bulletin 739, p. 77-116.

Imlay, R. W., 1953, Callovian (Jurassic) ammonites from the United States and Alaska. Part 2. Alaska Peninsula and Cook Inlet regions: U.S. Geological Survey Professional Paper 249-B, p. 41-108.

Kellum, L. B., Daviess, S. N., and Swinney, C. M., 1945, Geology and oil possibilities of the southwestern part of the Wide Bay anticline, Alaska: U.S. Geological Survey open-file report, 17 p.

Martin, G. C., 1926, The Mesozoic stratigraphy of Alaska: U.S. Geological Survey Bulletin 776, 493 p.

Mutti, Emiliano, and Ricci Lucci, Franco, 1972, Le torbidite dell'Appennino setentrionale introduzione all'analisi de facies: Societa Geologica Italiana Memoir, v. 11, p. 161-199 translated by Tor H. Nilsen, 1978, Turbidites of the northern Apennines: Introduction to facies analysis: American Geological Institute Reprint Series 3 (reprinted from International Geology Review, v. 20, no. 2, p. 125-166)

Smith, W. R., 1926, Geology and oil developments of the Cold Bay district, Alaska, in Mineral resources of Alaska: Report on progress of investigations in 1924: U.S. Geological Survey Bulletin 783, p. 63-88.

The 1912 eruption in the Valley of Ten Thousand Smokes, Katmai National Park: A summary of the stratigraphy and petrology of the ejecta

By Wes Hildreth, Judith E. Fierstein, Anita Grunder[1], and Larry Jager[2]

Our reexamination of the 20th century's most voluminous eruption, the 1912 outburst in the Valley of Ten Thousand Smokes (VTTS), was initiated primarily to provide modern petrochemical data on a strongly zoned calcic magmatic system; the splendid exposures soon stimulated a complementary study of the emplacement and welding of the tuff (area 2, fig. 19).

The approximately 15 km^3 of magma erupted from the Novarupta caldera at the head of the VTTS on June 6-8, 1912, generated about 20 km^3 of air-fall tephra and 11 to 15 km^3 of ash-flow tuff within 60 hours. Three discrete periods of ash fall recorded at Kodiak correlate with plinian tephra layers in the VTTS that were respectively designated A, C-D, and F-G by Curtis (1968). As much as 80 percent of the ash-flow volume was emplaced as a single flow unit, which divided into graded subunits only distally, where velocity gradients that developed in the halting flow promoted internal shear and segregation. This main flow unit is widely overlain by two to four smaller flow units of restricted areal extent, and these units are, in turn, capped by the stratified air fall, layers C through H.

The sequence of ash flows overlapped with but outlasted pumice fall A, and terminated within about 20 hours of the initial outbreak and before pumice fall C. Layer B is a composite veneer that is laterally equivalent to the ash flows, and layers E and H consist mostly of vitric dust that settled during lulls after each of the three plinian eruptive intervals. Truncation of Falling Mountain, a precaldera dacite dome adjacent to the 1912 vent, took place on the first day, because the inboard brow of its caldera-rim scarp lacks layer A and is mantled only by layer B and later tephra units. These units filled and obscured the caldera, but concentric and radial fissures outline a 6-km^2 depression. Subsequent growth of the Novarupta lava dome and its ejecta ring was complete when the VTTS was discovered in 1916 (Griggs, 1922).

At Mount Katmai, 10 km east of Novarupta, a second caldera (about 600 m deep and also about 6 km^2 in area) is thought to have collapsed during these events, apparently owing to some sort of hydraulic connection with the venting magmatic system. The floor of Katmai caldera is similar in elevation to the preeruptive 1912 vent. Observations by Griggs (1922) and Fenner (1923, 1930) on the behavior of beheaded glaciers, intracaldera fumaroles, and the caldera-lake level during 1916-23 support the inferred 1912 age of Katmai caldera. All known ejecta, however, appear to have vented at Novarupta. A 20-m-thick pumiceous debris-flow deposit at the southwest base of Mount Katmai (Fenner, 1950, pl. 1; Curtis, 1968, p. 201) resembles an ash-flow tuff but consists of tephra that remobilized down a single steep canyon—as shown by uncharred wood, the absence of degassing features, and a ratio of pumice-clast types unlike that of any 1912 ash flow but identical to that of the bulk pumice fall on Mount Katmai. An andesitic tuff just inside the northwest rim of Katmai caldera (Curtis, 1968, p. 204) is a poorly sorted fall unit of pre-1912 age, zoned from nonwelded material to a dense agglutinate. The "horseshoe island" on the Katmai caldera floor (Griggs, 1922; Fenner, 1930, 1950) was a severely eroded platy dacite lava that plots off the 1912 compositional trends (fig. 22) and may or may not have been erupted in 1912.

Mingling of three distinctive magmas, both as liquids and as chilled ejecta, took place during the eruption, although there is no approach to homogenization between sharply defined bands in the mixed ejecta. Pumice in the initial plinian fall is 100 percent rhyolite, but the later fall units (C-H) atop the ash-flow sheet are more than 98 percent light-grey dacite. Black andesitic scoria is common only late in the ash-flow sequence and in thin near-vent deposits interbedded with the dacite tephra layers, although traces of such scoria occur in most emplacement units. For the whole eruption, rhyolite:dacite:andesite proportions are 40:50:10. Banded pumice, less than 10 percent of all ejecta, consists of every combination but is predominantly rhyolite-andesite. Pumice counts at more than 150 localities show the first half of the ash-flow sequence to be 91 to 98 percent rhyolite; successive pulses were alternately enriched in either dacite or andesite, as rhyolite declined to less than 2 percent. The rhyolite-poor ash flows late in the sequence were less mobile and were progressively channeled by ongoing compaction. Novarupta dome, the final unit emplaced, consists of high-silica rhyolite contaminated by 1 to 2 percent of lithic debris and dacitic phenocrysts and by about 5 percent of well-defined bands of dacite.

After traveling about 16 km from the vent, the main ash flow was too deflated and sluggish to surmount a 20-m-high moraine perpendicular to its path. Parts of the flow penetrated gaps in the moraine, and

[1]Department of Geology, Stanford University, Stanford, CA 94305.
[2]Mill Valley, CA 94941.

one tongue continued 5 km downvalley, engulfing and charring trees but not toppling all of them.

At a point only 10 km from the vent, where the VTTS narrows slightly, the main ash flow formed primary depositional ridges that stand as much as 15 m above its otherwise smooth surface. In the same area, the moving flows left thin veneers of poorly sorted but fines-enriched tuff that feather up the valley walls to elevations 30 to 40 m higher than the general level of the adjacent valley-filling ash-flow sheet. In the upper VTTS, however, the "high sand mark" (Griggs, 1922; Fenner, 1923) is not a veneer but a marginal bench formed in thick tuff largely by differential compaction; the 30- to 60-m-elevation difference between the valley floor and the fissured hingeline of the bench suggests a thickness of 150 to 250 m for the tuff in the upper VTTS, in agreement with Curtis' (1968) estimate from comparative stream profiles.

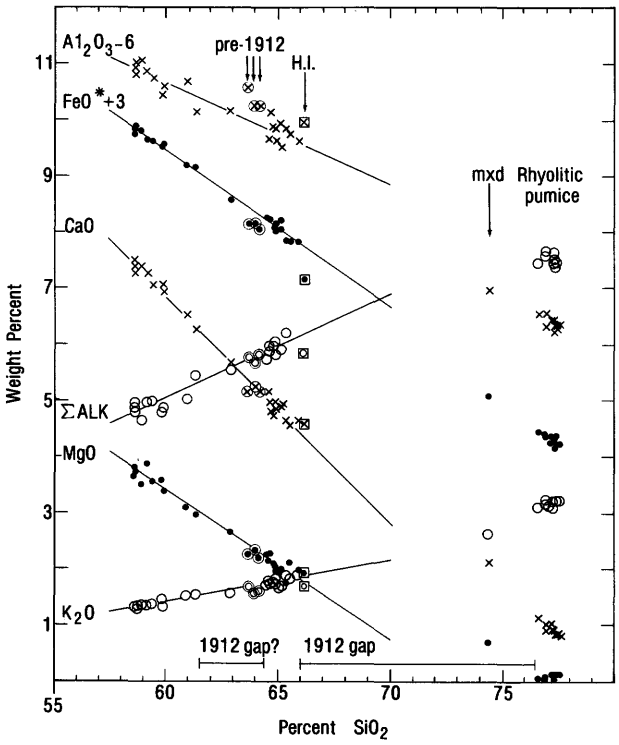

Figure 22.—Variations of major elements (in weight percent) for materials from the June 1912 eruption in the Valley of Ten Thousand Smokes (VTTS); new X-ray fluorescence analyses by U.S. Geological Survey laboratories, Menlo Park, Calif., and Denver, Colo. For internal comparability, all data are normalized to 100 percent, excluding H_2O and CO_2 but including halogens and 30 trace oxides. Pileup of points at 77.1 to 77.6 percent SiO_2 represents 11 analyses of rhyolitic pumice. Most samples are 1912 pumice and scoria from air-fall and ash-flow emplacement units, except: (1) mxd, Fenner's (1923) analysis of rhyolitic lava slightly contaminated by coeruptive dacite in the Novarupta dome—new analyses of least contaminated bands in the dome are plotted here at 65.1 and 76.9 percent SiO_2; and (2) H.I., Fenner's (1950) analysis of horseshoe-island lava on Katmai caldera floor. Pre-1912 points are for precaldera lava domes, Falling Mountain and Mount Cerberus, and a fluvially stratified deposit of pumice lapilli in lower VTTS, which plot, respectively, at 64.2, 64.0, and 63.7 percent SiO_2 and partly occupy a possible second compositional gap apparent in the 1912 zonation. Note that linear-regression lines fit 1912 andesite-dacite data rather well but do not project directly toward rhyolite data arrays.

In the lower VTTS, the distally thinning rhyolite-rich tuff is wholly nonwelded, and its base is widely exposed. In the central VTTS, gorges floored in partially welded tuff have reached a maximum measured depth of 33 m; some of these gorges had been incised to more than 20 m within 5 years after the eruption (Griggs, 1922). In the upper VTTS, high-temperature andesite-rich flow units that were emplaced late in the ash-flow sequence created partially welded tuff and sillar that are widely exposed.

Debris flows of remobilized rhyolitic tephra locally swept onto the ash-flow surface from surrounding mountainsides before the emplacement of dacitic fall units C through H. Flooding from the adjacent glaciers locally created a few meters of fluvial deposits, but within several hours such runoff was suppressed and overwhelmed by the heavy fallout of dacitic pumice. After the dacitic eruptions, phreatic explosions in the ash-flow sheet created dozens of craters, the fringing surge deposits of which contain ejected blocks of tuff more densely welded than any part of the primary material yet exposed. Deposits from one cluster of craters dammed a 1-km-long lake in upper Knife Creek, where more than 15 m of pumiceous diamicton and mud accumulated atop the tuff. Breaching of this lake caused a catastrophic flood that stripped the ash-flow surface in the central VTTS, deposited a sheet of distinctive debris as much as 50 m higher than the ash-flow surface on the banks of lower Windy Creek, and carried 50-cm blocks of welded tuff more than 20 km to the lowermost VTTS, where the flood deposit is as much as 6 m thick. All these events took place before the incision of gorges in the tuff, presumably in the summer of 1912.

Phenocryst contents (by weight) of the ejecta are: rhyolite 0.5 to 2 percent, and dacite and andesite, 30 to 40 percent. All the ejecta contain plagioclase, hypersthene, titanomagnetite, ilmenite, apatite, and pyrrhotite; a trace of olivine (Fo_{75-79}) occurs in the scoria. Quartz is present and augite absent only in the rhyolite. The zoning ranges of rhyolitic plagioclase (An_{25-28}) and orthopyroxene (En_{49-51}) do not overlap those of dacitic phenocrysts (An_{34-71}, En_{59-67}). The quartz-free dacitic magma is clearly not a product of direct mixing between the rhyolitic and andesitic magmas.

Chemical analyses (fig. 22) show the SiO_2 contents (anhydrous) to be: rhyolite, 77.0±.6 percent, dacite, 64.5 to 66 percent, and andesite, 58.5 to 61.5 percent. The dacitic and andesitic ejecta contrast in color and density, and it remains uncertain whether they form a compositional continuum; so far, only one

1912 sample (a medium-grey pumice block in the topmost ash-flow unit) falls in the range 61.5 to 64.5 percent SiO_2 (fig. 22), despite concerted search for such material. Analyses reported by Fenner (1923, 1950) within the range 66 to 76 percent SiO_2 were of mixed lava and of bulk tephra that mechanically fractionated and (or) mixed during emplacement. Ample data confirm the large compositional gap between the rhyolitic and intermediate magmas. The selected compositional parameters listed below illustrate the contrast between the rhyolitic and intermediate ejecta erupted in 1912:

	Rhyolite	Dacite-andesite
CaO (wt pct)——	0.84-0.96	4.6-7.4
K_2O (wt pct)——	3.1-3.3	1.3-1.9
Fe/Mg————	>15	2.2-3.4
K/Na————	.82-0.87	.40-0.53
Rb/Sr————	1.2-1.5	.06-0.13
V/Ni————	<1	5-10
Ba/Sr————	18-25	1.6-2.7
Eu/Eu^*————	.5-0.6	.8-1.15
Zn/Cu————	5.0-8.5	1.5-3.3
Ba (ppm)———	950-1,025	400-600

Despite this compositional gap, 80 titanomagnetite-ilmenite temperatures (Buddington and Lindsley, 1964; Carmichael, 1967) show a continuous range: rhyolite, 805°-850°; dacite, 855°-955°; and andesite, 955°-990°C. ^{18}O fractionations of 3.9 to 4.2 permil between quartz and titanomagnetite support these values, as do measurements of the homogenization temperatures of vapor-glass inclusions in 1912 quartz phenocrysts by Clocchiatti (1972). Continuity in T and f_{O_2} for the entire sequence, and continuous variation in phenocrystic compositions in the crystal-rich andesitic and dacitic magmas, support the concept of a single zoned system; as does the similarity of all the 1912 ejecta in $^{87}Sr/^{86}Sr$ ratio (0.7036), K/Ba ratio (about 25), Ce/Yb ratio (about 9), La/Sm ratio (about 3), Th/U ratio (2.2), and $\delta^{18}O_{plag}$ (6.1-6.4 permil in rhyolite, 5.8-6.1 permil in dacite and andesite).

If the rhyolitic liquid separated from dacitic magma, extraction was so efficient that no dacitic phenocrysts were retained and no 66- to 76-percent-SiO_2 compositions were created; if the liquid were a partial meltof roof rocks atop an intermediate magma body, then such rocks had no Sr-isotopic contrast with the andesitic-dacitic magma and clearly did not include the Jurassic arkosic or granitic basement. The presence of Holocene domes of pre-1912 dacite (Falling Mountain and Mount Cerberus, fig. 22) adjacent to the 1912 vent suggests that the 6 km^3 (or more) of high-silica rhyolitic magma (a composition rare in the Aleutian arc) was generated within a few thousand years. The 1912 vent is semiencircled by a cluster of andesitic stratocones and is as close to Mageik, Trident, and Griggs volcanoes as it is to Mount Katmai. Although Quaternary basalt is not known to have erupted here, the intrusion of basaltic magma probably sustains the greater-VTTS magmatic system (see Hildreth, 1981, fig. 15).

Acknowledgments.—We are grateful to Dan Kosco, Terry E. C. Keith, Peter Shearer, and the late David A. Johnston for collaboration, debate, and hauling rocks; and to I. S. E. Carmichael for microprobe facilities and 1976 field expenses under National Science Foundation Grants EAR-74-12782 and EAR-78-03648.

REFERENCES CITED

Buddington, A. F., and Lindsley, D. H., 1964, Iron-titanium oxide minerals and synthetic equivalents: Journal of Petrology, v. 5, no. 2, p. 310-357.

Carmichael, I. S. E., 1967, The iron-titanium oxides of salic volcanic rocks and their associated ferromagnesian silicates: Contributions to Mineralogy and Petrology, v. 14, no. 1, p. 36-64.

Clocchiatti, R., 1972, Les cristaux de quartz des ponces de la Vallée des Dix Milles Fumées (Katmai, Alaska) [Quartz crystals from pumice of the Valley of Ten Thousand Smokes (Katmai, Alaska)]: Paris, Comptes Rendus Hebdomadaires des Séances de l'Académie des Sciences, ser. D, v. 274, no. 23, p. 3037-3040.

Curtis, G. H., 1968, The stratigraphy of the ejecta from the 1912 eruption of Mount Katmai and Novarupta, Alaska, in Studies in volcanology: A memoir in honor of Howel Williams: Geological Society of America Memoir 116, p. 153-210.

Fenner, C. N., 1923, The origin and mode of emplacement of the great tuff deposit in the Valley of Ten Thousand Smokes: Washington, National Geographic Society Contributed Technical Papers, Katmai Series, no. 1, 74 p.

——1930, Mt. Katmai and Mt. Mageik: Zeitschrift für Vulkanologie, v. 13, no. 1, p. 1-24.

——1950, The chemical kinetics of the Katmai eruption: American Journal of Science, v. 248, no. 9, p. 593-627 (pt. 1); no. 10, p. 697-725 (pt. 2).

Griggs, R. F., 1922, The Valley of Ten Thousand Smokes: Washington, National Geographic Society, 341 p.

Hildreth, Wes, 1981, Gradients in silicic magma chambers: Implications for lithospheric magmatism: Journal of Geophysical Research, v. 86, no. B11, p. 10153-10192.

EAST-CENTRAL ALASKA

(Figure 23 shows study areas discussed)

New ages of radiolarian chert from the Rampart district, east-central Alaska

By David L. Jones, Norman J. Silberling, Robert M. Chapman, and Peter Coney

Reconnaissance geologic studies in 1981 north and south of the Yukon River in the Rampart district

(Tanana and Livengood quadrangles; area 10, fig. 23) resulted in collections of radiolarian chert from several different terranes (fig. 24). Because the rocks in the Rampart district are poorly fossiliferous and structurally complex, little is presently known concerning the stratigraphic relations or ages of the

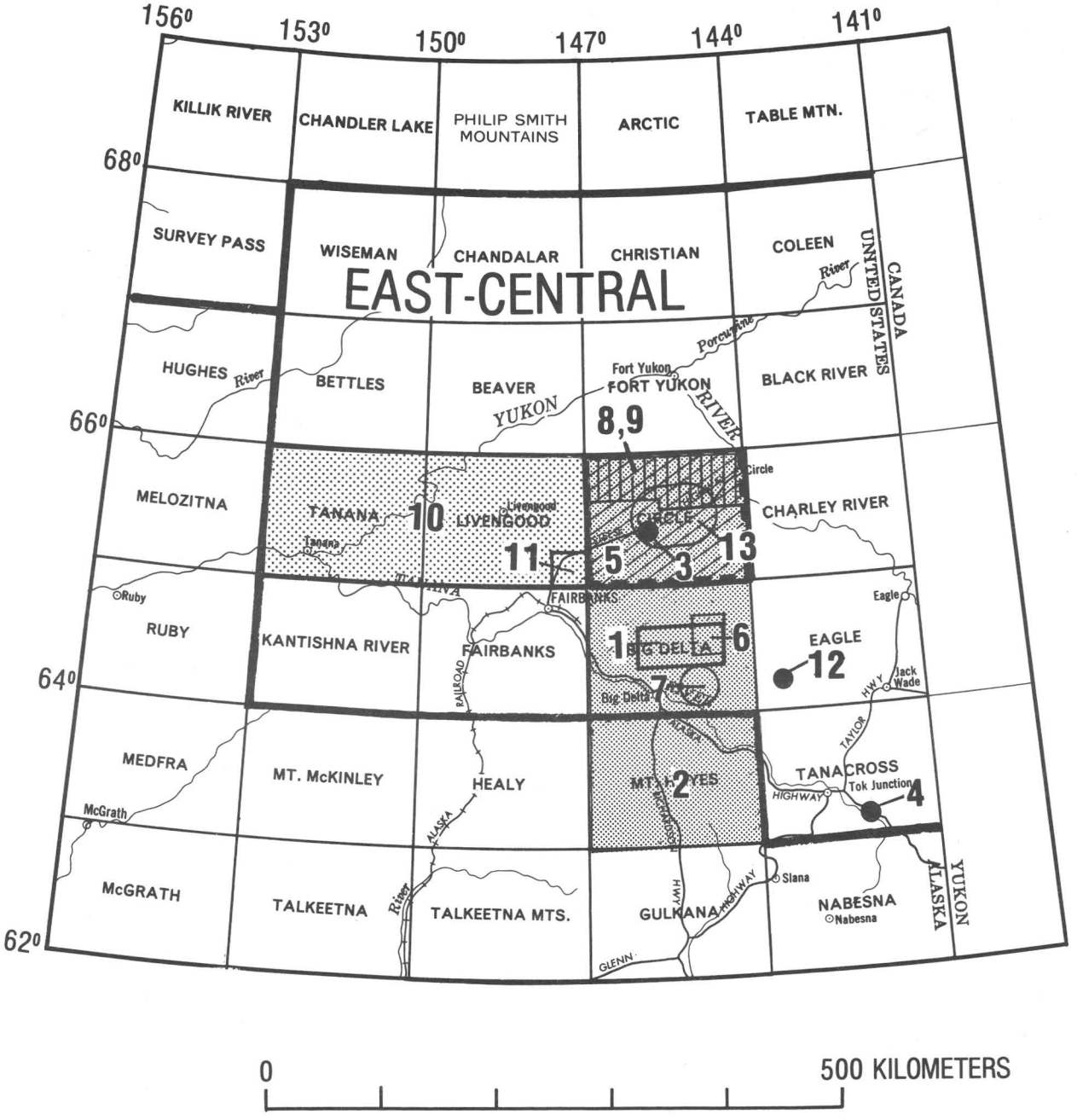

Figure 23.—Areas and localities in east-central Alaska discussed in this volume. A listing of authorship, applicable figures and tables, and article pagination (in parentheses) relating to the numbered areas follows. 1, Aleinikoff, Dusel-Bacon, and Foster, figure 27, tables 8 and 9 (p. 45-48); 2, Aleinikoff, Foster, and others, figures 25 and 26, table 7 (p. 43-45); 3, Burack and others, figure 32, table 12 (p. 54-57); 4, Carter and Galloway, figure 41 (p. 66-68); 5, Cushing and Foster, figures 39 and 40 (p. 64-65); 6, Dusel-Bacon and Bacon, figures 28 and 29 (p. 48-50); 7, Dusel-Bacon, figures 30 and 31, tables 10 and 11 (p. 50-54); 8, Foster, Cushing, and others, figure 38 (p. 62-64); 9, Foster, Weber, and Dutro, figures 36 and 37 (p. 60-62); 10, Jones and others, figure 24, table 6 (p. 39-43); 11, Laird and others, figures 33 through 35, table 13 (p. 57-60); 12, Weber and Ager, figures 42 and 43 (p. 68-70); 13, Yeend (p. 65-66).

various lithologic units present. Thus, ages derived from dating of radiolarian chert provide important new information necessary for correlating these rocks with nearby, better dated sections.

RAMPART GROUP

According to Mertie (1937), the Rampart Group consists of basaltic to andesitic flows; basaltic, andesitic, and rhyolitic tuff and breccia; and lesser amounts of interbedded chert, shale, argillite, and limestone. No type section has been established and the stratigraphic and structural relations of these heterogeneous rock types remain unclear. Certainly, some rocks, such as the rhyolite tuff and breccia exposed southwest of Rampart, should be excluded from the group because they appear to be Cenozoic and to overlie unconformably the more complexly deformed older rocks.

Only two fossil localities, both near Point No Point on the Yukon River, were known previously from the Rampart Group. The fossils consist mainly of bryozoans occurring as clasts in overturned prismatic limestone. According to Brosgé and others (1969), these bryozoans are probably Permian, and the pelecypod prisms may belong to the Permian bivalve genus Atomodesma. These fossils have served to assign a probable Permian age to the entire Rampart Group. Mafic intrusive rocks that cut the limestone-bearing bedded sedimentary and volcanic sequence described by Brosgé and others (1969) yield a Late Triassic or earliest Jurassic (210±6 m.y.) potassium-argon age.

Exposures of the Rampart Group both north and south of the Yukon River and west of Point No Point consist mainly of thin septa of red chert and argillite, maroon and green tuff, and minor volcanic graywacke, intruded by enormous volumes of mafic intrusive rocks, primarily diabase and gabbro but also including

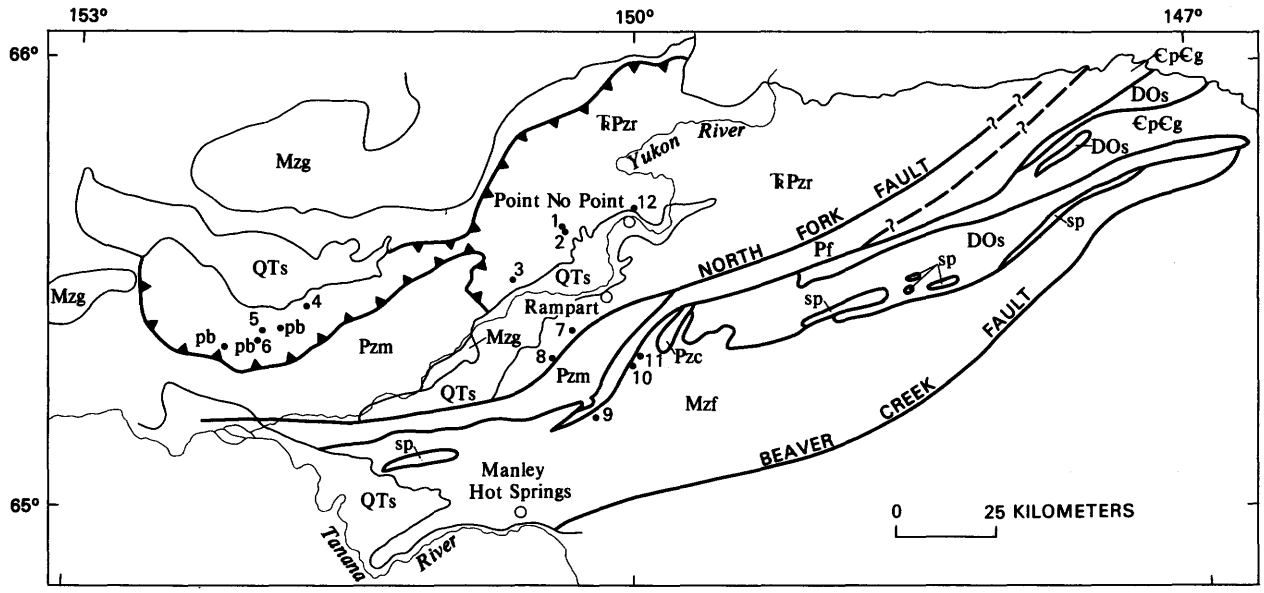

EXPLANATION

QTs	SEDIMENTARY DEPOSITS (QUATERNARY AND TERTIARY)
Mzg	GRANITIC ROCKS (MESOZOIC)—Mainly Cretaceous in age
Mzf	FLYSCH DEPOSITS AND QUARTZITE (MESOZOIC)
Pf	FLYSCH DEPOSITS (PERMIAN)
TrPzr	RAMPART GROUP, MAFIC INTRUSIVE ROCKS, AND BASALT (TRIASSIC? AND PALEOZOIC)
DOs	SEDIMENTARY AND MINOR VOLCANIC ROCKS (DEVONIAN TO ORDOVICIAN)
Pzm	METASEDIMENTARY ROCKS (LOWER? PALEOZOIC)—May include some Precambrian metasedimentary rocks
Pzc	CHERT, ARGILLITE, AND GABBRO (PALEOZOIC?)
€pEg	GRIT, QUARTZITE, AND SLATE (CAMBRIAN AND PRECAMBRIAN?)
sp	SERPENTINITE

Contact

Fault

Thrust fault—Sawteeth on upper plate

• 3 Radiolarian chert sample locality and number (see Table 6)

•pb Pillow basalt

Figure 24.—Geologic map of the Rampart district, east-central Alaska, showing locations of dated radiolarian-chert samples. Modified from Eberlein and others (1977).

massive basalt and minor ultramafic rocks. The ultramafic rocks are an olivine and clinopyroxene-rich differentiate of gabbro. Possibly as much as 80 to 90 percent of the exposed rock is igneous, and so the amount of sedimentary rock present in the Rampart Group is very small. Pillow basalt in the Rampart Group is also rare, although well-developed pillows were observed at several places (pb, fig. 24). The relations of the basalt to nearby red argillite and chert could not be established.

The Rampart Group, including the voluminous mafic intrusive rocks, structurally overlies undated mica schist, marble, and metachert of the Ruby terrane, as suggested by Patton and others (1977). The contact between these two assemblages is interpreted as a nearly flat fault, marked by an extensive zone of mylonite, above which the lower part of the Rampart Group is intensely sheared and disrupted. None of the mafic intrusive rocks that cut the Rampart Group occur in the metamorphic rocks of the Ruby terrane beneath this basal fault, and so faulting clearly postdates intrusion of the mafic rocks.

Chert sampled from the Rampart Group occurs in three lithic associations (fig. 24; table 6): (1) Red and black chert and red argillite without volcaniclastic rocks, in which the chert is Late Mississippian to Early Pennsylvanian(?) (locs. 2, 4, 5, 6, fig. 24); (2) red chert, red argillite, and green to gray tuff and volcaniclastic graywacke, in which the chert is Pennsylvanian(?) to Permian (fig. 24, locs. 1, 3, 7); and (3) fine-grained graywacke, argillite, and minor chert, undated (fig. 24, loc. 8).

In addition to these occurrences, loose blocks of red and green chert, as much as 0.5 m long, occur along the north bank of the Yukon River near Point No Point (loc. 12, fig. 24); these blocks contain well-preserved Late Triassic radiolarians. The source of the blocks has not yet been determined.

MESOZOIC FLYSCH BELT

A complexly deformed assemblage of graywacke, quartzite, argillite, and minor conglomerate forms an extensive belt trending more than 200 km northeast from the Tanana River (fig. 24). Although late Mesozoic fossils have long been known from this belt near Quail Creek in the Rampart district, radiolarian chert had not previously been reported from these predominantly clastic rocks. During our reconnaissance studies, two exposures of radiolarian chert of Late Triassic age were discovered. Locality 10 (fig. 24) consists of several tens of meters of black chert interbedded(?) with black siltstone and graywacke, and locality 11 (fig. 24) is a small rubbly exposure of chert in a fault zone separating vitreous quartzite from graywacke. In addition, chert clasts in conglomerate at locality 9 (fig. 24) yielded Late Triassic radiolarians.

CONCLUSIONS

Sedimentary rocks of the Rampart Group are dominantly deep water chert, argillite, andesitic volcaniclastic rocks, and very minor tuffaceous bioclastic limestone. Dated rocks range in age from Late Mississippian to Permian, and float blocks suggest the presence of Upper Triassic strata. The volcaniclastic rocks appear to be mainly Permian. All these sedimentary rocks are intruded by large sill-like bodies of mafic igneous rock, apparently largely sills, of probable latest Triassic age that may be feeders to scarce pillow flows. None of these rocks appears to be genetically related to ophiolite, and the presence of oceanic crust within the Rampart Group in the Rampart district is unsubstantiated. The Rampart Group structurally overlies metamorphosed sedimentary and igneous rocks of the Ruby terrane along a major thrust

Table 6.--Ages of radiolarians from chert localities in the Rampart district

Chert locality (fig. 24)	Field No.	Age	Remarks
4	81-JTN-37	Late Mississippian to Lower Pennsylvanian.	Rampart Group (nonvolcanic assemblage).
6	81-JTN-40	do.	
2	81-Ach-5A	do.	
5	79-Ach-89	do.	
7	81-JTN-3	Pennsylvanian to Permian---	Rampart Group (volcaniclastic assemblage).
1	81-JTN-23	do.	
1	81-JTN-24	Permian	
1	81-JTN-25	do.	
3	81-JTN-27	do.	
8	81-JTN-13	Unknown----------	Rampart Group (graywacke-argillite assemblage).
12	81-JTN-10	Late Triassic----------	Float, presumably from the Rampart Group but source unknown.
10	81-JTN-18	Late Triassic----------	Mesozoic flysch belt (clasts in conglomerate).
11	81-JTN-19	do.	
9	81-JTN-26	do.	

fault, and its depositional basement is absent. Radiolarian chert, structurally associated with graywacke and argillite of the Mesozoic flysch belt south of Rampart, is Triassic; its presence may indicate that clastic sedimentation within this belt commenced much earlier than hitherto suspected, although definite depositional relations of the chert and clastic rocks are not yet proved.

REFERENCES CITED

Brosgé, W. P., Lanphere, M. A., Reiser, H. N., and Chapman, R. M., 1969, Probable Permian age of the Rampart group, central Alaska: U.S. Geological Survey Bulletin 1294-B, p. B1-B18.

Eberlein, G. D., Gassaway, J. S., and Beikman, H. M., compilers, 1977, Preliminary geologic map of central Alaska: U.S. Geological Survey Open-File Report 77-168-A, scale 1:1,000,000.

Mertie, J. B., Jr., 1937, The Yukon-Tanana region, Alaska: U.S. Geological Survey Bulletin 872, 276 p.

Patton, W. W., Jr., Tailleur, I. L., Brosgé, W. P., and Lanphere, M. A., 1977, Preliminary report on the ophiolites of northern and western Alaska, in Coleman, R. G., and Irwin, W. P., eds., North American ophiolites: Oregon Department of Geology and Mineral Industries Bulletin 95, p. 51-57.

Isotopic evidence from detrital zircons for Early Proterozoic crustal material, east-central Alaska

By **John N. Aleinikoff, Helen L. Foster, Warren J. Nokleberg, and Cynthia Dusel-Bacon**

The ages of metamorphic rocks in east-central Alaska, especially in the Yukon-Tanana Upland, have been the subject of much conjecture for many years. Mertie (1937) concluded, on the basis of now-disproven stratigraphic relations, that all the crystalline schist with sedimentary protoliths (Birch Creek Schist of former usage) is Precambrian. Although the sedimentary history of those rocks has yet to be completely deciphered, there has been some progress both in determining the age of the parent material (provenance) and in bracketing the subsequent age(s) of metamorphism. This study (area 2, fig. 23) reports new isotopic analyses of detrital zircons that show evidence for Early Proterozoic sources of the sediment composing rocks in and adjacent to the Upland.

Zircons were extracted from four distinct quartzite units in three quadrangles, the Circle, Big Delta and Mount Hayes (fig. 25), encompassing an area of about 18,500 km^2, or approximately a fourth of the total area of the Upland. The zircon separates contain rounded, pitted, and frosted grains that are unequivocally detrital. Within each separate are several distinct populations, distinguishable primarily by color and shape. Because sedimentary rocks commonly are composed of material derived from several sources, it is likely that these separates contain zircons of different ages. We have endeavored to obtain, by careful handpicking, small samples (less than 5 mg) that probably are composed of zircons from a single source and thus, within each group, are of the same age.

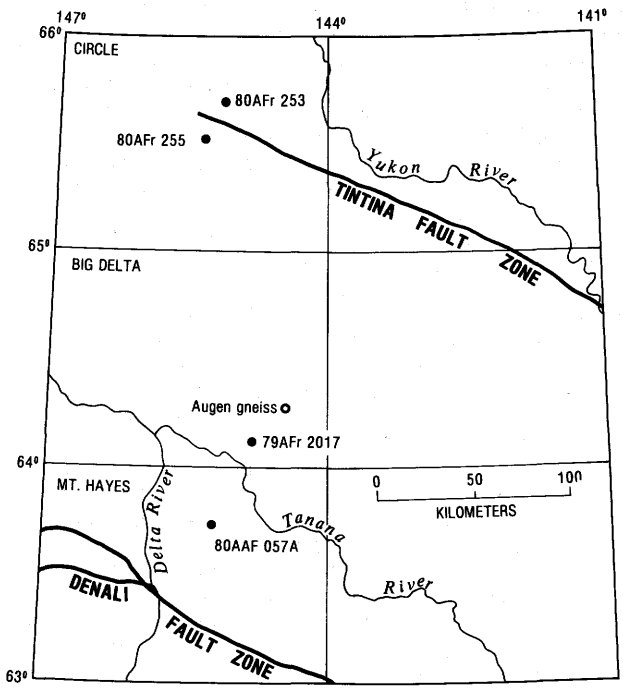

Figure 25.—Sketch map showing sample localities and numbers in the Circle, Big Delta, and Mount Hayes quadrangles, Alaska. Table 7 lists sample data.

Sample 80AFr 253 (table 7) is a weakly foliated grit characterized by rounded silt- to sand-size quartz grains in a sericitic matrix. Rocks of this type are found in the eastern and western Crazy Mountains and in the northwestern part of the Circle quadrangle on both sides of the Tintina fault zone, where they are interbedded locally with green and maroon argillite; the grit is tentatively considered to be Cambrian(?) because of the occurrence of the trace fossil Oldhamia (Churkin and Brabb, 1965). Sample 80AFr 255, from a strongly foliated quartzite and schist unit, is composed of fine-grained quartz, minor biotite, and muscovite containing scattered large (2-5 mm) gray, blue, and white quartz grains. This quartzitic unit, which ranges from greenschist- to epidote-amphibolite facies, is extensive in the central part of the Circle quadrangle south of the Tintina fault zone. Although these rocks could be higher grade equivalents of grits similar to sample 80AFr 253, the foliated quartzites have a more complex deformational and metamorphic history than the grit. Sample 79AFr 2017, from the southeastern part of the Big Delta quadrangle, is a foliated gray quartzite interbedded with quartz-mica schist and containing minor muscovite, biotite, and garnet. This rock tentatively has been interpreted as a wallrock for a large orthoaugen gneiss body of Early Mississippian (350 m.y.) age (Aleinikoff and others, 1981). Sample 80AAF 057A is a well-foliated pinkish quartzite containing minor muscovite and garnet, collected in the central part of the Mount Hayes quadrangle north of the Hines Creek strand of the Denali fault.

Within the largest size fraction of three of the samples (80AFr 255 excepted), two zircon populations

were analyzed for uranium and lead isotopes. In sample 80AFr 253, red and gray zircons were hand-picked from the (+150) size fraction. In sample 79AFr 2017, the two selected populations from the (+100) size fraction consisted of clear round zircons and black oblong zircons. Four splits were analyzed from sample 80AAF 057A, including clear round and dark oblong zircons from the (+100) size fraction, and clear round grains from the (-100+150) size fraction and the entire nonmagnetic portion (mostly clear) of the (-325) size fraction. Only pink round zircons were analyzed from sample 80AFr 255. All the samples from which dark (or gray) zircons were analyzed contained 8 to 10 times more uranium than the clear (or red) zircons. Directly correlative with this relatively high uranium concentration is the degree of discordance. As listed in table 7, the dark zircons have considerably younger lead-uranium ages than their clear counterparts. These data were not used in the best-fit line calculation (fig. 26) because they clearly show, by plotting far off the discordia, disturbance of their uranium-lead systematics sometime during the past 350 m.y.

In sharp contrast, the clear (and red) zircons form a linear array between about 350 and 2,250 m.y. (fig. 26). There is some scatter in the data, outside of analytical error, that may be due to lead loss during the early Paleozoic (during sedimentation), lead losses during the Cretaceous and (or) Tertiary (due to thermotectonic events), modern lead loss through dilatancy (Goldich and Mudrey, 1972), or different ages of the provenances. A best-fit line with 95-percent-confidence limits (Ludwig, 1980) was calculated through six nondark splits from the four detrital samples (table 7), plus five points from an orthoaugen gneiss (Aleinikoff and others, 1981). We chose to use the augen gneiss data because previous research has indicated that some of the zircons from this meta-igneous rock contain a large component of inherited radiogenic lead from an approximately 2,300-m.y.-old

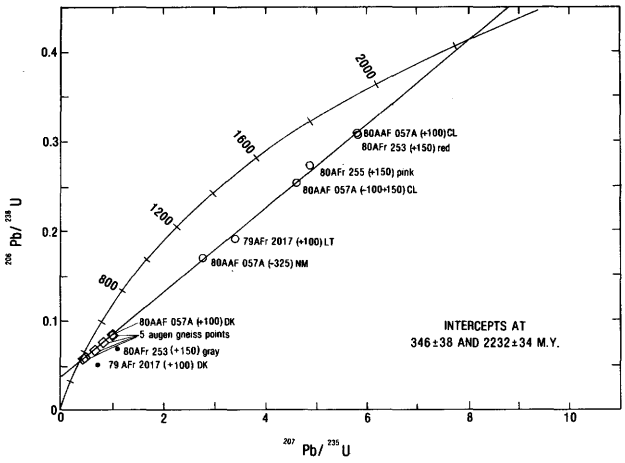

Figure 26.—Concordia plot of uranium-lead ratios in detrital zircons from quartzite and in igneous zircons from an augen gneiss, east-central Alaska. Table 7 lists sample data.

source. Intercepts from the best-fit line are 346±38 and 2,232±34 m.y.

We interpret these data as follows: Detritus from Early Proterozoic crustal rocks about 2,250 m.y. old was deposited probably during the latest Proterozoic and (or) earliest Paleozoic. Part of this package of sedimentary rocks was either partially melted or incorporated into a magma that formed the plutonic protolith of the augen gneiss about 350 m.y. B.P. Old detrital zircons were incorporated as cores around which younger magmatic rims of zircon grew. Metamorphism of the gneiss and at least the nearby quartzite (sample 79AFr 2017) protoliths may have been contemporaneous with emplacement of the magma, as

Table 7.--Uranium-lead isotopic data for detrital zircons, Yukon-Tanana Upland, east-central Alaska

[Constants used in calculation of ages: $^{235}U=0.98485\times10^{-9}$/yr, $^{238}U=0.155124\times10^{-9}$/yr, $^{235}U/^{238}U=1/137.88$ (Steiger and Jäger, 1977). LT, light; DK, dark; CL, clear; NM, nonmagnetic]

Sample	Size fraction	Lat N., long W.	Concentration (ppm)		Atomic percentage				Age (m.y.)		
			U	Pb	^{204}Pb	^{206}Pb	^{207}Pb	^{208}Pb	$\frac{^{206}Pb}{^{238}U}$	$\frac{^{207}Pb}{^{235}U}$	$\frac{^{207}Pb}{^{206}Pb}$
80AFr 253	(+150)red	65°42'30",	210.3	77.2	0.054	72.64	10.71	16.59	1,723	1,949	2,198
	(+150)gray	145°05'42"	1,500.8	131.1	.233	70.94	11.33	17.49	427	748	1,888
80AFr 255	(+150)pink	65°31'04", 145°31'22"	227.0	72.3	.042	74.53	10.19	15.23	1,558	1,797	2,086
79AFr 2017	(+100)LT	64°06'51",	134.5	32.5	.130	70.02	10.80	19.05	1,127	1,509	2,095
	(+100)DK	144°45'30"	1,049.8	59.5	.061	77.23	8.30	14.41	316	520	1,560
80AAf 057A	(+100)CL	62°42'27",	122.2	44.4	.034	73.76	10.49	15.72	1,737	1,948	2,179
	(+100)DK	145°10'38"	1,282.6	116.8	.115	80.37	8.83	10.69	515	721	1,427
	(-100+150)CL		200.7	758.2	.034	75.86	10.47	13.64	1,459	1,754	2,126
	(-325)NM		346.2	64.8	.028	78.33	9.71	11.93	1,010	1,352	1,944

suggested by coplanar foliation and the lower intercept (fig. 26), or after it cooled. The linear array of the uranium-poor detrital zircons, from widespread areas of the Yukon-Tanana Upland, suggests that this 350-m.y.-B.P. event was a large-scale, regional occurrence with major significance to the geology of the region. This conclusion is substantiated by many other ages of approximately 350 m.y. (J. N. Aleinikoff, unpub. data, 1981) on metaplutonic and metavolcanic rocks in the upland.

Although the above sequence of events may be applicable to one or more of the samples described, it is unlikely to be applicable to all of them because the Yukon-Tanana Upland probably is a composite terrane (Churkin and others, 1982). The samples are separated by at least one major fault system (the Tintina) and probably more. Although all the samples contain detrital Proterozoic zircons, not all these zircons may have come from the same source(s), and so the sedimentary rocks may not represent a single depositional sequence. However, the occurrence of these zircons in metasedimentary rocks from different terranes is significant because the age of about 2,250 m.y. for the provenance is uncommon for rocks of western North America. Thus, tectonic models for the accretion of terranes in Alaska should account for the source-rock age data. As yet, no Proterozoic metaigneous rocks have been found in the upland. Although no connection with the upland is presently apparent, we note that a thermal event at 2,300 m.y. B.P. is recorded in the area straddling the boundary between the Bear and Slave structural provinces in the Northwest Territories of Canada, approximately 1,500 km to the east (Frith and others, 1977). To the southeast, in the Yukon Territory and British Columbia, Tempelman-Kluit (1976) invoked a model that includes Late Proterozoic to Devonian sedimentation, followed by Late Devonian-Early Mississippian plutonism. The current concept of microplate accretionary tectonics in Alaska (see Jones and others, 1981) implies that terranes which in the past were juxtaposed may now be separated by vast distances. Thus, we suggest that the terrane(s) that now compose the upland might have originated several hundred kilometers to the east and (or) south.

REFERENCES CITED

Aleinikoff, J. N., Dusel-Bacon, Cynthia, Foster, H. L., and Futa, Kiyoto, 1981, Proterozoic zircon from augen gneiss, Yukon-Tanana Upland, east-central Alaska: Geology, v. 9, no. 10, p. 469-473.

Churkin, Michael, Jr., and Brabb, E. E., 1965, Occurrence and stratigraphic significance of Oldhamia, a Cambrian trace fossil, in east-central Alaska, in Geological Survey research 1965: U.S. Geological Survey Professional Paper 525-D, p. D120-D124.

Churkin, Michael, Jr., Foster, H. L., Chapman, R. M., and Weber, F. R., 1982 , Terranes and suture zones in east-central Alaska: Journal of Geophysical Research, v. 87, no. 5, p. 3718-3730.

Frith, Rosaline, Frith, R. A., and Doig, Ronald, 1977, The geochronology of the granitic rocks along the Bear-Slave Structural Province boundary, northwest Canadian Shield: Canadian Journal of Earth Sciences, v. 14, no. 6, p. 1356-1373.

Goldich, S. S., and Mudrey, M. G., Jr., 1975, Dilatancy model for discordant U-Pb zircon ages, in Tugarinov, A. I., ed., Recent contributions to geochemistry and analytical chemistry: New York, John Wiley & Sons, p. 466-470.

Jones, D. L., Silberling, N. J., Berg, H. C., and Plafker, George, 1981, Map showing tectonostratigraphic terranes of Alaska, columnar sections, and summary description of terranes: U.S. Geological Survey Open-File Report 81-792, 20 p, scale 1:2,500,000, 2 sheets.

Ludwig, K. R., 1980, Calculation of uncertainties of U-Pb isotope data: Earth and Planetary Science Letters, v. 46, no. 2, p. 212-220.

Mertie, J. B., Jr., 1937, The Yukon-Tanana region, Alaska: U.S. Geological Survey Bulletin 872, 276 p.

Steiger, R. H., and Jäger, Emilie, compilers, 1977, Subcommission on Geochronology: Convention on the use of decay constants in geo- and cosmochronology: Earth and Planetary Science Letters, v. 36, no. 3, p. 359-362.

Tempelman-Kluit, D. J., 1976, The Yukon Crystalline Terrane: Enigma in the Canadian Cordillera: Geological Society of America Bulletin, v. 87, no. 9, p. 1343-1357.

Uranium-lead isotopic ages of zircon from sillimanite gneiss and implications for Paleozoic metamorphism, Big Delta quadrangle, east-central Alaska

By John N. Aleinikoff, Cynthia Dusel-Bacon, and Helen L. Foster

As part of a continuing geochronologic study of igneous and metamorphic rocks in east-central Alaska, we have dated four samples of sillimanite gneiss and one sample of a crosscutting granite by the uranium-lead method. These samples were selected from some of the highest grade metamorphic rocks in the Yukon-Tanana Upland (area 1, fig. 23) whose protolith is considered to have been sedimentary rocks of Precambrian or Paleozoic age (Dusel-Bacon and Foster, 1983). Previous investigations (Aleinikoff and others, 1981) showed that early Proterozoic crustal material was involved in the formation of some of the Paleozoic and Mesozoic igneous rocks in this part of Alaska, but more data are needed on the age of metamorphism.

Four of the five rocks sampled were collected from a nearly circular body of sillimanite gneiss, approximately 600 km^2 in area, in the Big Delta quadrangle. We consider this body to be a gneiss dome on the basis of structure, mineral assemblages, and geothermometry (Dusel-Bacon and Foster, 1983). Foliation is subhorizontal in the central part of the body and dips outward at the margins; quartzite and marble are infolded locally. Metamorphic grade increases inward from pelitic schist that contains all three aluminosilicate polymorphs in apparent equilibrium, to sillimanite gneiss in the central part. Partial melting may have occurred near the center, as suggested by garnet-biotite equilibrium temperatures and the occurrence of migmatite.

The fifth sample was collected from an east-west-trending area of sillimanite gneiss that crops out

east of the gneiss dome and is separated from it by the northeast-trending Shaw Creek fault. The sillimanite gneiss on both sides of the fault is petrographically similar was probably continuous before faulting. The sense and extent of movement along the Shaw Creek fault required for the palinspastic reconstruction agree with the 50 km of left-lateral movement postulated by Griscom (1980), primarily on the basis of aeromagnetic data.

Three samples of sillimanite gneiss from the gneiss dome were studied, including one sample (80AFr 114) from an area of "typical" sillimanite gneiss and two samples from a locality where partial melting may have occurred. One of these samples (81ADb 35A) is another "typical" sillimanite gneiss; the other (81ADb 35B) is a weakly foliated equigranular granitic rock, possibly a leucosome in the sillimanite gneiss. An unfoliated crosscutting granite was sampled (79AFr 2010) to provide evidence for a minimum age of the gneiss. Finally, a sample (81ADb 38A) of what appears both in hand sample and thin section to be "typical" sillimanite gneiss from east of the Shaw Creek fault was studied for comparison with those from the gneiss dome.

Table 8 lists major-element analyses for the three samples of sillimanite gneiss. The chemical compositions of the rocks are compatible with a sedimentary protolith proposed for the gneiss, in that potassium is greater than sodium, magnesium greater than calcium, and normative quartz close to or greater than the 50-percent value considered to indicate a sedimentary protolith (Mason, 1966, p. 249). Normative quartz values, calculated on the assumption that two-thirds of the iron is ferric, are: 49 percent (sample 81ADb 35A); 59 percent (80AFr 114); and 52 percent (81ADb 38A). The major-element abundances for a sample of the sillimanite gneiss collected east of the fault (81ADb 38A) are intermediate between those for the two samples from the gneiss dome for all elements except Na_2O and MnO and thus are permissive evidence for these areas having had the same protolith.

The intent of this study was to determine the age(s) of metamorphism of the sillimanite gneiss bodies and to examine the morphology of their zircons. Zircons were extracted from approximately 40 kg of rock and processed by routine ion exchange (modified from Krogh, 1973) for the separation of uranium and lead isotopes; these elements were analyzed on a 30-cm NBS mass spectrometer with digital control and data processing.

Interpretation of zircon morphology is particularly important for this study because of the possible occurrence of both detrital and metamorphic populations. In sample 80AFr 114, about 25 percent of the +150 size fraction are clear euhedral crystals with length-to-width (l/w) ratios of 1 to 3; approximately 50 percent of the crystals are brown in color, subhedral to euhedral, with partly pitted faces and an l/w ratio of 1 to 5; and the remaining 25 percent are broken and (or) rounded brown grains. In the finer grain sizes, at least 75 percent of the grains are clear and euhedral, whereas 25 percent or less are brown and partly rounded. Although euhedral zircons that are unequivocally detrital in origin have been found in metasedimentary rocks (Grauert and others, 1973), this is not generally the case. We presumed that the clear euhedral zircons grew during metamorphism, and so we selected those zircons in the +150 size fraction and the entire population in the -325+400 and -400 size fractions of sample 80AFr 114 for analysis. In sample 81ADb 35A, greater than 75 percent of the zircons are clear and euhedral, with an l/w ratio of 1 to 3, whereas less than 25 percent are subhedral and brown. Although the yield of zircons in sample 81ADb 35B was very small, most were euhedral and light brown. Although many of the zircons in sample 81ADb 38A are detrital, in marked contrast to the other sillimanite gneiss samples, a few clear euhedral crystals are also present; these were the only zircons analyzed from this sample. Sample 79AFr 2010, an unfoliated granite, contains zircons that range in color from clear to light brown; all are euhedral, and the l/w ratio ranges from 2 to 8. There is no optical evidence for cores or overgrowths.

Table 8 .--Major-element data for selected samples of sillimanite gneiss from the Big Delta quadrangle, Alaska

[All analyses in weight percent by quantitative X-ray spectroscopy]

Sample	81ADb 35A	81ADb 36A	81ADb 38A
SiO_2	69.3	79.0	74.7
Al_2O_3	14.9	9.65	10.5
Total Fe (as Fe_2O_3)	6.21	3.43	5.49
MgO	2.18	1.20	1.81
CaO	.41	.84	.77
Na_2O	.66	1.02	1.14
K_2O	3.53	2.89	3.34
TiO_2	.76	.52	.75
P_2O_5	.05	.07	.05
MnO	.06	.04	.08
Loss on ignition	1.58	.81	.81
Total	99.64	99.47	99.44

Table 9 lists the isotopic data plotted in figure 27. The most geologically reasonable interpretation of these data (fig. 27) involves calculating the best-fit line through only the upper four data points for the coarsest size fractions of zircons from all three sillimanite gneiss samples (80AFr 114, 81ADb 35A, 81ADb 38A). The discordia through these points has concordia intercepts of 302±156 and 2,383±398 m.y. The three lower data points, from two finer grained zircon fractions from sillimanite gneiss (sample 80AFr 114) and one coarse fraction from the probable leucosome (sample 81ADb 35B), were not used in determining the discordia. The zircons from these fractions contain

significantly more uranium (738-1,009 ppm U, in comparison with 289-501 ppm U in the upper four data points), and so they probably lost relatively more lead as the result of a well-documented regional thermal event about 115 m.y. B.P. (Aleinikoff and others, 1981; J. N. Aleinikoff, unpub. data, 1981; M. A. Lanphere and others, oral commun., 1982; J. N. Aleinikoff, unpub. data, 1981).

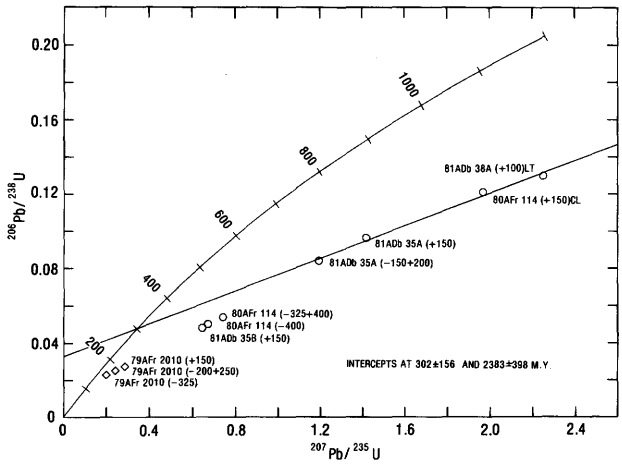

Figure 27.—Concordia plot of zircon from sillimanite gneiss (circles) and crosscutting granite (diamonds). Best-fit line calculated through four upper sillimanite gneiss points.

The upper-intercept age of 2,383±398 m.y. indicates the provenance age of the sedimentary protolith of the sillimanite gneiss. This age is not unexpected because most upper-intercept ages on metamorphic rocks in the Yukon-Tanana Upland, interpreted to be inheritance and provenance ages, are Early Proterozoic (Aleinikoff and others, 1981, 1983). Analyses of zircons from the Mount Hayes quadrangle (J. N. Aleinikoff, unpub. data, 1981) also indicate that 2.0-b.y.-old primary igneous and detrital zircons are present in that part of the Upland. Thus, the age of the inherited material could range from 2.0 to 2.3 b.y. (Aleinikoff and others, 1981).

We propose that the lower concordia intercept of 302±156 m.y. reflects the growth of metamorphic zircons during the Paleozoic or Mesozoic. The large uncertainty is probably due to inheritance of radiogenic lead from a heterogeneous population of Proterozoic zircons and (or) multiple episodes of post-metamorphism lead loss. The most likely cause of such lead loss is the intrusive event that produced the crosscutting granite (sample 80AFr 2010). If a discordia were calculated through the three granite data points, it would have a lower concordia intercept of 116±3 m.y., interpreted as the age of crystallization. Its upper-intercept age of approximately 2 b.y. would indicate inheritance of Early Proterozoic material, a likely source of which would be the zircons from the sillimanite gneiss. The large uncertainty in the lower-intercept age of the chord calculated through the upper four sillimanite gneiss points (fig. 27) can be more tightly constrained by the age limits we have placed on dynamothermal metamorphism in the Yukon-Tanana Upland on the basis of additional geochronologic data from related parts of the Upland: Metamorphism is post-345-m.y.-B.P. intrusion of augen

Table 9.--U-Pb-isotopic data for zircons from sillimanite gneiss and granite, Big Delta quadrangle, east-central Alaska

[Constants used in calculation of ages: $^{235}U=0.98485\times10^{-9}/yr$, $^{238}U=0.155124\times10^{-9}/yr$, $^{235}U/^{238}U=1/137.88$ (Steiger and Jäger, 1977). LT, light; CL, clear]

Sample	Size fraction	Lat N., long W.	Concentrations (ppm)		Atomic percent				Age (m.y.)		
			U	Pb	^{204}Pb	^{206}Pb	^{207}Pb	^{208}Pb	$\frac{^{206}Pb}{^{238}U}$	$\frac{^{207}Pb}{^{235}U}$	$\frac{^{207}Pb}{^{206}Pb}$
81AFr 114	(+150)CL	64°34'15",	289	39.8	0.015	75.83	9.15	15.01	736	1,105	1,926
	(-325+400)	145°38'10"	738	43.2	.048	79.45	8.70	11.79	336	566	1,646
	(-400)		741	39.5	.022	80.63	8.25	11.10	313	524	1,596
81ADb 35A	(+150)	64°26'46",	469	50.8	.062	77.30	9.12	13.51	592	898	1,752
	(-150+200)	145°45'26"	501	46.2	.043	78.95	8.76	12.24	519	799	1,688
81ADb 35B	(+150)	64°26'46", 145°45'26"	1,009	51.3	.018	81.21	8.25	10.52	301	508	1,596
81ADb 38A	(+100)LT	64°38'16", 144°43'10"	339	51.2	.036	74.48	9.86	15.62	787	1,198	2,042
79AFr 2010	(+150)	64°37'50",	2,040	57.1	.051	84.47	7.24	8.24	172	258	1,124
	(-200+250)	145°40'20"	2,189	55.2	.051	86.15	6.85	6.95	159	224	974
	(-325)		2,435	53.8	.027	88.44	6.18	5.35	144	189	792

gneiss and pre-210-m.y.-B.P. intrusion of the unmetamorphosed Taylor Mountain batholith (Aleinikoff and others, 1981).

In conclusion, our interpretation of the data presented above is as follows: (1) Pre-350 m.y. B.P.—deposition of the protolith of the sillimanite gneiss containing detrital zircons from provenance(s) ranging in age from about 2.0 to 2.3 b.y.; (2) between 350 and 210 m.y. B.P.—high-grade dynamothermal metamorphism formed the gneiss and new euhedral zircons which contain inherited Proterozoic radiogenic lead; (3) about 115 m.y. B.P.—a thermal event that partially reset zircons in the gneiss and resulted in emplacement of the crosscutting granite. Because a strong dynamothermal event at about 350 m.y. B.P. is indicated by independent lines of evidence (J. N. Aleinikoff, unpub. data, 1981; J. K. Mortensen, oral commun., 1981), metamorphism of the sillimanite gneiss probably occurred at that time. Subsequent lead loss, coupled with inheritance, has caused the present scatter in the data. When these data are integrated into the growing body of radiometric data for the upland, there appears to be considerable evidence that a major metamorphic event occurred during the Early Mississippian, followed by Mesozoic and Cenozoic thermal events.

REFERENCES CITED

Aleinikoff, J. N., Dusel-Bacon, Cynthia, Foster, H. L., and Futa, Kiyoto, 1981, Proterozoic zircon from augen gneiss, Yukon-Tanana Upland, east-central Alaska: Geology, v. 9, no. 10, p. 469-473.

Aleinikoff, J. N., Foster, H. L., Nokleberg, W. J., and Dusel-Bacon, Cynthia, 1983, Isotopic evidence from detrital zircons for Early Proterozoic crustal material, east-central Alaska, in Coonrad, W. L., and Elliott, R. L., eds., The United States Geological Survey in Alaska: Accomplishments during 1981: U.S. Geological Survey Circular 868, p. 43-45.

Churkin, Michael, Jr., Foster, H. L., Chapman, R. M., and Weber, F. R., 1982, Terranes and suture zones in east-central Alaska: Journal of Geophysical Research, v. 87, no. 5, p. 3718-3730.

Dusel-Bacon, Cynthia, and Foster, H. L., 1983, A sillimanite gneiss dome in the Yukon Crystalline Terrane, east-central Alaska: Petrography and garnet-biotite geothermometry: U.S. Geological Survey Professional Paper 1170-E, p. E1-E25.

Grauert, B. W., Hanny, Rudolf, and Soptrajanova, Gorica, 1973, Age and origin of detrital zircons from the pre-Permian basements of the Bohemian Massif and the Alps: Contributions to Mineralogy and Petrology, v. 40, no. 2, p. 105-130.

Griscom, Andrew, 1979, Aeromagnetic map and interpretation of the Big Delta quadrangle, Alaska: U.S. Geological Survey Open-File Report 78-529-B, 11 p.

Krogh, T. E., 1973, A low-contamination method for hydrothermal decomposition of zircon and extraction of U and Pb for isotopic age determinations: Geochimica et Cosmochimica Acta, v. 37, no. 3, p. 485-494.

Ludwig, K. R., 1980, Calculation of uncertainties of U-Pb isotope data: Earth and Planetary Science Letters, v. 46, no. 2, p. 212-220.

Mason, Brian, 1966, Principles of geochemistry: New York, John Wiley and Sons, 329 p.

Concordant bands of augen gneiss within metasedimentary rocks in the Big Delta C-2 quadrangle, east-central Alaska

By Cynthia Dusel-Bacon and Charles R. Bacon

Augen gneiss is a fairly common rock type in the amphibolite-facies metamorphic rocks of the Yukon-Tanana Upland and crops out both as large bodies (max 700-km^2 area) and, locally, as concordant bands (commonly less than 1 m thick) within similarly metamorphosed and cataclasized metasedimentary and (or) metavolcanic rocks. Determination of protoliths for this augen gneiss has been complicated by observations of these two modes of occurrence. Study of a large area (area 7, fig. 23) of augen gneiss in the southeastern part of the Big Delta quadrangle (Dusel-Bacon and Aleinikoff, 1980; Aleinikoff and others, 1981) supports a plutonic origin for this batholith-size body. Evidence for a plutonic origin consists of: (1) the large extent and uniform granitic composition of the body; (2) a contact with metasedimentary wallrocks that dips steeply and is strongly discordant to regional subhorizontal foliation where mapped along part of one margin of the augen gneiss body; (3) the presence of fine-grained inclusions, believed to be xenoliths, within the gneiss; (4) concentricity of zones of plagioclase and biotite inclusions in some of the more idiomorphic less deformed augen; and (5) the euhedral shape of most accessory zircons.

A small area in the Big Delta C-2 quadrangle (area 6, fig. 23) approximately 25 km north of the margin of the large orthoaugen gneiss body, was revisited in June 1981 to examine concordant layers of augen gneiss within the metasedimentary rocks (fig. 28). The thickest (approx 20-100 m) layer of augen gneiss (stippling, fig. 28) appears to be a sill that intruded a sequence of sedimentary rocks now metamorphosed to interlayered quartz-mica schist, quartz-ofeldspathic biotite gneiss, diopside-bearing marble, and biotite-hornblende schist. Coexisting andalusite and sillimanite in one sample of staurolite-garnet-biotite-white mica schist suggest that metamorphic pressures were less than, and temperatures greater than, those of the aluminum silicate triple point (0.38 GPa and approx 500°C, Holdaway, 1971). Foliations in the augen gneiss and adjacent layers are essentially parallel to one another and to mutual lithologic contacts. The general strike of foliation and contacts is N. 15° W.,and the dip 25°-40° E., although attitudes vary somewhat owing to subsequent deformation, as evidenced by crenulations in the micaceous layers and isoclinal folds (mostly less than about 1 m in wavelength and amplitude). This band of augen gneiss is considered to be a sill because its texture and composition resemble those of the large augen gneiss body. In both areas, the augen gneiss is characterized by as much as 25 percent potassium feldspar porphyroclasts, up to 7 cm long, set in a medium-grained partially

recrystallized cataclastic matrix of quartz+plagioclase+biotite+white mica and minor potassium feldspar. The porphyroclasts (augen) in rocks from both areas are fairly densely packed and show the effects of bunching up and deformation of preexisting lath-shaped megacrysts (fig. 29A). Inclusions of biotite, arranged in concentric zones within augen similar to those in the metaplutonic body, were also observed in the sill (loc. 1, fig. 28).

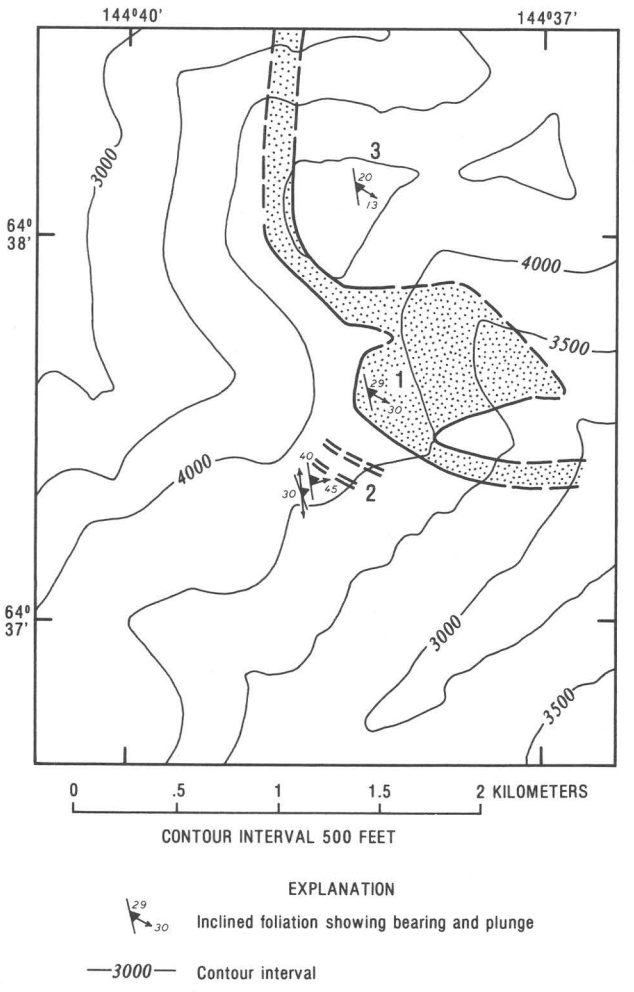

Figure 28.—Geologic sketch map of part of Big Delta C-2 quadrangle, showing relations between bands of augen gneiss and intervening metasedimentary rocks. Stippling denotes thick orthoaugen gneiss sill at locality 1 (fig. 29A); dashed lines outline thin orthoaugen gneiss sills at locality 2. Fine-grained augen gneiss occurs at locality 3 (fig. 29B).

Two thin bands of augen gneiss (approx 1 m thick) in which the augen are smaller but similar to those in the thick sill crop out nearby (dashed lines, loc. 2, fig. 28); these bands are also tentatively interpreted as sills. Augenlike clots of potassium feldspar, less than 1 cm long, occur in some layers of pelitic schist and biotite gneiss between and below the two thin augen gneiss sills; these porphyroblastic clots probably formed during metamorphism.

A third, and most enigmatic, textural type of augen gneiss lies above the thick sill (loc. 3, fig. 28), in an area composed of the metasedimentary-rock sequence previously described. This augen gneiss occurs as thin (approx 1 m thick) layers in which nearly perfect eye-shaped feldspar augen (1-3 cm long, avg approx 1.5 cm long) are evenly scattered in a fine-grained matrix of quartz+plagioclase+potassium feldspar+biotite+white mica (fig. 29B). The augen gneiss is overlain by biotite-hornblende schist that contains scattered clots and thin laminae of feldspar. Foliation in the augen gneiss parallels that in the adjacent rocks and the layering. The texture of this augen gneiss, however, differs from that of the metaplutonic augen gneiss and the nearby sill (compare figs. 29A and 29B) in that: (1) The augen are almost perfectly eye shaped and do not appear to be broken and sheared lath-shaped megacrysts; (2) the augen are less abundant (10 percent versus 25 percent), and the potassium feldspar/plagioclase ratio of the matrix higher (0.64 versus 0.32), than in the nearby sill; (3) no concentric zones of mineral inclusions were observed in any of the augen; and (4) the augen appear to be eye shaped in all visible sections and do not have a randomly oriented euhedral outline in a plane perpendicular to both foliation and lineation, as in certain excellent exposures of the metaplutonic augen gneiss.

These textural differences can be explained by two different mechanisms for formation of the augen at the third locality. In the first mechanism, the textural differences could be functions of the degree of penetrative deformation. The augen gneiss layer at the third locality could have been intruded as a sill, and, as a result of severe cataclasis, the original phenocrysts (which may have been relatively small originally) were comminuted into their present shape. Perhaps the scattered, sparsely distributed, well-formed augen were the largest phenocrysts in the original rock, and smaller ones are now part of the matrix. The survival of the largest megacrysts as more idiomorphic coherent augen and the granulation of the smaller ones are features that are commonly observed in the large body of orthoaugen gneiss. Modes of augen gneiss from the sill (loc. 1, fig. 28) and the fine-grained layer (loc. 3) were determined to compare bulk compositions and to evaluate the possibility that the textural differences are due to comminution and (or) to variations in phenocryst size and abundance. The modes for the sill (total kf=31, pl=29, qz=30, bt=9, mu=1 percent) and the augen gneiss layer (total kf=28, pl=25, qz=36, bt=9, mu=2 percent) are similar and consistent with the hypothesis that the textural differences are due to comminution alone. More than half (57 percent) of the total amount of potassium feldspar in the enigmatic layer is in the recrystallized cataclastic matrix, and much less of the total (31 percent) in the matrix of the sill sample.

In the second mechanism, the fine-grained augen gneiss could be porphyroblastic arkosic metasedimentary layers, rather than metaigneous sills. Similarity of modal compositions would be explained by the fact that analyses of granitic and arkosic rocks are commonly difficult to distinguish. The incipient clots of

feldspar that developed in quartz-mica schist and gneiss near the contacts of the two bands of augen gneiss (dashed lines, loc. 2) might represent the beginning stages of the same phenomenon. The association of those clots with the narrow bands considered to be sills may indicate that intrusion of the augen gneiss sills, formation of porphyroblasts, and cataclasis were all closely related in time. The perfect eye shape of most augen could be evidence that growth of porphyroblasts and modification of their shape by cataclasis was contemporaneous. Petrographic examination of the fine-grained augen gneiss in question, as well as study of the metamorphic textures of the cataclasized rocks in the upland in general, indicates that cataclasis and neocrystallization were closely linked. However, because the timing of regional metamorphism and cataclasis subsequent to intrusion of the augen gneiss (about 350 m.y. B.P. for the large body of augen gneiss) is still uncertain within about a 150-m.y. interval (Aleinikoff and others, 1981), a genetic relation between intrusion of the augen gneiss protolith and possible porphyroblastic formation of other augen gneiss layers is only speculative.

The various layers at the localities described are examples of the textural end members in the porphyroclastic to possibly porphyroblastic origin of augen gneiss in the upland. The sill of augen gneiss, which is the first such intrusive layer that we have recognized, may be similar to other layers of augen gneiss whose interlayering with metasedimentary rocks was previously interpreted to suggest a sedimentary protolith. The incipient clots of feldspar in pelitic metasedimentary rocks near the narrow bands of augen gneiss are evidence that the formation of feldspar porphyroblasts in metasedimentary rocks may be a plausible explanation for some augen gneiss layers, and the augen gneiss layer at the last locality described is a good example of the equivocal textures of the "grey" area between the two end members.

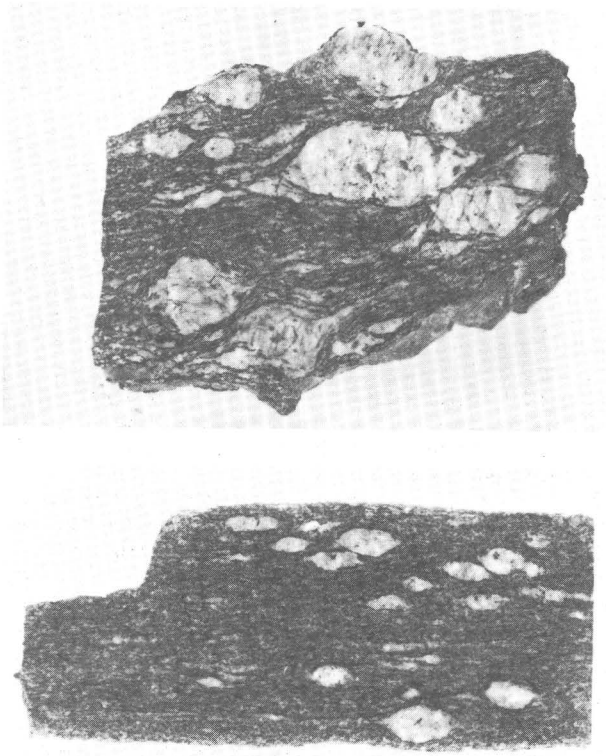

Figure 29.—Slabs of augen gneiss from localities in Big Delta C-2 quadrangle. A, Orthoaugen gneiss from thick sill at locality 1 (fig. 28). Note fracturing and cataclastic deformation of originally idiomorphic megacrysts, and apparent rotation of some smaller megacrysts. Largest auge is 12 cm long. B, Enigmatic fine-grained augen gneiss from locality 3 (fig. 28). In outcrop, augen are more evenly spaced than in this sample. Diagonal-stacking alinement of augen, which is common in coarse-grained orthoaugen gneiss, may be evidence for porphyritic-sill protolith. Largest auge is 1.25 cm long.

REFERENCES CITED

Aleinikoff, J. N., Dusel-Bacon, Cynthia, Foster, H. F., and Futa, Kiyoto, 1981, Proterozoic zircon from augen gneiss, Yukon-Tanana Upland, east-central Alaska: Geology, v. 9, no. 10, p. 469-473.

Dusel-Bacon, Cynthia, and Aleinikoff, J. N., 1980, Proterozoic cataclastic augen gneiss in the southeastern part of the Big Delta quadrangle, Yukon-Tanana Upland, east-central Alaska [abs.]: Geological Society of America Abstracts with Programs, v. 12, no. 3, p. 104-105.

Holdaway, M. J., 1971, Stability of andalusite and the aluminum silicate phase diagram: American Journal of Science, v. 271, no. 2, p. 97-131.

Trace-element evidence for the tectonic affinities of some amphibolites from the Yukon-Tanana Upland, east-central Alaska

By Cynthia Dusel-Bacon

Amphibolite occurs throughout the Yukon-Tanana Upland, interlayered with metasedimentary and metaigneous rocks of Precambrian(?) and Paleozoic age. There has been considerable speculation as to the origins of the various amphibolite layers and their geologic significance. Amphibolite may result from: (1) Metamorphism of basic igneous rocks, (2) metamorphism of calcareous or dolomitic shale, or (3) metasomatism involving the exchange of significant amounts of nonvolatile constituents (Preto, 1970). On the basis of trace-element evidence obtained in the preliminary study reported here, basaltic protoliths are indicated for amphibolite of the Yukon-Tanana Upland.

In the amphibolite-grade terrane of the southeastern part of the Big Delta quadrangle (area 7, fig. 23), amphibolite is commonly interlayered with quartzofeldspathic gneiss and schist that are near the margins of, and probably wallrock for, a batholith-size body of orthoaugen gneiss of Late Devonian-Early Mississippian age (Aleinikoff and others, 1981). Samples from amphibolite layers at three different localities around the augen gneiss pluton were chemically

analyzed to determine whether immobile minor- and trace-element contents might be diagnostic of the origin of these layers. Table 10 lists locations and modal analyses of the three amphibolite and two associated gneiss samples, and table 11 lists major-, minor-, and trace-element data. Features characteristic of metasomatic amphibolite (Orville, 1969, p. 84) are absent at the three localities sampled, and a metasomatic origin is considered highly unlikely.

Lithologic interlayering at the first locality (sample 4017B) suggests a volcanic origin for the amphibolite layer. The sample is from a 10-m-thick layer of amphibolite with minor interlayered plagioclase-rich bands. Thin biotite-rich layers occur at several levels in the amphibolite outcrop; these layers might represent thin sedimentary laminae deposited between layers of mafic tuff. Zircon uranium-lead systematics that indicate an inherited older (sedimentary?) component in this amphibolite sample (J. N. Aleinikoff, written commun., 1981) are also compatible with a bedded-tuff protolith. A 10-m-thick layer of homogeneous biotite-hornblende felsic gneiss (sample 4017A) containing flattened lenses of a more mafic composition overlies the amphibolite. Lenses, with a flattening ratio of about 1:20, make up as much as 50 percent of the exposure in some layers but generally constitute only about 5 percent. The lenses appear to be monolithologic and may have originated as mafic inclusions in a silicic lava flow. A total of 1 m of augen gneiss (sample 4017C) of probable igneous origin is exposed beneath the sampled amphibolite.

The other two amphibolite samples were collected about 30 km northwest of sample 4017. Sample 4024J is from a concordant band of amphibolite, several tens of meters thick, that occurs within an area of quartzofeldspathic gneiss and garnetiferous quartz-mica schist near the north contact of a large orthoaugen gneiss body. Sample 4026B was collected from an adjacent parallel ridge 2.5 km to the southwest at a 1- to 2-m-thick outcrop of amphibolite containing a few thin interlayered feldspathic bands. Pelitic schist and biotite gneiss, as well as a thin layer of marble, crop out nearby on the ridge. Similar amphibolite occurs around the margins of a small foliated serpentinite body 2.5 and 3.5 km west of the localities of samples 4026B and 4024J, respectively.

Leake (1964, p. 247) stated that high Cr contents (about 250 ppm) are excessive for pelite-dolomite mixtures but are appropriate for orthoamphibolite. Thus, the 311-ppm Cr content of sample 4026B probably indicates an igneous origin. The Cr contents of the other two samples (195 and 180 ppm) are well within the range of values for basalt but are also within the highest part of the range of possible shale-carbonate mixtures (Evans and Leake, 1960, p. 357) and are, therefore, nondiagnostic.

The TiO_2 contents of the amphibolites fall in the uppermost range for pelite-carbonate mixtures but low in the range for basalt (Evans and Leake, 1960, p. 356; Nockolds, 1954, p. 1021). Although some pelite has TiO_2 contents as high as about 2 weight percent, pelite generally is appreciably poorer in TiO_2 (avg 0.82 weight percent) (Evans and Leake, 1960). When pelite is diluted by mixture with dolomite, which is very poor in TiO_2, the resultant mixture will be lower in TiO_2. Thus, if the amphibolite were of sedimentary parentage, the sediment was unusually titaniferous.

The Niggli k value (Barth, 1962), based primarily on the ratio of K_2O to K_2O+Na_2O, was considered by Evans and Leake (1960, p. 356) to be greater than 0.50 in amphibolite derived from the metamorphism of mixtures of clay and dolomite. Although the k values for the amphibolite samples of this study are considerably lower (0.09, 0.14, and 0.18 for samples 4024J, 4026B, and 4017B, respectively) and thus might be used as

Table 10.--Modal analyses of amphibolite and associated gneiss samples from the Big Delta quadrangle, Yukon-Tanana Upland

[All modes in volume percent, based on 1,500 data points. Sample 4017A was inclusion free. tr, trace]

	Amphibolite			Gneiss	
Sample	4024J	4026B	4017B	4017A	4017C
Lat. N	64°23'11"	64°22'34"	64°08'40"	64°08'40"	64°08'40"
Long. W	144°37'52"	144°41'18"	144°26'30"	144°26'30"	144°26'30"
Quartz	--	1	--	33	49
Plagioclase	30	32	26	35	6
K-feldspar	--	--	--	12	35
Biotite	--	5	--	10	6
White mica	--	--	tr	--	--
Actinolitic hornblende	55	56	63	6	--
Chlorite	--	--	2	2	3
Epidote	9	tr	tr	tr	tr
Clinozoisite	--	tr	tr	tr	tr
Clinopyroxene	--	--	tr	--	--
Sphene	3	5	8	1	tr
Apatite	1	--	--	tr	--
Allanite	--	--	--	--	tr
Rutile/opaque minerals	2	--	--	--	--

evidence for an igneous protolith, the known mobility of alkali elements during metamorphism renders this criterion virtually meaningless.

Table 11.--Major-, minor-, and trace-element data for amphibolite and associated gneiss samples from the Big Delta quadrangle, Yukon-Tanana Upland

[All major and minor elements in weight percent, determined by quantitative X-ray spectroscopy. All trace elements in parts per million, determined by instrumental neutron activation, except Nb, which was determined by spectrophotometry]

	Amphibolite			Gneiss	
Sample----------	4024J	4026B	4017B	4017A	4017C
	Major and minor elements				
SiO_2----------	47.6	49.9	51.0	69.3	75.6
Al_2O_3----------	14.3	15.4	14.8	14.1	12.6
Fe_2O_3----------	12.16	8.97	9.47	4.66	2.48
MgO----------	6.7	7.1	7.8	1.2	.2
CaO----------	9.4	10.5	11.9	4.6	1.0
Na_2O----------	3.5	3.3	2.8	2.6	2.6
K_2O----------	.51	.80	.96	2.22	4.86
TiO_2----------	1.54	1.18	1.46	.39	.27
P_2O_5----------	.14	.17	.22	.08	.06
MnO----------	.19	.12	.14	.08	.04
Loss on fusion--	3.5	3.0	---	---	.3
Total------	99.5	100.4	100.6	99.2	100.0
	Trace elements				
Sc----------	39.9	29.2	36.0	17.2	12.0
Cr----------	195	311	180	25.9	3.5
Co----------	34.3	38.9	36.1	8.7	1.7
Zn----------	82	84	78	47	56
Rb----------	9	20	31	92	155
Zr----------	64	110	110	138	277
Nb----------	5.4	16	20	7.8	27
Sb----------	.6	.8	.6	.8	.4
Cs----------	.4	.7	.8	2.7	1.6
Ba----------	200	93	211	655	1470
La----------	3	17	20	24	86.5
Ce----------	10	32	37	46	165
Nd----------	10	17	20	21	68
Sm----------	3.3	3.9	4.8	4.3	13.5
Eu----------	1.12	1.07	1.19	.68	1.18
Gd----------	3.6	3.6	4.4	4.0	10.5
Tb----------	.91	.53	.57	.60	1.44
Ho----------	.7	.4	.5	.7	1.4
Tm----------	.32	.26	.20	.30	.46
Yb----------	3.4	1.8	1.9	2.5	3.2
Lu----------	.50	.27	.29	.37	.46
Hf----------	2.1	2.5	2.6	3.5	7.4
Ta----------	.50	1.09	1.36	.69	1.74
Th----------	.4	4.3	2.9	8.4	22.6
U----------	.7	1.1	.8	2.3	2.4

Of all the criteria just discussed, only the high Cr content of sample 4026B is clearly outside the area of overlap between a possible shale-carbonate mixture and basalt and appears to be fairly definitive of an igneous origin. More diagnostic, however, are the abundances of the trace elements Sc, Co, and the rare-earth elements (REE's). Shaw and Kudo (1965) determined that Sc and Co are the elements that best discriminate between known orthoamphibolites and para-amphibolites. Average Sc values for orthoamphibolites and para-amphibolites were determined to be 30 and 5 ppm, respectively. The Sc contents of the Big Delta samples (29-40 ppm) are closest to the orthoamphibolite average and higher than all the para-amphibolite values reported by Shaw and Kudo (1965). The Sc contents of the amphibolite samples listed in table 10 are also higher than the range of values for shale-carbonate mixtures (Evans and Leake, 1960, p. 357). The Co contents (table 10) are closest to the ortho-amphibolite average (37 ppm) and higher than all but one para-amphibolite value (avg 14 ppm) of Shaw and Kudo (1965, p. 431). The Co contents of the Big Delta amphibolite samples are in the middle of the range for basalt but also overlap the upper limit for shale-carbonate mixtures (Evans and Leake, 1960, p. 357).

REE concentrations provide the most definitive geochemical evidence for an igneous origin of the amphibolite samples of this study because REE's have been shown in many studies to remain relatively immobile during metamorphism and alteration (e.g., Frey and others, 1968; Garcia, 1978). Figure 30 plots the chondrite-normalized REE patterns for the three amphibolite samples, as well as those for the presumed metavolcanic and orthoaugen gneiss that overlie and underlie sample 4017B. Figure 31 plots the REE patterns of a North American shale composite (Haskin and others, 1966b) and several basaltic-magma types for comparative purposes. The REE pattern of the shale composite was found by Haskin and others (1966a, p. 271) to be indistinguishable from the patterns for average REE contents in limestone, sandstone, graywacke, and ocean sediment to within a ±10-15 percent experimental uncertainty.

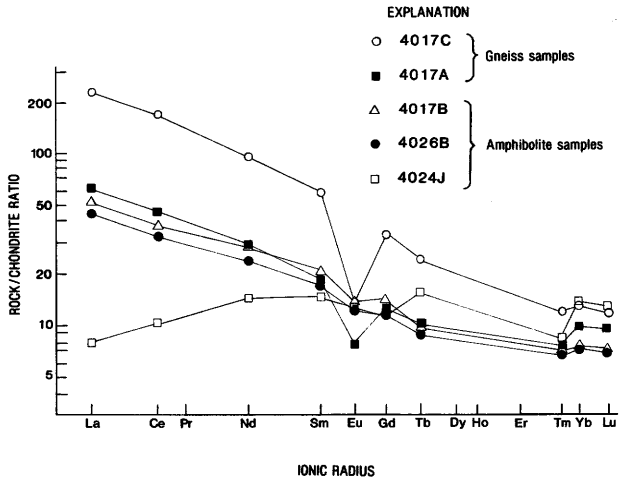

Figure 30.--Chondrite-normalized rare-earth-element contents versus ionic radius for amphibolite (samples 4017B, 4024J, 4026B) and interlayered gneiss (samples 4017A, 4017C). Chondrite concentrations from Leedey chondrite of Masuda and others (1973). Apparent negative Tm anomaly is probably due to analytical error.

All three amphibolite samples are depleted in REE's relative to the composite sedimentary pattern. The depletion in light rare-earth elements (LREE's) and the convex-upward REE distribution of sample 4024J differ most markedly from the shale pattern but

are typical of both ocean-floor basalt (OFB) and island-arc tholeiite (IAT). Similar patterns have been shown for pillow lavas and diabase dikes associated with the Bay of Islands ophiolite suite in Newfoundland by Suen and others, 1978, who pointed out that the REE data are inadequate to distinguish between such tectonic environments as deep-oceanic ridges, small ocean basins, or young island arcs. According to the Ti-Cr discrimination diagram of Pearce (1975), in which island-arc tholeiite is distinguishable chemically from ocean-floor basalt by its low Ti and Cr contents, all three amphibolite samples plot in the OFB field. However, this criterion alone is probably insufficient to determine the parentage of metamorphosed or altered volcanic rocks (Garcia, 1978).

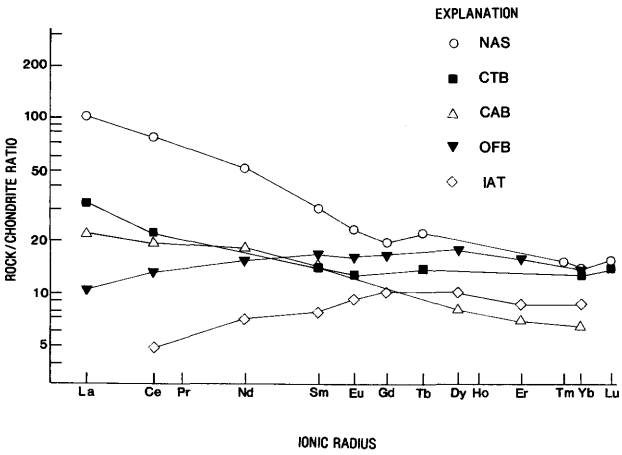

Figure 31.---Chondrite-normalized rare-earth-element patterns for a composite of North American shale (NAS) (Haskin and others, 1966b) and representative basalt. Data sources for basalt: Calc-alkaline island-arc basalt (CAB) from Okmok, Alaska (Arth, 1981, fig. 5); continental tholeiitic basalt (CTB) (Gottfried and others, 1977); and island-arc tholeiite (IAT) and ocean-floor basalt (OFB) (Garcia, 1978, fig. 6).

The REE patterns for samples 4026B and 4017B differ from that of the other amphibolite sample in that they are enriched in LREE's. Their patterns more closely resemble those of calc-alkaline basalt (CAB) or continental tholeiitic basalt (CTB). The REE patterns of the interlayered samples (4017A, 4017B, 4017C) may be related by differentiation within continental crust because the general trend of such processes is for the REE contents to increase, the Ce/Yb ratio to increase, and the Eu anomaly to become more negative with increasing SiO_2 content (Arth, 1981); although REE patterns alone are insufficient to determine the composition and relations of the protoliths.

At present, a unique tectonic environment for the basaltic protoliths of the amphibolite samples of this study cannot be defined. Neither the relative age and tectonic relations between the three amphibolite samples nor the modes of emplacement (that is, lava flow, tuff, or intrusion) of their protoliths are known. In the case of the LREE-depleted sample (4024J), lithologic association suggests that OFB may be a more reasonable choice for the protolith than IAT. The small foliated serpentinite body nearby, as well as other small ultramafic masses infolded in the schist and gneiss associated with the amphibolite around the augen gneiss body, is permissive but not conclusive evidence for the presence of oceanic material because these ultramafic bodies have not been studied in detail and may have had other origins. Although an OFB affinity seems more likely for sample 4024J, an IAT protolith cannot be completely discounted. In the latter case, the association of sample 4024J with the other two samples (with REE patterns similar to those of CAB) could conceivably be explained by the fact that the composition of volcanic-arc rocks ranges from low-potassium tholeiite, through calc-alkaline rocks, to shoshonite both in time (in which tholeiite is typical of the earliest eruptions) and in space (in which tholeiite occurs closest to the trench) (Pearce and Cann, 1973). However, because the REE patterns of calc-alkaline and continental tholeiitic basalt are similar (fig. 31), it is equally plausible that the protoliths of samples 4017B and 4026B may have been generated by continental (rifting?) volcanism.

The interpretation of these amphibolite samples as metamorphosed continental tholeiitic basalt is consistent with the continental nature of most of the crystalline rocks of the Yukon-Tanana Upland. That the tectonic environment was predominantly continental is shown by the abundance of quartzose and pelitic rocks, large augen gneiss bodies containing more than 70 percent SiO_2, and the possible presence of siliceous volcanic protoliths, such as I propose for gneiss sample 4017A. This continental material is now known to have been derived from a very old source. Uranium-lead data on zircon separates from the large augen gneiss body in the Big Delta quadrangle indicate that its Devonian plutonic protolith was either derived from or contaminated by Proterozoic crustal rocks (Aleinikoff and others, 1981), and uranium-lead data from metasedimentary rocks nearby and in other parts of the Yukon-Tanana Upland also indicate that these rocks contain Proterozoic detritus (Aleinikoff and others, this volume). At present, the data are insufficient to answer such fundamental questions as "Do the large bodies of augen gneiss represent the deeply eroded plutonic roots of a Devonian magmatic arc that developed off cratonic North America?" and "Are the mafic and felsic volcanic protoliths of this study the extrusive equivalents of the Devonian-Mississippian plutons?" Additional uranium-lead data (J. N. Aleinikoff, unpub. data, 1981) on zircon separates from several other metaigneous rocks, including amphibolite (sample 4017B) and felsic gneiss (sample 4017C), suggest that their protoliths formed during a Devonian volcanic-plutonic event and that at least some of the mafic and felsic volcanic protoliths were, indeed, formed during the same, possibly long-lived event.

The results of this preliminary study, though far from conclusive, suggest that: (1) the trace-element chemistry of the analyzed amphibolite samples indicates basaltic protoliths, (2) sample 4024J is the most "primitive" rock (IAT or OFB) of the three samples and interacted minimally with sialic crust (it also contains the least Rb, Nb, Th, U, and Ta), and (3) samples 4026B

and 4017B have a bigger crustal signature and thus are more like CAB and CTB. With more geochemical data and some warranted scepticism, the REE patterns and trace-element chemistry of orthoamphibolite of the Yukon-Tanana Upland, together with more detailed field mapping of these rocks, may provide valuable information about the tectonic history of this enigmatic terrane.

REFERENCES CITED

Aleinikoff, J. N., Dusel-Bacon, Cynthia, Foster, H. L., and Futa, Kiyoto, 1981, Proterozoic zircon from augen gneiss, Yukon-Tanana Upland, east-central Alaska: Geology, v. 9, no. 10, p. 469-473.

Aleinikoff, J. N., Foster, H. L., Nokleberg, W. J., and Dusel-Bacon, Cynthia, 1983, Isotopic evidence from detrital zircons for Early Proterozoic crustal material, east-central Alaska, in Coonrad, W. L., and Elliott, R. L., eds., The United States Geological Survey in Alaska—Accomplishments during 1981: U.S. Geological Survey Circular 868, p. 43-45.

Arth, J. G., 1981, Rare-earth element geochemistry of the island-arc volcanic rocks of Rabaul and Talasea, New Britain: Geological Society of America Bulletin, v. 92, no. 11, p. 858-863.

Barth, T. F. W., 1962, Theoretical petrology (2d ed.): New York, John Wiley, 416 p.

Evans, B. W., and Leake, B. E., 1960, The composition and origin of the striped amphibolites of Connemara, Ireland: Journal of Petrology, v. 1, no. 3, p. 337-363.

Frey, F. A., Haskin, M. A., Poetz, J. A., and Haskin, L. A., 1968, Rare earth abundances in some basic rocks: Journal of Geophysical Research, v. 73, no. 18, p. 6085-6098.

Garcia, M. O., 1978, Criteria for the identification of ancient volcanic arcs: Earth Science Reviews, v. 14, no. 2, p. 147-165.

Gottfried, David, Annell, C. S., and Schwarz, L. J., 1977, Geochemistry of subsurface basalt from the deep corehole (Clubhouse Crossroads corehole 1) near Charleston, South Carolina—magma type and tectonic implications: U.S. Geological Survey Professional Paper 1028-G, p. 91-113.

Haskin, L. A., Frey, F. A., Schmitt, R. A., and Smith, R. H., 1966a, Meteoritic, solar, and terrestrial rare-earth distributions, in Ahrens, L. H., Press, Frank, Runcorn, S. K., and Urey, H. C., eds., Physics and chemistry of the earth: New York, Pergamon, p. 167-321.

Haskin, L. A., Wildeman, T. R., Frey, F. A., Collins, K. A., Keedy, C. R., and Haskin, M. A., 1966b, Rare earths in sediments: Journal of Geophysical Research, v. 71, no. 24, p. 6091-6105.

Leake, B. E., 1964, The chemical distinction between ortho- and para-amphibolites: Journal of Petrology, v. 5, no. 2, p. 238-254.

Masuda, Akimasa, Nakamura, Noboru, and Tanaka, Tsuyoshi, 1973, Fine structures of mutually normalized rare-earth patterns of chondrites: Geochimica et Cosmochimica Acta, v. 37, no. 2, p. 239-248.

Nockolds, S. R., 1954, Average chemical compositions of some igneous rocks: Geological Society of America Bulletin, v. 65, no. 10, p. 1007-1032.

Orville, P. M., 1969, A model for metamorphic differentiation origin of thin-layered amphibolites: American Journal of Science, v. 267, no. 1, p. 64-86.

Pearce, J. A., 1975, Basalt geochemistry used to investigate past tectonic environments on Cyprus: Tectonophysics, v. 25, no. 1-2, p. 41-67.

Pearce, J. A., and Cann, J. R., 1973, Tectonic setting of basic volcanic rocks determined using trace element analyses: Earth and Planetary Science Letters, v. 19, no. 2, p. 290-300.

Preto, V. A. G., 1970, Amphibolites from the Grand Forks quadrangle of British Columbia, Canada: Geological Society of America Bulletin, v. 81, no. 3, p. 763-782.

Shaw, D. M., and Kudo, A. M., 1965, A test of the discriminant function in the amphibolite problem: Mineralogical Magazine, v. 34, no. 268, p. 423-435.

Suen, C. J., Frey, F. A., and Malpas, J., 1979, Bay of Islands ophiolite suite, Newfoundland: Petrologic and geochemical characteristics with emphasis on rare earth element geochemistry: Earth and Planetary Science Letters, v. 45, no. 2, p. 337-348.

Metamorphic petrology of the Table Mountain area, Circle quadrangle, Alaska

By Anna C. Burack, Jo Laird, Helen L. Foster, and Grant W. Cushing

Metamorphic rocks along the Pinnell Mountain trail, Circle B-4 quadrangle, Alaska (area 3, fig. 23; fig. 32), are part of a complexly deformed terrane of schist and quartzite of Paleozoic and (or) Precambrian age that are typical of much of the western Yukon-Tanana Upland (Foster and others, 1973). We have been studying the petrology of these rocks as a representative sample of this metamorphic terrane, and this report describes typical mineral assemblages and presents probable conditions of metamorphism. A knowledge of the metamorphic history may help in identifying the kind and extent of mineralization in the Table Mountain area.

The metamorphic rocks studied are divided into pelitic schist and quartzite, mafic schist, and calc-silicate rocks. A northeast-trending lineament, discernible on aerial photographs (fig. 32; Cushing and others, 1982), appears to separate rocks regionally metamorphosed to epidote-amphibolite facies (garnet grade) on the south from contact-metamorphosed rocks (biotite hornfels) on the north. The contact metamorphism, which is related to a small (approx 2-km^2 area) granodiorite pluton (fig. 32) has overprinted regional metamorphism of probable epidote-amphibolite facies (garnet grade). Several small epizonal felsic intrusions also crop out north of the lineament, mostly in the vicinity of Table Mountain (fig. 32).

Pelitic rocks south of the lineament are primarily composed of quartz+plagioclase+muscovite+chlorite+biotite+garnet; the plagioclase is commonly porphyroblastic. Coexisting with this epidote-amphibolite-facies assemblage, near the lineament

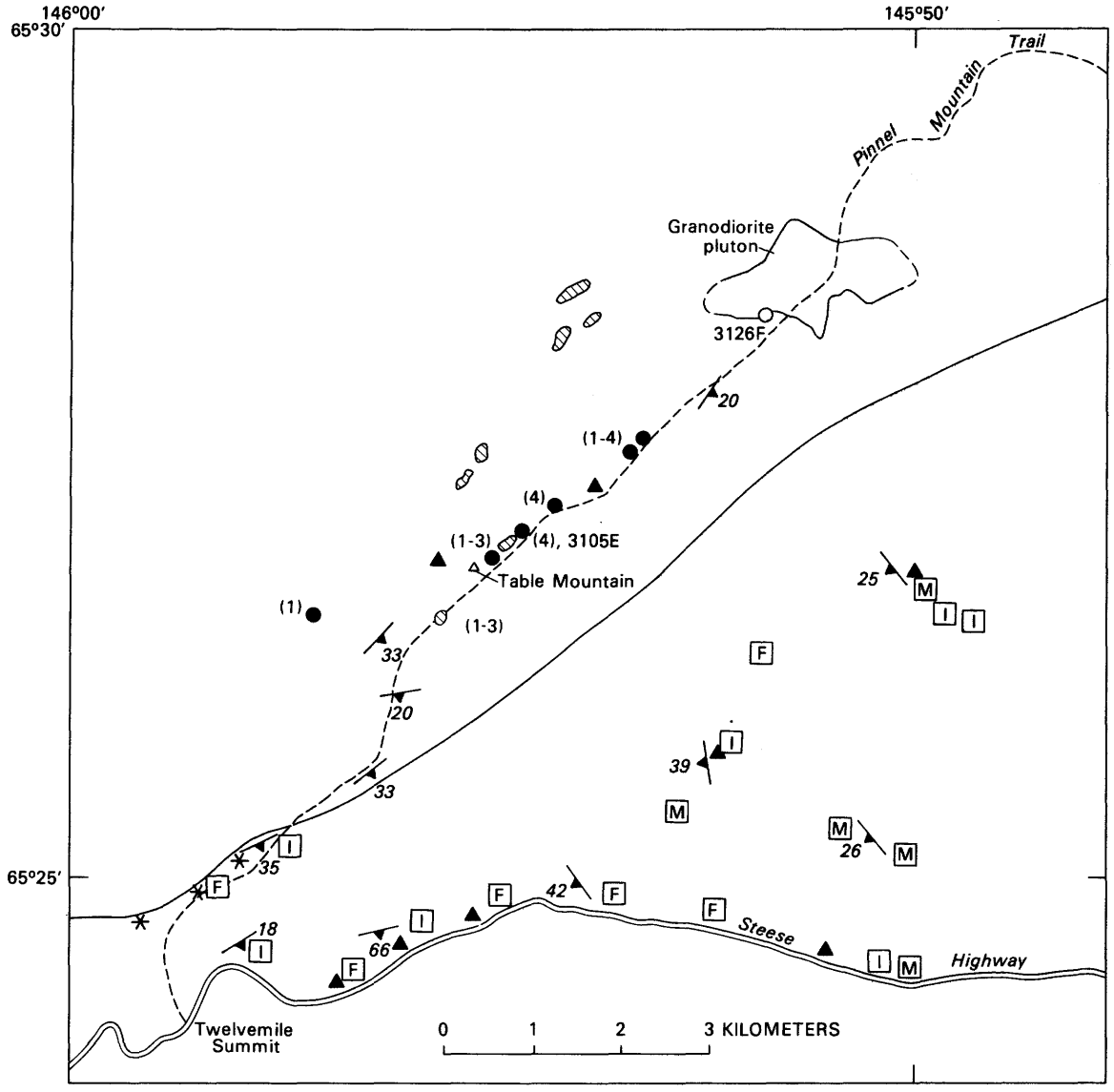

EXPLANATION

- Felsic intrusive rocks
- Biotite hornfels (sample 3126F analyzed by electron microprobe, table 12)
- Mafic rocks intercalated in pelitic rocks
- Calc-silicate rocks intercalated in pelitic rocks (sample 3105E analyzed by electron microprobe, table 12)

Pelitic rocks:

- Chloritoid-garnet-chlorite
- Chlorite-garnet-biotite
- F Fe-rich chlorite
- I Fe/Mg ratio in chlorite 1.0
- M Mg-rich chlorite

- 35 Strike and dip of foliation
- Lineament (interpreted from aerial photographs)

Figure 32.—Sketch map of study area, showing generalized geology and grade (biotite or garnet) of regional metamorphism in the Table Mountain area. Sample 3126F is biotite hornfels typical of pelitic rocks along the Pinnell Mountain trail northwest of lineament. Numbers in parentheses refer to calc-silicate assemblages discussed in text.

north of Twelvemile Summit (fig. 32), is a more aluminous quartz+plagioclase+muscovite+Fe-chlorite+chloritoid± garnet schist. These assemblages indicate garnet-grade medium-pressure facies-series metamorphism; they are stable from about 400°C at 0.1 to 0.4 GPa (limited by the breakdown of pyrophyllite) to 550°C at 0.7 GPa (using the petrogenetic grid of Labotka, 1981, fig. 11). An increase in metamorphic grade within this range of temperatures is seen toward the east, as indicated by increasingly Mg rich chlorite and Ca rich plagioclase in the less aluminous assemblage (fig. 32).

North of the lineament, the pelitic rocks are composed of quartz+plagioclase+muscovite+biotite+Fe-chlorite. Garnet is rare and occurs only in a few samples as resorbed grains or as inclusions in plagioclase. The porphyroblastic plagioclase resembles that of pelitic rocks south of the lineament. Two generations of biotite are present. The first occurs as alined inclusions in plagioclase that define a weak foliation, which were apparently formed during regional metamorphism. The second is randomly oriented biotite that crosses the early foliation and gives the rock a hornfelsic texture. These observations suggest that contact metamorphism was superimposed on a preexisting garnet-grade epidote-amphibolite-facies regional metamorphism. Contact effects do not extend south of the lineament.

Petrographic examination indicates that the plagioclase porphyroblasts are of albite in the pelitic schist south of the lineament near Twelvemile Summit, but farther east they are zoned and have albite cores (An_{0-1}) and oligoclase rims (An_{24-27}). In contrast, preliminary electron microprobe data (table 12) on zoned plagioclase from near the pluton indicate that the cores are An_{23-25} and the rims are An_1. More data are needed to determine whether this zoning is continuous and, if not, to assess whether the cores and rims represent polymetamorphism or equilibrium mineral growth across the peristerite gap, which would confine the metamorphic temperature to between approximately 400° and 550° (Smith, 1972, fig. 9). Metamorphic temperatures above 600° could not have been reached on either side of the lineament or else the pelitic rocks would have undergone partial melting.

South of the lineament, mafic schist contains amphibole+plagioclase+quartz+Mg-chlorite+biotite+epidote+garnet+sphene. Petrographic data suggest that the amphibole has an actinolite core and a hornblende rim and that the plagioclase porphyroblasts have cores of albite rimmed with oligoclase. Coexistence of hornblende with oligoclase is consistent with the garnet-oligoclase grade of the intercalated pelitic rocks (Laird, 1980, fig. 2).

Mafic rocks north of the lineament are mineralogically and texturally distinct. The assemblage is oligoclase+quartz+actinolite+biotite+epidote+sphene± Fe-chlorite. Garnet is rare and occurs as resorbed grains or as inclusions in plagioclase. Actinolite needles form small radial clusters; random orientations of white mica, biotite, and tourmaline imply contact metamorphism. Coexistence of actinolite with oligoclase rather than albite also indicates low-pressure facies series metamorphism (compare Laird, 1980, figs. 2, 5).

Calc-silicate rocks, which crop out only north of the lineament, include four thin-bedded mineral assemblages: (1) cryptocrystalline black marble, (2) clinohumite+forsterite+dolomite+calcite+Mg-chlorite+Mg-serpentine marble, (3) green actinolite+calcite+epidote+diopside+quartz+plagioclase+sphene fels with silky white tremolite layers, and (4) massive red-brown grossularite+green hedenbergite+quartz+calcite fels.

Table 12.--Representative electron microprobe analyses of pyroxene and garnet in calc-silicate fels and of plagioclase in pelitic hornfels from the Pinnell Mountain trail, Circle quadrangle, Alaska

[Wavelength-dispersive analyses on a CAMECA model MBX electron microprobe, using Tracor-Northern model TN-1310 automation, converted to weight percent according to the Bence-Albee technique with Albee-Ray correction factors. Accelerating voltage, 15 kV; sample current, 12 nA on brass; spot size, 16 μm for plagioclase (PLG) and 1 μm for garnet (GAR) and pyroxene (PYX). n.d., not determined. See figure 32 for sample localities. PYX, GAR, and PLG normalized to total cations of 4, 5, and 8, respectively; Al^{IV} and Al^{VI} assigned from assumed stoichiometry; Fe^{2+} and Fe^{3+} estimated from assumed charge balance]

Sample----------	80AFR3105E (Calc-silicate fels)				80AFR3126F (Pelitic hornfels)	
Mineral------	GAR			PYX	PLG	
	(core)	(rim)	(edge)		(core)	(rim)
Wavelength-dispersive analyses						
SiO_2---------	37.86	37.55	38.48	49.22	61.53	68.29
Al_2O_3--------	19.64	18.50	19.94	0.17	23.73	19.62
TiO_2---------	.80	.25	.26	.01	n.d.	n.d.
Cr_2O_3--------	.01	0	.03	0	n.d.	n.d.
Total Fe (as FeO)	4.77	9.50	11.24	24.44	.06	.14
MnO----------	.56	3.69	5.14	1.83	n.d.	n.d.
MgO----------	.08	0	0	1.89	n.d.	n.d.
CaO----------	36.39	30.79	26.44	23.85	5.25	.21
Na_2O---------	n.d.	n.d.	n.d.	0	8.88	11.88
K_2O----------	n.d.	n.d.	n.d.	n.d.	.20	.11
Anhydrous total	100.12	100.28	101.53	101.43	99.65	100.26
Structural formulas						
Si----------	2.88	2.90	2.95	1.97	2.73	2.97
Al^{IV}---------	.12	.10	.05	.01	1.24	1.01
Al^{VI}---------	1.64	1.58	1.76	0	---	---
Ti----------	.05	.01	.01	.0003	---	---
Cr----------	.001	0	.002	0	---	---
Fe^{3+}---------	.30	.49	.26	.05	.002	.005
Fe^{2+}---------	0	.12	.46	.77	---	---
Mn----------	.04	.24	.33	.06	---	---
Mg----------	.01	0	0	.11	---	---
Ca----------	2.97	2.55	2.17	1.02	.25	.01
Na----------	---	---	---	0	.76	1.00
K----------	---	---	---	---	.01	.01

Assemblage 2 may be described by the equilibrium forsterite+dolomite+H_2O=clinohumite+calcite+CO_2, which constrains the metamorphic temperature to a minimum of about 450°C (Rice, 1980). Absence of evidence of partial melting of the intercalated pelitic rocks sets the upper temperature limit at 600°C. This range of metamorphic temperatures is consistent with assemblages 3 and 4 and with the presence of calcite+quartz rather than wollastonite (Winkler, 1979, figs. 9-5, 9-6, 10-2). Low values of

X_{CO_2} are indicated by coexisting grossularite+quartz (Winkler, 1979, fig. 10-2).

Assemblage 4 contains discontinuously zoned garnets. Relatively unzoned birefringent cores consist of 83 mol percent grossular (gr), 15 mol percent andradite (an), 1 mol percent spessartine (sp), and no almandine (al) (table 12). Isotropic rims are zoned outward from $gr_{62}an_{25}sp_{8}al_{4}$ to $gr_{60}an_{13}al_{15}sp_{11}$. The core may have formed during regional metamorphism of Fe- and Al-rich carbonate rocks. The rims could have formed during the contact-metamorphic event at the expense of earlier formed Fe- and Mn-bearing minerals, or the cores and rims may both have formed during the same event by a discontinuous reaction.

Alternatively, semiquantitative emission-spectroscopy analyses of calc-silicates from Table Mountain suggest that they are enriched in Zn, Sn, W, and Cu and may thus have undergone metasomatism from fluids emanating from the nearby granodiorite pluton and (or) epizonal felsic intrusions. However, the sequence of assemblages 1 through 4 is observed in the same order at three separate localities (fig. 32), a result that could be due to thermal metamorphism of compositionally distinct layers.

Contact-metamorphic assemblages and textures are observed along the Pinnell Mountain trail as far as 6 km southwest of the granodiorite pluton mapped in the northeastern part of the study area (fig. 32). Because this is too large a contact aureole for such a small pluton, a larger, felsic pluton underlying the area is suggested. The small felsic intrusions may well be related to such a body.

REFERENCES CITED

Cushing, G. W., Foster, H. L., Laird, Jo, and Burack, A. C., 1982, Description and preliminary interpretation of folds and faults in a small area in Circle B-4 and B-5 quadrangles, Alaska, in Coonrad, W. L., ed., The United States Geological Survey in Alaska: Accomplishments during 1980: U.S. Geological Survey Circular 844, p. 56-58.

Foster, H. L., Weber, F. R., Forbes, R. B., and Brabb, E. E., 1973, Regional geology of the Yukon-Tanana Upland, Alaska, in Pitcher, M. G., ed., Arctic geology: American Association of Petroleum Geologists Memoir 19, p. 388-395.

Labotka, T. C., 1981, Petrology of an andalusite-type regional metamorphic terrane, Panamint Mountains, California: Journal of Petrology, v. 22, no. 2, p. 261-296.

Laird, Jo, 1980, Phase equilibria in mafic schist from Vermont: Journal of Petrology, v. 21, no. 1, p. 1-37.

Rice, J. M., 1980, Phase equilibria involving humite minerals in impure dolomitic limestones, part I: Calculated stability of clinohumite: Contributions to Mineralogy and Petrology, v. 71, no. 3, p. 219-235.

Smith, J. V., 1972, Critical review of synthesis and occurrence of plagioclase feldspars and a possible phase diagram: Journal of Geology, v. 80, no. 5, p. 505-525.

Winkler, H. G. F., 1979, Petrogenesis of metamorphic rocks (5th ed.): New York, Springer-Verlag, 348 p.

Amphibole eclogite in the Circle quadrangle, Yukon-Tanana Upland, Alaska

By Jo Laird, Helen L. Foster, and Florence R. Weber

Petrographic and electron-microprobe analyses of a sample of mafic schist collected north of Twin Buttes, Circle A-6 quadrangle, Yukon-Tanana Upland (area 11, fig. 23; fig. 33), show it to be eclogite near the boundary of Groups B and C of Coleman and others (1965). Estimated conditions of metamorphism are 600°±50°C and 1.35±0.15 GPa. This eclogite is on strike with that reported by Swainbank and Forbes (1975) from the nearby Fairbanks district (fig. 33).

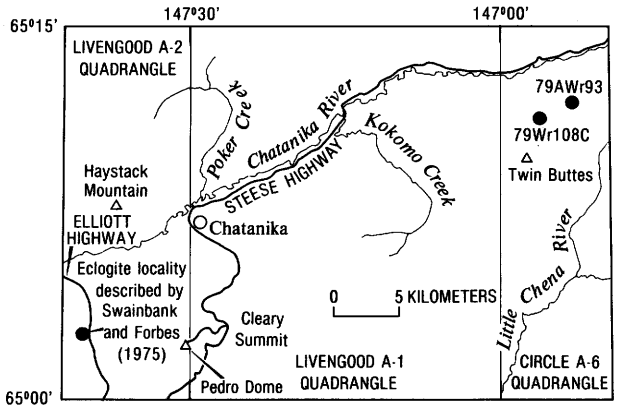

Figure 33.—Eclogite localities in eastern part of Livengood (A-2) quadrangle and western part of Circle (A-6) quadrangle.

The sample studied (79AWr108C, fig. 33) is from a mafic layer within quartz+white mica+garnet (somewhat retrograded to chlorite) schist and quartzite. Where the contact is visible, the foliation has the same orientation in both the mafic and pelitic layers, which appear to have been metamorphosed together. The mafic layer cuts across the foliation and is more massive in the interior, an observation suggesting that its protolith was a dike.

In general, the mafic layer is medium grained, medium green, massive to foliated, containing medium-green pyroxene, dark-blue-green amphibole, reddish-brown garnet porphyroblasts as large as 3 mm across, quartz, a pale-yellow epidote-group mineral, white mica, and gold-colored sulfides. Similar rocks occur as rubble on the adjacent ridges to the west and east.

Petrographically the sample is composed (in estimated modal percent) of: garnet (25), clinopyroxene (25), quartz (20), clinoamphibole (10), clinozoisite (10), white mica (10), rutile (1), and sulfide (trace). The clinopyroxene is colorless and is surrounded and cut by cryptocrystalline material that may be similar to the symplectite described by other workers as an alteration product of eclogitic omphacite. Amphibole shows colorless to pale-blue-gray pleochroism except in a few places next to garnet, where a colorless to

blue-green pleochroic rim is developed. Elongate grains of white mica, pyroxene, clinozoisite, and amphibole define a weak foliation. Garnet occurs as subhedral to euhedral porphyroblasts and commonly contains inclusions of rutile, quartz, white mica, and clinozoisite. Quartz is strained.

Table 13 lists representative analyses by electron microprobe, as well as operating conditions and assumptions used for normalizing each mineral to a structural formula. Figure 34 plots the compositional ranges for amphibole (AMP), garnet (GAR), and pyroxene (PYX).

The PYX is omphacite, ranging from $jd_{45}wo_{26}en_{22}fs_6cats_1$ to $jd_{40}ac_7wo_{25}en_{23}fs_2cats_3$. Grains are somewhat acmite richer toward their margins. Pale-blue-gray pleochroic AMP is barroisite to alumino-barroisite. Minor zoning toward Al^{IV}- and Al^{VI}-poorer margins is noted. The most aluminous interior composition has the formula: $(Na_{0.16}K_{0.07})(Ca_{1.28}Na_{0.72})-(Mg_{2.76}Mn_{0.01}Fe^{2+}_{0.65}Fe^{3+}_{0.53}Cr_{0.01}Ti_{0.04}Al_{1.02})-(OH)_{1.86}$, and the least aluminous edge composition has the formula: $(Na_{0.19}K_{0.03})(Ca_{1.20}Na_{0.80})-$

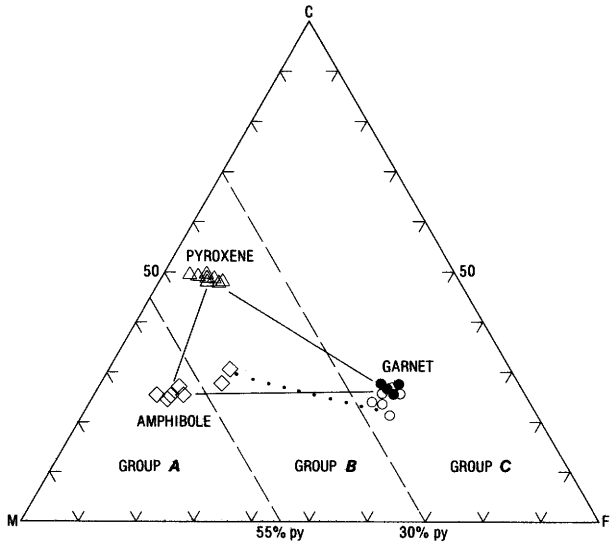

Figure 34.--Electron-microprobe analyses (in mole percent) of amphibole (AMP), garnet (GAR), and pyroxene (PYX) in sample 79AWr108c (fig. 33). Solid tielines connect coexisting compositions probably representing peak of metamorphism; dotted tieline shows coexisting compositions of late-stage amphibole rims in contact with Ca-poor edges of GAR. Dashed lines at 30 and 55 percent pyrope (py) divide GAR compositions into groups A, B, and C eclogites as defined by Coleman and others (1965). Dots, interior compositions of GAR. F=al+sp in GAR, fs+mn in PYX, and Fe^{2+}+Mn in AMP; C=gr+an+uv in GAR, wo in PYX, and Ca in AMP. M=py in GAR, en in PYX, and Mg in AMP. Mn and Cr contents of all analyses are minor (see table 13).

Table 13.--Eclogite compositional data determined by electron-microprobe analyses of amphibole (AMP), muscovite (MUS), clinozoisite (CZO), pyroxene (PYX), and garnet (GAR) in sample 79AWr108C

[Wavelength-dispersive analyses obtained with a CAMECA model MBX electron microprobe with Tracor Northern model TN-1310 automation, converted to weight percent by the Bence and Albee (1968) technique, using Albee and Ray (1970) correction factors. Accelerating voltage, 15 kV; sample current, 12 nA on brass; spot size, 19 μm for MUS and 1 μm for other minerals. n.d., not determined. PYX normalized to 4 total cations, GAR and CZO to 8 total cations, and AMP and MUS to 13 and 6 total cations less (Na+K+Ca), respectively. Al^{IV}, Al^{VI}, and Na^{VIII}, and Na^{XII} assigned from assumed stoichiometry. Fe^{2+} and Fe^{3+} estimated from assumed charge balance, according to the method of Laird and Albee (1981, app. 1). Na^{VIII} refers to the M4 and M2 sites in AMP and PYX, respectively; Na^{XII} refers to the A site in AMP and the 12-fold site in MUS. End members in mole percent, assigned sequentially downward from structural formulas; other ratios in atomic percent]

Mineral	AMP	AMPrim	MUS	CZO	PYX	GAR
Point	A0301	D2401	A1201	A0102	A0202	A1003
Major- and minor-element analyses						
SiO_2	49.46	42.57	48.50	38.35	55.64	38.70
Al_2O_3	12.86	15.45	28.53	31.62	11.14	21.91
TiO_2	.29	.23	.39	.08	0.11	.04
Cr_2O_3	.01	0	.04	.02	0.06	.04
Total Fe (as FeO)	7.92	12.71	1.69	1.93	3.81	23.97
MnO	.05	.15	.03	.03	0.04	.46
MgO	14.01	10.63	2.74	.04	8.42	5.89
CaO	8.24	9.39	0	24.21	13.62	9.26
Na_2O	3.75	3.24	.98	n.d.	6.70	n.d.
K_2O	.39	.60	9.17	n.d.	n.d.	n.d.
F	.21	0	.13	n.d.	n.d.	n.d.
Cl	0	.12	.02	n.d.	n.d.	n.d.
Anhydrous total	97.19	95.09	92.22	96.27	99.53	100.28
Structural formulas						
Si	6.96	6.32	3.31	2.97	1.98	2.98
Al^{IV}	1.04	1.68	.69	.03	.02	.02
Al^{VI}	1.09	1.02	1.60	2.85	.45	1.98
Ti	.03	.03	.02	.004	.003	.002
Cr	.002	0	.002	.001	.002	.003
Fe^{3+}	.31	.57	.05	.13	.02	.03
Fe^{2+}	.62	1.01	.05	0	.09	1.51
Mn	.006	.02	.002	.002	.001	.03
Mg	2.94	2.35	.28	.005	.45	.68
Ca	1.24	1.49	0	2.01	.52	.77
Na^{VIII}	.76	.51	---	---	.46	---
Na^{XII}	.26	.43	.13	---	---	---
K	.07	.11	.80	---	---	---
F	.09	0	.03	---	---	---
Cl	0	.03	.002	---	---	---
End members						
$NaFeSi_2O_6$ (ac)					2.3	---
$NaCrSi_2O_6$ (ur)					.2	---
$NaAlSi_2O_6$ (jd)					43.8	---
$Mg_2Si_2O_6$ (en)					22.4	---
$Fe_2Si_2O_6$ (fs)					4.5	---
$Mn_2Si_2O_6$ (mn)					.1	---
$CaTiAl_2O_6$ (Ti cats)					.3	---
$CaAlSiAlO_6$ (cats)					1.2	---
$Ca_2Si_2O_6$ (wo)					25.3	---
$Mg_3Al_2Si_3O_{12}$ (py)						22.7
$Fe_3Al_2Si_3O_{12}$ (al)						50.7
$Mn_3Al_2Si_3O_{12}$ (sp)						1.0
$Ca_3Cr_2Si_3O_{12}$ (uv)						.1
$Ca_3Fe_2Si_3O_{12}$ (an)						1.7
$Ca_3Al_2Si_3O_{12}$ (gr)						23.8
Other ratios						
K/(K+Na+Ca)			86.0			
Na/(K+Na+Ca)			14.0			
$Al^{VI}/(Al^{VI}+Fe^{3+}+Ti+Cr)$				95.6		
$Fe^{3+}/(Al^{VI}+Fe^{3+}+Ti+Cr)$				4.2		
$Ti(Al^{VI}Fe^{3+}+Ti+Cr)$				.2		

$(Mg_{3.09}Fe^{2+}_{0.69}Fe^{3+}_{0.21}Ti_{0.01}Al_{0.98})Si_{7.34}Al_{0.66})$-$O_{22}F_{0.11}(OH)_{1.89}$. Blue-green pleochroic rims are distinguished by enrichment in Fe^{2+}, Fe^{3+}, and Ca (table 13), and compositions range from magnesiohornblende to tschermakitic hornblende.

GAR becomes slightly less calcic toward the grain margins (fig. 34). The least calcic composition, represented by the formula $Fe^{2+}_{1.54}Mg_{0.75}Mn_{0.03}$-$Ca_{0.63}Al_{1.98}Fe^{3+}_{0.06}Si_{2.95}Al_{0.05}O_{12}$, is from the edge of a grain at its contact with a blue-green pleochroic AMP rim. The $Fe^{3+}/(Al^{VI}+Fe^{3+}Ti+Cr)$ ratio in clinozoisite (CZO) is small and ranges from 3.0 to 4.5 atom percent. White mica is muscovite showing considerable phengite substitution. The K/(K+Na+Ca) ratio ranges from 81.6 to 86.0 atom percent, and the Ca/(K+Na+Ca) ratio is no more than 0.9 percent.

On the basis of GAR composition (fig. 34), this eclogite falls within group C (eclogites from alpine-type orogenic terranes) of Coleman and others (1965) but is near the "contact" with group B (eclogite from gneiss and migmatite terranes). Coexisting GAR and omphacite compositions are also comparable to those at the group C/group B boundary (compare fig. 34 with Coleman and others, 1965, fig. 11). On the basis of omphacite composition, the eclogite is similar to eclogites from high-pressure metamorphic terranes, whereas the distribution of Fe^{2+}/Mg between GAR and PYX suggests amphibolite- or granulite-facies terranes (Miyashiro, 1973, figs. 12-4, 12-5).

The occurrence of biotite+feldspar+quartz+garnet+white mica gneiss (sample 79AWr93, fig. 33) associated with eclogite-appearing rubble suggests group B affinities. Further petrographic and electron-microprobe studies of the mineralogic variations in the eclogitic rocks represented and in the associated pelitic and felsic rocks are planned to test this hypothesis.

Figure 35 illustrates our best estimate of the pressure (P) and temperature (T) of metamorphism on the basis of the experimental data presently available. The omphacite+quartz assemblage constrains P to above the jd_{45} isopleth for the reaction albite=jadeite+quartz. T is constrained by the Fe^{2+}/Mg distribution between GAR and PYX but must be less than the high T estimates from the Ellis and Green (1979) calibration because the eclogite appears to be intercalated with pelitic schist, which would have partially melted if T were above that of the reaction muscovite+K-feldspar+albite+quartz+vapor = liquid—just above 600°C for these pressures (Thompson and Algor, 1977, fig. 8). Using the muscovite-paragonite solvus of Eugster and others (1972) gives a minimum T of about 530°C, but the magnitude of the effect of phengite substitution on this solvus is unknown.

The only eclogites previously described from the Yukon-Tanana Upland are group C eclogites (Swainbank and Forbes, 1975) in the Fairbanks district, about 39 km southwest of the eclogite locality near Twin Buttes (fig. 33). These Fairbanks district eclogites are distinct from the sample studied in that: (1) Their GAR is almandine richer but pyrope poorer; (2) their PYX is jadeite poorer, and $K_D=(Fe^{2+}/Mg)_{GAR/PYX}$ is greater; (3) their AMP is less aluminous and sodic and is calcic rather than sodic-calcic; and (4) calcite, plagioclase, and sphene occur in some samples. Differences 1 through 3 suggest metamorphism at lower T and P for the Fairbanks eclogites, which is consistent with the estimates of 540° to 590°C and 0.55 to 0.75 GPa by Swainbank and Forbes (1975).

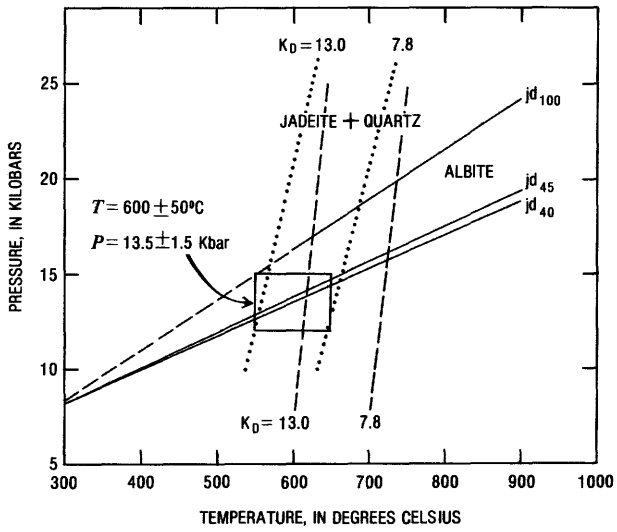

Figure 35.—Estimated pressure (P) and temperature (T) (within box) of metamorphism for sample 79AWr108c (fig. 33). P,T stability for reaction albite=jadeite+quartz is from Holland (1980). jd_{40} and jd_{45} isopleths, representing minimum and maximum jadeite contents observed in omphacite, calculated from model of Holland (1979, 1980). Lines of constant $K_D=Fe^{2+}/Mg)_{GAR/PYX}$, representing minimum and maximum values observed, extrapolated from Raheim and Green (1974) (dotted lines) and Ellis and Green (1979) (dashed lines).

Whole-rock analyses of the Fairbanks district eclogites indicate sedimentary protoliths. However, the distinction in mineral assemblage (difference 4) and the field relations suggest that an igneous protolith is more probable for the eclogite near Twin Buttes.

Swainbank and Forbes (1975) suggested that the Fairbanks district eclogite terrane is a tectonic window. Occurrence of brecciated rocks about 1.6 km south of the eclogite and associated pelitic schist and quartzite near Twin Buttes suggests a possible tectonic contact with the pelitic, mafic, and calc schist and quartzite to the south. Fairly good preservation in the sample from near Twin Buttes except for formation of cryptocrystalline material around the PYX and blue-green rims on the AMP (possibly associated with Tertiary plutonism) suggests that this eclogite was exhumed quickly. More detailed mapping and petrologic study are required to test this hypothesis, to determine the relation of this eclogite and associated rocks to adjacent metamorphic terranes, including that of the Fairbanks district, and to further assess its geologic implications.

REFERENCES CITED

Albee, A. L., and Ray, Lily, 1970, Correction factors for electron probe microanalysis of silicates, oxides, carbonates, phosphates, and sulfates: Analytical Chemistry, v. 42, no. 12, p. 1408-1414.

Bence, A. E., and Albee, A. L., 1968, Empirical correction factors for the electron microanalysis of silicates and oxides: Journal of Geology, v. 76, no. 4, p. 382-403.

Coleman, R. G., Lee, D. E., Beatty, L. B., and Brannock, W. W., 1965, Eclogites and eclogites: Their differences and similarities: Geological Society of America Bulletin, v. 76, no. 5, p. 483-508.

Ellis, D. J., and Green, D. H., 1979, An experimental study of the effect of Ca upon garnet-clinopyroxene Fe-Mg exchange equilibria: Contributions to Mineralogy and Petrology, v. 71, no. 1, p. 13-22.

Eugster, H. P., Albee, A. L., Bence, A. E., Thompson, J. B., Jr., and Waldbaum, D. R., 1972, The two-phase region and excess mixing properties of paragonite-muscovite crystalline solutions: Journal of Petrology, v. 13, no. 1, p. 147-179.

Holland, T. J. B., 1979, Reversed hydrothermal determination of jadeite-diopside activities [abs.]: Eos (American Geophysical Union Transactions), v. 60, no. 18, p. 405.

———1980, The reaction albite=jadeite+quartz determined experimentally in the range 600-1200°C: American Mineralogist, v. 65, no. 1-2, p. 129-134.

Laird, Jo, and Albee, A. L., 1981, High-pressure metamorphism in mafic schist from northern Vermont: American Journal of Science, v. 281, no. 2, p. 97-126.

Miyashiro, Akiho, 1973, Metamorphism and metamorphic belts: New York, Wiley, 492 p.

Raheim, Arne, and Green, D. H., 1974, Experimental determination of the temperature and pressure dependence of the Fe-Mg partition coefficient for coexisting garnet and clinopyroxene: Contributions to Mineralogy and Petrology, v. 48, no. 3, p. 179-203.

Swainbank, R. C., and Forbes, R. B., 1975, Petrology of eclogitic rocks from the Fairbanks district, Alaska, in Forbes, R. B., ed., Contributions to geology of the Bering Sea Basin and adjacent regions: Geological Society of America Special Paper 151, p. 77-123.

Thompson, A. B., and Algor, J. R., 1977, Model systems for anatexis of pelitic rocks; I. Theory of melting reactions in the system $KAlO_2$-$NaAlO_2$-Al_2O_3-SiO_2-H_2O: Contributions to Mineralogy and Petrology, v. 63, no. 3, p. 247-269.

Paleozoic limestones of the Crazy Mountains and vicinity, Circle quadrangle, east-central Alaska

By Helen L. Foster, Florence R. Weber, and J. Thomas Dutro, Jr.

The Crazy Mountains, in the northern part of the Circle quadrangle (area 9, fig. 23), could have been named by a geologist because of their numerous geologic puzzles. The many prominent limestone outcrops are among the enigmas to be solved.

Steep-sided light-colored limestone outcrops are visible across the landscape of both the eastern and western Crazy Mountains for many kilometers. One limestone unit in the eastern Crazy Mountains can be traced from a fairly broad outcrop area in the east,

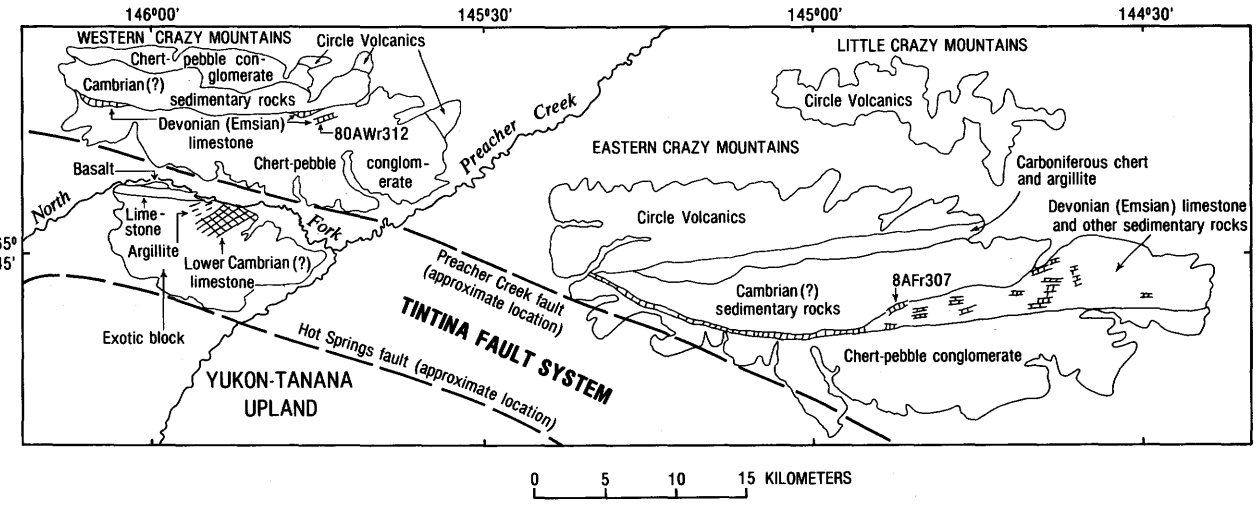

Figure 36.—Sketch map showing sample localities and numbers and location of Emsian limestone and associated sedimentary rocks and Lower Cambrian(?) limestone in vicinity of the eastern Crazy Mountains, Circle quadrangle, Alaska.

westward into a narrow band that extends cross country along a nearly straight course for more than 19 km (fig. 36). In the western Crazy Mountains, similar-appearing limestone occurs in several outcrops, possibly isolated by faulting or erosion.

Most of the large outcrops (fig. 37) in the eastern Crazy Mountains weather gray and are of medium-light-gray to medium-gray limestone with yellowish-brown mottling. A minor amount of dark-gray limestone occurs locally, and a few dark-gray smooth-surfaced dolomite beds are interlayered. The limestone is fine grained with incipient recrystallization; it is generally massive but may be thin bedded locally. Commonly, small white calcite veins and veinlets lace the outcrop. The limestone generally has a spongy-appearing solution-pitted surface; rillenstein and other small solution features occur.

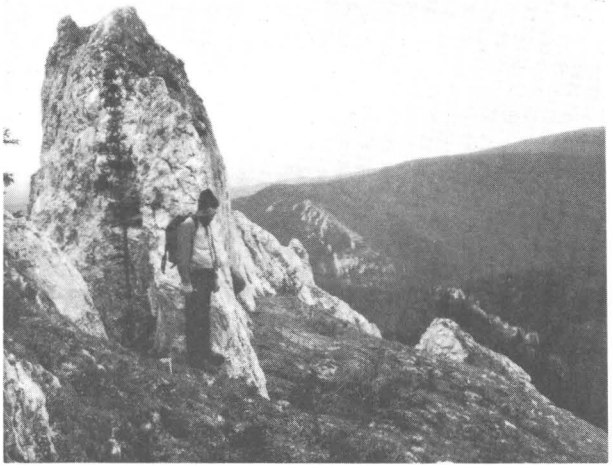

Figure 37.—Typical outcrop of Emsian limestone in the eastern Crazy Mountains. View westward.

At two localities, corals that were collected in 1980 suggest an Early Devonian age. These corals were identified by W. A. Oliver, Jr., who reported from one locality: "80A Fr 307 (USGS 10314-SD), sec. 8, T. 10 N., R. 14 E.; Circle C-2 quadrangle. Alveolites sp., Favosites sp., Pachyfavosites sp., Striatopora sp. (in the sense of Oliver and others, 1975, pl. 10), Thamnopora sp., Martinophyllum sp., and cf. Taimyrophyllum sp." Oliver reported a Siegenian-early Eifelian age range for the corals, indicating that closely related species of Martinophyllum and cf. Spongonaria are Emsian.

Also present are indeterminate bryozoans and the two-holed crinoid ossicle Gasterocoma bicaula Johnson and Lane. J. T. Dutro , Jr., indicated an Emsian-early Eifelian agerange for the distinctive crinoid ossicle; the consensus is that the most likely age is Emsian (late Early Devonian). An Emsian age is also supported by data from conodonts (Anita Harris, oral commun., 1981). Fieldwork in 1981 shows that much of the limestone in the eastern Crazy Mountains, on trend with locality 10314-SD, contains the two-holed crinoids and that the entire outcrop belt may reasonably be dated by this collection as probable Emsian.

Another collection, 80A Wr 312 (USGS 10315-SD), to the west in the Circle D-4 quadrangle, western Crazy Mountains (fig. 36), contains, according to Oliver: Amphipora, Striatopora, Syringopora, cf. Pseudoplasmopora, and cf. Spinolasma. This collection is also Early Devonian but may be slightly older than collection 10314-SD. Conodonts also indicate a slightly older age for this limestone (Anita Harris, oral commun., 1981).

The stratigraphic and structural relations of the rocks adjoining the limestone are unclear. In the eastern Crazy Mountains, the limestone, on the south, has a covered contact with a thick coarse chert-pebble conglomerate of unknown age and attitude. To the north, the limestone lies in apparently unconformable (covered) contact with a sequence of rocks including a thick very dark gray, nearly black arenaceous limestone, olive, green, maroon, and gray argillite, a few thin beds of chert, and a thick section of quartzite and siltstone. Olive argillite has yielded the Early Cambrian trace fossil Oldhamia (Churkin and Brabb, 1965). The nature of both the north and south contacts of this limestone is uncertain, and neither unconformities nor fault contacts completely satisfy the mapped geologic relations.

Faunal evidence for post-Devonian rocks in the main part of the Crazy Mountains is absent, except for the occurrence of late Paleozoic and early Mesozoic radiolarians (D. L. Jones and others, written commun., 1981) in chert associated with mafic igneous rocks that crop out in the northern part of the study area and are included in the Circle Volcanics (Mertie, 1937).

A different sequence of limestone and clastic rocks crops out on the south bank of the North Fork of Preacher Creek, just south of the western Crazy Mountains. In exposures along the high bluff, about 300 m of massive-appearing bedded limestone contains pisolites, spongelike bodies, and possible archaeocyathids. This limestone weathers medium gray and is cream colored on some vertical surfaces; it is generally medium gray on fresh surfaces and is fine grained but mostly recrystallized. The limestone beds are 2.5 to 30 cm thick. Medium-gray very fine grained limy mudstone, some of which is finely laminated with millimeter-thick tan-colored siliceous layers, is locally interbedded. Thin bands of black chert nodules or lenses also occur, but they are rare. Stylolites are present in some of the very fine grained limy mudstone.

This limestone, on the west side, is in probable fault contact with red and green argillite, dark-gray to black limestone, dolomite, and basalt, including pillow basalt. Its lithology and possible faunal content suggest a correlation with the Lower Cambrian Funnel Creek limestone of the Tatonduk River area (Brabb, 1967). The adjacent rocks have lithologies suggestive of part of the Tindir Group (Proterozoic). Although these rocks include maroon and green argillite, they are unlike any other lithologic sequence seen in the Yukon-Tanana Upland. The block containing this unusual group of rocks appears to be exotic: it might have moved in from the southeast, possibly caught up between two fault strands of the Tintina fault system (fig. 36).

More detailed geologic mapping, stratigraphic work, and fossil collecting must be done before the puzzling stratigraphy and structure are unraveled, but a start has been made in deciphering the complex geologic relations in the Crazy Mountains.

REFERENCES CITED

Brabb, E. E., 1967, Stratigraphy of the Cambrian and Ordovician rocks of east-central Alaska: U.S. Geological Survey Professional Paper 559-A, p. A1-A30.

Churkin, Michael, Jr., and Brabb, E. E., 1965, Occurrence and stratigraphic significance of Oldhamia, a Cambrian trace fossil, in east-central Alaska, in Geological Survey research 1965: U.S. Geological Survey Professional Paper 525-D, p. D120-D124.

Mertie, J. B., Jr., 1937, The Yukon-Tanana region, Alaska: U.S. Geological Survey Bulletin 872, 276 p.

Oliver, W. A., Jr., Merriam, C. W., and Churkin, Michael, Jr., 1975, Ordovician, Silurian, and Devonian corals of Alaska: U.S. Geological Survey Professional Paper 823-B, p. 13-44.

Late Paleozoic and early Mesozoic radiolarians in the Circle quadrangle, east-central Alaska

By Helen L. Foster, Grant W. Cushing, Florence R. Weber, David L. Jones, Benita Murchey, and Charles D. Blome

Late Paleozoic and early Mesozoic radiolarians have been found in slightly metamorphosed chert north of the Tintina fault system in the Circle quadrangle (area 8, fig. 23). During the course of reconnaissance geologic mapping, 32 chert samples were collected. Subsequently processed to determine their radiolarian content, 11 samples yielded radiolarians whose age could be determined, and 16 other samples contained radiolarians that were either nondiagnostic or too poorly preserved for identification. Most of the samples containing identified radiolarians, which were from areas mapped as the Circle Volcanics (Mertie, 1937) in the northern part of the eastern Crazy and Little Crazy Mountains, indicate that these rocks include chert of two distinct ages—Late Mississippian or Early Pennyslvanian, and Middle and Late Triassic. Thus, the age of the Circle Volcanics is here considered to be late Paleozoic and Triassic.

Radiolarians were identified from chert samples associated with mafic igneous rocks included in the Circle Volcanics (Mertie, 1937). These samples are from several localities on the Yukon River, in the eastern Crazy Mountains, and in the Little Crazy Mountains (fig. 38). Along the east bank of the Yukon River in the Circle C-1 quadrangle (locs. 1, 2, fig. 38, Area A), the radiolarian chert is interlayered with fine-grained basalt. Underlying the basalt and chert is a sequence of layered gabbro with alternating plagioclase-rich and plagioclase-poor layers. The chert contained "Spongodiscaceid gen. nov. (tetrahedral)" (Holdsworth and Jones, 1980) and "Parahagiastriids" (Holdsworth and Jones, 1980), which indicate a latest Mississippian or Early Pennsylvanian age.

In the central part of the eastern Crazy Mountains, radiolarian chert occurs in a 1.5-km-wide easterly trending band that lies north of arenite, argillite, and black arenaceous limestone of Cambrian(?) age (fig. 38, area A). Although black chert appears to be the dominant rock type in this band, the radiolarians are found in interlayered gray chert. Locally the chert is finely banded, light and medium gray and black; gray argillite occurs in at least one locality. At the westernmost radiolarian locality (80AWr91C) in this band, the fossils are Albaillella sp. (an undescribed Late Mississippian species) and Paronaella impella Ormiston and Lane, which are considered Late Mississippian. At a second locality to the east (80AWr272) the chert contains "Spongodiscaceid gen. nov. (tetrahedral)" (Holdsworth and Jones, 1980), which is considered to be latest Late Mississippian or Early Pennsylvanian. Two other localities (80AFr2084, 80AWr279A) in this band yield very poorly preserved Spumellariina, the age of which is uncertain, but may be Carboniferous. These radiolarians help define this band of Carboniferous(?) chert, which appears to lie beyond the south boundary of mafic intrusive and volcanic rocks comprising the Circle Volcanics. Because of poor exposures and covered contacts, the relation of these chert units to the Circle Volcanics to the north is not known, although they may be part of the Circle Volcanics. A thrust fault is postulated to separate this Carboniferous(?) chert unit from the lower Paleozoic sedimentary rocks farther to the south.

To the north of the band of Carboniferous(?) rocks just described, chert is found in contact with gabbro and basalt (Circle Volcanics). The radiolarians in these rocks (locs. 7, 8, fig. 38, Area A) are not yet described but are recognized as Late Triassic.

In the Little Crazy Mountains, basalt and gabbro similar to that of the eastern Crazy Mountains has minor amounts of chert in contact with it. Most of the chert layers are thin and discontinuous. The color is dominantly gray, but red and black chert also are found; the gray chert commonly weathers white or very light gray. In the eastern part of the Little Crazy Mountains, radiolarians were found in a sequence of gray and bleached white ribbon chert, with layers of chert ranging from 2 to 18 cm in thickness but averaging about 5 cm. A section of about 2.5 m of chert is exposed here, and the outcrop is about 170 m long, the largest outcrop of chert seen in the Little Crazy Mountains. Chert collected from the top of the sequence (loc. 9, sample number 81AFr223D) contains Paronaella impella Ormiston and Lane, Albaillella sp., and Spongotripus sp; the chert at the base of the sequence 2.5 m below (loc. 9, sample number 81AFr223E) contains Paronaella impella Ormiston and Lane. These radiolarians indicate that chert of this outcrop is most likely Late Mississippian.

A chert outcrop (loc. 10) about a kilometer west of locality 9 (fig. 38, Area A) contains Capnodoce sp. aff. C. anapetes DeWever, Capnodoce sp., ?Canoptum sp., and Quasipetasus sp,. which indicate a Late Triassic (late Karnian to Middle Norian) age. Chert in the eastern part of the Little Crazy Mountains 12 km to the east (loc. 81AFr228B) contains ?Archaeospongoprunum japonicum Nabaseko and Nishimura, Triassocampe sp., and other undescribed spumellariinids. A Middle Triassic (Ladinian) and Late Triassic (early Karnian) age is indicated for this chert.

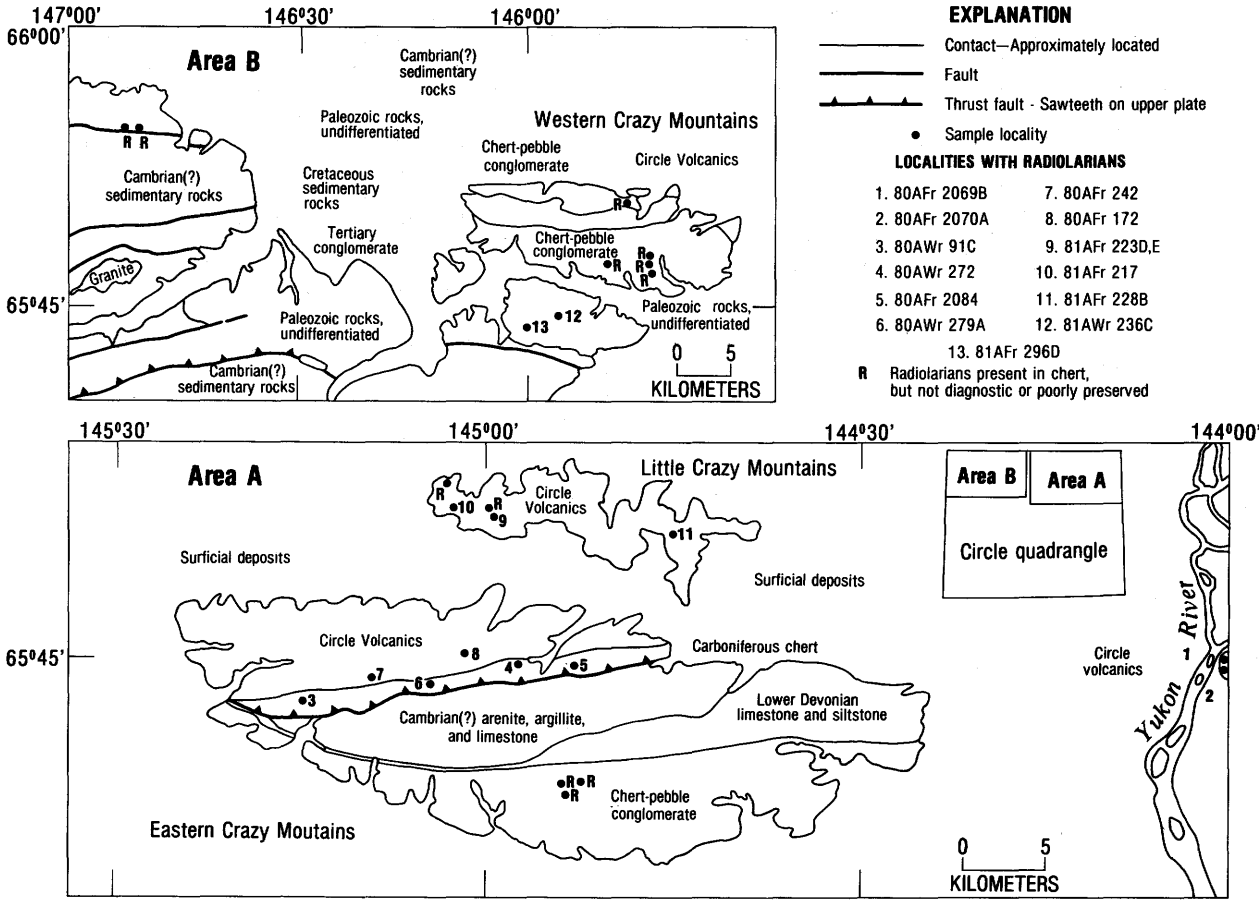

Figure 38.—Geologic maps showing radiolarian-chert localities in two areas in northern part of the Circle quadrangle.

Thus, the Crazy Mountains and the Little Crazy Mountains have chert bearing both Mississippian and Triassic radiolarians. The chert units of both ages are similar in appearance and in their relation to the basalt and gabbro with which they are associated; and the igneous rocks, though as yet little studied, do not display any easily observable lithologic differences, and radiometric-age determinations for them are unavailable. At present, the two chert units and related mafic igneous rocks within the Circle Volcanics are not separately mappable.

Nondiagnostic radiolarians were found in the chert in the Circle C-4 quadrangle south of the Crazy Mountains (loc. 12, sample number 81AWr236C, fig. 38, Area B). The common occurrence of some of the undescribed spumellariinids in this sample in Mississippian chert suggests a Mississippian age for these. A second locality (loc. 13, sample number 81AFr296D) 2 km to the southwest of locality 12 has only nondiagnostic poorly preserved spumellariinids. This chert is also associated with mafic igneous rocks and a complex section of sedimentary rocks (Foster and others, 1983). Radiolarians that are either nondiagnostic or too poorly preserved to identify are also found in three localities in the southern part of the eastern Crazy Mountains, at five localities in the western Crazy Mountains, and at two localities in the Circle D-6 quadrangle.

Because of the scarcity of fossils in the Circle quadrangle, identification of radiolarians from chert is of major significance in deciphering the geologic relations and history, particularly of the Crazy Mountains and Little Crazy Mountains areas. The radiolarians from the Circle Volcanics along the Yukon River and in the Little Crazy Mountains indicate a terrane that includes at least two widely separated times of chert deposition—Late Mississippian or Early Pennsylvanian, and Middle and Late Triassic. Because these two groups of chert units within the Circle Volcanics and their associated igneous rocks cannot presently be distinguished from each other in the field and the relation of the Carboniferous(?) chert unit to the south is not known, the geology and history of this terrane require additional study.

REFERENCES CITED

Foster, H. L., Weber, F. R., and Dutro, J. T., Jr., 1983, Paleozoic limestones of the Crazy Mountains and vicinity, Circle quadrangle,

east-central Alaska, in Coonrad, W. L., and Elliott, R. L., eds., The United States Geological Survey in Alaska: Accomplishments during 1981: U.S. Geological Survey Circular 868, p. 60-62.

Holdsworth, B. K., and Jones, D. L., 1980, A provisional Radiolaria biostratigraphy, Late Devonian through Late Permian: U.S. Geological Survey Open-File Report 80-876, 32 p.

Mertie, J. B., Jr., 1937, The Yukon-Tanana region, Alaska: U.S. Geological Survey Bulletin 872, 276 p.

Structural observations in the Circle quadrangle, Yukon-Tanana Upland, Alaska

By Grant W. Cushing and Helen L. Foster

Folds and associated planar structures observed in the metamorphic rocks of the Circle quadrangle south of the Tintina fault (area 5, fig. 23) during the course of reconnaissance geologic mapping are being analyzed to help determine the deformational history of the metamorphic terrane of the Yukon-Tanana Upland. The study has concentrated on minor folds, ranging in wavelength and amplitude from a few centimeters to several meters, which are believed to be related to large-scale regional structures throughout most of the quadrangle.

The metamorphic terrane consists of interlayered quartzite, quartzitic schist, pelitic schist and gneiss, marble, amphibolite, and greenschist. These rocks range in metamorphic grade from middle greenschist to upper amphibolite facies. The protoliths were dominantly sedimentary rocks and probably Precambrian and (or) Paleozoic.

Four distinct deformational events are recognized in the metamorphic rocks on the basis of fold styles and the type and orientation of planar and linear features (fig. 39). The first recognized deformational event (D_1) produced a penetrative schistosity that is parallel or subparallel to gently dipping axial planes of rarely observed tight to isoclinal recumbent folds. This schistosity (S_1) commonly parallels compositional layering and is everywhere prevalent in the metamorphic rocks.

The folds associated with the second deformational event (D_2) are ubiquitous and vary considerably both in style and size. Fold styles range from tight to isoclinal recumbent and include rounded and chevron-fold hinges; folds range in amplitude and wavelength from microscopic to several meters. A second schistosity (S_2) has developed locally owing to mechanical rotation of the preexisting S_1 schistosity. In the pelitic rocks, this S_2 schistosity is observed only rarely, as an axial planar fabric, and in quartzite and carbonate rocks it is incipient to absent. The orientation of the S_2 schistosity is generally subhorizontal to horizontal and thus essentially parallels the S_1 fabric. At some fold hinges, these two schistosities can be differentiated; the folds associated with this second event deform the S_1 schistosity and compositional layering (fig. 39).

Several zones have been recognized throughout the quadrangle where folds of this generation (D_2) are particularly conspicuous; these zones are typically characterized by complexly folded large torlike outcrops. One such zone has been traced southwestward in the Circle B-4, B-5, and A-6 quadrangles; other, smaller zones have also been recognized in the higher grade rocks to the southeast. The fold styles and orientations of planar features in the highly folded zones do not significantly differ from those of rocks in the adjacent areas. A possible explanation for these highly folded zones is that they occur on the noses of large recumbent folds, where minor folds are abundant owing to thickening of the fold hinge. The less folded sections are on the limbs of large structures, where minor folds are less abundant and the gently dipping foliation results from the recumbence of large-scale folds. This interpretation does not preclude the possibility of tectonic movement between the lower limb and nose of the recumbent fold.

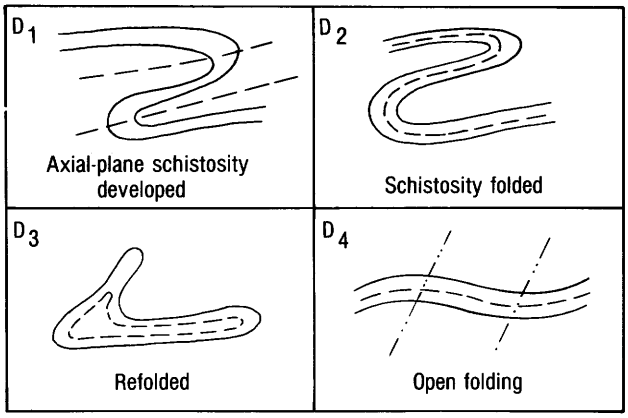

Figure 39.—Schematic representation of results of four deformational events in the Circle quadrangle, Alaska. Solid lines represent compositional layering, dashed lines show schistosity, dash and double dot lines indicate cleavage subparallel to axial plane of D_4 folds.

Structural features of a third deformational event (D_3) are difficult to distinguish from features of the D_2 event because the fold styles and orientations of axial planes are similar. The folds of the D_3 generation are recumbent, tight to isoclinal, and, where observed, have a horizontal or gently dipping axial plane. These folds, like D_2 folds, rarely have an axial-planar cleavage. Because the style of both the D_2 and D_3 folds are so similar, the two folds are distinguishable only in a few fortuitously oriented outcrops. Commonly, two sets of recumbent folds are observed, but their relative age cannot everywhere be determined. In one outcrop in the Circle B-2 quadrangle, one set of fold axes trend from N. 30° to 50° E. and plunge from 0° to 5° SW.; the other set of fold axes trend from N. 30° to 60° W., with no significant plunge.

In many outcrops, the D_3 deformational event is evidenced by convergent foliation surfaces, but very

few fold closures are preserved. In several places, the D_2 fold traces are deformed by the later D_3 folds, and the resulting interference forms are distinctive (fig. 39). In one locality in the Circle A-2 quadrangle, gneissic banding outlines a closed interference figure in two dimensions (fig. 40). This structure is situated in the nose of a recumbent D_2 fold. D_3 isoclinal folding is also suggested at this locality by foliation surfaces converging at a high angle to the axis of the recumbent fold. The angle between fold axes of the D_2 recumbent and D_3 isoclinal folds is interpreted to be between 60° and 110°. Ramsay (1962), in discussing the interference patterns produced by the superposition of folds of similar style, concluded that closed shapes are formed when the shear direction of the second fold is close to the axial plane of the first fold, as is the case just described in the Circle quadrangle.

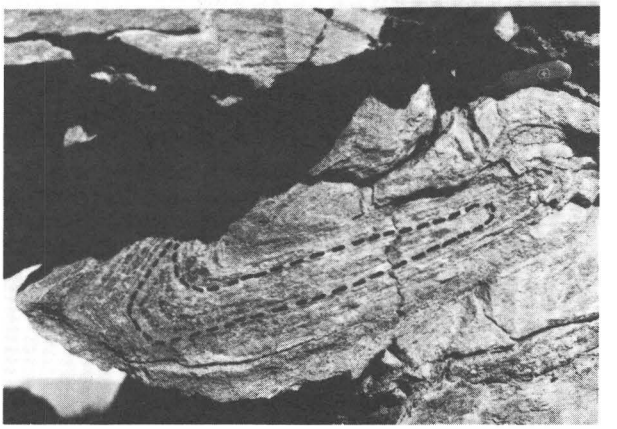

Figure 40.—Closed interference figure (dashed lines) formed by refolding of D_2 folds by third deformational event (D_3). Knife near upper right corner of photograph is approximately 8 cm long.

Structural features of the fourth deformational event (D_4) are characterized by gentle and open folds that deform all previous structures and range from open symmetric to asymmetric kink folds, with wavelengths and amplitudes generally less than 50 cm but as large as 5 m. The interlimb angle of these folds is generally greater than 120°, and they have a steeply dipping axial plane. Generally associated with the D_4 folds is a slip cleavage that is subparallel to the axial plane. D_4 folds are recognized in many localities throughout the Circle quadrangle but are not ubiquitous.

The minor folds and associated planar structures in this part of the Yukon-Tanana Upland are believed to be related to regional-scale recumbent folds. The widespread occurrence of such large recumbent folds explains the subhorizontal to gently dipping attitude of the foliation and compositional layering seen throughout the area. Although differences in intensity and apparent complexity of folding are observed, we tentatively conclude that the major metamorphic units in the quadrangle have undergone the same deformational events. Field observation and orientation diagrams suggest that recumbent D_2 folds are generally predominant, although in a few areas the D_3 recumbent folds may be most evident. For example, in the central part of the quadrangle the most conspicuous set of folds have northwesterly trending axes and are probably of the D_2 generation. In the southeastern part of the quadrangle, however, folds have northeasterly trending axes and may be of the D_3 generation. One explanation for such a local predominance of D_3 recumbent folds may be that the relative intensities of the two deformational events (D_2 and D_3) varied regionally.

REFERENCE CITED

Ramsay, J. G., 1962, Interference patterns produced by the superposition of folds of similar type: Journal of Geology, v. 70, no. 4, p. 466-481.

Gold in Tertiary(?) rocks, Circle quadrangle, Alaska

By Warren E. Yeend

Gold was panned from several deposits of Tertiary(?) conglomerate within the so-called Tintina fault zone in the Circle quadrangle (area 13, fig. 23). Although gold was previously recovered from Tertiary rocks in neighboring quadrangles (Mertie, 1938), none had been reported from Tertiary rocks of the Circle quadrangle.

Pink sandy conglomerate exposed on a tributary of Albert Creek and described by Weber and Foster (1982) has yielded several small "colors" in two separate pan samples. The poorly to moderately consolidated conglomerate and sandstone, which appear to dip as much as 55° SE., weather to hogbacks paralleling the northeastward strike. A pebble count (100 clasts) from the conglomerate produced: 44 of quartzite, including "quartz eye" quartzite; 37 of white quartz; 9 of weathered schistose quartzite; and 10 of chert. A thin layer of brown silt overlies what may be a pediment surface developed on the eroded tilted beds.

Rocks of possible Tertiary age are present near the south fault(?) boundary of the Tintina fault zone. They are exposed in a placer-mine pit near the junction of Crooked and Sawpit Creeks, and within a backhoe trench on the fan of Deadwood Creek near where the Hot Springs fault(?) crosses Deadwood Creek. The Tertiary(?) conglomerate on Crooked Creek is bright orange to orange brown, in marked contrast to the drab gray overlying gravel. The mining operator scrapes off the overlying 2 to 3 m of low-value gray gravel to mine this underlying unit. The gold values appear to be concentrated in pockets in the conglomerate; these pockets may be as large as 200 m^3 in volume and run as high as \$8/m^3 (\$400/troy oz). There are no nuggets; the gold is all fine, thin, and flaky. The conglomerate contains well-rounded cobbles of chert and quartzite as the primary rock types. The schist has been almost completely broken down by weathering. Zones exist where the cobbles are coated by a sooty black substance, probably a manganese-iron oxide.

Holes as much as 5 m deep within the weathered conglomerate have been dug by the miners, but the presence of large volumes of subsurface water makes mining difficult at this depth. One local miner stated that an early-day miner sank a shaft 25 m in the Tertiary(?) conglomerate without reaching its base. The conglomerate is truncated by a fault (Hot Springs fault?) near Crooked Creek.

Orange-brown clayey weathered (Tertiary?) conglomerate is exposed at the base of a backhoe trench excavated in the fan gravel of Deadwood Creek. Here, the Tertiary(?) conglomerate is overlain by about 2 m of silty gray-brown gold-bearing fan gravel. Clasts in the orange-brown material are generally 5 cm in diameter or smaller, composed of 90 to 95 percent weathered quartzite and schist and 5 to 10 percent quartz. A total of 12 gold "colors" were panned from a sample collected at the contact of the gray gravel with the underlying orange-brown conglomerate, and 2 "colors" were panned from the weathered conglomerate itself approximately 48 cm below this contact.

Although Tertiary(?) clastic rocks in the Circle quadrangle appear to be restricted to the Tintina fault zone, when initially deposited they probably covered areas beyond the fault zone. If so, these rocks most likely were a source for much of the gold occurring in the Holocene alluvium that has supplied the Circle district placer miners with a gold resource for more than 80 years.

REFERENCES CITED

Mertie, J. B., Jr., 1938, Gold placers of the Fortymile, Eagle, and Circle districts, Alaska: U.S. Geological Survey Bulletin 897-C, p. 133-261.

Weber, F. R., and Foster, H. L., 1982, Tertiary(?) conglomerate and Quaternary faulting in the Circle quadrangle, Alaska, in Coonrad, W. L., ed., The United States Geological Survey in Alaska: Accomplishments during 1980: U.S. Geological Survey Circular 844, p. 58-61.

Lacustrine and eolian deposits of Wisconsin age at Riverside Bluff in the upper Tanana River valley, Alaska

By L. David Carter and John P. Galloway

Riverside Bluff (loc. 4, fig. 23), a 40-m-high cutbank on the northeast side of the Tanana River near Riverside Lodge, about 50 km southeast of Tok (Tanacross A-3 quadrangle, lat 63°09'38" N., long 142°06'25" W.), is one of the few readily accessible localities in this area at which Quaternary deposits are both thick and well exposed. Part of the bluff was described by Fernald (1965a), but he did not identify lacustrine beds and could not directly date eolian deposits in the section. Here, we present two radiocarbon dates for the eolian part of the section as well as evidence that some of the bluff deposits are lacustrine in origin, and comment on the possible significance of these lacustrine beds to the late Quaternary history of the upper Tanana Valley.

The part of the bluff in which Quaternary deposits are well exposed extends from Bitters Creek downstream about 1.5 km. Fernald (1965a) described the bluff materials near Bitters Creek as consisting of 4.5 m of compacted sand, silt, and muck that is unconformably overlain by 24 m of fluvial sand and silt and some fine to coarse rubble. Overlying this fluvial material is 6 m of eolian sand, above which is as much as 6 m of alluvial-colluvial sand, silt, organic material, and fine rubble. Fernald (1965a, p. C122) reported radiocarbon ages of 1,520 to 6,200 years for the uppermost alluvial-colluvial materials, of 25,800 years in the upper part of the fluvial deposits, and of greater than 42,000 years on wood from the basal sand, silt, and muck. Fernald (1965a) proposed that the basal unit was deposited during the last or Sangamon Interglaciation and correlated the fluvial and overlying eolian deposits with the deposits of the Jatahmund Lake Glaciation, which he presumed to be equivalent to the entire Wisconsinan Stage. He equated the 25,800-year age to a Wisconsinan interstadial.

We examined the bluff about 1.25 km downstream from Bitters Creek, near where a small unnamed stream enters the Tanana River. Here, the silty sand to sandy silt that makes up the bluff deposits can be divided into 11 units on the basis of sedimentary structures (fig. 41). We correlate unit 1 with Fernald's (1965a) basal unit and agree that it is most likely of last interglacial age. Units 2 through 5 are probably equivalent to his overlying "fluvial" deposits, but we believe that a significant part of the deposits which we examined are lacustrine in origin. We correlate units 6 through 9 with Fernald's eolian deposits, and unit 10 with the alluvial-colluvial upper part of his section. The volcanic ash beneath the modern turf is probably the White River Ash Bed (Péwé, 1975), a widespread member of the Engineer Loess in east-central Alaska and the adjacent Yukon Territory that is about 1,400 years old.

The eolian part of the section is about 10 m thick and consists of dune slipface deposits with large-scale high-angle cross-stratification (units 7, 9) and of interdune-pond deposits composed of laminated silty sand (units 6, 8). Radiocarbon ages of 12,230±120 years (USGS-1037) and 11,880±180 years (I-11,704), determined on plant remains collected from the pond deposits, indicate that the eolian beds are late Wisconsinan, as Fernald (1965a) suggested, and agree well with radiocarbon ages of 12,400, 11,250, and 8,200 years obtained by Fernald (1965b) on organic materials associated with stabilized eolian sand at nearby localities in the upper Tanana Valley. Bedding attitudes in the dune-slipface deposits of N. 22° E., 27° SE., in unit 7 and of N. 17° E., 30° SE., in unit 9 indicate upvalley dune migration, as do the slipface orientations of stabilized dunes on top of the bluff and elsewhere in the upper Tanana Valley.

Our contention that lacustrine beds are present below the eolian deposits is based on sediment composition and structure. Units 2 and 5, which are 9 and 1.5 m thick, respectively, consist of silty sand containing angular granules and pebbles of locally derived schist and granite. Beds are a few centimeters to about 10 cm thick and exhibit tabular crossbedding, trough crossbedding, lenticular bedding, and minor horizontal bedding. Unit 3, which is 6 m thick, consists of sets that are each about 1 m thick. Each set generally contains a lower zone of laminated sand and silt as much as 0.5 m thick, and an upper zone of silty sand with tabular crossbedding. The laminae are of

even thickness and conform to irregularities in the bed on which they were deposited. These irregularities, which occur within the laminated zones, appear to be isolated ripples of coarser sand. We interpret the laminae to be draped lamination, as described by Gustavson and others (1975). The tops of sets are sometimes marked by one or more thin layers that contain angular granules and pebbles of schist and granite; some sets contain sand- or pebbly-sand-filled channels at their tops. Unit 4, also 6 m thick, consists of laminated to thin-bedded sand and silt, and contains a few zones of sinusoidal ripple marks (Jopling and Walker, 1968). As in unit 3, the laminae conform to bed irregularities and are here interpreted as draped lamination.

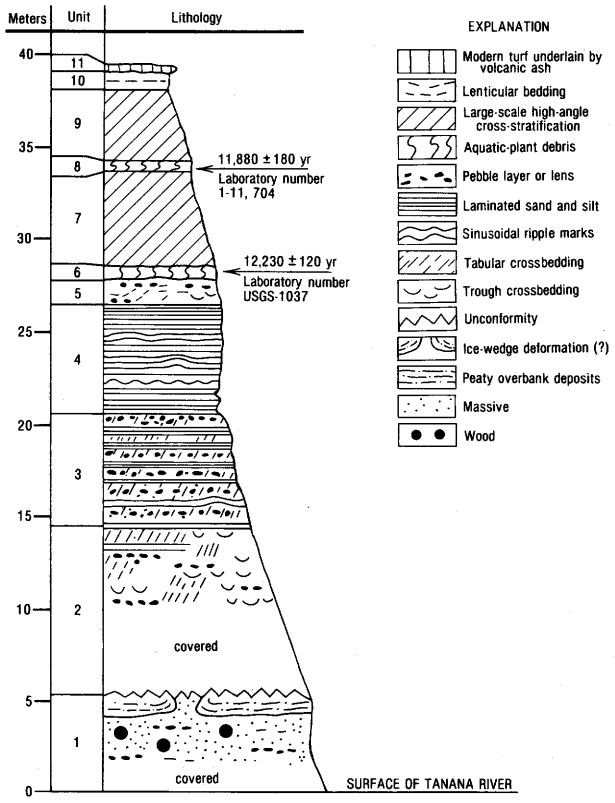

Figure 41.—Quaternary stratigraphic section and radiocarbon ages at Riverside Bluff.

Units 2 and 5 apparently contain only sediment transported by traction and are probably fluvial deposits. However, we believe that unit 4 is lacustrine, and unit 3 probably also. The sinusoidal ripple marks in unit 4 and the draped lamination in units 3 and 4 indicate deposition from suspension (Jopling and Walker, 1968; Gustavson and others, 1975), which can occur in a body of standing water or from overbank floodwaters. However, draped laminae deposited from floodwaters generally occur in the form of thin sets at the top of flood-formed sedimentation units that commonly include sediment which was transported as traction load. The thickness and uniformity of unit 4 strongly suggest deposition in a lake. In unit 3, the occurrence of the draped laminae at the base of individual sedimentation units is the reverse of the sequence to be expected in flood deposits; however, such an occurrence was reported in sediment deposited from density currents in glaciolacustrine deltas (Gustavson and others, 1975). Channels and thin layers of angular granules and pebbles at the tops of sedimentation units may represent rapid lowering of water level.

We found no organic remains of any kind in units 2 through 5 and believe that these deposits were formed entirely during a glacial episode. The last major glacial advance in the Alaska Range probably began about 25,000 years B.P. (Hamilton, 1982) and was separated from an early advance of the Wisconsin Glaciation by a long interstadial interval, the informally designated Boutellier interval (Hopkins, 1983), that began at least 49,000 years B.P. Therefore, we believe that units 2 through 5 are either about 25,000 years old or younger, or older than 49,000 years.

Because of the absence of organic materials, the lacustrine beds cannot be directly related to Fernald's (1965a) radiocarbon date of 25,800±800 years, although he reported that the material dated was fine organic debris collected 14 m below the top of the bluff and 6 m below the base of the eolian deposits. An equivalent position in our section would be in the middle or lower part of unit 4. Thus, the lacustrine beds may be about 25,000 or 26,000 years old. Although Fernald (1965a) related this age to interstadial conditions, it could as easily be related to the early phase of the late part of the Wisconsin Glaciation. Also, deposits of this age may simply not be present in the part of the bluff that we measured, and the lacustrine beds may be early Wisconsinan.

Although we are unsure of the regional significance of the lacustrine beds in the absence of further work, the features of the Tanana River valley downriver between Dot Lake and the Johnson River suggest a possible explanation for the occurrence of these beds. Here, in one of the narrowest parts of the valley, ice-scoured granitic bedrock is exposed across the Tanana River valley except for the part occupied by the modern river. Both sides of this part of the valley are steep and linear and appear to have been trimmed by ice. Thus, during at least one glacial episode, the flow of the Tanana River either was completely blocked or profoundly impeded by glacial ice. Such an event could create a large lake in the upper Tanana River valley, and we believe that the lacustrine beds exposed in Riverside Bluff record one or more large ice-dammed lakes.

REFERENCES CITED

Fernald, A. T., 1965a, Glaciation in the Nabesna River area, upper Tanana River valley, Alaska, in Geological Survey research 1965: U.S. Geological Survey Professional Paper 525-C, p. C120-C123.

——1965b, Recent history of the upper Tanana River lowland, Alaska, in Geological Survey research 1965: U.S. Geological Survey Professional Paper 525-C, p. C124-C127.

Gustavson, T. C., Ashley, G. M., and Boothroyd, J. C., 1975, Depositional sequences in glaciolacustrine deltas, in Jopling, A. V., and McDonald, B. C., eds., Glaciofluvial and glaciolacustrine sedimentation: Society of Economic Paleontologists and Mineralogists Special Publication 23, p. 264-280.

Hamilton, T. D., 1982, A late Pleistocene glacial chronology for the southern Brooks Range: Stratigraphic record and regional significance: Geological Society of America Bulletin, v. 93, no. 8, p. 700-716.

Hopkins, D. M., 1982, Aspects of the paleogeography of Beringia during the late Pleistocene, in Hopkins, D. M., Mathews, J. V., Jr., Schweger, C. E., and Young, S. B., eds., Paleoecology of Beringia: New York, Academic Press, p. 3-28.

Jopling, A. V., and Walker, R. B., 1968, Morphology and origin of ripple-drift cross-lamination with examples from the Pleistocene of Massachusetts: Journal of Sedimentary Petrology, v. 38, no. 4, p. 971-984.

Péwé, T. L., 1975, Quaternary stratigraphic nomenclature in unglaciated central Alaska: U.S. Geological Survey Professional Paper 862, 32 p.

Glacial-lake deposits in the Mount Harper area, Yukon-Tanana Upland

By Florence R. Weber and Thomas A. Ager

During the past year, two new ^{14}C ages and pollen data have thrown light on some events in the Pleistocene history of the Yukon-Tanana Upland. Woody debris within a volcanic ash layer previously described (Weber, 1982) has been dated, as well as some organic material from farther down in the same section. The locality with the new ages is an actively thawing 15-m-high cutbank in unconsolidated sediment on the Middle Fork of the Fortymile River about 16 km southeast of Mount Harper (loc 12, fig. 23; fig. 42). Mount Harper, with an elevation of 1,994 m, is the highest point in the Yukon-Tanana Upland and has repeatedly supported active glacial systems.

The lower 3 to 6 m of the dated cutbank section (fig. 43) is made up of stratified polymictic gravel and lenticular coarse sand, including subrounded cobbles and boulders as large as 25 cm in diameter. The larger clasts are mainly of granitic and other igneous rocks but also include gneiss, augen gneiss, quartzite, and some schist. Locally at the top of this lower section is as much as 30 cm of sand. In places, several centimeters of this sand and gravel is oxidized orange.

The overlying 9 to 10 m in the middle and upper part of the section (fig. 43) is made up of alternating thin layers of sand and silt. The sand is coarse and gravelly, but, in contrast to the lower part of the section, the gravel is made up of angular bits of schist or quartzite and contains no igneous rocks. The metamorphic-rock clasts are mostly about 2.5 cm in diameter; the largest schist clast observed was 20 cm in diameter, although such large flat angular fragments are very rare. Much fine dark organic material is mixed in the silty layers, particularly near the base.

The top meter of the entire section is loess containing some organic material, but because of frost mixing it is unclear whether the contact is sharp or gradational between the loess and the underlying sand and silt. Close to the bottom of this meter of loess is a layer of white volcanic ash 3 to 15 cm thick (here informally designated as the Mount Harper ash).

Studies in the Mount Harper area of the upland indicate three major glacial advances, which, for convenience, are here designated I, II, and III, from oldest to youngest. Figure 42 maps the extent of recognized glacial advances in the Mount Harper area. The glacier of maximum extent (I) in valley X (fig. 42) opposite the mouth of Molly Creek extended down to and blocked the valley of the Middle Fork of the Fortymile River in two separate episodes. Episode IB is recognized by a well-defined inner terminal moraine. Instead of typical irregular morainal topography, however, the upper surface of this feature is weathered to a terrace of low relief because of its age; such level morainal surfaces are characteristic of older glacial advances in the upland. Moraine of the earlier episode (IA) is no longer extant, but its presence is defined by erratic boulders at an elevation of slightly more than 900 m, by a concentration of large lag boulders in the stream valleys, and only locally by topographic form.

A large lake, here informally named "Lake Harper," formed when the Middle Fork was blocked by glacial ice extending from valley X. The approximate shoreline of Lake Harper is drawn at the 900-m contour (fig. 42); at its maximum extent the water level was probably somewhat higher. Outwash of the advance I glaciers in valleys Y and Z (fig. 42) discharged into the lake and formed alluvial fans. A smaller lake may have formed in the lower valley of Molly Creek, which was also blocked by valley X ice advances.

The flat floor of the Lake Harper basin, approximately 40 km^2 in area, at present is covered with unconsolidated sand and gravel. The gravel, mostly of schist or schistose gneiss, is evidently derived from the local bedrock. A few thin sand and clay layers occur under loess capping the low bluffs that stand slightly above the flats.

The cutbank is in sediment making up the floor of the valley. The basal stratified gravel and sand are thought to represent a distal part of the outwash fan of valley Z, probably of glacial episode IA. The large amount of granite in this gravel indicates that the gravel came from the Mount Harper area to the west. Metamorphic rocks surround and probably underlie much of the Lake Harper basin. Granite is found only near Mount Harper at the head of the glacial valleys and at the far southward reaches of the Middle Fork drainage (Foster, 1976). This gravel was exposed and oxidized after glacial episode IA.

A sharp break occurs at the top of the oxidized gravel, above which a thick succession of finely layered organic and fine-grained glacial-silt lakebeds was deposited. This lake (Lake Harper) formed against the terminal moraine of glacial episode IB. A ^{14}C age on fine woody debris collected from near the base of the lakebed section is older than 50,300 years (USGS 1122).

A pollen sample (80A Wr 332A) from essentially this dated horizon contains abundant fine woody debris and well-preserved pollen. The fossil assemblage includes pollen of spruce (Picea), birch (Betula sp.), alder

(Alnus sp.), heaths (Ericaceae, Empetrum), willow (Salix sp.) and spores of Sphagnum and ferns. This pollen assemblage is nearly identical to assemblages of middle to late Holocene age in the Tanana River valley and adjacent Yukon-Tanana Upland (Matthews, 1974; Ager, 1975). The pollen assemblage is interpreted to represent taiga (northern boreal forest) vegetation that probably grew in valleys of the Yukon-Tanana Upland during an interglacial or warm interstadial before 50,300 years B.P.

The volcanic ash (Mount Harper ash) in the loess at the top of the section has been dated from fine woody debris contained within it at 21,410±190 years (USGS 1123), an age that falls within the last glacial interval of the Pleistocene (approx 25,000-14,000 years B.P.). A sediment sample from near the top of the ash layer contains a pollen assemblage of grass (Gramineae), sedge (Cyperaceae), small amounts of birch (Betula spp.), heath, and various herbs (e.g. Artemisia, Caryophyllaceae, Ranunculaceae, Epilobium, Phlox). Sphagnum spores are also present in the sample. Trace amounts of spruce pollen may represent contaminants, reworked older pollen, or wind-transported pollen from distant sources. This assemblage is interpreted to represent herb-shrub tundra. Tundra vegetation is consistent with the full-glacial age suggested by the ash-layer radiocarbon age of 21,410±190 years. Similar full-glacial pollen assemblages have been reported from the Tanana River valley and adjacent upland (Matthews, 1970, 1974; Ager, 1975).

It is important to know the actual age of the older-than-50,300-year sample. Is it early Wisconsinan or older? Some evidence suggests that it is older than Wisconsinan. The upper valleys in valley X (fig. 42) show evidence of two major glacial advances, II and III,

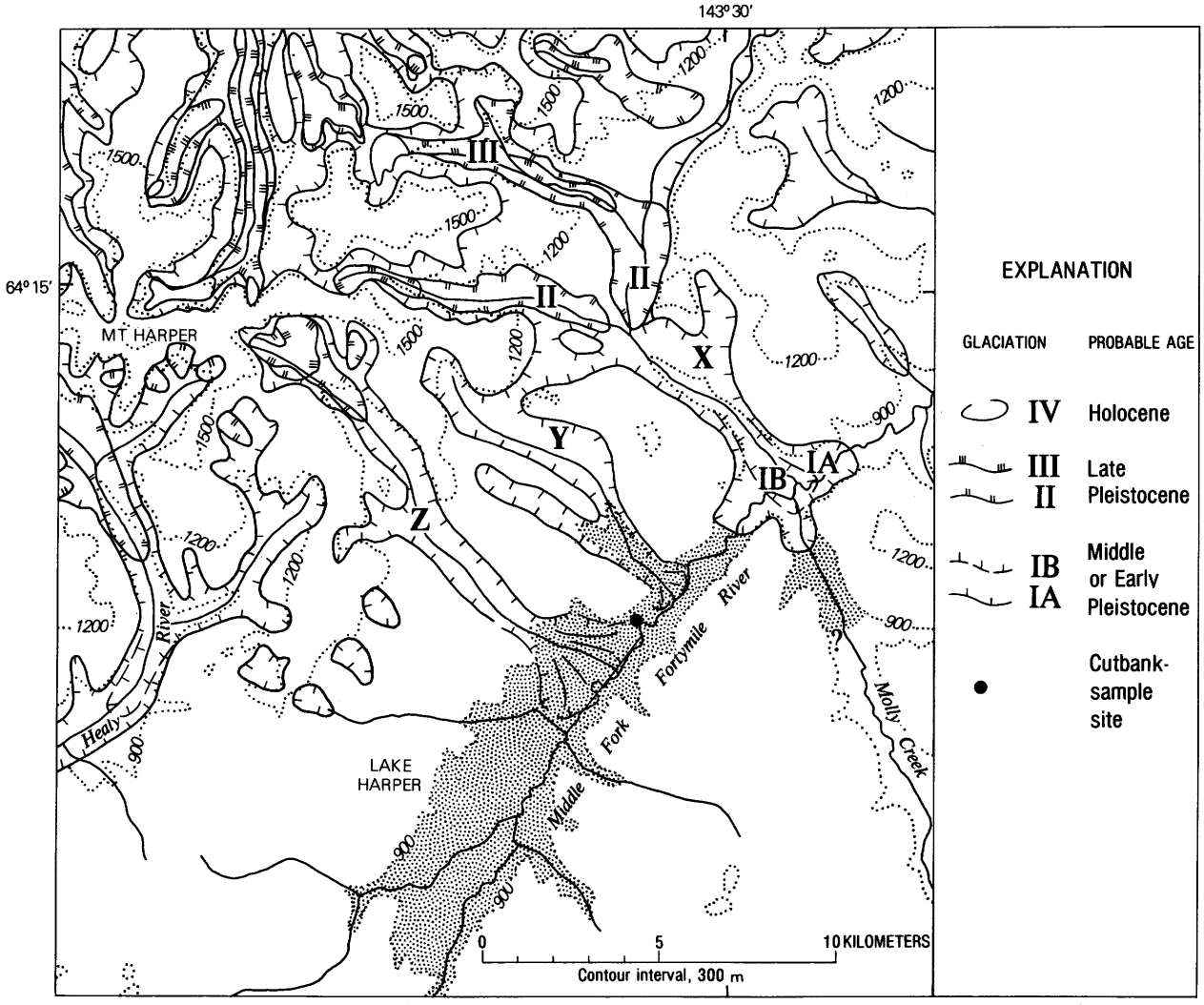

Figure 42.—Mount Harper region, Yukon-Tanana Upland, showing limits of glacial advances (IA-IV), approximate extent of glacial Lake Harper (stippled area), valleys referred to in text (X, Y, Z), and location of cutbank section and dated samples in figure 43.

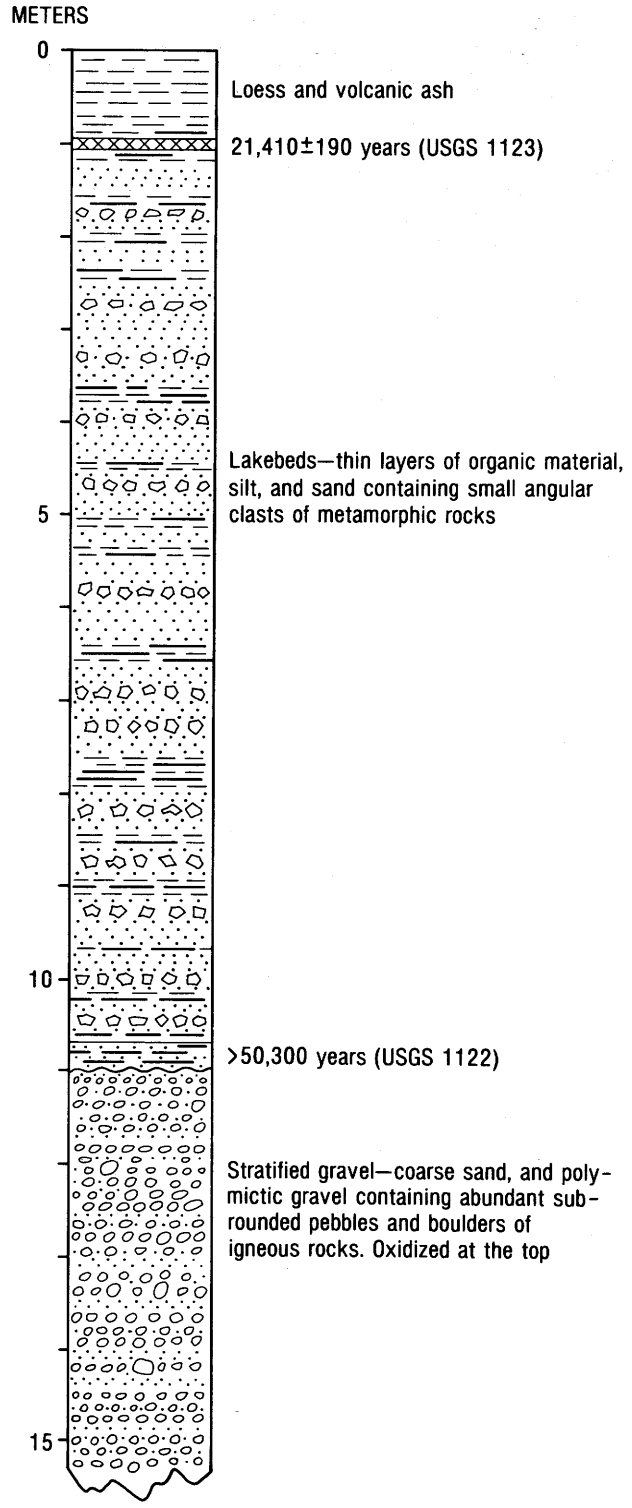

Figure 43.—Composite cutbank section of Pleistocene deposits on the Middle Fork of the Fortymile River, showing positions of C^{14}-dated samples.

that postdate advance I. Although advances II and III each had several episodes similar to episodes IA and IB, these episodes are not delineated in this report. Deposits of advances II and III are conspicuous throughout the upland and have physical characteristics similar to those of deposits of the Delta (Illinoian) and Donnelly (Wisconsinan) Glaciations in the nearby Alaska Range (Péwé,1975). Recently, Weber and others (1981) suggested that the Delta Glaciation may be early Wisconsinan in age instead of Illinoian. Our best guess is that in the Mount Harper area, glacial advance III is equivalent to the Donnelly and II to the Delta (both late Pleistocene), and that advance I was middle Pleistocene or older. Figure 42 also maps a fourth (IV) postglacial cirque-forming event.

REFERENCES CITED

Ager, T. A., 1975, Late Quaternary environmental history of the Tanana valley, Alaska: Columbus, Ohio State University, Institute of Polar Studies Report 54, 117 p.

Foster, H. L., compiler, 1976, Geologic map of the Eagle quadrangle, Alaska: U.S. Geological Survey Miscellaneous Investigations Series Map I-922, scale 1:250.000.

Matthews, J. V., Jr., 1970, Quaternary environmental history of interior Alaska—pollen samples from organic colluvium and peats: Arctic and Alpine Research, v. 2, no. 4, p. 241-251.

——1974, Wisconsin environment of interior Alaska—pollen and macro-fossil analysis of a 27 meter core from the Isabella basin (Fairbanks, Alaska): Canadian Journal of Earth Sciences, v. 11, no. 6, p. 828-841.

Péwé,T. L., 1975, Quaternary geology of Alaska: U.S. Geological Survey Professional Paper 835, 145 p.

Weber, F. R., 1982, Two new tephra localities in the Yukon-Tanana Upland, in Coonrad, W. L., ed., The United States Geological Survey in Alaska: Accomplishments during 1980: U.S. Geological Survey Circular 844, p. 61-62.

Weber, F. R., Hamilton, T. D., Hopkins, D. M., Repenning, C. A. and Haas, Herbert, 1981, Canyon Creek—a Late Pleistocene vertebrate locality in interior Alaska: Journal of Quaternary Research, v. 16, no. 2, p. 167-180.

SOUTHERN ALASKA

(Figure 44 shows study areas discussed)

Stratigraphy, petrology, and structure of the Pingston terrane, Mount Hayes C-5 and C-6 quadrangles, eastern Alaska Range, Alaska

By Warren J. Nokleberg, Carl E. Schwab, Ronny T. Miyaoka, and Carol L. Buhrmaster

The Pingston tectonostratigraphic terrane forms a major part of the northern Alaska Range, according to Jones and others (1981), who delineated the areal extent and stratigraphy of the terrane. The Pingston

terrane extends at least 300 km to the west, beyond Mount McKinley, and about 100 km to the southeast (Jones and others, 1981). Part of this terrane occurs in a fault-bounded block immediately south of the Hines Creek fault in the western part of the Mount Hayes quadrangle, where it is structurally juxtaposed against rocks of the Yukon-Tanana Upland to the north, which, in this area, consists of the schist of Jarvis Creek (area 13, fig. 44; fig. 45). The Pingston terrane is bounded to the south by the intensely deformed McKinley terrane and by numerous fault-bounded slivers of highly deformed and metamorphosed flysch of presumed Jurassic or Cretaceous age (Jones and others, 1981).

Far to the west of the Mount Hayes quadrangle, the Pingston terrane has been described as an intensely deformed suite of deep-water upper Paleozoic phyllite and chert, minor limestone, and Triassic black argillite, gray limestone, and calcareous siltstone and sandstone intruded by younger diabase and gabbro dikes and sills (Jones and others, 1981). Previous studies of the Pingston terrane in the western part of the Mount Hayes and eastern part of the Healy quadrangles indicate that the terrane consists of varying amounts of highly deformed and metamorphosed limestone, black shale and phyllite, argillite, graywacke, conglomerate, and submarine basalt (Wahrhaftig and others, 1975) or varying amounts of metavolcanic rock, metatuff, pillow greenstone, and sparse marble (Sherwood and Craddock, 1979).

Recent field, petrologic, and structural studies of the Pingston terrane in the Mount Hayes C-5 and C-6 quadrangles reveal that in this area the terrane: (1) has a highly distinctive stratigraphy, age, petrology (relict textures, relict minerals, and metamorphic facies), and structure; and (2) differs markedly from that described in previous studies. These more recent studies indicate that the major rock types, in order of decreasing abundance, are meta-andesite, metadacite and metarhyodacite flows and (or) tuff, metabasalt, metagabbro, metavolcanic graywacke, metagraywacke, metasiltstone, metaquartzite or metachert, and very sparse marble. Table 14 lists the general petrography of the major rock units in the Pingston

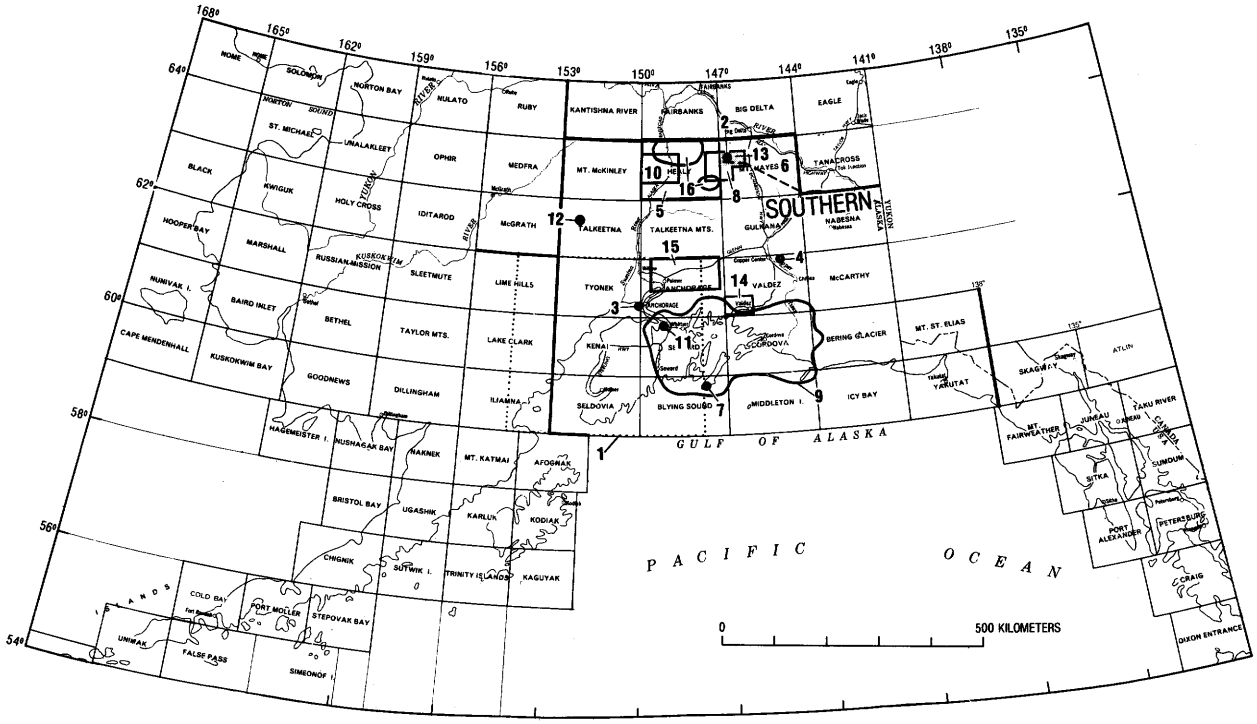

Figure 44.—Areas and localities in southern Alaska discussed in this volume. A listing of authorship, applicable figures and tables, and article pagination (in parentheses) relating to the numbered areas follows. 1, Ager and Sims, figure 65 (p. 103-105); 2, Aleinikoff and Nokleberg, figure 46, table 15 (p. 73-75); 3, Bartsch-Winkler and Schmoll, figures 66 through 70 (p. 105-108); 4, Connor, figure 64 (p. 102-103); 5, Csejtey and others, figure 49 (p. 77-79); 6, Curtin and others, figure 58 (p. 92-93); 7, Dumoulin and Miller, figures 47 and 48 (p. 75-77); 8, Evenson and others, figures 59 through 61 (p. 94-95); 9, Goldfarb, figure 57, tables 18 and 19 (p. 89-92); 10, Hillhouse and Gromme, figures 50 and 51 (p. 80-82); 11, Kachadoorian and Ovenshine, figure 71 (p. 109-110); 12, Mamay and Reed, figures 62 and 63 (p. 98-102); 13, Nokleberg and others, figure 45, table 14 (p. 70-73); 14, Pickthorn and Silberman, figures 54 through 56 (p. 86-89); 15, Silberman and Grantz, figures 52 and 53, tables 16 and 17 (p. 82-86); 16, Yeend (p. 95-98).

terrane. Igneous rocks and sedimentary rocks derived from igneous material make up about two thirds, and pelitic and calcareous rocks as much as one-third, of the total succession.

Because of intense deformation, a definite stratigraphy cannot be established for the Pingston terrane in the study area. However, the abundance of metavolcanic rock and of metasedimentary rock derived from volcanic material, as well as the presence of lesser schist, quartzite, and marble, suggests that the original stratigraphy consisted of a succession of submarine volcanic rocks and rocks derived from volcanic material, as well as lesser shale, chert or quartzite, and limestone, probably deposited in a submarine island-arc environment. The age of the Pingston terrane in the Mount Hayes and Healy quadrangles is not well established. Recent U-Pb geochronologic studies of a metarhyodacite from the Mount Hayes C-6 quadrangle indicate a 373±7-m.y. (Devonian) age of extrusion for the protolith of the metarhyodacite (Aleinikoff and Nokleberg, 1983).

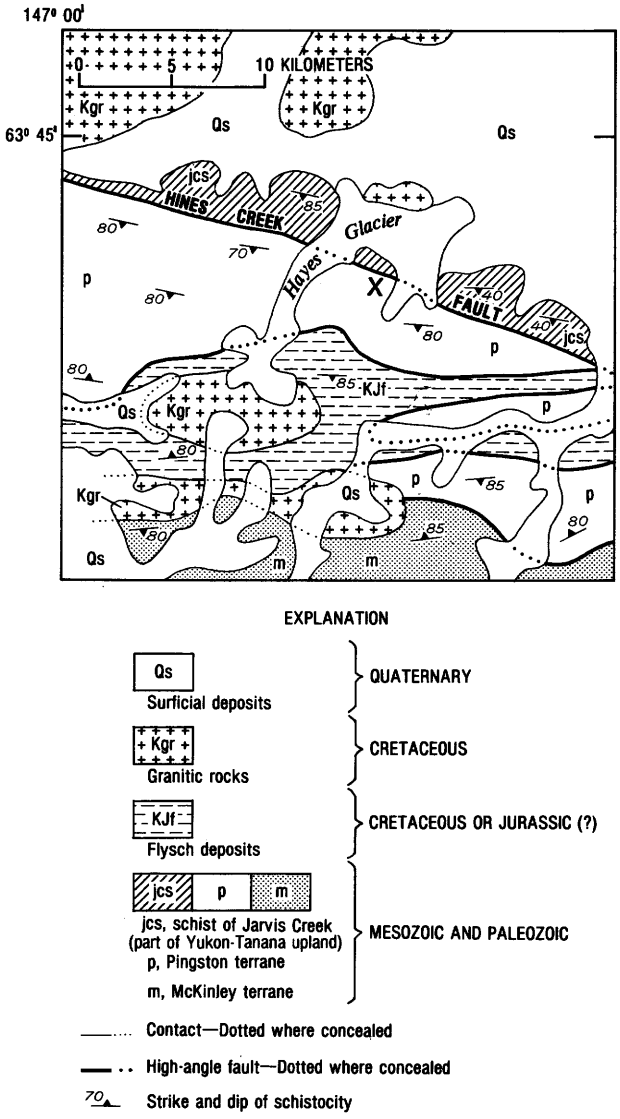

Figure 45.—Simplified geologic map of parts of the Mount Hayes C-5 and C-6 quadrangles, eastern Alaska Range, Alaska. X denotes site of metarhyodacite sample 80AAF039A, dated by U-Pb methods on zircon at 373±7 m.y. (Aleinikoff and Nokleberg, 1983).

In determining the origin of the Pingston terrane, the more important units are the metavolcanic rocks and the metavolcanic graywacke (table 14). The major relict minerals in the metavolcanic rocks are albite-rich plagioclase, quartz, and potassium feldspar. Evidence of an igneous origin for these rocks consists of abundant complex twinning in plagioclase, local normal and delicate oscillatory zoning in plagioclase, local well-preserved euhedral outlines of feldspar, and sparse resorbed outlines and embayments in quartz. The matrix and relict phenocrysts are intensely deformed. The matrix commonly consists of an intensely deformed and schistose aggregate of mainly metamorphic mica, feldspar, epidote, and chlorite. The matrix exhibits a well-developed schistosity defined by parallel-alined mica and elongate quartz and feldspar, and by a strong preferred orientation of quartz and feldspar crystallographic axes. The relict phenocrysts are generally fractured, granulated, or crushed and have been generally rotated into orientations parallel to schistosity. Locally, schistosity crosscuts the relict phenocrysts. Metamorphism of the Pingston terrane under conditions approximating upper greenschist facies is indicated by the occurrence of metamorphic epidote, chlorite, actinolite, biotite, and albite-rich plagioclase in rocks of appropriate compositions (table 14). Hornblende in the metagabbro probably formed during replacement of clinopyroxene during hydrothermal alteration. Partial replacement of hornblende by chlorite and actinolite indicates that the amphibole has been metamorphosed under conditions approximating greenschist facies.

Petrologic analysis indicates that the metavolcanic rocks of the Pingston terrane range in composition mainly from andesite and dacite to rhyodacite, latite, and trachyte. Local grading into keratophyre is suggested by locally low quartz content (as low as 5 modal percent) and by abundant relict phenocrysts of albite-rich plagioclase. Chemical analyses of the metavolcanic rocks give the following ranges (in weight percent) for selected oxides: SiO_2, 56.3 to 75.7; CaO, 0.57 to 5.73; Na_2O, 2.75 to 4.50; and K_2O, 2.06 to 4.90.

The Pingston terrane is intensely deformed. Bedding in former volcanic and sedimentary rocks is generally transposed to foliation that consists of deformed elongate lenses of various rock types. The most common structures are isoclinal folds and a pervasive axial-plane schistosity. Schistosity, defined by alined mica and deformed feldspar and quartz augen, occurs subparallel to the transposed bedding except in the cores of folds. Fold-axial planes and schistosity generally strike west-northwest and dip 40°-80° S. (fig. 45). Adjacent to the Hines Creek fault (fig. 45), the various rock units commonly are intensely cleaved and sheared. Along the fault is local structural imbrication of the schist of Jarvis Creek with various rock

Table 14.--General petrography of major rock units in the Pingston terrane, Mount Hayes C-5 and C-6 quadrangles, eastern Alaska Range

Unit	Major minerals (minor minerals)	Grain size, texture, structure, replacements, alterations
Meta-andesite, metalatite, metadacite, and metarhyodacite.	Plagioclase, quartz, white mica, chlorite, biotite, actinolite, K-feldspar (epidote, carbonate, sphene, clay, opaque minerals).	0.2-0.3 mm matrix, 0.5-8.0 mm relict phenocrysts. Schistose. Relict plagioclase, quartz, and K-feldspar phenocrysts. Matrix of schistose quartz, white mica, plagioclase, epidote, and chlorite. Plagioclase with normal and oscillatory zoning. Local embayed quartz. Feldspar partly replaced by white mica and epidote.
Quartz-mica schist (metagraywacke).	Quartz, white mica, biotite, chlorite, carbonate, opaque minerals, plagioclase (sphene, pyrite).	0.02-0.5 mm. Schistose. Folded schistosity. Granulated quartz. Relict quartz and plagioclase phenocrysts. Cataclastic zones. Local blastomylonite. Plagioclase partly replaced by white mica.
Amphibolite (metagabbro and metadiabase).	Plagioclase, hornblende, actinolite, biotite, chlorite (white mica, quartz, carbonate, epidote, sulfides, sphene).	0.05-2.75 mm. Schistose. Local folded schistosity. Relict ophitic texture. Complex twinning and normal and oscillatory zoning in plagioclase. Clinopyroxene replaced by hornblende and actinolite. Plagioclase replaced by white mica. Hornblende replaced by epidote, chlorite, and actinolite.
Quartz-mica-graphite schist (metasiltstone).	Quartz, white mica, carbonate, graphite, biotite, chlorite (plagioclase, opaque minerals, K-feldspar, clinozoisite).	0.02-0.35 mm matrix, quartz porphyroblasts as large as 1.0 mm. Schistose. Folded schistosity. Granulated quartz. Cataclastic zones. Local blastomylonite. Minor quartz porphyroblasts.
Quartzite (metachert or quartzite).	Quartz (white mica, chlorite, pyrite, opaque minerals).	0.05-0.4 mm. Schistose. Granulated quartz with strong preferred orientation. Folded schistosity. Local cataclastic zones. Local blastomylonite.

units of the Pingston terrane. Local multiple deformation of the Pingston terrane is indicated by refolding of schistosity into isoclinal folds.

In summary, protoliths of the Pingston terrane in the western part of the Mount Hayes quadrangle consist of an assemblage composed of andesite through rhyodacite, shale, chert, and limestone deposited in a submarine island-arc environment. At least a part of the volcanic-rock sequence was erupted during the Devonian. Subsequently, the volcanic- and sedimentary-rock sequence was strongly deformed and metamorphosed. The stratigraphy, age, petrology, and structure of the Pingston terrane in the western Mount Hayes quadrangle differ greatly from those previously reported.

REFERENCES CITED

Aleinikoff, J. N., and Nokleberg, W. J., 1983, Uranium-lead geochronology of a metarhyodacite from the Pingston terrane, Mount Hayes C-6 quadrangle, eastern Alaska Range, Alaska, in Coonrad, W. L., and Elliott, R. L., eds., The United States Geological Survey in Alaska: Accomplishments during 1981: U.S. Geological Survey Circular 868, p. 73-75.

Jones, D. L., Silberling, N. J., Berg, H. C., and Plafker, George, 1981, Map showing tectonostratigraphic terranes of Alaska, columnar sections, and summary description of terranes: U.S. Geological Survey Open-File Report 81-792, 20 p., scale 1:2,500,000, 2 sheets.

Sherwood, K. W., and Craddock, Campbell, 1979, General geology of the central Alaska Range between the Nenana River and Mount Deborah: Alaska Division of Geological and Geophysical Surveys Open-File Report AOF-116, 22 p.

Wahrhaftig, Clyde, Turner, D. L., Weber, F. R., and Smith, T. E., 1975, Nature and timing of movement on the Hines Creek strand of the Denali fault system, Alaska: Geology, v. 3, no. 8, p. 463-466.

Uranium-lead geochronology of a metarhyodacite from the Pingston terrane, Mount Hayes C-6 quadrangle, eastern Alaska Range

By John N. Aleinikoff and Warren J. Nokleberg

The Pingston tectonostratigraphic terrane consists of a unique assemblage of highly deformed and fault-bounded rocks that occur in an elongate belt immediately south of the Hines Creek fault in the west-central part of the Mount Hayes quadrangle (fig. 45). The Pingston terrane extends at least 300 km to the west, beyond Mount McKinley, and about 100 km to the southeast, according to Jones and others (1981), who defined and described the terrane. Recent studies by Nokleberg and others (1983) show that in the Mount

Hayes C-5 and C-6 quadrangles, the Pingston terrane consists predominantly of varying proportions of metaandesite, metadacite, metarhyodacite flows and (or) metatuff, metabasalt, metavolcanic graywacke, metagraywacke, metasiltstone, quartzite or metachert, and sparse marble. The terrane in these two quadrangles is intensely deformed, with isoclinal folds of various sizes and a pervasive axial-plane schistosity. Axial planes of folds and schistosity generally strike west-northwest and dip 35°-40° S. In this area, the Pingston terrane is bounded on the north by the Hines Creek fault, which marks the south boundary of the Yukon-Tanana Upland (Wahrhaftig and others, 1975; Gilbert, 1977; Sherwood and Craddock, 1979; Nokleberg and others, 1983), and on the south by the intensely deformed McKinley terrane and by numerous fault-bounded slivers of highly deformed and metamorphosed flysch of presumable Jurassic or Cretaceous age (Jones and others, 1981; Nokleberg and others, 1983).

To better define and describe this terrane, we identified and sampled a metarhyodacite (field No. 80AAF039A) from an area about 65 m south of the Hines Creek fault for zircon U-Pb geochronologic studies (loc. 2, fig. 44). The metarhyodacite contains relict phenocrysts of potassium feldspar, plagioclase, and sparse quartz in a fine-grained schistose matrix. Relict phenocrysts of potassium feldspar are slightly predominant over those of plagioclase. Igneous parentage for the metarhyodacite is indicated by abundant complex twinning of plagioclase, local normal and delicate oscillatory zoning in plagioclase, local well-preserved euhedral outlines of feldspar, and sparse resorbed outlines and embayments in quartz. The matrix is a schistose aggregate of metamorphic minerals, consisting of potassium feldspar, plagioclase, quartz, white mica, biotite, epidote, and accessory carbonate and opaque minerals. A chemical analysis gave: 65.0 weight percent SiO_2, 1.66 weight percent CaO, 4.50 weight percent Na_2O, and 4.90 weight percent K_2O. This analysis and modal data indicate a rhyodacitic composition for the protolith.

Local variation of the metamorphic rocks in the Pingston terrane into quartz latite and, possibly, quartz keratophyre is indicated by quartz (as low as 5 modal percent), albite-rich plagioclase, a relatively low percentage of CaO, and relatively high percentages of Na_2O and K_2O. Generally in the metavolcanic rocks, the relict phenocrysts range as large as 8.0 mm in diameter, whereas the matrix has an average grain size of 0.05 to 0.2 mm. Both the matrix and relict phenocrysts are intensely deformed. The matrix exhibits well-developed schistosity defined by parallel-alined mica, elongate quartz and feldspar, and a strongly preferred orientation of quartz and feldspar crystallographic axes. The relict phenocrysts are commonly fractured, granulated, or crushed, and many have been rotated into positions with their long dimensions parallel to the schistosity. Locally, the schistosity crosscuts the relict phenocrysts. Many of the relict feldspar phenocrysts are partially altered to a mixture of very fine grained epidote and white mica.

Zircons extracted from approximately 35 kg of rock are pinkish gray, and at least 50 percent of the grains are broken fragments. The euhedral grains are stubby and have a maximum length-to-width ratio of 3:1. Less than 10 percent of all the grains contain opaque inclusions. Three size fractions of the sample were analyzed for uranium and lead isotopes (fig. 46; table 15). Standard isotope-dilution techniques were used, modified from Krogh (1973), and isotopic ratios

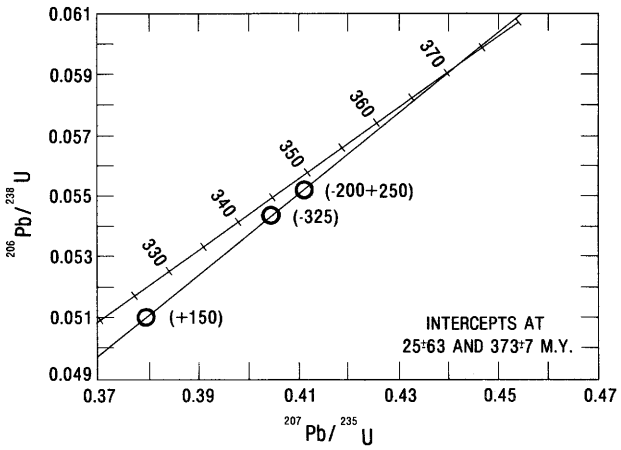

Figure 46.—Concordia diagram of U-Pb-isotopic data from zircons in metarhyodacite (field No. 80AAF039A, fig. 45), Mount Hayes C-6 quadrangle, eastern Alaska Range, Alaska. Least-squares best-fit line through three zircon points indicates an extrusive igneous age of 373±7 m.y.

Table 15.--U-Pb isotopic-age determinations on zircons from the Pingston terrane, Mount Hayes C-6 quadrangle, eastern Alaska Range, Alaska

[Sample: Field No. 80AAF039A, lat 63°41'00" N., long 146°40'41" W.]

Size fraction	Concentration (ppm)		Atomic percent				Age (m.y.)		
	U	Pb	^{204}Pb	^{206}Pb	^{207}P	^{208}Pb	$\frac{^{206}Pb}{^{238}U}$	$\frac{^{207}Pb}{^{235}U}$	$\frac{^{207}Pb}{^{206}Pb}$
(<150)	119.8	7.32	0.071	73.19	4.98	21.76	321	327	369
(<200>250)	135.0	8.80	.045	73.82	4.65	21.49	347	350	372
(<325)	154.1	9.85	.029	73.80	4.41	21.77	341	345	370

were measured on a 12-in. mass spectrometer with on-line digital processing. All three size fractions have nearly identical $^{207}Pb/^{206}Pb$ ages, ranging from 369 to 372 m.y. (table 15); the U-Pb ages range from about 320 to 350 m.y. (table 15). This age variation does not follow the ordinary dependency on uranium concentration, which, in this sample, is extremely low, ranging from about 120 to 154 ppm and increasing with decreasing grain size. A best-fit line (Ludwig, 1980) through the data points yields concordia intercepts of 373±7 m.y. and 256±3 m.y. (fig. 46). We interpret these data to indicate that the protolith for the metarhyodacite was erupted during the Late Devonian. The lower-intercept age reflects either modern lead loss due to dilatancy (Goldich and Mudrey, 1972) or, possibly, late Mesozoic and Tertiary movement, metamorphism, and deformation of rocks along the Hines Creek fault.

Most of the rocks of the Pingston terrane to the west in the Healy quadrangle or near Mount McKinley have been assigned a late Paleozoic and Triassic age, mainly on the basis of conodonts (Sherwood and Craddock, 1979; Reed and Nelson, 1980; Jones and others, 1981). The age of the relatively younger diabase and gabbro is assumed to be middle or late Mesozoic. Before our study, no metavolcanic rock from the Pingston terrane had been dated. Our data show that an important component of the Pingston terrane consists of former siliceous volcanic rock of Late Devonian age. On the basis of lithology, metamorphic grade, and structure, we interpret the metarhyodacite to be an important constituent of the terrane in the western part of the Mount Hayes quadrangle (Nokleberg and others, 1983). This report suggests that the age of at least a part of the Pingston terrane is Late Devonian and thereby extends the age range of the terrane and revises the stratigraphy of the terrane to include former siliceous volcanic rock.

REFERENCES CITED

Gilbert, W. G., 1977, General geology and geochemistry of the Healy D-1 and southern Fairbanks A-1 quadrangles and vicinity, Alaska: Alaska Division of Geological and Geophysical Surveys Open-File Report 105, 13 p.

Gilbert, W. G., and Redman, Earl, 1977, Metamorphic rocks of the Toklat-Teklanika Rivers area, Alaska: Alaska Division of Geology and Geophysical Surveys Geologic Report 50, 13 p.

Goldich, S. S., and Mudrey, M. G., Jr., 1972, Dilatancy model for discordant U-Pb zircon ages, in Tugarinov, A. I., ed., Recent contributions to geochemistry and analytical chemistry: New York, John Wiley & Sons, p. 466-470.

Jones, D. L., Silberling, N. J., Berg, H. C., and Plafker, George, 1981, Map showing tectonostratigraphic terranes of Alaska, columnar sections, and summary description of terranes: U.S. Geological Survey Open-File Report 81-792, 20 p., scale 1:2,500,000, 2 sheets.

Krogh, T. E., 1973, A low-contamination method for hydrothermal decomposition of zircon and extraction of U and Pb for isotopic age determinations: Geochimica et Cosmochimica Acta, v. 37, no. 3, p. 485-494.

Ludwig, K. R., 1980, Calculation of uncertainties of U-Pb isotope data: Earth and Planetary Science Letters, v. 46, no. 2, p. 212-220.

Nokleberg, W. J., Buhrmaster, C. L., and Schwab, C. E., 1983, Stratigraphy, petrology, and structure of the Pingston terrane, Mount Hayes C-5 and C-6 quadrangles, eastern Alaska Range, in Coonrad, W. L., and Elliott, R. L., eds., The United States Geological Survey in Alaska: Accomplishments during 1981: U.S. Geological Survey Circular 868, p. 70-73.

Reed, B. L., and Nelson, S. W., 1980, Geologic map of the Talkeetna quadrangle, Alaska: U.S. Geological Survey Miscellaneous Investigations Series Map I-1174, 15 p., scale 1:250,000.

Sherwood, K. W., and Craddock, Campbell, 1979, General geology of the central Alaska Range between the Nenana River and Mount Deborah: Alaska Division of Geological and Geophysical Surveys Open-File Report AOF-116, 22 p.

Wahrhaftig, Clyde, Turner, D. L., Weber, F. R., and Smith, T. E., 1975, Nature and timing of movement on the Hines Creek strand of the Denali fault system, Alaska: Geology, v. 3, no. 8, p. 463-466.

The Jeanie Point complex revisited

By Julie A. Dumoulin and Martha L. Miller

The so-called Jeanie Point complex is a distinctive package of rocks within the Orca Group, a Tertiary turbidite sequence. The rocks crop out on the southeast coast of Montague Island, Prince William Sound, approximately 3 km northeast of Jeanie Point (loc. 7, fig. 44). These rocks consist dominantly of fine-grained limestone and lesser amounts of siliceous limestone, chert, tuff, mudstone, argillite, and sandstone (fig. 47). The Jeanie Point rocks also differ from those typical of the Orca Group in their fold style. Thus, the Orca Group of the area is isoclinally folded on a large scale (tens to hundreds of meters), whereas the Jeanie Point rocks are tightly folded on a 1- to 3-m-wavelength scale (differences in rock competency may be responsible for this variation in fold style).

Helwig and Emmet (1981) first described these rocks and interpreted them as an accreted terrane of pelagic origin. They suggested "* * * the complex could represent a separate terrane and/or a separate basement to the Orca Group" (Helwig and Emmet, 1981, p. 28). Our studies suggest that the Jeanie Point rocks are interbedded with the Orca Group and may have formed in a small marginal basin.

The Jeanie Point rocks crop out along the shoreline on two prominent points and include about 0.8 km of tidal-flat and cliff exposures (fig. 48). The rocks are structurally complex; a best estimate of their stratigraphic thickness is 100 to 300 m. Beds are commonly 2 to 10 cm thick and, though folded, are laterally continuous. The dominant rock type is micritic to slightly coarser grained limestone containing few to abundant planktic and scarce benthic foraminifers. Recrystallized and (or) replaced radiolarian tests are present but not abundant in the micrite. A subordinate rock type consists of chert containing few to abundant

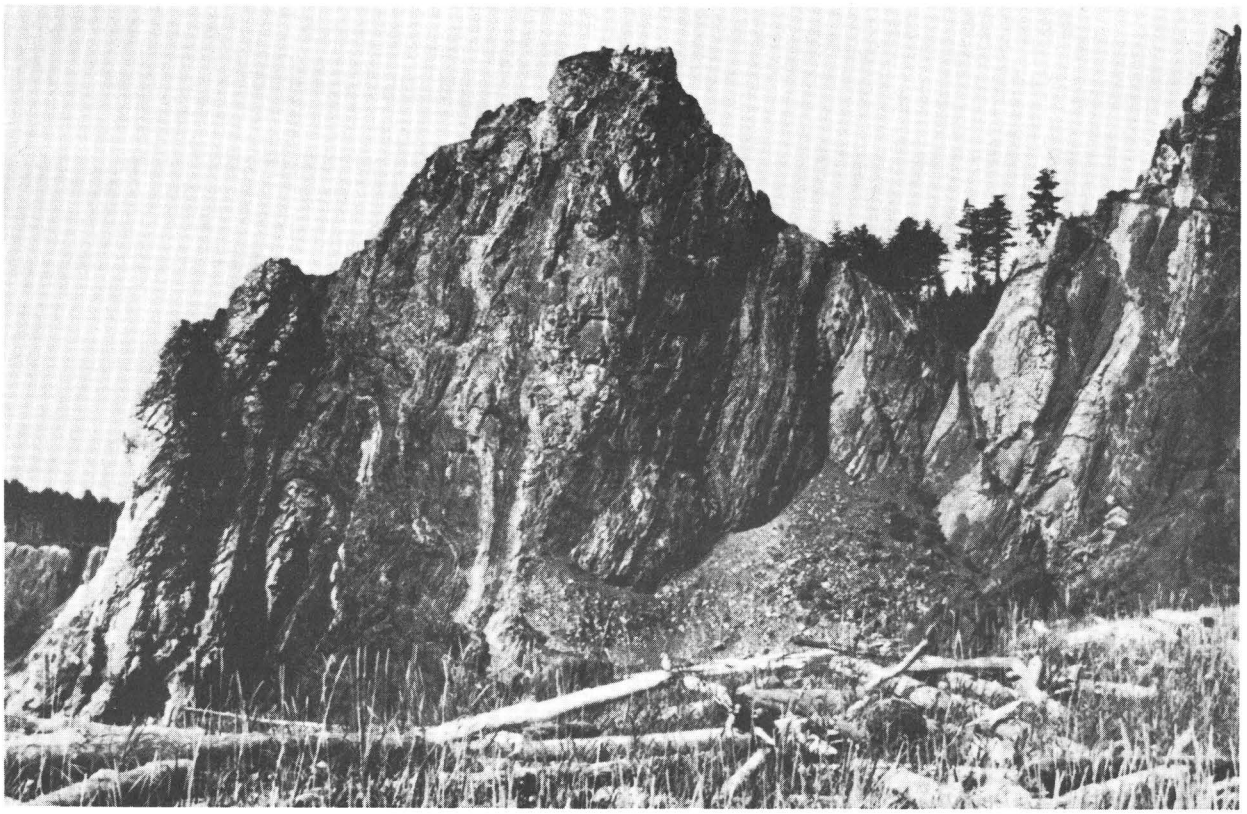

Figure 47.—Prominent outcrop of interbedded limestone, chert, and tuff of the Jeanie Point complex on Montague Island. Bluff is approximately 32 m high.

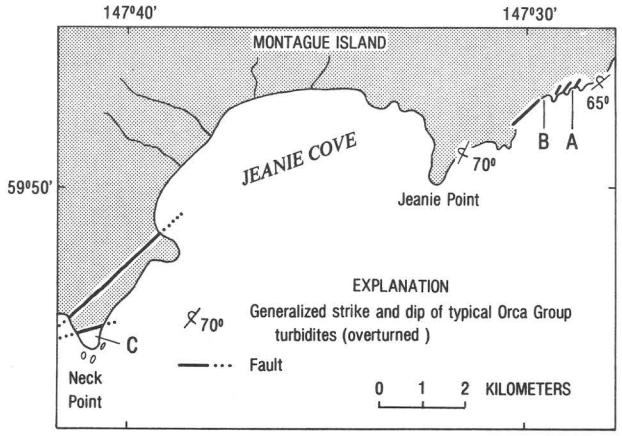

Figure 48.—Sketch map of Jeanie Cove area on southeast coast of Montague Island. Rocks of the Jeanie Point complex crop out between shoreline localities A and B. Hemipelagic to pelagic sedimentary rocks crop out at Neck Point (loc. C). Turbidites typical of the Orca Group underlie rest of area (stippling).

radiolarian tests in various states of preservation. In some samples, the radiolarian tests and fragments have been pyritized; pyrite also occurs as cubes and laminae throughout the cherty rocks. In two chert samples, glauconite fills radiolarian tests and occurs in irregular to rounded grains. The siliceous limestone exhibits all compositional gradations between predominantly calcareous micrite and chert. In places, the silica and carbonate occur in millimeter-thick alternating layers and laminae; poorly preserved radiolarian and foraminiferal tests occur in these mixed rocks. The rocks appear to have undergone a diagenetic silicification like that described by Wachs and Hein (1974) for the Calera Limestone of the Franciscan Complex. They suggested that secondary silica was added to limestone before lithification and that radiolarians may have provided nuclei for the silica addition. They ascribed complete transformation from a limestone bed to a chert bed to this mechanism.

Tuff and tuffaceous mudstone, in beds 1 to 3 cm thick, are minor parts of the Jeanie Point rocks. Petrographic inspection reveals brown glassy fragments and silt in a cryptocrystalline to glassy matrix. Less common are basaltic rock fragments with a hyalopilitic to pilotaxitic texture.

Black argillite occurs as interbeds within the Jeanie Point rocks but is concentrated in two thick sequences, one of which may be as much as 50 m thick. No internal bedding planes are obvious in either of these sequences. Argillite from typical Orca Group sedimentary rocks occurs in layers less than 5 cm thick and represents the top parts of turbidite beds. The argillite of the Jeanie Point rocks seems to represent deposition under oxygen-poor conditions because it contains abundant diagenetic pyrite and little evidence of indigenous fauna or bioturbation.

Thin lenses of carbonate packstone to wackestone occur sparsely throughout the Jeanie Point rocks. These rocks show grading on a millimeter to centimeter scale and contain silt- to sand-size clasts in a micritic matrix. The clasts consist of skeletal debris, angular quartz, and volcanic fragments, including glass. These calcareous rocks could be small-scale locally derived turbidites or hemipelagic sediment reworked by bottom currents (Kelts and Arthur, 1981).

Clastic rocks of a less local provenance than those discussed above also occur in the Jeanie Point rocks. A few thin beds of fine- to medium-grained sandstone, rich in lithic clasts, that closely resemble turbidites of the Orca Group on Montague Island are interbedded with Jeanie Point carbonate rocks at two localities. Sandstone rich in lithic clasts also occurs as clastic dikes, containing as much as 20 percent sparry-calcite cement, that are found throughout the Jeanie Point rocks but seem to be most abundant in the argillite-rich intervals.

Helwig and Emmet (1981) reported that the Jeanie Point complex is fault bounded. It is cut by northeasterly trending faults that parallel the neotectonic faults on this part of Montague Island. In fact, a probable fault slice of turbidite is exposed in the tidal flats between the two prominent points. In places, this turbidite slice is olistostromal; irregular blocks of sandstone and mudstone, as much as several meters across, occur in a mudstone matrix. However, the Jeanie Point rocks are not actually fault bounded; although faults are present near their borders, the Jeanie Point rocks lie on both sides of these faults and are interbedded with the apparently typical Orca Group turbidites. This relation is most evident at the northeasternmost of the two prominent points mentioned above.

Our structural and lithologic data suggest that the Jeanie Point rocks do not represent an exotic terrane or an older basement for the Orca Group. Interbeds of Jeanie Point limestone and typical Orca Group turbidites at the northeast margin of the complex argue against a fault-slice origin. Furthermore, substantial intervals of pelagic to hemipelagic rocks are known elsewhere within typical Orca Group turbidites; examples include the sequences on Hawkins and Hinchinbrook Islands (Winkler, 1976), at Gravina Point and Point Martin in the Cordova quadrangle, and at Neck Point on Montague Island, just 9 km southwest of Jeanie Point (loc. C, fig. 48).

These occurrences negate the uniqueness of the Jeanie Point rocks within the Orca Group. The hemipelagic composition of the rocks suggests that they were deposited in a slope environment in a small, restricted basin. Winkler (1976) suggested that the fine-grained carbonate rocks of Hinchinbrook Island were deposited in the shadow of local volcanic barriers. Temporary volcanic barriers may have provided protection from the influx of terrigenous sediment and allowed the Jeanie Point sediment to accumulate.

REFERENCES CITED

Helwig, James, and Emmet, Peter, 1981, Structure of the Early Tertiary Orca Group in Prince William Sound and some implications for the plate tectonic history of southern Alaska: Alaska Geological Society Journal, v. 1, p. 12-35.

Kelts, Kerry, and Arthur, M. A., 1981, Turbidities after ten years of deep sea drilling—wringing out the mop?, in Warme, J. E., Douglas, R. G., and Winterer, E. L., eds., The Deep Sea Drilling Project: A decade of progress: Society of Economic Paleontologists and Mineralogists Special Publication 32, p. 91-127.

Wachs, Daniel, and Hein, J. R., 1974, Petrography and diagenesis of Franciscan limestones: Journal of Sedimentary Petrology, v. 44, no. 4, p. 1217-1231.

Winkler, G. R., 1976, Deep-sea fan deposition of the lower Tertiary Orca Group, eastern Prince William Sound, Alaska: U.S. Geological Survey Open-File Report 76-83, 20 p.

Occurrence of the Cantwell(?) Formation south of the Denali fault system in the Healy quadrangle, southern Alaska

By Béla Csejtey, Jr., Warren E. Yeend, and David J. Goerz III

The Denali fault system is one of the most conspicuous structural features of southern Alaska; its northward-convex trace trends more than 1,200 km across the entire width of the State (Grantz, 1966). This system has been previously described as a major strike-slip feature with possibly as much as several hundreds of kilometers of Cenozoic right-lateral offset (for example, Forbes and others, 1974).

In more recent years, an informal but important consideration in the tectonic evaluation of the Denali fault system was the assumption that continental rocks of the Paleocene (Wolfe and Wahrhaftig, 1970, p. A46) Cantwell Formation, which underlie large areas north of the McKinley fault of the Denali system near its apex, are absent south of it. Earlier reports by Capps (1933, 1940) of outcrops of the Cantwell Formation south of the Denali fault system, in the southwestern part of the Healy quadrangle, have been informally discredited by many geologists. Our current reconnaissance geologic investigations in the Healy quadrangle (area 5, fig. 44) suggest that the Cantwell Formation occurs south of the Denali fault system, as originally mapped by Capps. This occurrence south of the McKinley fault (fig. 49) is based on plant-fossil evidence and on the lithologic and stratigraphic similarities of these rocks to the typical Cantwell north of the fault.

The proposed correlation lends credence to the tectonic interpretation that no more than about 10 km of Cenozoic right-lateral offset has occurred along the central section of the Denali fault system in Alaska (Csejtey and others, 1982). This interpretation of limited right-lateral Cenozoic offset is based on the occurrence of the same Triassic and Lower Cretaceous units on both sides of the McKinley fault, and on the continuity of a belt of Upper Cretaceous metamorphic rocks that extends across the Denali fault system in the eastern part of the Healy quadrangle (fig. 49; Csejtey and others, 1982). Here, we briefly describe the probable Cantwell Formation south of the Denali fault and, for comparison, some of the Cantwell strata to the north. Figure 49 shows the localities of the described stratigraphic sections and rock samples.

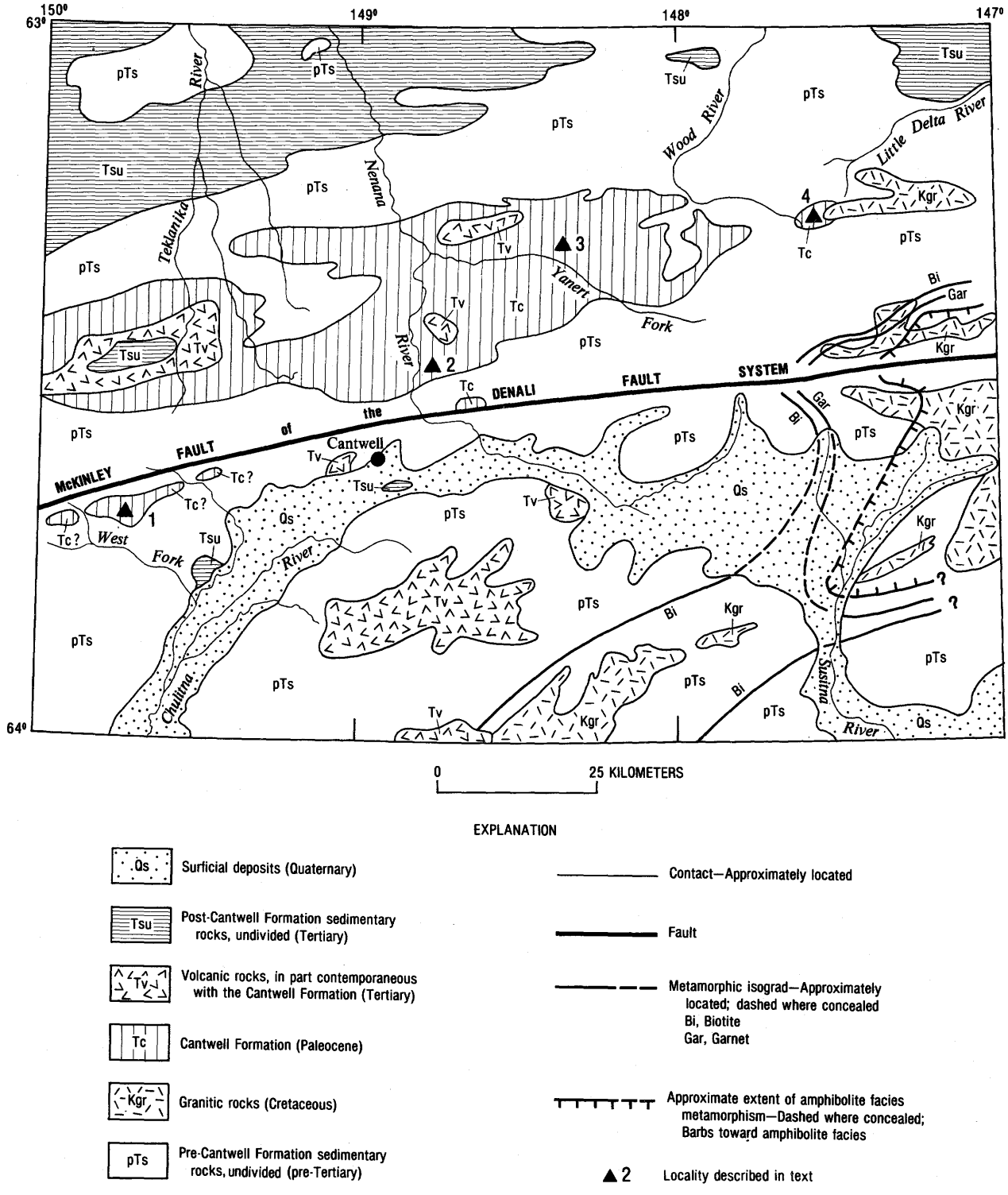

Figure 49.—Generalized geologic map showing Cretaceous plutonic rocks and the McKinley fault in the Healy quadrangle, southern Alaska. Geology in part after Capps (1933), Wolfe and Wahrhaftig (1970), Beikman and others (1977), and Csejtey and others (1982).

The Cantwell(?) Formation south of the McKinley fault composes a flat-lying or gently dipping sequence of conglomerate with intercalated sandstone and siltstone. This sequence rests with angular unconformity on intensely deformed Lower Cretaceous flysch deposits and is exposed in a narrow band of erosional remnants along ridgetops near the headwaters of the West Fork of the Chulitna River, in the southwestern part of the Healy quadrangle (fig. 49). Although the top of the sequence is nowhere exposed, a maximum thickness of about 100 to 150 m still remains. At locality 1 (fig. 49) the conglomerate is whitish gray and poorly to moderately well cemented, with a chalky sand and clay matrix. The clasts are clay coated, subangular to well rounded, and commonly between 1 and 3 cm in diameter, although some are as much as 10 cm across. Most clasts consist of white quartz and gray and black chert, but some are of gray quartzite, pink fine-grained sandstone, light-green and medium-brown chert, and fine-grained chert conglomerate. The conglomerate of the sequence forms massive apparently lenticular layers, a few to several tens of meters thick. The intercalated sandstone and siltstone occur in beds as much as a few meters thick, are gray and brown, and contain carbonized plant fragments, some of which have been identified by J. A. Wolfe (oral commun., 1982) as Metasequoia occidentalis (Newberry) Chaney. This species, which indicates an early Tertiary age, is part of the flora of the Cantwell Formation north of the McKinley fault (Wolfe and Wahrhaftig, 1970; Wolfe and Tanai, 1980).

North of the McKinley fault, the main body of the Cantwell Formation forms a broad east-west-trending belt. According to Wolfe and Wahrhaftig (1970), the formation here consists predominantly of interbedded conglomerate, sandstone, argillite, shale and a few coalbeds. Locally, it contains some flows and related tuff of mafic to intermediate composition. The formation is also intruded by numerous dikes and sills ranging in composition from diabase to rhyolite. Bedding is generally massive. The maximum preserved thickness of the formation north of the McKinley fault is about 3,000 m. Everywhere north of the McKinley fault, the generally gently deformed Cantwell Formation rests with pronounced angular unconformity on intensely deformed older rocks of Precambrian(?) to Early Cretaceous age.

At locality 2, the Cantwell Formation consists of fine- to medium-grained arkose. The fine-grained variety is gray to black and is extremely indurated, breaking with great difficulty. The medium-grained arkose is well sorted and contains grains of gray quartz, feldspar weathering to chalky-white clay, and dark-colored chert, and (or) quartz.

A grayish-brown moderately well indurated massive conglomerate with a "salt and pepper" coarse-sand matrix is present at locality 3. The subangular to well-rounded pebbles, as much as 3 cm in diameter, are composed of gray-green sandstone, dark gray and black chert, white to gray quartz, gray quartzite(?), and gray to black argillite. The matrix is a coarse sand of chert, quartz, quartzite(?) and (or) argillite(?), and weathered feldspar. Iron-oxide coatings are present on some of the grains. Also at locality 3 is a medium-grained "salt-and-pepper" arkose containing a few pebbles and granules. The sand grains are of gray, gray-green, or black chert, gray to white quartz, feldspar weathering to white clay minerals, quartzite(?), and argillite(?). Gray to black argillite containing carbonized fragments of Metasequoia(?) sp. completes the Cantwell sequence at locality 3.

A massive mottled-gray-white-brown moderately well-indurated to well-indurated conglomerate occurs at locality 4. The subangular to well-rounded pebbles consist of white quartz and gray and brown phyllite and quartzite. Most of the pebbles are 1 to 2 cm in diameter, but some are as large as 7 cm in diameter. Generally very little matrix is present. Some of the rock samples from this locality appear to have been sheared by postdepositional deformation.

The correlation of the Cantwell Formation across the McKinley fault, based on stratigraphic and lithologic similarities, should be regarded as probable and not as certain. Nevertheless, the proposed correlation, in conjunction with the continuity of a Cretaceous metamorphic belt across the McKinley fault and the occurrence of the same geologic formations on both sides of this fault, tends to support the interpretation of limited Cenozoic dextral offset along the Denali fault system (Csejtey and others, 1982). The disparity in the volumes of the Cantwell Formation exposed on opposite sides of the McKinley fault can be explained by south-side-up vertical separation along the fault during post-Cantwell time.

REFERENCES CITED

Beikman, H. M., Holloway, C. D., and MacKevett, E. M., Jr., 1977, Generalized geologic map of the eastern part of southern Alaska: U.S. Geological Survey Open-File Report 77-169-B, scale 1:1,000,000.

Capps, S. R., 1933, The eastern portion of Mount McKinley National Park, in Mineral resources of Alaska: Report on progress of investigations in 1930: U.S. Geological Survey Bulletin 836, p. 219-345.

——1940, Geology of the Alaska Railroad region: U.S. Geological Survey Bulletin 907, 201 p.

Csejtey, Béla, Jr., Cox, D. P., Evarts, R. C., Stricker, G. D., and Foster, H. L., 1982, The Cenozoic Denali fault system and the Cretaceous accretionary development of southern Alaska: Journal of Geophysical Research, v. 87, no. B5, p. 3741-3754.

Forbes, R. B., Smith, T. E., and Turner, D. L., 1974, Comparative petrology and structure of the Maclaren, Ruby Range, and Coast Range belts: Implications for offset along the Denali fault system [abs.]: Geological Society of America Abstracts with Programs, v. 6, no. 3, p. 177.

Grantz, Arthur, 1966, Strike-slip faults in Alaska: U.S. Geological Survey open-file report, 82 p.

Wolfe, J. A., and Tanai, Toshimasa, 1980, The Miocene Seldovia Point flora from the Kenai Group, Alaska: U.S. Geological Survey Professional Paper 1105, 52 p.

Wolfe, J. A., and Wahrhaftig, Clyde, 1970, The Cantwell Formation of the central Alaska Range, in Cohee, G. V., Bates, R. G., and Wright, W. B., Changes in stratigraphic nomenclature by the U.S. Geological Survey, 1968: U.S. Geological Survey Bulletin 1294-A, p. A41-A46.

Paleomagnetic latitude of Paleocene volcanic rocks of the Cantwell Formation, central Alaska

By John W. Hillhouse and Sherman Grommé

The Cantwell basin in the central Alaska Range consists of the Cantwell Formation, which includes, in its upper part, calc-alkaline volcanic rocks and intrusive rocks (the Teklanika Formation of Gilbert and others, 1976). Figure 50 shows the present distributions of the volcanic and sedimentary rocks of the Cantwell Formation. Potassium-argon ages determined from the extrusive and intrusive rocks, which range from 41.8 to 60.6 m.y., are considered to be minimum ages at least in part (Hickman, 1974; Gilbert and others, 1976). These ages accord with the Paleocene age of plant fossils in the Cantwell Formation (Wolfe and Wahrhaftig, 1970; Wolfe, 1972). The entire Cantwell Formation has been extensively folded and faulted, and local angular unconformities occur between the volcanic and sedimentary rocks.

We collected paleomagnetic samples at 19 sites (area 10, fig. 44; fig. 50); each site is a separate lava flow or welded tuff and is represented by eight samples. Except for site 17, which was completely remagnetized by lightning, the paleomagnetic data are of high quality. The structural dips at the various localities, which range from 21° to 54°, provide an excellent test of whether the magnetization in the rocks was acquired before their deformation. The angular standard deviation of the 18 mean onsite directions is 29.4°; after restoration of the bedded rocks to the original horizontal by rotation around the strike, this angular standard deviation is reduced to 12.4°, which is a typical value representing geomagnetic secular variation. We conclude that the natural magnetization

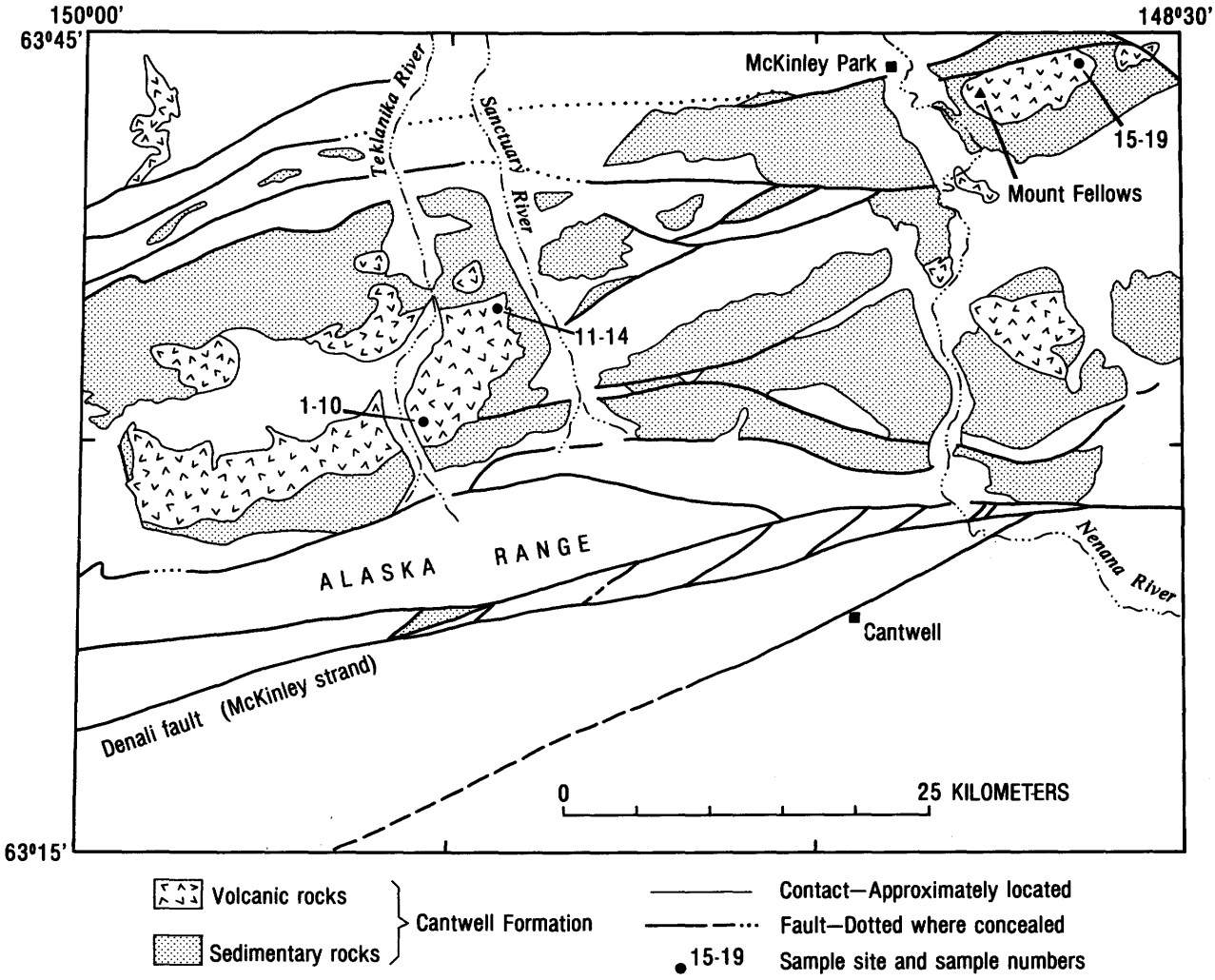

Figure 50.—Cantwell basin area, showing locations of paleomagnetic sampling sites (dots) in volcanic rocks of the Cantwell Formation. Pre-Tertiary and post-Paleocene rocks are not differentiated. Geology from Jones and others (1983).

in the 18 lava flows is thermoremanent magnetization acquired during initial cooling. All the lavas exhibited reversed polarity, as is appropriate for their age because Paleocene time was dominated by periods of reversed geomagnetic polarity (Ness and others, 1980).

The paleomagnetic inclinations in these rocks range from -65.8° to -87.6°, and the paleomagnetic pole calculated from the 18 sites (pole 1, fig. 51) is close to northwestern Alaska at lat 70.0° N., long 165.4° W., with a 95-percent-confidence radius of 10.0°. Figure 51 compares this pole with Cretaceous and Paleocene poles from cratonic North America. Somewhat surprisingly, the Cantwell pole is much closer to the Cretaceous reference pole (135-78 m.y. B.P.) than to the Paleocene reference pole (67-61 m.y. B.P.). This difference could be accounted for if the Cantwell volcanic rocks were, in fact, slightly older than the age range of the Paleocene reference because the interval from latest Cretaceous to early Paleocene was a time of rapid apparent polar wander for the North American craton. The paleomagnetic latitude of the Cantwell, calculated according to the improved method of Kono (1980), is 83.0°, with a 95-percent-confidence deviation of ±9.7°. The locus of this paleolatitude is shown as a dashed circle in figure 51 around the location of the basin in which the Cantwell Formation was deposited. The result is the same as when poles are compared: The paleolatitude is what would be expected for Cretaceous time and somewhat, but not significantly, high for Paleocene time.

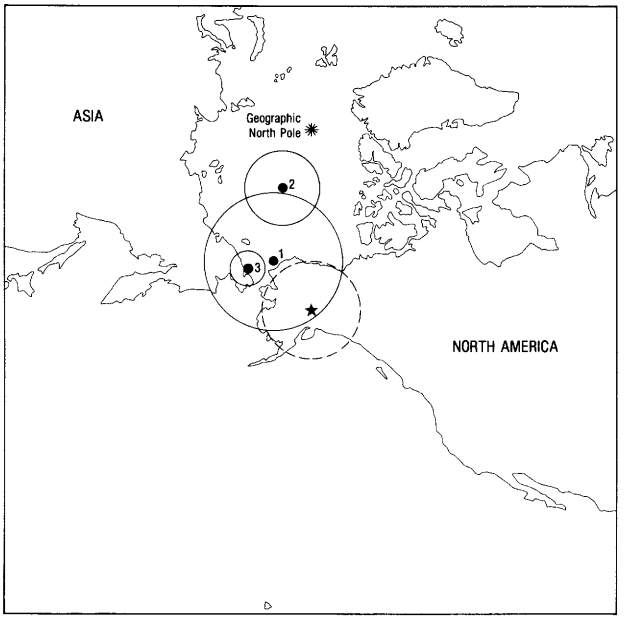

Figure 51.—Locations of paleomagnetic poles in North America, with 95-percent-confidence circles: 1, volcanic rocks of the Paleocene Cantwell Formation; 2, Paleocene intrusive rocks in Montana (Jacobson and others, 1980); 3, Cretaceous pole for North American craton (Mankinen, 1978). Star denotes study area. Dashed circle is locus of poles corresponding to mean geomagnetic latitude of the Cantwell Formation according to Kono's (1980) statistical method.

The timing of accretion of tectonostratigraphic terranes in Alaska is constrained by this new paleolatitude determination. From paleomagnetic and geologic evidence, the general pattern of accretion of terranes south of the Denali fault has been one of northward movement: for example, Wrangellia (Hillhouse, 1977; Csejtey and others, 1982), the Peninsular terrane (Stone and Packer, 1979), and the Chugach terrane (Grommé and Hillhouse, 1981). The volcanic rocks of the Cantwell are just north of the McKinley strand of the Denali fault (fig. 50) and overlie the Pingston and McKinley terranes, which are also bounded on the south by the McKinley strand of the Denali fault (Jones and others, 1982). These terranes and, by implication, other terranes to the north, such as the Nixon Fork and Yukon-Tanana terranes, have undergone no northward displacements greater than about 500 km since Paleocene time. Moreover, recently discovered evidence that strike-slip movement on the McKinley strand has been minimal (Csejtey and others, 1982, 1983) likewise implies that the northward movement and accretion of Wrangellia and the Peninsular terrane were complete by Paleocene time.

REFERENCES CITED

Csejtey, Béla, Jr., Cox, D. P., Evarts, R. C., Stricker, G. D., and Foster, H. L., 1982, The Cenozoic Denali fault system and the Cretaceous accretionary development of southern Alaska: Journal of Geophysical Research, v. 87, no. 5, p. 3741-3754.

Csejtey, Béla, Jr., Yeend, W. E., and Goerz, D. J., III, 1983, Occurrence of probable Cantwell Formation rocks south of the Denali fault system in the Healy quadrangle, south-central Alaska, in Coonrad, W. L., and Elliott, R. L., eds., The United States Geological Survey in Alaska: Accomplishments during 1981: U.S. Geological Survey Circular 868, p. 77-79.

Gilbert, W. G., Ferrell, V. M., and Turner, D. L., 1976, The Teklanika Formation—a new Paleocene volcanic formation in the central Alaska Range: Alaska Division of Geological and Geophysical Surveys, Geologic Report 47, 16 p.

Grommé, C. S., and Hillhouse, J. W., 1981, Paleomagnetic evidence for northward movement of the Chugach terrane, southern and southeastern Alaska, in Albert, N. R. D., and Hudson, Travis, eds., The United States Geological Survey in Alaska: Accomplishments during 1979: U.S. Geological Survey Circular 823-B, p. B70-B72.

Hickman, R. G., 1974, Structural geology and stratigraphy along a segment of the Denali Fault system, central Alaska Range: Madison, University of Wisconsin, Ph. D. thesis, 276 p.

Hillhouse, J. W., 1977, Paleomagnetism of the Triassic Nikolai Greenstone, McCarthy quadrangle, Alaska: Canadian Journal of Earth Sciences, v. 14, no. 11, p. 2578-2592.

Jacobson, D., Beck, M. E., Jr., Diehl, J. F., and Hearn, B. C., Jr., 1980, A Paleocene paleomagnetic pole for North America from alkalic intrusions, central Montana: Geophysical Research Letters, v. 7, no. 7, p. 549-552.

Jones, D. L., Silberling, N. J., and Coney, P. J., 1983, Tectonostratigraphic and interpretive bedrock geologic map of the Mt. McKinley region, Alaska: U.S. Geological Survey Open-File Report 83-11, scale 1:250,000.

Jones, D. L., Silberling, N. J., Gilbert, W. G., and Coney, P. J., 1982, Character, distribution, and tectonic significance of accretionary terranes in the central Alaska Range: Journal of Geophysical Research, v. 87, no. 5, p. 3709-3717.

Kono, Masaru, 1980, Statistics of paleomagnetic inclination data: Journal of Geophysical Research, v. 85, no. B7, p. 3878-3882.

Mankinen, E. A., 1978, Paleomagnetic evidence for a Late Cretaceous deformation of the Great Valley sequence, Sacramento Valley, California: U.S. Geological Survey Journal of Research, v. 6, no. 3, p. 383-390.

Ness, Gordon, Levi, Shaul, and Couch, Richard, 1980, Marine magnetic anomaly timescales for the Cenozoic and Late Cretaceous: A precis, critique, and synthesis: Reviews of Geophysics and Space Physics, v. 18, no. 4, p. 753-770.

Stone, D. B., and Packer, D. R., 1979, Paleomagnetic data from the Alaska Peninsula: Geological Society of America Bulletin, v. 90, no. 6, p. 545-560.

Wolfe, J. A., 1972, An interpretation of Alaskan Tertiary floras, in Graham, Alan, ed., Floristics and paleofloristics of Asia and eastern North America: Amsterdam, Elsevier, p. 201-233.

Wolfe, J. A. and Wahrhaftig, C. A., 1970, The Cantwell Formation of the central Alaska Range, in Cohee, G. V., Bates, R. G., and Wright, W. B., Changes in stratigraphic nomenclature by the U.S. Geological Survey, 1968: U.S. Geological Survey Bulletin 1294-A, p. A41-A46.

Paleogene volcanic rocks of the Matanuska Valley area and the displacement history of the Castle Mountain fault

By Miles L. Silberman and Arthur Grantz

Primitive strontium-isotopic composition and overall bimodal distribution of silica in upper Paleocene and Eocene subalkalic tholeiitic to calc-alkaline basalt and low-potassium rhyolite of the Matanuska Valley and southern Talkeetna Mountains (area 15, fig. 44; fig. 52) suggest that these rocks were derived from the mantle with little contamination by continental crust. The volcanic rocks consist of rhyolite tuff and ash flows, as well as basalt flows and dikes, in the nonmarine Arkose Ridge Formation of the southwestern Talkeetna Mountains; of subaerial basalt and andesite flows, tuff, and mafic intrusions in the southeastern Talkeetna Mountains; and of felsic and mafic dikes, sills, and small plutons in the Matanuska Valley. Figure 53 shows the generalized geology of the area in which the volcanic rocks occur and the localities sampled for potassium-argon-age determinations and for chemical and strontium-isotopic analysis. Tables 16 and 17 list the analytical results.

The volcanic-rock-bearing terranes lie adjacent to or astride the Castle Mountain fault system, which forms the physiographic and structural boundary between the Talkeetna Mountains on the north and the lower and middle reaches of the Matanuska Valley on the south (figs. 52, 53). The Arkose Ridge Formation lies along the north side of the fault, opposite the lower and middle Matanuska Valley, where it contacts coeval but lithologically distinct coal-bearing strata of the Chickaloon Formation (Winkler, 1978). According to J. A. Wolfe (written commun., 1981), both the Chickaloon and Arkose Ridge Formations contain fossil plants of late Paleocene age. The volcanic suite of the southeastern Talkeetna Mountains consists of a thick sequence of flows and pyroclastic rocks, which are preserved only on the north side of the Castle Mountain fault system, and of mafic intrusions, which occur on both sides of the major Caribou (northern) strand of this fault system.

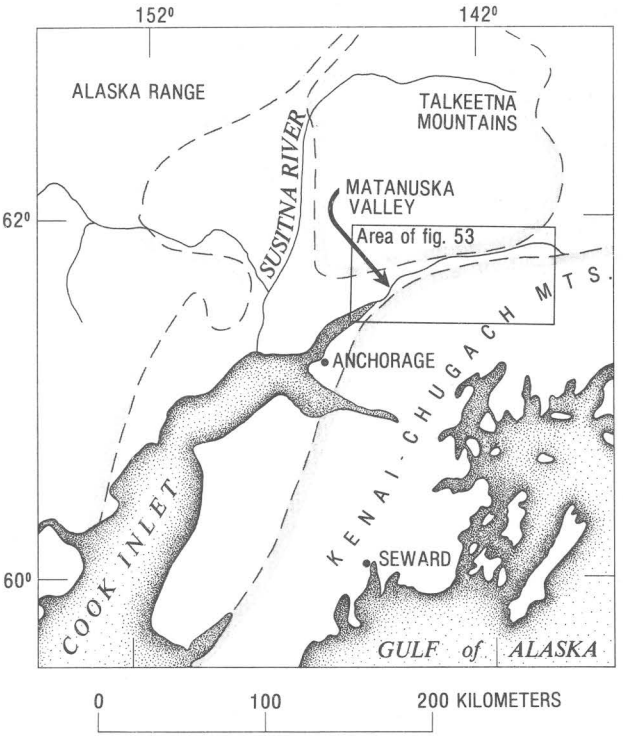

Figure 52.—Index map of part of southern Alaska, showing location of Matanuska Valley area included in figure 53 and major physiographic features in surrounding region.

Potassium-argon ages of three basalt flows, two rhyolite tuff units and ash flows in the lower part of the Arkose Ridge Formation, and a basalt dike near the middle of the formation range from 45.5±1.8 to 56.2±1.7 m.y. These data (table 16) suggest that the age of the Arkose Ridge Formation is included within the interval latest Paleocene to middle Eocene, which is similar to the age indicated by the plant fossils.

Slightly younger potassium-argon ages were obtained on the intrusive volcanic rocks in the Matanuska Valley. Felsic intrusions, a basalt sill, and hornfelsed

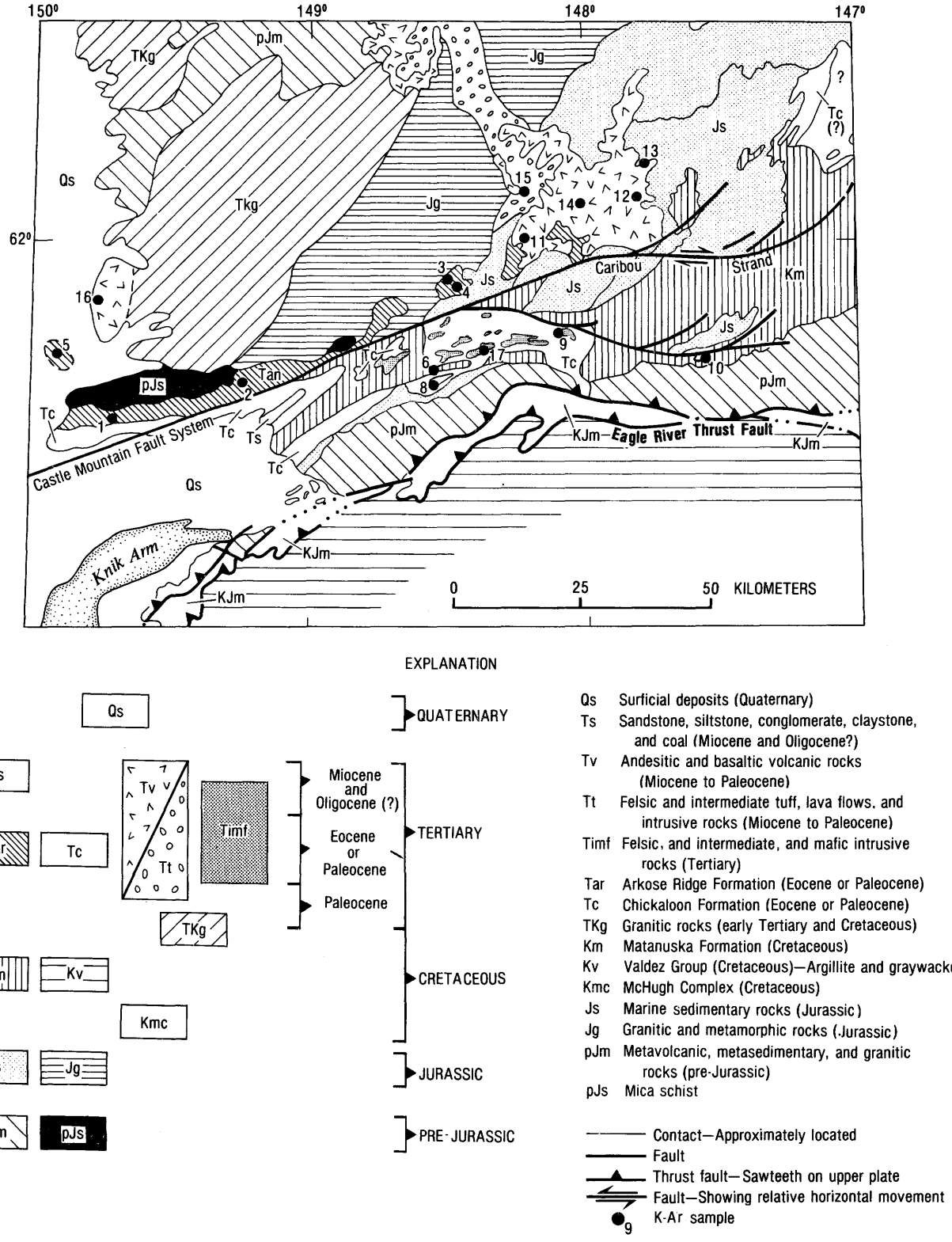

Figure 53.—Geologic sketch map of the Matanuska Valley and part of surrounding region, southern Alaska (modified from Beikman, 1974), showing 16 sample sites where volcanic rocks were collected for age determinations and other analyses (see tables 16, 17).

Upper Cretaceous shale in contact with a large felsic stock yielded potassium-argon ages of 37.5±1.2 to 45.5±2.3 m.y., which correspond to the late Eocene. These ages are compatible with the late Paleocene age of the fossil plants in the Chickaloon Formation (J. A. Wolfe, written commun., 1981), which these volcanic rocks intrude.

Table 16.--Potassium-argon ages of volcanic rocks from the Matanuska Valley and southern Talkeetna Mountains

[Potassium and argon analyses by isotope-dilution/mass-spectrometric techniques; analysts, U.S. Geological Survey, Menlo Park, Calif., and Kruger Enterprises, Cambridge, Mass.]

Map No. (fig. 53)	Field No.	Rock type	Material analyzed	K_2O (wt pct)	Age (m.y.)
		Arkose Ridge Formation			
1	77AGz-AR3	Basalt flow	Whole rock	0.43	50.0±2.5
2	77AGz-AR10	Basalt dike	do	.28	46.1±2.8
3	78ASi-M23	Rhyolite tuff	do	8.43	50.5±1.5
4	79AGz-38A	--do--	do	1.95	45.5±1.8
	79AGz 38B	Rhyolite ash-flow tuff.	Alkali feldspar.	3.31	51.4±1.5
5	78ASi-M19	Basalt flow	Whole rock	.28	56.2±1.7
[1]16	78ASi-M21	--do--	do	1.90	51.8±1.6
		Intrusive volcanic rocks of the Matanuska Valley			
6	78ASi-M6	Rhyolite dike	Whole rock	0.91	40.0±1.6
7	78ASi-M8	Dacite dike	do	1.10	43.5±1.7
8	78ASi-M22A	Rhyolite stock	do	1.70	37.5±1.2
	78ASi-M7	Slide block of hornfelsed shale of the Matanuska Formation in contact with rhyolite stock at locality 8.	do	2.05	40.0±1.2
9	78ASi-M45	Basalt sill	do	.13	40.9±1.6
10	79AG-112	Dacite stock	do	.67	45.5±2.3
		Volcanic rocks of the southeastern Talkeetna Mountains			
11	79AGz-112	Basalt flow	Whole rock	0.20	[2]60.1±4.6
12	79AGz-107	Andesite flow	do	1.50	48.4±2.4
13	79AGz-106	Basalt flow	do	.39	55.5±3.5
14	79AGz-102	Plug	do	.42	46.7±2.3
15	79AGz-116	Pyroclast in tuff breccia.	do	1.78	43.6±2.2

[1]Assignment to Arkose Ridge formation tentative.

[2]Data somewhat uncertain owing to low K_2O content.

Potassium-argon ages of volcanic rocks in the southeastern Talkeetna Mountains—43.6±2.2 to 60.1±4.6 m.y. (late Paleocene to late Eocene)—essentially overlap the potassium-argon ages of samples from the Arkose Ridge Formation (table 16). Stratigraphic relations in the southeastern Talkeetna Mountains, however, contradict the age equivalency of these volcanic rocks and the Arkose Ridge Formation. The Talkeetna Mountains volcanic rocks overlie generally gently deformed fluviatile gravel that rests unconformably on the strongly folded and faulted rocks of the Chickaloon Formation. Because plant fossils suggest that the Chickaloon and the Arkose Ridge are coeval, we had expected to obtain ages from the southeastern Talkeetna Mountains volcanic rocks that were somewhat younger than those in the Arkose Ridge. Possibly the contradiction is due to a large uncertainty in the 60.1-m.y. age for the southeastern Talkeetna Mountains volcanic rocks, caused by its large content of potassium and radiogenic argon. Excluding this determination, the age for the volcanic rocks would range from 43.6±2.2 to 55.5±3.5 m.y., or from latest Paleocene to late Eocene. This age range would permit the volcanic rocks of the southeastern Talkeetna Mountains to be younger than the Arkose Ridge Formation, but it would certainly not prove that they are, in fact, younger. The age determinations do, however, indicate that the interval between deposition of the Arkose Ridge Formation and the volcanic rocks was short.

All the dated southeastern Talkeetna Mountains samples are from bedded volcanic rocks, and a plug intruding them, from the north side of the Castle Mountain fault system. These bedded volcanic rocks are absent south of the main northern (Caribou) strand of this fault system. In the southeastern Talkeetna Mountains, however, just east of the area shown in figure 53, mafic dikes and sills in the underlying country rock have a contiguous distribution both north and south of the Caribou fault (Grantz, 1965). Contiguity, lithology, and the observation (Grantz, 1960) that the mafic dikes on opposite sides of the fault have the same strong west-northwestward preferred orientation suggest that these dikes form a related volcanic field. None of these eastern dikes have yet been dated, and so we cannot compare their ages to those of the volcanic rocks discussed here, although Grantz (1960) assigned them to the Eocene.

The three suites of volcanic rocks in the Matanuska Valley area have an essentially bimodal distribution of silica, with peaks between 45 to 53 and 69 to 78 percent SiO_2, although some intermediate compositions also occur. Strontium-isotopic ratios of six samples of volcanic rock from the Matanuska Valley and from the Arkose Ridge Formation range from 0.7037 to 0.7042; one sample from the southwestern Talkeetna Mountains is slightly more radiogenic ($^{87}Sr/^{86}Sr$=0.7047). This rock, which may be part of the Arkose Ridge Formation, rests on granitic rocks through which it was probably extruded; it may be slightly contaminated by the probably more radiogenic strontium of the granite. The strontium-isotopic ratios are fairly primitive and nearly as low as those measured in igneous rocks from ensimatic island arcs or along continental margins, where the crust is young (Peterman and Hedge, 1974). We believe that these low isotopic ratios are consistent with derivation of the magmas from the upper mantle, with minimal strontium-isotope exchange with older crustal rocks. Preliminary rare-earth-element data suggest little fractionation for the more mafic rocks at shallow crustal levels but are inconsistent for the more felsic varieties (M. L. Silberman and K. J. Wenrich, unpub. data, 1981).

The strontium-isotopic ratios for the volcanic rocks of the Matanuska Valley area contrast sharply

Table 17.--Strontium-isotopic analyses and selected chemical data for volcanic rocks of the Matanuska Valley and southern Talkeetna Mountains

[See figure 53 for location of samples. Analyses by solid-source mass spectrometry; analyst, D. G. Brookins. $^{87}Sr/^{86}Sr$ ratio normalized to $^{87}Sr/^{86}Sr=0.1194$. E and A, $SrCO_3=0.7080\pm 0.0001$. Decay constant for ^{87}Rb, 1.42×10^{-11} yr^{-1}. Analytical uncertainty, ±0.03 percent. $(\ )_m$, measured ratio; $(\ )_o$, ratio corrected for age of rock. SiO_2 analyses by X-ray fluorescence; analysts: V. McDaniel, G. Kawakita, and D. Hopping]

Map No. (fig. 53)	Field No.	Rock type	SiO_2 (wt pct)	Rb (ppm)	Sr (ppm)	$(^{87}Sr/^{86}Sr)_m$	$(^{87}Sr/^{86}Sr)_o$
		Arkose Ridge Formation					
1	77AGz-AR3	Basalt flow------	47.92	5	370	0.7042	0.7042
5	78ASi-M19	do----------	45.9	10	500	.7041	.7041
16	78ASi-M21	do----------	50.46	29	640	.7084	.7047
		Intrusive volcanic rocks of the Matanuska Valley					
8	78ASi-M22A	Rhyolite stock---	74.80	49	54	0.7056	0.7042
9	78ASi-M45	Basalt sill------	49.9	10	183	.7042	.7047
10	78ASi-M9	Dacite stock-----	69.31	25	115	.7041	.7037
17	78ASi-M12	Basalt sill------	46.40	10	102	.7037	.7036

with the higher (0.706-0.707) values measured in sandstone of the Orca and Valdez Groups and in the granodiorite believed to be anatectically derived from them. According to Hudson and others (1979), the anatexis followed subduction and accretion of the Orca and Valdez Groups (Chugach and Prince William terranes) to coastal southern Alaska during the Late Cretaceous or early Tertiary (MacKevett and Plafker, 1974; Plafker and others, 1977). It appears unlikely that the volcanic rocks of the Matanuska Valley area originated from melting of older crustal material. Instead, their strontium-isotopic ratios and geologic setting suggest that these rocks were emplaced in a continental margin with young crust. This crust was composed of allochthonous terranes that had been accreted and welded by plutonism to nuclear Alaska during Late Cretaceous and Paleocene time, and it included thick prisms of newly deposited Paleocene and Eocene continental sedimentary rocks. At least some of these volcanic rocks may be the remnants of a late Paleocene and Eocene arc that was emplaced on this young continental margin in response to subduction in the present Gulf of Alaska-Chugach Mountains area.

The age and stratigraphic and structural relations of the volcanic and sedimentary rocks of the Matanuska Valley area also help constrain the history of movement on the Castle Mountain fault system. Juxtaposition of the coeval, but lithologically distinct, Arkose Ridge and Chickaloon Formations indicates that large-scale strike-slip motion on the Castle Mountain right-lateral fault was post-late Paleocene (fossil-plant-assemblage ages) and (or) post-early or middle Eocene (potassium-argon ages of volcanic rocks within and intruding these formations). Contiguity and similar structural orientation of the mafic dike field across the eastern part of the Caribou strand of the Castle Mountain fault system (Grantz, 1960) suggest that this strike-slip motion was largely complete during the Eocene, although this suggestion requires confirmation from radiometric ages of some of these dikes. Felsic stocks, plugs, and dikes occur on both sides of the Castle Mountain strand of the fault system in the upper Matanuska Valley (Detterman and others, 1976). South of the Castle Mountain strand, these rocks have been radiometrically dated at late Eocene (table 16). If, as we suspect, the felsic rocks north and south of the strand are coeval, then these relations would support the proposed minimum age of large-scale right-lateral motion on the fault system. None of our data preclude postintrusive large-scale mainly vertical motion on the fault system.

The potassium-argon ages reported here, within the context of the geology of the Matansuka Valley area, suggest that volcanism and major lateral slip on the Castle Mountain fault system were both largely Eocene events. Strong temporal association is supported by the previously noted west-northwestward preferred orientation of the Eocene mafic dikes in the southeastern Talkeetna Mountains. The trend of these dikes indicates that at the time of their emplacement, the maximum and minimum principal stresses in the region were generally horizontal, with the maximum stress oriented west-northwest-east-southeastward. This orientation is appropriate for right-lateral movement on the high-angle to vertical east-northeast-trending Castle Mountain fault system.

REFERENCES CITED

Beikman, H. M., compiler, 1974, Preliminary geologic map of the southeast quadrant of Alaska: U.S. Geological Survey Miscellaneous Field Studies Map MF-612, scale 1:1,000,000, 2 sheets.

Detterman, R. L., Plafker, George, Tysdal, R. G., and Hudson, Travis, 1976, Geology and surface features along part of the Talkeetna segment of the Castle Mountain-Caribou fault system: U.S. Geological Survey Miscellaneous Field Studies Map MF-738, scale 1:63,360.

Grantz, Arthur, 1960, Generalized geologic map of the Nelchina area, Alaska, showing igneous rocks and larger faults: U.S. Geological Survey Miscellaneous Geologic Investigations Series Map I-312, scale 1:96,000.

———1965, Geologic map and cross sections of the Nelchina area, south-central Alaska: U.S. Geological Survey open-file report, scale 1:63,360, 4 sheets.

Hudson, Travis, Plafker, George, and Peterman, Z. E., 1979, Paleogene anatexis along the Gulf of Alaska margin: Geology, v. 7, no. 12, p. 573-577.

MacKevett, E. M., Jr., Plafker, George, 1974, The Border Ranges fault in south-central Alaska: U.S. Geological Survey Journal of Research, v. 2, no. 3, p. 323-329.

Peterman, Z. E., and Hedge, C. E., 1974, Isotopes in nature, pt. B of Strontium, sec. 38 of Wedepohl, K. H., ed., Handbook of geochemistry: Berlin, Springer-Verlag, p. 38-B-1 to 38-B-14.

Plafker, George, Jones, D. L., and Pessagno, E. A., Jr., 1977, A Cretaceous accretionary flysch and melange terrane along the Gulf of Alaska margin, in Blean, K. M., ed., The United States Geological Survey in Alaska: Accomplishments during 1976: U.S. Geological Survey Circular 751-B, p. B41-B43.

Winkler, G. R., 1978, Framework grain mineralogy and provenance of sandstone from the Arkose Ridge and Chickaloon Formations, Matanuska Valley, in Johnson, K. M., ed., The United States Geological Survey in Alaska: Accomplishments during 1977: U.S. Geological Survey Circular 772-B, p. B70-B73.

Structural relations and fluid-inclusion data for mineralized and nonmineralized quartz veins in the Port Valdez gold district, Valdez quadrangle, southern Alaska

By William J. Pickthorn and Miles L. Silberman

The Port Valdez district is one of several gold districts, including the Port Wells, Girdwood, Hope-Sunrise, Moose Pass, and Nuka Bay, located within the Valdez Group around Prince William Sound. The gold occurs in epigenetic hydrothermal quartz veins, a few of which have been mined on a small scale. Total production for the district is probably less than 100,000 troy oz (Berg and Cobb, 1967). At its peak of activity, the district comprised a belt more than 40 km long from the westernmost occurrence at Columbia Glacier to east of Valdez Glacier, and more than 12 km wide from the shore of Port Valdez to beyond the head of Mineral Creek (area 14, fig. 44; fig. 54). Brooks (1912) considered that these limits of mineral occurrence were determined only by accessibility and exposure and that the district should be considered a geographic rather than a geologic province.

The Valdez Group, dominantly graywacke, argillite, slate, and minor greenstone, is the major component of the Chugach terrane (Plafker and others, 1977; Winkler and others, 1981). This terrane was juxtaposed against the North American Continent during Late Cretaceous and (or) early Tertiary time (MacKevett and Plafker, 1974). Penetrative deformation during accretion resulted in tight folding of the rocks and

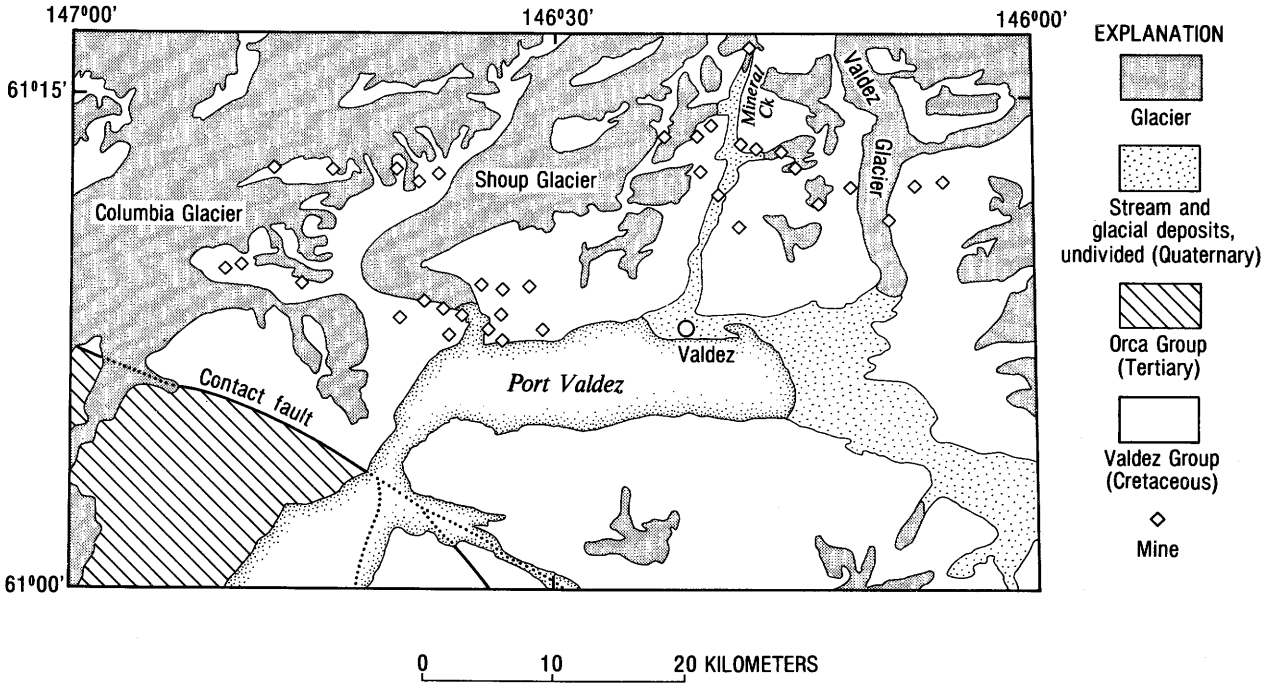

Figure 54.—Generalized geologic map showing approximate location of individual mines in Port Valdez gold district (Cobb and Matson, 1972; Winkler and others, 1981).

development of axial-plane cleavage in which the dominantly steep east-west-trending structures were overturned slightly to the south (Brooks, 1912; Berg and others, 1972). Locally the rocks have been metamorphosed to lower greenschist facies.

Gold deposits in the Port Valdez district occur as fissure veins in faults, fractures, and shear zones, principally along the axes and upper limbs of overturned anticlinal structures (Brooks, 1912). Thus, the mineral occurrences are located in distinct local belts (fig. 54). The occurrence and grade of gold mineralization appear to be unrelated to host-rock lithology but may correlate with the more disturbed and sheared areas.

Two fairly distinct types of quartz veins are found in the Port Valdez area. The first type consists of thin (generally less than 10 cm thick) irregular veins that principally parallel regional cleavage. These veins, and similar cleavage-localized quartz veins in the Hope-Sunrise district (Mitchell, 1979; Mitchell and others, 1981), are considered to be a result of metamorphic-segregation processes (Robin, 1979). The metamorphic quartz is white, massive, fine grained, and tightly frozen to the wallrock. Pyrite, the only sulfide mineral observed, in some places is found along the edges of veins and in wallrock fragments within the veins. Calcite is a common vein constituent. Most often these veins are found along cleavage or bedding planes, and seldom as joint and fracture fillings.

The second type of veins are those associated with gold mineralization. Such veins are coarse grained, vuggy, iron stained, and commonly shattered, with well-developed shears on one or both walls. These veins, ranging from several centimeters to a meter in width, are discontinuous (commonly separated along strike by great distances of barren shattered country rock), podiform, and most commonly occur as fracture fillings in joints and faults that crosscut and, in many places, offset metamorphic-segregation veins and regional cleavage. Figure 55 illustrates the difference in orientation for the mineralized veins and the cleavage-localized metamorphic-segregation quartz veins. A few mineralized veins are also found in shear zones along bedding planes and contacts. The mineralized veins are all postfolding. Structural features suggest that mineralization occurred along joints and faults which opened during relaxation of the compressive forces and (or) uplift, as was the case at Hope-Sunrise (Mitchell and others, 1981). The absence of wallrock alteration or mineralization suggests that the mineralized veins formed at a temperature below or equal to that of metamorphism.

Vein mineralogy consists of quartz, chloritized wallrock inclusions, calcite, sulfides, free gold, and minor albite (Brooks, 1912; Johnson, 1915). The sulfide minerals pyrite, galena, sphalerite, chalcopyrite, stibnite, pyrrhotite, and arsenopyrite (Brooks, 1912; Johnson, 1915), as well as free gold, are found associated with late-stage quartz, in microfractures, and in open cavities. Together, the sulfides generally make up less than 3 percent of the ore. Mine reports indicate that mineralization is discontinuous along strike but commonly is found in steeply dipping pipelike shoots.

Fluid inclusions in the metamorphic-segregation and mineralized veins have different characteristics.

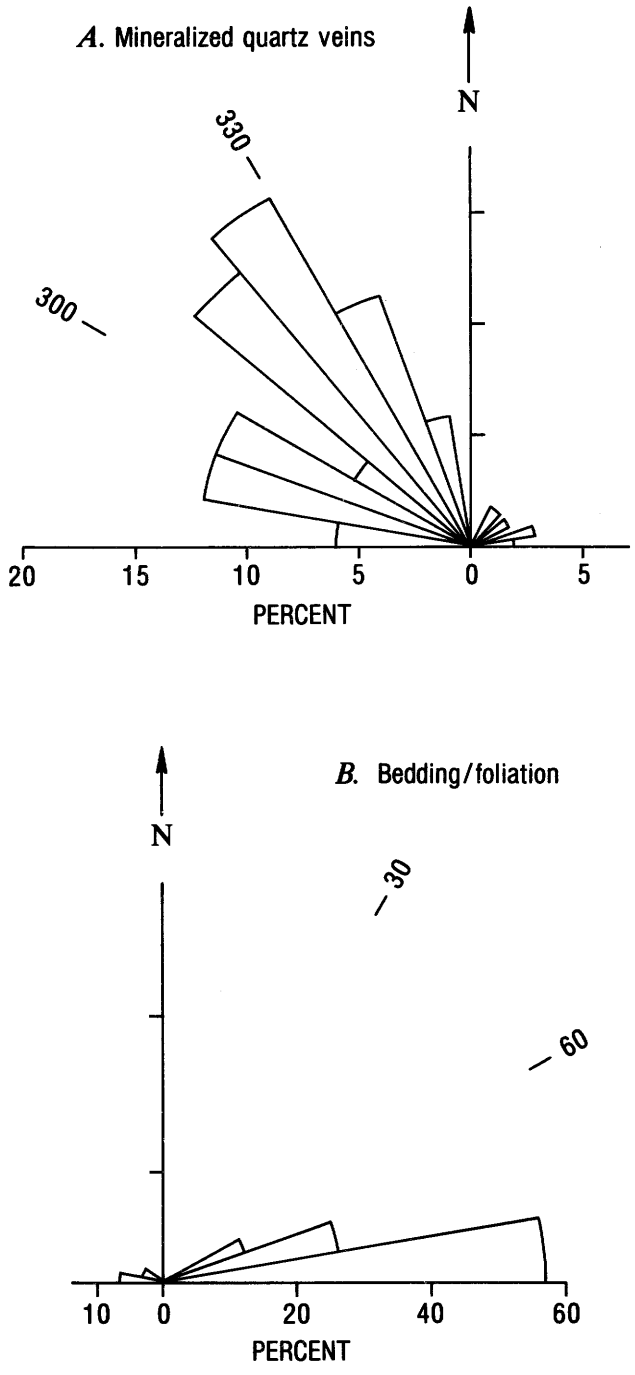

Figure 55.—Rose diagrams showing orientation and percentage of measured occurrences within each 10° of azimuth for mineralized quartz veins (A) and bedding/foliation (B) for mines in Port Valdez gold district, Alaska. Data from Brooks (1912), Johnson (1915), and this study.

In the metamorphic quartz, primary inclusions are small (generally less than 5 μm diam), and are liquid dominated; the volume of the vapor phase is estimated

at 15 to 20 percent. Primary inclusions in the mineralized samples vary considerably in size and commonly range as large as 10 μm in diameter, some even larger. These inclusions are principally liquid dominated, with varying liquid-to-vapor ratios, but are in part vapor dominated. Secondary inclusions are flattened or elongate, with very little or no vapor phase, and are easily recognized as occurring along healed fractures. Pseudosecondary inclusions are common in the mineralized quartz. A total of 36 samples of the two types of quartz veins were examined.

Figure 56 plots the filling temperatures, uncorrected for pressure, of both types of quartz veins. Inclusions in the metamorphic quartz have a narrow range of homogenization temperatures centering about 170°C; actual formation temperature, by addition of a correction for confining pressure, are higher (Roedder, 1979). Homogenization temperatures of inclusions in the mineralized-vein samples vary widely. Samples from the mineralized quartz veins were divided into two groups: (1) Quartz from the edge or other unmineralized areas of the veins, and (2) late-stage quartz directly associated with mineralization. Inclusions in the unmineralized samples are liquid dominated and have a narrow range of homogenization temperatures near 150°C. In the mineralized quartz the inclusions are both liquid and vapor dominated. Homogenization temperatures for inclusions that fill to the fluid phase range over 100°C, as high as 240°C. Vapor-dominated inclusions could not be measured because of inadequate lighting, which made it impossible to determine the homogenization point. This wide variation in homogenization temperatures and the presence of simultaneously formed liquid- and vapor-dominated inclusions suggest that the inclusions formed from a medium in which both liquid and vapor were present, that is, that the hydrothermal fluid was boiling (Roedder, 1979, p. 697). If boiling occurred, the actual temperature of formation would be that indicated from co-homogenizing liquid- and vapor-dominated inclusions and would probably be in the range of or slightly lower than the 240°C observed (Roedder, 1972, 1979). Homogenization temperatures for the two quartz-vein types are fairly consistent districtwide and do not appear to be related to elevation.

Salinity measurements by freezing point depression for inclusions in the metamorphic quartz show a tight grouping in the range 8.5-10 weight percent NaCl equivalent. In contrast, inclusions in the mineralized-vein samples have salinities less than 6.5 weight percent NaCl equivalent; however, precise measurements were impossible owing to the formation of metastable superheated ice, caused by low salinity and complete filling of the cavity by the ice upon freezing (Roedder, 1967, 1972).

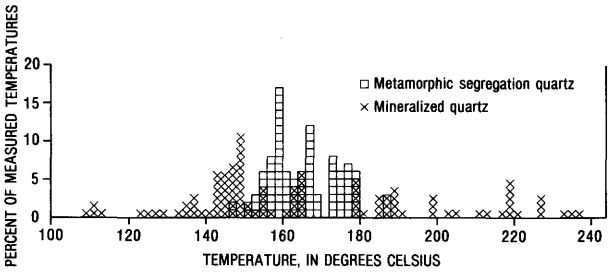

Figure 56.—Fluid-inclusion filling temperatures, uncorrected for pressure, in metamorphic-segregation- and mineralized-quartz-vein samples, Port Valdez gold district, southern Alaska.

The source of the ore constituents and hydrothermal fluids is still under investigation, but we suggest two possible derivation mechanisms. Boyle (1979) showed that such sedimentary rocks as those of the Valdez Group can contain considerable gold. During metamorphism, the gold, along with other ore constituents (sulfur, base metals, and carbon), can be mobilized through diffusion and (or) mass transfer and deposited in suitable chemical or structural traps. Henley and others (1976) suggested that the gold-quartz and scheelite-quartz lodes in the Haast Schist, Otago district, New Zealand, were formed by such a process. Upward migration of the Otago fluids was in response to opening of structures during uplift and unloading of the schist terrane; deposition was due to lowering of temperature as the fluids migrated into lower grade (greenschist facies) rocks, and to reaction with these rocks.

An alternative explanation for the generation of the mineralized veins may be a mechanism similar to that described for lode deposits in the Hope-Sunrise district, northern Kenai Peninsula (Mitchell and others, 1981; Silberman and others, 1981). Hope-Sunrise is similar in host-rock, structural, and mineralogic characteristics to Port Valdez: Unmineralized cleavage, localized quartz, and mineralized crosscutting fissure- and fault-localized veins. Stable-isotope analyses reported by the above-mentioned workers suggest a dominance of meteoric water in the ore-forming fluid. These workers suggested that accretion of the Valdez Group to the North American Continent was followed by high-grade metamorphism and partial melting of lower parts of the sedimentary wedge (Hudson and others, 1979), grading upward to lower-greenschist and upper-zeolite-facies metamorphism in the upper part. After metamorphism, uplift and dilation allowed meteoric waters to circulate to depth along fractures and faults. Hydrothermal-convection cells were probably formed, heated and driven by the still-hot high-grade and granitized rocks. Ore constituents were leached from the metamorphosed sediment and deposited as fissure veins in the lower temperature rocks.

The two processes—fluid migration versus hydrothermal leaching—may not be mutually exclusive. At Port Valdez, fluids generated by metamorphic dehydration at depth may have ascended and mixed with circulating meteoric fluids; the resulting dilution and decrease in temperature and pressure would have caused deposition in the open structures. The low temperatures and salinities of fluid inclusions in the mineralized veins may reflect this process.

REFERENCES CITED

Berg, H. C., and Cobb, E. H., 1967, Metalliferous lode deposits of Alaska: U.S. Geological Survey Bulletin 1246, 254 p.

Berg, H. C., Jones, D. L., and Richter, D. H., 1972, Gravina-Nitzotin belt—tectonic significance of an upper Mesozoic sedimentary and volcanic sequence in southern and southeastern Alaska, in Geological Survey research 1972: U.S. Geological Survey Professional Paper 800-D, p. D1-D24.

Boyle, R. W., 1979, The geochemistry of gold and its deposits: Geological Survey of Canada Bulletin 284, 585 p.

Brooks, A. W., 1912, Gold deposits near Valdez, in Mineral resources of Alaska: Report on progress of investigations in 1911: U.S. Geological Survey Bulletin 520, p. 108-130.

Cobb, E. H., and Matson, N. A., compilers, 1972, Metallic mineral resources map of the Valdez quadrangle, Alaska: U.S. Geological Survey Miscellaneous Field Studies Map MF-438, scale 1:250,000.

Henley, R. W., Norris, R. J., and Paterson, C. J., 1976, Multistage ore genesis in the New Zealand geosyncline—a history of post-metamorphic lode emplacement: Mineralium Deposita, v. 11, no. 1, p. 180-196.

Hudson, Travis, Plafker, George, and Peterman, Z. E., 1979, Paleogene anatexis along the Gulf of Alaska margin: Geology, v. 7, no. 12, p. 573-577.

Johnson, B. L., 1915, The gold and copper deposits of the Port Valdez district, in Mineral resources of Alaska: Report on progress of investigations in 1914: U.S. Geological Survey Bulletin 622, p. 140-188.

MacKevett, E. M., Jr., and Plafker, George, 1974, The Border Ranges fault in south-central Alaska: U.S. Geological Survey Journal of Research, v. 2, no. 3, p. 323-329.

Mitchell, P. A., 1979, Geology of the Hope-Sunrise (gold) mining district, north-central Kenai Peninsula, Alaska: Stanford, Calif., Stanford University, M. Sc. thesis, 123 p.

Mitchell, P. A., Silberman, M. L., and O'Neil, J. R., 1981, Genesis of gold vein mineralization in an Upper Cretaceous turbidite sequence, Hope-Sunrise district, southern Alaska: U.S. Geological Survey Open-File Report 81-103, 18 p.

Plafker, George, Jones, D. L., and Pessagno, E. A., Jr., 1977, A Cretaceous accretionary flysch and melange terrane along the Gulf of Alaska margin, in Blean, K. M., ed., The United States Geological Survey in Alaska: Accomplishments during 1976: U.S. Geological Survey Circular 751-B, p. B41-B43.

Robin, P. Y. F., 1979, Theory of metamorphic segregation and related processes: Geochimica et Cosmochimica Acta, v. 43, no. 10, p. 1587-1600.

Roedder, Edwin, 1967, Metastable superheated ice in liquid-water inclusions under high negative pressure: Science, v. 155, no. 3768, p. 1413-1416.

——1972, Composition of fluid inclusions, chap. JJ of Fleischer, Michael, ed., Data of geochemistry (6th ed.): U.S. Geological Survey Professional Paper 440-JJ, p. JJ1-JJ164.

——1979, Fluid inclusions as samples of ore fluids, in Barnes, H. L., ed., Geochemistry of hydrothermal ore deposits (2d ed.): New York, John Wiley, p. 684-780.

Silberman, M. L., Mitchell, P. A., and O'Neil, R., Jr., 1981, Isotopic data bearing on the origin and age of the epithermal lode gold deposits in the Hope-Sunrise mining district, northern Kenai Peninsula, Alaska, in Albert, N. R. D., and Hudson, Travis, eds., The United States Geological Survey in Alaska: Accomplishments during 1979: U.S. Geological Survey Circular 823-B, p. B81-B84.

Winkler, G. R., Silberman, M. L., Grantz, Arthur, Miller, R. J., and MacKevett, E. M., Jr., 1980, Geologic map and summary geochronology of the Valdez quadrangle, southern Alaska: U.S. Geological Survey Open-File Report 80-892-A, scale 1:250,000, 2 sheets.

A preliminary geochemical interpretation of the Chugach Wilderness, southern Alaska

By Richard J. Goldfarb

A geochemical survey is currently being conducted in the Chugach Wilderness, southern Alaska (area 9, fig. 44), as part of the U.S. Geological Survey-Forest Service's mineral resource appraisal program. Most of the Chugach Wilderness is contained within the Seward and Cordova 1:250,000-scale quadrangles (fig. 57). These two quadrangles were previously sampled on a reconnaissance basis by the Los Alamos National Laboratory (LANL) for the U.S. Department of Energy's National Uranium Resource Evaluation (NURE) program. Neutron-activation analysis was used to determine the concentrations of 32 elements (Al, Au, Ba, Ca, Ce, Cl, Co, Cr, Cs, Dy, Eu, Fe, Hf, K, La, Lu, Mg, Mn, Na, Rb, Sb, Sc, Sm, Sr, Ta, Tb, Th, Ti, V, Yb, U, Zn) and X-ray fluorescence spectroscopy to determine the concentrations of 9 other elements (Ag, Bi, Cd, Cu, Nb, Ni, Pb, Sn, W). Geochemical interpretations of these LANL stream-sediment data bases for the Seward and Cordova quadrangles (U.S. Department of Energy, 1981, 1982) are being used to supplement the current study in the Chugach Wilderness. Statistical interpretation of the LANL data is aiding in the recognition of target areas, justifying more detailed fieldwork.

An R-mode factor analysis with varimax was run on analytical data from the 498 stream-sediment samples collected by LANL from the Cordova quadrangle. Applying the principles of matrix algebra, R-mode factor analysis is used to reduce an extensive data matrix into a much smaller factor matrix of intercorrelated variables (see Joreskog and others, 1976); "varimax" refers to orthogonal rotation of the factor axes to obtain a better fit to the variable (element) clusters. R-mode factor analysis was used to find the groupings of associated elements that are characteristic of various localities within the quadrangle. A five-factor model was used that explained 68 percent of the overall data variance. Table 18 lists these factors and the approximate locations of the sites with highest factor scores.

The suite of rare-earth elements constituting factor 1 (table 18) appears to be characteristic of the phyllite and schist (Winkler and Plafker, 1981) that crop out in the northeast corner of the quadrangle. In

addition, this factor generally defines the Tertiary pluton and the Orca Group of the peninsula east of Port Gravina. Samples from this peninsula show U/Th ratios greater than 1, as well as relatively low K concentrations. A radiometric survey of the area (U.S. Department of Energy, 1978) indicated a preferred equivalent-uranium (eU) anomaly just north of Sheep Bay.

Factor 2 consists of predominantly siderophilic elements and correlates well with known copper occurrences in the Ellamar-Port Fidalgo region. This factor is also important in an area north of Cordova, near Ibeck and Power Creeks, and at Mount Kelly. The Ibeck claims in this area contain veins carrying native copper within the Orca Group (Grant and Higgins, 1910). High scores on this factor near the Copper River delta may represent cation adsorption onto mud rich in organic material. The importance of factor 2 along the west side of the Copper River, north of Allen Glacier, possibly reflects a high percentage of mafic metavolcanic rocks within sedimentary rocks of the Valdez Group.

Factor 4 represents a belt of potassium-rich samples extending through Hinchinbrook Island, from English Bay northeastward to Dan Bay, into the southern Heney Range. This area, also strongly enriched in sodium and chlorine, may represent clay-rich zones within marine sedimentary rocks of the Orca Group.

High concentrations of arsenic, cesium, and zinc are associated with factor 5. This factor forms a belt along the coastline, from Port Fidalgo southeastward through many of the Copper River delta sloughs, possibly reflecting sorption of these elements by clays. Within this factor trend are smaller clusters of samples highly anomalous in either zinc or arsenic. Samples enriched in zinc were obtained from streams draining Mount Eccles, just south of Cordova, and from the north tip of Hawkins Island. Followup work may locate sulfides associated with scattered outcrop areas of oceanic tholeiite that have been noted between Cordova and Hinchinbrook Island (S. W. Nelson, oral commun., 1981). A well-defined arsenic anomaly, with some associated gold, is located in the McKinley Peak area, an area already recognized as containing pyrite, arsenopyrite, and free gold in quartz veins and graywacke of the Orca Group (Cobb, 1979). A distinctive arsenic anomaly lies within the Silver Glacier area, to the west of Ellamar, at elevations above the many base-metal occurrences in the region. The occurrence

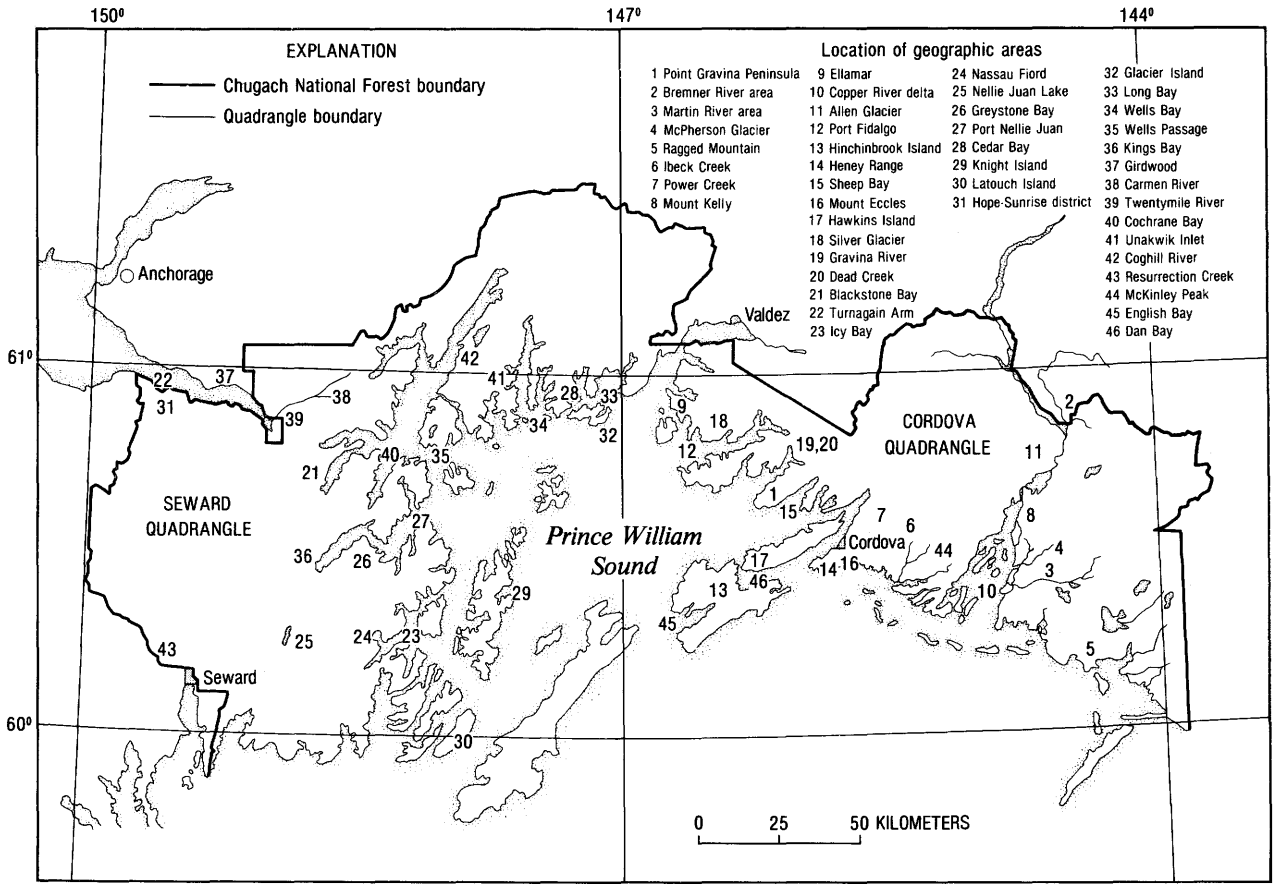

Figure 57.—Prince William Sound region, showing boundaries of Seward and Cordova quadrangles and Chugach National Forest. Numbers indicate approximate locations of geographic areas referred to in text.

of arsenic with gold, tungsten, and copper between the Gravina River and Dead Creek suggests a relation to localized zones of volcanic rocks within the Valdez Group and (or) to a presently unknown granitic body. The south half of the Gravina Point peninsula, already mentioned as having possible uranium occurrences, is also anomalous in arsenic where volcanic rocks have been observed (S. W. Nelson, oral commun., 1981) in the Orca Group section.

Table 18.--Results of a five-factor R-mode factor analysis of data from 498 stream-sediment samples from the Cordova quadrangle

Factor	Significant elements	Locations
1	U, Zr, Ce, Dy, Hf, La, Lu, Sm, Th, Yb, ±Eu	Point Gravina Peninsula. Bremner River region. Martin River region (specifically, south of McPherson Glacier and northwest side of Ragged Mountain).
2	Cu, Ni, Co, Cr, Fe, Mg, Sc, V, Mn, ±Ti	North of Cordova (especially Ibeck and Power Creeks and Mount Kelly). Ellamar. Copper River delta. Copper River, north of Allen Glacier (west side). South side of Port Fidalgo.
3	Au, Sb, Sr, Ta, Tb	No specific locations (erroneously high concentrations related to analytical problems).
4	K±Ba±Al, Na	Zone down central Hinchinbrook Island and into southern Heney Range. Scattered throughout Martin River region.
5	As, Cs, Zn±Rb	Zone along coast from Port Fidalgo through Copper River delta.

An R-mode factor analysis with varimax was run on analytical data from 405 of the 465 stream sediment samples collected from the Seward quadrangle by LANL (60 samples that lacked X-ray fluorescence data were excluded). Table 19 lists the factors (obtained from the four-factor model that was used) responsible for approximately 60 percent of the overall data variance.

The suite of elements constituting factor 1 (table 19) may reflect clay-rich units within areas underlain by the Valdez and Orca Groups of the Seward quadrangle (Tysdal and Case, 1979), as well as several granitic bodies. Factor 2 reflects a distinct enrichment of siderophilic elements in sedimentary rocks of the Valdez Group, relative to the Orca Group and the McHugh Complex. The siderophilic association also occurs around the Knight Island and LaTouche Island copper deposits. However, most sample volumes from these islands were too small for accurate analytical measurement by LANL's techniques and thus could not be used for statistical interpretation. To a lesser extent, this same association of enriched siderophilic elements (factor 2) is observed in factor analysis of stream-sediment and heavy-mineral-concentrate data from recent U.S. Geological Survey studies in the Seward quadrangle (O'Leary and others, 1978).

Factor 3 (table 19) partly defines scattered lode-gold deposits in the Hope-Sunrise gold district; it also defines anomalous antimony along the contact between the Orca and Valdez Groups, from Wells Passage southward to Kings Bay. Factor 3 is significantly anomalous in the Glacier Island-Long Bay-Wells Bay region. The presence of tungsten anomalies in this same region, in an area partly underlain by the Cedar Bay Granite, might be related to contact metamorphism as well as to exotic glacial debris within the greenstone area of Glacier Island. This observation contrasts with the findings of Tripp and Crim (1978), who did not recognize scheelite here but discovered significant amounts west of Unakwik Inlet, in an area where LANL data do not show tungsten.

Uranium values as high as 75 ppm associated with factor 4 (table 19) are scattered throughout the area underlain by the Valdez Group terrane east of Resurrection Creek, within the Hope-Sunrise mining district; U/Th ratios exceed 15 in some samples. These high concentrations of uranium are unusual for sedimentary marine environments and require further investigation.

Table 19.--Results of a four-factor R-mode analysis of data from 405 stream-sediment samples from the Seward quadrangle

Factor	Significant elements	Locations and (or) source-rock unit
1	Na±Li, Al, Hf, Th+Be, Ba, Ce, K, Sc, Ti, Yb	Southwest Blackstone Bay. Eastern Turnagain Arm. Nassau Fiord in Icy Bay. Southwest of Nellie Juan Lake. Granitic rocks south of Greystone Bay, Port Nellie Juan. Granite of Cedar Bay.
2	Cu, Fe, V, Sc±Ni, Cr, Mg, Mn, Ti	Valdez Group sedimentary rocks (relative to Orca Group sedimentary rocks). Knight-LaTouche Islands.
3	Au, Sb±Zn, Cl	Hope-Sunrise district. Glacier Island-Long Bay-Wells Bay. Wells Passage south to Kings Bay. Knight Island. Girdwood area. South Fork Upper Carmen and Twenty Mile Rivers. Cochrane Bay. North Unakwik Inlet west to Coghill River.
4	U±Ce, Cs, Eu, La, ±Th	East of Resurrection Creek within Hope-Sunrise district.

REFERENCES CITED

Cobb, E. H., 1979, Summary of references to mineral occurrences (other than mineral fuels and construction materials) in the Cordova quadrangle, Alaska: U.S. Geological Survey Open-File Report 79-973, 74 p.

Grant, U. S., and Higgins, D. F., 1910, Reconnaissance of the geology and mineral resources of Prince William Sound, Alaska: U.S. Geological Survey Bulletin 443, 89 p.

Joreskog, K. G., Klovan, J. E., and Reyment, R. A., 1976, Geological factor analysis: Amsterdam, Elsevier, 178 p.

O'Leary, R. M., Cooley, E. F., Day, G. W., McDougal, C. M., Tripp, R. B., and Crim, W. D., 1978, Spectrographic and atomic-absorption analyses of geochemical samples from the Seward and Blying Sound quadrangles, Alaska: U.S. Geological Survey Open-File Report 78-1102, 59 p.

Tripp, R. B., and Crim, W. D., 1978, Mineralogical maps showing distribution and abundance of gold, scheelite, chalcopyrite, arsenopyrite, minium and sapphire corundum in heavy-mineral concentrates in the Seward and Blying Sound quadrangles, Alaska: U.S. Geological Survey Miscellaneous Field Studies Map MF-880-G, scale 1:250,000, 2 sheets.

Tysdal, R. G., and Case, J. E., 1979, Geologic map of the Seward and Blying Sound quadrangles, Alaska: U.S. Geological Survey Miscellaneous Investigations Series Map I-1150, 12 p., scale 1:250,000.

U.S. Department of Energy, 1978, NURE aerial gamma-ray and magnetic reconnaissance survey, Chugach-Yakutat area, Alaska—Bering Glacier, Icy Bay, Valdez, Cordova, Mt. Saint Elias, and Yakutat quadrangles, vol. 1—Narrative report: Huntington Valley, Pa., LKB Resources, Inc., Bendix Open-File Report GJBX-127 (78), variously paged.

——1981, Uranium hydrogeochemical and stream sediment reconnaissance of the Cordova NTMS quadrangle, Alaska: Grand Junction, Colo., Bendix Field Engineering Corp. Report GJBX-185 (81), 65 p.

——1982, Uranium hydrogeochemical and stream sediment reconnaissance of the Seward NTMS quadrangle, Alaska: Grand Junction, Colo., Bendix Field Engineering Corp. Report GJBX-142 (82), 129 p.

Winkler, G. R., and Plafker George, 1981, Geologic map and cross sections of the Cordova and Middleton Island quadrangles, Alaska: U.S. Geological Survey Open-File Report 81-1164, 25 p., scale 1:250,000.

Geochemically anomalous areas north of the Denali fault in the Mount Hayes quadrangle, southern Alaska

By Gary C. Curtin, Richard B. Tripp, Richard M. O'Leary, and David L. Huston

We have recently completed fieldwork for reconnaissance geochemical studies of the Mount Hayes quadrangle (area 6, fig. 44). These studies included the collection and analysis of composite samples of minus-80-mesh stream sediment and heavy-mineral concentrates of stream sediment at 795 sites on small tributary streams (drainage basins ranging in area from 3 to 13 km^2). Composite samples of minus-80-mesh sediment and heavy-mineral concentrates of glacial debris were also collected at 116 sites on small tributary glaciers (drainage basins ranging in area from 3 to 13 km^2). For the purposes of the reconnaissance studies, analytical data from glacial-debris samples were combined with those from stream-sediment samples because statistical analysis of the data showed that these two media are chemically similar within the study area. A sample-site map and analytical data from geochemical studies in the Mount Hayes quadrangle have recently been published (O'Leary and others, 1982).

The reconnaissance studies were made to outline mineralized areas and to aid in defining the type of mineral occurrences within these areas. Preliminary evaluation of the chemical data for elements of interest was based on the selection of threshold values at approximately the 90th percentile of the total sample population. Preliminary results have revealed several areas where anomalous amounts of various metals in the sample media coincide with known mineral occurrences in the terranes south of the Denali fault (Cobb, 1972), and indicate areas of possible mineral occurrences north of the Denali fault (fig. 58) that are discussed herein. Mineralogic examination of the heavy-mineral concentrate has aided in determining the mineral residence of the metals of interest at a large number of the sampled localities.

In the southeastern part of the Mount Hayes quadrangle, north of the Denali fault, anomalous values of silver (10-20 ppm), lead (1,000-2,000 ppm), zinc (700-1,500 ppm), and copper (1,000-1,500 ppm) in heavy-mineral-concentrate samples delineate areas characterized by massive sulfide occurrences, mainly in the schist of Jarvis Creek. These areas are also outlined by anomalous amounts of silver (1-5 ppm), lead (150-300 ppm), zinc (150-300 ppm), copper (150-500 ppm), and molybdenum (5-10 ppm) in minus-80-mesh stream-sediment samples. The geochemically anomalous localities are between the West Fork and the Robertson River, and in the drainages of Rumble Creek, the Tok River, and Dry Tok Creek (fig. 58). Galena, sphalerite, chalcopyrite, and scheelite were observed in the heavy-mineral concentrates from these areas. Other areas in the central and western parts of the quadrangle are characterized by similar geochemical anomalies that may delineate additional massive sulfide occurrences in the metavolcanic units of the Jarvis Creek or adjacent terranes.

In the central part of the quadrangle, anomalous values of silver (10-100 ppm), lead (1,000-7,000 ppm), zinc (500-1,500 ppm), and arsenic (2,000-20,000 ppm), mainly in heavy-mineral-concentrate samples, target additional areas of mineralized rock. These samples were collected from the tributaries of the Gerstle River and in the vicinity of Mount Hajdukovich (fig. 58). Chalcopyrite, galena, sphalerite, and arsenopyrite were observed in the heavy-mineral concentrates from this area. To the west, anomalously high values of silver (0.7-5 ppm), lead (150-300 ppm), zinc (150 ppm), and molybdenum (5-15 ppm) occur mainly in minus-80-mesh stream-sediment samples from an area extending from just west of Hayes Glacier to Trident Glacier (fig. 58). Pyrite, chalcopyrite, sphalerite, and arsenopyrite were observed in several of the associated heavy-mineral concentrates. In addition, the discovery of cobbles of massive pyrrhotite containing pods of chalcopyrite, sphalerite, and galena on one of the moraines of Trident Glacier (Evenson and others, 1983) indicates the presence of massive sulfide occurrences in this terrane.

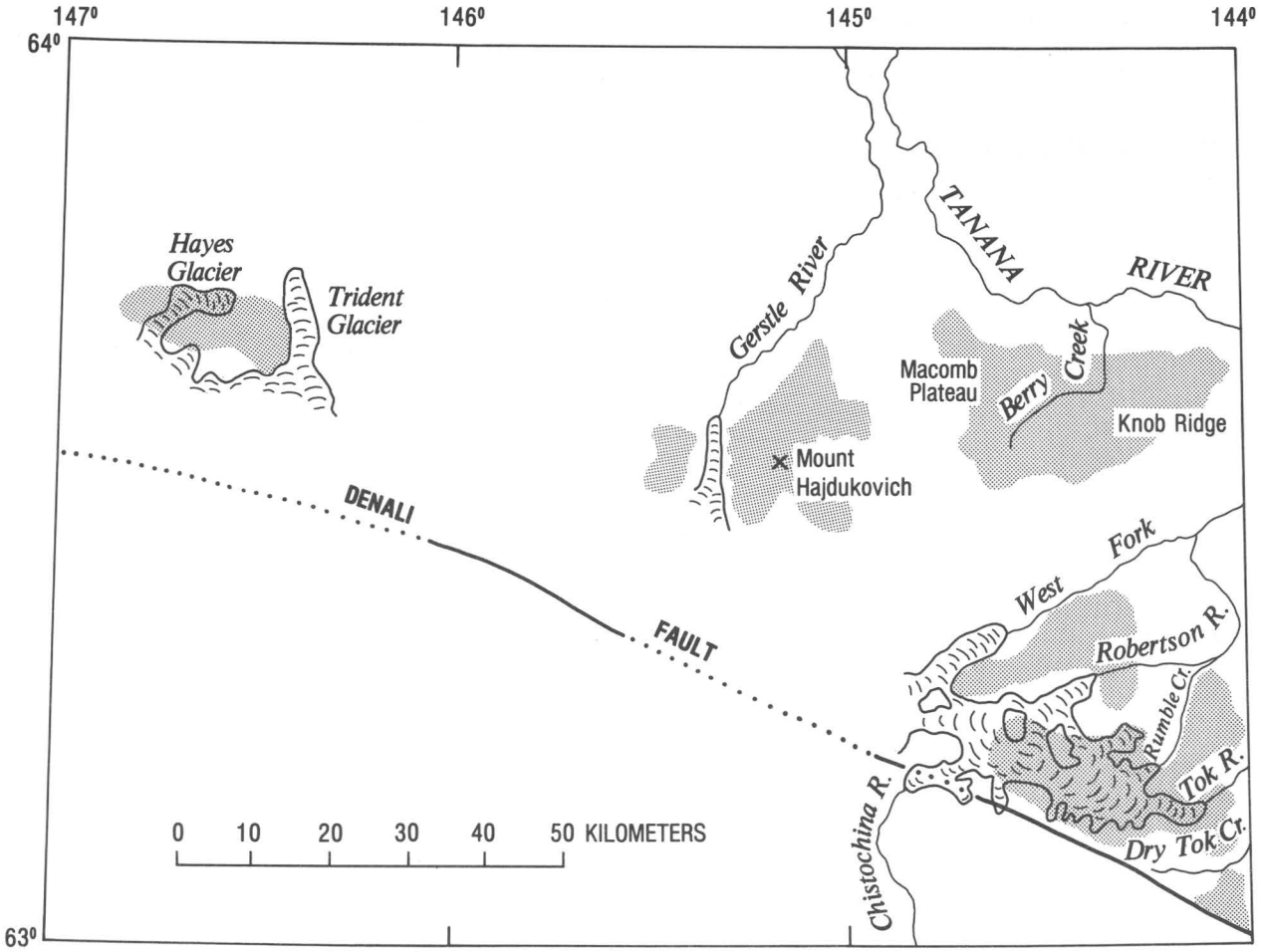

Figure 58.—Sketch map of Mount Hayes quadrangle, showing selected geochemically anomalous areas (stipling) north of Denali fault.

In the vicinity of the Macomb Plateau, Berry Creek, and Knob Ridge in the eastern part of the quadrangle (fig. 58), anomalously high tin (greater than 2,000 ppm), tungsten (10,000 ppm), and antimony (700 ppm) values in heavy-mineral-concentrate samples suggest greisen occurrences in this terrane. The highest tin values detected in minus-80-mesh stream-sediment (200-500 ppm) are in two samples collected from Berry Creek. These samples also contain large amounts of silver (1-7 ppm), lead (150 ppm), zinc (150-300 ppm), and tungsten (1,000 ppm). Tin values of greater than 2,000 ppm occur in the associated heavy-mineral-concentrate samples together with anomalous amounts of silver (20-100 ppm), copper (1,000-1,500 ppm), lead (1,000-2,000 ppm), and zinc (1,000-1,500 ppm). Mineralogic examination of these heavy-mineral-concentrate samples confirmed the presence of cassiterite, scheelite, and fluorite, all common minerals in greisen occurrences, together with gold, chalcopyrite, and galena.

REFERENCES CITED

Cobb, E. H., compiler, 1972, Metallic mineral resources map of the Mount Hayes quadrangle, Alaska: U.S. Geological Survey Miscellaneous Field Studies Map MF-414, scale 1:250,000.

Evenson, E. B., Stephens, G. C., Weber, F. R., King, H. D., and Detra, D. E., 1983, Mineral exploration and reconnaissance bedrock mapping using active alpine glaciers, Mount Hayes and Healy quadrangles, southern Alaska, in Coonrad, W. L., and Elliott, R. L., eds., The United States Geological Survey in Alaska: Accomplishments during 1981: U.S. Geological Survey Circular 868, p. 94-95.

O'Leary, R. M., Risoli, D. A., Curtin, G. C., Tripp, R. B., McDougal, C. M., and Huston, D. L., 1982, Final analytical results of stream sediment, glacial debris and non-magnetic heavy-mineral concentrate samples from the Mount Hayes quadrangle, Alaska: U.S. Geological Survey Open-File Report 82-325, 128 p.

Mineral exploration and reconnaissance bedrock mapping using active alpine glaciers, Mount Hayes and Healy quadrangles, southern Alaska

By Edward B. Evenson, George C. Stephens, F. R. Neher, Harley D. King, and David E. Detra

We conducted a detailed sampling program of the supraglacial debris load of Susitna Glacier, Mount Hayes B-6 and C-6 and Healy B-1 and C-1 quadrangles (area 8, fig. 44; fig. 59), during August 1981. This program involved the refinement of an application of techniques initiated during the Trident Glacier Project (Evenson and others, 1982). The principal project objective remained the same—the rapid and accurate evaluation of mineral potential, particularly metallic-mineral resources. Situated in the same alpine massif and sharing ice divides with the Trident Glacier system (192-km^2 catchment area), the Susitna Glacier system drains a 288-km^2 catchment area; it has 69 distinct medial moraines.

Methodologies employed for delineation of these medial moraines and establishment of their points of origin were the same as those utilized in the Trident Glacier Project. Modification and refinement of techniques, based on the results and interpretations from Trident Glacier, consisted primarily of revisions of sampling schemes to yield a more time efficient field program with minimal loss of interpretative accuracy. This year, pebble, cobble, and boulder fractions were identified, examined, and quantified in the field, whereas in 1980 pebbles were collected for subsequent analysis. Representative samples of each rock type and sand-size and finer (silt and clay size) fractions were again collected as previously described (Evenson and others, 1982). These modifications realized a 50-percent reduction in the time required for field examination of the supraglacial debris load. The samples and data collected on Susitna Glacier are presently being analyzed and interpreted.

Assessment and interpretation of lithologic data (pebble, cobble, and boulder suites) collected during the Trident Glacier investigation concerned: (1) lithologic composition, (2) structural interpretation, and (3) identification of visible mineralization. Lithologic differentiation was based on field and laboratory identification of the cobble and boulder fraction of the supraglacial debris load. Coupled with determination

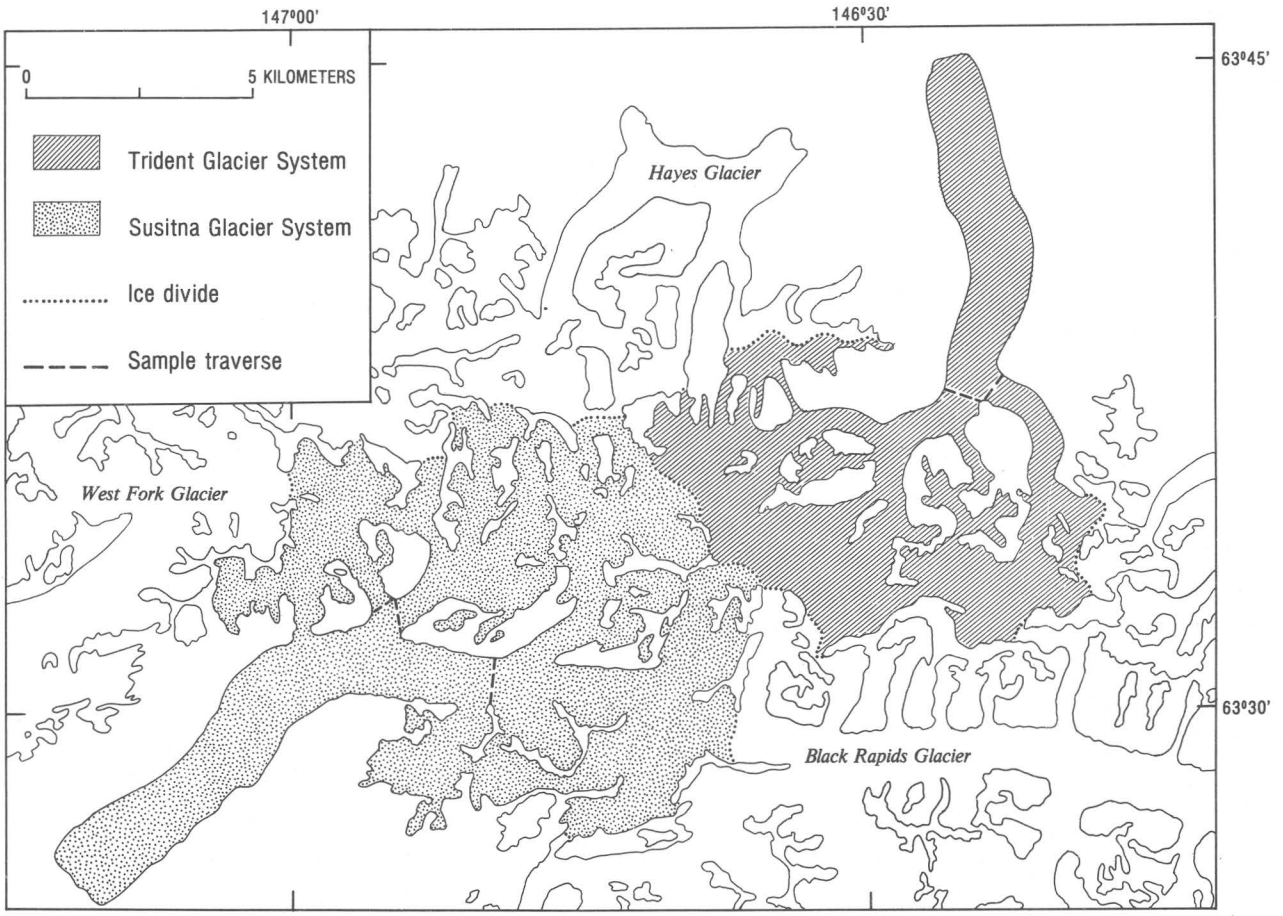

Figure 59.—Sample-traverse routes on Trident and Susitna Glaciers, Mount Hayes quadrangle, Alaska.

of relative lithologic abundances within moraines and conventional airphoto interpretation of morainal origin, major bedrock units were identified, and their distribution delineated to produce a generalized lithologic map. Morainal debris represented regional and contact(?)-metamorphic rocks and hypabyssal to plutonic igneous rocks; no sedimentary rocks were observed.

Structural interpretations were based primarily on observation and analysis of planar features (joints, small faults, veins, and dikes) and minor folds visible in individual constituents of the boulder- and, to some extent, the cobble-size fractions of the morainal material. Fold styles, relative abundance of planar features, type of igneous contacts, and crosscutting relations were combined with other observations (lithologic differentiation, visible mineralization, and airphoto data) to delineate the style and orientation of major structures and stratigraphic relations. On the basis of an integration of these observations, the catchment area is composed of well-foliated isoclinally-folded east-west-trending schist and phyllite with minor interlayered quartzite and marble, discordantly intruded by one granitic and one gabbroic igneous body.

The evaluation of mineral potential involved two distinct but complementary lines of investigation: (1) identification of metallic minerals in the pebble-, cobble-, and boulder-size fractions; and (2) a 31-element semiquantitative spectrographic analysis of the nonmagnetic heavy-mineral separate from the sand-size fraction of each sample. Pyrite was the dominant metallic mineral identified, both disseminated and as thin (0.5-1.0 mm thick) veinlets. Much of this pyrite is directly related to metamorphism of the host rock but is not related to potential ore-bearing systems. Significant amounts of copper mineralization, in the form of chalcopyrite, bornite, azurite, and malachite, were found in the coarser fractions from several moraines. This mineralization was observed as finely disseminated chalcopyrite within the metasedimentary rocks or, more commonly, as vein fillings, commonly associated with quartz and pyrite. A boulder of massive sulfide (chalcopyrite, arsenopyrite, bornite, and other sulfide minerals), measuring 15 by 20 cm and weighing 18 kg, that was recovered from the eastern tributary indicates that concentrations of massive sulfides exist in the catchment area. Tungsten and molybdenum mineralization (scheelite and powellite) was identified during microscopic and ultraviolet examination of the nonmagnetic heavy-mineral separates (R. B. Tripp, written commun., 1981).

Evaluation of the semiquantitative-spectrographic-analysis data was based on the selection of 11 metallic elements (Ag, As, Cr, Cu, Mo, Ni, Pb, Sb, Sn, W, Zn) representative of ore-mineral assemblages. Two histograms were prepared for each element: (1) a frequency histogram showing the concentration (in parts per million) from the lowest to highest values (fig. 60A), and (2) a plot of anomalous occurrence versus identified source moraine on the glacier (fig. 60B). The concentration histogram was utilized to semiquantitatively delineate anomalous concentration values, defined as those values lying above an abrupt break in slope of a curve fitted to each set of data. The anomalous occurrence-versus-source moraine histogram (fig. 60B) diagrams the source-area spatial relation of anomalous values. Four major types of anomalies were identified: (1) a multielement (Cu, Ag, Pb, Zn, Sb, Ni) anomaly, (2) a tungsten-molybdenum anomaly, (3) a silver-lead anomaly, and (4) two spatially discrete chromium anomalies (figs. 60B, 61).

Two exploration targets were outlined through integration of visible-mineralization observations and geochemical analyses. The first target is the multielement anomaly area (1, figs. 60B, 61), in which the copper mineralization is attributed to a hydrothermal-vein system genetically related to a monzonite-granodiorite complex. On the basis of composition, texture, and the apparent absence of widespread hydrothermal-alteration effects in the plutonic rocks, the likelihood of a well-developed porphyry system is small. The second target, the tungsten-molybdenum-anomalous area (2, figs. 60B, 61), is interpreted to be derived from a skarn deposit spatially associated with the gabbroic intrusive complex. The chromium-anomalous area (3, figs. 60B, 61) is interpreted to reflect the relatively high chromium content of a gabbroic intrusive body. The silver-lead-anomalous area (4, figs. 60B, 61) is based on values from only one moraine and is, therefore, assigned a low exploration-target priority.

REFERENCE CITED

Evenson, E. B., Stephens, G. C., Curtin, G. C., and Tripp, R. B., 1982, Geochemical exploration using englacial debris, in Coonrad, W. L., ed., The United States Geological Survey in Alaska: Accomplishments during 1980: U.S. Geological Survey Circular 844, p. 108-109.

Placers and placer mining in the Healy quadrangle, southern Alaska

By Warren E. Yeend

Gold was originally discovered on Valdez Creek in 1903, and soon afterward the buried "Tammany Channel" was determined to contain rich concentrations of placer gold. Approximately 27,000 troy oz of gold has been produced from the channel (Smith, 1981); however, a substantial part of the buried channel is still unmined. The channel is very steep sided, similar to the present Valdez Creek. Where mined, it appears as a gorge, 45 to 60 m deep and at least 90 m across at the top. The upper part of the channel and the surrounding bedrock bench is mantled with a blanket of glacial drift, as much as 23 m thick. As much as 15 m of the buried alluvial channel gravel may be gold bearing. Smith (1970) conducted a seismic-refraction survey to locate additional buried incised channels in the Valdez Creek area. He identified a deposit, described as the Denali bench gravels, containing more than 27 million m^3 of auriferous gravel.

A buried gold-bearing gravel-filled channel in the Valdez Creek drainage is currently being mined on a moderately large scale by the Denali Mining Co. A large washing plant that was assembled in summer 1980 has subsequently been put into operation processing the gold-bearing gravel in the buried "Tammany Channel."

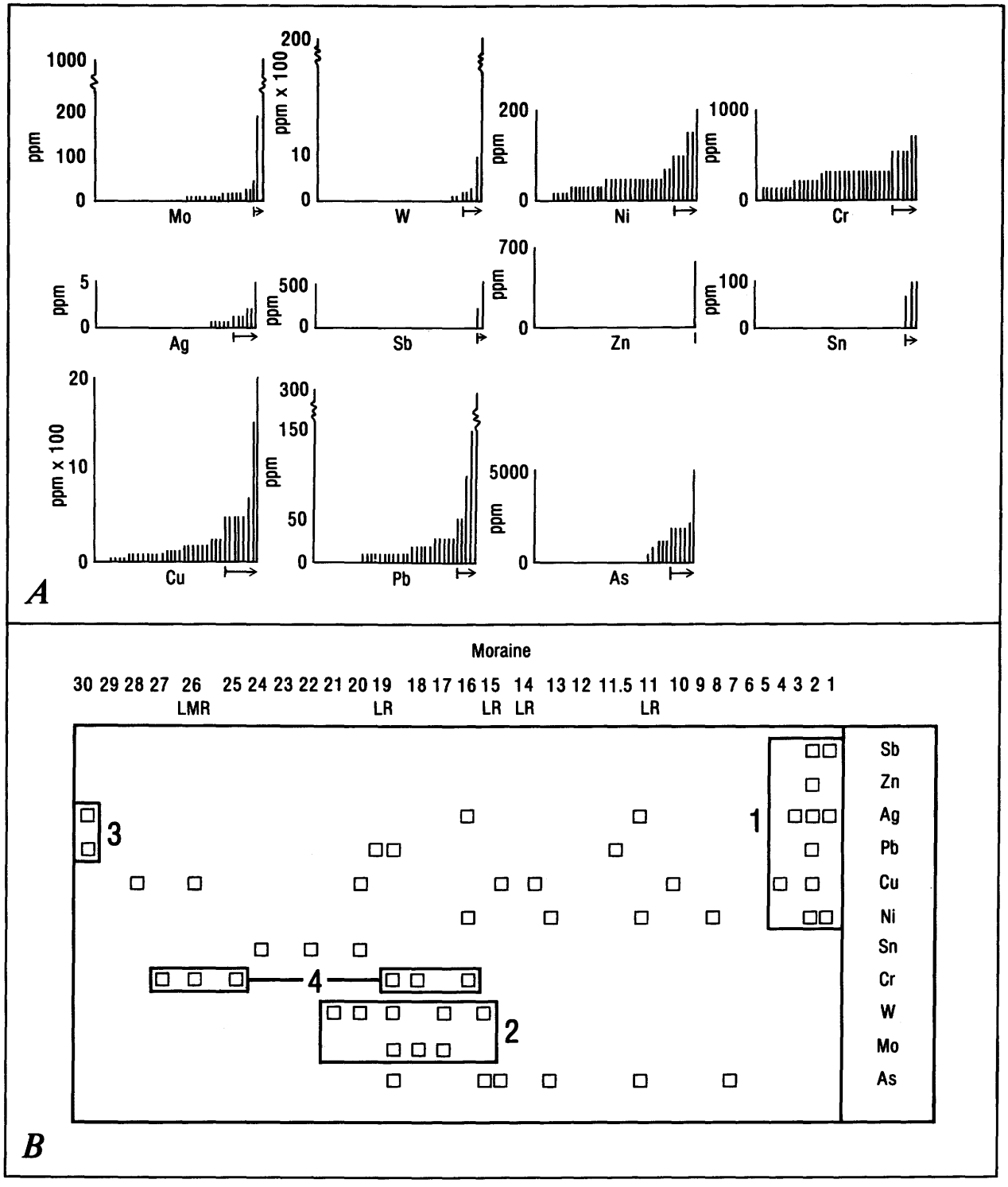

Figure 60.—Semiquantitative-spectrographic-analysis data for selected metallic elements. A, Frequency distribution of concentrations in parts per million (ppm) and limits of anomalous concentrations (arrows). B, Spatial relation of anomalous concentrations to moraine source areas and exploration-target areas (boxes) adjacent to the Trident Glacier, Alaska. See text for discussion.

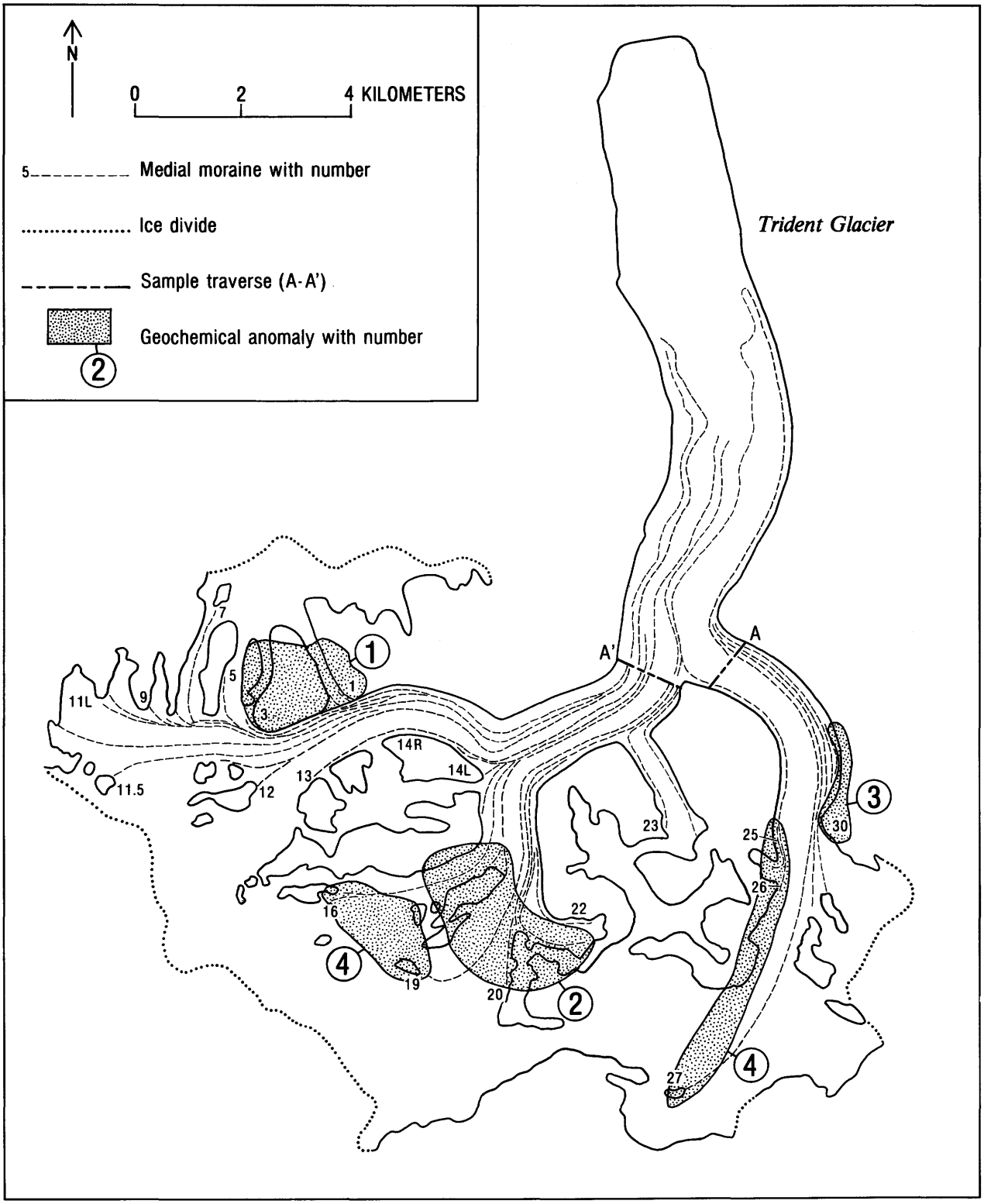

Figure 61.—Trident Glacier, showing medial moraines sampled on traverse A-A' and geochemically anomalous exploration-target areas inferred from samples (see fig. 60B). Key moraines are numbered progressively from west to east side of glacier system. Some moraines are designated as right limit (R) or left limit (L) where they originate from a common source area.

Smaller placer mines are active on Valdez Creek itself and several of its tributaries. Values in the Valdez Creek drainage range from $4.00 to $15.00/$m^3$ (at $400.00/troy oz of gold). Gold from the Valdez Creek area is typically oatmeal size, smaller, and commonly much flattened with rounded edges. Colors range from lemon yellow to a rich golden brown and reddish brown (iron stained). Gold was panned as far east as Pass Creek on the extreme east boundary of the Healy quadrangle.

Several small lode-gold mines are located in the surrounding Clearwater Mountains. These lodes and, possibly, other undiscovered lode-gold deposits in the area are most likely the source for the placer gold in the Valdez Creek drainage.

An area of the old Bonnifield mining district, described by Capps (1912), lies at the north edge of the Healy quadrangle. Mining operations on Totatlanika and Platt Creeks, near the north-central boundary of the quadrangle, and on Portage Creek in the northwest corner of the quadrangle are small scale and generally employ 2 to 5 people per operation.

Capps (1912, p. 43) pointed out that the workable placers in this northern district have all been found in areas that drain terrain presently or originally covered by the upper Tertiary Nenana Gravel, and he postulated that "* * * doubtless a reconcentration of the gold from these gravels has produced most of the present placer deposits, although some gold may have been contained in the lower Tertiary beds and have been reconcentrated * * *." This would seem to be a correct assessment of the gold source in this area, substantiated by the fact that I panned gold from the Lignite Creek Formation-Nenana Gravel (Tertiary formations) contact near where the main highway to Fairbanks crosses Panguingue Creek. In the Mount Hayes quadrangle, directly east of the Healy quadrangle, gold is present in conglomerate of early Tertiary(?) age (Yeend, 1981). It seems increasingly clear that gold has been recycled through the Tertiary continental deposits before its incorporation into the Holocene placers throughout much of interior Alaska.

REFERENCES CITED

Capps, S. R., 1912, The Bonnifield region, Alaska: U.S. Geological Survey Bulletin 501, 64 p.

Smith, T. E., 1970, Gold resource potential of the Denali bench gravels, Valdez Creek mining district, Alaska, in Geological Survey research 1970: U.S. Geological Survey Professional Paper 700-D, p. D146-D152.

——1981, Geology of the Clearwater Mountains, south-central Alaska: Alaska Division of Geological and Geophysical Surveys Geologic Report 60, 72 p.

Yeend, Warren, 1981, Placer gold deposits, Mount Hayes quadrangle, Alaska, in Albert, N. R. D., and Hudson, Travis, eds., The United States Geological Survey in Alaska: Accomplishments during 1979: U.S. Geological Survey Circular 823-B, p. B68.

Permian plant megafossils from the conglomerate of Mount Dall, central Alaska Range

By Sergius H. Mamay and Bruce L. Reed

Only a few occurrences of late Paleozoic plant megafossils are known in Alaska. Before the discovery of Permian plant fossils in the conglomerate of Mount Dall in the central Alaska Range (previously assigned to the Middle Pennsylvanian by Reed and Nelson, 1977, 1980), no credible Pennsylvanian or Permian plants had been reported. The sole report of a Pennsylvanian Calamites ambiguus fragment from the Alaska Peninsula (Eichwald, 1871, pl. 4, fig. 9) has never been properly corroborated. Sparse but significant Devonian plants have been documented (Mamay, 1963; Churkin and others, 1969), and small but stratigraphically informative collections of Early Mississippian plants are made occasionally, especially in the Brooks Range. The paleobotany of the Pennsylvanian and Permian of Alaska, however, has been enigmatic until recently. This report describes a small collection of plant fossils that provides a limited but intriguing insight into that late Paleozoic hiatus.

These fossils were collected in 1976 by B. L. Reed, R. L. Detterman and S. W. Nelson while investigating the geology of the Talkeetna quadrangle in the central Alaska Range (area 12, fig. 44). The fossiliferous shale and siltstone are exposed south of the Denali fault, about 5.2 km N. 76° E. from Mount Dall (at lat 63°25'52" N., long 152°11'40" W., in the SE1/4NW1/4 sec. 23, T. 29 N., R. 16 W., Talkeetna C-5 quadrangle) at about 1,525-m elevation. They occur within a thick (min 1,500 m) sequence of chiefly terrestrial conglomerate, sandstone, siltstone, and shale. The unit consists largely of massive lenticular beds of conglomerate and sandstone, with numerous cut-and-fill channels; the top is not exposed. This unit has been informally called the conglomerate of Mount Dall by Reed and Nelson (1977). The lower part is believed to be gradational downward into a depositionally and structurally complex terrane of mostly marine flyschoid sedimentary rocks containing fossil marine invertebrates of Devonian, Mississippian, and Pennsylvanian age (Reed and Nelson, 1977). Before the 1976 investigations in the Talkeetna quadrangle, the sedimentary rocks south of the Denali fault in the Mount Dall area were regarded as part of a sequence of upper Mesozoic graywacke and argillite, and any unit of conglomerate was assumed to be Late Cretaceous or Tertiary. The fossil plants discussed here, however, establish a late Paleozoic age and a continental origin for at least parts of the conglomerate of Mount Dall. The conglomerate and flyschoid sediment are part of the Mystic tectonostratigraphic terrane (Jones and others, 1981).

The fossils, which were found in the upper half of the conglomerate, are most abundant in a hard fine-grained dark-gray irregularly bedded matrix. About 20 small to medium-size slabs (approx 4-30 cm in maximum dimension) containing discernible plant parts constitute the collection. Some of these slabs contain only a single leaf fragment; others have sufficiently abundant interbedded plant parts to suggest the original presence of a fairly luxuriant growth of vegetation near the site of deposition. All the specimens are fragmentary; the largest is 28 cm long by 2 cm wide.

Most specimens represent detached leaflets or partial fronds; some, still problematic, may be stems. The specimens are preserved mostly as impressions, although a few have adherent areas of coalified organic residue. Foliar outlines are well defined in most specimens; more importantly, the veins of some specimens were originally stout enough that they remain in clear relief. Thus, regardless of their generally inferior preservation, the fossils retain enough characteristic features that the following forms are recognizable:

1. Pecopteris spp.: This complex of fernlike foliage is common in Pennsylvanian and Permian sedimentary rocks and constitutes a dominant element in many of the coal floras. It is also conspicuous in the Alaskan flora; half or more of the determinable specimens are pecopterids. Three species are apparently present. Most of the specimens are referable to the common species P. arborescens Schlotheim (fig. 62A). The specimen shown in figure 62B may, with reasonable assurance, be referred to P. hemitelioides Brongniart. A third species, P. unita Brongniart, is represented by the frond fragment shown in figures 62E and 62F.
2. Cyclopteroid pinnules (figs. 62C, 62D): The five specimens representing this generalized morphologic format are not generically identifiable because of their fragmentary condition. In the absence of demonstrable apical parts, generic identification of these basal fragments is at best, speculative; possibly they are Cyclopteris Brongniart, Angaropteridium Zalessky, or Cardioneura Zalessky.
3. Zamiopteris sp.: The specimens shown in figures 62G through 62I represent the most remarkable element in the Alaskan assemblage. These are long linear or linear-lanceolate symmetrical and petiolate leaves with entire margins, acute apices, open venation, and a resemblance to Glossopteris foliage in general outline. The leaves are clearly within the circumscription of the genus Zamiopteris Schmalhausen (1879), originally described on the basis of leaves (Z. glossopteroides Schmalhausen) from Permian rocks near Ssuka, U.S.S.R. Subsequently, at least 20 species have been described, one from Korea and the others from the U.S.S.R., all characteristically Permian. The most recent account of Zamiopteris (Zimina, 1977) records several species in the Lower and Upper Permian of the Far Eastern floral province, near Vladivostok.

A few indeterminate specimens make up the remainder of the collection, all narrow linear fragments with more or less parallel ribbing. One quite large (2 by 28 cm) fragment may be an unusual zamiopterid element; another fragment, with faint but seemingly regular parallel ribbing, possibly represents a cordaitean leaf fragment. There is no evidence of lepidophytes or arthrophytes.

These fossils, which represent the first post-Mississippian Paleozoic plants found in Alaska, add an important element to the sparse pre-Cenozoic paleobotanic history of the State. Furthermore, they are critical in geologic dating of the conglomerate of Mount Dall because of the rarity of fossils in that unit. The pecopterids are stratigraphically long ranging (Middle Pennsylvanian to Permian) but are doubtless younger than Mississippian, and the material of Pecopteris unita in the Alaskan collection has an interestingly close resemblance to what probably is a superfluous species, P. niamdensis Zalessky, most recently reported by Fefilova (1973, p. 88, pl. 23) from the Permian of the Pechora basin, U.S.S.R. The cyclopteroid specimens are not stratigraphically definitive because they resemble long-ranging late Paleozoic taxa with approximately the same vertical distributions as those of the pecopterids concerned here. The Alaskan specimens of Zamiopteris, however, serve as a common stratigraphic denominator because the occurrence of this genus is restricted to rocks of Permian age in Siberia, where it occurs mainly in the upper part of the Lower Permian and the lower part of the Upper Permian (S. V. Meyen, oral commun., 1979).

Thus, the evidence favors a Permian age assignment for the Alaskan plant fossils. The zamiopterid specimens were previously misinterpreted as cordaitean leaves, and a Pennsylvanian age was assigned to the conglomerate of Mount Dall (Reed and Nelson, 1977, 1980; Reed and others, 1979). This age was also applied by Dutro and Jones (1979) in a report discussing Carboniferous strata in Alaska. The recognition of Zamiopteris, however, necessitates assignment of the plant-bearing beds of the conglomerate of Mount Dall to the Permian. Pending the collection of larger, more varied assemblages, it seems judicious to regard the present material as no younger than Early Permian.

These Alaskan plants are of further interest in that they are the first North American flora of Permian age known north of the Dunkard basin (lat approx 40° N.). As shown in figure 63, only a few areas that yield Permian plants are known in North America; these areas are concentrated chiefly in the Southwestern United States, where three distinct Permian floral provinces are recognized (Read and Mamay, 1964), each on the basis of a single characteristic genus (Gigantopteris, Glenopteris, and Supaia). The geographically isolated Alaskan flora shares a strong pecopterid element with those North American floras far to the south. However, by virtue of its distinguishing component—Zamiopteris—the Alaskan flora clearly constitutes an eastward extension of the Permian flora of Angaraland, the greater part of northeastern Asia. It now seems reasonable to anticipate the discovery, in Alaska and, possibly, at more southerly North American sites, of additional Permian taxa characteristic of the Angara flora.

Geographic proximity of the Alaskan plant occurrence to East Asia contributes to the accumulation of widely cited evidence for Paleozoic unity of the major landmasses and subsequent drifting of the continents. Long ago, White (1912, p. 513-514) commented on the presence of Chinese and Uralian elements in the Permian floras of the Southwestern United States and speculated regarding plant migration from China to North America by way of "the north Pacific (Alaskan) route." Interestingly, White was then referring obliquely to a "supercontinent" ("* * * since the land migration of the Chinese types could hardly have been accomplished without the aid of essential continuity of environmental conditions * * *"), in which East Asia and western Alaska were joined, substantially as later depicted in the Wegenerian Pangaea

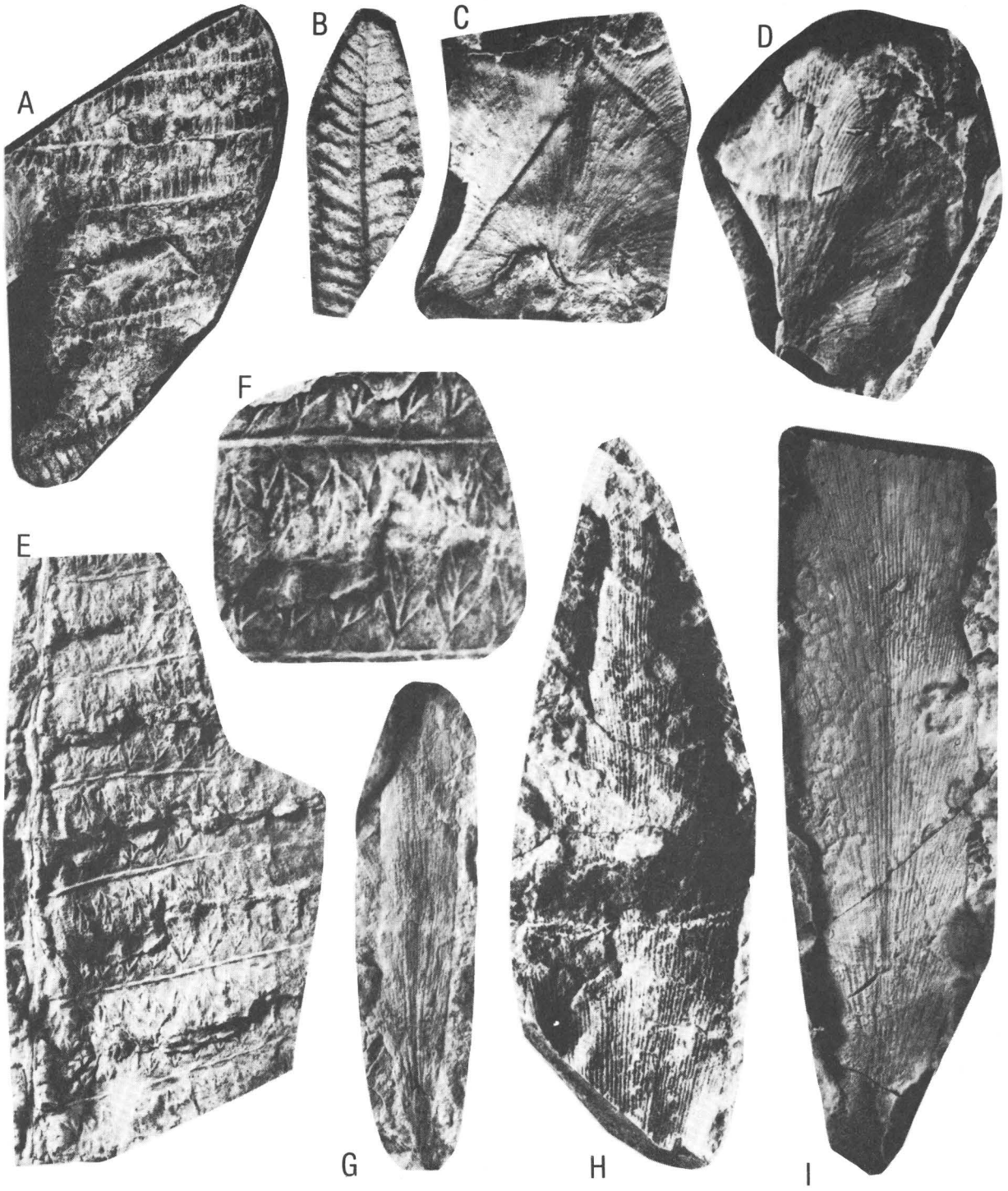

Figure 62.—Plant fossils from the conglomerate of Mount Dall, Talkeetna quadrangle, Alaska. A, Several pinnae of Pecopteris cf. P. arborescens Schlotheim, x1: USNM 312727. B, Pinna of Pecopteris cf. P. hemitelioides Brongniart, x1; USNM 312728. C, D, Cyclopteroid pinnule fragments, x2: C, USNM 312729; D, USNM 312730. E, F, Pecopteris unita Brongniart: E, parts of several pinnae, x2; USNM 312731; F, part of E enlarged to x4, showing ultimate venation characteristic of the species. G, H, I, Incomplete leaves of Zamiopteris sp., all x2: G, USNM 312732; H, USNM 312733; I, USNM 312734, showing glossopteroid petiolate leaf form, absence of midrib, and closely spaced open gently arched venation.

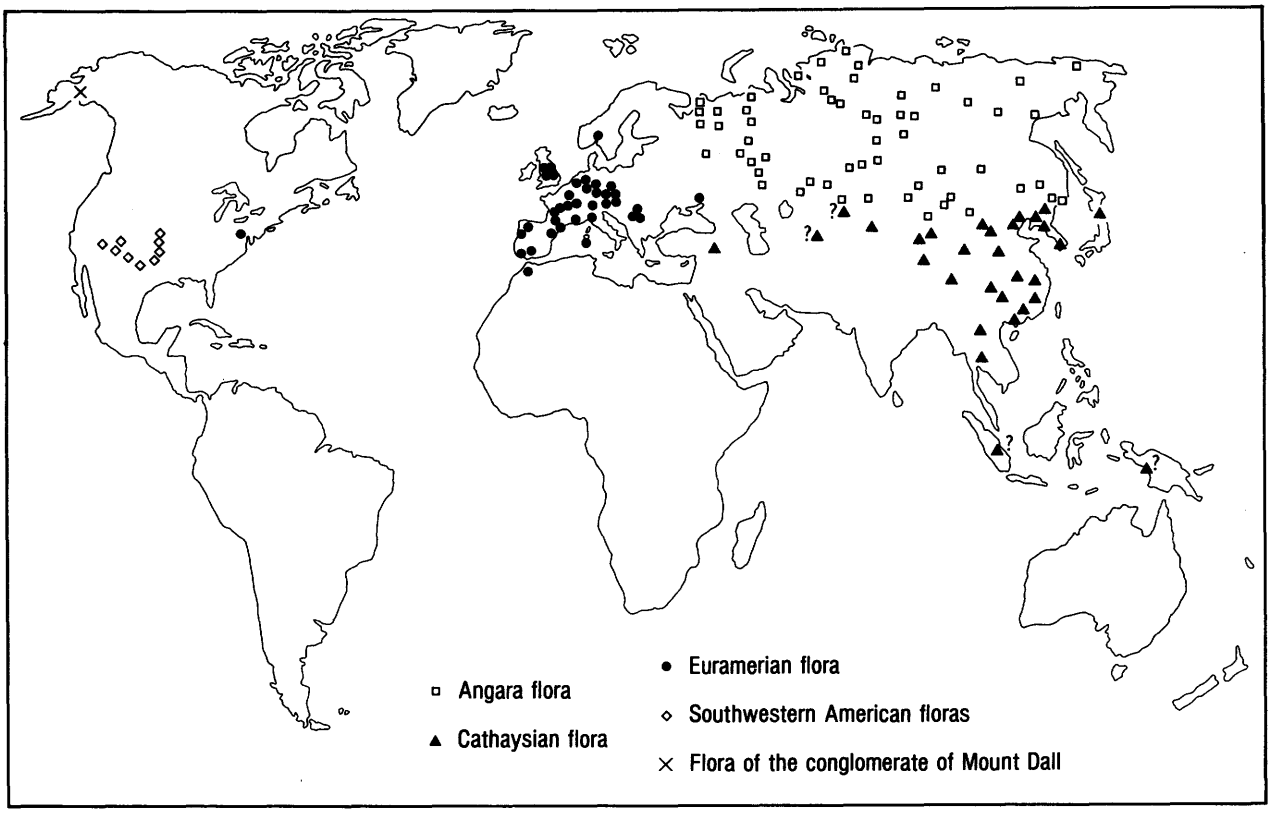

Figure 63.—Distribution of northern Permian floras (modified from Chaloner and Meyen, 1973, fig. 3).

(Hallam, 1975, p. 9). Such a geographic pattern would, indeed, have provided the pathway necessary for eastward dispersal of Asiatic plants and could have resulted in this Alaskan outpost of the Angara flora.

Alternatively, this paleophytogeographic circumstance can also be interpreted in the light of recent concepts of accretionary tectonostratigraphic terranes (Jones and others, 1977, 1981; Dutro and Jones, 1979; Jones and Silberling, 1979; Beck and others, 1980; Coney and others, 1980; Ben-Avraham, 1981), which indicate that southern Alaska is an amalgamation of allochthonous continental and oceanic terranes, some of which have been rafted for thousands of kilometers and accreted to their present positions. The conglomerate of Mount Dall lies in the Mystic terrane (Jones and others, 1981), a fault-bounded exotic block that probably was accreted to this part of Alaska between post-Early Cretaceous and early Tertiary time (Reed and others, 1979). The distribution of Zamiopteris and associated plant taxa may be an important key to the history and interpretation of accretionary terranes in this part of Alaska, and an East Asian origin for the Mystic terrane merits consideration.

REFERENCES CITED

Beck, Myrl, Cox, Allan, and Jones, D. L., 1980, Mesozoic and Cenozoic microplate tectonics of western North America: Geology, v. 8, no. 9, p. 454-456.

Ben-Avraham, Zvi, 1981, The movement of continents: American Scientist, v. 69, no. 3, p. 291-299.

Chaloner, W. G., and Meyen, S. V., 1973, Carboniferous and Permian floras of the northern continents, in Hallam, Anthony, ed., Atlas of palaeobiogeography: Amsterdam, Elsevier, p. 169-186. pls. 1-4.

Churkin, Michael, Jr., Eberlein, G. D., Hueber, F. M., and Mamay, S. H., 1969, Lower Devonian land plants from graptolite shale in south-eastern Alaska: Palaeontology, v. 12, no. 4, p. 559-573.

Coney, P. J., Jones, D. L., and Monger, J. W. H., 1980, Cordilleran suspect terranes: Nature, v. 288, no. 5789, p. 329-333.

Dutro, J. T., Jr., and Jones, D. L., 1979, Paleotectonic setting of the Carboniferous in Alaska [abs.]: International Congress of Carboniferous Stratigraphy and Geology, 9th, Washington, D.C., and Urbana, Ill., 1979, Abstracts, p. 58-59.

Eichwald, Eduard von, 1871, [Geognostic-paleontologic remarks on the Mangishlak Peninsula and the Aleutian Islands]: Académie Impériale des Sciences de St. Petersbourg Mémoires, v. 27, no. 4, p. 1-200, pls. 1-20 [in Russian].

Fefilova, L. A., 1973, [Permian pteridophyta from the north of the pre-Uralian depression]: Leningrad, U.S.S.R., Academy of Sciences, Geological Institute, Publisher "Nauka," p. 1-192, pls. 1-42 [in Russian].

Hallam, Anthony, 1975, Alfred Wegener and the hypothesis of continental drift: Scientific American, v. 232, no. 2, p. 88-97.
Jones, D. L., and Silberling, N. J., 1979, Mesozoic stratigraphy—the key to tectonic analysis of southern and central Alaska: U.S. Geological Survey Open-File Report 79-1200, 37 p.
Jones, D. L., Silberling, N. J., Berg, J. C., and Plafker, George, 1981, Map showing tectonostratigraphic terranes of Alaska, columnar sections, and summary description of terranes: U.S. Geological Survey Open-File Report 81-792, 20 p., scale 1:2,500,000.
Jones, D. L., Silberling, N. J., and Hillhouse, J., 1977, Wrangellia—a displaced terrane in northwestern North America: Canadian Journal of Earth Sciences, v. 14, no. 11, p. 2565-2577.
Mamay, S. H., 1963, Occurrence of Pseudobornia Nathorst in Alaska: Palaeobotanist, v. 11, no. 1-2, p. 19-22.
Neuburg, M. F., 1948, [Upper Paleozoic flora of the Kusnetzk basin]: Moscow, U.S.S.R., Academy of Sciences, Palaeontological Institute, v. 12, no. 3, pt. 2, p. 1-342, pls. 1-73 [in Russian].
Read, C. B., and Mamay, S. H., 1964, Upper Paleozoic floral zones and floral provinces of the United States, with a Glossary of stratigraphic terms, by G. C. Keroher: U.S. Geological Survey Professional Paper 454-K, p. K1-K35, pls. 1-19.
Reed, B. L., Curtin, G. C., Griscom, Andrew, Nelson, S. W., Singer, D. A., and Steele, W. C., 1979, The Alaskan Mineral Resource Assessment Program: Background information to accompany folio of geologic and mineral resource maps of the Talkeetna quadrangle, Alaska: U.S. Geological Survey Circular 775, 17 p.
Reed, B. L., and Nelson, S. W., 1977, Geologic map of the Talkeetna quadrangle, Alaska: U.S. Geological Survey Miscellaneous Field Studies Map MF-870-A, scale 1:250,000.
———1980, Geologic map of the Talkeetna quadrangle, Alaska: U.S. Geological Survey Miscellaneous Investigations Series Map I-1174, scale 1:250,000.
Schmalhausen, Johannes, 1879, Beiträge zur Jura-Flora Russlands [Contributions to the Jurassic flora of Russia]: Académie Impériale des Sciences de St. Petersbourg Mémoires, v. 27, no. 4, p. 1-96, pls. 1-16.
White, David, 1912, The characters of the fossil plant Gigantopteris Schenk and its occurrence in North America: U.S. National Museum Proceedings, v. 41, p. 493-516, pls. 43-49.
Zimina, V. G., 1977, [Flora of the Early and the beginning of the Late Permian of the South Primor'e]: Moscow, U.S.S.R., Academy of Sciences, Publisher "Nauka," p. 1-126, 20 pls. [in Russian].

A middle Wisconsin pollen record from the Copper River basin, Alaska

By Cathy L. Connor

A 150-m-thick section, exposed by the Dadina River approximately 16 km from its confluence with the Copper River (loc. 4, fig. 44; Valdez D-3 quadrangle), provides an excellent record of middle and late Wisconsin sedimentation on the western flank of Mount Wrangell. A silty clay interval rich in organic material within this river-bluff exposure yielded a radiocarbon age of 30,670±1,050 years. Samples from this interval were analyzed for palynomorphs. Preliminary data indicate that a spruce (Picea)-dominated woodland with intermixed shrub tundra was established by 30,000 years B.P. in the eastern Copper River basin.

This section (fig. 64) contains four distinct glacial-till units that are separated by sediment representing fluvial, lacustrine, and subglacial environments of deposition. The pollen source beds stratigraphically overlie the second oldest till and have an upper boundary delineated by a conspicuous seepline 54 m above river level. This silty-clay interval, 7 m thick, is impermeable to ground water moving through the overlying strata. The gradational boundary between the till and silty-clay unit reflects ablation of glacial ice and onset of shallow standing-water conditions that were ideal for the growth of peat-forming plants. Upward in the section, immediately above the seepline contact, 3.4 m of white horizontally laminated ashy sand and interbedded clay coarsen upward into lithic and pumice-bearing channeled sand. This sediment indicates sufficient increase in water depth upsection to accommodate a sudden influx of volcanically derived material, presumably representing an ash eruption of Mount Wrangell.

A total of 10 grab samples from a 4.3-m-thick zone within the silty-clay interval were analyzed for fossil spores and pollen, using methods developed by C. E. Schweger for alluvial sediment (Matthews, 1974). Preliminary data indicate a dominance of spruce (Picea), as high as 46 percent, followed by sedge (Cyperaceae), 13 percent; birch (Betula), 7 percent; willow (Salix), 4 percent; and alder (Alnus), 3 percent in the samples counted. Herbaceous plants, such as Artemisia, members of the family Caryophyllaceae, Potentilla, and Saussurea are sparse (1-3 percent) as individual groups but make up as much as 20 percent of the pollen. Spore-producing plants, such as Sphagnum and Lycopodium, make up 8 to 27 percent of the total palynomorphs counted and increase in abundance above the radiocarbon-dated horizon. Those intervals above the radiocarbon-dated horizon also show a decrease in spruce pollen, to a low of 15 percent.

Palynomorphs became very sparse at the upper seep-zone contact where an increase in water depth is indicated by a transition from silty humus deposits to finely laminated silt and clay. The newly inundated site received pollen and spores that had been abraded during transport and diluted by the inflowing sediment. Recovery of usable and sufficient numbers of palynomorphs became particularly difficult in this type of sedimentary environment.

These data suggest that a present-day type of lowland spruce forest with patches of shrub and tundra was extant during middle Wisconsin time in the Dadina River area. This information corroborates the concept of large ice-free areas for much of the Copper River basin during the late Pleistocene, as put forth by Ferrians and Nichols (1965), and extends the record of vegetational history in this area backward approximately 18,000 years beyond that described by Ager and

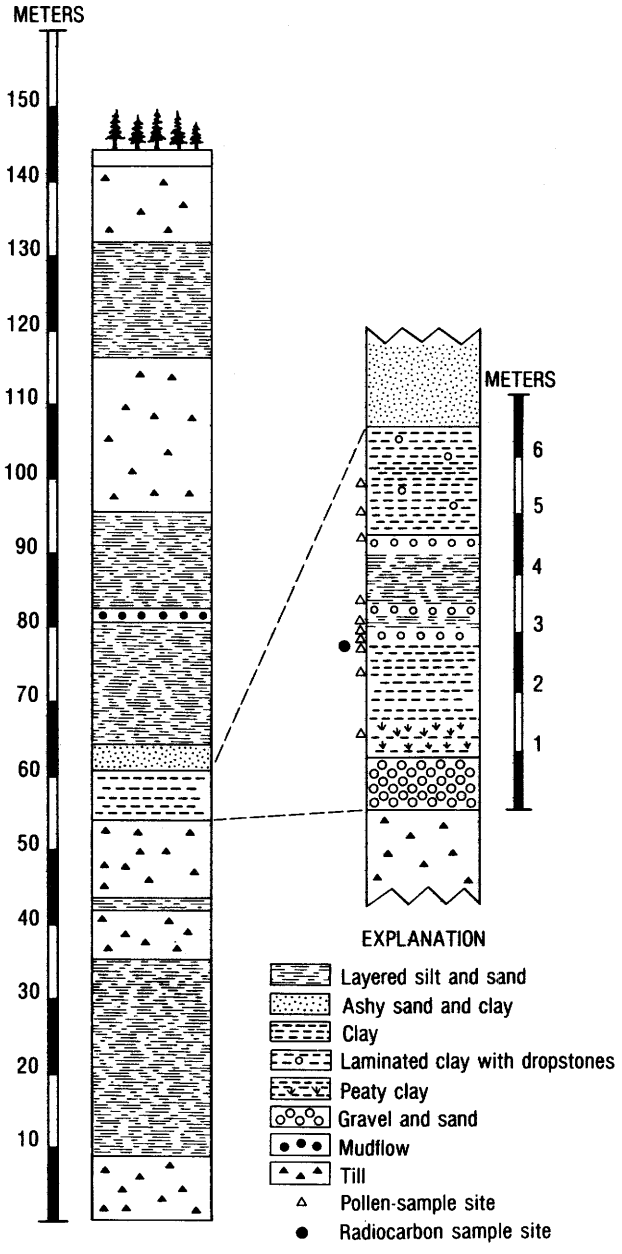

Figure 64.—Quaternary section measured in a Dadina River bluff, Copper River basin (lat 61°51'50" N., long 144°50'20" W., Valdez D-3 quadrangle).

Sims (1981) for the Tangle Lakes area on the north edge of the basin. The Dadina River pollen data also agree with those of Matthews (1974), whose work in the Isabella basin near Fairbanks provided the first evidence for an Alaskan middle Wisconsin interstadial period between 35,000 and 32,000 years B.P. In addition, the timing of this interstadial in the Copper River basin is recorded in two peat horizons on the Sanford River north of the Dadina River. These peat deposits yielded radiocarbon ages of 28,000±1,000 and 31,300± 1,000 years, interpreted by Ferrians and Schmoll (1957) as representing a low stand of proglacial Lake Ahtna, a late Pleistocene water body that formed in the basin when advancing ice in the Chugach Mountains created an ice dam which blocked the main drainageway out of the basin, and that covered more than 1,600 km^2 of the Copper River basin.

Absence of continuous river-bluff exposures and frequent facies changes within exposures make stratigraphic correlation across the basin somewhat speculative. Thus, the radiocarbon sample from the Dadina section may well record the initiation of a small pond or miniproglacial lake that was not connected to a major basinwide water body. Ongoing work will continue to evaluate pollen and sedimentologic data in this area.

REFERENCES CITED

Ager, T. A. and Sims, J. D., 1981, Holocene pollen and sediment record from the Trangle Lakes area, central Alaska: Palynology, v. 5, p. 85-98.

Ferrians, O. J., Jr., and Nichols, D. R., 1965, Copper River Basin, in Schultz, C. B., and Smith, H. T. U., eds.: International Association for Quaternary Research Congress, 7th, Lincoln, Nebr., Guidebook for Field Conference F, Central and South-Central Alaska, p. 93-114.

Ferrians, O. J., Jr., and Schmoll, H. R., 1957, Extensive proglacial lake of Wisconsin age in the Copper River Basin of Alaska [abs.]: Geological Society of America Bulletin, v. 68, no. 12, pt. 2, p. 1726.

Matthews, J. V., 1974, Wisconsin environment of interior Alaska: pollen and macrofossils analysis of a 27 meter core from the Isabella basin (Fairbanks, Alaska): Canadian Journal of Earth Sciences, v. 11, no. 6, p. 828-841.

Postglacial pollen and tephra records from lakes in the Cook Inlet region, southern Alaska

By Thomas A. Ager and John D. Sims

During the last major glacial interval of the Pleistocene, the mountains rimming Cook Inlet were extensively glaciated, and glaciers flowed into the region's lowlands. In central Cook Inlet, a large lake was formed when glaciers from the southern Kenai Mountains merged with glaciers flowing from the Alaska Peninsula and dammed Cook Inlet to the north (Karlstrom, 1964).

Evidence from several areas of Alaska and adjacent parts of Canada suggests that deglaciation began earlier than 14,000 years B.P. (Hopkins, 1973, 1979; Denton, 1974). In south-central Alaska, deglaciation continued over several thousand years, during which time a number of climatic oscillations occurred (Karlstrom, 1964).

In an effort to reconstruct the history of environmental changes during and after deglaciation, we obtained sediment cores from five lakes in the Cook Inlet region (area 1, fig. 44; fig. 65). Cores are currently being analyzed for sediment type, fossil-pollen assemblages, and tephra content, and core segments are being radiocarbon dated to provide a regional chronology of environmental changes and ash falls.

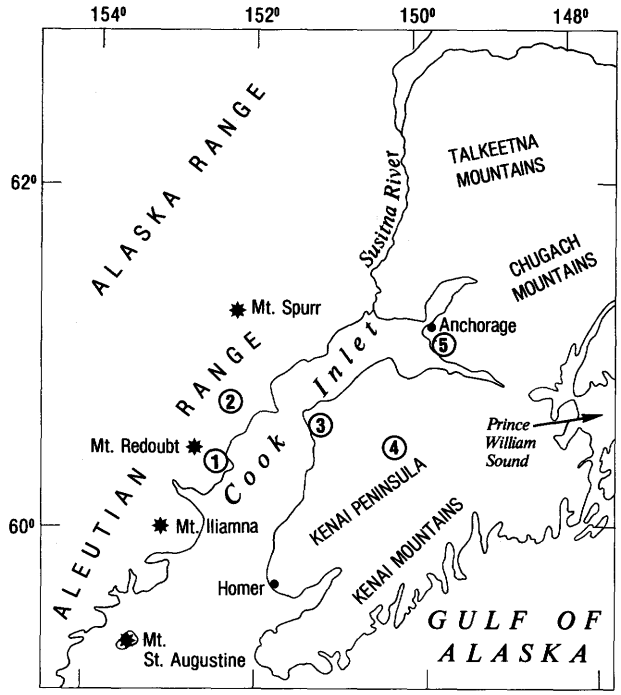

Figure 65.—Sketch map of Cook Inlet region, showing major Quaternary volcanoes (stars) and approximate locations of lakes where bottom-sediment cores were taken: 1, Bear Lake; 2, Big River Lakes; 3, Upper Salamatof Lake; 4, Hidden Lake; and 5, Hideaway Lake.

All the lakes cored thus far from the region contain two or more tephra layers. The shallower lakes generally preserve only the thicker tephra layers; many thin tephra layers are destroyed or obscured by sediment mixing due to wave action, bottom currents, and burrowing organisms. The deeper lakes in the region contain the most complete tephra records. A core from Hidden Lake (fig. 65, no. 4) in the central Kenai Peninsula (Rymer and Sims, 1982), for example, contains at least 10 tephra layers; an additional 7 thin light-colored laminae that may also be tephra have not yet been examined microscopically. Four radiocarbon ages from the Hidden Lake core permit preliminary dating of individual tephra layers by extrapolation of sedimentation rates between dated core segments. This procedure suggests that ash falls occurred on the central Kenai Peninsula about 300, 2,880, 3,900, 6,560, 8,210, 8,370, 11,360, 13,700, 14,500, and 14,700 years B.P. The last two dates are particularly speculative because no radiocarbon data are available from the lowermost part of the core owing to low organic content, although the sedimentary structures and composition in that part of the core suggest a rapid sedimentation rate.

No single lake, however, can provide a complete record of the ash falls for the entire region because ash plumes commonly pass over only parts of south-central Alaska. Many ash clouds from volcanic eruptions on the southern Alaska Peninsula and the Aleutian Islands are swept southeastward into the Gulf of Alaska and entirely bypass the Cook Inlet region. Ash falls from volcanoes along the west side of Cook Inlet (such as Mount St. Augustine, Mount Iliamna, Mount Redoubt, and Mount Spurr) are most likely to be represented in the region's lakes (fig. 65), although volcanic ash from more distant sources may also occasionally fall on the Cook Inlet region.

Pollen analysis of the sediment core from Hidden Lake permits the reconstruction of a regional vegetation history spanning more than 14,000 years (Ager and Sims, 1981b; Ager, 1983), the oldest continuous late Quaternary pollen record yet obtained from anywhere in south-central or southeastern Alaska. The earliest recorded vegetation to appear was an herb-shrub tundra that developed soon after glacial ice retreated from the western Hidden Lake area more than 14,000 years B.P. By about 13,700 years B.P., mesic shrub tundra developed that included dwarf birch (Betula nana), ericales (Ericaceae, Empetrum nigrum), and willow (Salix spp.). Poplar (Populus spp.) began to spread into the area by about 10,400 years B.P. The regional vegetation soon developed into a mosaic of shrub tundra communities interspersed with thickets of willow and scattered stands of poplar. Alder shrubs (Alnus spp.) spread rapidly in the region between about 10,000 and 9,500 years B.P. The first conifers to invade the region were spruce (Picea), which appeared abruptly at Hidden Lake about 8,400-8,000 years B.P. These first invading spruce were probably white spruce (Picea glauca), which apparently spread very rapidly (approx 0.3-0.4 km/yr) southward from the Tanana Valley in interior Alaska (Ager, 1975) through the mountain passes of the Alaska Range (Ager and Sims, 1981a) and the Talkeetna and Chugach Mountains.

Previous investigations of pollen profiles from peat cores collected along the south and east coast of the Kenai Peninsula and in Prince William Sound (Heusser, 1960) suggest that coastal forests consisting primarily of Sitka spruce (Picea sitchensis), smaller amounts of mountain hemlock (Tsuga mertensiana), and some western hemlock (T. heterophylla) reached those areas from the east during middle Holocene time. Pollen of Picea glauca and P. sitchensis cannot yet be differentiated, and so it is unclear when elements of the coastal forest reached the east edge of Hidden Lake on the west flank of the Kenai Mountains. The first appearance of traces of pollen of mountain hemlock in the Hidden Lake core at about 5,000-4,000 years B.P. may indicate that at least some elements of the coastal Sitka spruce-hemlock forest reached the Hidden Lake area about that time.

Other cores of lacustrine sediment were obtained near Kenai on the Kenai Peninsula, near Anchorage in upper Cook Inlet, and in the vicinity of Mount Redoubt on the west side of Cook Inlet (fig. 65) in March 1981 by T. A. Ager, James Reihle, and Susan Bartsch-Winkler. Preliminary analysis of these cores reveals that pollen of Alnus occurs in the lowest pollen-bearing sediment of the cores. This observation suggests that the maximum age of the cores is probably less than 10,000 years, on the basis of the pollen zonation and chronology established for the Hidden Lake core.

REFERENCES CITED

Ager, T. A., 1975, Late Quaternary environmental history of the Tanana Valley, Alaska: Columbus, Ohio State University, Institute of Polar Studies Report 54, 117 p.

——1983, Holocene vegetational history of Alaska, in Wright, H. E., Jr. ed., Late-Quaternary environments the United States; volume 2, The Holocene: Minneapolis, University of Minnesota Press, p. 128-141 [in press].

Ager, T. A., and Sims, J. D., 1981a, Holocene pollen and sediment record from the Tangle Lakes area, Alaska: Palynology, v. 5, p. 85-98.

——1981b, Late Quaternary pollen record from Hidden Lake, Kenai Peninsula, Alaska [abs.]: American Association of Stratigraphic Palynologists Annual Meeting, 14th, New Orleans, La., 1981, Program and Abstracts, p. 8-9.

Denton, G. H., 1974, Quaternary glaciations of the White River Valley, Alaska, with a regional synthesis for the northern St. Elias Mountains, Alaska and Yukon Territory: Geological Society of America Bulletin, v. 85, no. 6, p. 871-892.

Heusser, C. J., 1960, Late Pleistocene environments of North Pacific North America: New York, American Geographical Society Special Publication 35, 308 p.

Hopkins, D. M., 1973, Sea level history in Beringia during the last 250,000 years: Quaternary Research, v. 3, no. 4, p. 520-540.

——1979, Landscape and climate of Beringia during late Pleistocene and Holocene time, in Laughlin, W. S., and Harper, A. B., eds., The first Americans: Affinities and adaptations: New York, Gustav Fischer, p. 15-40.

Karlstrom, T. N. V., 1964, Quaternary geology of the Kenai Lowland and glacial history of the Cook Inlet region, Alaska: U.S. Geological Survey Professional Paper 443, 69 p.

Rymer, M. J., and Sims, J. D., 1982, Lake-sediment evidence for the date of deglaciation of the Hidden Lake area, Kenai Peninsula, Alaska: Geology, v. 10, no. 6, p. 314-316.

Convoluted beds in late Holocene intertidal sediment at the mouth of Knik Arm, upper Cook Inlet, Alaska

By Susan Bartsch-Winkler and Henry R. Schmoll

Convoluted and contorted intertidal sand-and-mud bedded sequences of the present-day and recent past are exposed in upper Cook Inlet at the mouth of Knik Arm, just southwest of Point Woronzof (loc. 3, fig. 44; fig. 66). These intertidal deposits, which are exposed at low tide in eroded bluffs approximately 10.5 m high, are completely covered by tidewater at high tide (fig. 67). The bluffs are scoured by channeled tidal currents that enter and leave Knik Arm through a narrows formed by Point MacKenzie on the north and Point Woronzof on the south.

The contorted sequences have abrupt boundaries at their base and top and are separated from other contorted sequences by flat-lying planar-bedded sequences. Each sequence varies in thickness both laterally and vertically over the 10-m-high exposure. At the base of each convoluted sequence is a rapid gradation (less than 2 cm) upward into beds that are severely deformed; that is, the contortions appear to have formed along a single bedding plane, and the entire overlying unit to have undergone considerable disruption (fig. 68). Discordances are present at the top of the convoluted sequences where, in some places, the contorted beds are truncated by overlying planar beds (fig. 69); discordances also exist within the convoluted sequences where contorted beds are truncated by contorted beds (fig. 68). Each convoluted unit resulted from one or more postdepositional events that preceded burial by the overlying planar-bedded sequences.

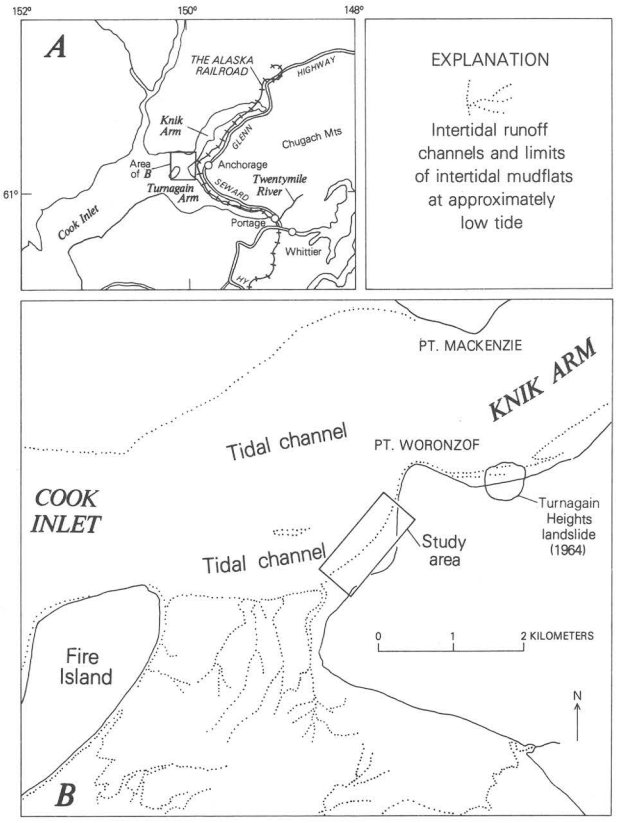

Figure 66.—Index map of upper Cook Inlet region, showing location of study area and approximate distribution of intertidal mudflats at low tide.

Several beds of peat or other concentrated organic matter, only a few millimeters thick, occur within the mud-sand sequence. A sample from the lowest organic bed observed, about 1 m above the base of the exposure, yielded a ^{14}C age of 3,280±90 years (Teledyne Isotopes, laboratory No. I-11,706). A similar age has been obtained on intertidal deposits in a comparable stratigraphic sequence near Goose Bay, about 25 km to the north. Although small peatballs, as large as about 15 cm in diameter, are presently being eroded

Figure 67.—Intertidal bluffs composed of unconsolidated silt and sand aggregate about 9 m in height from surface of water to tidal flats. Bluffs are result of erosion by tidewater flowing in a channel extending from Knik Arm to upper Cook Inlet.

from bluff deposits stratigraphically above the dated bed (fig. 70B), the absence of outcrops of older peat within or near the study area, as well as the similarity of ages determined on deposits in comparable stratigraphic positions, suggests that the age reported is closely contemporaneous with the enclosing deposits.

Landsliding or slumping is probably the primary mechanism by which these sedimentary deposits were deformed, but the events triggering the slumping are speculative. Possible triggering events include: (1) Earthquakes in the area, (2) undercutting of the sediment by channels, or (3) increase in the slope of local intertidal zones created by channel development. Other deformational mechanisms include (1) ice loading in the winter months and (2) wave-induced liquefaction.

Anchorage and upper Cook Inlet are in a tectonically active region characterized by frequent earthquakes and nearby volcanic activity. Ground shaking of saturated unconsolidated sediment, such as that in the intertidal zones, results in extensive slumping and (or) landsliding. Hansen (1966) documented the major Turnagain Heights landslide (fig. 66) in the 1964 Alaska earthquake (Richter magnitude, 8.5). Tectonic events resulting in inplace deformation by dewatering or liquefaction could presumably be recognized in the soft sediment as convoluted layers, and a minimum number of earthquake events could be determined by counting the number of disturbed beds separated by undisturbed beds. Such studies have been undertaken in lake deposits in southern California and on the Kenai Peninsula, 50 km south of the study area (Sims, 1973; Rymer and Sims, 1976).

Blocks of ice, which incorporate layers of intertidal sand and mud, may grow to house-size dimensions over the course of the winter. These blocks are grounded on the higher intertidal mudflats at low tide (tidal channels are left ice free). At low tide, the weight of these blocks could significantly increase pore pressure in the underlying saturated sediment and cause dewatering and soft-sediment deformation. Convoluted bedding resulting from ice loading would be localized in the higher intertidal sandbars, which receive greater numbers of and larger iceblocks. The

Figure 68.—Planar and convoluted bedding in sediment exposed in intertidal bluff. Dashed lines are along discontinuities within contorted sequence.

deformed deposits near Anchorage, however, extend into the active tidal zone, where ice loading does not occur.

Swift silt-laden high-density currents and rapidly changing water levels in a macrotidal environment, such as the regime of upper Cook Inlet, may create frictional drag on the cohesive but saturated surface sediment and cause liquefaction and soft-sediment deformation. The resulting features have been documented in other macrotidal settings (Bay of Fundy; Dalrymple, 1979), but they are on a smaller scale and have a larger proportion of undisturbed sequences than those observed near Anchorage.

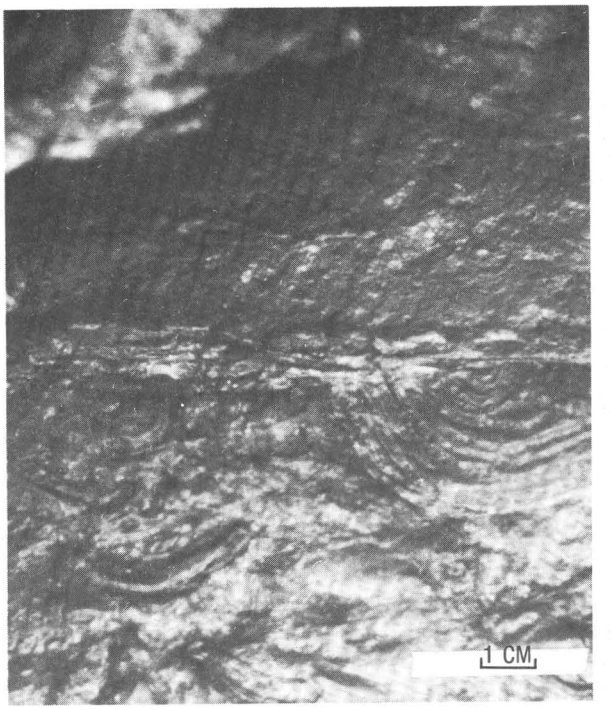

Figure 69.—Planar-bedded sequence truncating an underlying convoluted sequence.

Channel undercutting can result in landsliding and slumping of unsupported deposits and creation of bluffs like those under study. Channel development could cause an increase in the surface slope of the deposit that may, in turn, cause instability in the saturated sediment and "creep" of the sediment channelward, with the attendant development of contorted bedding. Small-scaled convoluted beds, similar to those seen near Anchorage, have been observed adjacent to channels in the present-day intertidal silt at Portage, about 80 km southeast of the study area (fig. 66A), but we were unable to detect the presence of channels in the deposits at Anchorage or Portage. The channels may be destroyed by slumping.

REFERENCES CITED

Dalrymple, R. W., 1979, Wave induced liquefaction; a modern example from the Bay of Fundy: Sedimentology, v. 26, no. 6, p. 835-844.

Hansen, W. R., 1966, Effects of the earthquake of March 27, 1964, at Anchorage, Alaska: U.S. Geological Survey Professional Paper 542-A, p. A1-A68.

Rymer, M. J., and Sims, J. D., 1976, Preliminary survey of modern glaciolacustrine sediments for earthquake-induced deformational structures, south-central Alaska: U.S. Geological Survey Open-File Report 76-373, 20 p.

Sims, J. D., 1973, Earthquake-induced structures in sediments of Van Norman Lake, San Fernando, California: Science, v. 182, no. 4108, p. 161-163.

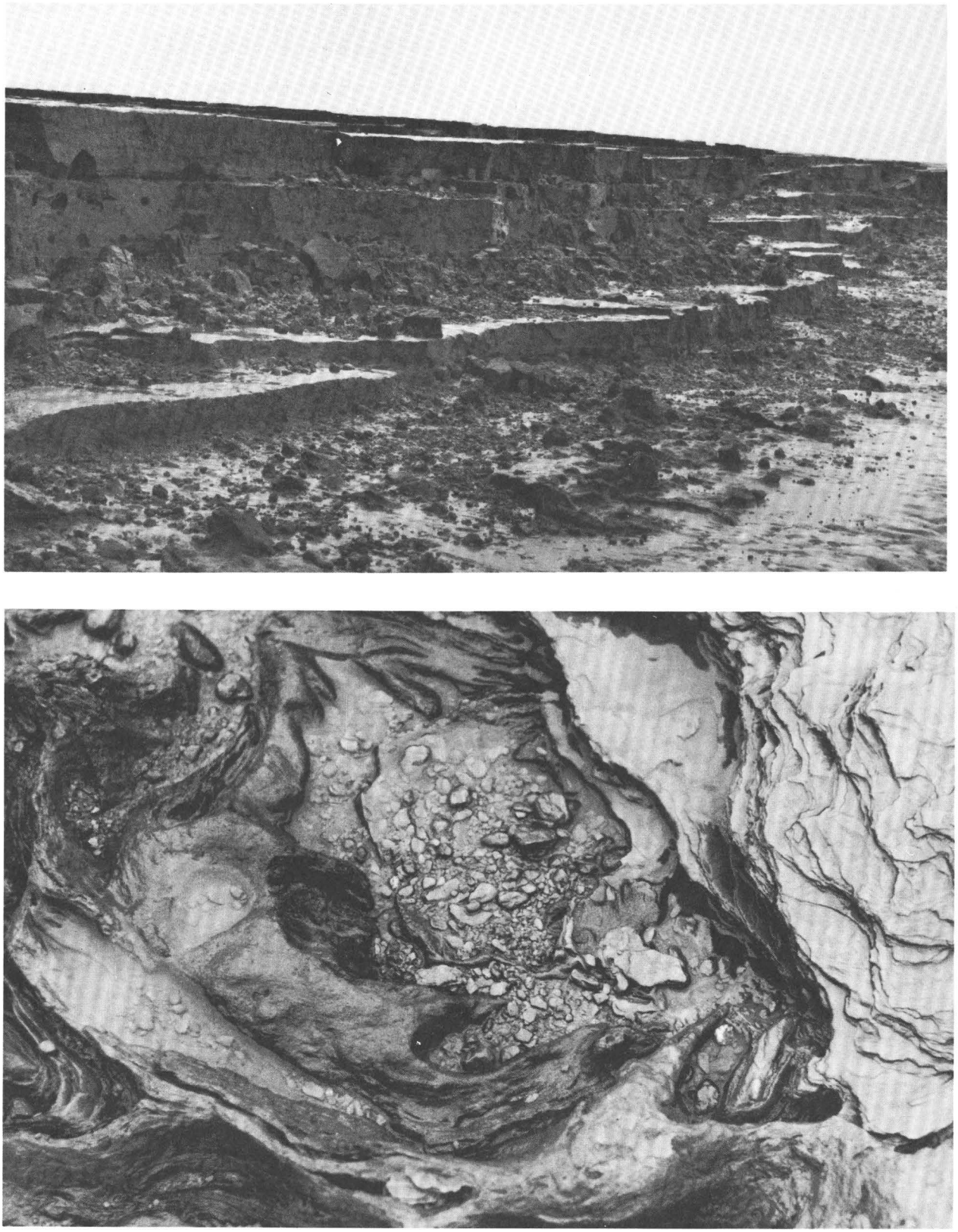

Figure 70.—Products of erosion of intertidal bluffs. A, Slump blocks of flat-lying saturated cohesive mud and sand, as large as approximately 2 m in maximum dimension. B, Mudballs and peatballs, as large as about 15 cm in diameter, eroded from contorted sequences.

Natural restoration from the effects of the 1964 earthquake at Portage, southern Alaska

By Reuben Kachadoorian and A. Thomas Ovenshine

During the 1964 Alaska earthquake, the land in the Portage area (loc. 11, fig. 44) subsided about 2 m owing to local and regional subsidence (Kachadoorian, 1968; McCulloch and Bonilla, 1970). An area of about 18 km^2 was lowered into the intertidal zone of the Turnagain Arm (Ovenshine and others, 1976), and the encroaching tidal waters killed forest, shrub, and grassland communities that the Portage area supported. These tidal waters also caused rapid sedimentation in the area, and by 1974 about 20×10^6 m^3 of silt had accumulated in a layer averaging 1.5 m in thickness (Ovenshine and others, 1976).

Geologic data available on the pre-1964 earthquake sediment in the Portage area suggest that the cycle of subsidence and restoration had occurred at least twice previously during Holocene time (Ovenshine and others, 1976). To determine the rate of sedimentation and the time required for restoration at Portage due entirely to sedimentation, Ovenshine and Kachadoorian (1976, fig. 18) developed a model based on data from the cycle initiated by the 1964 earthquake. The data available to develop this model for estimating the rate of sedimentation were that: (1) The total subsidence was about 2 m, and (2) the average thickness of sediment accumulated during the 10-year period 1964-74 was 1.55 m.

The sedimentation model (fig. 71) derived by Ovenshine and Kachadoorian predicts the total thickness of sediment accumulated at any given time after the 1964 earthquake. The curve is based on the equation

$$A = S(1 - e^{kt}),$$

where A is the total thickness of sediment accumulated at time t, S is the total subsidence due to the 1964 earthquake, k=-0.1492, and t is the time (in years) since 1964. The value of the constant k was determined for S=2 m, A=1.55 m, and t=10 years. (In Ovenshine and Kachadoorian's report, the minus sign was inadvertently omitted in the value given for the constant k.) The curve generated by the model (3, fig. 71; Ovenshine and Kachadoorian, 1976, fig. 18) predicts that sedimentation in the Portage area will cease by the year 2014 and will be approximately 98-percent complete by 1989.

Results of recent investigations by Bartsch-Winkler and Garrow (1982) and ourselves indicate that sedimentation in the Portage area had stopped by summer 1981. Bartsch-Winkler and Garrow have concluded that the Portage area was in the final reconstruction phase of the sedimentation cycle in summer 1980. We observed the presence of lush vegetation and the occurrence of Succinea sp. (a freshwater gastropod) on the higher mudflats during summer 1981. These observations indicate that sedimentation had stopped in Portage by 1981, or about 23 years sooner than predicted by Ovenshine and Kachadoorian (1976).

Curve 3 (fig. 71), derived from Ovenshine and Kachadoorian's sedimentation model, indicates that by 1980 about 1.80 m of sedimentation would have occurred in the Portage area, or about 20 cm less than the 2.0 m of subsidence to which the area was subjected. Actually, only 1.75 m of sedimentation had occurred by 1980. Apparently, either the model is incorrect, or some physical factor is responsible for this discrepancy. The discrepancy is due to post-earthquake tectonic rebound, as reported by Brown and others (1977). No rebound was measured at Portage between 1964 and 1968, and about 20 cm of rebound occurred between 1968 and 1975 (curve 5, fig. 71; Brown and others, 1977, fig. 2). We have, however, extrapolated the curve from the years 1975-82 on the basis of an analysis of Brown and others' data. Curve 1 (fig. 71), which represents the ground-surface elevation relative to the post-1964 surface elevation, is based on the addition of curve 3 (predicted amount of sedimentation from equation 1) and curve 5 (amount of tectonic uplift after 1964). This curve, which intersects the 2.0-m (amount of subsidence at Portage) line at mid-1978, indicates that sedimentation should have stopped at that time. Field data indicated that some sedimentation was occurring during summer 1978, albeit slight.

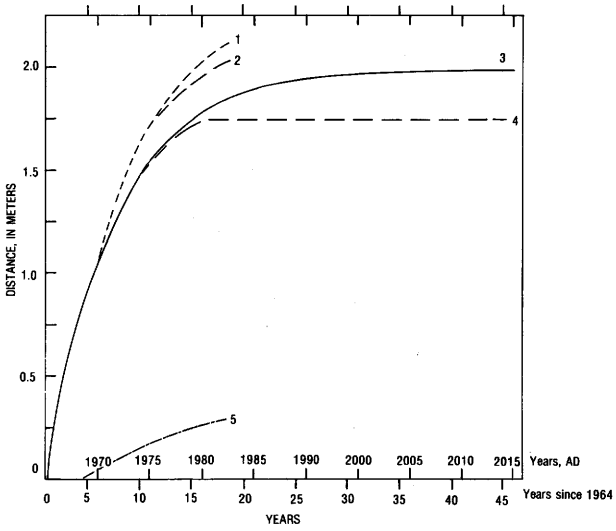

Figure 71.—Rate of sedimentation, amount of uplift, and sediment-surface elevation relative to post-1964 earthquake elevation. Curve 1, sediment-surface elevation based on addition of curves 3 and 5; curve 2, actual sediment-surface elevation based on addition of curves 4 and 5; curve 3, predicted amount of sedimentation from equation $A = S(1 - e^{kt})$; curve 4, actual amount of sedimentation; curve 5, tectonic uplift in Portage area.

Ovenshine and Kachadoorian's (1976) model sedimentation-rate curve was based on an assumption of no tectonic uplift and thus does not consider the effect of tectonic uplift on the sedimentation rate. Any uplift of the Portage area would naturally slow down the sedimentation to a rate below that predicted by the model. The equation on which the predictive

curve is based indicates that 6.1 cm of sedimentation should have occurred in the 1-year period between 1974 and 1975; however, we measured only 5 cm of sedimentation for this period. Although Ovenshine and Kachadoorian did not consider this difference to be significant, we now believe that the difference of 1.1 cm of sedimentation is due to tectonic uplift. An analysis of the predictive-model sedimentation-rate curve and the uplift curve, extended to 1982, indicates that by 1980 the amount of actual sedimentation at Portage was 5 cm less than predicted: The actual sedimentation curve (4, fig. 71) indicates that 1.75 m of sedimentation occurred by 1980 instead of the 1.80 m predicted. Curve 2 (fig. 71), which represents the actual ground-surface elevation relative to the post-1964 earthquake ground elevation, is based on the addition of the tectonic-uplift curve (5) and the actual-sedimentation curve (4). Curve 2, which intersects the 2.0-m line in the year 1980, indicates that sedimentation stopped in the Portage area in 1980, as suggested by field data. The slope of curve 2 becomes the same as that of the uplift curve after deposition stopped in 1980.

On the basis of the data available, we believe that the model proposed by Ovenshine and Kachadoorian (1976) was a valid approach to estimate the time required for natural restoration due only to sedimentation from the effects of the 1964 earthquake at Portage, Alaska.

REFERENCES CITED

Bartsch-Winkler, S. R., and Garrow, H. C., 1982, Depositional system approaching maturity at Portage Flats, in Coonrad, W. L., ed., The United States Geological Survey in Alaska: Accomplishments during 1980: U.S. Geological Survey Circular 844, p. 115-117.

Brown, L. D., Reilanger, R. E., Holdhal, S. R., and Balazs, E. I., 1977, Post seismic crustal uplift near Anchorage, Alaska: Journal of Geophysical Research, v. 82, no. 23, p. 3369-3378.

Kachadoorian, Reuben, 1968, Effects of the earthquake of March 27, 1964, on the Alaska highway system: U.S. Geological Survey Professional Paper 545-C, p. C1-C66.

McCulloch, D. S., and Bonilla, M. G., 1970, Effects of the earthquake of March 27, 1964, on the Alaska Railroad: U.S. Geological Survey Professional Paper 545-D, p. D1-D161.

Ovenshine, A. T., and Kachadoorian, Reuben, 1976, Estimate of the time required for natural restoration of the effects of the 1964 earthquake at Portage, in Cobb, E. H., ed., The United States Geological Survey in Alaska: Accomplishments during 1975: U.S. Geological Survey Circular 733, p. 53-54.

Ovenshine, A. T., Lawson, D. E., and Bartsch-Winkler, Susan, 1976, The Placer River Formation—intertidal sedimentation caused by the Alaska earthquake of March 27, 1964: U.S. Geological Survey Journal of Research, v. 4, no. 2, p. 151-162.

SOUTHEASTERN ALASKA

(Figure 72 shows study areas discussed)

Progress in lead/uranium zircon studies of lower Paleozoic rocks of the southern Alexander terrane

By Jason B. Saleeby[1], George E. Gehrels[1], G. Donald Eberlein, and Henry C. Berg

Geologic mapping and zircon lead/uranium geochronologic studies on southern Prince of Wales Island and southern Annette Island (area 10, fig. 72; fig. 73) have delineated a regional metaigneous complex that

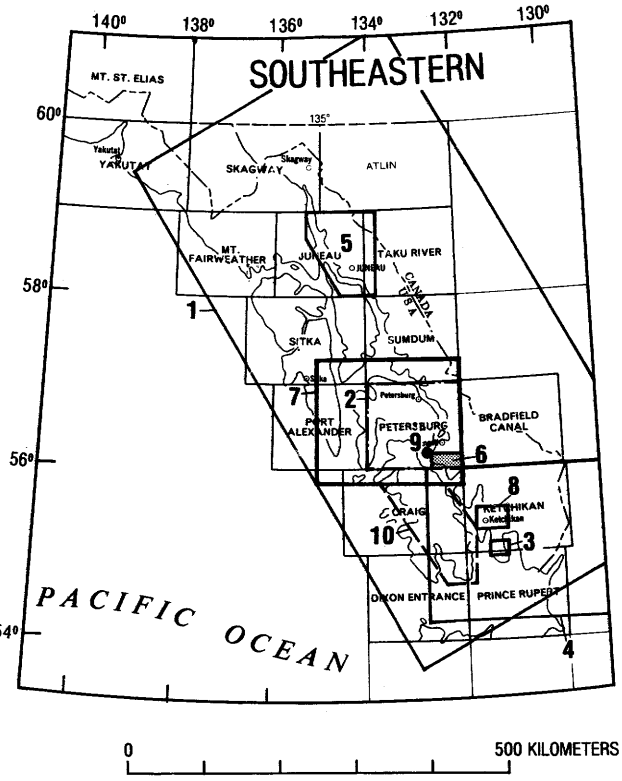

Figure 72.—Areas and localities in southeastern Alaska discussed in this volume. A listing of authorship, applicable figures and tables, and article pagination (in parentheses) relating to the numbered areas follows. 1, Brew and Ford, figure 79 (p. 120-124); 2, Burrell, figures 80 and 81 (p. 124-126); 3, Gehrels and others, figure 75 (p. 113-115); 4, Gehrels and Taylor, figures 86 through 89 (p. 134-136); 5, Himmelberg and others, figure 85 (p. 131-134); 6, Hunt, figures 83 and 84 (p. 128-131); 7, Karl, figures 76 and 77 (p. 115-117); 8, Koch and Elliott, figure 82 (p. 126-128); 9, Panuska and others, figure 78, tables 20 and 21 (p. 117-120); 10, Saleeby and others, figures 73 and 74 (p. 110-113).

[1]Division of Geological and Planetary Sciences, California Institute of Technology, Pasadena, CA 91125.

ties these two areas together during Ordovician and, possibly, earlier time. Important phases of this complex are varitextured hornblende diorite, quartz diorite, diorite-basite migmatite, dioritic agmatite, trondhjemite, and minor gabbro, pyroxenite, and mafic dike rock. Metamorphic-mineral assemblages and fabrics indicate metamorphism to greenschist to amphibolite facies under both static and dynamic conditions. On Prince of Wales Island, such rocks intrude the Wales Group and parts of the Descon Formation and age-equivalent eugeosynclinal strata. On Annette Island, Wales Group-type rocks occur as screens and small pendants in similar metaigneous rocks (Gehrels and others, 1983).

Geochronologic work has focused on trondhjemitic and quartz dioritic members of the complex. Figure 74 summarizes the preliminary lead/uranium zircon data. Apparent concordance in age is defined $^{206}Pb/^{238}U$ data point for a particular fraction; such ages approximate the time of igneous crystallization. Concordance is defined as clustering (within analytical uncertainty) of $^{206}Pb/^{238}U$ ages on multiple fractions that each show apparent concordance. Such systematics define tight igneous-age constraints bounded by the total range of the $^{206}Pb/^{238}U$-age uncertainties. Igneous-age constraints on discordant fractions can be derived only by considering the total data set and depend on the model chosen for the discordance mechanism. The data summarized in figure 74 reveal both a distinct pattern in regional-scale zircon behavior and important igneous-age constraints on the metaigneous complex.

Zircon discordance is widespread throughout the metaigneous complex, although the discordance mechanism is not yet understood. The pattern of discordant $^{207}Pb/^{206}Pb$ ages falling within the range of the concordant ages, independent of dispersion in the corresponding $^{206}Pb/^{238}U$ ages, points to a late-stage lead-loss (or uranium gain) mechanism. Although such a mechanism would do little to change the isotopic composition of the lead, it could upset the lead/uranium ratios significantly. Thus, by this mechanism the $^{207}Pb/^{206}Pb$ ages of the discordant samples also approximate the igneous-crystallization ages. Although Saleeby and Eberlein (1981) suggested that discordance in most of the Prince of Wales Island

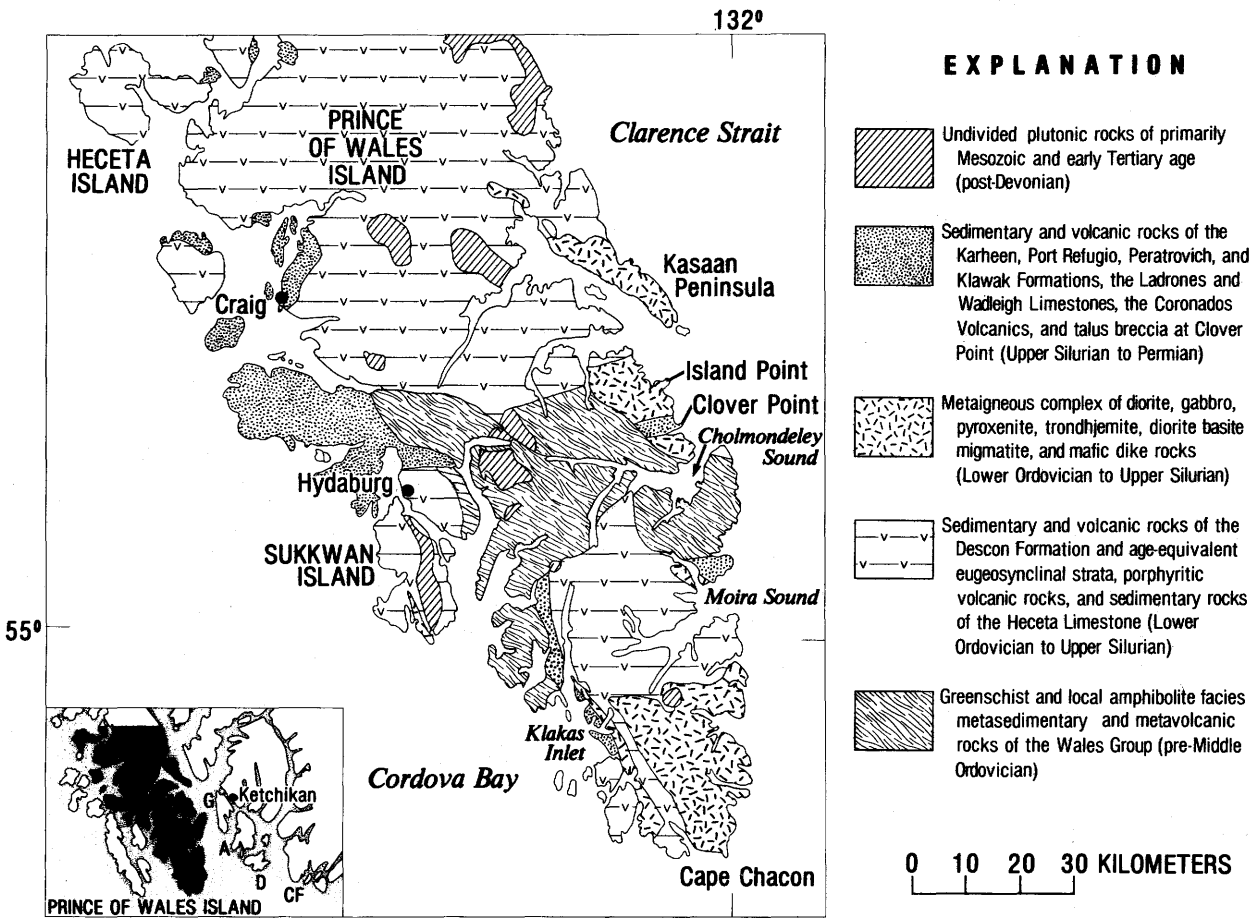

Figure 73.—Geologic sketch map of southern Prince of Wales Island (from G. D. Eberlein, unpub. data, 1981) and index map showing Prince of Wales Island and several Alexander terrane localities discussed in text: A, Annette Island; CF, Cape Fox area; D, Duke Island; G, Gravina Island.

samples is related to widespread mafic-dike emplacement, subsequent work on both Prince of Wales and Annette Islands suggests otherwise. In particular, even though samples from both islands show similar discordance patterns, crosscutting mafic dikes are rare on Annette Island in comparison with Prince of Wales Island. Furthermore, although restriction of the main dike swarms to the Paleozoic rocks suggests a Paleozoic age, it is unlikely that dike emplacement could account for a late-stage disturbance.

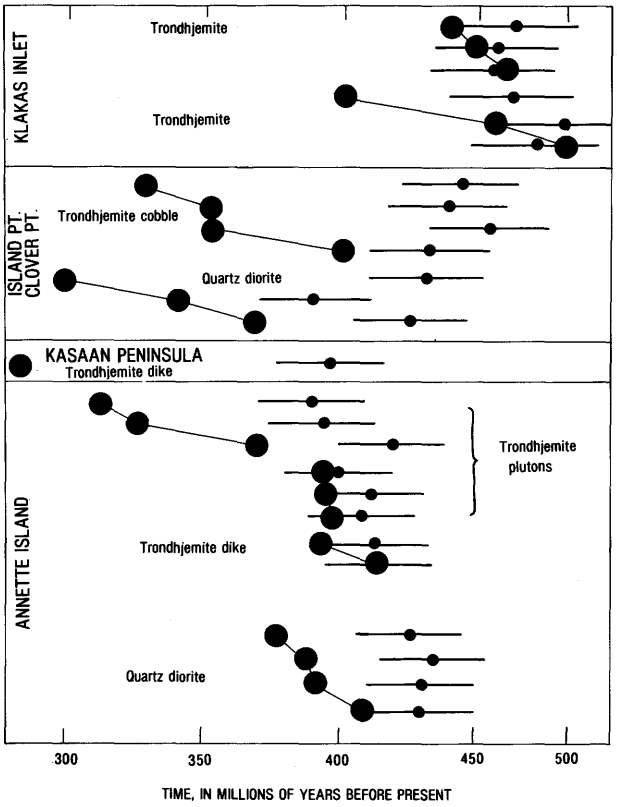

Figure 74.—Zircon $^{206}Pb/^{238}U$ and $^{207}Pb/^{207}Pb$ ages on rock samples from localities (fig. 73) in the southern Alexander terrane. Large dots, $^{206}Pb/^{238}U$ ages, with diameters approximating analytical uncertainties; small dots, $^{207}Pb/^{206}Pb$ ages, with line lengths showing analytical uncertainties. Links between $^{206}Pb/^{238}U$ dots denote multiple-fraction analyses from cogenetic suites.

The oldest metaigneous rocks dated are the trondhjemite of Klakas Inlet. The five fractions showing apparent concordance and the systematics of the discordant fractions indicate igneous ages in the range 450-500 m.y. The Klakas Inlet trondhjemite occurs as a kilometer-scale homogeneous mass and as meter-scale dikes and screens within sheeted mafic dikes. Contradictory intrusive relations (mafic dikes cutting trondhjemite and trondhjemite dikes cutting mafic dikes) suggest that the Klakas Inlet mafic dikes are cogenetic with the trondhjemite. Detailed relations between the trondhjemite/mafic-dike assemblage and the adjacent Wales Group are unclear owing to complex intrusive patterns along their contact zone that may involve younger igneous rocks.

The youngest rocks dated are the trondhjemitic plutons and dikes of Annette Island. Concordant and discordant ages from these rocks indicate igneous crystallization at about 400 m.y. B.P. Detailed mapping by Gehrels and others (1983) indicates that the Annette Island trondhjemite intrudes both metadioritic and Wales Group-type assemblages. A quartz dioritic phase of the metadioritic wallrock assemblage yields an age array suggesting an igneous age in the range 400-500 m.y.

Detailed age constraints cannot be placed at this time on the trondhjemite and quartz diorite samples from the Kasaan Peninsula and Clover Point-Island Point areas. The Kasaan Peninsula trondhjemite sample is from a series of dikes and pods that occur in gabbro-diorite and sets of locally sheeted basaltic dikes. The $^{207}Pb/^{206}Pb$ age on the trondhjemite suggests that igneous crystallization took place about 400 m.y. B.P. Quartz diorite of the Island Point area to the south is the youngest phase from a complex mixture of metadioritic, gabbroic, and pyroxenitic rocks; the $^{207}Pb/^{206}Pb$ ages suggest an igneous age in the range 400-450 m.y.

Sand- to boulder-size debris of diorite, gabbro, and pyroxenite from the Island Point assemblage constitutes an ancient talus-slope breccia exposed from the vicinity of Clover Point for about 2 km northward. Important additional clastic components consist of rare trondhjemite and mafic-dike-rock clasts and blocks of Lower(?) Devonian limestone. Discordant $^{207}Pb/^{206}Pb$ ages on zircon from a large trondhjemite cobble suggest an igneous age of about 450 m.y., not unlike that of the Klakas trondhjemite. The Klakas Inlet trondhjemite and its related mafic dike rock were unroofed and shed as coarse detritus during Early Devonian time, as is shown by a zone of highly shattered trondhjemite along the eastern part of Klakas Island that grades into an ancient talus breccia similar to that exposed at Clover Point. The Klakas Inlet breccia is depositionally overlain by Lower Devonian grit and shale. Although the age of the Clover Point breccia is not known, crosscutting mafic dikes that are widespread in Paleozoic rocks on Prince of Wales Island also crosscut the breccia. The breccia is tentatively considered an expression of the same mid-Paleozoic tectonic event that unroofed the Klakas Inlet trondhjemite and rocks of the metaigneous complex on Annette Island (Gehrels and others, 1983).

The metaigneous rocks described above and by Gehrels and others (1983) may constitute a major and fundamentally important lithologic constituent of the southern Alexander terrane. Published field and age data (MacKevett, 1963; Lanphere and others, 1964; Berg, 1973; Koch and others, 1977) and our own reconnaissance work suggest that such metaigneous rocks underlie parts of Gravina and Duke Islands, the Cape Fox area on the mainland, and southernmost Prince of Wales Island. Furthermore, dioritic, gabbroic, and pyroxenitic members of the metaigneous complex are apparently of the proper age and composition to be

genetically related to volcanic rocks of the Descon Formation. Thus, better resolution of igneous ages in conjunction with field and petrologic studies will provide critical information on the petrologic development of the southern Alexander terrane as well as additional criteria for defining the limits of this terrane.

REFERENCES CITED

Berg, H. C., 1973, Geology of Gravina Island, Alaska: U.S. Geological Survey Bulletin 1373, 41 p.

Gehrels, G. E., Saleeby, J. B., and Berg, H. C., 1983, Geologic framework of Paleozoic rocks on southern Annette and Hotspur Islands, in Coonrad, W. L., and Elliott, R. L., eds., The United States Geological Survey in Alaska: Accomplishments during 1981: U.S. Geological Survey Circular 868, p. 113-115.

Koch, R. D., Elliott, R. L., Smith, J. G., and Berg, H. C., 1977, Metamorphosed trondhjemite of the Alexander terrane in Coast Range plutonic complex, in Blean, K. M., ed., The United States Geological Survey in Alaska: Accomplishments during 1976: U.S. Geological Survey Circular 751-B, p. B72-B74.

Lanphere, M. A., MacKevett, E. M., Jr., and Stern, T. W., 1964, Potassium-argon and lead-alpha ages of plutonic rocks, Bokan Mountain area, Alaska: Science, v. 145, no. 3633, p. 705-707.

MacKevett, E. M., Jr., 1963, Geology and ore deposits of the Bokan Mountain uranium-thorium area, southeastern Alaska: U.S. Geological Survey Bulletin 1154, 125 p.

Saleeby, J. B., and Eberlein, G. D., 1981, An ensimatic basement complex and its relation to the early Paleozoic volcanic-arc sequence of southern Prince of Wales Island, southeastern Alaska [abs.]: Geological Society of America Abstracts with Programs, v. 13, no. 2, p. 104.

Geologic framework of Paleozoic rocks on southern Annette and Hotspur Islands, southern Alexander terrane

By George E. Gehrels[1], Jason B. Saleeby[1], and Henry C. Berg

Paleozoic and Mesozoic rocks on Annette Island (area 3, fig. 72) constitute one of the southeasternmost exposures of the Alexander terrane—a displaced tectonic fragment that underlies much of southeastern Alaska (Jones and others, 1972). Detailed geologic mapping and preliminary uranium-lead geochronologic studies demonstrate that Annette Island is underlain by a Silurian and older volcanic-plutonic complex and a superjacent sequence of Devonian and younger sedimentary and volcanic rocks (fig. 75). Three distinct lithologic assemblages have been recognized in the volcano-plutonic complex, including: (1) pre-Late Ordovician metasedimentary and metavolcanic rocks, (2) Late Ordovician and Silurian dioritic intrusive rocks, and (3) Silurian trondhjemites that intrude both of the above assemblages.

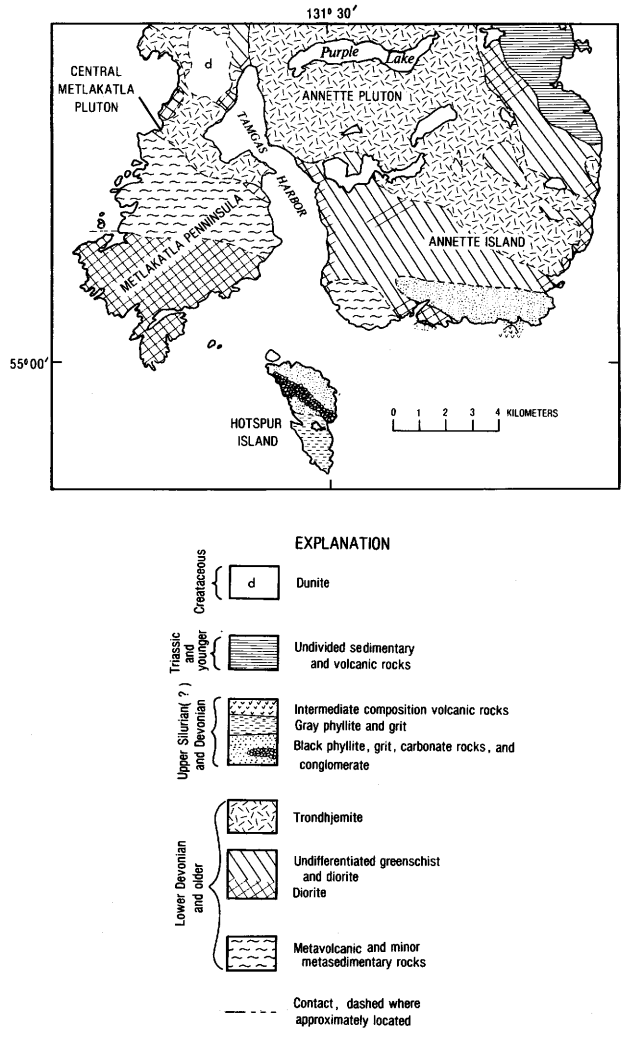

Figure 75.—Geologic sketch map of southern Annette and Hotspur Islands, southeastern Alaska (modified from Berg, 1972).

The oldest assemblage in the study area includes pre-Late Ordovician silicic to intermediate-composition metavolcanic and minor metasedimentary rocks (fig. 75). In most areas these rocks are moderately to intensely deformed and are metamorphosed to greenschist and locally amphibolite facies. Locally, however, primary structures such as graded bedding in mudstone turbidites and fragmental textures in tuff breccia are preserved. The silicic volcanic rocks are generally subordinate to the intermediate composition rocks, and consist of layered and finely laminated tuffs. Orange-weathering, coarsely recrystallized

[1]Division of Geological and Planetary Sciences, California Institute of Technology, Pasadena, CA 91125.

marble is also locally present in this assemblage. The deformation and metamorphism of these rocks occurred in part prior to the emplacement of dioritic dikes and stocks, although in most areas the younger diorites share these deformational fabrics.

A heterogeneous assemblage of dioritic rocks intrudes and disrupts the older metavolcanic and metasedimentary rocks on Annette Island (fig. 75). Textural varieties in this assemblage include massive hornblende diorite and quartz diorite, layered diorite-basite migmatite, and dioritic agmatite. Migmatitic varieties have tabular blocks of fine-grained metabasite lying concordantly within medium-grained diorite; these tabular blocks probably include both fragments of wallrock and disrupted synplutonic dikes. The agmatite ranges from dikelets of fine- to medium-grained diorite intruding relatively intact country rock to swarms of xenoliths in a dioritic matrix. Sharp angular contacts and the absence of widespread ductile deformation in both the migmatite and agmatite indicate that these units formed in rather shallow-level plutonic environments. In contrast, ductile shear zones and local gneissic banding in coarse-grained hornblende diorite on the southern Metlakatla Peninsula may record emplacement at greater depth. Our preliminary uranium-lead geochronological studies suggest that the dioritic rocks were emplaced in the 430-450 m.y. range.

Large trondhjemitic plutons underlie much of Annette Island and intrude both the dioritic and older metamorphic rocks (fig. 75). These plutons generally consist of medium- to coarse-grained trondhjemite, with minor phases ranging in composition from quartz diorite to granite (Berg, 1972). Preliminary uranium-lead analyses of zircon from the trondjemitic rocks (fig. 75) indicate igneous ages in the range 405-420 m.y.

Sedimentary and volcanic rocks rest unconformably on dioritic rocks on southern Annette Island and underlie much of Hotspur Island (fig. 75). At the base of this sequence is a very thin conglomerate containing clasts of the dioritic assemblage. Above this basal conglomerate is a sequence of interbedded black phyllite, siltstone, sandstone, and minor limestone, conglomerate containing large intraformational olistoliths in a grit matrix, and gray phyllite and grit. The sedimentary sequence on Hotspur Island is capped by intermediate-composition pillow flows, lapilli tuff, and interbedded tuff and black phyllite. Megafossils demonstrate a Devonian (and possible Late Silurian(?)) age for the lower part of the section (Berg, 1972), but the age of the volcanic rocks is unknown.

Along the east side of Annette Island, Ordovician-Silurian plutonic rocks are overlain directly by Upper Triassic sedimentary and volcanic rocks (fig. 75). The lack of Devonian strata in this area may be due to non-deposition or to a post-Devonian pre-Late Triassic erosional event. Because the Triassic rocks appear to have undergone the same moderate deformation and low-grade metamorphism as the Devonian rocks, this speculative erosional event was probably not accompanied by major deformation or metamorphism. The low-grade metamorphism which is apparent in the Devonian and Triassic rocks is also evident in Jurassic and Cretaceous rocks on eastern Annette Island and may be related to the late Mesozoic or Tertiary thermal activity described by Gehrels and Taylor (1983).

The Devonian and older rocks on Annette Island are quite similar to coeval rocks on Prince of Wales Island (Saleeby and others, 1983, fig. 73). The pre-Late Ordovician metavolcanic and metasedimentary rocks on Annette Island resemble rocks in both the Wales Group and the Descon Formation on Prince of Wales Island (Herreid and others, 1978). Dioritic and trondhjemitic intrusives are also similar lithologically and have comparable uranium-lead ages (Saleeby and others, 1983, fig. 74). Superjacent Upper Silurian(?) and Devonian rocks on Annette and Hotspur Islands resemble strata in the Klakas Inlet area (Herreid and others, 1978) and in the Craig area (Eberlein and Churkin, 1970) of Prince of Wales Island. The post-Devonian sedimentary rocks on central Prince of Wales Island, however, are absent on Annette Island. This difference may be due to nondeposition and (or) an erosional event on Annette Island between Devonian and Late Triassic time.

The above general correlations suggest that parts of Annette and Prince of Wales Islands are underlain by similar volcano-plutonic and superjacent Devonian rocks. The difference in Paleozoic stratigraphy between the two areas can be reasonably attributed to facies changes and (or) erosional events, rather than to evolution in different tectonic environments, as tentatively suggested by Berg and others (1978). Thus, Annette and Prince of Wales Islands probably evolved in the same general marine volcanoplutonic province during Devonian and earlier time.

Acknowledgments.—Financial support for this research was partly provided by the Division of Geological and Planetary Sciences, California Institute of Technology (contribution No. 3721); the Geological Society of America; and Sigma Xi, the scientific research society.

REFERENCES CITED

Berg, H. C., 1972, Geologic map of Annette Island, Alaska: U.S. Geological Survey Miscellaneous Geologic Investigations Series Map I-684, 8 p., scale 1:63,360.

Berg, H. C., Jones, D. L., and Coney, P. J., 1978, Map showing pre-Cenozoic tectonostratigraphic terranes of southeastern Alaska and adjacent areas: U.S. Geological Survey Open-File Report 78-1085, scale 1:1,000,000, 2 sheets.

Eberlein, G. D., and Churkin, Michael, Jr., 1970, Paleozoic stratigraphy in the northwest coastal area of Prince of Wales Island, southeastern Alaska: U.S. Geological Survey Bulletin 1284, 67 p.

Gehrels, G. E., and Taylor, H. P., 1983, Fossil hydrothermal systems in the Ketchikan area, southeastern Alaska, in Coonrad, W. L., and Elliott, R. L., eds., The United States Geological Survey in Alaska: Accomplishments during 1981: U.S. Geological Survey Circular 868, p. 134-136.

Herried, Gordon, Bundtzen, T. K., and Turner, D. L., 1978, Geology and geochemistry of the Craig C-2 quadrangle and vincinity, Prince of Wales Island, southeastern Alaska: Alaska Division of Geological and Geophysical Surveys Geologic Report 48, 49 p.

Jones, D. L., Irwin, W. P., and Ovenshine, A. T., 1972, Southeastern Alaska—a displaced continental fragment?, in Geological Survey research 1972: U.S. Geological Survey Professional Paper 800-B, p. B211-B217.

Saleeby, J. B., Gehrels, G. E., Eberlein, G. D., and Berg, H. C., 1983, Progress in Pb/U zircon studies of Lower Paleozoic rocks of the southern Alexander terrane, in Coonrad, W. L., and Elliott, R. L., eds., The United States Geological Survey in Alaska: Accomplishments during 1981: U.S. Geological Survey Circular 868, p. 110-113.

Recognition of the Burnt Island Conglomerate on the Screen Islands, southeastern Alaska

By Susan M. Karl

The Screen Islands represent the easternmost boundary of Alexander terrane rocks where they occur in Clarence Strait between Prince of Wales and Etolin Islands, southeastern Alaska (area 7, fig. 72; fig. 76). Detailed mapping, new paleontologic ages, and tectonic setting support correlation of the rocks on the Screen Islands with the Upper Triassic Burnt Island Conglomerate (Muffler, 1967) of Keku Strait. With this designation, the rocks on the Screen Islands represent the southernmost known occurrence of the Burnt Island Conglomerate and imply a relation between the Clarence Strait and Keku Strait fault zones.

LITHOLOGY

The rocks on the Screen Islands consist of conglomerate, calcareous sandstone (calcarenite), calcareous siltstone (calcisiltite), and limestone (fig. 77). The base of the conglomerate is not exposed. The conglomerate is interbedded with, and grades upward into, calcarenite, which is overlain by calcisiltite and silty limestone, and calcareous lithic sandstone.

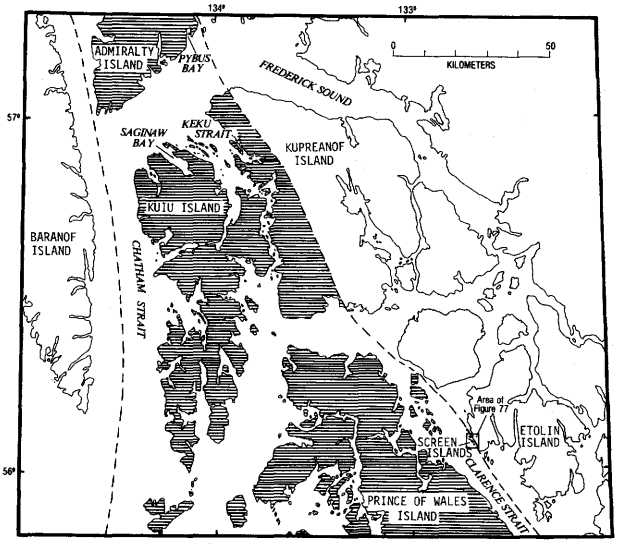

Figure 76.—Alexander terrane (shaded area between dashed lines) in vicinity of the Screen Islands and Keku Strait (modified from Berg and others, 1978).

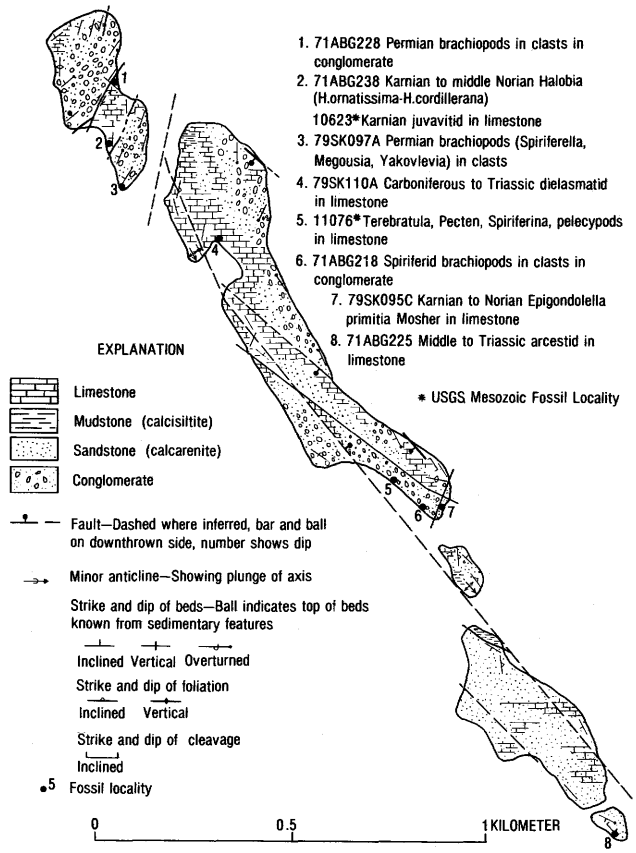

Figure 77.—Lithologic map of the Screen Islands (Petersburg A-3 quadrangle), southeastern Alaska, showing fossil localities. See figure 76 for location.

The conglomerate is a well-bedded poorly sorted bimodal chert, volcanic-rock, and limestone-cobble conglomerate. The matrix resembles the tan- to brown-weathering medium- to coarse-grained calcarenite and calcareous lithic sandstone that the conglomerate grades upward into. The clasts consist predominantly of: well-rounded white spirifirid-brachiopod-bearing chert cobbles; angular to plastically deformed masses of limestone, calcisiltite, calcarenite, calcareous lithic sandstone, finely laminated shale, and siltstone; and subordinate angular to subrounded pebbles and cobbles of tuff and felsic, intermediate, and mafic volcanic rocks. No plutonic- or metamorphic-rock clasts were observed in the conglomerate or in the sandstone matrix. The bimodality of the conglomerate is defined by the two main clast populations: The rounded chert and volcanic-rock cobbles, and the angular deformed masses of calcarenite and calcareous mudstone.

Bedding in the conglomerate ranges from graded beds, several centimeters thick, to massive layers, tens of meters thick. Well-defined crosslaminations and channel-scour features indicate that these beds face upward.

The sandstone is light brown and consists predominantly of angular clasts of calcite in a calcareous cement (calcarenite). Clast types include sparsely distributed angular limpid embayed quartz with straight extinction, euhedral plagioclase feldspar, angular to subrounded intermediate to mafic volcanic-rock fragments, calcareous mudstone, and rare cubes of pyrite. The sandstone beds range from a centimeter to several meters in thickness; they are typically massive but locally trough crossbedded and, in places, graded.

The limestone is light to medium gray and locally sandy or silty. It may be massive or brecciated but is generally well-bedded. Bedding is on a centimeter scale and defined by thin layers of mudstone or calcarenite; some layers are graded. Millimeter- to centimeter-thick wisps and wavy to convoluted stringers of siltstone and sandstone suggest soft-sediment deformation within limestone layers. The limestone is locally isoclinally folded, and in some places these folds lose their integrity and grade into intraformational conglomerate, which is a matrix-poor "jigsaw puzzle" limestone breccia.

The southernmost of the Screen Islands is composed of light-gray fine- to medium-grained calcareous lithic sandstone turbidites. Beds average several centimeters to tens of centimeters in thickness. Graded crosslaminated and convolute layers are common. Interbeds consist of calcareous mudstone. These rocks are folded and faulted against sandy limestone to the northeast. Turbidite features were not observed in sandstone elsewhere on the Screen Islands.

AGE

Numerous fossil collections on the Screen Islands have yielded an equivocal distribution of ages (fig. 77). The oldest fossils are predictably found in the white well-rounded chert cobbles in the conglomerate. These fossils are mainly brachiopods, including Spirifirella and the linoproductids Megousia and, possibly, Yakovlevia, considered to be Late Permian (J. T. Dutro, Jr., written commun., 1979). A fragment of a probable Septacamera is similar to those described (J. T. Dutro, Jr., written commun., 1979) from the Halleck Formation, a Permian unit that crops out in Saginaw Bay and Keku Strait. The chert clasts could also have been derived from the Pybus Formation, a cherty carbonate unit that has been recognized on East Island, a few kilometers west of the Screen Islands in Clarence Strait (Michael Churkin, Jr., written commun., 1979), as well as in Keku Strait and Pybus Bay (fig. 76).

The intercalated and overlying sandstone and limestone on the Screen Islands yielded an ammonite of late Karnian age (Buddington and Chapin, 1929), a terebratuloid brachiopod of Carboniferous to Triassic age, Late Triassic Halobia (N. J. Silberling, written commun., 1980), and the conodont Epigondolella primitia Mosher of late Karnian to early Norian age (Bruce Wardlaw, written commun., 1980). The Late Triassic age of the sandstone and limestone associated with the conglomerate suggests that the Permian cobbles in the conglomerate were redeposited. Because no major unconformity has been observed and the limestone appears to be intercalated with the conglomerate, a Late Triassic depositional age seems reasonable for these rocks.

SEDIMENTARY ENVIRONMENT

Sedimentary structures, such as well-developed crossbedding in the conglomerate and sandstone as well as common sedimentary breccia in the limestone, suggest a high-energy environment and a proximal sedimentary facies for the sequence of rocks on the Screen Islands. Sedimentary structures and lithologic characteristics suggest a change in depositional environment from a high-energy setting to a quieter, possibly deeper water setting for the limestone higher in the section.

The conglomerate is the oldest unit, and its substrate is not exposed. The conglomerate is locally well bedded but in other places is massive and contains slumped blocks of sandstone or limestone, as much as 50 m long. The composition of the conglomerate varies in the percentage of mature clasts and in the proportions of chert, mudstone, volcanic rock, limestone, and sandstone. These variations, which are not systematic either laterally or vertically, appear to reflect changes in a local source. The composition of the matrix of the conglomerate is slightly more consistent but also varies from place to place in the proportions of calcite, lithic fragments, quartz, feldspar, and delicate fossil fragments.

The absence of any plutonic- or metamorphic-rock clasts in the conglomerate and sandy matrix suggests that this unit was deposited in a basin which was controlled by a local source and which was small enough or offshore far enough to be effectively isolated from terrigenous or continental influence. The rounding of the chert and volcanic-rock clasts, as well as the older age of the chert clasts, suggests reworking from underlying units; the abundance of plastically deformed sandstone and limestone clasts also suggests reworking from within the unit, in the form of slumping and soft-sediment deformation. A high-energy environment is favored over long-distance travel for the rounding of the chert and volcanic-rock clasts, owing to the homogeneity of clast composition. Common slumped masses and large blocks indicate a tectonically active environment. The angularity of the grains in the matrix of the conglomerate and in the overlying sandstone and limestone suggests rapid deposition from a nearby source.

A reasonable explanation for the bimodality of this deposit might be rapid accumulation in a small basin adjacent to tectonically active volcanic islands. These islands may have been established by uplift of Upper Permian marine deposits and subsequent growth of felsic to mafic, but dominantly intermediate, volcanic centers. Uplift is indicated by the absence of latest Permian through Middle Triassic fossils, an implied unconformity. Paleontologic information indicates that the rocks on the Screen Islands were deposited during Late Triassic time. Contemporary volcanic activity is suggested by the common clear

angular volcanic quartz (Folk, 1968) and euhedral feldspar, and the abundance of soft-sediment deformation. Quiet intervals may be reflected by the accumulation of the well-bedded silty limestone. Although fossils are common in this limestone, they are pelagic types, including ammonoids and belemnoids, rather than fossils typical of carbonate-bank deposits. Even bedding, absence of upper-flow-regime sedimentary structures, and fine grain size suggest deposition in moderately deep water. Recent faulting and jumbling of the sequence preclude estimates of section thickness and any distinction between sedimentary versus tectonic repetition of section; however, the three rock types are all interbedded, and the limestone seems to increase in abundance upsection. The structurally highest and apparently youngest rocks in the Screen Islands appear to be the calcareous turbidites on the southernmost island; this observation, also made by Buddington and Chapin (1929), suggests a deepening environment and a change in depositional regime.

DEFORMATION

The conglomerate, sandstone, limestone, and mudstone have been jostled by strike-slip faulting into a relation other than that in which they were originally deposited. Considerable shearing is associated with the faulting, generally northwest-southeastward, parallel to the trend of Clarence Strait, although the deformation is not penetrative. Clasts in the conglomerate are neither broken nor flattened, although the matrix may appear sheared within shear zones. Original textures and structures of rocks between faults and shear zones are generally well preserved.

C. S. Grommé and J. W. Hillhouse drilled three holes in the best dated and structurally most coherent limestone section on the Screen Islands for a paleomagnetic study. Their results, however, did not pass the fold test; that is, the scatter in the data increased when the rocks were unfolded. They concluded (J. W. Hillhouse, oral commun., 1981) that the magnetization in these rocks is postfolding and, therefore, not primary.

Although faulting has been significant on the Screen Islands, no metamorphic minerals have been observed, and the rocks are entirely unmetamorphosed. The conodont-color-alteration index of 3.0 indicates maximum host-rock temperatures of 110° to 200° C, which is unusually low for rocks in this part of southeastern Alaska (Bruce Wardlaw, written commun., 1980).

CORRELATION

Nearly identical conglomerate, sandstone, and limestone coeval with the rocks on the Screen Islands have been observed in Keku Strait, to the northwest of Clarence Strait, along the same general structural trend. These similar rocks in Keku Strait, which were described by Muffler (1967), compose the Burnt Island Conglomerate of the Hyd Group. In fact, the rocks on the Screen Islands resemble the Burnt Island Conglomerate, as well as the basal breccia of the Hyd Formation (Loney, 1964) of the Pybus Bay area on Admiralty Island (fig. 76), so closely in age, lithology, and structural setting that the rocks on the Screen Islands are herein assigned to the Burnt Island Conglomerate of the Hyd Group (Muffler, 1967).

The Hyd Group is a component of the Alexander terrane, which forms a belt of Paleozoic and lower Mesozoic rocks in southeastern Alaska. Hillhouse and Gromme (1980) drilled basalt of the Hound Island Volcanics (an Upper Triassic formation overlying the Burnt Island Conglomerate in Keku Strait, also included in the Hyd Group); their paleomagnetic results indicate that the Alexander terrane apparently has not moved northward with respect to the North American craton since Late Triassic time (Hillhouse and Grommé,1980).

REFERENCES CITED

Berg, H. C., Jones, D. L., and Coney, P. J., 1978, Map showing pre-Cenozoic tectonostratigraphic terranes of southeastern Alaska and adjacent areas: U.S. Geological Survey Open-File Report 78-1085, scale 1:1,000,000, 2 sheets.

Buddington, A. F., and Chapin, Theodore, 1929, Geology and mineral deposits of southeastern Alaska: U.S. Geological Survey Bulletin 800, 398 p.

Folk, R. L., 1968, Petrology of sedimentary rocks: Austin, Tex., Hemphill's, 170 p.

Hillhouse, J. W., and Grommé, C. S., 1980, Paleomagnetism of the Triassic Hound Island Volcanics, Alexander terrane, southeastern Alaska: Journal of Geophysical Research, v. 85, no. B5, p. 2594-2602

Loney, R. A., 1964, Stratigraphy and petrography of the Pybus-Gambier area, Admiralty Island, Alaska: U.S. Geological Survey Bulletin 1178, 103 p.

Muffler, L. J. P., 1967, Stratigraphy of the Keku Islets and neighboring parts of Kuiu and Kupreanof Islands, southeastern Alaska: U.S. Geological Survey Bulletin 1241-C, p. C1-C52.

A preliminary paleomagnetic study of the Gravina-Nutzotin belt, southern and southeastern Alaska

By Bruce C. Panuska[1], John E. Decker[2], and Henry C. Berg

The Gravina-Nutzotin belt consists of an Upper Jurassic through Lower Cretaceous sequence of andesite and flysch in southern and southeastern Alaska. These rocks constitute an overlap assemblage, deposited on both Wrangellia and the Alexander terrane (Berg and others, 1972), and thus provide a minimum age of amalgamation of these two terranes. We selected an interbedded sedimentary and volcanic sequence from the Gravina-Nutzotin belt on Marsh Island for paleomagnetic study (loc. 9, fig. 72). The

[1]Geophysical Institute, University of Alaska, and Alaska Division of Geological and Geophysical Surveys, College, Alaska.

[2]Alaska Division of Geological and Geophysical Surveys, College, Alaska.

purpose of this study was to determine whether reliable paleomagnetic data can be acquired from the Gravina-Nutzotin belt in southeastern Alaska that will aid in the resolution of the much-debated time of accretion of southern Alaska terranes. We chose Marsh Island for three reasons: (1) The age of the rocks is precisely known (Albian); (2) ancient horizontal and stratigraphic younging directions can be determined from bedding; and (3) the rocks are known to be the least recrystallized part of the Gravina-Nutzotin belt in southeastern Alaska.

A total of 33 samples were collected from four beds at two localities (fig. 78). Bed 1 is a 50- to 60-cm-thick medium-grained lithic sandstone, interbedded with graded turbidites and shale. Beds 2 through 4 are poorly sorted coarse-grained tuffaceous pebbly sandstone containing angular clasts of green volcanic rock, interbedded with graded turbidites, shale, and massive volcanic mudflow deposits containing volcanic blocks as much as 5 m wide. Bed 1 was sampled at regular intervals (17 samples) for a distance of about 10 meters between two andesite dikes, which were also sampled, to determine whether the unit had been thermally remagnetized by the dikes. Beds 2 through 4 (loc. 2, fig. 78) were sampled at a locality 0.5 km away from bed 1. The 2.54-cm-diameter cores were cut into 2-cm lengths. All samples were subjected to stepwise thermal demagnetization. Replicates of these samples were subjected to stepwise alternating field (A.F.) cleaning procedures; all magnetization measurements were made on a cryogenic magnetometer. In general, the cleaning procedure ended when the magnetization appeared to reach a stable end point and was below 10 percent of the natural remanent magnetization (NRM) or the initial magnetic-intensity value, or when unstable magnetic behavior became apparent. Each bed represents an instant in geologic time; therefore, the sample directions were averaged by bed to provide a spot reading of the geomagnetic field.

Samples from bed 1 responded well to thermal demagnetization. Stable magnetic directions appeared at unblocking temperatures of 450° to 500°C (table 20). The two samples collected from one dike did not yield a reliable magnetic direction. Two of the three samples from the second dike, however, yielded stable directions that are similar to the magnetic direction of the nearest sandstone sample in bed 1, 2 cm away. We conclude that the second dike thermally remagnetized bed 1 near the contact but that the thermal effect of the dike dissipated within 2 m. Bed 1 thus passes the baked-contact test (McElhinny, 1973). Most of the samples from bed 1 and the two dikes underwent rotational remanent magnetization (RRM) at coercivities of 20 to 80 mT during A.F. treatment or did not reach a stable end point, and so these A.F. data were not used in calculation of the ancient-field direction. One sample, however, did reach a stable end point and yielded a magnetic direction similar to that of its thermally demagnetized counterpart.

Cores from beds 2 through 4 responded well to the A.F. cleaning but behaved erratically during thermal treatment. A few of the A.F.-demagnetized samples were suspected of acquiring RRM at coercivities of 30 to 50 mT. Most of the samples displayed a stable magnetic direction before suspected RRM obscured the NRM; these directions were comparable to RRM-free samples in the same bed. One thermally treated sample cleaned to a stable end point that compared well with its A.F.-demagnetized replicate.

To estimate the average Albian (Early Cretaceous) geomagnetic field, the mean of the four bed means was calculated (table 21). The mean magnetic direction for the Marsh Island site was found not to coincide with the present field. Also, the $\underline{k}$-value (Fisher's precision parameter; see McElhinny, 1973) for the mean of the bed means, corrected for tilting, was greater than the individual bed $\underline{k}$-value. Because the bedding attitudes vary by only 5°, a realistic fold test is not possible.

Having passed the baked-contact test, and in view of the absence of present-field signature, we consider the magnetic directions from Marsh Island to represent a measure of the ancient (Albian) geomagnetic field. However, because only four beds or time horizons are represented, it may be that the secular variation of the geomagnetic field was not averaged out. Therefore, we regard these results as preliminary and likely to be modified somewhat by more complete sampling of stratigraphic section.

Within the limitations of this study, we offer two possible interpretations of the mean magnetic direction. The first interpretation assumes that the magnetic vector obtained from the Marsh Island samples represents original detrital remanent magnetization (DRM). If so, then the equivalent paleolatitude of the vector inclination is 10°. Moreover, because these rocks are Albian, they were almost certainly deposited within the Cretaceous long-normal-polarity interval (Irving and Pullaiah, 1976). As such, the vector polarity is unambiguous and represents 10° north of the paleoequator. Even if this paleolatitude estimate is slightly in error, owing to a poor time averaging of the geomagnetic field, the estimate still suggests that the Gravina-Nutzotin belt and, thus, Wrangellia and the Alexander terrane were far south of their present latitude during Early

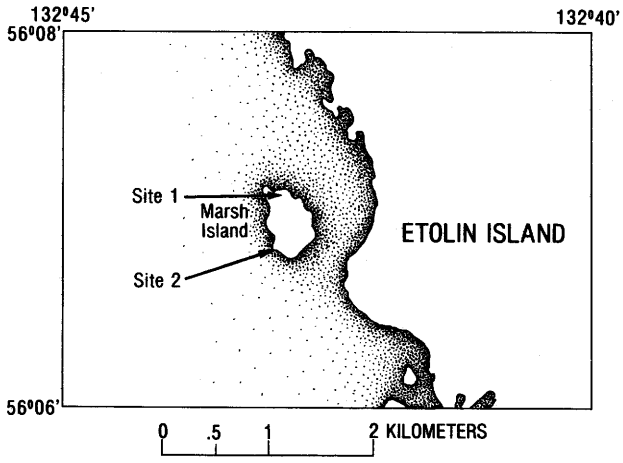

Figure 78.—Part of the Petersburg A-3 quadrangle, showing locations of paleomagnetic-sample sites on Marsh Island.

Cretaceous time. Similarly, the report of low paleolatitudes (approx 20°) from the Nutzotin Mountains sequence of the Gravina-Nutzotin belt (Packer and Stone, 1974; Stone and others, 1982) allows the possibility that these terranes did not accrete to North America until post-Early Cretaceous time. However, this conclusion is contrary to the interpretation of Hillhouse and Grommé(1980) based on a more complete paleomagnetic study of the Hound Island Volcanics. Their data suggest that the Alexander terrane has not moved northward relative to cratonal North America since before Late Triassic time. This conflict could be resolved by accepting the reversed (Southern Hemisphere) polarity of the Hound Island Volcanics as the correct magnetic direction (Stone and others, 1982).

Table 20.--Paleomagnetic data of selected Gravina-Nutzotin belt rocks on Marsh Island

[Stratigraphic declination (D) and inclination (I) of vector corrected for tilt of bedding, in degrees. A.F., peak alternating-field intensity]

Bed	Sample	Stratigraphic D	Stratigraphic I	Demagnetization temperature (°C)	A.F. (mT)	Intensity (10^{-6} emu/cm^3)	Comments
1	4B	35	42	500	--	2.26	---
1	5A	40	28	450	--	4.17	---
1	6A	41	57	500	--	4.33	---
1	7A	29	53	450	--	8.01	---
1	8A	44	32	450	--	4.15	---
1	9A	60	39	450	--	10.1	---
1	10A	63	33	450	--	9.66	---
1	11A	55	24	500	--	5.25	---
1	13A	41	23	400	--	2.92	---
1	14A	43	25	500	--	7.41	---
1	16A	60	35	500	--	3.13	---
1	17A	52	28	500	--	2.47	---
1	19A	24	58	550	--	26.5	Remagnetized by dike.
Dike	21A	14	57	500	--	2.02	---
Dike	22A	19	57	500	--	3.09	---
2	2B	62	11	---	10	5.35	---
2	3B	63	12	---	10	4.78	---
2	4B	32	26	---	20	4.05	---
2	5B	73	29	---	5	7.91	---
3	6B	54	10	---	10	5.73	---
3	7B	56	17	---	10	6.01	---
3	8B	55	21	---	10	7.18	---
3	9B	51	15	---	30	5.09	---
4	11B	67	8	---	10	8.00	---
4	12B	54	9	---	10	6.49	---

Table 21.--Mean paleomagnetic data on four Gravina-Nutotin belt beds on Marsh Island

[Geographic declination (D) and inclination (I) of onsite vector direction with respect to present north and horizontal. Stratigraphic declination (D) and inclination (I) of vector corrected for tilt of bedding. $\underline{K}$, Fisher's precision parameter; α_{95}, radius of 95-percent-confidence circle; $\overline{VGP}$, virtual geomagnetic pole. All directional and VGP values in degrees]

Bed	Number of samples	Geographic D	Geographic I	Stratigraphic D	Stratigraphic I	$\underline{K}$	α_{95}	VGP Long-itude	VGP Lati-tude	$\underline{K}$	α_{95}
1	12	197	67	48	35	33.8	7.0	344	40	39.3	6.4
2	4	140	67	58	20	18.9	16.1	340	26	20.2	15.6
3	4	129	71	54	16	260.4	4.3	344	26	775.9	2.5
4	2	113	63	61	9	79.1	11.1	340	20	84.1	10.8
Mean of 4 beds--		143	70	56	20	44.9	10.5	342	28	86.5	7.5

The second interpretation assumes that the mean magnetic vector obtained from the Marsh Island samples represents thermal remanent magnetization acquired during an unknown postdepositional thermal event. Unpublished paleomagnetic data (C. S. Grommé and J. W. Hillhouse, oral commun., 1982) from northern Prince of Wales Island, Etolin Island, and the Screen Islands, indicate magnetic vectors, uncorrected for tectonic tilt, that point steeply downward to the southeast, similar to the Marsh Island directions. The important points are that: (1) The localities which Grommè and Hillhouse sampled surround the Marsh Island locality (fig. 78), and (2) rocks of different ages and varying bedding attitudes all show the same anomalous magnetic direction. When corrected for tectonic tilt, the Marsh Island, Prince of Wales Island, Etolin Island, and Screen Islands vectors diverge from their common down-to-the-southeast orientation and thus, taken together, fail the fold test. The obvious conclusion is that a regional post-Albian remagnetization affected all the above sample sites. However, the steep down-to-the-southeast direction does not correspond to any known or suspected post-Albian geomagnetic field, assuming that the sample sites have been in their present orientation and at their present latitude since Albian time. Therefore, if post-Albian regional remagnetization in southeastern Alaska is to be assumed, additional postremagnetization regional tilting, rotation, and (or) translation is required to establish the necessary correspondence between known geomagnetic-field directions and the measured sample directions.

In summary, our data indicate that the dikes that cut the Marsh Island section of the Gravina-Nutzotin belt did not remagnetize these beds, and so the beds pass the baked-contact test. Nonetheless, we cannot rule out the possibility of regional remagnetization. Further sampling is required to distinguish between the two interpretations for the origin of the magnetization described above.

REFERENCES CITED

Berg, H. C., Jones, D. L., and Richter, D. H., 1972, Gravina-Nutzotin belt--tectonic significance of an upper Mesozoic sedimentary and volcanic sequence in southern and southeastern Alaska, in Geological Survey research 1972: U.S. Geological Survey Professional Paper 800-D, p. D1-D24.

Hillhouse, J. W., and Grommé, C. S., 1980, Paleomagnetism of the Triassic Hound Island Volcanics, Alexander terrane, southeastern Alaska: Journal of Geophysical Research, v. 85, no. B5, p. 2594-2602.

Irving, Edward, and Pullaiah, Guntur, 1976, Reversals of the geomagnetic field, magnetostratigraphy, and relative magnitude of paleosecular variation in the Phanerozoic: Earth-Science Reviews, v. 12, no. 1, p. 35-64.

McElhinny, M. W., 1973, Paleomagnetism and plate tectonics: London, Cambridge University Press, 358 p.

Packer, D. R., and Stone, D. B., 1974, Paleomagnetism of Jurassic rocks from southern Alaska and their tectonic implications: Canadian Journal of Earth Science, v. 11, no. 7, p. 976-997.

Stone, D. B., Panuska, B. C., and Packer, D. R., 1982, Paleolatitude versus time for southern Alaska: Journal of Geophysical Research, v. 87, no. 5, p. 3697-3707.

The northern Coast plutonic-metamorphic complex, southeastern Alaska and northwestern British Columbia

By David A. Brew and Arthur B. Ford

INTRODUCTION

The northern Coast plutonic-metamorphic complex is but one segment of an 8,000-km-long batholithic complex that extends the length of the North American Cordillera from Baja California to the Aleutian Islands. As described here, the northern Coast plutonic-metamorphic complex (area 1, fig. 72) lies between lat 55° and 60° N. The adjacent segment to the north has been described only in reports concerned with regional geology (Kindle, 1953; Muller, 1954, 1967; Christie, 1957; Wheeler, 1961, 1963; Campbell and Dodds, 1975, 1978, 1979); the adjacent segment to the south was described by Hutchison (1970) and Roddick and Hutchison (1974) as well as depicted on various regional geologic maps.

Different segments of the Cordilleran batholithic complex have significantly different features. This report documents the main characteristics and inferred evolutionary history of the northern Coast plutonic-metamorphic complex that should facilitate comparisons between segments.

The Coast plutonic-metamorphic complex is defined here more or less according to the usage of Douglas and others (1970) and Brew (1981) but not that of Brew and Ford (1978). Thus, the northern Coast plutonic-metamorphic complex includes not only the dominantly granitic and gneissic rocks of the Coast Mountains, but also the metamorphic rocks adjacent to both sides. This definition poses no problems so far as the northeast limit of the complex is concerned because there the outer contact of the low-pressure facies-series metamorphic rocks adjoining the northeasternmost plutons is relatively clear.

The southwest limit of the northern Coast plutonic-metamorphic complex, however, is difficult to place because the medium-pressure facies-series metamorphic rocks that contact the granitic and gneissic rocks of the northern Coast plutonic-metamorphic complex decrease in grade to the southwest and appear to form a single wide metamorphic and deformation belt. As noted below, there may, instead, be two belts of different ages side by side. Figure 79 shows this wide area of medium-pressure low- to medium-temperature metamorphism as the informally named western metamorphic zone; it has as its southwest limit the southwesternmost contacts of flysch units within the Upper Jurassic(?) to middle Cretaceous Gravina belt (Berg and others, 1978). The reason for selecting this boundary is twofold: (1) The generally low grade metamorphism in these units appears to grade northeastward into the higher grade metamorphism in the granitic and gneissic rocks of the northern Coast plutonic-metamorphic complex; and (2) the deformational

history here is complicated, similar to that in the higher grade rocks, and apparently differs from that to the southwest In some places, however, the actual west limit of metamorphism and deformation is known to lie to the east of the boundary selected here.

The first part of this report describes the northern Coast plutonic-metamorphic complex as it now exists; the second part is a brief speculation on the driving forces behind its evolution and their relation to the accretion of the Chugach terrane (Plafker and others, 1977). Throughout this report, the reader should bear in mind that most of the events inferred from the geologic record occurred elsewhere than at the present position of the northern Coast plutonic-metamorphic complex. Some of the earlier events may have transpired thousands of kilometers away, but no consistent paleomagnetic evidence exists to establish control on movements.

DESCRIPTION

Throughout the northern region, the Coast plutonic-metamorphic complex can be divided into four more or less parallel zones (fig. 79), described here from southwest to northeast as the western metamorphic zone, the central metamorphic zone, the central granitic zone, and the eastern metamorphic zone. These four zones have been subdivided locally according to the proportions of intrusive and metamorphic rocks and of different metamorphic-rock types. The ages of metamorphism and intrusion differ in part between these zones.

The western metamorphic zone consists mostly of progressively metamorphosed (higher grade to the northeast) low- to intermediate-temperature low- to high-pressure facies-series metamorphic rocks, scattered mesozonal to epizonal granitic bodies, and rare concentrically zoned mafic-ultramafic masses. Rare fossils indicate that the protolith ranges in age from at least Permian to middle Cretaceous. Various compositions are present: The Lower Permian rocks are dominantly greenstone/greenschist, limestone/marble, and slate/phyllite/semischist; the Upper Triassic rocks are greenstone/greenschist, slate/phyllite, and minor limestone/marble; and the Jurassic(?) to middle Cretaceous rocks are metaconglomerate/slate/phyllite/semischist derived from a flysch wedge, and greenstone/greenschist derived from volcanic flows and breccia.

Various plutons are scattered throughout the zone. The crosscutting concentrically zoned mafic-ultramafic bodies that intrude these rocks, which were described by Taylor (1967), belong to the Klukwan-Duke Island belt of Brew and Morrell (1980a); they are probably 100 to 110 m.y. old (Lanphere and Eberlein, 1966). Generally concordant granitic bodies consist dominantly of diorite, quartz diorite, monzodiorite, and granodiorite, probably 80 to 90 m.y. old; they belong to the Admiralty-Revillagigedo belt (Brew and Morrell, 1980; Burrell, 1983) and have hornfels aureoles associated with them. Crosscutting granitic bodies, consisting mostly of biotite granite, granodiorite, and quartz monzodiorite but including significant amounts of syenite, monzonite, and monzodiorite, belong to the Kuiu-Etolin intrusive belt (Brew and others, 1979; Brew and Morrell, 1980a; Brew and others, 1981; Hunt, 1983); they are probably 20 to 25 m.y. old and are epizonal.

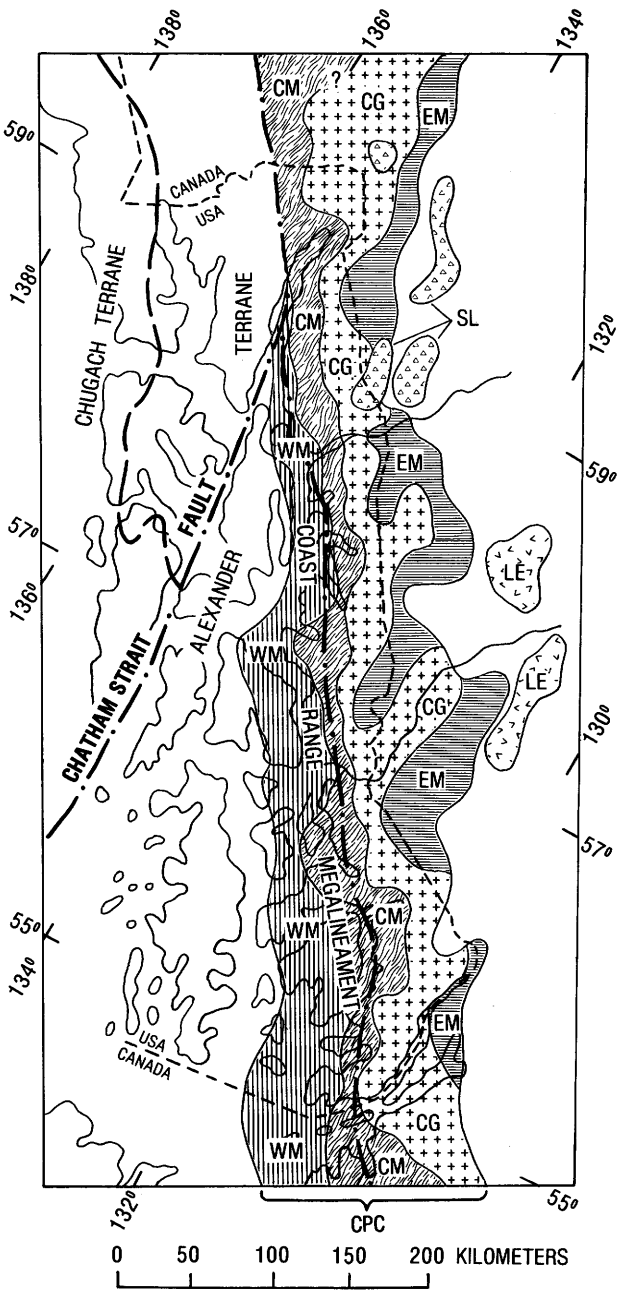

Figure 79.—Northern Coast plutonic-metamorphic complex (CPC), southeastern Alaska and northwestern British Columbia, showing zones and units as follows: WM, western metamorphic zone; CM, central metamorphic zone; CG, central granitic zone; EM, eastern metamorphic zone; SL, Sloko Volcanics; LE, Level Mountain and Mount Edziza volcanic fields. Boundaries are approximately located.

The central metamorphic zone consists of abundant synkinematic to postkinematic mesozonal to

epizonal granitic bodies, mixed with intermediate-temperature intermediate- to high-pressure facies-series rocks. The ages of the protoliths are not known, but a 140-m.y. age (Smith and others, 1979) has been determined for some orthogneiss masses. Most of the metamorphic rocks consist of migmatite, biotite schist, gneissose schist, biotite gneiss, marble, and large orthogneiss units. The protoliths of the migmatite, schist, and paragneiss cannot be unequivocally determined, but they probably were dominantly clastic sedimentary rocks and limestone containing only minor amounts of volcanic material; their age is not known. The most important intrusive unit is the conspicuous tonalite sill that runs almost the whole length of southeastern Alaska (Brew and others, 1976; Brew and Ford, 1981). This sill and some nearby less continuous dominantly granodiorite sills make up the Coast plutonic-metamorphic complex sill belt (Brew and Morrell, 1980a). Some evidence suggests that these sills are probably 55 to 60 m.y. old (J. G. Smith, oral commun., 1979; Smith and others, 1979).

The central granitic zone consists of generally crosscutting mostly unfoliated granodiorite and quartz monzodiorite plutons, with subordinate screens and pendants of metamorphic rocks like those in the central metamorphic zone to the southwest. Most of these plutons, which are about 50 m.y. old wherever they have been dated (Brew and others, 1977; Wilson and others, 1979; Forbes and Engels, 1970), are mesozonal to epizonal. They define the Coast plutonic-metamorphic complex belt I (Brew and Morrell, 1980a). Mapping in progress near the Stikine River suggests that these bodies may in part be closely related to some of the granodiorite sills within the Coast plutonic-metamorphic complex sill belt in the central metamorphic zone (S. M. Karl, unpub. data, 1981). The Sloko Volcanics (fig. 79) of British Columbia, which is approximately coeval, is interpreted to be the extrusive equivalent (Souther, 1971).

Several 20- to 30-m.y.-old granite and granodiorite plutons occur in the Behm Canal belt (Brew and Morrell, 1980a), which overlaps both the central granitic and the central metamorphic zones. These epizonal bodies, which are notable for their sparseness and their association with molybdenite deposits (Hudson and others, 1979), somewhat resemble those noted above in the Kuiu-Etolin belt within the western metamorphic zone.

The eastern metamorphic zone consists of low- to high-temperature generally low pressure facies-series metamorphic rocks and scattered to abundant epizonal granitic bodies. This zone is separated from the central granitic zone because (1) it is dominantly metamorphic and (2) the metamorphism differs; the boundary between the two zones is both arbitrary and gradational. The granitic rocks in the eastern zone resemble those in the central granitic zone, whereas the metamorphic rocks are dominantly hornfels derived from protoliths of intermediate to mafic volcanic, semipelitic, and carbonate composition. The age of the protoliths are not known everywhere, although Carboniferous, Permian, and Triassic rocks are present at some localities.

Not far northeast of the Coast plutonic-metamorphic complex (fig. 79) are the extensive late Miocene to Pleistocene volcanic fields of Level Mountain and Mount Edziza (Souther and others, 1979). They apparently have no counterparts within the Coast plutonic-metamorphic complex except, possibly, for some dikes, although they are probably related to the general evolution of the complex.

A few Holocene basalt flows occur within the boundaries of the Coast plutonic-metamorphic complex but show no clear relation to the complex. They are as young as 360 years B.P. (Elliott and others, 1981), and more flows can probably be expected to be erupted in the future.

The three most significant structural features in the northern Coast plutonic-metamorphic complex are (1) the Chatham Strait fault (fig. 79), (2) the Coast Range megalineament (CRML), and (3) a narrow linear area straddling the boundary between the western and central metamorphic zones in which the deformation and metamorphism were apparently most intense. The Chatham Strait fault to the north (Ovenshine and Brew, 1972; Sonnevil, 1981) truncates the southwest margin of the Coast plutonic-metamorphic complex. The CRML is a profound structural element (Brew and Ford, 1978) that probably has a long and complex history. Because of map scale, the CRML is locally shown on figure 79 as the boundary between the western and central metamorphic zone; in those places, the CRML actually lies within the western metamorphic zone but close to the boundary with the central zone. Although the narrow linear area of intense deformation and metamorphism is probably related to the CRML, this area may simply mark the locus of greater uplift of the Coast plutonic-metamorphic complex. Other structural boundaries stated to be present in the Coast plutonic-metamorphic complex, such as tectonostratigraphic-terrane contacts (Berg and others, 1978), either coincide with the CRML, are not verifiable in the field, or are related to sedimentary, intrusive, or metamorphic processes that are only indirectly linked to the accretion of the exotic Chugach terrane to the west (fig. 79).

INTERPRETATION

The Coast plutonic-metamorphic complex is interpreted to have resulted primarily from the effects of a major Cretaceous and early Tertiary accretional event that occurred about 100 km to the southwest, at which time the Chugach terrane became attached to the Alexander and Wrangellia terranes (Plafker and others, 1977). The effects of that distant event were superposed on both upper Paleozoic and lower Mesozoic Alexander-terrane rocks and on an upper Mesozoic overlap assemblage (the Gravina belt) that probably accumulated in a rifted backarc environment. These effects are interpreted to include two ages of penetrative deformation, two ages of progressive metamorphism, four main intrusive events, and sporadic volcanism. The main part of the Alexander terrane, which intervenes between the Coast plutonic-metamorphic complex and the accreted Chugach terrane to the southwest, apparently was less

affected than were its margins, although it was the site of Early Cretaceous and middle Tertiary intrusions and of Tertiary volcanism. There is no convincing evidence for imbricate collision/subduction zones (Godwin, 1975).

MINERAL DEPOSITS

Mineral deposits are more common along the northeast side of the Coast plutonic-metamorphic complex than elsewhere, possibly because of the higher structural levels preserved there. They include polymetallic hydrothermal and porphyry copper deposits. In the western metamorphic belt, along the southwest side are several types of deposits: (1) Pre-Coast plutonic-metamorphic complex volcanogenic base-metal deposits, (2) similar base-metal deposits remobilized during deformation and metamorphism, (3) magmatic deposits associated with mafic-ultramafic intrusions, and (4) postdeformational gold-silver veins.

The relative abundance of mineral deposits here adjacent to the most deformed and metamorphosed part of the Coast plutonic-metamorphic complex, in comparison with other areas to the southwest and northeast (Berg and others, 1981), suggests that (1) the differential uplift which brought the linear most deformed and metamorphosed part to the surface also stripped off any deposits that were present at higher levels, or (2) significant metallization occurred adjacent to that part during the complex history of deformation, metamorphism, and intrusion. Porphyry molybdenum deposits are associated with the 20- to 30-m.y.-old intrusions, which may occur anywhere in the Coast plutonic-metamorphic complex.

REFERENCES CITED

Berg, H. C., Decker, J. E., and Abramson, B. S., 1981, Metallic mineral deposits of southeastern Alaska: U.S. Geological Survey Open-File Report 81-122, 136 p.

Berg, H. C., Jones, D. L., and Coney, P. J., 1978, Map showing pre-Cenozoic tectonostratigraphic terranes of southeastern Alaska and adjacent areas: U.S. Geological Survey Open-File Report 78-1085, scale 1:1,000,000, 2 sheets.

Brew, D. A., 1981, The Coast plutonic complex in southeastern Alaska and northwestern British Columbia [abs.]: Geological Association of Canada, Annual Meeting, Vancouver, British Columbia, Canada, 1981, Programme and Abstracts, p. 9-10.

Brew, D. A., Berg, H. C., Morrell, R. P., Sonnevil, R. A., Hunt, S. J., and Huie, Carl, 1979, The Tertiary Kuiu-Etolin volcanic-plutonic belt, southeastern Alaska, in Johnson, K. M., and Williams, J. R., eds., The United States Geological Survey in Alaska: Accomplishments during 1978: U.S. Geological Survey Circular 804-B, p. B129-B130.

Brew, D. A., and Ford, A. B., 1978, Megalineament in southeastern Alaska marks southwest edge of Coast Range batholithic complex: Canadian Journal of Earth Sciences, v. 15, no. 11, p. 1763-1772.

——1981, The Coast plutonic complex sill, southeastern Alaska, in Albert, N. R. D., and Hudson, Travis, eds., The United States Geological Survey in Alaska: Accomplishments during 1979: U.S. Geological Survey Circular 823-B, p. B96-B99.

Brew, D. A., Ford, A. B., Grybeck, Donald, Johnson, B. R., and Nutt, C. J., 1976, Key foliated quartz diorite sill along southwest side of Coast Range complex, northern southeastern Alaska, in Cobb, E. H., ed., The United States Geological Survey in Alaska: Accomplishments during 1975: U.S. Geological Survey Circular 733, p. 60.

Brew, D. A., Grybeck, Donald, Johnson, B. R., Jachens, R. C., Nutt, C. J., Barnes, D. F., Kimball, A. L., Still, J. C., and Rataj, J. L., 1977, Mineral resources of the Tracy Arm-Fords Terror Wilderness study area and vicinity, Alaska: U.S. Geological Survey Open-File Report 77-649, 282 p.

Brew, D. A., and Morrell, R. P., 1980a, Intrusive rocks and plutonic belts of southeastern Alaska, U.S.A.: U.S. Geological Survey Open-File Report 80-78, 34 p.

———1980b, Preliminary map of intrusive rocks in southeastern Alaska: U.S. Geological Survey Miscellaneous Field Investigations Map MF-1048, scale 1:1,000,000.

Brew, D. A., Sonnevil, R. A., Hunt, S. J., and Ford, A. B., 1981, Newly recognized alkali granite stock, southwestern Kupreanof Island, Alaska, in Albert, N. R. D., and Hudson, Travis, eds., The United States Geological Survey in Alaska: Accomplishments during 1979: U.S. Geological Survey Circular 823-B, p. B108-B109.

Burrell, P. D., 1983, Cretaceous plutonic rocks, Mitkof and Kupreanof Islands, Petersburg quadrangle, southeastern Alaska, in Coonrad, W. L., and Elliott, R. L., eds., The United States Geological Survey in Alaska: Accomplishments during 1981: U.S. Geological Survey Circular 868, p. 124-126.

Campbell, R. B., and Dodds, C. J., 1975, Operation Saint Elias, Yukon Territory in Report of activities: Geological Survey of Canada Paper 75-1A, p. 51-53.

——1978, Operation Saint Elias, Yukon Territory, in Current research: Geological Survey of Canada Paper 78-1A, p. 35-41.

——1979, Operation Saint Elias, British Columbia, in Current research: Geological Survey of Canada Paper 79-1A, p. 17-20.

Christie, R. L., 1957, Bennett, British Columbia: Geological Survey of Canada Map 19-1957, scale 1:250,000.

Douglas, R. J. W., Gabrielse, Hubert, Wheeler, J. O., Stott, D. F., and Belyea, H. R., 1970, Geology of western Canada, in Douglas, R. J. W., ed., Geology and economic minerals of Canada: Geological Survey of Canada Economic Geology Report 1, p. 365-488.

Elliott, R. L., Koch, R. D., and Robinson, S. W., 1981, Age of basalt flows in the Blue River valley, Bradfield Canal quadrangle, in Albert, N. R. D., and Hudson, Travis, eds., The United States Geological Survey in Alaska: Accomplishments during 1979: U.S. Geological Survey Circular 823-B, p. B115-B116.

Forbes, R. B., and Engels, J. C., 1970, K^{40}/Ar^{40} age relations of the Coast Range batholith and related rocks of the Juneau Icefield area, Alaska: Geological Society of America Bulletin, v. 81, no. 2, p. 579-584.

Godwin, C. I., 1975, Imbricate subduction zones and their relationship with Upper Cretaceous to Tertiary porphyry deposits in the Canadian Cordillera: Canadian Journal of Earth Sciences, v. 12, no. 8, p. 1362-1378.

Hudson, T. L., Smith, J. G., and Elliott, R. L., 1979, Petrology, composition, and age of intrusive rocks associated with the Quartz Hill molybdenite deposit, southeastern Alaska: Canadian Journal of Earth Sciences, v. 16, no. 9, p. 1805-1822.

Hunt, S. J., 1983, Preliminary study of a zoned leucocratic granite body on central Etolin Island, southeastern Alaska, in Coonrad, W. L., and Elliott, R. L., eds., The United States Geological Survey in Alaska: Accomplishments during 1981: U.S. Geological Survey Circular 868, p. 128-131.

Hutchison, W. W., 1970, Metamorphic framework and plutonic styles in the Prince Rupert region of the Central Coast Mountains, British Columbia: Canadian Journal of Earth Sciences, v. 7, no. 2, p. 376-405.

Kindle, E. D., 1953, Dezadeash map-area, Yukon Territory: Geological Survey of Canada Memoir 268, 68 p, scale 1:253,400.

Lanphere, M. A., and Eberlein, G. D., 1966, Potassium-argon ages of magnetite-bearing ultramafic complexes in southeastern Alaska [abs.], in Abstracts for 1965: Geological Society of America Special Paper 87, p. 94.

Muller, J. E., 1953, Preliminary map, Kluane Lake (west half), Yukon Territory (descriptive notes): Geological Survey of Canada Paper 53-20, 9 p., scale 1:253,400, 2 sheets.

———1967, Kluane Lake map-area, Yukon Territory: Geological Survey of Canada Memoir 340, 137 p., scale 253,400, 2 sheets.

Ovenshine, A. T., and Brew, D. A., 1972, Separation and history of the Chatham Strait fault, southeast Alaska, North America: International Geological Congress, 24th, Montreal, Quebec, Canada, 1972, Proceedings, sec. 3, p. 245-254.

Plafker, George, Jones, D. L., and Pessagno, E. A., Jr., 1977, A Cretaceous accretionary flysch and melange terrane along the Gulf of Alaska margin, in Blean, K. M., ed., The United States Geological Survey in Alaska: Accomplishments during 1976: U.S. Geological Survey Circular 751-B, p. B41-B43.

Roddick, J. A., and Hutchison, W. W., 1974, Setting of the Coast Plutonic Complex, British Columbia: Pacific Geology, v. 8, p. 91-108.

Smith, J. G., Stern, T. W., and Arth, J. G., 1979, Isotopic ages indicate multiple episodes of plutonism and metamorphism in the Coast Mountains near Ketchikan, Alaska [abs.]: Geological Society of America Abstracts with Programs, v. 11, no. 7, p. 519.

Sonnevil, R. A., 1981, The Chilkat-Prince of Wales plutonic province, southeastern Alaska, in Albert, N. R. D., and Hudson, Travis, eds., The United States Geological Survey in Alaska: Accomplishments during 1979: U.S. Geological Survey Circular 823-B, p. B112-B115.

Souther, J. G., 1971, Geology and ore deposits of Tulsequah map-area, British Columbia: Geological Survey of Canada Memoir 362, 84 p.

Souther, J. G., Brew, D. A., and Okulitch, A. V., 1979, Geology of Iskut River, British Columbia-Alaska, Geological Atlas, NTS 104, 114: Geological Survey of Canada Map 1418A, scale 1:1,000,000.

Taylor, H. P., 1967, The zoned ultramafic complexes of southeastern Alaska, in Wyllie, P. J., ed., Ultramafic and related rocks: New York, John Wiley, p. 97-121.

Wheeler, J. O., 1961, Whitehorse map-area, Yukon Territory: Geological Survey of Canada Memoir 312, 156 p., scale 1:253,400, 2 sheets.

———1963, Kaskawulsh map-area, Yukon Territory: Geological Survey of Canada Map 1134-A, scale 1:253,400.

Wilson, F. H., Dadisman, S. V., and Herzon, P. L., 1979, Map showing radiometric ages of rocks in southeastern Alaska: U.S. Geological Survey Open-File Report 79-594, 33 p, scale 1:1,000,000.

Cretaceous plutonic rocks, Mitkof and Kupreanof Islands, Petersburg quadrangle, southeastern Alaska

By Peter D. Burrell

Reconnaissance geologic mapping and preliminary petrologic studies of a group of similar granitic bodies in a northwest-trending belt in the eastern part of the Petersburg quadrangle (area 2, fig. 72) suggest that these bodies can be divided into subgroups which are mineralogically similar but texturally distinct. These rocks are all part of the Admiralty-Revillagigedo plutonic belt, which extends from Ketchikan to Juneau, outboard of the Coast plutonic complex; they intrude metamorphic rocks of the Gravina-Nutzotin belt (Brew and Morrell, 1980).

These granitic bodies occur as stocks of varying areal extent. They are relatively resistant and form mountains that rise steeply above the surrounding country rock. These mountains are heavily vegetated, and exposures are poor except on near-vertical mountain slopes, above tree line, and along the intertidal zone. The country rocks intruded include biotite (±garnet) schist, semischist, and phyllite. The intrusions are generally discordant except on central Mitkof Island, where they appear to be concordant. Narrow contact aureoles, locally containing andalusite, were created by these intrusions.

The stocks of body 1 (fig. 80) on the central Lindenberg Peninsula and at Horn Mountain are crowded plagioclase-porphyritic quartz monzodiorite to quartz diorite (see fig. 81 for modal compositions of all bodies). The close spacing (crowding) of the plagioclase phenocrysts (max 12 mm diam) gives the mafic minerals an interstitial appearance. The dominant mafic mineral is hornblende; biotite and epidote/clinozoisite are present in lesser amounts. Both primary and secondary epidote are present in these rocks. The quartz and potassium feldspar are

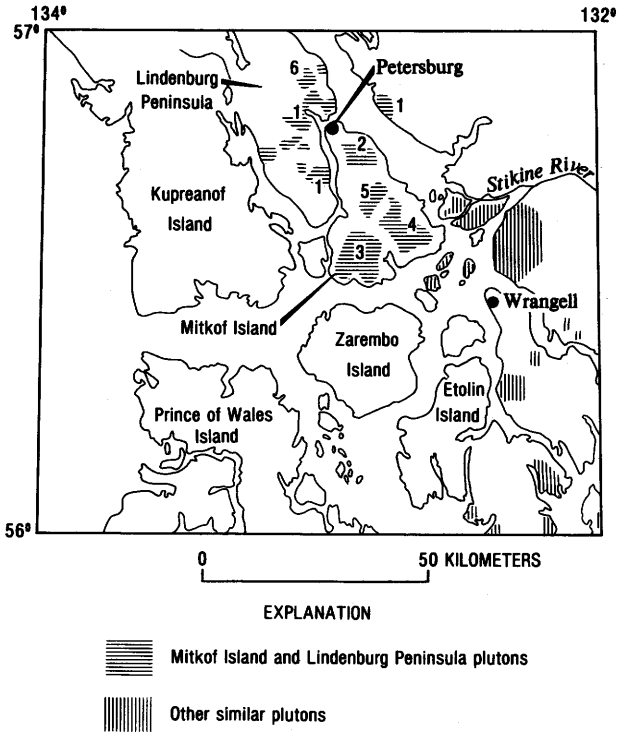

Figure 80.—Petersburg quadrangle, showing approximate locations of Cretaceous and Cretaceous(?) granitic plutons. Numbers refer to granitic bodies described in text and figure 81.

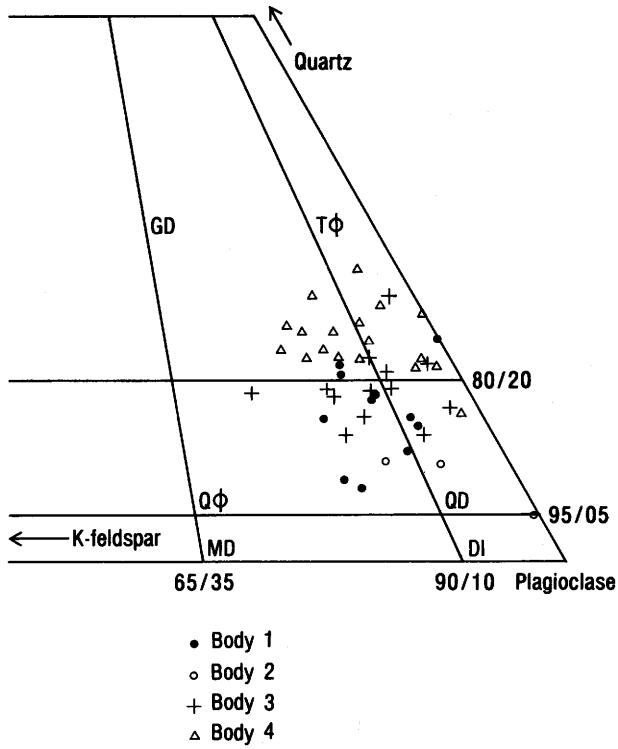

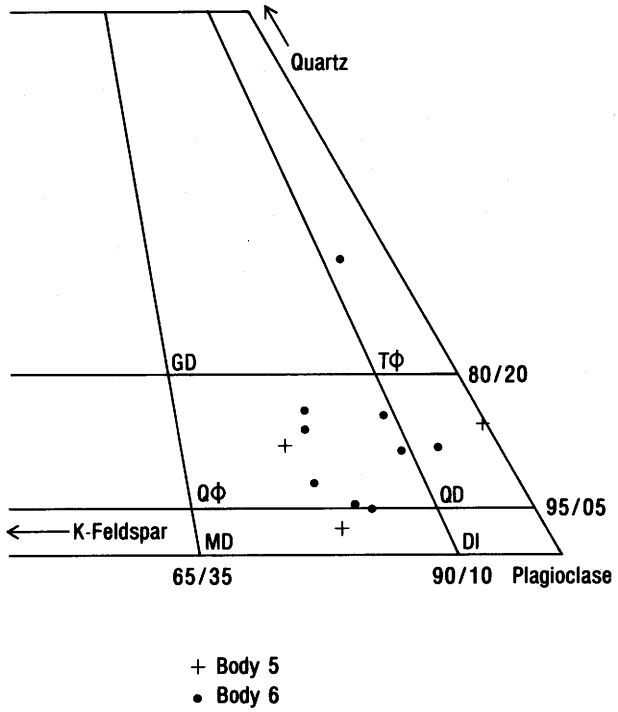

Figure 81.—Modal compositions of granitic rocks of Cretaceous and Cretaceous(?) age from the Lindenberg Peninsula and Mitkof Island (see fig. 80 for locations). DI, diorite; GD, granodiorite; MD, monzodiorite; QD, quartz diorite; QØ, quartz monzodiorite; TØ, tonalite.

anhedral and crystallized interstitially. Sphene and apatite are common accessory minerals. The color index for these rocks ranges from 17 to 27. The margins of stocks composing body 2 are characterized by fine-grained mafic minerals and (garnet)-muscovite-epidote-biotite aplite dikes of granitic composition.

Body 2, on northern Mitkof Island and the east coast of the Lindenberg Peninsula, is mineralogically similar to body 1, although it is generally more mafic. The color index ranges from 32 to 52. Mafic minerals generally are more clustered together, and the plagioclase phenocrysts are smaller than those in body 1. The rocks are crowded plagioclase-porphyritic quartz monzodiorite and quartz diorite.

Body 3, on southern Mitkof Island, also has the crowded-plagioclase texture, although it is not everywhere porphyritic. Parts of this body are inequigranular and contain seriate plagioclase. The mineralogy differs in that biotite and quartz are more abundant than in body 1. Hornblende is the dominant mafic mineral, although biotite is more prevalent toward the center of several stocks. Compositions of these rocks range from quartz monzodiorite to tonalite, and their color indices from 30 to 49. Aplite dikes, similar to those of body 1, are present in the contact zones of the southern part of this body.

Body 4, on Mitkof Island, differs texturally from the crowded-plagioclase unit. Most of these rocks are

foliated and inequigranular and contain seriate plagioclase, although local variation to porphyritic as well as equigranular texture occurs. The mineralogy of this body is the same as that of the crowded-plagioclase bodies. Biotite and hornblende are the dominant mafic minerals, although their proportions vary. Primary epidote, sphene, and apatite are also present. The composition of body 4 ranges from granodiorite to tonalite, and the color index from 24 to 35. Rocks from the east margin contain anhedral red-orange garnets associated with the mafic minerals.

Body 5, on central Mitkof Island, is anomalous in comparison with the surrounding stocks. Hornblende is generally the dominant mafic mineral, although biotite is locally present in equal amounts. Hornblende occurs as anhedral crystals, commonly clustered together. In about half the rocks studied, the hornblende has relict pyroxene cores, and much of it is poikilitic, with enclosed quartz, feldspar, and opaque minerals. Primary epidote is a minor phase in some rocks. Plagioclase, as small twinned and zoned laths grown together, forms the bulk of the groundmass. These rocks are inequigranular foliated monzodiorite to quartz diorite; the color index ranges from 34 to 55. An arc of inequigranular crowded-plagioclase quartz monzodiorite and quartz diorite crops out along the north edge of this body.

Body 6, on the northern Lindenberg Peninsula, is much like body 5. The rocks are mostly foliated inequigranular quartz monzodiorite, and the color index ranges from 32 to 51. Hornblende, the dominant mafic mineral, ranges from small discrete subhedral crystals to larger anhedral crystals, with inclusions of quartz and feldspar and commonly relict pyroxene cores. Primary epidote is present in very small amounts. Plagioclase is twinned and zoned, and commonly exhibits a seriate texture. Sphene and apatite are common accessory minerals.

Mapping is incomplete southeast of Mitkof Island, and the plutons there have been compared with the Mitkof Island and Lindenberg Peninsula plutons by reconnaissance mapping only. Rocks observed in the southeastern part of the area include epidote(±garnet)-hornblende-biotite granodiorite, tonalite, and quartz diorite with inequigranular to porphyritic textures.

A recent potassium-argon age determination on hornblende from body 4 yielded an age of 89.1 m.y. (Marvin Lanphere, written commun., 1982). Bodies 1 through 4 are correlated with similar porphyritic and inequigranular rocks in the Bradfield Canal 1:250,000-scale quadrangle, which were also dated at approximately 90 m.y. by potassium-argon methods (R. D. Koch, oral commun., 1982).

The Mitkof Island and Lindenberg Peninsula plutons may represent a complex intrusive sequence. Bodies 1 through 4, though exhibiting limited textural differences that range from crowded porphyry to inequigranular, have similar mineralogies and are likely to be coeval; they are herein considered to constitute a distinct group. Bodies 5 and 6 compose a second distinct group; poikilitic hornblende with pyroxene cores, an inequigranular texture, and a plagioclase-dominant groundmass distinguish them from bodies 1 through 4. Despite these observed differences, however, the presence of primary epidote and the generally similar compositions and structural settings indicate that these two groups of plutonic bodies may be genetically related.

REFERENCE CITED

Brew, D. A., and Morrell, R. P., 1980, Intrusive rocks and plutonic belts of southeastern Alaska, U.S.A.: U.S. Geological Survey Open-File Report 80-78, 34 p.

Late Oligocene gabbro near Ketchikan, southeastern Alaska

By Richard D. Koch and Raymond L. Elliott

A large elongate gabbro complex, here referred to informally as the gabbro of Ketchikan Lakes, is exposed over an irregular area, 7 by 16 km, in the vicinity of Ketchikan Lakes just north and east of the town of Ketchikan (area 8, fig. 72; fig. 82). Originally believed to be mainly granodiorite and quartz diorite with a small area of leucogabbro (Berg and others, 1978), this heterogeneous pluton consists entirely of various gabbroic rocks.

Composition varies considerably across this complex, with a crude zonation, with a small slightly offcenter core area of olivine-bearing two-pyroxene gabbro, wholly enclosed by an area of biotite-hornblende-two-pyroxene gabbro. A third, discontinuous zone of quartz-bearing gabbro underlies two large areas at the northwest and southeast ends of the complex. A few samples from this outermost zone also contain minor amounts of potassium feldspar. Compositions vary within, as well as among, these zones. Contacts between the zones were not observed in the field and are presumed to be gradational.

Quartz-free gabbroic rocks from the olivine-bearing core zone and from much of the surrounding area contain biotite, hypersthene, hornblende, and augite. The color index for these rocks ranges from about 15 to 50 and is generally 30 or less; thus, the rocks are largely leucogabbro. Relative abundances of the mafic minerals vary considerably from place to place; clinopyroxene exceeds orthopyroxene in all but one sample (norite).

The color index for the quartz-bearing gabbro ranges from about 12+ to 35 and is mostly less than 30 (leucogabbro). Many of these quartz-bearing rocks contain clinopyroxene, hornblende, biotite, and little or no orthopyroxene; a few contain only hornblende and biotite as mafic minerals.

Most of the gabbro is massive, fine to medium grained, seriate to relatively equigranular, with a hypidiomorphic-granular texture. Foliation, formed by alinement of plagioclase and mafic minerals, is poorly developed in a few places, and diabasic and rarer allotriomorphic-granular textures also occur.

Quartz, where it occurs, forms small interstitial grains that constitute less than 5 percent of the rock. Potassium feldspar occurs in only a few places, as small untwinned anhedral interstitial grains.

Plagioclase forms anhedral to euhedral crystals, but the texture of almost all the gabbro is dominated by subhedral plagioclase as equant to, more commonly, elongate laths with a length-to-width ratio of 4:1 to

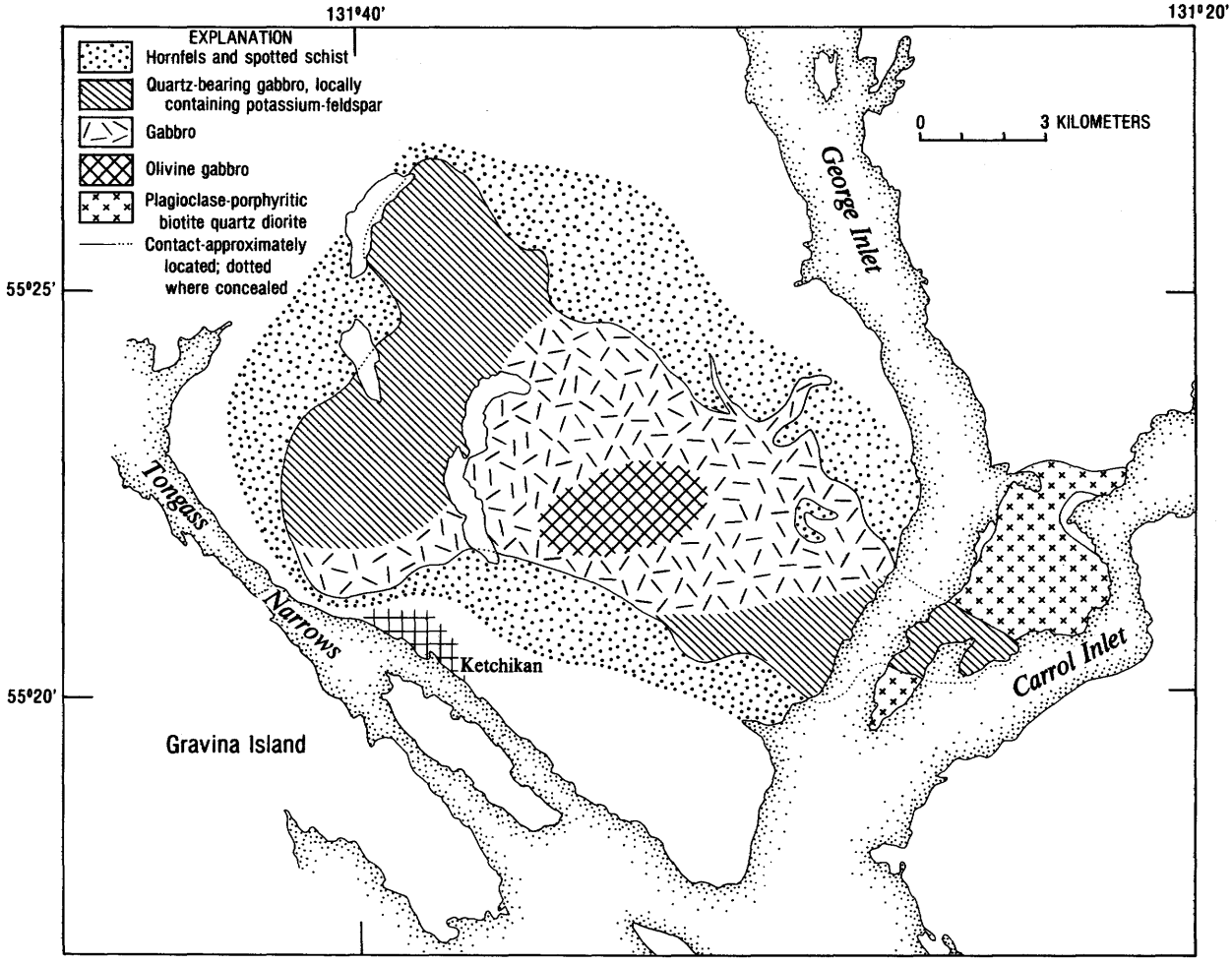

Figure 82.—Geologic sketch map of gabbro complex near Ketchikan, Alaska.

2:1, rarely as small as 6:1. Fine albite twinning is common in most plagioclase crystals; Carlsbad twinning is also common, and pericline twinning occurs in minor amounts in most of the samples examined. The plagioclase crystals are unzoned to very strongly zoned; zoning is gradational progressive (normal), progressive concentric stepped, and locally oscillatory with as many as 6 or more cycles. Composition of most grains lies toward the calcic end of the range An_{27} to An_{80}, which is the optically measurable range of the most strongly zoned crystals. A few grains in samples from throughout the complex have a clear untwinned core area with high relief, yellow interference colors, and irregular fractures. These cores are probably early-formed and partially resorbed plagioclase of extremely calcic composition, probably close to pure anorthite. The plagioclase commonly has myrmekitic borders where it contacts potassium feldspar.

Mafic minerals make up from about 12 to at least 50 percent of the rock, and the relative proportions of different mafic minerals vary markedly from place to place. With local exceptions, however, a crudely sequential change in these relative proportions appears to occur from the olivine-bearing core area to the quartz-bearing outer areas. In the core area, the mafic assemblage includes olivine, orthopyroxene, clinopyroxene, hornblende, and biotite. Away from the core area there is generally a diminishment and, finally, loss of the mafic minerals olivine, orthopyroxene, and clinopyroxene, commonly in that order.

The pyroxenes are anhedral to subhedral and commonly form cores in brown hornblende or are rimmed by brown hornblende, with sharp or gradational boundaries between the two minerals. The brown hornblende is anhedral to subhedral and generally within the medium-grained size range; it locally forms large poikilitic crystals with many pyroxene inclusions. Biotite is strongly colored dark reddish brown.

Opaque minerals occur as discrete disseminated anhedra in trace amounts to 7 percent of the rock in a few places. Where the opaque minerals are abundant, they also form densely packed inclusions in pyroxene. Apatite occurs in most samples as trace amounts of

tiny euhedra. Sphene anhedra and zircon are also present in trace amounts in some of the quartz-bearing samples.

Alteration of primary minerals is slight throughout most of the complex but is locally significant. Most feldspar is clear, with only scattered trace amounts and local small patches of sericite. In only a very few localities, the rock contains strongly sericitized plagioclase and (or) shows notable alteration of pyroxene and brown hornblende to colorless and pale-green secondary amphibole. Primary textures are intact throughout the complex, and no penetrative deformation is evident.

The gabbro intrudes greenschist-facies metavolcanic and metasedimentary rocks of dominantly pelitic and semipelitic composition, and plagioclase-porphyritic garnet-bearing biotite-quartz diorite of probable middle Cretaceous age. Contacts are sharp where observed, and several large dikes extend outward from the main complex. In small areas near some contacts, the gabbro is loaded with country-rock xenoliths. Thermal metamorphism of the schist has resulted in a zone of hornfels and spotted schist, ranging from less than 0.5 to nearly 3 km in apparent width. The broadest areas of contact-metamorphosed rocks may be underlain by gabbro. Immediately adjacent to the contact, the country rocks reached pyroxene-hornfels facies. The gabbro is cut by highly leucocratic (color index, 1-3) fine-grained allotriomorphic biotite granodiorite dikes. Because no known felsic igneous rocks of Tertiary age occur in the vicinity and because the apparent compositional-differentiation(?) trend of the gabbroic rocks is clearly toward rock of a composition similar to that of the granodiorite, these dikes probably represent a late-stage differentiate of the gabbro.

The aeromagnetic pattern over this gabbro complex is distinctly bimodal (U.S. Geological Survey, 1977). Most of the body has a flat, featureless magnetic expression indistinguishable from the regional aeromagnetic pattern. A conspicuous elongate 230-mGal anomaly is located over the southwestern part of the complex, at the corner of the complex that was originally mapped as leucogabbro (Berg and others, 1978). The proportion of opaque minerals in this part of the complex is low, as in most of the gabbro, and the source of this anomaly is not known.

The gabbro may have been intruded in several discrete but closely timed pulses, the evidence for which includes: (1) The irregular pattern of compositional zoning is reversed from that which normal on-site differentiation and cooling would create; (2) the aeromagnetic pattern of the complex is distinctly bimodal; (3) strong textural variations within some small areas may reflect separate intrusive pulses; and (4) the granodiorite dikes, interpreted as a differentiate of the gabbro, represent a discrete (the last) intrusive pulse.

Constraints on the age of this gabbro include: (1) The unmetamorphosed (undeformed and generally unaltered) condition of the gabbro and contact metamorphism of the surrounding schist, whose metamorphic age is pre-middle Cretaceous and possibly pre-latest Jurassic; (2) intrusion of gabbro into plagioclase-porphyritic garnet-bearing biotite-quartz diorite of probable middle Cretaceous age (Berg and others, 1978; Smith and Diggles, 1978); (3) potassium-argon determinations on biotite and hornblende from a sample of quartz-bearing augite-biotite-hornblende leucogabbro (sample 75SJ417; originally called granodiorite by Smith and Diggles, 1978) yield ages of 23.2± 0.70 and 24.9±0.75 m.y., respectively. The probable intrusive age of the gabbro is late Oligocene.

REFERENCES CITED

Berg, H. C., Elliott, R. L., Smith, J. G., and Koch, R. D., 1978, Geologic map of the Ketchikan and Prince Rupert quadrangles, Alaska: U.S. Geological Survey Open-File Report 78-73-A, scale 1:250,000.

Smith, J. G., and Diggles, M. F., 1981, Potassium-argon determinations in the Ketchikan and Prince Rupert quadrangles, southeastern Alaska: U.S. Geological Survey Open-File Report 78-73-N, 16 p.

U.S. Geological Survey, 1977, Aeromagnetic map of the Ketchikan, Prince Rupert, and northeastern Craig quadrangles, Alaska: Open-File Report 77-359, scale 1:250,000.

Preliminary study of a zoned leucocratic-granite body on central Etolin Island, southeastern Alaska

By Susan J. Hunt

Several similar-appearing leucocratic granitic bodies have been mapped within the Kuiu-Etolin volcanic-plutonic belt (Brew and others, 1979, 1981) in the Petersburg quadrangle. These bodies have been tentatively assigned an age of 19 to 23 m.y. on the basis of potassium-argon ages of 19.7 m.y. on biotite from a leucocratic quartz monzonite on southern Etolin Island (Koch and others, 1977) and of 21.5 m.y. on biotite from a granitic rock on northwestern Etolin Island (Ken Fink, oral commun., 1978), as well as on comparison with Miocene plutons to the southeast in the Ketchikan and Prince Rupert quadrangles (Berg and others, 1978). Detailed petrographic study of rocks from the largest and most complex of these plutons, on central Etolin Island, has revealed some unusual features that provide insight into the probable origin of these distinctive bodies.

This pluton, herein referred to informally as the Burnett Inlet body, underlies about 250 km^2 of central Etolin Island between Anita Bay and the south boundary of the Petersburg quadrangle (area 6, fig. 72; fig. 83). The body intrudes a sequence of metamorphosed turbidites and mafic to intermediate volcanic rocks, probably Jurassic to middle Cretaceous (Berg and others, 1972). The country rocks are also intruded by bodies of garnet-bearing plagioclase-porphyritic tonalite to quartz diorite, believed to be approximately 90 m.y. old, which crop out east of Menefee Inlet and in the area around McHenry Inlet. Preliminary studies indicate that the Burnett Inlet body is zoned, with a homogeneous leucocratic granitic core zone and a complex inhomogeneous outer zone that includes rocks varying widely in lithology and texture. The relation between these two zones is not

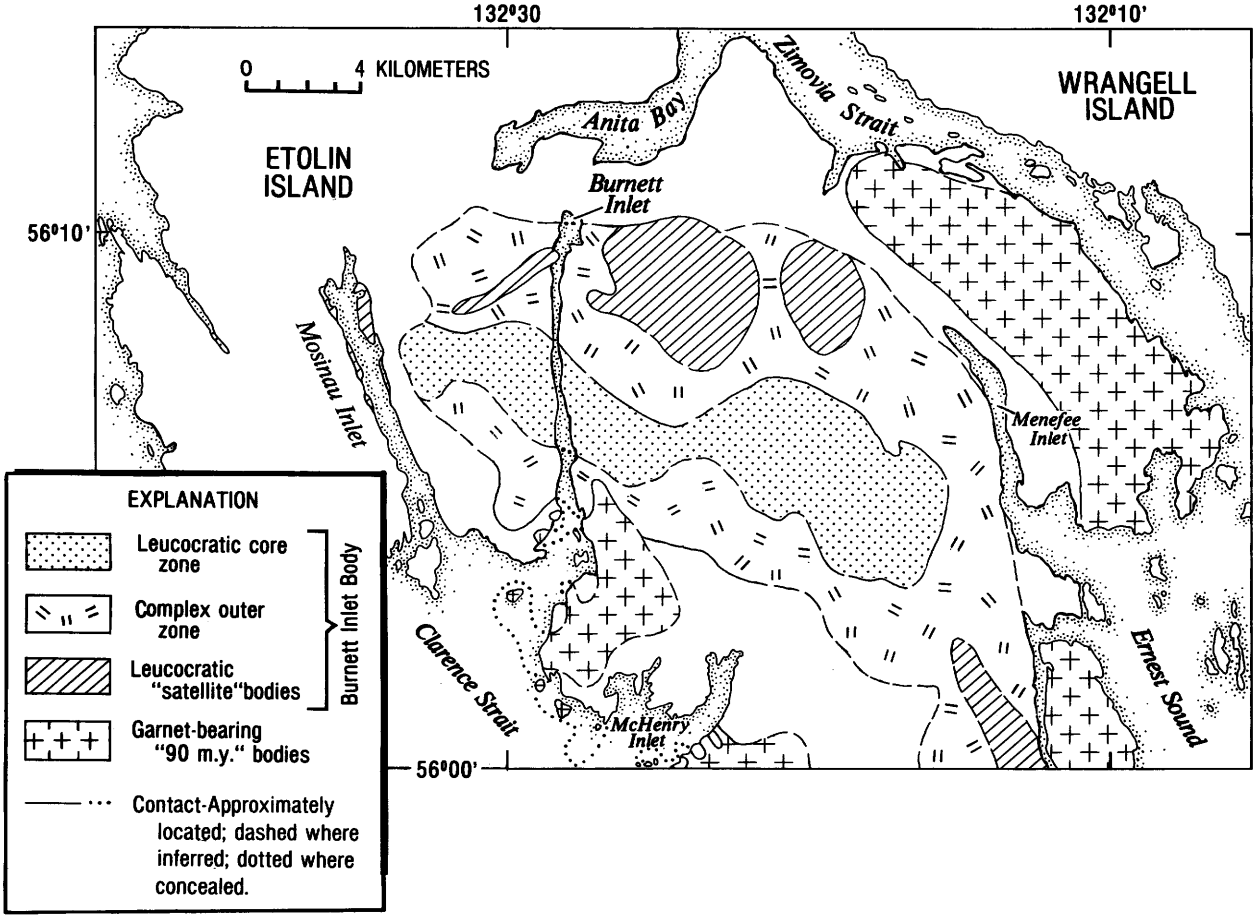

Figure 83.—Schematic geologic map of central Etolin Island in southeast corner of Petersburg quadrangle, showing Burnett Inlet body and adjacent older garnet-bearing plutons.

yet fully understood and is currently the subject of further study.

The core zone is composed of rocks that are distinctive and homogeneous in both texture and composition. Texturally, they are characterized by abundant miarolitic cavities and graphic intergrowths. The rocks are generally allotriomorphic and equigranular to seriate, with grain sizes ranging from medium to coarse. Modal analyses indicate that compositions range from granite, through quartz syenite, to alkali quartz syenite, according to the International Union of Geological Sciences (IUGS) classification (fig. 84). There is some uncertainty in these analyses, however, owing to the pervasive micrographic textures, which probably cause quartz to be undercounted in the mode. Extensive perthitic textures may also cause the same effect regarding plagioclase. Calculations on data from two core-zone samples for which major-element chemistry is available give normative compositions within the IUGS granite field (fig. 84).

The feldspar in the core-zone rocks is generally perthite, with only minor amounts of either plagioclase or potassium feldspar as separate phases. The color index is characteristically less than 5, although on the outer fringes of the core zone it may increase to between 8 and 12. In such samples, the proportion of plagioclase as a separate phase also increases, and the modal compositions become less alkalic (fig. 84). Throughout most of the core zone, the mafic phases consist of both biotite and green hornblende, which commonly are partially altered to chlorite. In the center of the zone, however, are regions containing only biotite, or biotite heavily altered to chlorite. Sphene, allanite, and secondary epidote occur locally; pyroxene and garnet are absent.

Surrounding the core zone on all but the west side (fig. 83) is a highly inhomogeneous and poorly defined zone made up of a wide variety of rock types. These rocks are distinguished from the core-zone rocks by a distinctly higher color index (20-40) that generally increases away from the core, by generally finer grain sizes, and by compositions that are generally plagioclase dominant. Modal compositions are predominantly quartz monzonite, with lesser quartz monzodiorite, quartz diorite, and diorite (fig. 84). Potassium feldspar is present in all but the most mafic samples, commonly as interstitial grains but in places

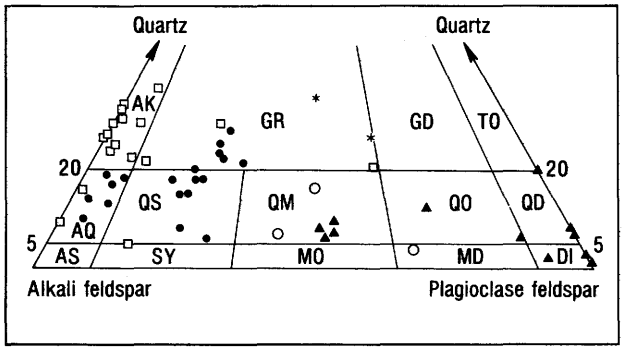

Figure 84.—Compositional diagram (from Streckeisen, 1973) showing modes of stained-slab samples from Burnett Inlet body on central Etolin Island (fig. 83). Asterisks denote normative compositions, as calculated from major-element chemistry for two core-zone samples, which are included for comparative purposes. AK, alkali granite; AQ, alkali quartz syenite; AS, alkali syenite; DI, diorite, GD, granodiorite; GR, granite; MD, monzodiorite; MO, monzonite; QD, quartz diorite; QM, quartz monzonite; QO, quartz monzodiorite; QS, quartz syenite; SY, syenite; TO, tonalite.

rimming and replacing plagioclase. Textures are generally equigranular, although several samples contain plagioclase phenocrysts. Clinopyroxene is almost ubiquitous and seems to be characteristic, although it commonly is partly replaced by biotite and hornblende. Epidote is a minor secondary mineral, and garnet is absent.

Within this generally more mafic outer zone are several occurrences of leucocratic alkali granite ("satellite" bodies, fig. 83). Although these rocks grossly resemble rocks from the core zone in both texture and composition, modal analyses indicate a much lower plagioclase content, and so these rocks mostly fall into the alkali granite and alkali quartz syenite fields (fig. 84). Texturally, the rocks are generally coarser grained, and miarolitic cavities and graphic intergrowths are not so abundant as in the core zone itself. Further distinguishing these rocks is a suite of unusual mafic minerals, including sodic amphibole, iron-rich pyroxene, and iron-rich olivine (fayalite), which may occur in addition to the more common biotite, hornblende, and allanite. Fluorite also occurs locally.

Further studies are now underway to explore the relations, both temporal and genetic, between the various rock types in the Burnett Inlet body. Common brecciation of the rocks in the outer zone and their diking by more leucocratic rock types, especially near the contacts of the two zones, suggest that the leucocratic core-zone rocks are younger than and were emplaced into the more mafic rocks of the outer zone. Although the exact relation between the core-zone rocks and the "satellite" bodies of alkali granite within the outer zone is unclear, they appear to be genetically similar. The leucocratic diking in the outer zone may be in part related to these "satellite" bodies. Preliminary plots of modal compositions (fig. 84), as well as initial results from whole-rock chemical analyses, suggest trends that may reflect differentiation between the various rock types in this body. Further analyses of field relations and of petrographic and chemical data are necessary to explore this possibility.

The characteristic textural properties of the core zone of the Burnett Inlet body suggest that the leucocratic rocks were emplaced at fairly shallow depths. Both the numerous miarolitic cavities and extensive graphic intergrowths indicate shallow emplacement as well as late-stage magmas rich in water and other volatile materials. The strongly perthitic composition of the feldspar in the core zone is consistent with fairly rapid cooling from hypersolvus temperatures of a single feldspar phase that later exsolved to perthite. This evidence, as well as the abundance of upper Tertiary volcanic rocks within the Kuiu-Etolin volcanic-plutonic belt, seems to support the suggestion that the Burnett Inlet body represents one of several late Tertiary eruptive centers within this belt (Brew and others, 1981).

REFERENCES CITED

Berg, H. C., Elliott, R. L., Smith, J. G., and Koch, R. D., 1978, Geologic map of Ketchikan and Prince Rupert quadrangles, Alaska: U.S. Geological Survey Open-File Report 78-73-A, scale 1:250,000.

Berg, H. C., Jones, D. L., and Richter, D. H., 1972, Gravina-Nutzotin belt—tectonic significance of an upper Mesozoic sedimentary and volcanic sequence in southern and southeastern Alaska, in Geological Survey research 1972: U.S. Geological Survey Professional Paper 800-D, p. D1-D24.

Brew, D. A., Berg, H. C., Morrell, R. P., Sonnevil, R. A., Hunt, S. J., and Huie, Carl, 1979, The Tertiary Kuiu-Etolin volcanic-plutonic belt, southeastern Alaska, in Johnson, K. M., and Williams, J. R., eds., The United States Geological Survey in Alaska: Accomplishments during 1978: U.S. Geological Survey Circular 804-B, p. B129-B130.

Brew, D. A., Sonnevil, R. A., Hunt, S. J., and Ford, A. B., 1981, Newly recognized alkali granite stock, southwestern Kupreanof Island, Alaska, in Albert, N. R. D., and Hudson, Travis, eds., The United States Geological Survey in Alaska: Accomplishments during 1979: U.S. Geological Survey Circular 823-B, p. B108-B109.

Koch, R. D., Smith, J. G., and Elliott, R. L., 1977, Miocene or younger strike-slip(?) fault at Canoe Passage, southeastern Alaska, in Blean, K. M., ed., The United States Geological Survey in Alaska: Accomplishments during 1976: U.S. Geological Survey Circular 751-B, p. B76.

Streckeisen, A. L., chairman, 1973, Plutonic rocks—classification and nomenclature recommended by the IUGS Subcommission on the Systematics of Igneous Rocks: Geotimes, v. 18, no. 10, p. 26-30.

Progressive metamorphism of pelitic rocks in the Juneau area, southeastern Alaska

By Glen R. Himmelberg, Arthur B. Ford, and David A. Brew

A regional metamorphic terrane, containing mineral assemblages that reflect conditions of metamorphism ranging from prehnite-pumpellyite to upper amphibolite facies, is exposed along the west margin of the Coast Range batholith in southeastern Alaska (area 5, fig. 72; fig. 85). Buddington and Chapin (1929) first reported on this metamorphic belt, and Forbes (1959) documented the first appearance of the Barrovian index minerals biotite, garnet, staurolite, kyanite, and sillimanite in a transect of the metamorphic belt along Blackerby Ridge. More recently, mineral isograds have been mapped over a broad area from Taku Inlet to Berners Bay and Lynn Canal (fig. 85); the isogradic surfaces dip moderately to steeply northeast (Ford and Brew, 1973, 1977; Brew and Ford, 1977). Several new occurrences of index minerals found during 1979 and 1981 fieldwork have led to slight revision of previously mapped isograds.

The metamorphic belt consists dominantly of intermixed pelitic and semipelitic metasedimentary rocks and mafic metavolcanic and intrusive rocks. Impure calcareous metasedimentary rocks, quartzite, and quartz dioritic and granodioritic orthogneiss are also present. The diversity of intermixed bulk compositions in an area of excellent exposures provides an excellent opportunity to study details of progressive metamorphism. This report is specially concerned with the mineral assemblages and the chemistry of garnet and biotite in the pelitic rocks along Heintzleman Ridge near Juneau, Alaska (fig. 85). Mineral assemblages and rock types there resemble those on Blackerby Ridge, but the mineral zones are broader owing to lower dip of the isogradic surfaces.

Listed below for each zone are the pelitic-mineral assemblages containing the maximum number of coexisting phases. Any combination of a smaller number of phases from the limiting assemblage is possible. On the basis of textural criteria, all phases in an assemblage are tentatively interpreted to be in equilibrium. The order in which the minerals are listed carries no implications.

Zone		Assemblage
Biotite——	1	Quartz-muscovite-chlorite-biotite.
—Do——	2	Quartz-muscovite-biotite-epidote-calcite-dolomite.
Garnet——	3	Quartz-muscovite-chlorite-biotite.
—Do——	4	Quartz-muscovite-biotite-garnet-plagioclase.
Staurolite—	5	Quartz-muscovite-chlorite-biotite-garnet-staurolite.
—Do——	6	Quartz-muscovite-biotite-garnet-staurolite-plagioclase.
Kyanite——	7	Quartz-muscovite-biotite-garnet-staurolite-kyanite-plagioclase.
Sillimanite—	8	Quartz-muscovite-biotite-garnet-sillimanite-plagioclase.
—Do——	9	Muscovite-biotite-sillimanite-corundum-plagioclase.

In those assemblages where plagioclase does not occur as a phase in the maximum-phase assemblage, it may be present in some of the reduced-phase assemblages. In addition, all the assemblages may contain accessory minerals, such as magnetite, ilmenite, sphene, apatite, zircon, and tourmaline. Kyanite also occurs in assemblage 8 but shows reaction to sillimanite. Consideration of the number of phases and components suggests that all these assemblages formed under divariant or higher variance conditions. Chloritoid is not known on Heintzleman Ridge but has been found at two nearby localities (inset, fig. 85).

The textural occurrence of primary metamorphic minerals is as follows. Chlorite and muscovite generally occur as small laths parallel to and defining the schistosity. Biotite in the garnet zone, the staurolite zone, and part of the kyanite zone occurs as porphyroblasts as well as small plates parallel to the schistosity. The porphyroblasts contain an internal schistosity (S_i), well defined by strings of quartz inclusions and opaque dust, at a high angle to the external schistosity (S_e). In most samples, S_i appears to be a relict of an earlier deformation; this observation suggests that the porphyroblasts grew after the early deformation but before the deformation which created the dominant S_e. Rarely, the biotite porphyroblasts show a sense of rotation suggesting that some may have grown syntectonically with the formation of S_e. In several samples, the biotite porphyroblasts are eye shaped, with the long dimension parallel to S_e; these porphyroblasts, which also have S_i at an angle to S_e, are interpreted to have grown before the development of S_e and to have been bulk rotated into parallelism with S_e during the deformation that created S_e. In the upper kyanite zone and higher grades, the biotite occurs only as small plates that, along with muscovite, where present, define the schistosity. Garnet ranges in size from large porphyroblasts to small idioblastic grains. Garnet in some samples contains rotated S_i, which indicates growth syntectonic with the development of S_e, whereas garnet in other samples suggests growth before the development of S_e, and still others are nondiagnostic. The staurolite and kyanite porphyroblasts are commonly helicitic (S_i parallel to S_e), a feature indicating post-S_e growth. Sillimanite most commonly occurs as fibrolite parallel to the schistosity, although small prismatic grains are also present. Sillimanite replaces kyanite and is commonly found in biotite. Quartz and plagioclase form granoblastic polygonal aggregates.

Biotite in 26 samples and garnet in 19 samples have been chemically analyzed with an electron microprobe. In the lower biotite zone, the biotite is green, whereas all other biotite is brown or reddish brown. Green and brown biotite isograds have been mapped (Ford and Brew, 1973, 1977; Brew and Ford, 1977). The green color of biotite is generally attributed to ferric-iron content (Deer and others, 1962), a distinction that cannot be made with the electron microprobe. If O_2 were an inert component during metamorphism, the ferric-iron content and, presumably, the green versus brown color would be a function of bulk composition and not indicate conditions of metamorphism. Biotite shows quite a large range in 100Mg/(Mg+Fe+Mn) of 30.9 to 71.6; however, there is no correlation between this ratio and metamorphic grade. TiO_2 content ranges from approximately 1.2 to 3.2 weight percent; although the TiO_2 content in biotite in the sillimanite zone is

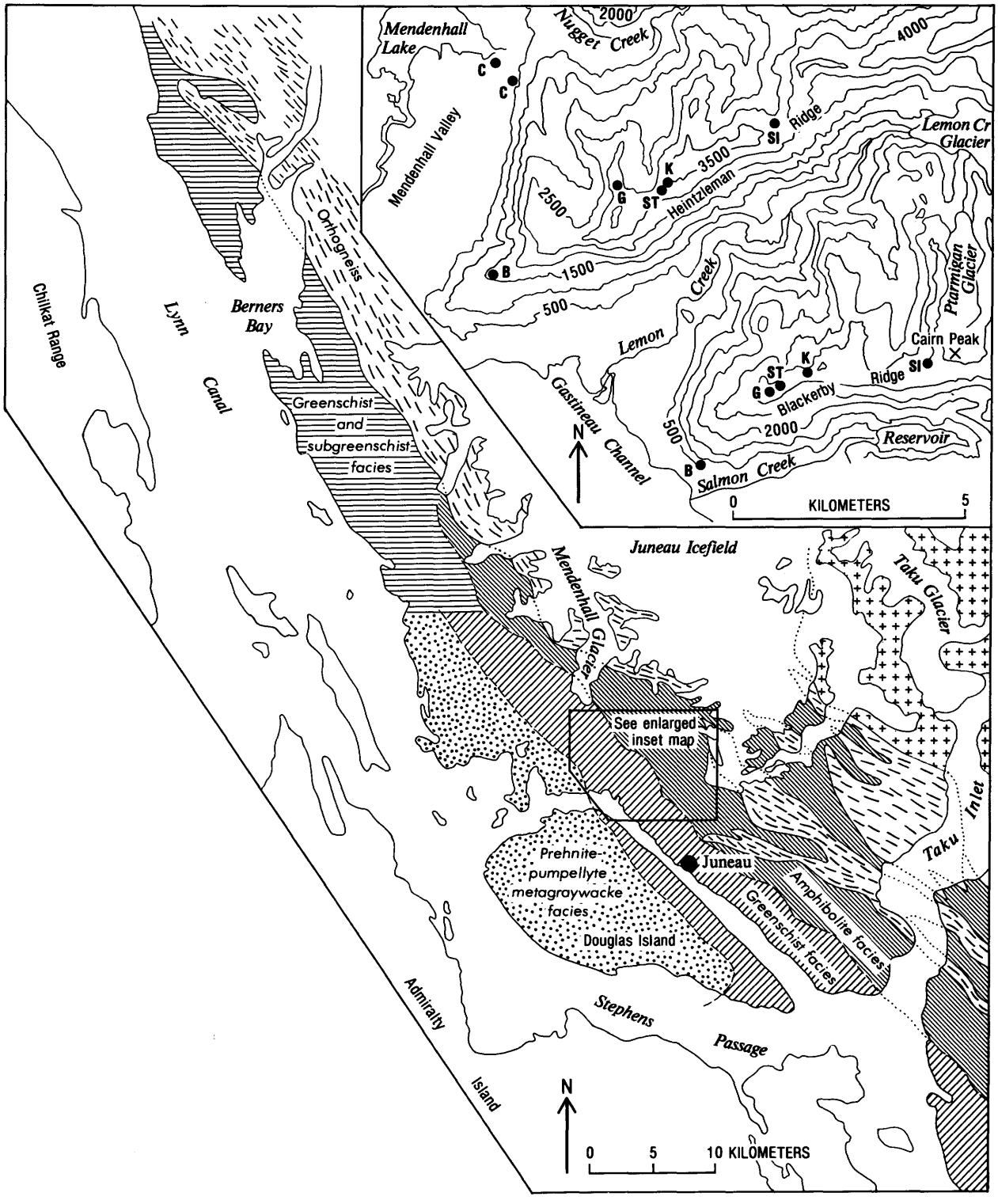

Figure 85.--Sketch map of Juneau area, showing regional distribution of metamorphic facies and relation to plutonic units of west margin of Coast Mountains batholithic complex. Dashed-line pattern shows approximate foliation trends in orthogneiss plutons. Crosses denote little-foliated posttectonic granitic pluton. Inset topographic map (500-ft contours) shows first occurrences in northeastward transects on Heintzleman and Blackerby Ridges of biotite (B), garnet (G), staurolite (ST), kyanite (K), and sillimanite (SI), and occurrences of chloritoid (C).

generally higher than in lower grade biotite, some exceptions occur. We emphasize that generally the compositional variation occurs in mineral assemblages with fewer than the maximum number of coexisting phases for the number of components. Therefore, the bulk chemistry of the individual rocks affects the composition of the minerals even at constant temperature and pressure. The influence of bulk chemistry is well illustrated in samples where biotite grains of markedly different chemical compositions are interlayered on a scale of millimeters. Retention of the biotite compositional differences also indicates that intergrain metamorphic diffusion has been restricted to a scale of millimeters or less. The biotite is chemically unzoned, and no compositional difference exists between biotite occurring as porphyroblasts or as small plates, nor between biotite in contact with different Fe-Mg aluminosilicates relative to matrix biotite. One exception is that the composition of biotite completely enclosed in garnet in the sillimanite zone differs significantly from that of biotite in the matrix.

Garnet compositional variation is complex, both within individual crystals and between crystals of different specimens. Most garnets are zoned. In the garnet zone, the staurolite zone, and part of the kyanite zone, garnet cores are generally lower in Fe and Mg and enriched in Mn relative to the margins, a well-established pattern generally considered to be normal (Hollister, 1966, 1969; Atherton, 1968; Yardley and others, 1980; Zen, 1981). In the higher grade rocks, garnet most commonly is reversely zoned; that is, the rims are generally enriched in Mn and depleted in Fe and Mg relative to the cores. This reverse zoning is generally attributed to elemental redistribution during retrograde cooling (Grant and Weiblen, 1971; Yardley and others, 1980). The major compositional variation of the garnet is in the almandine component (55.7-73.9 percent) and in the spessartine component (3.6-20.9 percent). The garnets, as well as the biotite, show no compositional variation reflecting metamorphic grade. Compositional variation in the garnets is also a function of bulk-composition control.

We have calculated temperatures of equilibration from the distribution of Fe and Mg between garnet and biotite in 19 specimens, using the empirical calibration of Thompson (1976) and the experimental calibration of Ferry and Spear (1978). Use of garnet-rim compositions in the calculations where garnet showed normal zoning assumes that the rims are in equilibrium with the other phases. For garnets with reverse zoning, the core compositions were assumed to yield the best maximum temperature. A minimum pressure of 0.55 GPa (the Al_2SiO_5 triple point, according to Richardson and others, 1969) was used in the Ferry and Spear geothermometer; we consider this pressure to be a reasonable minimum because the progressive metamorphism proceeds from the kyanite stability field into the sillimanite stability field. Temperatures calculated from the two geothermometers agree within 10°C for temperatures below 550°C; above 550°C the temperatures calculated from the Thompson geothermometer are 25° to 50°C lower. The natural biotite and garnet from Heintzleman Ridge depart significantly in Al^{VI}+Ti and Ca+Mn content, respectively, from the synthetic biotite and garnet used in the Ferry and Spear experimental calibration. Nevertheless, the temperatures calculated from both geothermometers are reasonable for the metamorphic progression from lower to upper amphibolite facies.

The calculated temperature ranges from approximately 495°C in the lower garnet zone to 690°C in the sillimanite zone, using the Thompson calibration, and from 495°C to 750°, using the Ferry and Spear calibration. A temperature calculated from a garnet-biotite pair, where the biotite is completely enclosed in the garnet, yields a value 100°C lower than that calculated from a garnet-matrix/biotite pair. This difference suggests that the biotite enclosed in garnet has a lower grade composition frozen in and, as suggested by Fletcher and Greenwood (1979) for a similar case, that progressive metamorphism in the strict sense has taken place.

REFERENCES CITED

Atherton, M. P., 1968, The variation in garnet, biotite, and chlorite composition in medium grade pelitic rocks from the Dalradian, Scotland, with particular reference to the zonation in garnet: Contributions to Mineralogy and Petrology, v. 18, no. 4, p. 347-371.

Brew, D. A., and Ford, A. B., 1977, Preliminary geologic and metamorphic-isograd map of the Juneau B-1 quadrangle, Alaska: U.S. Geological Survey Miscellaneous Field Studies Map MF-846, scale 1:31,680.

Buddington, A. F., and Chapin, Theodore, 1929, Geology and mineral deposits of southeastern Alaska: U.S. Geological Survey Bulletin 800, 398 p.

Deer, W. A., Howie, R. A., and Zussman, J., 1962, Rock forming minerals; volume 3, Sheet silicates: New York, John Wiley, 270 p.

Ferry, J. M., and Spear, F. S., 1978, Experimental calibration of the partitioning of Fe and Mg between biotite and garnet: Contributions to Mineralogy and Petrology, v. 66, no. 2, p. 113-117.

Fletcher, C. J. N., and Greenwood, H. J., 1979, Metamorphism and structure of Penfold Creek area, near Quesnel Lake, British Columbia: Journal of Petrology, v. 20, no. 4, p. 743-794.

Forbes, R. B., 1959, The geology and petrology of the Juneau Ice Field area, southeastern Alaska: Seattle, University of Washington, Ph. D. thesis, 261 p.

Ford, A. B., and Brew, D. A., 1973, Preliminary geologic and metamorphic-isograd map of the Juneau B-2 quadrangle, Alaska: U.S. Geological Survey Miscellaneous Field Studies Map MF-527, scale 1:31,680.

———1977, Preliminary geologic and metamorphic-isograd map of northern parts of the Juneau A-1 and A-2 quadrangles, Alaska: U.S. Geological Survey Miscellaneous Field Studies Map MF-847, scale 1:31,680.

Grant, J. A., and Weiblen, P. W., 1971, Retrograde zoning in garnet near the second sillimanite isograd: American Journal of Science, v. 270, no. 4, p. 281-296.

Hollister, L. S., 1966, Garnet zoning: An interpretation based on Rayleigh fractionation model: Science, v. 154, no. 3757, p. 1647-1651.

——1969, Contact metamorphism in the Kwoiek area of British Columbia: An end member of the metamorphic process: Geological Society of America Bulletin, v. 80, no. 12, p. 2465-2494.

Richardson, S. W., Gilbert, M. C., and Bell, P. M., 1969, Experimental determination of kyanite-andalusite and andalusite-sillimanite equilibrium; the aluminum silicate triple point: American Journal of Science, v. 267, no. 3, p. 259-272.

Thompson, A. B., 1976, Mineral reactions in pelitic rocks: II. Calculation of some P-T-X(Fe-Mg) phase relations: American Journal of Science, v. 276, no. 4, p. 425-454.

Yardley, B. W. D., Leake, B. E., and Farrow, C. M., 1980, The metamorphism of Fe-rich pelites from Connemara, Ireland: Journal of Petrology, v. 21, no. 2, p. 365-399.

Zen, E-an, 1981, Metamorphic mineral assemblages of slightly calcic pelitic rocks in and around the Taconic allochthon, southwestern Massachusetts and adjacent Connecticut and New York: U.S. Geological Survey Professional Paper 1113, 128 p.

Fossil hydrothermal systems in the Ketchikan area, southeastern Alaska

By George E. Gehrels[1] and Hugh P. Taylor, Jr.[1]

The Coast plutonic complex is a belt of metamorphic and predominantly Cretaceous and Tertiary plutonic rocks that extends along the length of western British Columbia and eastern southeast Alaska. Magmatic and thermal activity in this belt produced a large metamorphic aureole along the western edge of the batholith, and fueled immense hydrothermal circulation systems to the east in British Columbia (Taylor and Magaritz, 1978). Oxygen-isotope analyses reported herein demonstrate that extensive hydrothermal systems also existed west of the batholith in the Ketchikan area, and suggest that this hydrothermal activity was fueled by thermal events in the Coast plutonic complex.

Fossil hydrothermal systems have been detected in southernmost southeastern Alaska (area 4, fig. 72) by measuring the oxygen-isotopic composition of coexisting quartz and plagioclase in lower Paleozoic trondhjemitic rocks. Empirical and experimental evidence demonstrates that the isotopic composition of plagioclase may change quite readily in the presence of hot aqueous fluids, whereas coexisting quartz retains an igneous isotopic composition or changes only slightly (Criss and Taylor, 1983). The relative isotopic compositions of quartz and feldspar can therefore be used to infer the nature and extent of interaction between a rock body and circulating hydrothermal fluids. The oxygen-isotopic composition of these minerals is expressed as $\delta^{18}O$, which is the permil (parts per thousand) difference in $^{18}O/^{16}O$ ratio between the mineral and standard mean ocean water (SMOW), a standard with $\delta^{18}O=0.0$ permil. Previous studies have shown that the $\delta^{18}O$ values of quartz are typically 8 to 10 permil in trondhjemitic rocks which have not interacted substantially with hydrothermal fluids, and the coexisting plagioclase is typically 1.0±.3 permil lower in $\delta^{18}O$ than the quartz (Taylor, 1974). If the difference between the quartz and plagioclase ($\Delta^{18}O_{Q-pl}$) is less than 1.0±0.3 permil, the rock probably interacted with fluids that were fairly heavy (possibly marine, magmatic or metamorphic in origin) and (or) at fairly low temperatures. For $\Delta^{18}O_{Q-pl}$ greater than 1.0±0.3 permil, the fluids were probably fairly light (meteoric) and (or) at fairly high, but still subsolidus, temperatures. The actual isotopic composition and temperature are difficult to constrain.

We analyzed samples from various distances west of the Coast plutonic complex (fig. 86) to determine the type and extent of hydrothermal activity around the large batholithic belt. Figure 87 plots the isotopic composition of quartz and plagioclase in each sample, and figure 88 plots the variations in $\Delta^{18}O_{Q-pl}$ as a function of the distance of the sample locality from the western edge of the batholith. As seen on figure 87, three samples from Annette and Gravina Islands have $\Delta^{18}O_{Q-pl}$ values of 1.0± 0.3 permil, whereas samples both to the east and west have values outside the range of "normal" plutonic compositions. Figure 88 shows that the variations in $\Delta^{18}O_{Q-pl}$ in this suite are a function of the distance of the sample locality from the west edge of the Coast plutonic complex. Because this approximately linear relation is exhibited by the isotopically disturbed samples as well as those with "normal" igneous fractionations, we propose that all of the trondhjemite samples analyzed in this study have interacted with circulating hydrothermal fluids.

The isotopic variations plotted in figure 88 can be best explained by isotopic exchange between the trondhjemitic rocks and a hydrothermal system, or set of systems, in which the conditions of alteration changed progressively from east to west. Calculations based on the fractionation factor between feldspar and water (O'Neil and Taylor, 1967) show that if the plagioclase (albite-oligoclase) in all the samples reached isotopic equilibrium with circulating fluids of a given composition, the temperatures of interaction would have been about 70°C higher for the Cape Fox samples than for the Prince of Wales samples (fig. 86). Similarly, for a given temperature of interaction, the hydrothermal fluids would have been about 3 permil lighter at Cape Fox than on Prince of Wales Island. Although exact temperatures and water compositions have not been determined, these isotopic variations reflect interaction with fairly heavy hydrothermal fluids that became progressively lighter and (or) hotter toward the east.

Several different oxygen- and hydrogen-isotope studies have documented fossil hydrothermal systems within and along the east side of the Coast plutonic complex (Taylor and Magaritz, 1978). In the Prince Rupert area (fig. 86), this hydrothermal activity extended many kilometers eastward into the

[1]Division of Geological and Planetary Sciences, California Institute of Technology, Pasadena, CA 91125.

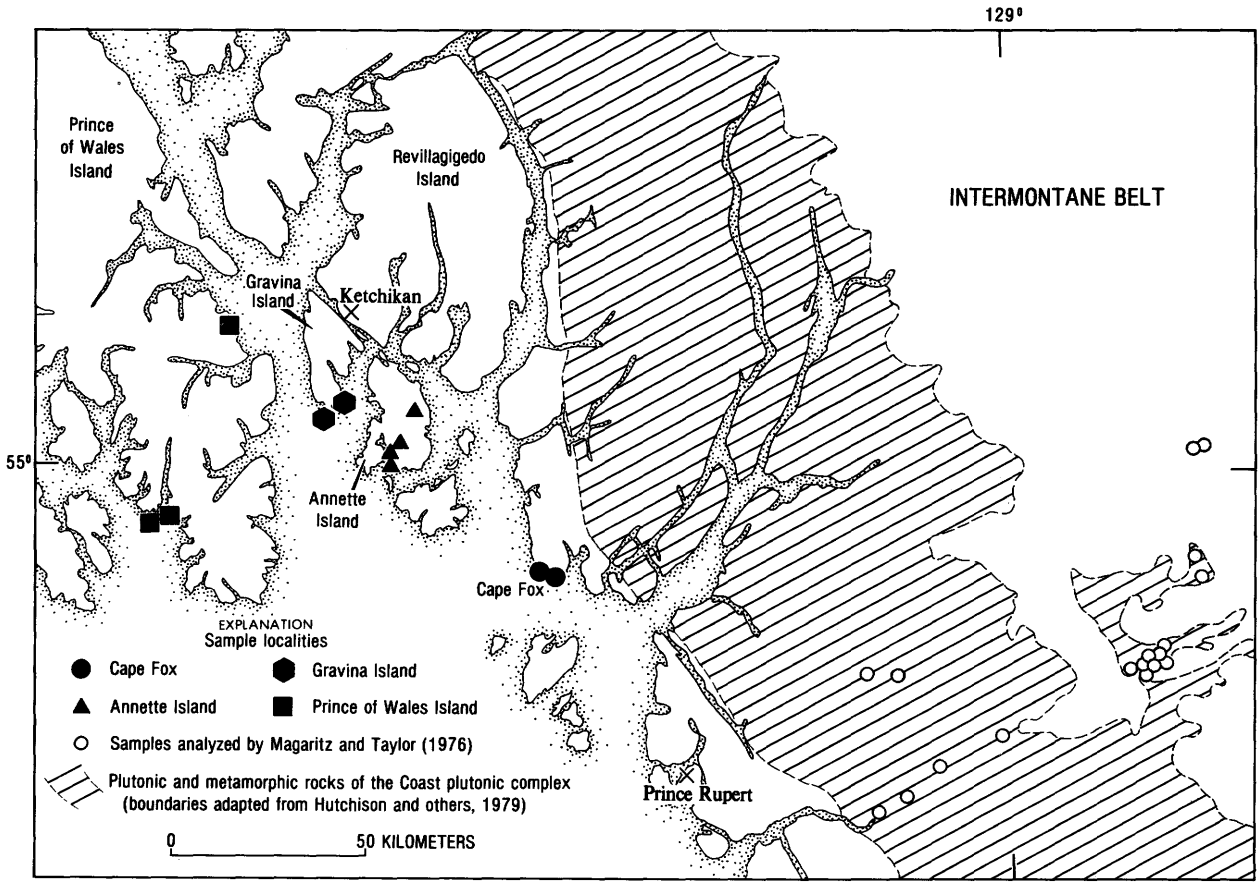

Figure 86.—Ketchikan area, showing locations of samples utilized for oxygen-isotope analyses and approximate distribution of plutonic and metamorphic rocks of the Coast plutonic complex.

intermontane belt and was fueled by the emplacement of Eocene plutons and dikes (Magaritz and Taylor, 1976). Figure 89 compares the isotopic variations within and east of the Coast plutonic complex near Prince Rupert (Magaritz and Taylor, 1976), with those measured in this study. The approximately linear relation between $\Delta^{18}O_{Q\text{-}pl}$ and the distance of the sample locality from the west edge of the batholith may be fortuitous, or this relation may be the isotopic signature of hydrothermal activity that circulated progressively lighter waters toward the east. A somewhat similar gradient in hydrothermal-fluid composition was recognized along a traverse across Vancouver Island and the southern part of the Coast plutonic complex (Taylor and Magaritz, 1978). Both of these inferred $\delta^{18}O_{H_2O}$ gradients are similar to the present-day variation in surface-water composition across southeastern Alaska and western British Columbia (Taylor, 1974, fig. 6).

On the basis of the geologic and isotopic relations described above, we infer that the oxygen-isotopic variations in the Ketchikan area may record interaction with huge hydrothermal systems which were driven by thermal events in the Coast plutonic complex. These isotopic relations also suggest that on the west side of the study area, fairly heavy fluids were involved—possibly marine or metamorphic in origin. Toward the east, the circulating fluids became lighter and were at least in part of meteoric origin on the east side of the Coast plutonic complex (Taylor and Magaritz, 1978). Investigations are currently in progress on the composition and age of the hydrothermal systems within and west of the batholithic belt, and on the relation between this hydrothermal activity and the mineralization history of southeastern Alaska.

Acknowledgments.—We thank Jason B. Saleeby and Henry C. Berg for the samples analyzed in this study. Financial support for this research was provided by National Science Foundation Grant EAR-7816874, awarded to H. P. Taylor, Jr. This is contribution No. 3722 of the Division of Geological and Planetary Sciences, California Institute of Technology, Pasadena, CA 91125.

REFERENCES CITED

Criss, R. E., and Taylor, H. P., 1983, An $^{18}O/^{16}O$ and D/H study of Tertiary hydrothermal systems in the southern half of the Idaho Batholith:

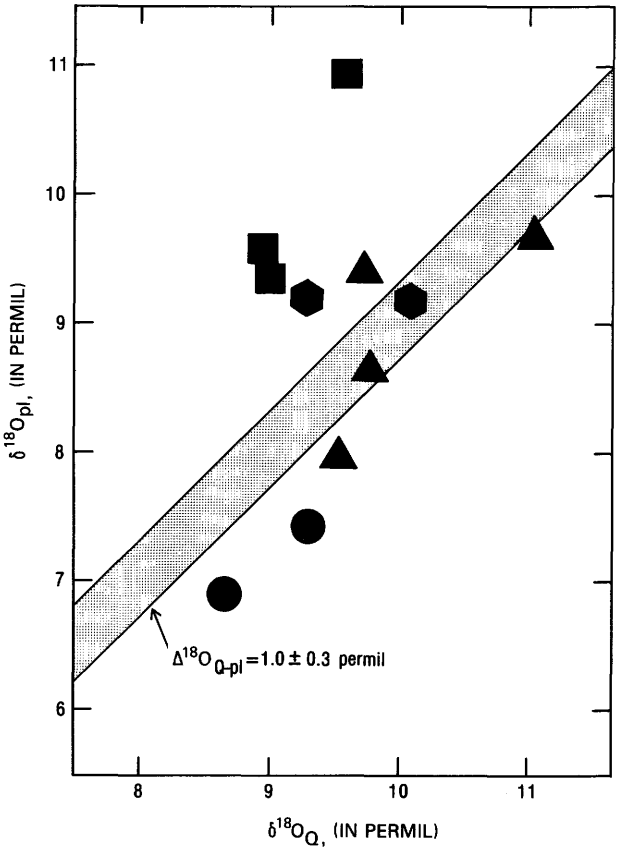

Figure 87.—$\delta^{18}O$ of quartz (Q) versus $\delta^{18}O$ of plagioclase (pl), relative to range of values for unaltered trondhjemitic rocks (shading). Circles, Cape Fox; squares, Prince of Wales Island; triangles, Annette Island; hexagons, Gravina Island. Size of symbol is approximately 2σ (±0.1 permil) analytical uncertainty.

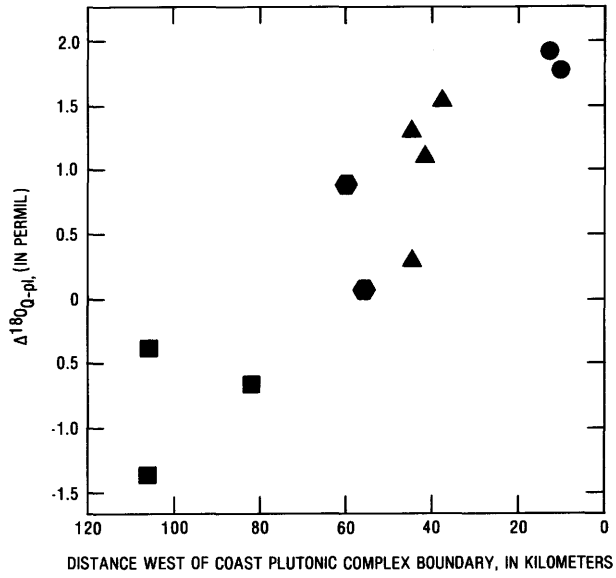

Figure 88.—$\Delta^{18}O/^{16}O$ fractionation between quartz and plagioclase ($\Delta^{18}O_{Q-pl}$) of analyzed samples versus distance of sample locality west of Coast plutonic complex boundary. Circles, Cape Fox; squares, Prince of Wales Island; triangles, Annette Island; hexagons, Gravina Island.

Geological Society of America Bulletin, v. 94, no. 5, p. 640-663..

Hutchison, W. W., Berg, H. C., and Okulitch, A. V., 1979, Skeena River geologic map: Geological Survey of Canada Map 1385A, scale 1:1,000,000.

Magaritz, Mordeckai, and Taylor, H. P., 1976, $^{18}O/^{16}O$ and D/H studies along a 500 km traverse across the Coast Range batholith and its country rocks, central British Columbia: Canadian Journal of Earth Sciences, v. 13, no. 11, p. 1514-1536.

O'Neil, J. R., and Taylor, H. P., Jr., 1967, The oxygen isotope and cation exchange chemistry of feldspars: American Mineralogist, v. 52, no. 9-10, p. 1414-1437.

Taylor, H. P., Jr., 1968, The oxygen isotope geochemistry of igneous rocks: Contributions to Mineralogy and Petrology, v. 19, no. 1, p. 1-71.

———1974, The application of oxygen and hydrogen isotope studies to problems of hydrothermal alteration and ore deposition: Economic Geology, v. 69, no. 6, p. 843-883.

Taylor, H. P., Jr., and Magaritz, Mordeckai, 1978, Oxygen and hydrogen isotope studies of the Cordilleran batholiths of western North America, in Robinson, B. W., ed., Stable isotopes in the earth sciences: New Zealand Department of Scientific and Industrial Research Bulletin, v. 220, p. 151-173.

OFFSHORE ALASKA

(Figure 90 shows study areas discussed)

Paleoenvironmental analysis of the ostracodes in Quaternary sediment from cores taken near Icy Bay, Gulf of Alaska

By Elisabeth M. Brouwers

The Continental Shelf south of Icy Bay (area 1, fig. 90; fig. 91) is a region of contrasting offshore sedimentation rates, ranging from areas of nondeposition near Cape Yakataga to areas with sedimentation rates as high as 18 mm per yr (Molnia and others, 1980). I have examined the ostracode faunas in four cores from this region (fig. 92) with several goals in mind: (1) To establish whether the cores in the area of high sedimentation rates can be correlated; (2) to determine whether any climatic cycles are evident that are comparable to the high-resolution onshore dendrochronology records; (3) to determine the Holocene/Pleistocene boundary in the core taken off Cape Yakataga; and (4) to establish

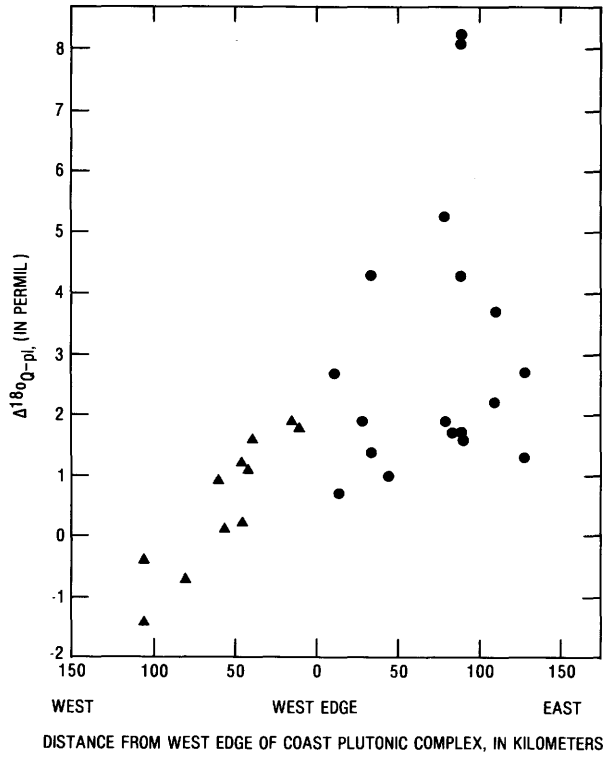

Figure 89.—$\Delta^{18}O/^{16}O$ fractionation between quartz and plagioclase ($\Delta^{18}O_{Q-pl}$) of analyzed samples versus distance of sample locality from the west edge of the Coast plutonic complex. Triangles, samples analyzed in this study; dots, samples analyzed by Magaritz and Taylor (1976).

whether any major geotechnical trends are paralleled by faunal trends.

Initial sample sizes and vertical spacing of samples were limited by availability of material from the cores; thus, all the ostracode assemblages contain small numbers of individuals. The ostracode fauna from each sample was tabulated and compared with the distinct depth assemblages I have determined for the modern ostracode faunas in this region.

The cores were taken in water depths of 82 to 156 m, which incorporates the middle neritic (50-100 m) and outer neritic (100-200 m) depth zones. The present environmental conditions for middle neritic depths include moderate variation in annual bottom temperatures (2°-8°C) and slight variation of bottom salinity (31-32 ppt) (Royer, 1975). In contrast, the outer neritic zone is slightly more stable, with maximum annual bottom-temperature variations of 2° to 6°C, though primarily from 2° to 4°C, and bottom salinity of about 32 parts per thousand. Winter downwelling and storms further cause an overturn of low-temperature surface waters to the bottom.

The ostracode faunas from cores 709C, 711, and 715 have been interpreted to represent two components. The first component (A) consists of a fauna that presently lives in this region in an environment of deeper middle neritic to shallow outer neritic conditions. In addition, a large number of inner neritic ostracode species occur in this component; some of these species are probably living at the edge of their habitat, whereas others are being transported in by downslope sediment movement. The transportation aspects are well illustrated by selective movement of the lighter, smaller juvenile specimens (Brouwers, 1980). Component A comprises the upper parts of cores 709C, 715, and 704B and all of core 711 (fig. 92).

The second component (B) consists of an ostracode fauna that lives today primarily in outer neritic depths, where the annual-bottom-temperature variation is reduced and summer maximum temperatures are lower. Aspects of the shallower neritic depths are greatly reduced and may be largely accounted for by offshore transport and by species living at the edge of their habitats. Component B occurs at the bottoms of cores 709C and 715. This subtle change in fauna can be interpreted to represent a different thermal regime than that which prevails today; this difference could be due to either colder temperatures or lesser variation in the annual range of bottom temperature.

High-resolution climatic cycles (on the order of the 50-year cycles determined by dendrochronology) were not observed in the cores. I interpret this result as due to two factors. First, the sample sizes were too small to make the desired larger, more representative counts of the ostracode populations. Second, and more importantly, the offshore environment is more ameliorated in comparison with to the onshore cycles. The mixing by current systems and winds and the large water masses involved do not respond so quickly to smaller scale changes in seasonal climates, especially in depths of greater than 100 m. A better area to look for these changes in the marine record is in shallow bays. However, nearly all the bays in the Gulf of Alaska have short (less than 100 years) records because of the presence of more advanced glaciers and consequent bottom scouring during the 20th century.

Core 704B was subsampled because it was taken in an area of nondeposition, and the likelihood of occurrence of the Holocene/Pleistocene boundary in this core was large. The upper part of this core can be correlated in terms of similar environment with component A of the other three cores; below this interval are several ostracode species that have not been documented to date as living today in the Gulf of Alaska, and are interpreted as being fossil (that is, extinct in this region) (component C). These fossil species have been found in colder environments, such as the southern Bering Sea. In addition, a lower sedimentation rate is indicated by the greater number of adult versus juvenile specimens, especially in comparison with the other three cores. Primarily on the basis of the presence of these fossil species and, to a lesser extent, the appearance of a change of preservation of the specimens, this lower interval of the core suggests that older, probable Pleistocene sediment is present, dating from an environment with colder water conditions.

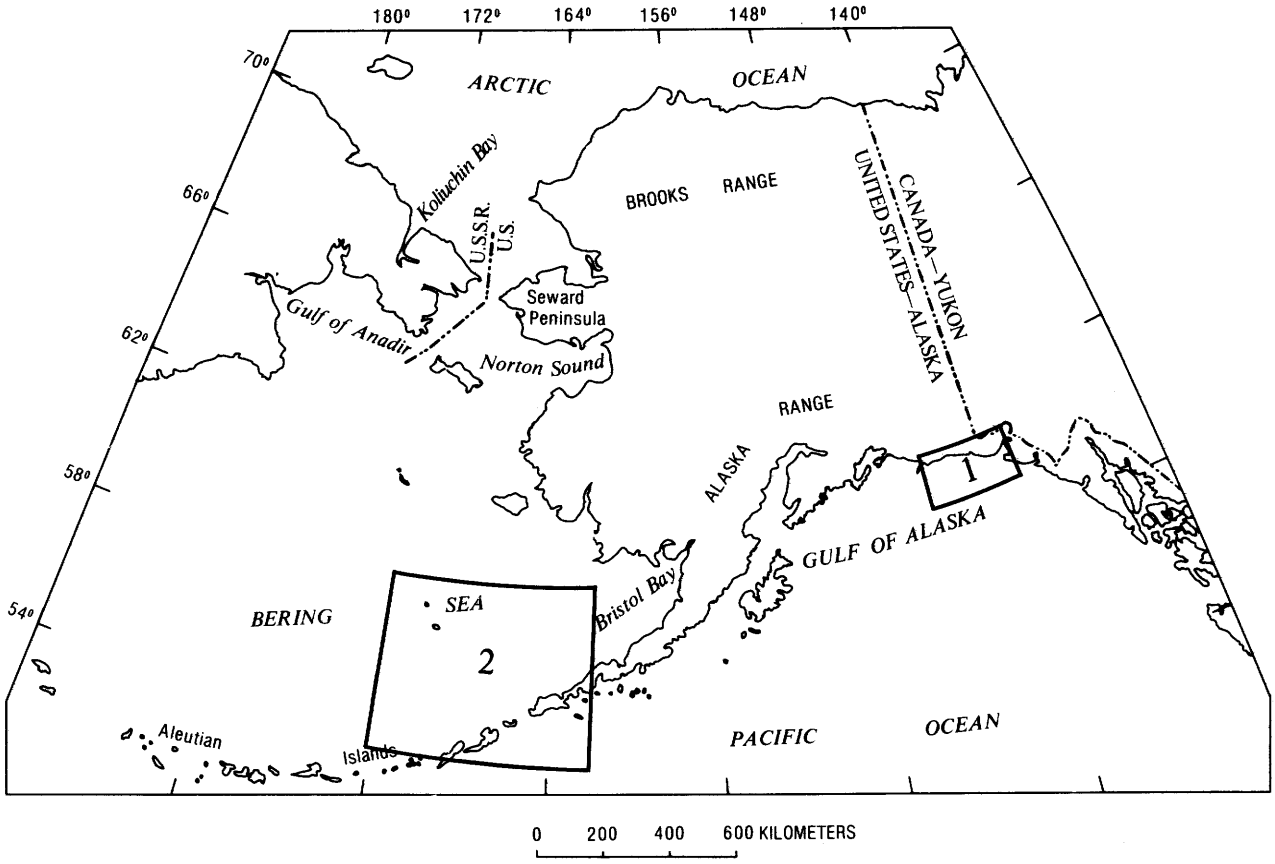

Figure 90.—Offshore areas discussed in this volume. A listing of authorship, applicable figures, and article pagination (in parentheses) relating to the numbered areas follows. 1, Brouwers, figures 91 and 92 (p. 136-139); 2, Brouwers and McDougall, figures 93 and 94 (p. 140-141).

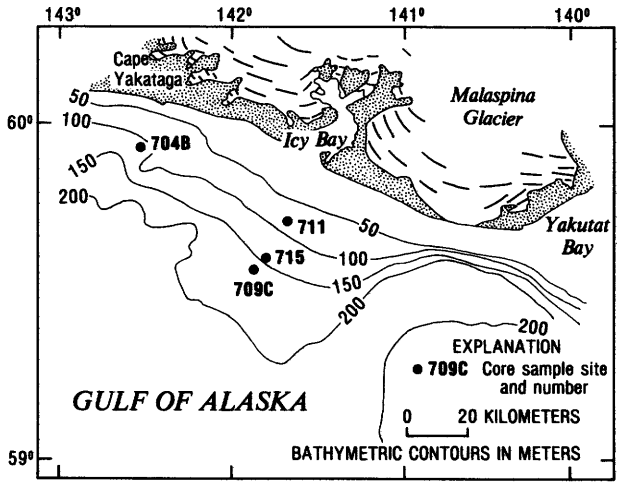

Figure 91.—Bathymetric map of part of the Continental Shelf south of Icy Bay, showing the four gravity-core bottom-sediment-sample sites (modified from Carlson and others, 1978, fig. 2).

REFERENCES CITED

Brouwers, E. M., 1980, Distribution of Holocene ostracodes in the eastern Gulf of Alaska: A zoogeographic, ecologic, and biosedimentologic analysis [abs.]: University of Colorado, Institute of Arctic and Alpine Research, Arctic Workshop, 9th, Boulder, Colo., 1980, p. 5-6.

Carlson, P. R., Levy, W. P., Molnia, B. F., and Hampson, J. C., Jr., 1978, Geotechnical properties of sediments from the continental shelf south of Icy Bay, northeastern Gulf of Alaska: U.S. Geological Survey Open-File Report 78-1071, 29 p.

Molnia, B. F., Levy, W. P., and Carlson, P. R., 1980, Map showing Holocene sedimentation rates in the northeastern Gulf of Alaska: U.S. Geological Survey Miscellaneous Field Studies Map MF-1170, scale 1:500,000.

Royer, T. C., 1975, Seasonal variations of waters in the northern Gulf of Alaska: Deep-Sea Research and Oceanographic Abstracts, v. 22, no. 6, p. 403-416.

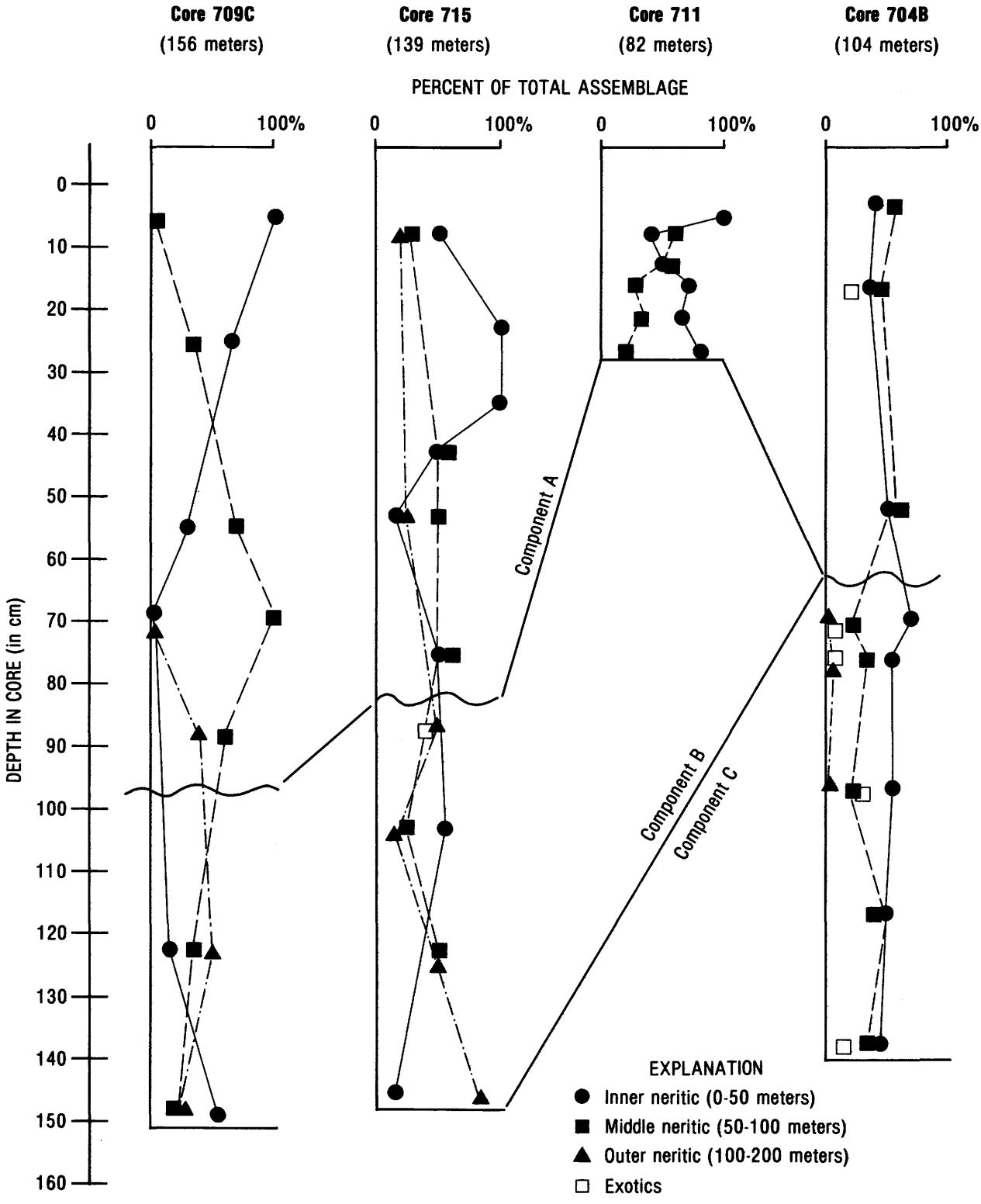

Figure 92.—Stratigraphic distribution of ostracode faunas (components A-C) as a percentage of total sample. Wavy lines indicate approximate boundaries between different assemblages; solid lines connecting cores mark correlation of similar faunas. Water depth of core is given in parentheses below core number.

Preliminary analysis of microfauna from selected bottom grab samples, southern Bering Sea

By Elisabeth M. Brouwers and Kristin McDougall

The ostracode and foraminifer faunas were examined from 14 Van Veen samples from the Continental Shelf adjacent to the Pribilof and Aleutian Islands (area 2, fig. 90; fig. 93). These faunas represent two distinct assemblages, one from the Pribilof Islands and the other from the Aleutians Islands.

The Pribilof Islands ostracode assemblage contains a mixture of species, some presently living in the region and other fossil species representing a cooler environment. Endemic ostracode species are "Acanthocythereis" dunelmensis, "Leguminocythereis" sp. D, Pectocythere aff. P. quadrangulata, and Krithe sp. On the basis of their modern geographic ranges, these species indicate a cold-temperate to subfrigid marine climate; the Pribilof Islands today have a mean sea-surface temperature range of 1° to 9°C.

Organic stains were not used, and so living and fossil benthic foraminifers are difficult to distinguish in the Pribilof Islands samples. Buliminella elegantissima, Elphidiella hannai, Nonionella puchella, Trichohylinus columbiensis, and T. ornatissima probably represent the living fauna. These benthic foraminiferal species indicate shallow cold-temperate waters and agree with the ostracode data. These occurrences near the Pribilof Islands approximate the north limits of the cold-temperate ostracode and foraminifer ranges. The fossil species lived in colder water conditions than are currently found near the Pribilofs; this observation suggests a colder thermal regime for the Pribilofs during the time of deposition. Elphidium clavatum is the principal indicator of fossil species and cold-arctic waters. The mixture of modern temperate species with arctic species supports previous interpretations that the shelf sediment near the Pribilof Islands contains mixed modern and relict elements.

The Aleutian Islands ostracode assemblage consists entirely of fossil species. We interpret the

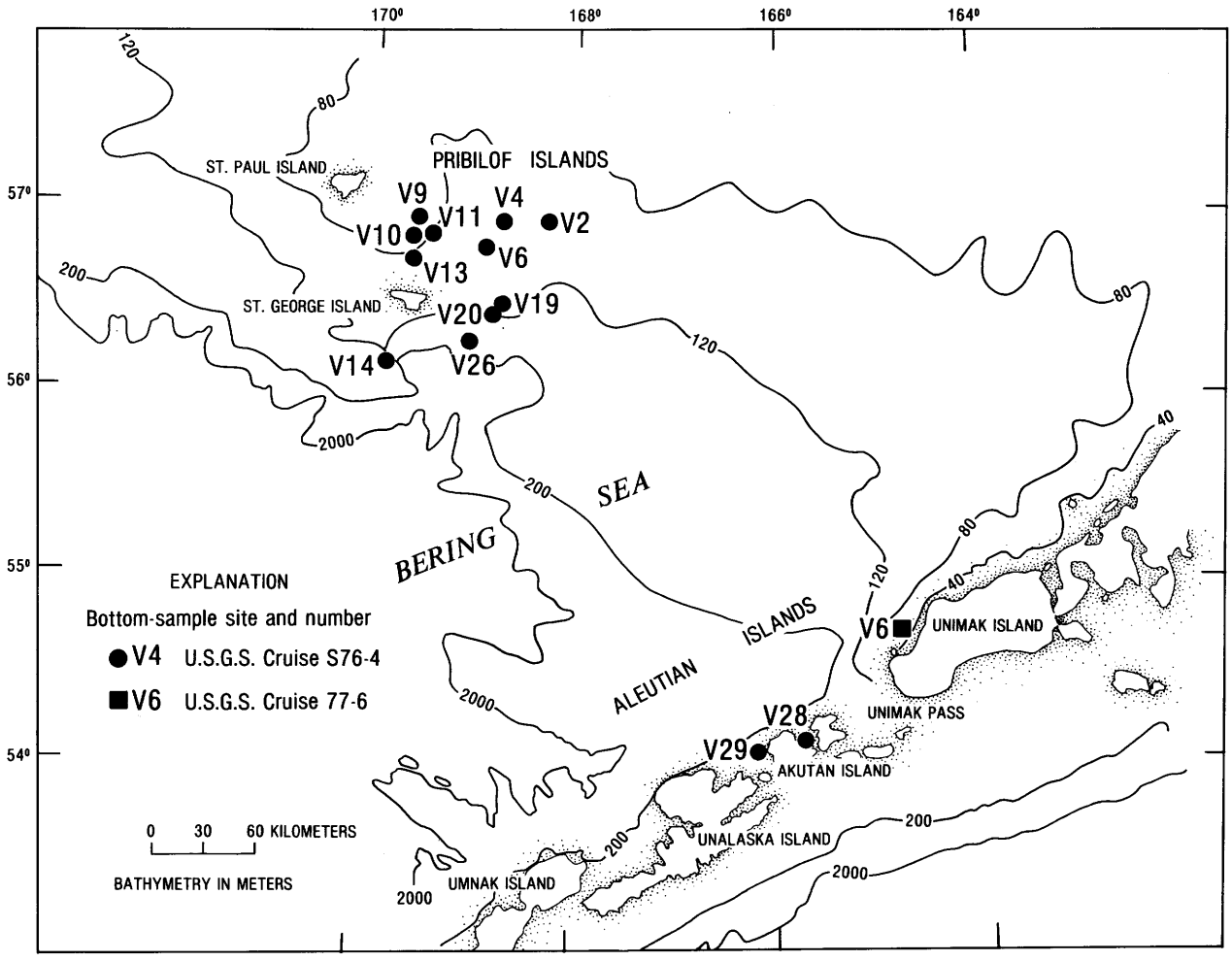

Figure 93.—Part of Bering Sea, showing bottom-sample sites near Pribilof and Aleutian Islands (modified from Gardner and others, 1979, figs. 4, 5).

ostracode fauna in these samples to consist of a mixture of three components representing three distinct zoogeographic provinces (fig. 94). The first component is thought to be a shallow-water assemblage of cold-temperate species from the Aleutian Province, which extends today from near Vancouver Island to Bristol Bay. Numerous phytal forms (Pontocypris, Sclerochilus, Paracytherois, Paradoxostoma, and Xestoleberis) indicate deposition within the photic zone. Several of the cold-temperate indicator species are known to be living in the Gulf of Alaska and near the Pribilof Islands.

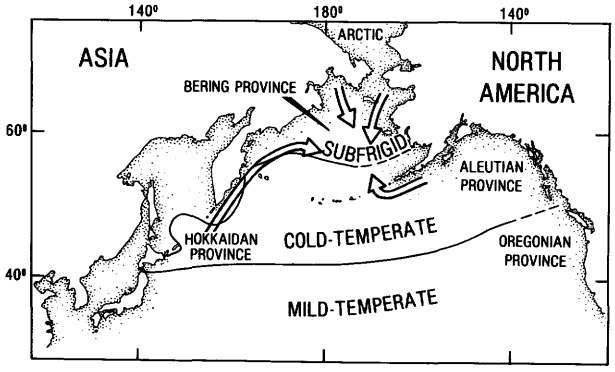

Figure 94.—North Pacific Ocean (modified from U.S. Navy, Chief of Naval Operations, 1977), showing modern boundaries of cold-temperate and subfrigid marine climates. Cold-temperature zone is termed the Hokkaidan Province in the western Pacific and the Aleutian Province in the eastern Pacific; subfrigid zone is termed the Bering Province. Arrows indicate interpreted origins of fossil faunas occurring in Aleutian Island samples (fig. 93).

The second component is represented by species that are very similar to western Pacific faunas from the cold-temperate Hokkaido Province. The ostracodes are congeneric with ostracode assemblages occurring along Japan and the Kuril Islands (for example, Finmarchinella [Barentsovia], Bythocytheromorpha, and Pectocythere). Because so few Quaternary microfaunas have been documented from the western Pacific, it is difficult to determine whether these forms are conspecific.

The third component has a modern distribution in colder water (subfrigid to frigid marine climates) than is currently present in the Aleutians. We interpret the presence of this component to indicate that the thermal regime at the time of deposition of these species was much colder. This colder water fauna has migrated from the Bering and Arctic Provinces of Asia and North America, and includes the ostracode species Elofsonella concinna neoconcinna, Finmarchinella (Barentsovia) barentzovoensis, and Eucytheridea punctillata.

Benthic foraminiferal assemblages from the Aleutian Islands samples contain numerous fossil species as well as cold-temperate species indigenous to the North Pacific. Elphidium clavatum is a common member of these assemblages and, in conjunction with E. bartletti, E. orbiculare, E. subarcticum, and Buccella frigida, represents the cold-arctic fauna which existed in this area during the glacial episodes. The occurrence of Cassidulina californica, Elphidiella groenlandica, and numerous other neritic species indicates the presence of cold-temperate Pacific faunas. These benthic foraminiferal species, like the cold-temperate ostracode species, are presently living in the Gulf of Alaska. Again, because organic stain was not used, it is unknown whether these species were living there at the time of collection.

This analysis suggests that: (1) During the Pleistocene, cold-arctic waters extended as far south as the Aleutian Islands; and (2) during the Holocene, cold-temperate water masses from the North Pacific have extended as far north as the Pribilof Islands.

REFERENCES CITED

Gardner, J. V., Vallier, T. L., Dean, W. E., Kvenvolden, K. A. and Redden, G. D., 1979, Sedimentology and geochemistry of surface sediments and the distribution of faults and potentially unstable sediments, St. George Basin region of the outer continental shelf, southern Bering Sea: U.S. Geological Survey Open-File Report 79-1562, 89 p.

U.S. Navy, Chief of Naval Operations, 1977, Marine climatic atlas of the world; volume 2, North Pacific Ocean: Washington, Naval Weather Service Detachment Report NAVAIR 50-1C-529, 388 p.

Reports on Alaska published by the U.S. Geological Survey in 1981

Compiled by Edward H. Cobb

Affolter, R. H., Simon, F. O., and Stricker, G. D., 1981, Chemical analyses of coal from the Healy, Kenai, Seldovia, and Utukok River 1:250,000 quadrangles, Alaska: U.S. Geological Survey Open-File Report 81-654, 88 p.

Albert, N. R. D., and Hudson, Travis, eds., 1981, The United States Geological Survey in Alaska: Accomplishments during 1979: U.S. Geological Survey Circular 823-B, p. B1-B151.

Aleinikoff, J. N., Dusel-Bacon, Cynthia, and Foster, H. L., 1981, Geochronologic studies in the Yukon-Tanana Upland, east-central Alaska, in Albert, N. R. D., and Hudson, Travis, eds., The United States Geological Survey in Alaska: Accomplishments during 1979: U.S. Geological Survey Circular 823-B, p. B34-B37.

Atwood, T. J., Bruns, T. R., Carlson, P. R., Molnia, B. F., and Plafker, George, 1981, Bathymetric maps of the northern Gulf of Alaska: U.S. Geological Survey Miscellaneous Field Studies Map MF-859, scale 1:250,000, 3 sheets.

Barnes, D. F., 1981, Gravity measurements useful in exploration and evaluation of the Nimiuktuk barite deposit, in Albert, N. R. D., and Hudson, Travis, eds., The United States Geological

Survey in Alaska: Accomplishments during 1979: U.S. Geological Survey Circular 823-B, p. B15-B17.

Bartsch-Winkler, Susan, and Huffman, A. C., 1981a, Compositional variation in sandstones of the Nanushuk Group, Arctic North Slope, in Albert, N. R. D., and Hudson, Travis, eds., The United States Geological Survey in Alaska: Accomplishments during 1979: U.S. Geological Survey Circular 823-B, p. B6-B8.

——1981b, Petrography of the Nanushuk Group and Torok Formation: U.S. Geological Survey Open-File Report 81-1222, 62 p.

Berg, H. C., 1981, Upper Triassic volcanogenic massive sulfide metallogenic province identified in southeastern Alaska, in Albert, N. R. D., and Hudson, Travis, eds., The United States Geological Survey in Alaska: Accomplishments during 1979: U.S. Geological Survey Circular 823-B, p. B104-B108.

Berg, H. C., Decker, J. E., and Abramson, B. S., 1981, Metallic mineral deposits of southeastern Alaska: U.S. Geological Survey Open-File Report 81-122, 136 p.

Bird, K. J., 1981a, Petroleum exploration of the North Slope in Alaska, U.S.A.: U.S. Geological Survey Open-File Report 81-227, 43 p.

——1981b, Machine-generated displays of well logs and lithology from selected wells of the North Slope of Alaska: 10 wells from the western part of the National Petroleum Reserve in Alaska (NPRA): U.S. Geological Survey Open-File Report 81-1032, 6 p. + 10 sheets.

——1981c, Machine-generated displays of well logs and lithology from selected wells on the North Slope of Alaska: 26 wells from the northern part of the National Petroleum Reserve in Alaska (NPRA): U.S. Geological Survey Open-File Report 81-1033, 6 p. + 26 sheets.

——1981d, Machine-generated displays of well logs and lithology from selected wells on the North Slope of Alaska: 11 wells from the northeastern part of the National Petroleum Reserve in Alaska (NPRA): U.S. Geological Survey Open-File Report 81-1034, 6 p. + 11 sheets.

——1981e, Machine-generated displays of well logs and lithology from selected wells on the North Slope of Alaska: 15 wells from the southeastern part of the National Petroleum Reserve in Alaska (NPRA): U.S. Geological Survey Open-File Report 81-1035, 6 p. + 15 sheets.

——1981f, Machine-generated displays of well logs and lithology from selected wells on the North Slope of Alaska: seven wells from the east-central North Slope: U.S. Geological Survey Open-File Report 81-1036, 6 p. + 7 sheets.

Bolm, J. G., 1981, Preliminary unevaluated map (1974) showing amounts of uplift in lower Cook Inlet, Alaska: U.S. Geological Survey Open-File Report 81-324, scale 1:190,000.

Bouma, A. H., 1981, Submarine topography and physiography of lower Cook Inlet, Alaska: U.S. Geological Survey Open-File Report 81-1335, 28 p.

Bowsher, A. L., and Tailleur, I. L., 1981a, Availability of petrographic thin-section slides from the Fortress Mountain Formation, central North Slope, Alaska: U.S. Geological Survey Open-File Report 81-1094, 7 p.

——1981b, Availability of cores and cuttings from the Ellesmerian strata of 16 test wells of National Petroleum Reserve in Alaska: U.S. Geological Survey Open-File Report 81-1171, 5 p.

Bowsher, A. L., Tailleur, I. L., and Gibson, H. A., 1981, Availability of petrographic thin-sections from thirty-five wells from National Petroleum Reserve in Alaska, North Slope, Alaska: U.S. Geological Survey Open-File Report 81-1307, 8 p.

Brew, D. A., and Ford, A. B., 1981, The Coast plutonic complex sill, southeastern Alaska, in Albert, N. R. D., and Hudson, Travis, eds., The United States Geological Survey in Alaska: Accomplishments during 1979: U.S. Geological Survey Circular 823-B, p. B96-B99.

Brew, D. A., Sonnevil, R. A., Hunt, S. J., and Ford, A. B., 1981, Newly recognized alkali granite stock, southwestern Kupreanof Island, Alaska, in Albert, N. R. D., and Hudson, Travis, eds., The United States Geological Survey in Alaska: Accomplishments during 1979: U.S. Geological Survey Circular 823-B, p. B108-B109.

Brosgé, W. P., Reiser, H. N., and Dutro, J. T., Jr., 1981, Significance of Middle Devonian clastic rocks in the eastern Brooks Range, Alaska, in Albert, N. R. D., and Hudson, Travis, eds., The United States Geological Survey in Alaska: Accomplishments during 1979: U.S. Geological Survey Circular 823-B, p. B24-B26.

Brosgé, W. P., Reiser, H. N., Dutro, J. T., Jr., and Detterman, R. L., 1981, Organic geochemical data for Mesozoic and Paleozoic shales, central and eastern Brooks Range, Alaska: U.S. Geological Survey Open-File Report 81-551, 17 p.

Brouwers, E. M., 1981, Tabulation of the ostracode assemblages and associated organisms from selected bottom grab samples taken in the northeast Gulf of Alaska, F.R.S. Townsend Cromwell Cruise EGAL-75-KC, 1975: U.S. Geological Survey Open-File Report 81-1314, 134 p.

Bruns, T. R., Atwood, T. J., and Childs, J. R., 1981, Free-air gravity anomaly map, Cross Sound to Icy Bay, northern Gulf of Alaska: U.S. Geological Survey Miscellaneous Field Studies Map MF-1306, scale 1:500,000.

Bruns, T. R., Childs, J. R., and Atwood, Thomas, 1981, Free-air gravity anomaly map, Dixon Entrance to Cross Sound, northeastern Gulf of Alaska: U.S. Geological Survey Miscellaneous Field Studies Map MF-1307, scale 1:500,000.

Burrows, R. L., Emmett, W. W., and Parks, Bruce, 1981, Sediment transport in the Tanana River near Fairbanks, Alaska, 1977-79: U.S. Geological Survey Water-Resources Investigations 81-20, 56 p. also available as U.S. National Technical Information Service Report ADA-105 363 .

Camp Dresser and McKee, Inc., 1981, Permit requirements for energy and other natural resources for the State of Alaska: U.S. Geological Survey Open-File Report 81-1249, 91 p.

Carlson, P. R., and Karl, H. A., 1981a, Seafloor geo-

logic hazards, sedimentology, and bathymetry, Navarin basin province, northwestern Bering Sea: U.S. Geological Survey Open-File Report 81-1217, 149 p.

——1981b, High-resolution seismic reflection profiles: Navarin Basin province, northern Bering Sea, 1980: U.S. Geological Survey Open-File Report 81-1221, 3 p. + 1 pl.

Carter, L. D., and Robinson, S. W., 1981, Minimum age of beach deposits north of Teshekpuk Lake, Arctic Coastal Plain, in Albert, N. R. D., and Hudson, Travis, eds., The United States Geological Survey in Alaska: Accomplishments during 1979: U.S. Geological Survey Circular 823-B, p. B8-B9.

Carter, R. D., 1981, National Petroleum Reserve in Alaska—data release, in Albert, N. R. D., and Hudson, Travis, eds., The United States Geological Survey in Alaska: Accomplishments during 1979: U.S. Geological Survey Circular 823-B, p. B3-B4.

Case, J. E., 1981, Magnetic expression and mineralization of some Tertiary plutons on Prince William Sound and the Alaskan Peninsula, southern Alaska abs., in Silberman, M. L., Field, C. W., and Berry, A. L., eds., Proceedings of the symposium on mineral deposits of the Pacific Northwest: Geological Society of America, Cordilleran Section Meeting, Corvallis, Oreg., 1980: U.S. Geological Survey Open-File Report 81-355, p. 29-30.

Case, J. E., Barnes, D. F., Detterman, R. L., Morin, R. L., and Sikora, R. F., 1981, Gravity anomaly and interpretation map of the Chignik and Sutwik Island quadrangles, Alaska: U.S. Geological Survey Miscellaneous Field Studies Map MF-1053-J, 5 p., scale 1:250,000.

Case, J. E., Cox, D. P., Detra, D. E., Detterman, R. L., and Wilson, F. H., 1981, Maps showing aeromagnetic survey and geologic interpretation of the Chignik and Sutwik Island quadrangles, Alaska: U.S. Geological Survey Miscellaneous Field Studies Map MF-1053-B, 8 p., scale 1:250,000, 2 sheets.

Chapman, R. M., Churkin, Michael, Jr., Carter, Claire, and Trexler, J. H., Jr., 1981, Ordovician graptolites and early Paleozoic radiolarians in the Lake Minchumina area date a regional shale and chert belt, in Albert, N. R. D., and Hudson, Travis, eds., The United States Geological Survey in Alaska: Accomplishments during 1979: U.S. Geological Survey Circular 823-B, p. B30-B34.

Chapman, R. M., and Yeend, Warren, 1981, Geologic reconnaissance of the east half of Kantishna River quadrangle and adjacent areas, in Albert, N. R. D., and Hudson, Travis, eds., The United States Geological Survey in Alaska: Accomplishments during 1979: U.S. Geological Survey Circular 823-B, p. B30-B32.

Childs, J. R., Cooper, A. K., and Wright, A. W., 1981, Residual magnetic map of Umnak Plateau region, southeastern Bering Sea: U.S. Geological Survey Geophysical Investigations Map GP-939, scale 1:1,000,000.

Childs, J. R., Scholl, D. W., and Vallier, Tracy, 1981, Onshore and offshore studies, Amlia Island area, Aleutian Ridge, in Albert, N. R. D., and Hudson, Travis, eds., The United States Geological Survey in Alaska: Accomplishments during 1979: U.S. Geological Survey Circular 823-B, p. B134-B137.

Cobb, E. H., compiler, 1981, Reports on Alaska published by the U.S. Geological Survey in 1979, in Albert, N. R. D., and Hudson, Travis, eds., The United States Geological Survey in Alaska: Accomplishments during 1979: U.S. Geological Survey Circular 823-B, p. B138-B145.

Cobb, E. H., 1981a, Summaries of data on and lists of references to metallic and selected nonmetallic mineral occurrences in the Skagway quadrangle, Alaska, supplement to Open-File Report 78-316; part A—Summaries of data to January 1, 1980: U.S. Geological Survey Open-File Report 81-82-A, p. A1-A10.

——1981b, Summaries of data on and lists of references to metallic and selected nonmetallic mineral occurrences in the Skagway quadrangle, Alaska, supplement to Open-File Report 78-316; part B--Lists of references to January 1, 1980: U.S. Geological Survey Open-File Report 81-82-B, p. B1-B9.

——1981c, Summaries of data on and lists of references to metallic and selected nonmetallic mineral occurrences in the Mount Fairweather quadrangle, Alaska, supplement to Open-File Report 78-316; part A—Summaries of data to January 1, 1980: U.S. Geological Survey Open-File Report 81-249-A, p. A1-A20.

——1981d, Summaries of data on and lists of references to metallic and selected nonmetallic mineral occurrences in the Mount Fairweather quadrangle, Alaska, supplement to Open-File Report 78-316; part B—Lists of references to January 1, 1980: U.S. Geological Survey Open-File Report 81-249-B. p. B1-B15.

——1981e, Summaries of data on and lists of references to metallic and selected nonmetallic mineral occurrences in the Bendeleben quadrangle, Alaska, supplement to Open-File Report 75-429; part A—Summaries of data to January 1, 1980: U.S. Geological Survey Open-File Report 81-363-A, p. A1-A25.

——1981f, Summaries of data on and lists of references to metallic and selected nonmetallic mineral occurrences in the Bendeleben quadrangle, Alaska, supplement to Open-File Report 75-429; part B—Lists of references to January 1, 1980: U.S. Geological Survey Open-File Report 81-363-B, p. B1-B26.

——1981g, Summaries of data on and lists of references to metallic and selected nonmetallic mineral occurrences in the Teller quadrangle, Alaska, supplement to Open-File Report 75-587; part A--Summaries of data to January 1, 1980: U.S. Geological Survey Open-File Report 81-364-A, p. A1-A25.

——1981h, Summaries of data on and lists of references to metallic and selected nonmetallic mineral occurrences in the Teller quadrangle, Alaska, supplement to Open-File Report 75-587; part B--Lists of references to January 1, 1980: U.S.

Geological Survey Open-File Report 81-364-B, p. B1-B25.

——1981i, Selected Geological Survey, U.S. Bureau of Mines, and Alaska Division of Geological and Geophysical Surveys reports and maps on Alaska released during 1980, indexed by quadrangle: U.S. Geological Survey Open-File Report 81-442, 164 p.

——1981j, Summaries of data on and lists of references to metallic and selected nonmetallic mineral occurrences in the Solomon quadrangle, Alaska, supplement to Open-File Report 78-181; part A--Summaries of data to January 1, 1981: U.S. Geological Survey Open-File Report 81-504-A, p. A1-A30.

——1981k, Summaries of data on and lists of references to metallic and selected nonmetallic mineral occurrences in the Solomon quadrangle, Alaska, supplement to Open-File Report 78-181; part B--Lists of references to January 1, 1981: U.S. Geological Survey Open-File Report 81-504-B, p. B1-B36.

——1981l, Summaries of data on and lists of references to metallic and selected nonmetallic mineral occurrences in the Wiseman quadrangle, Alaska, supplement to Open-File Report 76-340; part A--Summaries of data to January 1, 1981: U.S. Geological Survey Open-File Report 81-732-A, p. A1-A21.

——1981m, Summaries of data on and lists of references to metallic and selected nonmetallic mineral occurrences in the Wiseman quadrangle, Alaska, supplement to Open-File Report 76-340; part B—Lists of references to January 1, 1981: U.S. Geological Survey Open-File Report 81-732-B, p. B1-B21.

——1981n, Summaries of data on and lists of references to metallic and selected nonmetallic mineral occurrences in the Tanana quadrangle, Alaska, supplement to Open-File Report 77-432; part A--Summaries of data to June 1, 1981: U.S. Geological Survey Open-File Report 81-1313-A, p. A1-A23.

——1981o, Summaries of data on and lists of references to metallic and selected nonmetallic mineral occurrences in the Tanana quadrangle, Alaska, supplement to Open-File Report 77-432; part B--Lists of references to June 1, 1981: U.S. Geological Survey Open-File Report 81-1313-B, p. B1-B26.

——1981p, Summaries of data on and lists of references to metallic and selected nonmetallic mineral occurrences in the Livengood quadrangle, Alaska, supplement to Open-File Report 76-819; part A—Summaries of data to August 1, 1981: U.S. Geological Survey Open-File Report 81-1342-A, p. A1-A48.

——1981q, Summaries of data on and lists of references to metallic and selected nonmetallic mineral occurrences in the Livengood quadrangle, Alaska, supplement to Open-File Report 76-819; part B—Lists of references to August 1, 1981: U.S. Geological Survey Open-File Report 81-1342-B, p. B1-B54.

Cobb, E. H., and Chapman, R. M., 1981, Mineral occurrences (other than mineral fuels and construction materials) in the Kantishna River and Ruby quadrangles, Alaska: U.S. Geological Survey Open-File Report 81-170, 94 p.

Cobb, E. H., and Mayfield, C. F., 1981a, Summaries of data on and lists of references to metallic and selected nonmetallic mineral occurrences in the Ambler River quadrangle, Alaska, supplement to Open-File Report 75-628; part A—Summaries of data to January 1, 1981: U.S. Geological Survey Open-File Report 81-570-A, p. A1-A13.

——1981b, Summaries of data on and lists of references to metallic and selected nonmetallic mineral occurrences in the Ambler River quadrangle, Alaska; supplement to Open-File Report 75-628; part B—Lists of references to January 1, 1981: U.S. Geological Survey Open-File Report 81-570-B, p. B1-B11.

Cobb, E. H., Mayfield, C. F., and Brosgé,W. P., 1981a, Summaries of data on and lists of references to metallic and selected nonmetallic mineral occurrences in eleven quadrangles in northern Alaska, supplement to Open-File Report 75-628; part A—Summaries of data to January 1, 1981: U.S. Geological Survey Open-File Report 81-767-A, p. A1-A24.

——1981b, Summaries of data on and lists of references to metallic and selected nonmetallic mineral occurrences in eleven quadrangles in northern Alaska, supplement to Open-File Report 75-628; part B—Lists of references to January 1, 1981: U.S. Geological Survey Open-File Report 81-767-B, p. B1-B14.

Cobb, E. H., and Miller, T. P., 1981a, Summaries of data on and lists of references to metallic and selected nonmetallic mineral occurrences in the Hughes, Kotzebue, Melozitna, Selawik, and Shungnak quadrangles, west-central Alaska, supplement to Open-File Report 75-627; part A—Summaries of data to January 1, 1981: U.S. Geological Survey Open-File Report 81-847-A, p. A1-A14.

——1981b, Summaries of data on and lists of references to metallic and selected nonmetallic mineral occurrences in the Hughes, Kotzebue, Melozitna, Selawik, and Shungnak quadrangles, west-central Alaska, supplement to Open-File Report 75-627; part B—Lists of references to January 1, 1981: U.S. Geological Survey Open-File Report 81-847-B, p. B1-B13.

Cobb, E. H., and Reed, B. L., 1981a, Summaries of data on and lists of references to metallic and selected nonmetallic mineral occurrences in the Iliamna, Lake Clark, Lime Hills, and McGrath quadrangles, Alaska, supplement to Open-File Report 76-485; part A—Summaries to January 1, 1981: U.S. Geological Survey Open-File Report 81-1343-A, p. A1-A25.

——1981b, Summaries of data on and lists of references to metallic and selected nonmetallic mineral occurrences in the Iliamna, Lake Clark, Lime Hills, and McGrath quadrangles, Alaska, supplement to Open-File Report 76-485; part B—Lists of references to January 1, 1981: U.S. Geological Survey Open-File Report 81-1343-B, p. B1-B20.

Coffman, J. L., and Stover, C. W., 1979, United States

earthquakes, 1977: U.S. National Technical Information Service Report PB-300 863, 81 p.

Coney, P. J., Silberling, N. J., Jones, D. L., and Richter, D. H., 1981, Structural relations along the leading edge of the Wrangellia terrane in the Clearwater Mountains, Alaska, in Albert, N. R. D., and Hudson, Travis, eds., The United States Geological Survey in Alaska: Accomplishments during 1979: U.S. Geological Survey Circular 823-B, p. B53, B56-B59.

Cooper, A. K., Marlow, M. S., Parker, A. W., and Childs, J. R., 1981, Structure-contour map on acoustic basement in the Bering Sea: U.S. Geological Survey Miscellaneous Field Studies Map MF-1165, scale 1:2,500,000.

Csejtey, Béla, Jr., and St. Aubin, D. R., 1981, Evidence for northwestward thrusting of the Talkeetna superterrane, and its regional significance, in Albert, N. R. D., and Hudson, Travis, eds., The United States Geological Survey in Alaska: Accomplishments during 1979: U.S. Geological Survey Circular 823-B, p. B49-B51.

Dahlin, D. C., Rule, A. R., and Brown, L. L., 1981, Beneficiation of potential platinum resources from southeastern Alaska: U.S. Bureau of Mines Report of Investigations 8553, 14 p.

Dearborn, L. L., and Schaefer, D. H., 1981, Surficial geophysical data for two cross-valley lines in the middle Eagle River valley, Alaska: U.S. Geological Survey Open-File Report 80-2000, 14 p.

Decker, John, and Johnson, B. R., 1981, The nature and position of the Border Ranges fault on Chichagof Island, in Albert, N. R. D., and Hudson, Travis, eds., The United States Geological Survey in Alaska: Accomplishments during 1979: U.S. Geological Survey Circular 823-B, p. B102-B104.

Decker, John, Mullen, M. W., and Schwab, C. E., 1981, Aeromagnetic profile map of southeastern Alaska: U.S. Geological Survey Open-File Report 81-505, scale 1:1,000,000.

Detra, D. E., Risoli, D. A., O'Leary, R. M., Hurrell, J. A., and Everman, W. E., 1981, Analytical data and statistical summary from the analyses of stream-sediment and heavy-mineral-concentrate samples collected in Bristol Bay, Ugashik, and Karluk quadrangles, Alaska: U.S. Geological Survey Open-File Report 81-963, 88 p.

Detterman, R. L., Allaway, W. H., Jr., O'Leary, R. M., Houston, David, and Risoli, D. A., 1981, Sample location map and analytical data for rock samples collected in 1980, Ugashik and Karluk quadrangles, Alaska: U.S. Geological Survey Open-File Report 81-173, scale 1:250,000.

Detterman, R. L., Allaway, W. H., Jr., and Rossiter, R. H., 1981, Locality map and scintillometer data for the Ugashik and Karluk quadrangles, Alaska: U.S. Geological Survey Open-File Report 81-253, scale 1:250,000.

Detterman, R. L., Case, J. E., Cox, D. P., Detra, D. E., Miller, T. P., and Wilson, F. H., 1981, The Alaskan Mineral Resource Assessment Program: Background information to accompany folio of geologic and resource maps of the Chignik and Sutwik Island quadrangles, Alaska: U.S. Geological Survey Circular 802, 16 p.

Detterman, R. L., Miller, T. P., Yount, M. E., and Wilson, F. H., 1981a, Geologic map of the Chignik and Sutwik Island quadrangles, Alaska: U.S. Geological Survey Miscellaneous Investigations Series Map I-1229, scale 1:250,000.

——1981b, Quaternary geologic map of the Chignik and Sutwik Island quadrangles, Alaska: U.S. Geological Survey Miscellaneous Investigations Series Map I-1292, scale 1:250,000.

Detterman, R. L., and Spicer, R. A., 1981, New stratigraphic assignment for rocks along Igilatvik (Sabbath) Creek, William O. Douglas Arctic Wildlife Range, Alaska, in Albert, N. R. D., and Hudson, Travis, eds., The United States Geological Survey in Alaska: Accomplishments during 1979: U.S. Geological Survey Circular 823-B, p. B11-B12.

Detterman, R. L., Yount, M. E., and Case, J. E., 1981, Megafossil sample locality map, checklists, and stratigraphic sections of the Chignik and Sutwik Island quadrangles, Alaska: U.S. Geological Survey Miscellaneous Field Studies Map MF-1053-N, scale 1:250,000, 2 sheets.

Dickenson, K. A., and Roberts, M. E., 1981, Summary of radiometric anomalies in Alaska—collected under contract with the U.S. Department of Energy: U.S. Geological Survey Open-File Report 81-428.

Dolton, G. L., Carlson, K. H., Charpentier, R. R., Coury, A. B., Crovelli, R. A., Frezon, S. E., Kahn, A. S., Lister, J. H., McMullin, R. H., Pike, R. S., Powers, R. B., Scott, E. W., and Varnes, K. L., 1981, Estimates of undiscovered recoverable resources of conventionally producible oil and gas in the United States, a summary: U.S. Geological Survey Open-File Report 81-192, 17 p.

Duffield, W. A., and Guffanti, Marianne, 1981, The geothermal research program of the U.S. Geological Survey: U.S. Geological Survey Open-File Report 81-564, 105 p.

Dutro, J. T., Jr., Armstrong, A. K., Douglass, R. C., and Mamet, B. L., 1981, Carboniferous biostratigraphy, southeastern Alaska, in Albert, N. R. D., and Hudson, Travis, eds., The United States Geological Survey in Alaska: Accomplishments during 1979: U.S. Geological Survey Circular 823-B, p. B94-B96.

Dutro, J. T., Jr., and Patton, W. W., Jr., 1981, Lower Paleozoic platform carbonate sequence in the Medfra quadrangle, west-central Alaska, in Albert, N. R. D., and Hudson, Travis, eds., The United States Geological Survey in Alaska: Accomplishments during 1979: U.S. Geological Survey Circular 823-B, p. B42-B44.

Egbert, R. M., 1981, Petrography and provenance of Upper Cretaceous sandstone from Saddle Mountain in the Iniskin-Tuxedni area, lower Cook Inlet, Alaska, in Albert, N. R. D., and Hudson, Travis, eds., The United States Geological Survey in Alaska: Accomplishments during 1979: U.S. Geological Survey Circular 823-B, p. B88-B90.

Egbert, R. M., and Magoon, L. B., 1981, Petrography,

provenance, and tectonic significance of Middle and Upper Jurassic sandstone from Tuxedni Bay, Cook Inlet, Alaska, in Albert, N. R. D., and Hudson, Travis, eds., The United States Geological Survey in Alaska: Accomplishments during 1979: U.S. Geological Survey Circular 823-B, p. B86-B88.

Elliott, R. L., Koch, R. D., and Robinson, S. W., 1981, Age of basalt flows in the Blue River valley, Bradfield Canal quadrangle, in Albert, N. R. D., and Hudson, Travis, eds., The United States Geological Survey in Alaska: Accomplishments during 1979: U.S. Geological Survey Circular 823-B, p. B115-B116.

Epstein, J. B., 1981, Map of the United States showing distances from urban areas having populations greater than 2,500: U.S. Geological Survey Open-File Report 81-157, scale 1:7,500,000.

Fabiano, E. B., and Peddie, N. W., 1981, Magnetic total intensity in the United States—Epoch 1980: U.S. Geological Survey Miscellaneous Investigations Series Map I-1370, scale 1:5,000,000.

Feulner, A. J., and Williams, J. R., 1981, Further notes on the ground-water supply beneath Selin Creek near Cape Lisburne, northwestern Alaska, in Albert, N. R. D., and Hudson, Travis, eds., The United States Geological Survey in Alaska: Accomplishments during 1979: U.S. Geological Survey Circular 823-B, p. B12-B14.

Fisher, M. A., Holmes, M. L., and Patton, W. W., Jr., 1981, Preliminary interpretation of the geologic structure beneath the northern Bering Sea shelf, including Norton Basin, in Albert, N. R. D., and Hudson, Travis, eds., The United States Geological Survey in Alaska: Accomplishments during 1979: U.S. Geological Survey Circular 823-B, p. B118-B121.

Fisher, M. A., Moore, G. W., von Huene, R oland , and McClellan, P. H., 1981, Map of marine magnetic data from Shelikof Strait to Sutwik Island, Alaska: U.S. Geological Survey Miscellaneous Field Studies Map MF-1227, scale 1:500,000.

Fisher, M. A., Patton, W. W., Jr., and Holmes, M. A., 1981, Geology and petroleum potential of the Norton basin area, Alaska: U.S. Geological Survey Open-File Report 81-1316, 51 p.

Ford, A. B., and Brew, D. A., 1981, Orthogneiss of Mount Juneau—an early phase of Coast Mountain plutonism involved in Barrovian regional metamorphism near Juneau, in Albert, N. R. D., and Hudson, Travis, eds., The United States Geological Survey in Alaska: Accomplishments during 1979: U.S. Geological Survey Circular 823-B, p. B99-B102.

Foster, H. L., 1981, A minimum age for Prindle Volcano, Yukon-Tanana Upland, in Albert, N. R. D., and Hudson, Travis, eds., The United States Geological Survey in Alaska: Accomplishments during 1979: U.S. Geological Survey Circular 823-B, p. B37-B38.

Gibson, H. A., and Bowsher, A. L., 1981, Availability of foraminifera and palynomorph reports from shothole samples of National Petroleum Reserve in Alaska: U.S. Geological Survey Open-File Report 81-1340, 3 p.

Gough, L. P., and Severson, R. C., 1981, Element concentrations in rehabilitation species from thirteen coal-stripmines in five western states and Alaska: U.S. Geological Survey Open-File Report 81-182, 110 p.

Grantz, Arthur, and Greenberg, Jonathan, 1981a, Map showing tracklines of high resolution Uniboom seismic reflection profiles collected August 26 through September 19, 1978, in the Chukchi Sea: U.S. Geological Survey Open-File Report 81-33, scale 1:000,000.

———1981b, Map showing tracklines of high-resolution Uniboom seismic reflection profiles collected August 25 through October 5, 1977, in the Beaufort Sea: U.S. Geological Survey Open-File Report 81-34, scales 1:500,000, 1:1,000,000.

Greenberg, Jonathan, Hart, P. E., and Grantz, Arthur, 1981, Bathymetric map of the continental shelf, slope, and rise of the Beaufort Sea north of Alaska: U.S. Geological Survey Miscellaneous Investigations Series Map I-1182-A, 6 p., scale 1:500,000.

Gromḿe, Sherman, and Hillhouse, J. W., 1981, Paleomagnetic evidence for northward movement of the Chugach terrane, southern and southeastern Alaska, in Albert, N. R. D., and Hudson, Travis, eds., The United States Geological Survey in Alaska: Accomplishments during 1979: U.S. Geological Survey Circular 823-B, p. B70-B72.

Grybeck, D. J., McDanal, S. K., Cooley, E. F., and O'Leary, R. M., 1981, Map of anomalous rock samples and histograms of trace metals in rocks of the Survey Pass quadrangle, Brooks Range, Alaska: U.S. Geological Survey Miscellaneous Field Studies Map MF-1176-E, scale 1:250,000.

Grybeck, D. J., and Nelson, S. W., 1981a, Map and interpretation of the structural geology of the Survey Pass quadrangle, Brooks Range, Alaska: U.S. Geological Survey Miscellaneous Field Studies Map MF-1176-B, scale 1:250,000.

———1981b, Mineral deposit map of the Survey Pass quadrangle, Brooks Range, Alaska: U.S. Geological Survey Miscellaneous Field Studies Map MF-1176-F, scale 1:250,000.

Guild, P. W., 1981a, Preliminary metallogenic map of North America: A numerical listing of deposits: U.S. Geological Survey Circular 858-A, p. A1-A93.

———1981b, Preliminary metallogenic map of North America: An alphabetical listing of deposits: U.S. Geological Survey Circular 858-B, p. B1-B72.

Guild, P. W., McCartney, W. D., Leech, G. B., Dengo, Gabriel, Ellitsgaard-Rasmussen, K., Salas, G. P., and Reyna, J. G., compilers, 1981, Preliminary metallogenic map of North America: U.S. Geological Survey, scale 1:5,000,000, 4 sheets.

Hamilton, T. D., 1980, Surficial geologic map of the Killik River quadrangle, Alaska: U.S. Geological Survey Miscellaneous Field Studies Map MF-1234, scale 1:250,000.

——1981a, Episodic Holocene alluviation in the central Brooks Range: Chronology, correlations, and climatic implications, in Albert, N. R. D., and Hudson, Travis, eds., The United States Geo-

logical Survey in Alaska: Accomplishments during 1979: U.S. Geological Survey Circular 823-B, p. B21-B24.

——1981b, Surficial geologic map of the Survey Pass quadrangle, Alaska: U.S. Geological Survey Miscellaneous Field Studies Map MF-1320, scale 1:250,000.

Hampton, M. A., 1981, Grain size and composition of seafloor sediment, Kodiak Shelf, Alaska: U.S. Geological Survey Open-File Report 81-659, 78 p.

Hampton, M. A., and Bouma, A. H., 1980, Notes on the acquisition of high-resolution seismic reflection profiles, side-scanning sonar records, and sediment samples from lower Cook Inlet and Kodiak Shelf, R/V SEA SOUNDER cruise S8-79-WG, July-August, 1979: U.S. Geological Survey Open-File Report 80-985, 52 p. (unnumbered).

Hampton, M. A., Johnson, K. H., Torresan, M. E., and Winters, W. J., 1981, Description of seafloor sediment and preliminary geo-environmental report, Shelikof Strait, Alaska: U.S. Geological Survey Open-File Report 81-1133, 87 p.

Hein, J. R., McLean, Hugh, and Vallier, T. L., 1981, Reconnaissance geologic map of Atka and Amlia Islands, Alaska: U.S. Geological Survey Open-File Report 81-159, scale 1:125,000.

Hessin, T. D., Speckman, W. S., Crenshaw, G. L., Hoffman, J. D., and Cooley, E. F., 1980, Analytical results of various types of samples taken in the West Chichagof-Yakobi Wilderness Study Area, Sitka quadrangle, southeastern Alaska: U.S. Geological Survey Open-File Report 80-905, 72 p.

Hillhouse, J. W., and Grommé, Sherman, 1981a, Paleolatitude of Trassic basalt in the Clearwater Mountains, south-central Alaska, in Albert, N. R. D., and Hudson, Travis, eds., The United States Geological Survey in Alaska: Accomplishments durin 1979: U.S. Geological Survey Circular 823-B, p. B55-B56.

——1981b, Paleomagnetic investigation in the Chulitna terrane, south-central Alaska, in Albert, N. R. D., and Hudson, Travis, eds., The United States Geological Survey in Alaska: Accomplishments during 1979: U.S. Geological Survey Circular 823-B, p. B58-B61.

Himmelberg, G. R., and Loney, R. A., 1981, Petrology of the ultramafic and gabbroic rocks of the Brady Glacier nickel-copper deposit, Fairweather Range, southeastern Alaska: U.S. Geological Survey Professional Paper 1195, 26 p.

Hitzman, M. W., 1981, Geology of the BT claim group, southwestern Brooks Range, Alaska, in Silberman, M. L., Field, C. W., and Berry, A. L., eds., Proceedings of the symposium on mineral deposits of the Pacific Northwest: Geological Society of America, Cordilleran Section Meeting, Corvallis, Oreg., 1980: U.S. Geological Survey Open-File Report 81-355, p. 17-28.

Hoare, J. M., and Jones, D. L., 1981, Lower Paleozoic radiolarian chert and associated rocks in the Tikchik Lakes area, southwestern Alaska, in Albert, N. R. D., and Hudson, Travis, eds., The United States Geological Survey in Alaska: Accomplishments during 1979: U.S. Geological Survey Circular 823-B, p. B44-B45.

Holser, A. F., Rowland, R. W., and Goud, M. R., 1981, A compilation of subsea energy and mineral resources of the United States including its possessions and trust territory of the Pacific Islands: U.S. Geological Survey Miscellaneous Field Studies Map MF-1360, scale 1:20,000,000.

Hoose, P. J., Steffy, D. A., and Lybeck, L. D., 1981, Isopach map of Quaternary and upper Tertiary strata, Norton Sound, Alaska: U.S. Geological Survey Open-File Report 81-723, scale 1:250,000.

Hudson, Travis, and Plafker, George, 1981, Emplacement age of the Crillon-La Perouse pluton, Fairweather Range, in Albert, N. R. D., and Hudson, Travis, eds., The United States Geological Survey in Alaska: Accomplishments during 1979: U.S. Geological Survey Circular 823-B, p. B90-B94.

Imlay, R. W., 1981, Early Jurassic ammonites from Alaska: U.S. Geological Survey Professional Paper 1148, 49 p. + 12 pls.

Jones, D. L., Berg, H. C., Coney, Peter, and Harris, Anita, 1981, Structural and stratigraphic significance of Upper Devonian and Mississippian fossils from the Cannery Formation, Kupreanof Island, southeastern Alaska, in Albert, N. R. D., and Hudson, Travis, eds., The United States Geological Survey in Alaska: Accomplishments during 1979: U.S. Geological Survey Circular 823-B, p. B109-B112.

Jones, D. L., Silberling, N. J., Berg, H. C., and Plafker, George, 1981, Map showing tectonostratigraphic terranes of Alaska, columnar sections, and summary description of terranes: U.S. Geological Survey Open-File Report 81-792, 20 p. + 2 pls., scale 1:2,500,000.

Jones, D. L., Silberling, N. J., Wardlaw, Bruce, and Richter, Don, 1981, Revised ages of Paleozoic and Mesozoic rocks in the Talkeetna quadrangle, south-central Alaska, in Albert, N. R. D., and Hudson, Travis, eds., The United States Geological Survey in Alaska: Accomplishments during 1979: U.S. Geological Survey Circular 823-B, p. B46-B49.

Jones, D. M., Kingston, M. J., Marlow, M. S., Cooper, A. K., Barron, J. A., Wingate, F. H., and Arnal, R. E., 1981, Age, mineralogy, physical properties, and geochemistry of dredge samples from the Bering Sea continental margin: U.S. Geological Survey Open-File Report 81-1297, 69 p.

Jones, D. R., and Morley, J. M., 1981, Equal-area base map of the Bering Sea; plate 2, Southern Bering shelf: U.S. Geological Survey Open-File Report 81-456, scale 1:1,000,000.

Jones, D. R., and Swenson, P. A., 1981, Equal-area base map of the Bering Sea; plate 4, Aleutian east: U.S. Geological Survey Open-File Report 81-458, scale 1:1,000,000.

Keefer, D. K., and Tannaci, N. E., 1981, Bibliography on landslides, soil liquefaction, and related ground failures in selected historic earthquakes: U.S. Geological Survey Open-File Report 81-572, 38 p.

Keith, T. E. C., Barnes, Ivan, and Foster, H. L., 1981, Laumontite occurrences in the Circle A-1 quadrangle, Alaska, in Albert, N. R. D., and Hudson, Travis, eds., The United States Geological Survey in Alaska: Accomplishments during 1979: U.S. Geological Survey Circular 823-B, p. B28-B29.

Keith, T. E. C., Foster, H. L., Foster, R. L., Post, E. V., and Lehmbeck, W. L., 1981. Geology of an alpine-type peridotite in the Mount Sorenson area, east-central Alaska: U.S. Geological Survey Professional Paper 1170-A, p. A1-A9.

Keith, T. E. C., Presser, T. S., and Foster, H. L., 1981, New chemical and isotope data for the hot springs along Big Windy Creek, Circle A-1 quadrangle, Alaska, in Albert, N. R. D., and Hudson, Travis, eds., The United States Geological Survey in Alaska: Accomplishments during 1979: U.S. Geological Survey Circular 823-B, p. B25, B27-B28.

Kisslinger, C., Billington, S., Bowman, R., Harrison, J. C., Ihnen, S., Meertens, C., Pohlman, J., Sougstad, K., and Morrissey, S. T., 1981, A field study of earthquake prediction methods in the central Aleutian Islands: U.S. Geological Survey Open-File Report 81-384, 51 p.

Kisslinger, C., Billington, S., Bowman, R., Ihnen, S., Cruz, G., Pohlman, J., Sougstad, K., and Morrissey, S. T., 1981, A field study of earthquake prediction methods in the central Aleutian Islands: U.S. Geological Survey Open-File Report 81-937, 57 p.

Koch, R. D., and Elliott, R. L., 1981a, Maps showing distribution and abundance of gold and silver in geochemical samples from the Bradfield Canal quadrangle, southeastern Alaska: U.S. Geological Survey Open-File Report 81-728-C, 2 sheets, scales 1:250,000, 1:500,000.

——1981b, Maps showing distribution and abundance of copper in geochemical samples from the Bradfield Canal quadrangle, southeastern Alaska: U.S. Geological Survey Open-File Report 81-728-D, scale 1:250,000, 4 sheets.

——1981c, Maps showing distribution and abundance of lead in geochemical samples from the Bradfield Canal quadrangle, southeastern Alaska: U.S. Geological Survey Open-File Report 81-728-E, scales 1:250,000, 1:500,000, 4 sheets

——1981d, Maps showing distribution and abundance of zinc in geochemical samples from the Bradfield Canal quadrangle, southeastern Alaska: U.S. Geological Survey Open-File Report 81-728-F, scales 1:250,000, 1:500,000, 4 sheets

——1981e, Maps showing distribution and abundance of molybdenum in geochemical samples from the Bradfield Canal quadrangle, southeastern Alaska: U.S. Geological Survey Open-File Report 81-728-G, scales 1:250,000, 1:500,000, 2 sheets.

——1981f, Maps showing distribution and abundance of tin in geochemical samples from the Bradfield Canal quadrangle, southeastern Alaska: U.S. Geological Survey Open-File Report 81-728-H, scales 1:250,000, 1:500,000, 2 sheets.

——1981g, Maps showing distribution and abundance of beryllium in geochemical samples from the Bradfield Canal quadrangle, southeastern Alaska: U.S. Geological Survey Open-File Report 81-718-I, scale 1:250,000, 2 sheets.

——1981h, Maps showing distribution and abundance of niobium in geochemical samples from the Bradfield Canal quadrangle, southeastern Alaska: U.S. Geological Survey Open-File Report 81-728-J, scales 1:250,000, 1:500,000, 2 sheets.

——1981i, Maps showing distribution and abundance of yttrium in geochemical samples from the Bradfield Canal quadrangle, southeastern Alaska: U.S. Geological Survey Open-File Report 81-728-K, scales 1:250,000, 1:500,000, 2 sheets.

Koch, R. D., Elliott, R. L., O'Leary, R. M., and Risoli, D. A., 1980, Trace-element data for rock samples from the Bradfield Canal quadrangle, southeastern Alaska: U.S. Geological Survey Open-File Report 80-910A, 256 p.

Koch, R. D., Elliott, R. L., and Rossiter, Richard, 1981, Total gamma ray intensities at ground stations in the Bradfield Canal quadrangle, southeastern Alaska: U.S. Geological Survey Open-File Report 81-840, scales 1:125,000, 1:250,000, 2 sheets.

Lahr, J. C., and Stephens, C. D., 1981, Review of earthquake activity and current status of seismic monitoring in the region of the Bradley Lake hydroelectric project, southern Kenai Peninsula, Alaska: U.S. Geological Survey Open-File Report 81-736, 21 p. + 12 figs.

Lange, I. M., Nokleberg, W. J., Plahuta, J. T., Krouse, H. R., Doe, B. R., and Jansons, Uldis, 1981, Isotopic geochemistry of stratiform zinc-lead-barium deposits, Red Dog Creek and Drenchwater Creek areas, northwestern Brooks Range, Alaska, in Silberman, M. L., Field, C. W., and Berry, A. L., eds., Proceedings of the symposium on mineral deposits of the Pacific Northwest: Geological Society of America, Cordilleran Section Meeting, Corvallis, Oreg., 1980: U.S. Geological Survey Open-File Report 81-355, p. 1-14.

Le Compte, J. R., 1981a, Maps showing interpretation of Landsat imagery of the Survey Pass quadrangle, Brooks Range, Alaska: U.S. Geological Survey Miscellaneous Field Studies Map MF-1176-H, scale 1:250,000, 2 sheets.

———1981b, Maps showing interpretation of Landsat imagery of the Medfra quadrangle, Alaska: U.S. Geological Survey Open-File Report 80-811-D, scale 1:250,000, 2 sheets.

———1981c, Map showing interpretation of Landsat imagery of the Valdez 1, x 3, quadrangle, southern Alaska: U.S. Geological Survey Open-File Report 80-892-F, scale 1:250,000.

———1981d, Maps showing interpretation of Landsat imagery of the Bradfield Canal quadrangle, southeastern Alaska: U.S. Geological Survey Open-File Report 81-728-L, scale 1:250,000, 2 sheets.

——1981e, Preliminary maps showing interpretation of Landsat imagery of the Healy quadrangle, Alaska: U.S. Geological Survey Open-File Report 81-768, scale 1:250,000, 2 sheets.

——1981f, Preliminary maps showing interpretation of Landsat imagery of the Ugashik and Karluk

quadrangles, Alaska: U.S. Geological Survey Open-File Report 81-776, scale 1:250,000, 2 sheets.

———1981g, Landsat features maps of the Circle quadrangle, Alaska: U.S. Geological Survey Open-File Report 81-782, scale 1:250,000, 2 sheets.

———1981h, Landsat features maps of the Petersburg quadrangle and vicinity, southeastern Alaska: U.S. Geological Survey Open-File Report 81-799, scale 1:250,000, 2 sheets.

———1981i, Landsat features maps of the Ketchikan and Prince Rupert quadrangles, Alaska: U.S. Geological Survey Open-File Report 81-1139, scale 1:250,000, 2 sheets.

Le Compte, J. R., and Steele, W. C., 1981a, Landsat data interpretation in the south-central Brooks Range and in southeastern Alaska, in Albert, N. R. D., and Hudson, Travis, eds., The United States Geological Survey in Alaska: Accomplishments during 1979: U.S. Geological Survey Circular 823-B, p. B1-B3.

———1981b, Maps showing interpretation of Landsat imagery of the Chignik and Sutwik Island quadrangles, Alaska: U.S. Geological Survey Miscellaneous Field Studies Map MF-1053-O, scale 1:250,000, 2 sheets.

Luepke, Gretchen, and Leong, K. W., 1981, Areal and textural distribution of particulate gold in sediments from Bluff Beach, Alaska: U.S. Geological Survey Open-File Report 81-1085, 39 p.

Luthy, S. T., Foster, H. L., and Cushing, G. W., 1981, Petrographic and chemical data on Cretaceous granitic rocks of the Big Delta quadrangle, Alaska: U.S. Geological Survey Open-File Report 81-398, 12 p.

Luttrell, G. W., Hubert, M. L., Wright, W. B., Jussen, V. M., and Swanson, R. W., 1981, Lexicon of geologic names of the United States for 1968-1975: U.S. Geological Survey Bulletin 1520, 342 p.

MacKevett, E. M., Jr., Armstrong, A. K., Potter, R. W., II, and Silberman, M. L., 1981, Kennecott-type copper deposits, Wrangell Mountains, Alaska—an update and summary [abs.], in Silberman, M. L., Field, C. W., and Berry, A. L., eds., Proceedings of the symposium on mineral deposits of the Pacific Northwest: Geological Society of America, Cordilleran Section Meeting, Corvallis, Oreg., 1980: U.S. Geological Survey Open-File Report 81-355, p. 50-51.

Madison, R. J., 1981, Effects of placer mining on hydrologic systems in Alaska—status of knowledge: U.S. Geological Survey Open-File Report 81-217, 25 p.

Marlow, M. S., Carlson, P., Cooper, A. K., Karl, H., McLean, H., McMullin, R., and Lynch, M. B., 1981, Hydrocarbon resource report for proposed OCS sale no. 83, Navarin Basin, Alaska: U.S. Geological Survey Open-File Report 81-252, 83 p.

McClellan, P. H., and Giovannetti, D. M., 1981, New invertebrate fossils, but still no land vertebrates, from nonmarine Tertiary rocks of the Kenai Peninsula, Alaska, in Albert, N. R. D., and Hudson, Travis, eds., The United States Geological Survey in Alaska: Accomplishments during 1979: U.S. Geological Survey Circular 823-B, p. B84-B86.

Menzie, W. D., Foster, H. L., and Mosier, D. L., 1981, Metalliferous mineral resource potential of the Big Delta quadrangle, in Albert, N. R. D., and Hudson, Travis, eds., The United States Geological Survey in Alaska: Accomplishments during 1979: U.S. Geological Survey Circular 823-B, p. B38-B39.

Meyer, William, and Patrick, Leslie, 1980, Effects of artificial-recharge experiments at Ship Creek alluvial fan on water levels at Spring Acres Subdivision, Anchorage, Alaska: U.S. Geological Survey Open-File Report 80-1284, 42 p.

Miller, T. P., and Lanphere, M. A., 1981, K-Ar age measurements on obsidian from the Little Indian River locality in interior Alaska, in Albert, N. R. D., and Hudson, Travis, eds., The United States Geological Survey in Alaska: Accomplishments during 1979: U.S. Geological Survey Circular 823-B, p. B39-B42.

Minsch, J. H., Stover, C. W., Person, W. J., and Smith, P. K., 1980, Earthquakes in the United States, July-September 1979: U.S. Geological Survey Circular 836-C, p. C1-C39.

Minsch, J. H., Stover, C. W., Reagor, B. G., and Smith, P. K., 1981, Earthquakes in the United States, July-September 1980: U.S. Geological Survey Circular 853-C, p. C1-C42.

Mitchell, P. A., Silberman, M. L., and O'Neil, J. R., 1981a, Genesis of gold vein mineralization in an Upper Cretaceous turbidite sequence, Hope-Sunrise district, southern Alaska: U.S. Geological Survey Open-File Report 81-103, 18 p.

———1981b, Genesis of gold vein mineralization in an Upper Cretaceous turbidite sequence, Hope-Sunrise district, southern Alaska, in Silberman, M. L., Field, C. W., and Berry, A. L., eds., Proceedings of the symposium on mineral deposits of the Pacific Northwest, Geological Society of America, Cordilleran Section meeting at Corvallis, Oregon, March 20-21, 1980: U.S. Geological Survey Open-File Report 81-355, p. 33-49 [also released as U.S. Geological Survey Open-File Report 81-103].

Molenaar, C. M., 1981a, Depositional history of the Nanushuk Group and related strata, in Albert, N. R. D., and Hudson, Travis, eds., The United States Geological Survey in Alaska: Accomplishments during 1979: U.S. Geological Survey Circular 823-B, p. B4-B6.

———1981b, Depositional history and seismic stratigraphy of Lower Cretaceous rocks, National Petroleum Reserve in Alaska and adjacent areas: U.S. Geological Survey Open-File Report 81-1084, 42 p.

Molenaar, C. M., Egbert, R. M., and Krystinik, L. F., 1981, Depositional facies, petrography, and reservoir potential of the Fortress Mountain Formation (Lower Cretaceous), central North Slope, Alaska: U.S. Geological Survey Open-File Report 81-967, 32 p.

Moll, E. J., Silberman, M. L., and Patton, W. W., Jr., 1981, Chemistry, mineralogy, and K-Ar ages of igneous and metamorphic rocks of the Medfra quadrangle, Alaska: U.S. Geological Survey

Open-File Report 80-811C, 19 p. + 2 sheets, scale 1:250,000, 2 sheets.

Molnia, B. F., 1981a, Distribution of gas-charged sediment and pockmarks in the northeastern Gulf of Alaska, Yakutat Bay to Cross Sound, in Albert, N. R. D., and Hudson, Travis, eds., The United States Geological Survey in Alaska: Accomplishments during 1979: U.S. Geological Survey Circular 823-B, p. B125-B126.

——1981b, Depth changes in Icy Bay, Alaska, caused by sedimentation and melting of ice-cored moraine, in Albert, N. R. D., and Hudson, Travis, eds., The United States Geological Survey in Alaska: Accomplishments during 1979: U.S. Geological Survey Circular 823-B, p. B125-B128.

Morley, J. M., and Jones, D. R., 1981a, Equal-area base map of the Bering Sea; plate 1, Northern Bering shelf: U.S. Geological Survey Open-File Report 81-455, scale 1:1,000,000.

_____1981b, Equal-area base map of the Bering Sea; plate 3, Bowers Ridge: U.S. Geological Survey Open-File Report 81-457, scale 1:1,000,000.

Morrissey, L. A., and Ennis, R. A., 1981, Vegetation mapping of the National Petroleum Reserve in Alaska using Landsat digital data: U.S. Geological Survey Open-File Report 81-315, 25 p.

Murchey, B. L., Swain, P. B., and Curtis, Steven, 1981, Late Mississippian to Pennsylvanian radiolarian assemblages in the Siksikpuk(?) Formation at Nigu Bluff, Howard Pass quadrangle, Alaska, in Albert, N. R. D., and Hudson, Travis, eds., The United States Geological Survey in Alaska: Accomplishments during 1979: U.S. Geological Survey Circular 823-B, p. B17-B19.

Nelson, G. L., 1981, Hydrologic reconnaissance near Fourth of July Creek, Seward, Alaska: U.S. Geological Survey Water-Resources Investigations 81-21, 14 p. [also available as U.S. National Technical Information Service Report PB-81 223 752].

Nelson, R. E., 1981, Paleoenvironments during deposition of a section of the Gubik Formation exposed along the lower Colville River, North Slope, in Albert, N. R. D., and Hudson, Travis, eds., The United States Geological Survey in Alaska: Accomplishments during 1979: U.S. Geological Survey Circular 823-B, p. B9-B11.

Nelson, S. W., and Grybeck, Donald, 1980, Geologic map of the Survey Pass quadrangle, Brooks Range, Alaska: U.S. Geological Survey Miscellaneous Field Studies Map MF-1176-A, scale 1:250,000, 2 sheets.

Nilsen, T. H., Brosgé, W. P., Dutro, J. T., Jr., and Moore, T. E., 1981, Depositional model for the fluvial Upper Devonian Kanayut Conglomerate, Brooks Range, Alaska, in Albert, N. R. D., and Hudson, Travis, eds., The United States Geological Survey in Alaska: Accomplishments during 1979: U.S. Geological Survey Circular 823-B, p. B20-B21.

Nilsen, T. H., Moore, T. E., Brosgé, W. P., and Dutro, J. T., Jr., 1981, Sedimentology and stratigraphy of the Kanayut Conglomerate and associated units, Brooks Range, Alaska—report of 1979 field season: U.S. Geological Survey Open-File Report 81-506, 39 p.

Nokleberg, W. J., Albert, N. R. D., Herzon, P. L., Miyaoka, R. T., and Zehner, R. E., 1981a, Recognition of two subterranes within the Wrangellia terrane, southern Mount Hayes quadrangle, Alaska, in Albert, N. R. D., and Hudson, Travis, eds., The United States Geological Survey in Alaska: Accomplishments during 1979: U.S. Geological Survey Circular 823-B, p. B64-B66.

——1981b, Cross section showing accreted Andean-type arc and island arc terranes in southwestern Mount Hayes quadrangle, Alaska, in Albert, N. R. D., and Hudson, Travis, eds., The United States Geological Survey in Alaska: Accomplishments during 1979: U.S. Geological Survey Circular 823-B, p. B66-B67.

O'Leary, R. M., Risoli, D. A., Curtin, G. C., and McDanal, S. K., 1981, Spectrographic and chemical analyses of stream-sediment and glacial-debris samples from Mt. Hayes quadrangle, Alaska: U.S. Geological Survey Open-File Report 81-226, 55 p.

Orlando, R. C., and Martin, E. A., 1981, Grain size data compilation and parameters of sediment samples, lower Cook Inlet, Alaska, 1976 through 1979: U.S. Geological Survey Open-File Report 81-827, 389 p.

Patrick, Leslie, 1981, Results of exploratory drilling at Point MacKenzie, Alaska, 1981: U.S. Geological Survey Open-File Report 81-1072, 8 p.

Patton, W. W., Jr., and Csejtey, Béla, Jr., 1981, Geologic map of St. Lawrence Island, Alaska: U.S. Geological Survey Miscellaneous Investigations Series Map I-1203, scale 1:250,000.

Petering, G. W., and Smith, T. N., 1981, Stratigraphic sections, Hallo Bay to Katmai Bay, Shelikof Strait, Alaska, 1979: U.S. Geological Survey Open-File Report 81-21.

Quinterno, Paula, Carlson, P. R., and Molnia, B. F., 1981, Benthic foraminifers as indicators of the Pleistocene-Holocene boundary in the eastern Gulf of Alaska, in Albert, N. R. D., and Hudson, Travis, eds., The United States Geological Survey in Alaska: Accomplishments during 1979: U.S. Geological Survey Circular 823-B, p. B128-B131.

Rappeport, M. L., 1981, Current meter observations within lower Cook Inlet, Alaska, 1978-1979 from R/V SEA SOUNDER, Pacific-Arctic Branch, U.S. Geological Survey: U.S. Geological Survey Open-File Report 81-49, 78 p.

Rau, W. W., 1981, Unusually diverse and well-preserved Eocene foraminifers in dredge samples from the eastern Gulf of Alaska continental slope, in Albert, N. R. D., and Hudson, Travis, eds., The United States Geological Survey in Alaska: Accomplishments during 1979: U.S. Geological Survey Circular 823-B, p. B131-B135.

Rearic, D. M., Barnes, P. W., and Reimnitz, Erk, 1981, Ice-gouge data, Beaufort Sea, Alaska, 1972-1980: U.S. Geological Survey Open-File Report 81-950, 8 microfiche cards.

Reed, K. M., ed., 1981, The U.S. Geological Survey in Alaska, 1981 programs: U.S. Geological Survey Circular 843, 111 p.

Reiser, H. N., Brosgé, W. P., Dutro, J. T., Jr., and Detterman, R. L., 1980, Geologic map of the Demarcation Point quadrangle, Alaska: U.S. Geological Survey Miscellaneous Investigations Series Map I-1133, scale 1:250,000.

Rigby, J. K., 1981, Cambrian sponges of the North American cordilleran region, in Taylor, M. E., ed., Short papers for the Second International Symposium on the Cambrian System, 1981: U.S. Geological Survey Open-File Report 81-743, p. 181-183.

Sable, E. G., Dutro, J. T., Jr., Mangus, M. D., and Morris, R. H., 1981, Geology of the Kukpowruk-Nuka Rivers region, northwestern Alaska: U.S. Geological Survey Open-File Report 81-1078, 240 p.

Samuels, W. B., and Hopkins, Dorothy, 1981, An oilspill risk analysis for the St. George basin, Alaska (proposed sale 70) Outer Continental Shelf lease area: U.S. Geological Survey Open-File Report 81-864, 89 p.

Samuels, W. B., and Lanfear, K. J., 1981, An oilspill risk analysis for the Norton Sound, Alaska (proposed sale 57) Outer Continental Shelf lease area: U.S. Geological Survey Open-File Report 81-320, 114 p.

Schmoll, H. R., Dobrovolny, Ernest, and Gardner, C. A., 1981, Preliminary geologic map of Fire Island, Municipality of Anchorage, Alaska: U.S. Geological Survey Open-File Report 81-552, 4 p., scale 1:25,000.

Schmoll, H. R., and Emanuel, R. P., 1981, Generalized geologic map and hydrologic properties of Potter Creek area, Municipality of Anchorage, Alaska: U.S. Geological Survey Open-File Report 81-1168, scale 1:25,000.

Schmoll, H. R., Yehle, L. A., and Gardner, C. A., 1981, Preliminary geologic map of the Congahbuna area, Cook Inlet region, Alaska: U.S. Geological Survey Open-File Report 81-429, 8 p., scale 1:63,360.

Schwab, C. E., Patton, W. W., Jr., and Moll, E. J., 1981, Mineral occurrence map of the Medfra quadrangle, Alaska: U.S. Geological Survey Open-File Report 80-811-B, scale 1:250,000, 2 sheets.

Scully, D. R., Krumhardt, A. P., and Kernodle, D. R., 1980, Data from a hydrologic reconnaissance of the Beluga, Peters Creek, and Healy coal areas, Alaska: U.S. Geological Survey Open-File Report 80-1206, 54 p.

Severson, R. C., and Gough, L. P., 1981, Chemical character of minesoils at one Alaskan and twelve western conterminous United States coal-stripmines: U.S. Geological Survey Open-File Report 81-243, 80 p.

Shew, Nora, and Wilson, F. H., 1981, Map and tables showing radiometric ages of rocks in southwestern Alaska: U.S. Geological Survey Open-File Report 81-886, 25 p., scale 1:1,000,000.

Silberling, N. J., Richter, D. H., and Jones, D. L., 1981, Recognition of the Wrangellia terrane in the Clearwater Mountains and vicinity, south-central Alaska, in Albert, N. R. D., and Hudson, Travis, eds., The United States Geological Survey in Alaska: Accomplishments during 1979: U.S. Geological Survey Circular 823-B, p. B51-B55.

Silberman, M. L., Field, C. W., and Berry, A. L., eds., 1981, Proceedings of the symposium on mineral deposits of the Pacific Northwest: Geological Society of America, Cordilleran Section Meeting, Corvallis, Oreg., 1980: U.S. Geological Survey Open-File Report 81-355, 345 p.

Silberman, M. L., MacKevett, E. M., Jr., Connor, C. L., Klock, P. R., and Kalechitz, Georgiana, 1981, K-Ar ages of the Nikolai Greenstone from the McCarthy quadrangle, Alaska—the "docking" of Wrangellia, in Albert, N. R. D., and Hudson, Travis, eds., The United States Geological Survey in Alaska: Accomplishments during 1979: U.S. Geological Survey Circular 823-B, p. B61-B63.

Silberman, M. L., MacKevett, E. M., Connor, C. L., and Matthews, Alan, 1981, Metallogenic and tectonic significance of oxygen isotope data and whole-rock potassium-argon ages of the Nikolai Greenstone, McCarthy quadrangle, Alaska, in Silberman, M. L., Field, C. W., and Berry, A. L., eds., Proceedings of the symposium on mineral deposits of the Pacific Northwest: Geological Society of America, Cordilleran Section Meeting, Corvallis, Oreg., 1980: U.S. Geological Survey Open-File Report 81-355, p. 52-73.

Silberman, M. L., Mitchell, P. A., and O'Neil, J. R., 1981, Isotopic data bearing on the origin and age of the epithermal lode gold deposits in the Hope-Sunrise mining district, northern Kenai Peninsula, Alaska, in Albert, N. R. D., and Hudson, Travis, eds., The United States Geological Survey Circular 823-B, p. B81-B84.

Smith, J. G., and Diggles, M. F., 1981, Potassium-argon determinations in the Ketchikan and Prince Rupert quadrangles, southeastern Alaska: U.S. Geological Survey Open-File Report 78-73-N, 16 p.

Smith, P. R., 1981, Geology update of the Quartz Hill molybdenum property near Ketchikan, Alaska abs., in Silberman, M. L., Field, C. W., and Berry, A. L., eds., Proceedings of the symposium on mineral deposits of the Pacific Northwest: Geological Society of America, Cordilleran Section Meeting, Corvallis, Oreg., 1980: U.S. Geological Survey Open-File Report 81-355, p. 31-32.

Snavely, P. D., Jr., Tiffin, D. L., Wagner, H. C., and Tompkins, D. H., 1981, Preliminary geologic interpretation of a seismic reflection profile across the Queen Charlotte Island fault system off Dixon Entrance, Canada-United States: U.S. Geological Survey Open-File Report 81-299, 12 p.

Sohl, N. F., and Wright, W. B., 1980, Changes in stratigraphic nomenclature by the U.S. Geological Survey, 1979: U.S. Geological Survey Bulletin 1502-A, p. A1-A138.

Sonnevil, R. A., 1981a, The Chilkat-Prince of Wales plutonic province, southeastern Alaska, in Albert, N. R. D., and Hudson, Travis, eds., The

United States Geological Survey in Alaska: Accomplishments during 1979: U.S. Geological Survey Circular 823-B, p. B112-B115.

———1981b, New data concerning the geology of the North Bradfield River iron prospect, southeastern Alaska, in Albert, N. R. D., and Hudson, Travis, eds., The United States Geological Survey in Alaska: Accomplishments during 1979: U.S. Geological Survey Circular 823-B, p. B117-B119.

Steffy, D. A., and Hoose, P. J., 1981, Map showing acoustic anomalies and near-surface faulting, Norton Sound, Alaska: U.S. Geological Survey Open-File Report 81-722, scale 1:250,000.

Steffy, D. A., and Lybeck, L. D., 1981, Map showing selected geologic features, Norton Sound, Alaska: U.S. Geological Survey Open-File Report 81-721, scale 1:250,000.

Steffy, D. A., Turner, B. W., and Lybeck, L. D., 1981, Bathymetric map of Norton Sound, Alaska: U.S. Geological Survey Open-File Report 81-719, scale 1:250,000.

Steffy, D. A., Turner, B. W., Lybeck, L. D., and Roe, J. T., 1981, Isopach map of Holocene sedimentary units, Norton Sound, Alaska: U.S. Geological Survey Open-File Report 81-720, scale 1:250,000.

Stephens, C. D., Fogelman, K. A., Lahr, J. C., Helton, S. M., Cancilla, R. S., Tam, Roy, and Freiberg, J. A., 1980, Catalog of earthquakes in southern Alaska, January-March 1980: U.S. Geological Survey Open-File Report 80-1253, 55 p.

Stephens, C. D., Lahr, J. C., and Rogers, J. A., 1981, Eastern Gulf of Alaska seismicity: Annual report to the National Oceanic and Atmospheric Administration for April 1, 1980, through March 31, 1981: U.S. Geological Survey Open-File Report 81-897, 32 p.

Stover, C. W., Hubiac, P., Minsch, J. H., and Person, W. J., 1980, Earthquakes in the United States, April-June 1979: U.S. Geological Survey Circular 836-B, p. B1-B34.

Stover, C. W., Minsch, J. H., Reagor, B. G., and Smith, P. K., 1981a, Earthquakes in the United States, October-December 1979: U.S. Geological Survey Circular 836-D, p. D1-D43.

———1981b, Earthquakes in the United States, January-March 1980: U.S. Geological Survey Circular 853-A, p. A1-A41.

Stover, C. W., Minsch, J. H., Smith, P. K., and Person, W. J., 1981, Earthquakes in the United States, April-June, 1980: U.S. Geological Survey Circular 853-B, p. B1-B53.

Swanson, R. W., Hubert, M. L., Luttrell, G. W., and Jussen, V. M., 1981, Geologic names of the United States through 1975: U.S. Geological Survey Bulletin 1535, 643 p.

Thor, D. R., and Nelson, C. H., 1981, Environmental geologic studies of the northern Bering Sea, in Albert, N. R. D., and Hudson, Travis, eds., The United States Geological Survey in Alaska: Accomplishments during 1979: U.S. Geological Survey Circular 823-B, p. B121-B122.

Toth, M. I., 1981, Petrology, geochemistry, and origin of the Red Mountain ultramafic body near Seldovia, Alaska: U.S. Geological Survey Open-File Report 81-514, 86 p.

Townshend, J. B., Papp, J. E., and Sauter, E. A., 1981a, Preliminary geomagnetic data, College, Observatory, Fairbanks, Alaska, March 1981: U.S. Geological Survey Open-File Report 81-300-C, 22 p. (unnumbered).

——1981b, Preliminary geomagnetic data, College Observatory, Fairbanks, Alaska, April 1981: U.S. Geological Survey Open-File Report 81-300-D, 22 p. (unnumbered).

——1981c, Preliminary geomagnetic data, College Observatory, Fairbanks, Alaska, May 1981: U.S. Geological Survey Open-File Report 81-300-E, 22 p. (unnumbered).

——1981d, Preliminary geomagnetic data, College Observatory, Fairbanks, Alaska, June 1981: U.S. Geological Survey Open-File Report 81-300-F, 20 p. (unnumbered).

——1981e, Preliminary geomagnetic data, College Observatory, Fairbanks, Alaska, July 1981: U.S. Geological Survey Open-File Report 81-300-G, 21 p. (unnumbered).

Townshend, J. B., Papp, J. E., Sauter, E. A., and Tilton, S. P., 1980a, Preliminary geomagnetic data, College Observatory, Fairbanks, Alaska, November 1980: U.S. Geological Survey Open-File Report 80-300-K, 21 p. (unnumbered).

——1980b, Preliminary geomagnetic data, College Observatory, Fairbanks, Alaska, December 1980: U.S. Geological Survey Open-File Report 80-300-L, 21 p. (unnumbered).

——1981a, Preliminary geomagnetic data, College Observatory, Fairbanks, Alaska, January 1981: U.S. Geological Survey Open-File Report 81-300-A, 21 p. (unnumbered).

——1981b, Preliminary geomagnetic data, College Observatory, Fairbanks, Alaska, February 1981: U.S. Geological Survey Open-File Report 81-300-B, 10 p. (unnumbered).

U.S. Geological Survey, 1980, Geological Survey research 1980: Professional Paper 1175, 459 p.

Varnes, K. L., Dolton, G. L., and McMullin, R. H., 1981, Oil and gas resource assessment areas, U.S. Geological Survey, Geologic Division, 1980, Alaska, Regions 1 and 1A: U.S. Geological Survey Open-File Report 81-84-A, scale 1:5,000,000.

White, E. R., compiler, 1981, Reports on Alaska published by U.S. Geological Survey authors in outside publications, 1979, in Albert, N. R. D., and Hudson, Travis, eds., The United States Geological Survey in Alaska: Accomplishments during 1979: U.S. Geological Survey Circular 823-B, p. B146-B149.

Whitney, J. W., and Thurston, D. K., 1981, Geologic constraints for petroleum development of the lower Cook Inlet, Alaska, Outer Continental Shelf lease area, in Albert, N. R. D., and Hudson, Travis, eds., The United States Geological Survey in Alaska: Accomplishments during 1979: U.S. Geological Survey Circular 823-B, p. B122-B125.

Wilcox, D. E., 1980, Geohydrology of the Delta-Clearwater area, Alaska: U.S. Geological

Survey Water-Resources Investigations 80-92, 26 p. [also available as U.S. National Technical Information Service Report PB-81 200 651].

Williams, J. R., and Coulter, H. W., 1981, Deglaciation and sea-level fluctuations in Port Valdez, Alaska, in Albert, N. R. D., and Hudson, Travis, eds., The United States Geological Survey in Alaska: Accomplishments during 1979: U.S. Geological Survey Circular 823-B, p. B78-B80.

Williams, J. R., and Johnson, K. M., 1980, Map and description of late Tertiary and Quaternary deposits, Valdez quadrangle, Alaska: U.S. Geological Survey Open-File Report 80-892-C, scale 1:250,000, 2 sheets.

——1981, Surficial deposits of the Valdez quadrangle, Alaska, in Albert, N. R. D., and Hudson, Travis, eds., The United States Geological Survey in Alaska: Accomplishments during 1979: U.S. Geological Survey Circular 823-B, p. B76-B78.

Wills, J. C., and Bolm, J. G., 1981, Preliminary unevaluated subsurface stratigraphic study (1976) of the lower Cook Inlet area, Alaska: U.S. Geological Survey Open-File Report 81-615, 4 p. + 18 pls.

Wilson, C. W., 1981, Bibligraphic references to Alaskan fossils, 1839-May 1979: U.S. Geological Survey Open-File Report 81-624, 72 p.

Wilson, F. H., 1981a, K-Ar ages on intrusive rocks and altered zones in the Chignik and Sutwik Island quadrangles, in Albert, N. R. D., and Hudson, Travis, eds., The United States Geological Survey in Alaska: Accomplishments during 1979: U.S. Geological Survey Circular 823-B, p. B45-B46.

——1981b, Map and table showing radiometric ages of rocks in the Aleutian Islands and Alaska Peninsula: U.S. Geological Survey Open-File Report 81-471, 23 p. + map, scale 1:1,000,000.

Wilson, F. H., and Shew, Nora, 1981, Map and tables showing preliminary results of potassium-argon age studies in the Circle quadrangle, Alaska, with a compilation of previous dating work: U.S. Geological Survey Open-File Report 81-889, scale 1:250,000.

Winkler, G. R., and MacKevett, E. M., Jr., 1981, Geologic map of the McCarthy C-7 quadrangle, Alaska: U.S. Geological Survey Geologic Quadrangle Map GQ-1533, scale 1:63,360.

Winkler, G. R., Miller, R. J., and Case, J. E., 1981, Blocks and belts of blueschist and greenschist in the northwestern Valdez quadrangle, in Albert, N. R. D., and Hudson, Travis, The United States Geological Survey in Alaska: Accomplishments during 1979: U.S. Geological Survey Circular 823-B, p. B72-B74.

Winkler, G. R., Miller, R. J., MacKevett, E. M., Jr., and Holloway, C. D., 1981, Map and summary table describing mineral deposits in the Valdez quadrangle, southern Alaska: U.S. Geological Survey Open-File Report 80-892-B, scale 1:250,000, 2 sheets.

Winkler, G. R., Miller, R. J., Silberman, M. L., Grantz, Arthur, Case, J. E., and Pickthorn, W. J., 1981, Layered gabbroic belt of regional extent in the Valdez quadrangle, in Albert, N. R. D., and Hudson, Travis, eds., The United States Geological Survey in Alaska: Accomplishments during 1979: U.S. Geological Survey Circular 823-B, p. B74-B76.

Winkler, G. R., and Plafker, George, 1981a, Tectonic implications of framework grain mineralogy of sandstone from the Yakutat Group, in Albert, N. R. D., and Hudson, Travis, eds., The United States Geological Survey in Alaska: Accomplishments during 1979: U.S. Geological Survey Circular 823-B, p. B68-B70.

——1981b, Geologic map and cross sections of the Cordova and Middleton Island quadrangles, southern Alaska: U.S. Geological Survey Open-File Report 81-1164, 25 p., scale 1:250,000.

Winkler, G. R., Silberman, M. L., Grantz, Arthur, Miller, R. J., and MacKevett, E. M., Jr., 1981, Geologic map and summary geochronology of the Valdez quadrangle, southern Alaska: U.S. Geological Survey Open-File Report 80-892-A, scale 1:250,000, 2 sheets.

Witmer, R. J., 1980, Availability of palynomorph and Foraminifera microscope slides from test wells of National Petroleum Reserve in Alaska: Group II: U.S. Geological Survey Open-File Report 81-13, 18 p.

——1981, Availability of palynomorph and Foraminifera microscope slides from test wells of National Petroleum Reserve in Alaska: Group III—final release: U.S. Geological Survey Open-File Report 81-1081, 14 p.

Witmer, R. J., Haga, Hideyo, and Mickey, M. B., 1981, Biostratigraphic report of thirty-three wells drilled from 1975 to 1981 in National Petroleum Reserve in Alaska: U.S. Geological Survey Open-File Report 81-1166, 47 p.

Witmer, R. J., Mickey, M. B., and Haga, Hideyo, 1981, Biostratigraphic correlations of selected test wells of National Petroleum Reserve in Alaska: U.S. Geological Survey Open-File Report 81-1165, 89 p. + 6 pls.

Yeend, Warren, 1981a, Placer gold deposits, Mount Hayes quadrangle, Alaska, in Albert, N. R. D., and Hudson, Travis, eds., The United States Geological Survey in Alaska: Accomplishments during 1979: U.S. Geological Survey Circular 823-B, p. B68.

——1981b, Placer gold deposits, Mount Hayes quadrangle, Alaska, in Silberman, M. L., Field, C. W., and Berry, A. L., eds., Proceedings of the symposium on mineral deposits of the Pacific Northwest: Geological Society of America, Cordilleran Section Meeting, Corvallis, Oreg., 1980: U.S. Geological Survey Open-File Report 81-355, p. 74-83.

Zimmerman, Jay, Frank, C. O., and Bryn, Sean, 1981, Mafic rocks in the Avan Hills ultramafic complex, De Long Mountains, in Albert, N. R. D., and Hudson, Travis, eds., The United States Geological Survey in Alaska: Accomplishments during 1979: U.S. Geological Survey Circular 823-B, p. B14-B15.

Reports on Alaska published by U.S. Geological Survey authors in outside publications, 1981

Compiled by Ellen R. White

Ager, T. A., and Sims, J. D., 1981, Holocene pollen and sediment record from the Tangle Lakes area, central Alaska: Palynology, v. 5, p. 85-98.

Aleinikoff, J. N., Dusel-Bacon, Cynthia, Foster, H. L., and Futa, Kiyoto, 1981, Proterozoic zircon from augen gneiss, Yukon-Tanana Upland, east-central Alaska: Geology, v. 9, no. 10, p. 469-473.

Barnes, P. W., and Reimnitz, Erk, 1981, Seabed changes resulting from combined sea ice and hydraulic processes on shelves of Arctic Basin: Example from Harrison Bay, Alaska [abs.]: American Association of Petroleum Geologists Bulletin, v. 65, no. 5, p. 895.

Ben-Avraham, Zvi, and Cooper, A. K., 1981a, Early evolution of the Bering Sea by collision of oceanic rises and North Pacific subduction zones: Geological Society of America Bulletin, v. 92, no. 7, p. 485-495.

——1981b, Early evolution of the Bering Sea by collision of oceanic rises and North Pacific subduction zones [summary]: Geological Society of America News and Information, v. 3, no. 9, p. 167.

Ben-Avraham, Zvi, Nur, A., Jones, D., and Cox, A., 1981, Continental accretion: From oceanic plateaus to allochthonous terranes: Science, v. 213, no. 4503, p. 47-54.

Berg, H. C., 1981, Metallogenesis in accreted terranes in southeastern Alaska [abs.]: Geological Association of Canada-Mineralogical Association of Canada-Canadian Geophysical Union Joint Annual Meeting, Calgary, Alberta, Canada, 1981, Program with Abstracts, v. 6, p. A-4.

Billington, Selena, Engdahl, E. R., and Price, Stephanie, 1981, Changes in the seismicity and focal mechanism of small earthquakes prior to an M_S 6.7 earthquake in the central Aleutian Island Arc, in Simpson, D. W., and Richards, P. G., eds., 1981, Earthquake prediction; an international review: Washington, American Geophysical Union, p. 348-356.

Bird, K. J., and Mamet, B. L., 1981, Carboniferous foraminifer Mediocris, first occurrence in northern Alaska [abs.]: Geological Society of America Abstracts with Programs, v. 13, no. 7, p. 410.

Blome, C. D., 1981, Middle Jurassic (Callovian) radiolaria from southern Alaska [abs.]: Geological Society of America Abstracts with Programs, v. 13, no. 7, p. 411.

Boucher, Gary, 1981, Digital high-resolution study of shallow frozen and gas-bearing layers, offshore Prudhoe Bay, Alaska [abs.]: Geophysics, v. 46, no. 4, p. 449-450.

Boucher, Gary, Reimnitz, Erk, and Kempema, E. W., 1981, Seismic evidence for an extensive gas-bearing layer at shallow depth, offshore from Prudhoe Bay, Alaska: Cold Regions Science and Technology, v. 4, no. 1, p. 63-71.

Bouma, Arnold, Sangrey, Dwight, Coleman, James, Prior, David, Trippet, Anita, Dunlap, Wayne, and Hooper, James, 1981, Offshore geologic hazards; a short course presented at Rice University, May 2-3, 1981 for the Offshore Technology Conference: Tulsa, Okla., American Association of Petroleum Geologists Education Course Note Series 18.

Box, Stephen, and Moore, J. C., 1981, Mesozoic tectonic framework, northern Bristol Bay, southwestern Alaska [abs.]: Eos (American Geophysical Union Transactions), v. 62, no. 45, p. 1038-1039.

Brew, D. A., 1981, The Coast plutonic complex in southeastern Alaska and northwestern British Columbia [abs.]: Geological Association of Canada Annual Meeting, Vancouver, British Columbia, Canada, 1981, Programme and Abstracts, p. 9-10.

Brewer, M. C., 1981, Arctic construction and environmental engineering for petroleum exploration on the National Petroleum Reserve in Alaska [abs.]: International Symposium on Arctic Geology, 3d, Calgary, Alberta, Canada, 1981 [Program with Abstracts], p. 32.

Bruns, T. R., Carlson, P. R., and Plafker, George, 1981, Structural deformation in northern Gulf of Alaska: Transition from transform to convergent plate motion [abs.]: American Association of Petroleum Geologists Bulletin, v. 65, no. 5, p. 907.

Buland, Ray, and Taggart, James, 1981, A mantle wave magnitude for the St. Elias, Alaska, earthquake of 28 February 1979: Seismological Society of America Bulletin, v. 71, no. 4, p. 1143-1159.

Callahan, J. E., 1981, Geology and quality of coal beds in the Cretaceous Corwin Formation in the northern foothills of western arctic Alaska [abs.]: International Symposium on Arctic Geology, 3d, Calgary, Alberta, Canada, 1981 [Program with Abstracts], p. 33.

Carlson, P. R., Karl, H. A., and Johnson, K. A., 1981, Morphology, sedimentology, and genesis of three large submarine canyons adjacent to Navarin Basin, Bering Sea [abs.]: American Association of Petroleum Geologists Bulletin, v. 65, no. 5, p. 909.

Carlson, P. R., Plafker, George, and Bruns, T. R., 1981, Fairweather fault on SE Alaska shelf [abs.]: Eos (American Geophysical Union Transactions), v. 62, no. 6, p. 60.

Carter, L. D., 1980, Tertiary tillites(?) on the northeast flank of Granite Mountain, central Alaska Range: Alaska Division of Geological and Geophysical Surveys Geologic Report 63, p. 23-27.

——1981, A Pleistocene sand sea on the Alaskan arctic coastal plain: Science, v. 211, no. 4480, p. 381-383.

Carter, L. D., and Galloway, J. P., 1981, Earth flows along Henry Creek, northern Alaska: Arctic, v. 34, no. 4, p. 325-328.

Chapman, R. M., 1981, Memorial to John B. Mertie, Jr.: Alaska Mines and Geology, v. 30, no. 1, p. 14-15.

Churkin, Michael, Jr., Soleimani, George, Carter, Claire, and Robinson, Rhoda, 1981, Geology of the Soviet Arctic: Kola Peninsula to Lena River,

in Nairn, A. E. M., Churkin, Michael, Jr., and Stehli, F. G., The ocean basins and margins: New York, Plenum Press, v. 5, p. 331-375.

Churkin, Michael, Jr., and Trexler, J. H., Jr., 1981a, Continental plates and accreted oceanic terranes in the Arctic, in Nairn, A. E. M., Churkin, Michael, Jr., and Stehli, F. G., eds., The ocean basins and margins; volume 5, The Arctic Ocean: New York, Plenum Press, p. 1-20.

——1981b, Plate accretion and Kula plate capture in the Arctic [abs.]: International Symposium on Arctic Geology, 3d, Calgary, Alberta, Canada, 1981 [Program with Abstracts], p. 35.

Clark, S. H. B., 1981, Guide to the bedrock geology along the Seward highway north of Turnagain Arm: Anchorage, Alaska Geological Society Publication 1, 36 p.

Cooper, A. K., Marlow, M. S., and Ben-Avraham, Zvi, 1981a, Multichannel seismic evidence bearing on the origin of Bowers Ridge, Bering Sea: Geological Society of America Bulletin, v. 92, no. 7, p. 474-484.

——1981b, Multichannel seismic evidence bearing on the origin of Bowers Ridge, Bering Sea [summary]: Geological Society of America News and Information, v. 3, no. 9, p. 167.

Cooper, A. K., Marlow, M. S., and Scholl, D. W., 1981, Prospective and future hydrocarbon provinces of Bering Sea, south of St. Lawrence Island [abs.]: Geophysics, v. 46, no. 44, p. 444.

Dearborn, L. L., 1981, Potential and developed water-supply sources in Alaska: Alaska Geological Society Journal, v. 1, p. 1-11.

Detterman, R. L., 1981, The Sadlerochit Group—Paleozoic-Mesozoic boundary in arctic Alaska [abs.]: International Symposium on Arctic Geology, 3d, Calgary, Alberta, Canada, 1981 [Program with Abstracts], p. 39.

Dinter, D. A., and Grantz, Arthur, 1981, Environmental geology of the Beaufort and Chukchi Seas of concern to petroleum development [abs.]: International Symposium on Arctic Geology, 3d, Calgary, Alberta, Canada, 1981 [Program with Abstracts], p. 41.

Dutro, J. T., Jr., 1981, Geology of Alaska bordering the Arctic Ocean, in Nairn, A. E. M., Churkin, Michael, Jr., and Stehli, F. G., eds., The ocean basins and margins; volume 5, The Arctic Ocean: New York, Plenum Press, p. 21-36.

Ellis, J. M., Hamilton, T. D., and Calkin, P. E., 1981, Holocene glaciation of the Arrigetch Peaks, Brooks Range, Alaska: Arctic, v. 34, no. 2, p. 158-168.

Field, M. E., 1981, Deposition on Pacific shelf edge: zone of contrasts [abs.]: American Association of Petroleum Geologists Bulletin, v. 65, no. 5, p. 924.

Field, M. E., Nelson, C. H., Cacchione, D. A., and Drake, D. E., 1981, Sand wave on an epicontinental shelf: Northern Bering Sea: Marine Geology, v. 42, no. 1-4, p. 233-258.

Fisher, M. A., 1981, Location of the Border Ranges fault southwest of Kodiak Island, Alaska: Geological Society of America Bulletin, v. 92, no. 1, p. 19-30.

Fisher, M. A., Bruns, T. R., and von Huene, Roland, 1981, Transverse tectonic boundaries near Kodiak Island, Alaska: Geological Society of America Bulletin, v. 92, no. 1, p. 10-18.

Fox, J. E., Lambert, P. W., and Pitman, J. K., 1981, Depositional environments and reservoir properties of sandstones of Lower Cretaceous Nanushuk and Upper Cretaceous Colville Groups, Umiat Test Well 11, National Petroleum Reserve, Alaska [abs.]: American Association of Petroleum Geologists Bulletin, v. 65, no. 5, p. 926.

Frohlich, Cliff, Billington, Selena, and Engdahl, E. R., 1981, Final results from the OBS experiments in the central Aleutians [abs.]: Eos (American Geophysical Union Transactions), v. 62, no. 17, p. 335-336.

Fujita, Kazuya, Engdahl, E. R., and Sleep, N. H., 1981, Subduction zone calibration and teleseismic relocation of thrust zone events in the central Aleutian Islands: Seismological Society of America, Bulletin, v. 71, no. 6, p. 1805-1828.

Gardner, J. V., and Vallier, T. L., 1981, Faulting in outer continental shelf of southern Bering Sea: American Association of Petroleum Geologists Bulletin, v. 65, no. 9, p. 1568-1573.

Grantz, Arthur, Eittreim, Stephen, and Whitney, O. T., 1981, Geology and physiography of the continental margin north of Alaska and implications for the origin of the Canada Basin, in Nairn, A. E. M., Churkin, Michael, Jr., and Stehli, F. G., eds., The ocean basins and margins; volume 5, The Arctic Ocean: New York, Plenum Press, p. 439-492.

Grantz, Arthur, and May, S. D., 1981a, Influence of rifting geometry on the structural development of the continental margin north of Alaska abs., in Continental margin processes: Hedberg Research Conference, Galveston, Tex., 1981, Program with Abstracts, p. 26.

——1981b, Influence of rifting geometry on the structural development of the continental margin north of Alaska [abs.]: International Symposium on Arctic Geology, 3d, Calgary, Alberta, Canada, 1981 [Program with Abstracts], p. 54.

Grantz, Arthur, and May, S. D., 1981, Origin of the Canada basin as inferred from the seismic geology of offshore northern Alaska abs., in The origin of the Arctic Ocean (Canada basin): Alaska Geological Society Mini Symposium, Anchorage, 1981, 2 p.

Gryc, George, and Tailleur, I. L., 1981, Recent exploration results in the National Petroleum Reserve in Alaska [abs.]: International Symposium on Arctic Geology, 3d, Calgary, Alberta, Canada, 1981 [Program with Abstracts], p. 55.

Hamilton, T. D., 1981, Multiple moisture sources and the Brooks Range glacial record [abs.]: Annual Arctic Workshop, 10th, Boulder, Colo., Abstracts, p. 16-18.

Hampton, M. A., and Kvenvolden, K. A., 1981, Geology and geochemistry of gas-charged sediment on Kodiak Shelf, Alaska: Geo-Marine Letters, v. 1, no. 2, p. 141-147.

Hampton, M. A., and Winters, W. J., 1981, Environmental geology of Shelikof Strait, OCS sale area

60, Alaska: Offshore Technology Conference, Houston, Tex., 1981, Proceedings, no. 13, v. 4, p. 19-3, OTC 4118.

Hill, Malcolm, Morris, Julie, and Whelan, Joseph, 1981, Hybrid granodiorites intruding the accretionary prism, Kodiak, Shumagin, and Sanak Islands, southwest Alaska: Journal of Geophysical Research, v. 86, no. 11, p. 10569-10590.

Hillhouse, J. W., and Grommé, C. S., 1981a, Limits to northward drift of the Paleocene Cantwell basin, central Alaska [abs.]: Eos (American Geophysical Union Transactions), v. 62, no. 45, p. 854.

——1981b, Review of paleomagnetic studies in arctic Alaska abs., in The origin of the Arctic Ocean (Canada basin): Alaska Geological Society Mini Symposium, Anchorage, 1981, 2 p.

Holmes, M. L., and Creager, J. S. 1981, The role of the Kaltag and Kobuk faults in the tectonic evolution of the Bering Strait region, in Hood, D. W., and Calder, J. A., eds., The eastern Bering shelf: Oceanography and resources: U.S. Department of Commerce, v. 1, p. 293-302.

Hopkins, D. M., and Herman, Y., 1981, Ice rafting, An indication of glaciation?: Science, v. 214, no. 4521, p. 688.

Hopkins, D. M., and Smith, P. A., 1981, Dated wood from Alaska and the Yukon: Implications for forest refugia in Beringia: Quaternary Research, v. 15, no. 3, p. 217-249.

Houtz, R. E., Eittreim, Stephen, and Grantz, Arthur, 1981, Acoustic properties of northern Alaska shelves in relation to the regional geology: Journal of Geophysical Research, v. 86, no. B5, p. 3935-3943.

Hudson, Travis, Arth, J. G., and Muth, K. G., 1981, Geochemistry of intrusive rocks associated with molybdenite deposits, Ketchikan quadrangle, southeastern Alaska: Economic Geology, v. 76, no. 5, p. 1225-1232.

Jones, D. L., Berg, H. C., and Nokleberg, Warren, 1981, Significance of tectonostratigraphic terranes to metallogenesis in Alaska [abs.]: Geological Association of Canada-Mineralogical Association of Canada-Canadian Geophysical Union Joint Annual Meeting, Calgary, Alberta, Canada, 1981, Program with Abstracts, v. 6, p. A-29.

Karl, H. A., and Carlson, P. R., 1981, Large sediment waves at the shelf edge, northern Bering Sea [abs.]: Geological Society of America Abstracts with Programs, v. 13, no. 7, p. 483.

Karlstrom, T. N. V., 1981, Detailed Holocene records of paleoclimate from western North America, marine-terrestrial correlations and glacioeustatic implications [abs.], in Mahaney, W. C., ed., Quaternary paleo-climate: Norwich, England, Geo Abstracts, p. 45-46.

Koski, R. A., and Rubin, J. S., 1981, Amorphous and crystalline ferromanganese deposits from seamounts in Gulf of Alaska [abs.]: American Association of Petroleum Geologists Bulletin, v. 65, no. 5, p. 945.

Kvenvolden, K. A. Redden, G. D., Thor, D. R., and Nelson, C. H. 1981, Hydrocarbon gases in near-surface sediment of the northern Bering Sea, in Hood, D. W., and Calder, J. A., eds., The eastern Bering shelf: Oceanography and resources: U.S. Department of Commerce, v. 1, p. 411-424.

Kvenvolden, K. A., Vogel, T. M., and Gardner, J. V., 1981, Geochemical prospecting for hydrocarbons in the outer continental shelf, southern Bering Sea, Alaska: Journal of Geochemical Exploration, v. 14, no. 2-3, p. 209-219.

Lange, I. E., Nokleberg, W. J., and Zehner, R. E., 1981, Mineralization of Late Paleozoic island arc rocks of Wrangellia terrane, Mount Hayes quadrangle, eastern Alaska Range, Alaska [abs.]: Geological Association of Canada-Mineralogical Association of Canada-Canadian Geophysical Union Joint annual Meeting, Calgary, Alberta, Canada, 1981, Program with Abstracts, v. 6, p. A-33.

Lantz, R. J., 1981, Barrow gas-fields—N. Slope, Alaska: Oil and Gas Journal, v. 79, no.13, p. 197-200.

Larsen, M. C., Nelson, C. H., and Thor, D. R. 1981, Sedimentary processes and potential geologic hazards on the sea floor of the northern Bering Sea, in Hood, D. W., and Calder, J. A., eds., The eastern Bering shelf: Oceanography and resources: U.S. Department of Commerce, v. 1, p. 247-261.

Magoon, L. B., and Claypool, G. E., 1981a, Petroleum geology of Cook Inlet Basin—an exploration model: American Association of Petroleum Geologists Bulletin, v. 65, no. 6, p. 1043-1061.

——1981b, Two oil types on North Slope of Alaska—implications for exploration: American Association of Petroleum Geologists Bulletin, v. 65, no. 4, p. 644-652.

Magoon, L. B., and Kirschner, C. E., 1981, Evolution of sedimentary systems during Mesozoic and Cenozoic in southern Alaska—an overview [abs.]: American Association of Petroleum Geologists Bulletin, v. 65, no. 5, p. 953.

Marincovich, Louie, Jr., 1981, Tyrannoberingius rex, a new genus and species of Miocene gastropod from Alaska: Journal of Paleontology, v. 55, no. 1, p. 176-179.

Marlow, M. S., Cooper, A. K., and Childs, Jonathan, 1981, Geophysical survey of Anadyr and Navarin Basins, northern Bering Sea [abs.]: American Association of Petroleum Geologists Bulletin, v. 65, no. 5, p. 953.

Marsh, S. P., and Cathrall, J. B., 1981, Geochemical evidence for a Brooks Range mineral belt, Alaska: Journal of Geochemical Exploration, v. 15, no. 1-3, p. 367-380.

Molnia, B. F., 1981, Distribution of continental shelf surface sedimentary units between Yakutat and Cross Sound, northeastern Gulf of Alaska: Alaska Geological Society Journal, v. 1, p. 60-65.

Nilsen, T. H., Moore, T. E., Brosgé, W. P., Dutro, J. T., Jr., Balin, D. F., and Johnson, S. V., 1981, Allochthonous Upper Devonian fluvial strata, northern Alaska [abs.]: International Symposium on Arctic Geology, 3d, 1981, Calgary, Alberta, Canada [Program with Abstracts], p. 96.

Nokleberg, W. J., and Zehner, R. E., 1981, Metallogeny of accreted Andean type arc and island arc terranes, Mount Hayes quadrangle, eastern Alaska Range, Alaska [abs.]: Geological Association of Canada-Mineralogical Association of Canada-

Canadian Geophysical Union Joint Annual Meeting, Calgary, Alberta, Canada, 1981, Program with Abstracts, v. 6, p. A-43.

Overstreet, W. C., and Chapman, R. M., 1981, Memorial to John Beaver Mertie, Jr., 1888-1980: Geological Society of America preprint, 8 p.

Patton, W. W., Jr., and Moll, E. J., 1981, A geologic transect between the Alaska Range and Norton Sound, western Alaska [abs.]: Geological Society of America Abstracts with Programs, v. 13, no. 7, p. 527.

Perkins, J. A., and Sims, J. D., 1981, Reconstruction of trends of annual temperature and snowfall in Alaska based on varve thickness in Skilak Lake, Alaska [abs.]: Geological Society of America Abstracts with Programs, v. 13, no. 7, p. 527-528.

Plafker, George, 1981, Late Cenozoic glaciomarine deposits of the Yakataga Formation, Alaska, in Hambrey, M. J., and Harland, W. B., eds., 1981, Earth's pre-Pleistocene glacial record: New York, Cambridge University Press, p. 694-699.

Plumley, P. W., Byrne, T. B., Coe, R. S., and Moore, J. C., 1981, Paleomagnetism of the Ghost Rocks volcanics on Kodiak indicates 24° northward displacement [abs.]: Eos (American Geophysical Union Transactions), v. 62, no. 45, p. 854.

Plumley, P. W., Coe, R. S., Patton, W. W., Jr., and Moll, E. J., 1981, Paleomagnetic study of the Nixon Fork Terrane, west-central Alaska [abs.]: Geological Society of America Abstracts with Programs, v. 13, no. 7, p. 530.

Quinterno, Paula, Blueford, J. R., and Baldauf, J. G., 1981, Micropaleontologic analysis of Navarin Basin, Bering Sea, Alaska [abs.]: American Association of Petroleum Geologists Bulletin, v. 65, no. 5, p. 975.

Reimnitz, Erk, and Barnes, P. W., 1981, Depositional complexities in sea-ice environment of Arctic shelves: Example from Harrison Bay, Alaska [abs.]: American Association of Petroleum Geologists Bulletin, v. 65, no. 5, p. 978.

Rice, D. D., and Claypool, G. E., 1981, Generation, accumulation, and resource potential of biogenic gas: American Association of Petroleum Geologists Bulletin, v. 65, no. 1, p. 5-25.

Saleeby, J. B., and Eberlein, G. D., 1981, An ensimatic basement complex and its relation to the early Paleozoic volcanic-arc sequence of southern Prince of Wales Island, southeastern Alaska [abs.]: Geological Society of America, Abstracts with Programs, v. 13, no. 2, p. 104.

Savage, N. M., 1981, A reassessment of the age of some Paleozoic brachiopods from southeastern Alaska: Journal of Paleontology, v. 55, no. 2, p. 353-369.

Scholl, D. W., Vallier, T. L., and Stevenson, A. J., 1981a, Arc, forearc, and trench sedimentation and tectonics, Amlia corridor, Aleutian subduction zone; preliminary results [abs.], in Continental margin processes: Hedberg Research Conference, Galveston, Tex., 1981, Program with Abstracts, p. 50-53.

——1981b, Geologic evolution of the Amlia corridor of the Aleutian Ridge [abs.]: Eos (American Geophysical Union Transactions), v. 62, no. 45, p. 1091.

Smith, T. N., and Petering, G. W., 1981, Petroleum potential of Shelikof Strait based on outcrops in Katmai National Monument, Alaska [abs.]: American Association of Petroleum Geologists Bulletin, v. 65, no. 5, p. 994.

Spencer, C. P., and Engdahl, E. R., 1981, Inversion for hypocenters and structure beneath the central Aleutian Island Arc [abs.]: Eos (American Geophysical Union Transactions), v. 62, no. 17, p. 335.

Swanson, S. E., Turner, D. L., Forbes, R. B., and Hopkins, D. M., 1981, Petrology and geochronology of Tertiary and Quaternary basalts from the Seward Peninsula, western Alaska [abs.]: Geological Society of America Abstracts with Programs, v. 13, no. 7, p. 563.

Thor, D. R., and Nelson, C. H. 1981a , Ice gouging on the subarctic Bering shelf, in Hood, D. W., and Calder, J. A., eds., The eastern Bering shelf: Oceanography and resources: U.S. Department of Commerce, v. 1, p. 247-261.

——1981b , Ice gouging on the subarctic Bering shelf, in Hood, D. W., and Calder, J. A., eds., The eastern Bering shelf: Oceanography and resources: U.S. Department of Commerce, v. 1, p. 279-291.

Till, A. B., 1981, Alpine-type garnet lherzolite from the Kigluaik Mountains, Seward Peninsula, Alaska [abs.]: Geological Society of America Abstracts with Programs, v. 13, no. 2, p. 110.

Vallier, T. L., Hein, J. R., McLean, Hugh, Scholl, D. W., and Friesen, W. B., 1981, Igneous rocks of Amlia Island: Implications for the early volcanic and tectonic histories of the Aleutian Island arc [abs.]: Eos (American Geophysical Union Transactions), v. 62, no. 45, p. 1092.

Vogel, T. M., Kvenvolden, K. A., Carlson, P. R., and others, 1981, Geochemical prospecting for hydrocarbons in Navarin basin province [abs.]: American Association of Petroleum Geologists Bulletin, v. 65, no. 5, p. 1004.

von Huene, Roland, Bruns, Terry, and Fisher, Michael, 1981, Subduction-related structure along eastern Aleutian Trench [abs.]: American Association of Petroleum Geologists Bulletin, v. 65, no. 3, p. 1004.

Weber, F. R., Hamilton, T. D., Hopkins, D. M., Repenning, C. A., and Haas, Herbert, 1981, Canyon Creek: A Late Pleistocene vertebrate locality in interior Alaska: Quaternary Research, v. 16, no. 2, p. 167-180.

Westgate, J. A., Matthews, J. V., Jr., and Hamilton, T. D., 1981, Old Crow tephra: A new Late Pleistocene stratigraphic marker across Alaska and the Yukon Territory [abs.]: Geological Society of America Abstracts with Programs, v. 13, no. 7, p. 579.

Whitney, J. W., Noonan, W. G., and Thurston, D. K., 1981, Stability of large sand waves in lower Cook Inlet, Alaska: Alaska Geological Society Journal, v. 1, p. 36-47.

Author Index

[Page number underscored indicates listed name is senior author; number in parentheses indicates listed name has authorship in more than one report on that page .]

GPO 787-042/124

BACK COVER

The back cover is a photograph of plant fossils from the conglomerate of Mount Dall in the Talkeetna quadrangle (see Mamay and Reed, this volume, fig. 62).